University of Rhode Island
DigitalCommons@URI

Open Access Dissertations

2020

FUNCTION AND VARIABILITY OF METABOLIC NETWORKS

Keith Dufault-Thompson
University of Rhode Island, keitht547@uri.edu

Follow this and additional works at: https://digitalcommons.uri.edu/oa_diss

Recommended Citation

Dufault-Thompson, Keith, "FUNCTION AND VARIABILITY OF METABOLIC NETWORKS" (2020). *Open Access Dissertations.* Paper 1220.
https://digitalcommons.uri.edu/oa_diss/1220

This Dissertation is brought to you by the University of Rhode Island. It has been accepted for inclusion in Open Access Dissertations by an authorized administrator of DigitalCommons@URI. For more information, please contact digitalcommons-group@uri.edu. For permission to reuse copyrighted content, contact the author directly.

FUNCTION AND VARIABILITY OF METABOLIC NETWORKS

BY

KEITH DUFAULT-THOMPSON

A DISSERTATION SUBMITTED IN PARTIAL FULFILLMENT OF THE

REQUIREMENTS FOR THE DEGREE OF

DOCTOR OF PHILOSOPHY

IN

CELL AND MOLECULAR BIOLOGY

UNIVERSITY OF RHODE ISLAND

2020

DOCTOR OF PHILOSOPHY DISSERTATION

OF

KEITH DUFAULT-THOMPSON

APPROVED:

Dissertation Committee:

Major Professor Ying Zhang

David R. Nelson

Tatiana Rynearson

Brenton DeBoef

DEAN OF THE GRADUATE SCHOOL

UNIVERSITY OF RHODE ISLAND

2020

ABSTRACT

The study of bacterial growth has highlighted the importance of metabolism in how microorganisms have evolved and how they survive in different conditions. The introduction of next-generation sequencing methods has allowed for the study of metabolism in new ways by predicting metabolic phenotypes based on gene annotations. The development of GEnome-scale models (GEMs) of metabolism from these annotations has provided another method to investigate microbial metabolism. An overview of GEM development and simulation methods is provided in Appendix I.

In Manuscript I, a GEM was developed for the psychrotolerant, piezotolerant, deep-sea bacteria *Shewanella piezotolerans* WP3. Despite the broad differences in environmental adaptations across the *Shewanella* genus, the WP3 model provided evidence of conserved energy production strategies that may contribute to these organisms' ability to survive in a broad range of environments. This model's application to study energy metabolism in WP3 demonstrated the utility of these models in the study of non-model organisms.

The mechanisms of environmental adaptation were further explored in Manuscript II, where a GEM of the psychrotolerant, deep-sea bacteria *Shewanella psychrophila* WP2, was used to investigate metabolic changes that occur during acclimation to different growth temperatures. This study combined transcriptomic analysis with an integrated modeling approach to provide a complete illustration of the changes that occur in various metabolic pathways at different temperatures. WP2 exhibited many of the common transcriptional responses to temperature seen in other

psychrophiles, and simulations with the GEM illustrated how these changes resulted in changes in energy and biomass production efficiency at non-optimal temperatures.

In Manuscript III, the concept of using metabolic reconstructions to study metabolism was extended from single organisms to the prokaryotic tree of life. In this study, the metabolic pathways of all prokaryotic organisms in the Kyoto Encyclopedia of Genes and Genomes (KEGG) database were analyzed as mathematical networks. Previously used network representation methods were compared to a new type of network generated through the use of the FindPrimaryPairs algorithm. The application of this algorithm provided insights into the influence of carbon, nitrogen, and phosphorus transfers in the metabolism. Further network analyses using networks generated from published GEMs also highlighted differences in the structure of core metabolic pathways required for growth versus non-essential pathways.

In conclusion, these studies have highlighted the use of GEMs and metabolic networks in the study of metabolism. The studies revealed metabolic features that play critical roles in the adaptations of *Shewanella* to different environments and may have broader implications for other deep-sea microorganisms. The broader context of metabolism structures across prokaryotes provided through a network-based approach shows promise in advancing the understanding of how metabolic pathways are organized and evolved.

ACKNOWLEDGEMENTS

I would like to thank my committee members, Dr. David Nelson and Dr. Tatiana Rynearson, for their help and guidance throughout my research. I also want to express my sincere gratitude to my advisor Dr. Ying Zhang. Her advice and guidance throughout my time in her lab have taught me how to conduct research rigorously and, more importantly, how to think like a scientist. I'd also like to thank my fellow lab members Zachary Pimentel, Christopher Powers, Jon Lund Steffensen, Dr Jing Wang, and Dr. Weishu Zhao for their discussions and collaboration throughout the years.

I thank my parents Amy and Sean for all of their support and guidance throughout the years, and I couldn't be where I am now without them. For my brother Ryan, I would like to thank him for always being a happy distraction when I needed it the most. Most of all, I'd like to thank my wonderful wife, Elizabeth, for always being there for me supporting me while I pursue my dreams.

PREFACE

This dissertation has been prepared in the manuscript format following the guidelines established by the Graduate School of the University of Rhode Island. Manuscript 1, "Genome-Scale Model of *Shewanella piezotolerans* Simulates Mechanisms of Metabolic Diversity and Energy Conservation", was published in mSystems in 2017, and involves the development and application of a Genome-scale model of metabolism to study the energy metabolism of the bacterium *Shewanella piezotolerans* WP3. Manuscript 2, "Reconstruction and analysis of a thermodynamically constrained metabolic models reveal mechanisms of metabolic remodeling under temperature perturbations of a deep-sea bacterium", is formatted for and will be submitted to PLOS Computational Biology and explores the metabolic responses of the deep sea piezophile, *Shewanella psychrophila* WP2, during acclimation to different growth temperatures. Manuscript 3, "Investigation of the Structure of Element Transfer Networks within Metabolism", is formatted for publication and will be submitted to Nature Communications and explores different ways to represent metabolism as mathematical networks. A summary of the overall conclusions and future directions for this work is provided in the Conclusions chapter. Appendix I contains an overview of Genome-scale model development and metabolic simulation methods.

TABLE OF CONTENTS

LIST OF TABLES

TABLES **PAGE**

MANUSCRIPT I

MANUSCRIPT II

LIST OF FIGURES

FIGURES **PAGE**

MANUSCRIPT I

MANUSCRIPT II

Introduction

Metabolism is a central component of biological sciences, influencing how they grow, survive in different conditions, and interact with other organisms. In total, the metabolism of an organism is made up of metabolic pathways consisting of individual reactions which an organism can use to consume and break down nutrients from the environment and convert them into energy, cellular biomass, and other products. In this dissertation, microbial metabolism is examined using a variety of approaches and from different perspectives. These studies highlight how the use of different methods to study metabolism can allow for the study of complex metabolic processes in organisms from traditionally difficult to study environments like the deep-sea. They also demonstrate that approaching metabolism from different perspectives can lead to new views that would be missed if the picture of metabolism was limited to what has been described in the textbook examples of metabolic pathways.

Up until recently the study of microbial metabolism has been limited to model organisms and culturing-based techniques, leading to a deep understanding of metabolism in these systems, but also to a limited view of the broader metabolic landscape. Before DNA and RNA sequencing methods became available, metabolism was mostly studied through culture-based methods where the response of an organism to the addition or loss of nutrients could be closely monitored in a controlled laboratory environment. While these methods provided a wealth of physiological information and set up the foundation of how metabolism is looked at up to modern times, they were limited in scope because only certain organisms like *Escherichia coli*

and *Saccharomyces cerevisiae* could be efficiently grown and studied in the laboratory [1–4]. The advancement of DNA sequencing technology in the late 20th century has expanded the view of metabolism from the small subset of model organisms to a wide range of organisms from different environments and from across the tree of life through genome sequencing [5]. The study of these genomes through gene annotation and comparative genomic analyses has allowed for the prediction of metabolic functions based on what genes are present in different genomes. These analyses have revealed an extreme degree of variation in metabolic pathways with even core metabolic pathways like glycolysis and the citric acid cycle having many different variations across the tree of life [6–8]. Genome sequencing and analysis alone provides a way to predict the metabolic potential of an organism, but recently using genome sequences to develop Genome-Scale Models (GEMs) of metabolism has become a popular method to extend functional predictions to simulations of growth.

GEMs have become increasingly popular tools to study the metabolism of organisms from all environments. These GEMs are computational representations of the metabolic functions of an organism based on their gene content and can be used to perform simulations of how an organism would grow and what pathways and reactions it would use. Modeling of metabolism started with the development of models for well-studied organisms like *E. coli [9]*, but since then GEMs have been developed and applied to organisms from all three domains of life and from a wide range of environments [10–12]. A major benefit of using GEMs in the study of metabolism has been in their application to non-model organisms. The development of GEMs for difficult to culture organisms has allowed for the prediction of the

metabolic phenotypes of these organisms providing insights into their evolution and ecological importance [13–15]. These models have also provided a new way to look at metabolism, with simulations showing how different metabolic pathways do not function in isolation but instead are connected at a genome-scale.

In this dissertation Genome-scale modeling of metabolism is applied to look at the metabolism of microorganisms from different perspectives. In Manuscript 1, "Genome-Scale Model of *Shewanella piezotolerans* Simulates Mechanisms of Metabolic Diversity and Energy Conservation", a GEM of the deep-sea bacteria *Shewanella piezotolerans* WP3 was developed and used to simulate its growth on different substrates. Through different modeling approaches the connections between carbon and energy metabolism in *S. piezotolernas* WP3 were studied, demonstrating the interdependence of different pathways and the importance of the global energy balancing mechanisms in the organism. In Manuscript II, "Metabolic Variations During Acclimation to Different Temperatures-a Case Study in the Psychrophilic Bacteria, *Shewanella psychrophila* WP2", the genome-scale modeling methods were extended to incorporate transcriptomic and thermodynamic data during the simulation of the growth of *Shewanella psychrophila* WP2 at different temperatures. This study highlights the importance of approaching metabolism from different perspectives, demonstrating the importance of an integrated view of metabolic changes at different growth temperatures. Lastly in Manuscript III, "Investigation of the Structure of Element Transfer Networks within Metabolism", metabolism is approached from a different perspective as a mathematical network. This study highlights the implications of using different network representation methods on how metabolic networks are

understood and interpreted. The continued application of the methods presented in these studies and others like them promises to advance the study of metabolism and continue to provide new ways to look at this central component of growth and evolution.

REFERENCES

1. Epstein SS. General Model of Microbial Uncultivability. In: Epstein SS, editor. Uncultivated Microorganisms. Berlin, Heidelberg: Springer Berlin Heidelberg; 2009. pp. 131–159.
2. Staley JT, Konopka A. Measurement of in situ activities of nonphotosynthetic microorganisms in aquatic and terrestrial habitats. Annu Rev Microbiol. 1985;39: 321–346.
3. Blount ZD. The natural history of model organisms: The unexhausted potential of E. coli. Elife. 2015;4: e05826.
4. Botstein D, Chervitz SA, Cherry JM. Yeast as a model organism. Science. 1997. pp. 1259–1260.
5. Land M, Hauser L, Jun S-R, Nookaew I, Leuze MR, Ahn T-H, et al. Insights from 20 years of bacterial genome sequencing. Funct Integr Genomics. 2015;15: 141–161.
6. Kopp D, Sunna A. Alternative carbohydrate pathways – enzymes, functions and engineering. Critical Reviews in Biotechnology. 2020. pp. 895–912. doi:10.1080/07388551.2020.1785386
7. Romano AH, Conway T. Evolution of carbohydrate metabolic pathways. Res Microbiol. 1996;147: 448–455.
8. Huynen MA, Dandekar T, Bork P. Variation and evolution of the citric-acid cycle: a genomic perspective. Trends Microbiol. 1999;7: 281–291.
9. Edwards JS, Palsson BO. The Escherichia coli MG1655 in silico metabolic genotype: its definition, characteristics, and capabilities. Proc Natl Acad Sci U S A. 2000;97: 5528–5533.
10. Oberhardt MA, Palsson BØ, Papin JA. Applications of genome-scale metabolic reconstructions. Molecular Systems Biology. 2009. p. 320. doi:10.1038/msb.2009.77

11. Durot M, Bourguignon P-Y, Schachter V. Genome-scale models of bacterial metabolism: reconstruction and applications. FEMS Microbiol Rev. 2009;33: 164–190.

12. Kim TY, Sohn SB, Kim YB, Kim WJ, Lee SY. Recent advances in reconstruction and applications of genome-scale metabolic models. Curr Opin Biotechnol. 2012;23: 617–623.

13. Thor S, Peterson JR, Luthey-Schulten Z. Genome-Scale Metabolic Modeling of Archaea Lends Insight into Diversity of Metabolic Function. Archaea. 2017;2017: 9763848.

14. Ates O, Oner ET, Arga KY. Genome-scale reconstruction of metabolic network for a halophilic extremophile, Chromohalobacter salexigens DSM 3043. BMC Syst Biol. 2011;5: 12.

15. Mangold S, Denis Y, Esparza M, Johnson DB, Bonnefoy V, Dopson M, et al. Anaerobic sulfur metabolism coupled to dissimilatory iron reduction in the extremophile Acidithiobacillus ferrooxidans. Appl Environ Microbiol. 2013;79: 2172–2181.

Manuscript I

Publication Status: Published in mSystems, 2017

Title: Genome-Scale Model of *Shewanella piezotolerans* Simulates Mechanisms of Metabolic Diversity and Energy Conservation

Keith Dufault-Thompson[1], Huahua Jian[2], Ruixue Cheng[2], Jiefu Li[2,3], Fengping Wang[2], and Ying Zhang[1#]

Author Affiliations:

1. Department of Cell and Molecular Biology, College of the Environment and Life Sciences, University of Rhode Island, 120 Flagg Rd., Kingston, 02881 RI, USA

2. State Key Laboratory of Microbial Metabolism, School of Life Sciences and Biotechnology, Shanghai Jiao Tong University, 800 Dongchuan Road, Shanghai 200240, P.R.China

3. Current address: Department of Biology, Stanford University, Stanford, 94305 CA, USA

Corresponding Author:

[#]Ying Zhang, University of Rhode Island, yingzhang@uri.edu

ABSTRACT

Shewanella piezotolerans WP3 (WP3) belongs to the Group 1 branch of the *Shewanella* genus and is a piezotolerant and psychrotolerant species isolated from the deep sea. In this study, a genome-scale model was constructed for WP3 using a combination of genome annotation, ortholog mapping, and physiological verification. The metabolic reconstruction contained 806 genes, 653 metabolites, and 922 reactions, including central metabolic functions that represented non-homologous replacements between the Group 1 and Group 2 *Shewanella*. Metabolic simulations with the WP3 model demonstrated consistency with existing knowledge about the physiology of the organism. A comparison of model simulations with experimental measurements verified the predicted growth profiles under increasing concentration of carbon sources. The WP3 model was applied to study mechanisms of anaerobic respiration through investigating energy conservation, redox balancing, and the generation of proton motive force. Despite being an obligate respiratory organism, WP3 was predicted to use substrate-level phosphorylation as the primary source of energy conservation in anaerobic conditions, a trait previously identified in other *Shewanella* species. Further investigation of the ATP synthase activity revealed a positive correlation between the availability of reducing equivalents in the cell and the directionality of ATP synthase reaction flux. Comparing the WP3 model with an existing model of a Group 2 species, *S. oneidensis* MR-1, revealed that the WP3 model demonstrated higher flexibility in ATP production in the anaerobic conditions. Such flexibility could be advantageous to WP3 for its adaptation to fluctuating availability of organic carbon sources in the deep sea.

IMPORTANCE

The well-studied nature of the metabolic diversity of *Shewanella* makes species from this genus a promising platform for investigating the evolution of carbon metabolism and energy conservation. The *Shewanella* phylogeny is diverged into two major branches, referred to as Group 1 and Group 2. While the genotype-phenotype connections of Group 2 species have been extensively studied with metabolic modeling, a genome-scale model has been missing for the Group 1 species. The metabolic reconstruction of *Shewanella piezotolerans* WP3 represented the first model of *Shewanella* Group 1 and the first model among piezotolerant and psychrotolerant deep sea bacteria. The model brought insights into the mechanism of energy conservation in WP3 under anaerobic conditions and highlighted its metabolic flexibility under diverse carbon sources. Overall, the model opens up new opportunities for investigating energy conservation and metabolic adaptation, and it provides a prototype for systems-level modeling of other deep-sea microorganisms.

INTRODUCTION

Members of the *Shewanella* genus are present in a wide range of environments including fresh and salt waters, food products, sewage systems, and deep sea sediments (1–3). The *Shewanella* genus is known to utilize diverse carbon sources and electron acceptors, leading to its broad adaptation to various environmental conditions (3–6). A 16S rDNA based phylogenetic reconstruction has revealed two major groups in the *Shewanella* genus (7). Generally, Group 1 includes species that are capable of

producing eicosapentaenoic acid (EPA) and are piezotolerant and psychrotolerant, such as *S. benthica* and *S. violacea*, which have been isolated from the deep sea. Group 2 species are generally pressure-sensitive and mesophilic and include *S. oneidensis*, *S. baltica,* and *S. putreficans*, which have been isolated from a variety of environments including freshwater lakes and spoiled meat products.

The ability of *Shewanella* species to utilize a broad range of electron acceptors makes this genus a target for studying metabolic energy conservation and anaerobic respiration. Several recent studies have focused on identifying the relative contributions of two distinct ATP-producing mechanisms (8–10), oxidative phosphorylation and substrate-level phosphorylation. Oxidative phosphorylation is typically associated with respiration, where the reduction of terminal electron acceptors is coupled to proton motive force (PMF) generation, and the PMF subsequently contributes to ATP synthesis via ATP synthase (ATPase). Substrate-level phosphorylation is associated with the production of ATP through direct transfer of a phosphoryl group to ADP through the action of enzymes like phosphotransacetylase (Pta) and acetate kinase (AckA). In *S. oneidensis* MR-1, substrate-level phosphorylation is the primary source of ATP during anaerobic growth, while ATPase has either minor contributions to ATP production or acts as an ATP driven proton pump that generates PMF (8). This is surprising given that *Shewanella* are obligated to utilize terminal electron acceptors when growing under anaerobic conditions. An understudied aspect of these features of metabolism is how ATP production, PMF generation, and redox reactions interact and jointly contribute to the utilization of metabolic pathways and energy conservation strategies in *Shewanella*.

Shewanella piezotolerans WP3, hereafter referred to as WP3, has been isolated from West Pacific sediment at a depth of 1914 m. It is piezotolerant and psychrotolerant, reflecting its adaptations to the deep sea environment (11). A 16S-based phylogeny suggests this organism belong to Group 1 of the *Shewanella* genus (12). The ability of WP3 to utilize diverse carbon sources and electron acceptors demonstrates a metabolic flexibility that is comparable with other *Shewanella* species (11, 13). The full genome of WP3 encodes diverse c-type cytochrome genes, which support anaerobic respiration using various terminal electron acceptors, such as nitrate, iron, trimethylamine N-oxide (TMAO), and dimethyl sulfoxide (DMSO) (13). WP3 is also known to produce EPA and alter its lipid content to contain more unsaturated and branched chain fatty acids in low temperature and high pressure environments (14). These features enlist WP3 as a good representative of the Group 1 *Shewanella* species.

GEnome-scale Models (GEMs) of metabolic networks have broad applications in phenotype prediction, evolutionary reconstruction, functional analysis, and metabolic engineering (15). By connecting a set of biochemical reactions with the enzymatic functions encoded in a genome, GEMs provide a framework for simulating the associations between genotypes and phenotypes (16–19). The reconstruction of genome-scale models can be challenging due to the complexity in managing diverse data sets and maintaining model consistency through iterative manual curations. These challenges have been addressed with the recent releases of tools and automated pipelines to facilitate the modeling process (20–23). GEMs are available for four Group 2 *Shewanella* species, including *S. oneidensis* MR-1, *S. denitrificans*,

Shewanella sp. MR-4, and *Shewanella* sp. W3-18-1 (24, 25), while currently no GEM is available for any Group 1 species.

This study focuses on WP3 as a prototype for metabolic modeling among Group 1 *Shewanella*. WP3 presents the conserved features of the Group 1 *Shewanella* (e.g., piezotolerance, psychrotolerance, EPA production, etc.) and is a well-studied species in this group. Previous studies have provided detailed evidence related to the function and annotation of multiple key metabolic pathways in WP3, including nitrate utilization (26), DMSO respiration (27), iron reduction and biomineralization (28–30), and fatty acid synthesis (14). In addition to functional annotations, extensive data is available on the expression of key metabolic genes, connecting individual pathways with their functional roles under changing environmental conditions (31–36). These studies provide a broad knowledgebase for constructing the WP3 GEM. Furthermore, WP3 has established protocols for genetic manipulations (37–40). The experimental accessibility of this organism would enable the verification of modeling outcomes and support future research of molecular adaptations through combined GEM simulation and experimental verification. Overall, WP3 serves as an ideal organism for modeling the metabolism of Group 1 species in the *Shewanella* genus.

In this study, a GEM of WP3 was constructed and applied in simulating the carbon metabolism and energy conservation under both aerobic and anaerobic conditions. The model was verified based on the known physiology of the organism and new experimental data. Evolutionary analysis of the central metabolic genes revealed non-homologous replacements between WP3 (and other Group1 species) and the Group 2 *Shewanella*. Comparing the WP3 model with the model of a Group 2

representative, *S. oneidensis* MR-1 (here referred to as MR-1), revealed similarities and differences between the two organisms in their aerobic growth and anaerobic energy conservation.

RESULTS

Phylogenetic position of *Shewanella piezotolerans* WP3

The phylogenetic positioning of *S. piezotolerans* WP3 was confirmed following a phylogenomic analysis using the protein sequences of 661 conserved single copy genes (CSCGs) in the full genomes of 24 *Shewanella* species and five closely related *Gammaproteobacteria* that served as the outgroup to the *Shewanella* genus (Materials and Methods). The phylogenomic reconstruction demonstrated the differentiation of the Group 1 and Group 2 *Shewanella* species into distinct evolutionary branches (Figure 1) and concurred with a previously published 16S rRNA gene based phylogeny (7). An exception to this concurrence was with the positioning of *S. amazonensis*, where the 16S rRNA gene based phylogeny located *S. amazonensis* in the Group 2 taxa (7) while the genome based phylogeny positioned *S. amazonensis* as one of the deepest branching species among all of the analyzed *Shewanella*. According to the genome-wide phylogeny, WP3 was located in the Group 1 branch with *S. pealeana* and *S. halifaxensis* as its closest neighbors. The four previously modeled *Shewanella* species were marked with blue stars to indicate their position on the phylogeny while WP3 was marked with a red star (Figure 1).

Genome-scale metabolic reconstruction of *Shewanella piezotolerans* WP3

The complete metabolic reconstruction of WP3, GEM-iWP3, was released in a public Git repository at https://github.com/zhanglab/GEM-iWP3. It contained 806 genes, 653 metabolites, and 922 metabolic reactions. The reconstruction was achieved in three steps. First, gene-protein-reaction (GPR) associations were incorporated through mapping orthologous genes to the existing *Shewanella* reconstructions (24, 25) (Materials and Methods). This identified 596 genes (619 reactions) that were conserved between WP3 and all four of the other modeled *Shewanella* species as well as 130 genes (131 reactions) that were conserved between WP3 and some (but not all) of the four previously modeled species, leading to the inclusion of 726 genes associated with 750 reactions in the WP3 reconstruction.

Next, the WP3 metabolic reconstruction was expanded through manual curation of the WP3 genome using information from published literature (12, 14, 41), protein domain conservation, and evidence from the genomic and functional context of the metabolic genes (42). This expansion led to the inclusion of another 137 reactions associated with new gene annotations and the addition of a periplasmic compartment to account for cellular localizations of nutrient transporters and electron transport reactions. For example, the carbohydrate utilization pathways were annotated based on prior study of sugar catabolism in *Shewanella* (41) and further verified based on predictions of protein localization in the cell (43–45) (Figure 2). The reduction of soluble electron acceptors, such as nitrate, nitrite, thiosulfate, and TMAO, were represented as periplasmic reactions, while the reduction of DMSO and oxidized metals, such as Fe (III), Mn (IV), uranium (VI), and chromium (VI), were represented as extracellular processes following existing knowledge of the cellular

compartmentalization of the different electron transport processes in *Shewanella* species (46–55). Putative outer membrane transporters were identified and curated to identify what genes were responsible for nutrient exchange between the extracellular space and periplasm. A number of non-specific porins were identified, including distant homologs to the *E. coli* OmpC and OmpF proteins (56), as well as a homolog to the OprF protein in *Pseudomonas* aeruginosa (57, 58). This analysis also identified functionally specific outer membrane proteins that were responsible for the uptake of carbohydrates (e.g. LamB and OprB), phosphate (OprP), cobalamin (BtuB*)*, long-chain fatty acids (FadL), and nucleosides (Tsx) (41, 59–63).

The assembly of cell components in WP3 was represented with the addition of 8 synthesis reactions. The biomass equation was introduced to represent the composition of cell mass, including carbohydrates, proteins, RNA, DNA, lipids, vitamins, and cofactors (Table S1). The stoichiometry of biomass equation was normalized to reflect the *mmol* concentration of individual components in one gram of cell dry weight (Materials and Methods). The composition of macromolecules, such as lipids, proteins, DNA, and RNA, were represented using equations that defined the composition of basic building blocks, such as fatty acids, amino acids, and nucleotides. The stoichiometry of these biosynthesis equations was determined according to existing *Shewanella* reconstructions and experimental measurements performed on WP3. Specifically, stoichiometry of the lipid biosynthesis equation (Table S2) was calibrated based on experimentally measured concentrations of saturated, unsaturated, and branched-chain fatty acids in WP3 (14).

The WP3 metabolic reconstruction also included three reactions for the diffusion of O_2, CO_2, and urea across the cell membrane, and 24 gap filling reactions for unblocking the production of biomass components. These gap filling reactions reflected knowledge gaps in the synthesis of biomass compounds, where the metabolic mechanisms were either unknown or not yet associated with any annotated genes in the WP3 genome. These gap filling reactions included dihydroneopterin mono- and tri-phosphate dephosphorylases, which were involved in the synthesis of the cofactor tetrahydrobiopterin, as well as glycolaldehyde dehydrogenase and 5,10-methylenetetrahydrofolate reductase, which were involved in folate metabolism. Three gap filling reactions were compound sinks that allowed for the removal of metabolic side products whose metabolic pathways are currently unknown and are not involved in other reactions in the metabolic network. These included sinks for the compound S-Adenosyl-4-methylthio-2-oxobutanoate, a side product in the synthesis of biotin.

Finally, 109 exchange reactions were defined to represent the exchange of nutrients and metabolic products in the simulated environment (Table S3). These included reactions for the uptake of carbon sources, electron acceptors, trace metals, and vitamin precursors, as well as the diffusion of metabolic byproducts. These exchange reactions were set to represent the basal constraints specified in Table S3 and were subsequently modified during metabolic simulations to represent different environmental conditions (Materials and Methods).

Evolution of central metabolic genes

During manual curation of the WP3 metabolic reconstruction, non-homologous genes were identified between WP3 and the previously modeled *Shewanella* species for carrying out central metabolic functions. These included acetylornithine deacetylase (*argE*), which was essential for the biosynthesis of arginine, and glucosamine-6-phosphate deaminase (*nagB*), which was essential for utilizing N-acetyl-D-glucosamine (GlcNac). Both genes were experimentally identified in MR-1 and were found to be non-homologous to the canonical genes in *E. coli* (64, 65). A broader comparison of the Group 1 and Group 2 *Shewanella* suggested that they were conserved within each group but had diverged between the two groups (Figure S1). Exceptions were found for the *argE* gene in *S. amazonensis*, *S. loihica* and *S. frigidimarina*, where the deep-branching *S. amazonensis* and *S. loihica* encoded both non-homologous copies of *argE*, and the Group 2 species *S. frigidimarina* encoded a single *argE* of the Group 1 type. The genomic contexts of *argE* and *nagB* were well conserved among the Group 1 species, while they were variable among the Group 2 species. Consistent with the observed variability of the genomic contexts, mobile element proteins were encoded in proximity to *argE* and *nagB* in MR-1, as well as an *argE* in *S. loihica* that is homologous to the Group 2 type. The Group 2 genes had a diverse origin, with the *argE* homologous to genes in *Klebsiella* and a limited subset of host-associated *Enterobacteriaceae*, and the *nagB* homologous to genes in the deep branching bacteria and archaea (65). In contrast, the Group 1 genes were conserved with evolutionarily related genera of *Shewanella*, such as *Marinomonas*, *Colwellia*, and *Pseudoalteromonas*. Taken together, the central metabolic genes *argE* and *nagB*

evolved from distinct origins among the *Shewanella* Group 1 and 2. The WP3 genome encoded the gene copies that were conserved in the Group 1 species.

Metabolic simulations match experimental growth measurements.

Simulations of biomass production with the WP3 metabolic model were consistent with the known physiology of this organism. This included utilizing glucose, lactate, maltose, and GlcNac as carbon sources, and using Fe(III), nitrate, nitrite, thiosulfate, TMAO, and DMSO as terminal electron acceptors for anaerobic respiration (13). From the metabolic simulations, 53 sole carbon sources supported biomass production of the WP3 model under aerobic conditions, including various carbohydrates, amino acids, nucleotides, and fatty acids (Figure 2 and Table S3).

To quantitatively evaluate the prediction of biomass concentrations by the WP3 metabolic model, batch cultures were set up using a minimal medium developed in this study to experimentally measure the growth of WP3 with sole carbon sources (Supplemental Text S1). The sole carbon sources examined in this study were pyruvate, glucose, maltose, and an amino sugar (GlcNac), and the experiments were carried out under aerobic conditions using oxygen as the sole terminal electron acceptor. The concentrations of carbon sources ranged between 2 mM and 40 mM in the experimental media. Cell growth was measured in three independent replicates and converted to biomass concentrations (Materials and Methods). Metabolic simulations were performed with the WP3 model to predict the biomass fluxes under the conditions defined by the experimental media. This was achieved by modifying the flux bounds of the exchange reactions in the model. The lower bound of exchange

reactions for carbon, nitrogen, sulfur, and phosphorous sources were specifically calibrated to reflect their concentrations in the minimal media (Table 1), the exchange of oxygen was unlimited to simulate aerobic respiration, and the lower and upper bounds of other exchange reactions were assigned based on default settings in the basal constraints (Table S3, Materials and Methods).

The biomass fluxes predicted by the model demonstrated overall consistency with experimentally measured biomass concentrations at the stationary phase (Figure 3). The quantitative values slightly deviated from experimental measurements at relatively low (i.e., 2 mM of pyruvate or glucose) or high carbon source concentrations. Experimental measurements showed that the biomass production stopped increasing when the concentration of sole carbon sources increased beyond 60 mM in the count of carbon elements [i.e., 20 mM, 10 mM, or 5 mM of pyruvate (3 Carbons), glucose (6 Carbons), or maltose (12 Carbons), respectively]. This trend was also seen in the WP3 model simulations. Further, under high concentrations of pyruvate, glucose, and maltose, metabolic simulations identified NH_4^+ as the limiting factor of biomass production. This was because the uptake of these carbon sources was limited by the uptake bound of the NH_4^+ exchange flux that corresponded to its concentration in the experimental media. Allowing for higher uptake of NH_4^+ by the model led to higher biomass production and higher uptake of these carbon sources. In contrast, the model was not limited by the availability of NH_4^+ when an amino sugar, GlcNac, was used as a sole carbon source. This was because each molecule of GlcNac produced one molecule of NH_4^+ during its utilization, providing additional nitrogen that could be used during growth. As a result, higher biomass was observed with

GlcNac as a carbon source, and this trend was seen in both the experimental measurements and the model simulations (Figure 3).

The aerobic growth of WP3 was also compared with MR-1 [model iMR1_799 (25)] based on simulations of growth on 28 sole carbon sources that have been experimentally confirmed to support growth in either WP3 (13) or MR-1 (24, 25) (Figure S2). The MR-1 model was able to utilize almost all the examined carbon sources except for maltose. The WP3 model, in contrast, was viable in maltose but was not able to utilize six carbon sources, including the amino acids asparagine and glutamine, the nucleic acids inosine and thymidine, and the small molecules ethanol and 2-oxoglutarate. Simulations of biomass production using the two models revealed that WP3 had slightly higher biomass yields than MR-1 with most of the growth supporting carbon sources, including carbohydrates, small carbon molecules, and amino acids, while MR-1 had slightly higher biomass yield when malate, adenosine, or deoxyadenosine were used as sole carbon sources.

Metabolic energy conservation of WP3.

The relative roles of oxidative and substrate-level phosphorylation were examined by simulating mutant models with reactions blocked from the two pathways, respectively (Figure 4, Materials and Methods). For measuring the role of oxidative phosphorylation, biomass production of the wild type (WT) model and a deletion mutant of ATP synthase (*Δatp*) was simulated using flux balance analysis (FBA) under both aerobic (O_2) and anaerobic (fumarate) conditions using either GlcNac or lactate as sole carbon sources. Under aerobic conditions, the *Δatp* mutant produced

less than half of the WT biomass, indicating that oxidative phosphorylation played an important role in the aerobic growth of WP3. Under anaerobic conditions, however, the biomass production was comparable between the WT and *Δatp* models, demonstrating that oxidative phosphorylation had only a minor role in supporting anaerobic growth (Figure 4B).

For measuring the role of substrate-level phosphorylation, FBA was performed with the WP3 WT model and three mutant models that represent the single deletion of phosphotransacetylase (*Δpta*) or acetate kinase (*ΔackA*), or the double deletion of both genes (*ΔptaΔackA*). When lactate was used as a sole carbon source, the WT model was able to produce non-zero biomass flux, while the *Δpta*, *ΔackA*, and *ΔptaΔackA* models had a maximum biomass flux of zero indicating that these mutants are not viable in the lactate media. When GlcNac was used as a sole carbon source, both the WT and mutant models were viable in the anaerobic media. Compared to the WT, *Δpta* had a slight decrease in biomass production (97% of the WT flux), and *ΔackA* and *ΔptaΔackA* resulted in a greater reduction of the biomass to less than 50% of the WT (Figure 4C). The decrease or inhibition of biomass production in the *ΔackA* and *ΔptaΔackA* mutants indicated an important role of substrate-level phosphorylation in supporting anaerobic growth of WP3.

Additional examination of the internal fluxes obtained from FBA revealed changes in ATP production, PMF generation, and redox functions in the WT and mutant models (Figure 4D). In the WT model, substrate-level phosphorylation mediated by AckA was used for ATP production, while oxidative phosphorylation via ATP synthase (ATPase) played a minor role in this process. The activity of formate

dehydrogenase (Fdh) was coupled with terminal electron acceptor reduction to generate PMF, and NADH dehydrogenase (Ndh) was used for reducing the quinone pool. In the *Δpta* model, reaction fluxes were redirected to xylulose-5-phosphate phosphoketolase (Xpk) from the pentose phosphate pathway so that substrate-level phosphorylation through AckA was maintained. This redirection resulted in reduced Fdh flux, potentially due to decreases in formate production, and increased Ndh flux, potentially for maintaining the redox activities in the electron transport chain. In the *ΔackA* and *ΔptaΔackA* models, a more significant shift was observed in the distribution of metabolic fluxes. The inhibition of AckA led to blockage of the upstream fluxes through Pta and Xpk, and increased flux through pyruvate kinase (Pyk) to partially compensate for the loss of AckA mediated ATP production.

Variability of the internal fluxes was further examined using flux variability analysis (FVA) with biomass production constrained to its maximum under each simulation condition (Supplemental Table S4). This revealed consistent flux values for all the above-mentioned reactions in the WT and *Δpta* models and for the ATPase, AckA, Pta, and Xpk reactions in the *ΔackA* and *ΔptaΔackA* models. However, the Pyk, Fdh, and Ndh reactions had variable fluxes in the *ΔackA* and *ΔptaΔackA* mutants, indicating that these mutants had alternative strategies for balancing the ATP production, PMF generation and redox activities in the cell.

ATPase activity and anaerobic growth of *Shewanella*

One surprising feature of the *Shewanella* anaerobic growth was the lack of oxidative phosphorylation via ATPase despite the obligate requirement for respiration through

terminal electron acceptors (8). To further investigate how the ATPase activity (i.e., in either ATP production or PMF generation directions) was related to the redox balancing of *Shewanella* during anaerobic respiration, the NAD^+/*NADH* homeostasis was modeled with a robustness analysis to simulate the connections between redox state (as measured by the differences in NAD^+ and *NADH* concentrations) and the activity of ATPase in both the WP3 and MR-1 models (Materials and Methods). The simulation demonstrated a positive correlation between the availability of reducing equivalents and the flux of ATPase reaction for both WP3 and MR-1 (Figures S3, S4). This indicated that when the system was provided with more reducing equivalents, the ATPase flux would increase, and activity would be shifted towards the ATP-producing direction. In contrast, when the system had less reducing equivalents, the ATPase flux would decrease, and activity would be flipped to the proton pumping and PMF-generating direction.

The comparison of redox states in WP3 and MR-1 models when ATPase reaction flux approached zero revealed metabolic differences between these two organisms across diverse carbon sources when using fumarate as the sole electron acceptor (Figure 5). The WP3 model produced excess reducing equivalents in a wide range of carbon sources, including amino sugars, small carbon compounds, amino acids, and nucleotides (Figure 5A). Considering the positive correlation of the redox state and the ATPase flux (Figures S3, S4), the excess reducing equivalents in WP3 could potentially enable the production of additional ATP via ATPase. The MR-1 model, in contrast, produced excess reducing equivalents only when specific carbon sources were provided, such as malate, aspartate, and serine. Thus, the ATPase could

have little contribution to the ATP production but may instead be used for PMF generation in MR-1. Overall, the two representatives of Group 1 and Group 2 *Shewanella*, WP3 and MR-1, demonstrated complex interactions of ATP generation, PMF generation, and redox balancing processes under anaerobic growth. The WP3 model displayed higher capacity than MR-1 in producing excess reducing equivalents in most of the examined carbon sources. This may provide additional advantages to WP3 in its natural environment by enabling additional ATP production when using a diverse range of carbon sources.

DISCUSSION

In this study, a genome-scale model was constructed for WP3, a piezotolerant and psychrotolerant representative of the Group 1 *Shewanella* species (Figure 1). Extensive annotations of the WP3 genome were incorporated into the metabolic reconstruction, and the carbon utilization reactions were curated based on the current literature available (Figure 2). A periplasmic compartment was introduced to the WP3 reconstruction to account for the cellular localization of carbon utilization and electron transport reactions. This represented a new component not previously included by other metabolic reconstructions of *Shewanella* species.

Evolutionary analysis of central metabolic genes in WP3 revealed instances of non-homologous replacements among the Group 1 and Group 2 *Shewanella*. The *argE* and *nagB* in WP3 and other Group 1 species were conserved within bacterial species closely related to *Shewanella*. Hence, they could represent the ancestral genes conserved during early differentiation of the *Shewanella* genus. The Group 2 copies of

these genes were adjacent to mobile genetic elements, suggesting a possible acquisition of these genes through horizontal gene transfer. Further, the conservation of these acquired genes across Group 2 species and their presence in a few Group 1 species suggested they could be introduced to the genome during early differentiation of the Group 2 *Shewanella*.

The WP3 model represented known physiology of this organism, including its growth under a wide variety of carbon sources and electron acceptors. A comparison of biomass production from model simulations and experimental measurements revealed that the WP3 model represented growth trends consistent with what was observed in experimental cultures using the sole carbon sources pyruvate, glucose, GlcNac, and maltose (Figure 3). The slight deviations from the experimental results under low or excess carbon concentrations could be attributed to the differential regulation of gene expressions but was beyond the scope of this study. Additional confidence in the WP3 model was established when it was applied for the prediction of growth-limiting nutrients. The prediction of NH_4^+ as the limiting nutrient when excess carbon source was provided was corroborated by the fact that the amide molecule, GlcNac, was able to overcome this growth limit by serving as both a carbon and a nitrogen source.

A comparison of the WP3 model with an existing model of a Group 2 representative, *S. oneidensis* MR-1, revealed similarities and differences in carbon utilization and energy conservation of these two organisms. While MR-1 lacked enzymes for utilizing maltose, WP3 lacked identified transporters that are required for utilizing six carbon sources, including the amino acids asparagine and glutamine, the

nucleic acids inosine and thymidine, and the small molecules ethanol and 2-oxoglutarate (Figure S2). The anaerobic energy conservation strategies of WP3 were explored by simulating the deletion of genes responsible for oxidative (*Δatp*) and substrate-level (*ΔackA, Δpta* and *ΔptaΔackA*) phosphorylation (Figure 4). Using GlcNac and lactate as sole carbon sources and fumarate as the sole electron acceptor, the biomass production and reaction flux distributions of WP3 wild type and mutant models revealed that substrate-level phosphorylation was the primary source of anaerobic energy conservation, a trait that has been noted in MR-1 (8, 10). This indicates the primary usage of substrate-level phosphorylation could be a conserved feature in the anaerobic respiration of both Group 1 and Group 2 and suggests that this feature could have evolved during the early differentiation of *Shewanella*.

Internal redox balancing has been shown to play critical roles in the ability for other organisms to utilize nutrients and is a major driver of changes in metabolic strategy (66–68). Simulation of the NAD^+/*NADH* homeostasis and its connections to the ATPase activity in WP3 and MR-1 provided insights into the complex interactions of ATP production, PMF generation, and redox balancing processes in *Shewanella*. While both the WP3 and MR-1 models presented a positive correlation between the availability of reducing equivalents and the reaction flux of ATPase (Figures S3, S4), the two models demonstrated distinct redox states when different carbon sources were utilized (Figure 5). The production of excess reducing equivalents was supported by a wide range of carbon sources in WP3 but was restricted to only a few carbon sources in MR-1. This suggested a capacity for WP3 to produce additional ATP via the ATPase activity and could potentially enable the adaptation of WP3 to the fluctuating

availability of carbon sources at the deep sea by maintaining ATP production when different carbon sources became available.

Overall, the WP3 model represents the first genome-scale model of the Group 1 *Shewanella* and a first model of piezotolerant and psychrotolerant deep-sea species. It opens up new opportunities for the future studies of environmental adaptation and metabolic pathway utilization, for example, through incorporating environment specific features like the altered fatty acid compositions in different temperature and pressure (14) or the differential expression of key metabolic genes in different environmental conditions (31, 33, 36). The WP3 model also provides a framework for integrating additional parameters, such as enzyme thermostability (69) or context-specific information (70) during the study of temperature and pressure adaptations. The experimental accessibility of WP3 would make it possible to verify extensions to the model. Finally, future studies combining molecular evolution and metabolic simulation of the Group 1 and Group 2 *Shewanella* could lead to a better understanding of bacterial adaptations to low temperature and high-pressure environments and permit the exploration of metabolic potentials at the deep sea.

MATERIALS AND METHODS

Ortholog mapping and phylogenomic reconstruction of the *Shewanella* genus

An updated phylogeny of the *Shewanella* genus was constructed based on conserved single-copy genes (CSCGs). A dataset of 24 *Shewanella* genomes was downloaded from the KEGG database (71). Five additional genomes were used as the outgroup for rooting the *Shewanella* phylogeny, including *Pseudoalteromonas haloplanktis*,

Colwellia psychrerythraea, *Psychromonas ingrahamii*, *Photobacterium profundum*, and *Moritella viscosa*. An initial ortholog mapping among these species was identified using a bi-directional best hit BLAST analysis as defined in a previous study (72). The ortholog mapping was further refined based on a consensus of additional evidence from other sources, including a published ortholog table of the *Shewanella* genus (25), the KEGG Orthology database (71), as well as automated predictions by OrthoMCL (73). From analyzing ortholog groups that were consistently defined by all the above-mentioned approaches, CSCGs were identified as the orthologs that occurred once and only once in each of the analyzed genomes. Individual alignments were constructed on the protein sequences of each CSCG using MUSCLE v3.8.31 (74). The alignments were then concatenated to create a master alignment of the CSCGs in *Shewanella* and the outgroups. RaxML v 8.2.3 (75) was used for reconstructing a maximum likelihood protein phylogeny using the JTT substitution model with the GAMMA model of rate heterogeneity. Branch support values were estimated by performing bootstrapping with 100 replications.

Development of the genome-scale metabolic reconstruction

The WP3 metabolic reconstruction was developed using the version v0.27 of the PSAMM software package (23). The reconstruction was represented in a YAML format that is designed to represent variable model definitions and simulation conditions. Simulations with the model were performed in PSAMM using the IBM ILOG CPLEX Optimizer version 12.6.2 linear programming solver. An initial reconstruction was first developed based on ortholog mapping to the existing

metabolic reconstructions of *S. oneidensis* MR-1, *Shewanella* sp. MR-4, *S. denitrificans* OS217, and *Shewanella* sp. W3-18-1 (25). The orthologs were identified according to a global mapping of ortholog clusters among all *Shewanella* (described in the above paragraph). Gene-protein-reaction (GPR) associations in the initial WP3 reconstruction were mapped from conserved genes in the modeled species following logic expressions that represent the "AND" and "OR" relationships of enzyme coding genes. The "AND" logic was used to indicate multiple subunits of an enzyme complex, and the "OR" logic was used to indicate alternative enzymes. A GPR association was introduced from existing reconstructions only if orthologs were identified in the WP3 genome for all subunits of at least one alternative enzyme. The WP3 reconstruction was further expanded through manual curation by referencing existing annotations in the KEGG (71), SEED (42), and BioCyc (76) databases. Additional considerations in the manual curation process included examining genomic context using the SEED viewer tool (77), searching for conserved sequence domains (78), and reviewing current literature (12, 14, 41, 79). Finally, metabolic gaps in the production of biomass components were identified using the PSAMM *gapfill* function (23). A number of gap filling reactions were included to enable biomass production with experimentally confirmed carbon sources and electron acceptors (13). These gap reactions were further scrutinized through manual inspection of the biosynthetic pathways leading to the various biomass components and were reviewed with the *fluxcheck* function using the "--unrestricted" option in PSAMM to confirm their flux consistency. Stoichiometric consistency of the model was validated by using the *masscheck* function in PSAMM. Additional verification of the formula and charge

balance was performed with *formulacheck* and *chargecheck* functions. By default, the exchange reactions, compound sources or sinks (e.g., 4HBASink, 5DRIB_Sink, and AMOB_Sink), macromolecular synthesis equations (e.g., Core_Biomass, Growth, and PASYN_WP3_20C), and reactions involving the acyl carrier protein or its apo form (e.g., ACPS1, ACPSc, and AGPEPHOS) were excluded from formula and charge checks due to the presence of undefined R or X groups in the metabolites.

Formulating the biomass objective function

A biomass equation was formulated in the WP3 reconstruction to simulate the production of components required for cell growth. The biomass equation incorporates the cellular composition of the total cellular carbohydrates, proteins, RNA, DNA, lipids, vitamins, and cofactors (Table S1). Biomass compositions from experimental measurements of WP3 and evolutionarily related species was used as references for formulating the stoichiometry of the biomass equation. First, the composition of carbohydrates, proteins, DNA, RNA, and lipids was estimated using approximations from *S. oneidensis* MR-1 (24, 25). The addition of vitamins and cofactors into WP3 biomass was achieved by using an approximation of the experimental measurements from *E. coli* as a representation of gram-negative bacteria (80). Further calibration of the biomass composition in WP3 involved formulating the stoichiometry of the phosphatidic acid synthase reactions according to experimental measurements of branched-chain, unsaturated, and saturated fatty acids in this organism (14) (Table S2). The overall biomass equation was scaled so that the stoichiometry of biomass components corresponds to their millimole ($mmol$) amounts in a gram of cell dry

weight (gDW). This calibration enabled the comparison of computationally simulated biomass productions with experimental measurements.

Formulating the basal constraints of metabolic simulations

A list of basal constraints was defined for exchange reactions in the model using lower and upper bounds specified in Table S3. The basal constraints were used to set default bounds for the uptake of nutrient sources and the removal of metabolic byproducts. For trace elements, vitamin precursors, and salts, the default bounds were unlimited on both directions; for metabolic byproducts, the lower bounds were set to zero while the upper bounds were unlimited, indicating that they can be freely released from the system. The basal constraints also defined exchange reactions for 71 potential carbon sources and 13 electron acceptors in the model. Uptake of carbon sources and electron acceptors was blocked in the basal constraints and was defined during individual simulations. Unless specified, in the simulations the lower bound of the sole carbon source was set to -10 to limit its uptake to 10 $mmol/L$, and uptake of the sole electron acceptor was unlimited.

Comparing WP3 metabolic simulations with experiments and the MR-1 model

The growth of WP3 when utilizing a variety of sole carbon sources was examined in aerobic batch cultures using 50 mL of LMO-812 minimal media (Supplemental Text S1) supplemented with alternative sole carbon sources at different concentrations (2 mM, 5 mM, 10 mM, 20 mM, or 40 mM). Cultures were grown in triplicate at 20 degrees Celsius and were continuously shaken at 200 rpm. The growth curve of WP3

was determined using turbidity measurements at 600 nm (OD_{600}). The growth measurements at early stationary phase were converted to gDW/L of biomass concentration using a previously determined correlation between OD_{600} and dry weight in *Shewanella* species (24). To simulate the experimental growth conditions, the PSAMM *fba* function was applied to perform FBA simulations using the biomass equation as the objective function. The exchange of carbon, nitrogen, sulfur, and phosphorous nutrients were constrained based on their availability in the experimental media (Table 1), the exchange of oxygen was unlimited to simulate aerobic respiration with oxygen as the sole electron acceptor, and other exchange reactions were defined with the basal constraints. The unit of the uptake fluxes was assigned to $mmol/L$, which corresponds to the unit of nutrient concentrations in the experimental media. Since the biomass equation in WP3 was calibrated to reflect the millimole ($mmol$) amounts of biomass components in a gram of cell dry weight (gDW), the biomass concentrations were predicted based on the biomass fluxes ($v_B\ gDW/L$).

Comparisons of the WP3 with the MR-1 model were performed by simulating the aerobic growth of the organisms using 28 sole carbon sources that have been experimentally confirmed to support growth in either WP3 (13) or MR-1 (24, 25) (Figure S2). The latest metabolic reconstruction of MR-1, iMR1_799 (25) was used in all MR-1 simulations performed in this study. The simulations with both models were set up using the basal constraints with default bounds for sole carbon sources (i.e., $[-10, 1000]$) and the sole electron acceptor, oxygen (i.e., $[-1000, 1000]$). The biomass yields were calculated through dividing the biomass flux by the uptake fluxes of carbon source and the electron acceptor.

Metabolic simulation of mutant phenotypes

Mutant strains of WP3 were simulated in the metabolic model by setting a flux limit of $[0, 0]$ for all reactions catalyzed by the gene being knocked out. A list of enzymes involved in ATP production, PMF generation, and redox activities was provided in Table 2 along with their corresponding reactions, functional roles, and gene associations in the WP3 model. Media conditions were set in the WP3 model using the basal constraints with uptake enabled for a sole carbon source (lactate or GlcNac) and a sole electron acceptor (O_2 or fumarate). The carbon source was constrained to a maximum uptake of $10\ mmol/L$, and the electron acceptor was unlimited. For simulations with fumarate as the electron acceptor the succinate/fumarate antiporter reaction, SUCFUMtdc, was blocked as it has been noted to be able to form artificial loops with other transporters (80) and the fumarate hydrogen symporters FUMt4 and FUMt4_2 were also blocked to prevent utilization of fumarate as an additional carbon source. When GlcNac was used as the sole carbon source, the lactate dehydrogenase and glycerol-3-phosphate dehydrogenase reactions were blocked to prevent the formation of artificial loops in NADH cycling. Metabolic reaction fluxes were determined by optimizing the biomass objective function using *fba* with the *l1min* loop removal approach implemented in PSAMM (23, 81). Additional analysis of flux variability was performed on internal reactions with the *fva* function in PSAMM by fixing the biomass flux to its maximum. The reaction flux for Fdh was calculated based on the sum of fluxes through the FDH9 and FDH10 reactions, and the reaction flux for Ndh was calculated based on the sum of fluxes through the NADH4,

NADH12, and NADH14 reactions. All other fluxes were directly obtained from the FBA and FVA simulations according to the reactions listed in Table 2.

Metabolic Simulations of the NAD^+/NADH homeostasis

The *NAD^+/NADH* homeostasis was used as an approximation for investigating redox states in the WP3 model and the MR-1 model, iMR1_799 (25). To simulate the *NAD^+/NADH* homeostasis, an artificial reaction, EQ1: $NAD^+ + H^+ <=> NADH$, was introduced to the model to account for differences in the concentrations of *NAD^+* and *NADH*. First, a robustness analysis was performed by varying the flux value of EQ1 while optimizing the biomass production. This was performed using the *robustness* function in PSAMM (23), where flux values of EQ1 were probed in the range of $[-10,10]$ at 500 steps. For each step, FBA simulation was performed with the *l1min* loop removal, and the simulated ATPase flux was plotted with the corresponding flux of EQ1 (Figures S3, S4). Next, a linear model was fit to the data using the equation: $v_{ATPase} = k \cdot v_{EQ1} + b$, where v_{ATPase} was the flux of the ATPase reaction and v_{EQ1} was the flux of the EQ1 reaction. To identify the connections between ATPase activity (i.e., ATP production or PMF generation) and the redox state of a cell, the intersection of the linear model with the EQ1-axis was used to determine the difference in *NAD^+* and *NADH* concentrations when the ATPase reaction flux approached zero. A negative intersection of the linear model on the EQ1-axis would indicate $[NAD^+] - [NADH] < 0$, suggesting the homeostasis was pushed towards generating more *NADH*; A positive intersection would indicate $[NAD^+] - [NADH] > 0$, suggesting that the homeostasis was pushed towards generating more *NAD^+*. Both

the WP3 and MR-1 models were simulated using basal constraints with the addition of fumarate as the anaerobic electron acceptor paired with one of 12 sole carbon sources that are growth supporting in both models (Figures 5, S3, and S4). The exchange flux of the sole carbon source was constrained to $[-10,1000]$, and the exchange of the electron acceptor was unlimited. The fumarate transport reactions SUCFUMtdc, FUMt4, and FUMt4_2 were blocked as mentioned above to avoid artificial loops and prevent the utilization of fumarate as an additional carbon source. The proton-pumping NADH dehydrogenase in MR-1 was blocked due to the lack of evidence of its participation in energy metabolism (8, 24, 25). All other internal reactions in WP3 and MR-1 models were constrained based on the reaction reversibility using default settings in PSAMM.

ACKNOWLEDGEMENTS

We thank the Chao Liu for the comparative analysis of *Shewanella* full genomes and thank Jon Steffensen for the technical support to the operation of PSAMM software package. We thank Dr. Margrethe H. Serres for constructive comments on the manuscript and for discussions about genome annotation of the *Shewanella* genus.

FUNDING INFORMATION

The metabolic modeling was supported by the National Science Foundation under Grant No. 1553211, a summer fellowship to KDT from the RI NSF EPSCoR Cooperative Agreement #EPS-1004057, and the USDA National Institute of Food and

Agriculture, Hatch fund, RI0015-H002, Accession No. 1007170. The experimental work was supported by the National Natural Science Foundation of China (Grant No. 31290232). Any opinions, findings, and conclusions or recommendations expressed in this material are those of the author(s) and do not necessarily reflect the views of the funders.

REFERENCES

1. Chilukuri LN, Bartlett DH. 1997. Isolation and characterization of the gene encoding single-stranded-DNA-binding protein (SSB) from four marine Shewanella strains that differ in their temperature and pressure optima for growth. Microbiology 143:1163–1174.

2. Konstantinidis KT, Serres MH, Romine MF, Rodrigues JLM, Auchtung J, McCue L-A, Lipton MS, Obraztsova A, Giometti CS, Nealson KH, Fredrickson JK, Tiedje JM. 2009. Comparative systems biology across an evolutionary gradient within the Shewanella genus. Proc Natl Acad Sci U S A 106:15909–15914.

3. Hau HH, Gralnick J a. 2007. Ecology and biotechnology of the genus Shewanella. Annu Rev Microbiol 61:237–58.

4. Fredrickson JK, Romine MF, Beliaev AS, Auchtung JM, Driscoll ME, Gardner TS, Nealson KH, Osterman AL, Pinchuk G, Reed JL, Rodionov D a, Rodrigues JLM, Saffarini D a, Serres MH, Spormann AM, Zhulin IB, Tiedje JM. 2008. Towards environmental systems biology of Shewanella. Nat Rev Microbiol 6:592–603.

5. Nealson KH, Scott J. 2006. Ecophysiology of the Genus Shewanella, p. 1133–1151. *In* Dworkin, M, Falkow, S, Rosenberg, E, Schleifer, K-H, Stackebrandt, E (eds.), The Prokaryotes: Volume 6: Proteobacteria: Gamma Subclass. Springer New York, New York, NY, NY.

6. Beliaev AS, Klingeman DM, Klappenbach JA, Wu L, Romine MF, Tiedje JM, Nealson KH, Fredrickson JK, Zhou J. 2005. Global transcriptome analysis of Shewanella oneidensis MR-1 exposed to different terminal electron acceptors. J Bacteriol 187:7138–7145.

7. Kato C, Nogi Y. 2001. Correlation between phylogenetic structure and function: Examples from deep-sea Shewanella. FEMS Microbiol Ecol.

8. Hunt KA, Flynn JM, Naranjo B, Shikhare ID, Gralnick JA. 2010. Substrate-

level phosphorylation is the primary source of energy conservation during anaerobic respiration of *Shewanella oneidensis* strain MR-1. J Bacteriol 192:3345–3351.

9. Pinchuk GE, Geydebrekht O V., Hill EA, Reed JL, Konopka AE, Beliaev AS, Fredrickson JK. 2011. Pyruvate and lactate metabolism by Shewanella oneidensis MR-1 under fermentation, oxygen limitation, and fumarate respiration conditions. Appl Environ Microbiol 77:8234–8240.

10. Kane AL, Brutinel ED, Joo H, Maysonet R, VanDrisse CM, Kotloski NJ, Gralnick JA. 2016. Formate metabolism in Shewanella oneidensis generates proton motive force and prevents growth without an electron acceptor. J Bacteriol 198:1337–1346.

11. Wang F, Wang P, Chen M, Xiao X. 2004. Isolation of extremophiles with the detection and retrieval of Shewanella strains in deep-sea sediments from the west Pacific. Extremophiles 8:165–168.

12. Wang F, Wang J, Jian H, Zhang B, Li S, Wang F, Zeng X, Gao L, Bartlett DH, Yu J, Hu S, Xiao X. 2008. Environmental adaptation: Genomic analysis of the piezotolerant and psychrotolerant deep-see iron reducing bacterium Shewanella piezotolerans WP3. PLoS One 3.

13. Xiao X, Wang P, Zeng X, Bartlett DH, Wang F. 2007. Shewanella psychrophila sp. nov. and Shewanella piezotolerans sp. nov., isolated from west Pacific deep-sea sediment. Int J Syst Evol Microbiol 57:60–65.

14. Wang F, Xiao X, Ou H-Y, Gai Y, Wang F. 2009. Role and regulation of fatty acid biosynthesis in the response of Shewanella piezotolerans WP3 to different temperatures and pressures. J Bacteriol 191:2574–84.

15. Bordbar A, Monk JM, King ZA, Palsson BO. 2014. Constraint-based models predict metabolic and associated cellular functions. Nat Rev Genet 15:107–20.

16. Orth JD, Thiele I, Palsson BØ. 2010. What is Flux Balance Analysis? Nat Biotechnol 28:245–8.

17. Burgard AP, Pharkya P, Maranas CD. 2003. OptKnock: A Bilevel Programming Framework for Identifying Gene Knockout Strategies for Microbial Strain Optimization. Biotechnol Bioeng 84:647–657.

18. Zomorrodi AR, Suthers PF, Ranganathan S, Maranas CD. 2012. Mathematical optimization applications in metabolic networks. Metab Eng.

19. Casey JR, Mardinoglu A, Nielsen J, Karl DM. 2016. Adaptive Evolution of Phosphorus Metabolism in Prochlorococcus. mSystems 1:e00065-16.

20. Henry CS, DeJongh M, Best AA, Frybarger PM, Linsay B, Stevens RL. 2010.

High-throughput generation, optimization and analysis of genome-scale metabolic models. Nat Biotechnol 28:977–982.

21. Schellenberger J, Que R, Fleming RMT, Thiele I, Orth JD, Feist AM, Zielinski DC, Bordbar A, Lewis NE, Rahmanian S, Kang J, Hyduke DR, Palsson BØ. 2011. Quantitative prediction of cellular metabolism with constraint-based models: the COBRA Toolbox v2.0. Nat Protoc 6:1290–1307.

22. Agren R, Liu L, Shoaie S, Vongsangnak W, Nookaew I, Nielsen J. 2013. The RAVEN Toolbox and Its Use for Generating a Genome-scale Metabolic Model for Penicillium chrysogenum. PLoS Comput Biol 9.

23. Steffensen JL, Dufault-Thompson K, Zhang Y. 2016. PSAMM: A Portable System for the Analysis of Metabolic Models. PLoS Comput Biol 12.

24. Pinchuk GE, Hill EA, Geydebrekht O V., de Ingeniis J, Zhang X, Osterman A, Scott JH, Reed SB, Romine MF, Konopka AE, Beliaev AS, Fredrickson JK, Reed JL. 2010. Constraint-based model of Shewanella oneidensis MR-1 metabolism: A tool for data analysis and hypothesis generation. PLoS Comput Biol 6:1–8.

25. Ong WK, Vu TT, Lovendahl KN, Llull JM, Serres MH, Romine MF, Reed JL. 2014. Comparisons of Shewanella strains based on genome annotations, modeling, and experiments. BMC Syst Biol 8:31.

26. Chen Y, Wang F, Xu J, Mehmood MA, Xiao X. 2011. Physiological and evolutionary studies of NAP systems in Shewanella piezotolerans WP3. ISME J 5:843–855.

27. Xiong L, Jian H, Zhang Y, Xiao X. 2016. The Two Sets of DMSO Respiratory Systems of Shewanella piezotolerans WP3 Are Involved in Deep Sea Environmental Adaptation. Front Microbiol 7:1418.

28. Yang XW, He Y, Xu J, Xiao X, Wang FP. 2013. The Regulatory Role of Ferric Uptake Regulator (Fur) during Anaerobic Respiration of Shewanella piezotolerans WP3. PLoS One 8.

29. Wu W, Li B, Hu J, Li J, Wang F, Pan Y. 2011. Iron reduction and magnetite biomineralization mediated by a deep-sea iron-reducing bacterium Shewanella piezotolerans WP3. J Geophys Res Biogeosciences 116.

30. Wu WF, Wang FP, Li JH, Yang XW, Xiao X, Pan YX. 2013. Iron reduction and mineralization of deep-sea iron reducing bacterium Shewanella piezotolerans WP3 at elevated hydrostatic pressures. Geobiology 11:593–601.

31. Li S, Xiao X, Sun P, Wang F. 2008. Screening of genes regulated by cold shock in Shewanella piezotolerans WP3 and time course expression of cold-regulated genes. Arch Microbiol 189:549–556.

32. Li S, Xiao X, Li J, Luo J, Wang F. 2006. Identification of genes regulated by changing salinity in the deep-sea bacterium Shewanella sp. WP3 using RNA arbitrarily primed PCR. Extremophiles 10:97–104.

33. Jian H, Li S, Feng X, Xiao X. 2016. Global transcriptome analysis of the heat shock response of the deep-sea bacterium Shewanella piezotolerans WP3. Mar Genomics 30:81–85.

34. Jian H, Hu J, Xiao X. 2015. Transcriptional profiling of CRP-regulated genes in deep-sea bacterium Shewanella piezotolerans WP3. Genomics data 5:51–3.

35. Jian H, Wang F. 2015. Microarray analysis of lexA gene deletion mutant of deep-sea bacterium Shewanella piezotolerans WP3 at low-temperature and high-pressure. Genomics Data 4:130–132.

36. Jian H, Xiong L, He Y, Xiao X. 2015. The regulatory function of LexA is temperature-dependent in the deep-sea bacterium Shewanella piezotolerans WP3. Front Microbiol 6:627.

37. Wang F, Wang F, Li Q, Xiao X. 2007. A novel filamentous phage from the deep-sea bacterium Shewanella piezotolerans WP3 is induced at low temperature. J Bacteriol 189:7151–7153.

38. Jian H, Xiao X, Wanga F. 2013. Role of filamentous phage SW1 in regulating the lateral flagella of shewanella piezotolerans strain WP3 at low temperatures. Appl Environ Microbiol 79:7101–7109.

39. Yang X-W, Jian H-H, Wang F-P. 2015. pSW2, a Novel Low-Temperature-Inducible Gene Expression Vector Based on a Filamentous Phage of the Deep-Sea Bacterium Shewanella piezotolerans WP3. Appl Environ Microbiol 81:5519–26.

40. Jian H, Xiong L, Xu G, Xiao X. 2016. Filamentous phage SW1 is active and influences the transcriptome of the host at high-pressure and low-temperature. Environ Microbiol Rep 8:358–362.

41. Rodionov D a, Yang C, Li X, Rodionova I a, Wang Y, Obraztsova AY, Zagnitko OP, Overbeek R, Romine MF, Reed S, Fredrickson JK, Nealson KH, Osterman AL. 2010. Genomic encyclopedia of sugar utilization pathways in the Shewanella genus. BMC Genomics 11:494.

42. Overbeek R, Begley T, Butler RM, Choudhuri J V., Chuang HY, Cohoon M, de Crécy-Lagard V, Diaz N, Disz T, Edwards R, Fonstein M, Frank ED, Gerdes S, Glass EM, Goesmann A, Hanson A, Iwata-Reuyl D, Jensen R, Jamshidi N, Krause L, Kubal M, Larsen N, Linke B, McHardy AC, Meyer F, Neuweger H, Olsen G, Olson R, Osterman A, Portnoy V, Pusch GD, Rodionov DA, Rül;ckert C, Steiner J, Stevens R, Thiele I, Vassieva O, Ye Y, Zagnitko O, Vonstein V. 2005. The subsystems approach to genome annotation and its use in the project

to annotate 1000 genomes. Nucleic Acids Res 33:5691–5702.

43. Imai K, Asakawa N, Tsuji T, Akazawa F, Ino A, Sonoyama M, Mitaku S. 2008. SOSUI-GramN: high performance prediction for sub-cellular localization of proteins in gram-negative bacteria. Bioinformation 2:417–21.

44. Yu NY, Wagner JR, Laird MR, Melli G, Rey S, Lo R, Dao P, Cenk Sahinalp S, Ester M, Foster LJ, Brinkman FSL. 2010. PSORTb 3.0: Improved protein subcellular localization prediction with refined localization subcategories and predictive capabilities for all prokaryotes. Bioinformatics 26:1608–1615.

45. Petersen TN, Brunak S, von Heijne G, Nielsen H. 2011. SignalP 4.0: discriminating signal peptides from transmembrane regions. Nat Methods 8:785–6.

46. Cruz-García C, Murray AE, Klappenbach JA, Stewart V, Tiedje JM. 2007. Respiratory nitrate ammonification by Shewanella oneidensis MR-1. J Bacteriol 189:656–662.

47. Gon S, Patte JC, Dos Santos JP, Méjean V. 2002. Reconstitution of the trimethylamine oxide reductase regulatory elements of Shewanella oneidensis in Escherichia coli. J Bacteriol 184:1262–1269.

48. Simpson PJL, Richardson DJ, Codd R. 2010. The periplasmic nitrate reductase in Shewanella: The resolution, distribution and functional implications of two NAP isoforms, NapEDABC and NapDAGHB. Microbiology.

49. Schuetz B, Schicklberger M, Kuermann J, Spormann AM, Gescher J. 2009. Periplasmic electron transfer via the c-type cytochromes Mtra and Fcca of Shewanella oneidensis Mr-1. Appl Environ Microbiol 75:7789–7796.

50. Burns JL, Dichristina TJ. 2009. Anaerobic Respiration of Elemental Sulfur and Thiosulfate by Shewanella oneidensis MR-1 Requires psrA, a phsA homolog of Salmonella typhimurium LT2. Appl Environ Microbiol 64:119–125.

51. Heidelberg JF, Paulsen IT, Nelson KE, Gaidos EJ, Nelson WC, Read TD, Eisen J a, Seshadri R, Ward N, Methe B, Clayton R a, Meyer T, Tsapin A, Scott J, Beanan M, Brinkac L, Daugherty S, DeBoy RT, Dodson RJ, Durkin a S, Haft DH, Kolonay JF, Madupu R, Peterson JD, Umayam L a, White O, Wolf AM, Vamathevan J, Weidman J, Impraim M, Lee K, Berry K, Lee C, Mueller J, Khouri H, Gill J, Utterback TR, McDonald L a, Feldblyum T V, Smith HO, Venter JC, Nealson KH, Fraser CM. 2002. Genome sequence of the dissimilatory metal ion-reducing bacterium Shewanella oneidensis. Nat Biotechnol 20:1118–1123.

52. Gralnick JA, Vali H, Lies DP, Newman DK. 2006. Extracellular respiration of dimethyl sulfoxide by Shewanella oneidensis strain MR-1. Proc Natl Acad Sci U S A 103:4669–74.

53. Coursolle D, Baron DB, Bond DR, Gralnick JA. 2010. The Mtr respiratory pathway is essential for reducing flavins and electrodes in Shewanella oneidensis. J Bacteriol 192:467–474.

54. Shi L, Rosso KM, Zachara JM, Fredrickson JK. 2012. Mtr extracellular electron-transfer pathways in Fe(III)-reducing or Fe(II)-oxidizing bacteria: a genomic perspective. Biochem Soc Trans 40:1261–7.

55. Coursolle D, Gralnick JA. 2012. Reconstruction of extracellular respiratory pathways for iron(III) reduction in Shewanella oneidensis strain MR-1. Front Microbiol 3.

56. Masi M, Pagès J-M. 2013. Structure, Function and Regulation of Outer Membrane Proteins Involved in Drug Transport in Enterobactericeae: the OmpF/C - TolC Case. Open Microbiol J 7:22–33.

57. Nikaido H. 2003. Molecular Basis of Bacterial Outer Membrane Permeability Revisited. Microbiol Mol Biol Rev 67:593–656.

58. Nestorovich EM, Sugawara E, Nikaido H, Bezrukov SM. 2006. Pseudomonas aeruginosa porin OprF. Properties of the channel. J Biol Chem 281:16230–16237.

59. Death A, Notley L, Ferenci T. 1993. Derepression of LamB protein facilitates outer membrane permeation of carbohydrates into Escherichia coli under conditions of nutrient stress. J Bacteriol 175:1475–1483.

60. Wylie JL, Worobec EA. 1995. The OprB porin plays a central role in carbohydrate uptake in Pseudomonas aeruginosa. J Bacteriol 177:3021–3026.

61. Moraes TF, Bains M, Hancock REW, Strynadka NCJ. 2007. An arginine ladder in OprP mediates phosphate-specific transfer across the outer membrane. Nat Struct Mol Biol 14:85–87.

62. Nieweg A, Bremer E. 1997. The nucleoside-specific Tsx channel from the outer membrane of Salmonella typhimurium, Klebsiella pneumoniae and Enterobacter aerogenes: Functional characterization and DNA sequence analysis of the tsx genes. Microbiology 143:603–615.

63. Shultis DD, Purdy MD, Banchs CN, Wiener MC. 2006. Outer Membrane Active Transport: Structure of the BtuB:TonB Complex. Science (80-) 312:1396–1399.

64. Deutschbauer A, Price MN, Wetmore KM, Shao W, Baumohl JK, Xu Z, Nguyen M, Tamse R, Davis RW, Arkin AP. 2011. Evidence-based annotation of gene function in Shewanella oneidensis MR-1 using genome-wide fitness profiling across 121 conditions. PLoS Genet 7.

65. Yang C, Rodionov DA, Li X, Laikova ON, Gelfand MS, Zagnitko OP, Romine MF, Obraztsova AY, Nealson KH, Osterman AL. 2006. Comparative Genomics and Experimental Characterization of N -Acetylglucosamine Utilization Pathway of Shewanella oneidensis. J Biol Chem 281:29872–29885.

66. Bruinenberg PM, de Bot PHM, van Dijken JP, Scheffers WA. 1983. The role of redox balances in the anaerobic fermentation of xylose by yeasts. Eur J Appl Microbiol Biotechnol 18:287–292.

67. Berríos-Rivera SJ, Bennett GN, San K-Y. 2002. Metabolic Engineering of Escherichia coli: Increase of NADH Availability by Overexpressing an NAD+-Dependent Formate Dehydrogenase. Metab Eng 4:217–229.

68. Hasegawa S, Uematsu K, Natsuma Y, Suda M, Hiraga K, Jojima T, Inui M, Yukawa H. 2012. Improvement of the redox balance increases L-valine production by Corynebacterium glutamicum under oxygen deprivation conditions. Appl Environ Microbiol 78:865–875.

69. Chang RL, Andrews K, Kim D, Li Z, Godzik A, Palsson BØ. 2013. Structural systems biology evaluation of metabolic thermotolerance in Escherichia coli. Science 340:1220–1223.

70. Töpfer N, Caldana C, Grimbs S, Willmitzer L, Fernie AR, Nikoloski Z. 2013. Integration of genome-scale modeling and transcript profiling reveals metabolic pathways underlying light and temperature acclimation in Arabidopsis. Plant Cell 25:1197–211.

71. Kanehisa M, Sato Y, Kawashima M, Furumichi M, Tanabe M. 2016. KEGG as a reference resource for gene and protein annotation. Nucleic Acids Res 44:D457–D462.

72. Zhang Y, Sievert SM. 2014. Pan-genome analyses identify lineage- and niche-specific markers of evolution and adaptation in Epsilonproteobacteria. Front Microbiol 5.

73. Li L, Stoeckert CJ, Roos DS. 2003. OrthoMCL: Identification of ortholog groups for eukaryotic genomes. Genome Res 13:2178–2189.

74. Edgar RC. 2004. MUSCLE: Multiple sequence alignment with high accuracy and high throughput. Nucleic Acids Res 32:1792–1797.

75. Stamatakis A. 2014. RAxML version 8: A tool for phylogenetic analysis and post-analysis of large phylogenies. Bioinformatics 30:1312–1313.

76. Caspi R, Billington R, Ferrer L, Foerster H, Fulcher CA, Keseler IM, Kothari A, Krummenacker M, Latendresse M, Mueller LA, Ong Q, Paley S, Subhraveti P, Weaver DS, Karp PD. 2016. The MetaCyc database of metabolic pathways and enzymes and the BioCyc collection of pathway/genome databases. Nucleic

Acids Res 44:D471–D480.

77. Overbeek R, Olson R, Pusch GD, Olsen GJ, Davis JJ, Disz T, Edwards RA, Gerdes S, Parrello B, Shukla M, Vonstein V, Wattam AR, Xia F, Stevens R. 2014. The SEED and the Rapid Annotation of microbial genomes using Subsystems Technology (RAST). Nucleic Acids Res 42.

78. Finn RD, Coggill P, Eberhardt RY, Eddy SR, Mistry J, Mitchell AL, Potter SC, Punta M, Qureshi M, Sangrador-Vegas A, Salazar GA, Tate J, Bateman A. 2016. The Pfam protein families database: Towards a more sustainable future. Nucleic Acids Res 44:D279–D285.

79. Serres MH, Riley M. 2006. Genomic analysis of carbon source metabolism of Shewanella oneidensis MR-1: Predictions versus experiments. J Bacteriol 188:4601–4609.

80. Orth JD, Conrad TM, Na J, Lerman J a, Nam H, Feist AM, Palsson BØ. 2011. A comprehensive genome-scale reconstruction of Escherichia coli metabolism--2011. Mol Syst Biol 7:535.

81. Candès EJ, Wakin MB, Boyd SP. 2008. Enhancing sparsity by reweighted L1 minimization. J Fourier Anal Appl 14:877–905.

Tables and Figures Manuscript I

Table 1. Exchange reaction constraints representing the concentrations of carbon, nitrogen, sulfur, and phosphorous sources in the minimal media of WP3 batch cultures. All other exchange reactions in the WP3 model were defined with settings in the basal constraints. The compounds pyruvate, glucose, maltose, and GlcNac, were used as sole carbon sources. The LB and UB columns indicated the lower and upper bounds of exchange reaction fluxes, where the negative values indicated that uptake of the nutrient was permitted. Concentrations of the sole carbon sources varied from 2 mM to 40 mM; the concentration of the sulfur, phosphorus, and nitrogen sources were set according to their concentration in the experimental media.

Nutrient Source	Compound Name	Media Concentraton	LB	UB
Carbon Sources	Glucose/Maltose/GlcNac/Pyruvate	2mM	-2.00	1000.00
		5mM	-5.00	1000.00
		10mM	-10.00	1000.00
		20mM	-20.00	1000.00
		40mM	-40.00	1000.00
Sulfur Source	SO4	9.8mM	-9.80	1000.00
Phophorus Source	PO4	0.7mM	-0.70	1000.00
Nitrogen Source	NH4	5.6mM	-5.60	1000.00

Table 2. Metabolic enzymes involved in ATP production and PMF generation (Figure 4) with their corresponding reactions, functional roles, and gene associations in the WP3 model.

Enzyme	Reactions	Function	Gene association
Pta	PTAr	Phosphotransacetylase	swp_1948
AckA	ACKr	Acetate kinase	swp_1949
ATPase	ATPS4r	ATP synthase	swp_5155 AND swp_5156 AND swp_5157 AND swp_5158 AND swp_5159 AND swp_5160 AND swp_5161
Pyk	PYK	Pyruvate kinase	swp_2388
Pfl	PFL	Formate C-acetyltransferase	swp_1952
Xpk	XPK	Xylulose-5-phosphate phosphoketolase	swp_3738
Ndh	NADH4, NADH12, NADH14	NADH dehydrogenase	swp_1298 OR swp_2117 OR swp_4014
Fdh	FDH9, FDH10	Formate dehydrogenase	(swp_5024 AND swp_5025 AND swp_5023) OR (swp_5027 AND swp_5028 AND swp_5029)

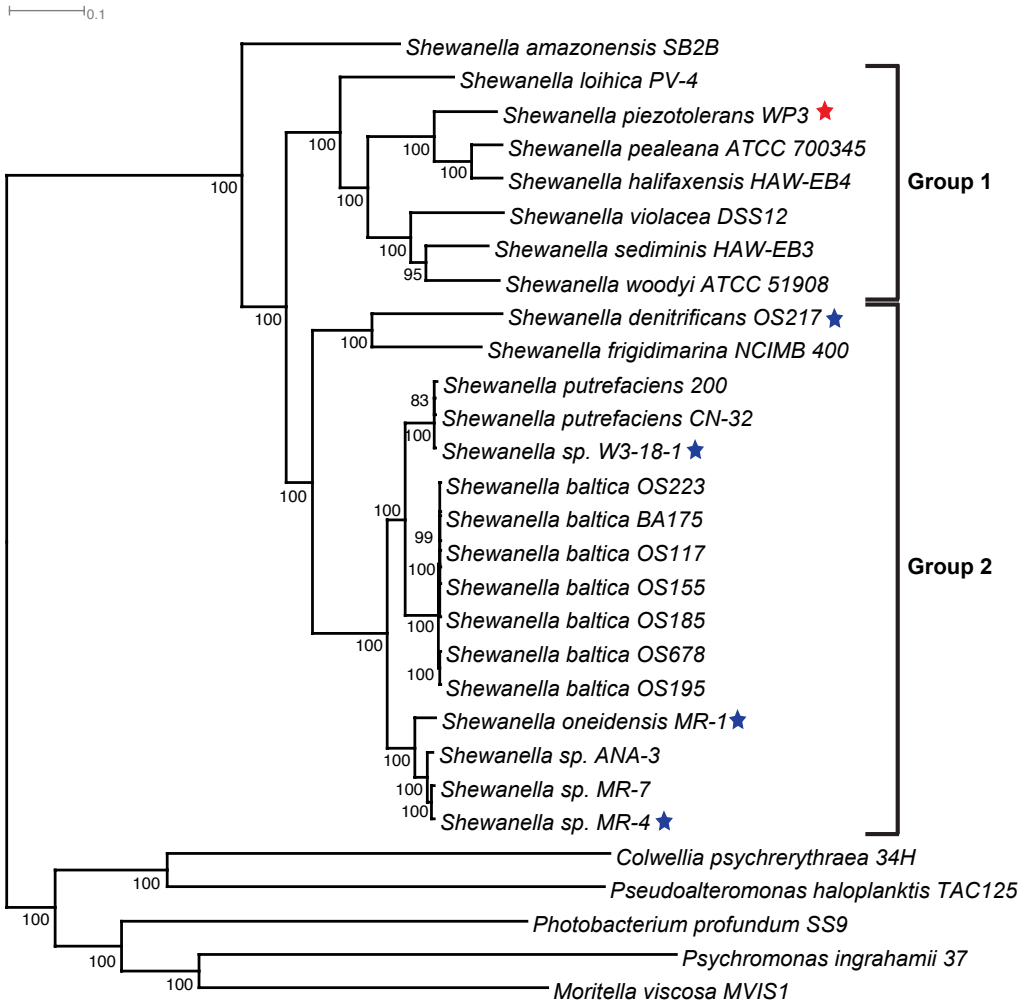

Figure 1. Phylogenetic reconstruction of the *Shewanella* genus based on the concatenated sequences of 661 conserved single copy genes identified in the full genomes of *Shewanella* and five outgroup species. Support values based on 100 iterations of bootstrapping were indicated as labels of the internal nodes. Only support values above 80 were shown. The four *Shewanella* species with available GEMs were marked with blue stars and WP3 was marked with a red star.

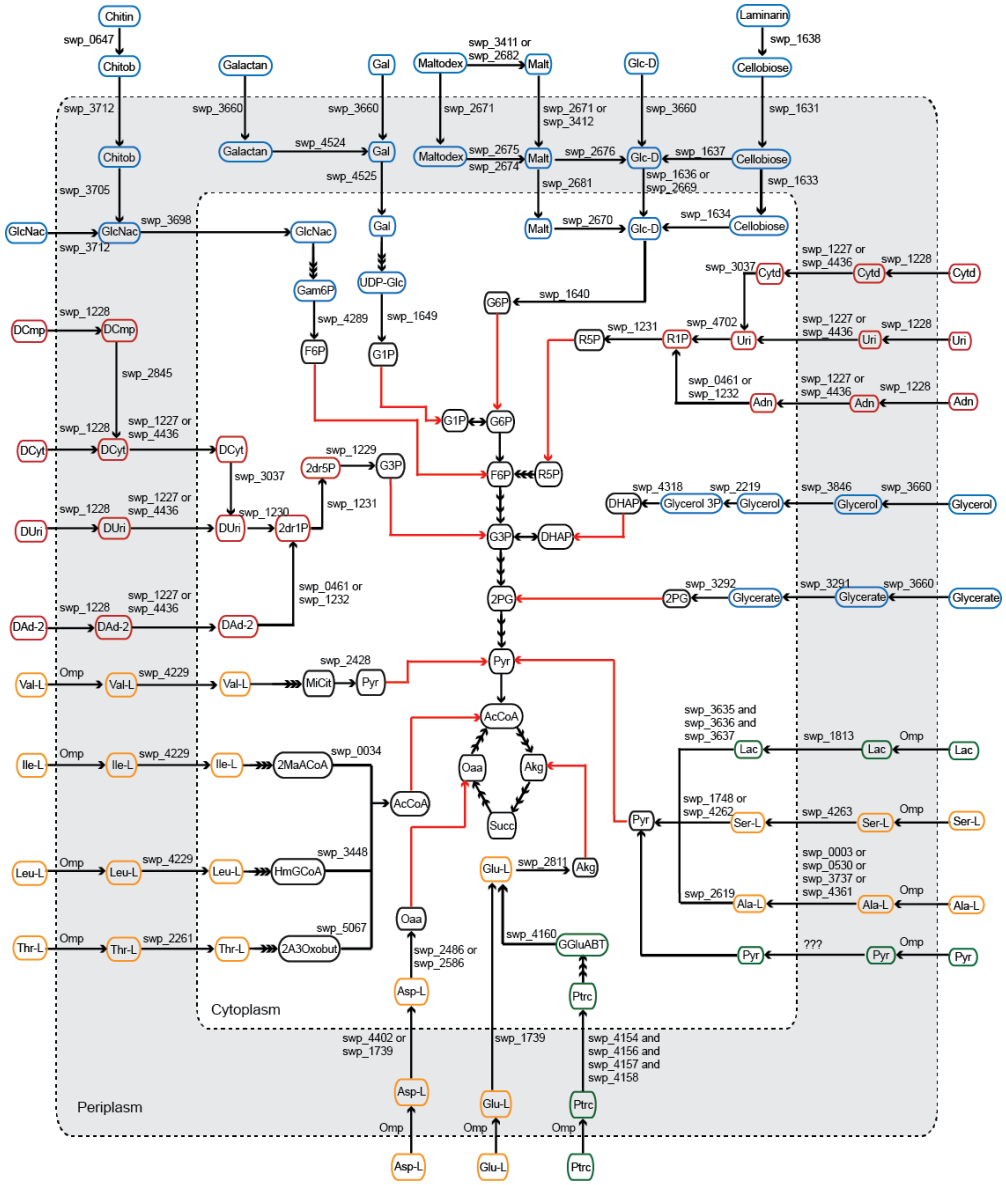

Figure 2. A schematic representation of the carbon utilization pathways for various carbohydrates and their derivatives (blue), amino acids (orange), nucleic acids (red), and small carbon molecules (green) as well as their links to the central carbon metabolism (red arrows). Metabolites were represented as ovals; metabolic and transport reactions were represented as links between metabolites. Triple arrows linking two compounds indicated that multiple reactions were involved in the conversion of one compound to the other. Genes coding for main metabolic steps of the carbon uptake pathways were indicated as labels on the links.

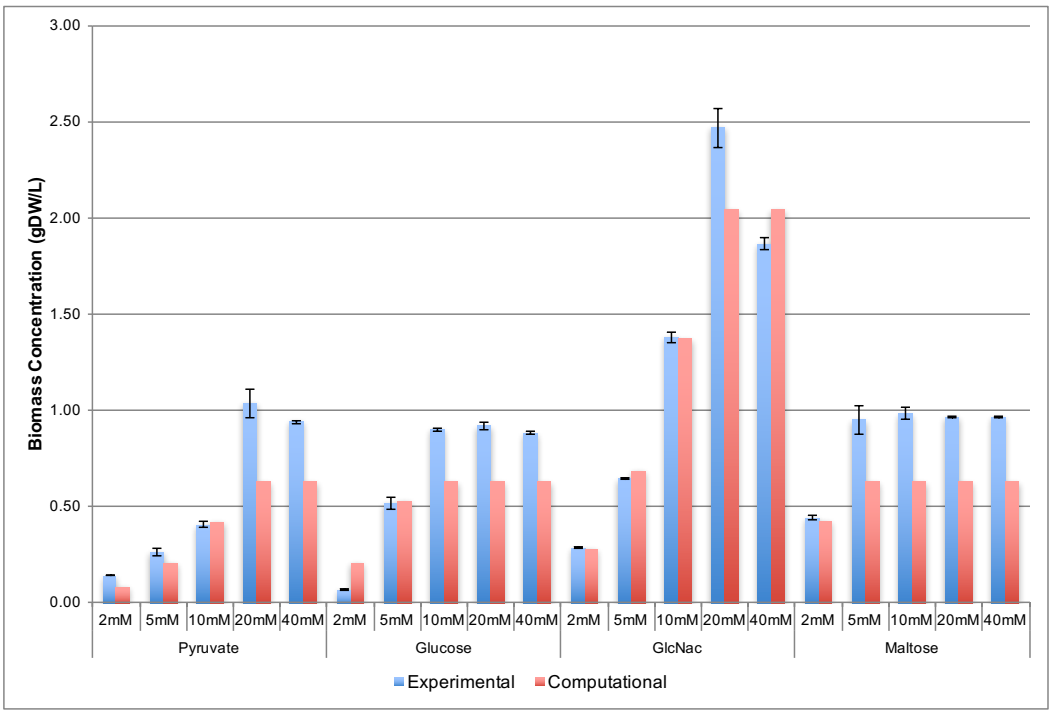

Figure 3. Comparison of experimentally measured and computationally simulated biomass production. Error bars represented the standard deviation of the experimentally measured biomass concentrations (*gDW/L*) from three independent replicates.

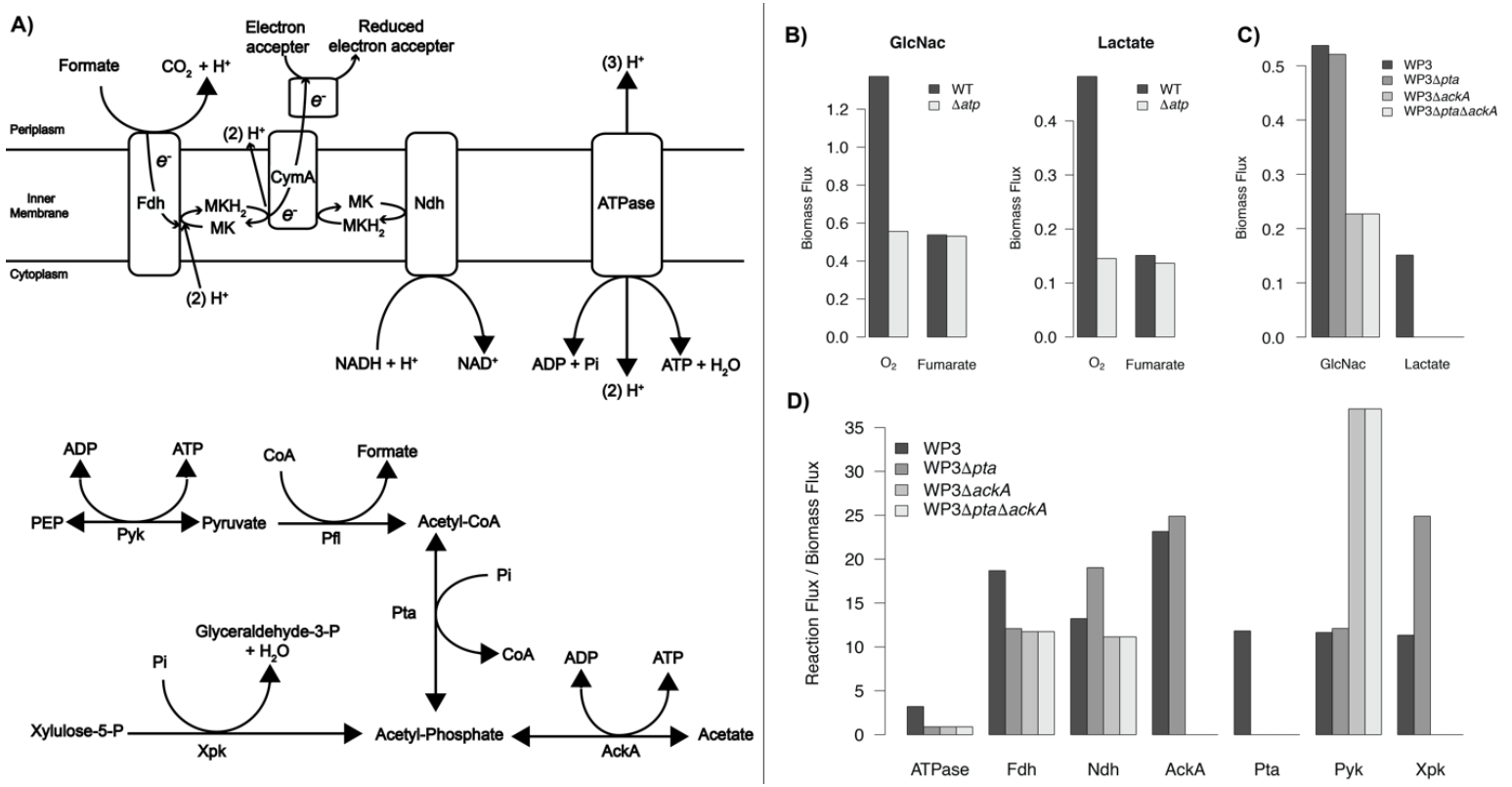

Figure 4. A) A schematic representation of key reactions involved in the production of ATP and PMF in WP3. B) Comparison of biomass fluxes in the wild type and the *Δatp* mutant models of WP3 with GlcNac or lactate as a sole carbon source in aerobic and anaerobic conditions. C) Biomass fluxes from anaerobic growth simulations of the WP3 wild type model and the mutant models *ΔackA*, *Δpta*, and *ΔptaΔackA* using GlcNac or lactate as a sole carbon source and fumarate as a sole electron acceptor. D) Internal reaction fluxes of the WP3 and mutant models from the simulations in C) using GlcNac as a sole carbon source. Abbreviations: MK–Menaquinone; CymA–Tetraheme c-type cytochrome; ATPase–ATP synthase; Fdh–Formate dehydrogenase; Ndh–NADH dehydrogenase; AckA–Acetate kinase; Pra–Phosphotransacetylase; Pyk–Pyruvate kinase; Xpk–Xylulose-5-phosphate phosphoketolase.

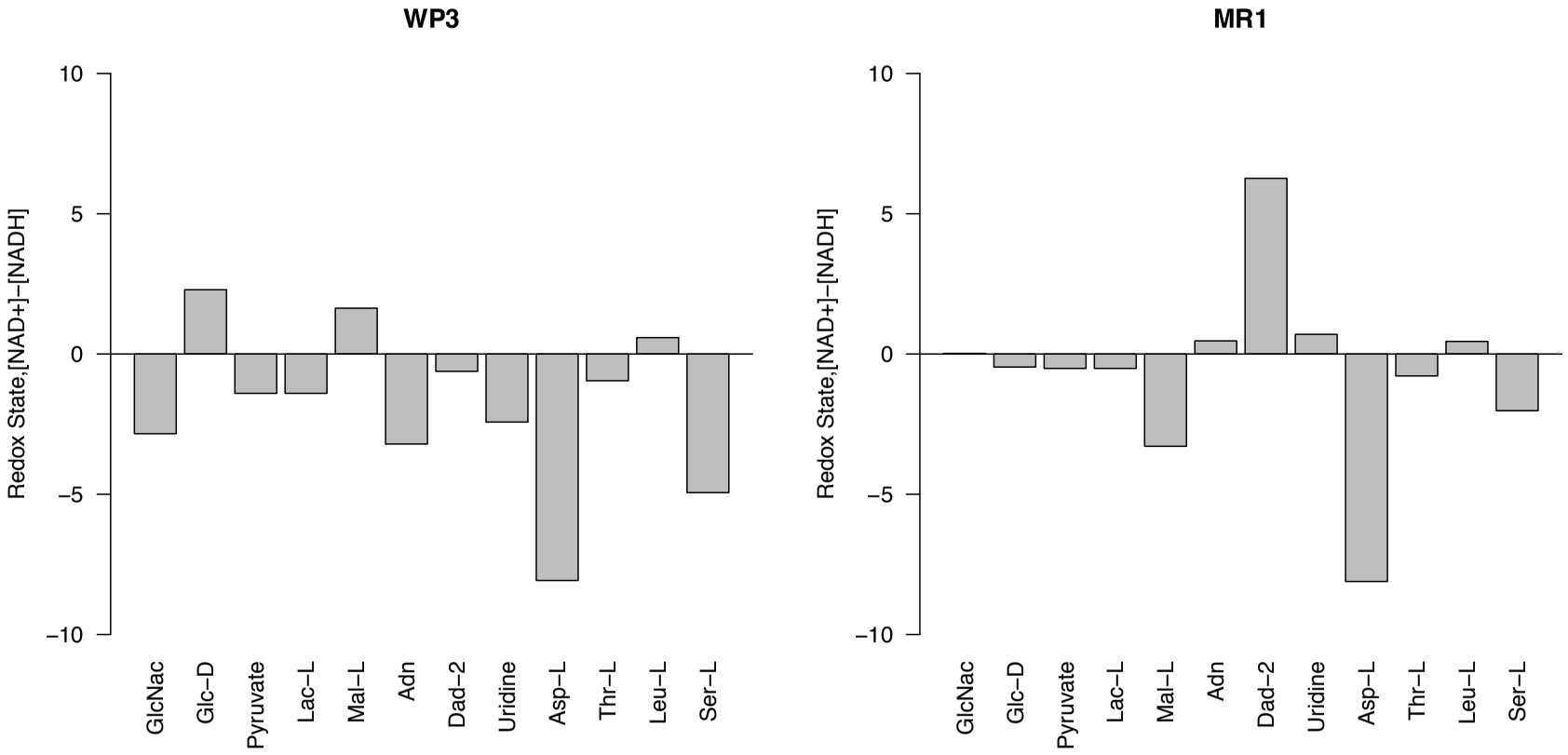

Figure 5. Comparison of the *NAD*$^+$/*NADH* homeostasis between A) WP3 and B) MR-1. The differences in *NAD*$^+$ and *NADH* concentrations were calculated from simulations under anaerobic conditions with fumarate as the terminal electron acceptor for each of the carbon sources shown (x-axis).

Supplemental Material Manuscript I:

Supplemental Text S1: Components of the LMO-812 minimal media used for culture-based experiments done with *Shewanella piezotolerans* WP3. Media components are adapted from a previously described defined marine media. Widdel, Friedrich. 2005. 8.1.1. Media for sulphate-reducing bacteria, p 102-104. In HERMES, Handbook of Methods for Microbial Ecology, Sept 2005 Edition.

LMO-812: Full Media
(Adjust final pH to 7.0 with Na_2CO_3 solution)

Component	Amount
Full Marine Salt Solution	950 mL
Trace Element Mixture	1 mL
Vitamin Mixture	1 mL
Thiamine Solution	1 mL
Vitamin B12 Solution	1 mL
$NaHCO_3$ Solution	20 mL

Full Marine Salt Solution

Component	Amount
Distilled Water	950 mL
NaCl	26.0 g
$MgCl_2 \cdot 6\ H_2O$	5 g
$CaCl_2 \cdot 2\ H_2O$	1.4 g
Na_2SO_4	4.0 g
NH_4Cl	0.3 g
KH_2PO_4	0.1 g
KCl	0.5 g

Trace Element Mixture
(Adjust final pH of solution to 6.0 with NaOH solution)

Component	Amount
Distilled Water	1000 mL
EDTA	5.2 g
H_3BO_3	10 mg
$MnCl_2 \cdot 4\ H_2O$	5 mg
$FeSO_4 \cdot 7\ H_2O$	2100 mg
$CoCl_2 \cdot 6\ H_2O$	190 mg
$NiCl_2 \cdot 6\ H_2O$	24 mg
$CuCl_2 \cdot 2\ H_2O$	10 mg
$ZnSO_4 \cdot 7\ H_2O$	144 mg
$Na_2MoO_4 \cdot 2\ H_2O$	36 mg

Vitamin Mixture

Component	Amount
Sodium Phosphate, 10 mM, pH 7.1	100 mL

4-Aminobenzoic acid	4 mg
D(+)-Biotin	1 mg
Nicotinic Acid	10 mg
D(+)-Pantothenic Acid, Calcium Salt	5 mg
Pyridoxine dihydrochloride	15 mg

Thiamine Solution

Component	**Amount**
Sodium Phosphate, 10 mM, pH 3.4	100 mL
Thiamine chloride dihydrochloride	10 mg

Vitamin B12 Solution

Component	**Amount**
Distilled Water	100 mL
Cyanocobalamin	5 mg

Bicarbonate Solution

Component	**Amount**
Distilled Water	1000 mL
$NaHCO_3$	84 g

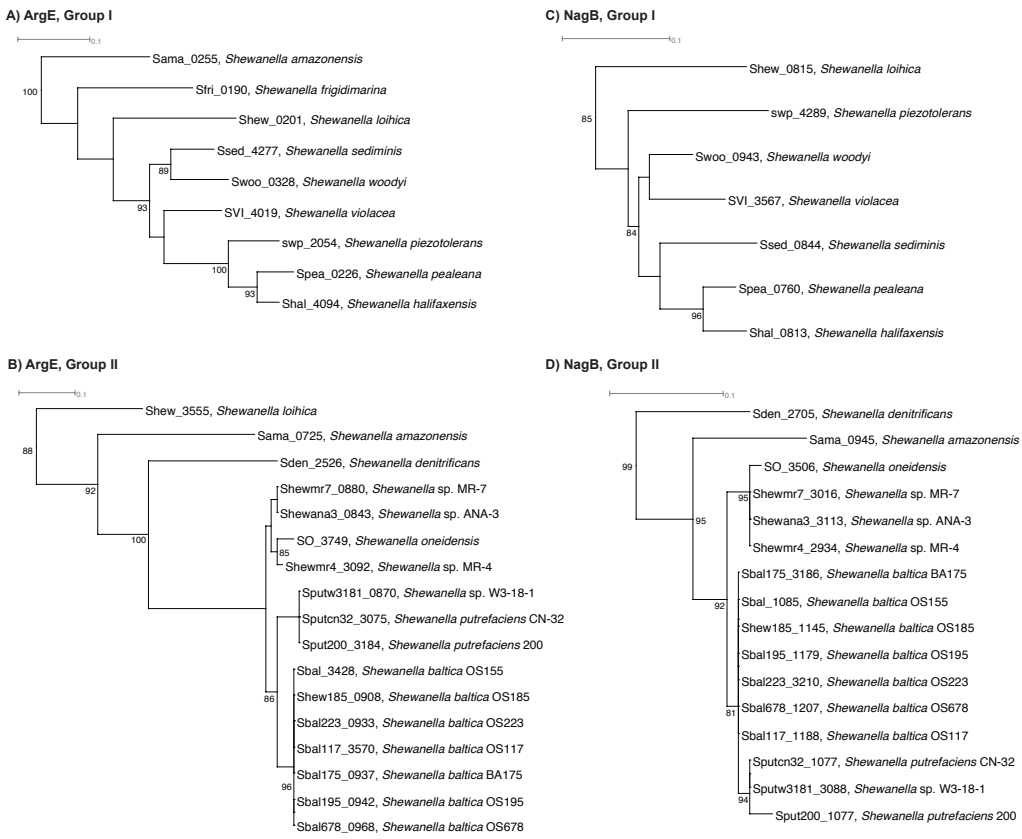

Supplemental Figure S1. Phylogenetic trees of ArgE and NagB proteins encoded in the genomes of Group 1 (A and C) and Group 2 (B and D) *Shewanella* species. Support values based on 100 iterations of bootstrapping were indicated as labels on the internal nodes. Only support values above 80 were shown. The Group 1 and Group 2 copies of the corresponding proteins had no detectable homology, indicating non-homologous replacements of the ArgE and NagB function in the two groups of *Shewanella*.

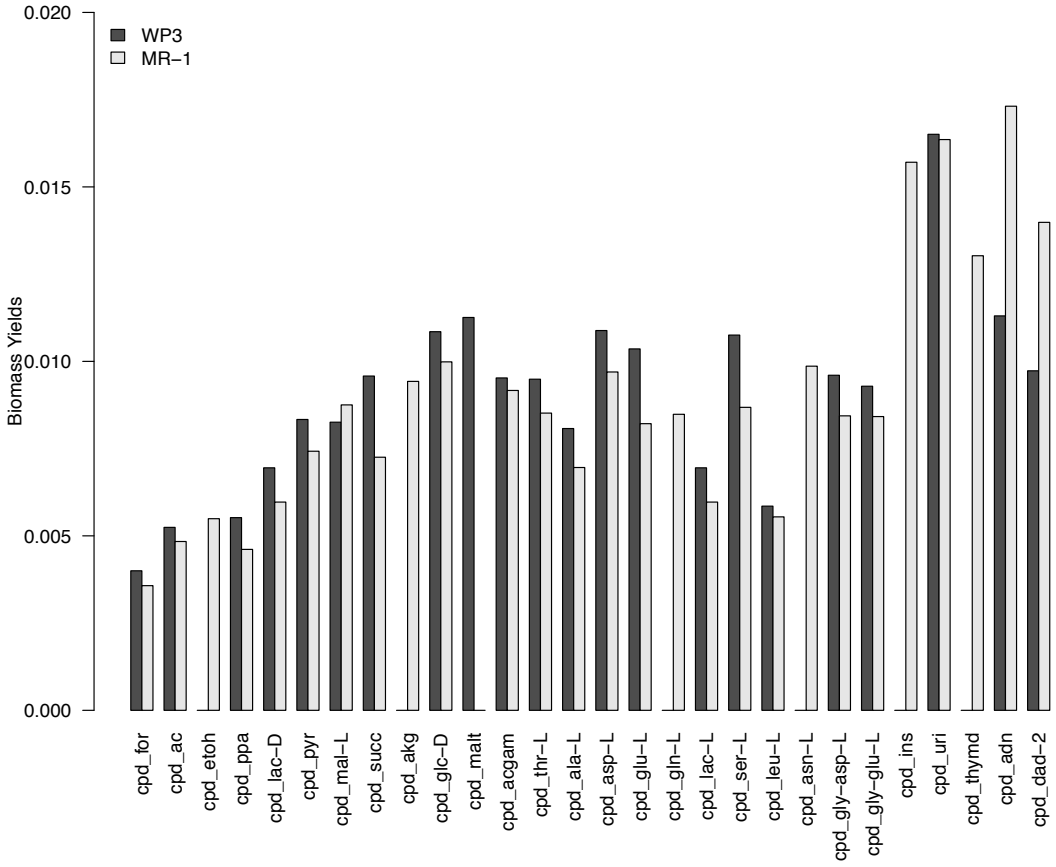

Supplemental Figure S2. Biomass yields for WP3 and MR-1 simulated across 28 carbon sources in aerobic conditions.

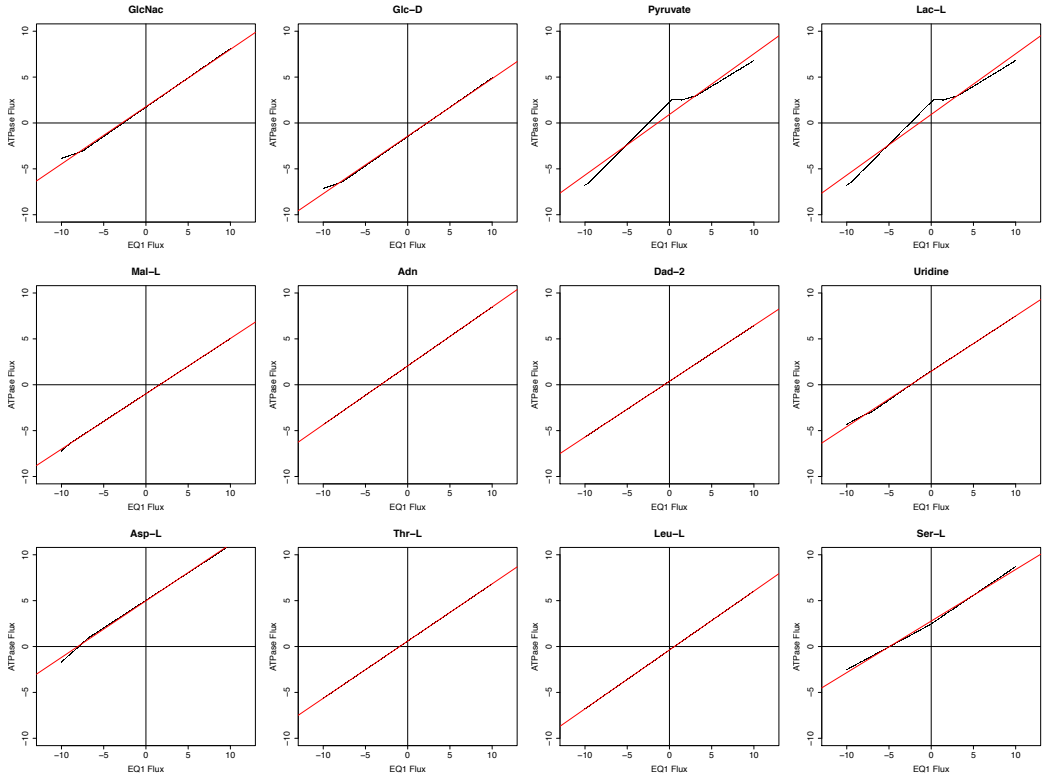

Supplemental Figure S3. Linear models for the prediction of *NAD*$^+$/*NADH* homeostasis in the WP3 model (Materials and Methods). Fluxes of the ATPase reaction (black dots) were plotted based on a robustness simulation across varied fluxes of the EQ1 reaction. Linear models (red lines) were fitted to the observed correlations between EQ1 and ATPase fluxes and was used to calculate the differences in *NAD*$^+$ and *NADH* concentrations where the ATPase flux approached zero.

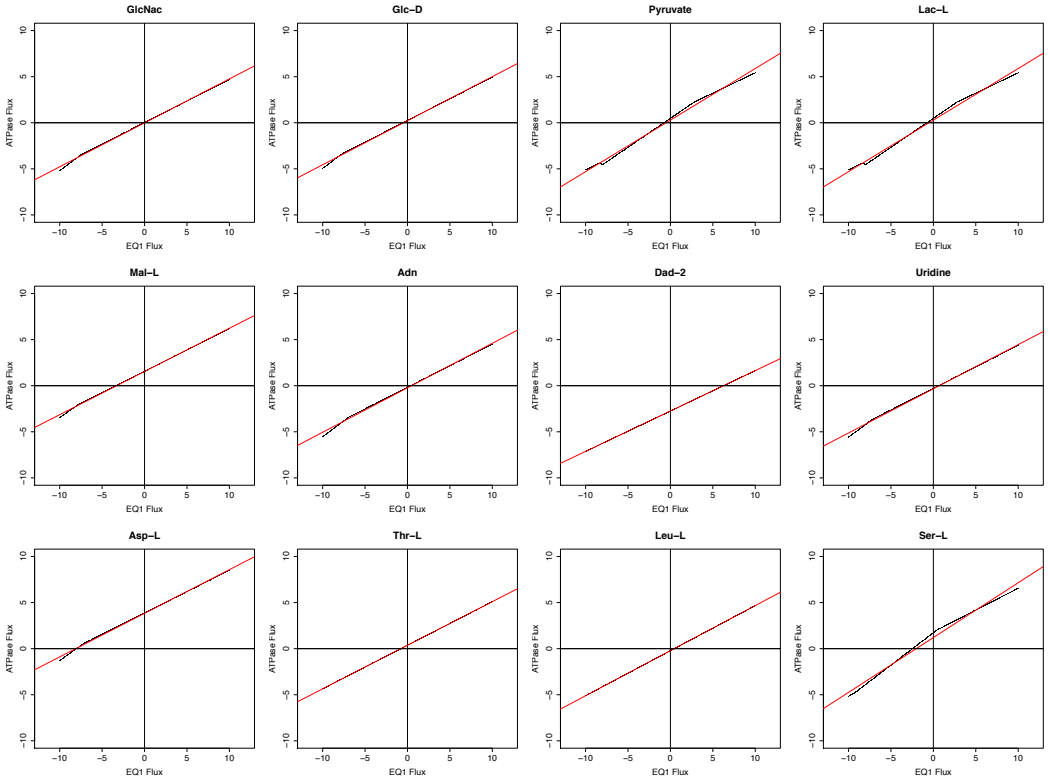

Supplemental Figure S4. Linear models for the prediction of *NAD*$^+$/*NADH* homeostasis in the MR-1 model (Materials and Methods). Fluxes of the ATPase reaction (black dots) were plotted based on a robustness simulation across varied fluxes of the EQ1 reaction. Linear models (red lines) were fitted to the observed correlations between EQ1 and ATPase fluxes and was used to calculate the differences in *NAD*$^+$ and *NADH* concentrations where the ATPase flux approached zero.

Manuscript II

Publication Status: Formatted for submission to PLOS Computational Biology

Title: Reconstruction and analysis of a thermodynamically constrained metabolic models reveal mechanisms of metabolic remodeling under temperature perturbations of a deep-sea bacterium

Keith Dufault-Thompson[1], Chang Nie[2], Fengping Wang[2], Ying Zhang[1#]

Author Affiliations:

1. Department of Cell and Molecular Biology, College of the Environment and Life Sciences, University of Rhode Island, 120 Flagg Rd., Kingston, 02881 RI, USA

2. State Key Laboratory of Microbial Metabolism, School of Life Sciences and Biotechnology, Shanghai Jiao Tong University, 800 Dongchuan Road, Shanghai 200240, P.R.China

Corresponding Author:

[#]Ying Zhang, University of Rhode Island, yingzhang@uri.edu

Abstract

Microbial acclimation to different environmental conditions can involve broad changes in gene expression and shifts in the utilization of metabolic pathways, but a systems-level view of these metabolic responses, however, is currently missing. In this study, an integrated metabolic modeling approach that combined transcriptomic and thermodynamic constraints was used to investigate the metabolic changes that occur during temperature acclimation to suboptimal (4 °C), optimal (15 °C), and supraoptimal (20 °C) temperatures in the deep-sea psychrophilic bacteria *Shewanella psychrophila* WP2. A comparison of the predicted growth at each temperature showed the 4 °C model to have a lower ability to produce both cellular biomass and energy, while the 20 °C model was able to produce energy at similar rates to the 15 °C model but was not able to efficiently use that energy to produce biomass. At 4 °C, thermodynamic changes were predicted to prevent the utilization of the payoff phase reactions of glycolysis, resulting in the utilization of less efficient pathways to produce both energy and metabolic precursors. At 20 °C, the model was predicted to use similar pathways to produce energy as the 15 °C model but was predicted to have higher flux through these pathways, resulting in less of the carbon source being used to produce biomass and more of it being secreted as acetate. The analysis of the differential expression of genes between the temperatures provided indications of stress at both 4 °C and 20 °C providing further context to the metabolic changes seen in the models. This study highlights how metabolic flexibility can allow organisms to remodel their growth to broad ranges of conditions and demonstrates the utility of modeling approaches that integrate multiple methods and sources of data.

Author Summary

Metabolic changes are a central component of any organism's ability to survive and adapt to changes in environmental conditions. This study combines modeling approaches that account for the effects of gene expression changes and reaction thermodynamics on metabolic pathways. Using this integrated modeling approach, growth of *Shewanella psychrophila* WP2 at non-optimal temperatures was simulated predicting global changes in pathway utilization and metabolic efficiency between the conditions. The changes in efficiency were contextualized by predicted differences in reaction thermodynamics, changes in pathway utilization, and observed differences in gene expression. Taken together the combination of modeling and gene expression analysis helps to build a systems level view of the metabolism of WP2 at different temperatures. Overall, this study highlights how diverse metabolic changes can be within an organism when exposed to different conditions and highlights the utility of modeling approaches that integrate multiple data sources in expanding and contextualizing these changes.

Introduction

Temperature is a major driving force in microbial growth and physiology, causing physical changes in cellular structures that cells respond and acclimate to. Physical changes in the cell include altered enzyme stability [1–3], differences in reaction kinetics [1], and altered membrane fluidity [4]. When experiencing changes in temperature, microbial cells adjust their physiology through the production of heat

shock and cold shock proteins [5], altered gene expression patterns [6–8], and the production of different kinds of membrane lipids [4,9]. Responses to temperature do not happen in isolation within the microbial cell and can often involve broader changes in metabolism as the organism shifts its growth strategies to acclimate to the new condition. Some microorganisms respond to temperature changes through the induction of specific stress responses, which allow for short-term survival in changing environments [5,10].

The metabolic changes that occur during growth at non-optimal temperatures in mesophilic microorganisms have been studied extensively, but the adaptations of psychrophilic organisms are less understood. Cold shock responses to low temperatures are not always seen in psychrophiles, with many strains showing constitutive expression of proteins typically associated with a cold shock response in mesophiles [11,12]. The metabolic changes that occur in psychrophiles in response to low-temperature conditions generally include a decreased utilization of central carbon and energy production pathways and increased utilization of branched-chain amino acid and unsaturated fatty acid metabolism [9,13–16], while the regulation of other metabolic pathways like amino acid, nucleotide biosynthesis, and vitamin metabolism is highly variable between strains [15]. While the response of psychrophiles to higher temperatures is much less understood, there has been evidence of a temperature-induced production of heat shock proteins [17] and broad changes in energy metabolism during high-temperature growth [18].

In addition to changes in specific metabolic pathways, global changes in the metabolic efficiency at different temperatures have been observed in many microbial

communities. Carbon Use Efficiency (CUE) is a measure of how much of a carbon growth substrate is used for growth versus how much of it is secreted as metabolic byproducts like carbon dioxide or acetate. Studies that have measured or estimated CUE in different microbes have shown that it varies broadly between microbial species [19] and that it can be altered by environmental factors like temperature [20–22], pH [23], and the availability of other nutrients [24]. While CUE has been extensively studied in many soil microbial communities, little is known about it in psychrophilic bacteria. Changes in temperature have also been shown to lead to altered ATP concentrations in the cell in psychrophilic bacteria with some strains showing a decrease in cellular ATP concentrations at low temperatures [18] and others showing increases in ATP concentration [25]. These broader measures in efficiency can provide important context to specific changes in metabolic pathway utilization, allowing for a broader perspective on the effects of temperature on physiology.

Bacteria from the Shewanella genus have long been studied because of their broad environmental adaptations and diverse metabolic capabilities [26–29]. Bacteria in this genus have been broadly classified into two clades, one with mostly psychrophilic deep-sea strains referred to as Group 1, and one clade with adaptations to a broader range of environments referred to as Group 2 [29]. Recent studies have rapidly expanded this genus introducing new strains from both groups from a variety of new environments [30–32]. While Group 2 *Shewanella* have been extensively studied for their uses in bioengineering [33–35], Group 1 *Shewanella* have recently become a focus of studies related to their environmental adaptations to low temperature and high pressure [7,36–40]. The Group 1 *Shewanella* strain *Shewanella*

psychrophila WP2 exhibits the hallmark metabolic versatility that is seen in many *Shewanella* and is a psychrophile, but its growth in different conditions has not been investigated [26]. WP2 was isolated from benthic sediment in the South China Sea where the ambient environmental temperature was approximately 4 °C [41]. Its optimal growth temperature has been determined to be between 10 °C and 15 °C with an overall growth supporting temperature range between 0 °C and 20 °C [26,41]. Understanding how this organism grows at different temperatures can provide insights into the adaptations found in the *Shewanella* genus and more broadly within psychrophiles.

Genome-scale metabolic modeling has become a common technique to investigate bacterial metabolism and advancements in the development of Genome-Scale Models (GEMs) of metabolism and methods to simulate growth have allowed for GEMs to be applied to increasingly complex questions. Traditional simulation methods utilize reaction stoichiometry during the maximization of growth [42,43]. These stoichiometry-based approaches, however, often result in large solution spaces due to the lack of specific constraints across metabolic pathways. Newer methods have extended this framework to incorporate additional constraints as a way to approach new biological problems. An increasingly popular approach has involved the introduction of transcriptomic constraints into GEMs allowing for the effects of complex environmental factors like temperature to be accounted for based on the gene expression changes that occur in the organism. These methods typically involve the introduction of new constraints into a GEM that relate the utilization of metabolic reactions to their gene expression. One type of approach applied in algorithms like E-

Flux [44] and iMTBGO [45] involves directly limiting metabolic fluxes proportionally to the expression of their associated genes. The other major type of approach involves utilizing the gene expression data to generate context-specific models based on the identification of highly and lowly expressed genes in the transcriptomes. This type of approach is applied in algorithms like GIMME [46], INIT [47]and StanDep [48] and they typically start with a full GEM and then attempt to remove reactions from the GEM if they are associated with lowly expressed genes. These methods used for the integration of transcriptional data into GEMs have the benefit of being able to account for the broad changes that can be captured in a transcriptomes of an organism growing at two temperatures, but they can only account for the factor of temperature indirectly through the gene expression changes.

Modeling methods have looked to address the effects of temperature directly through the incorporation of additional constraints into the model, rather than indirectly through data like gene expression. Because temperature can have such broad effects on an organism's physiology, the simulation methods that account for temperature have addressed a variety of different factors including enzyme stability and folding at different temperatures [49] and reaction thermodynamics [50,51] but these methods have not been broadly applied to look at changes in metabolism that occur between different growth temperatures and their application is often hampered by the availability of thermodynamic or kinetic data for reactions. One of these approaches, Thermodynamics-Based Metabolic flux Analysis (TMFA) involves the incorporation of metabolite concentrations, thermodynamic constraints, and temperature to simulate metabolism while accounting for the feasibility of metabolic

reactions in a GEM and has been applied to simulate growth in model organisms like *Eschericia coli* [50,51]. The use of computational methods to predict standard Gibbs Free Energy of Reaction values like the Group Contribution [52] and Component Contribution [53,54] methods has allowed for methods like TMFA to account for mode thermodynamic constraints in GEMs, even when experimental measurements of these values are not available. In this study the effects of temperature are addressed using a combination of TMFA to simulate specific changes in reaction thermodynamics at different temperature and Gene Inactivity Moderated by Metabolism and Expression (GIMME) to address the broader changes in gene expression between different temperatures and to fill in some gaps in pathway where thermodynamic data is missing. The combination of these methods allows for the development of temperature-dependent versions of an overall GEM, which can be used to simulate the effects of temperature on metabolism.

In this study, the metabolic response of the psychrophilic *Shewanella* strain *S. psychrophila* WP2 was examined by combining transcriptomics and thermodynamics-based genome-scale metabolic modeling. Transcriptomic profiles of the response of WP2 to growth at optimal, sub-optimal, and supraoptimal conditions revealed broad shifts in amino acid and nucleotide metabolism during non-optimal growth. Optimal growth was characterized by the high expression of genes in pathways typically associated with active growth. A modeling approach that combined transcriptomic and thermodynamic constraints into the WP2 GEM was used to simulate the growth of WP2 at optimal and non-optimal growth temperatures. These simulations revealed differences in metabolic pathway utilization at different temperatures, which explain

differences in the model's efficiency in converting the growth substrates to biomass and cellular energy. The simulations were further compared to the differential expression of genes in WP2 during growth at the three temperatures, providing a broader picture of how this organism's metabolism is remodeled during acclimation to different conditions.

Results

Temperature-dependent, thermodynamically constrained genome-scale models of WP2

The construction of temperature-dependent, thermodynamically constrained models was performed by integrating experimental growth measurements, thermodynamic properties of reactions, and gene expression profiles from optimal (15°C), supraoptimal (20°C), and suboptimal (4°C) temperatures (**Fig 1**). A GEM representing the complete metabolic potentials of WP2 was first developed, which contained 929 reactions, 789 genes, and 685 metabolites. The model represented the growth/no-growth phenotypes for all experimentally confirmed carbon sources (e.g., glucose, galactose, cellobiose, etc.) and electron acceptors (e.g., nitrate, TMAO, Fe^{3+}, etc.), with the exception of acetate and fumarate, where growth was not observed in a prior experiment but genes for the metabolism of acetate and fumarate were identified in the WP2 genome (**Table A in Data S1**).

The WP2 GEM served as the basis for predicting thermodynamic constraints and establishing the temperature-dependent models. The standard Gibbs free energy change of reactions ($\Delta_r G'^{\circ}$) was assigned to over 93% (868 reactions) of the 929

reactions included in the WP2 GEM using the group contribution approach [52]. Three temperature-dependent models were subset from the overall WP2 GEM based on the identification of actively expressed genes from the late exponential phase transcriptomes and by applying growth constraints based on the experimentally measured growth rates under the three temperatures (**Materials and Methods**). A total of 87 reactions were associated with lowly expressed genes across all three temperature conditions and were subsequently not included in any the temperature-dependent models. These included functions in cofactor biosynthesis, nucleotide salvage pathways, compound transport and alternative carbon metabolism, with their low expression levels likely driven by the experimental media rather than the temperature conditions. In addition, 27 reactions, while showing a low expression level of their genes in all three conditions, were included in the temperature-dependent models due to their essential roles in cell envelope biosynthesis, cofactor biosynthesis, and nucleotide metabolism. Of the three temperature-dependent models, the 15°C model was more streamlined and contained the lowest number of reactions based on gene expression data, while the 4°C model had the highest number of reactions, including functions that were absent in the 15°C and 20°C models, such as purine degradation, aromatic and branched-chain amino acid metabolism, alternative carbon metabolism, phosphate and sodium transporters, and two peroxidases (**Table B in Data S1**).

The integration of thermodynamic constraints with the temperature-dependent models was achieved through the application of the TMFA approach [50,51,55], which resulted in the prediction of reaction fluxes, metabolite concentrations, and the

Gibbs free energy change of reactions ($\Delta_r G'$). The concentration of 62 intracellular metabolites were predicted to be constrained across all three temperature-dependent models (**Table A in Data S2**). For example, the concentration of ATP was constrained towards the upper bounds and the concentrations of ADP, AMP, and phosphate were constrained towards the lower bounds of intracellular metabolite concentrations across all temperatures, indicating the potential importance of ATP production in WP2. The concentrations of central carbon metabolites, including glyceraldehyde-3-phosphate (G3P), phosphoenolpyruvate (PEP), malate, and 2-oxoglutarate (AKG), were differentially constrained in the different temperatures, highlighting potential temperature-dependent variations in the central metabolism of WP2 (**S1 Fig**).

Of the 671 thermodynamically constrained reactions that were in all three temperature-dependent models, 171 reactions were thermodynamically feasible in both directions (i.e., $\Delta_r G'$spanning a range from negative to positive values), 462 reactions were constrained as monodirectional, but the directionality was consistent across all three temperatures, and the remaining 38 reactions showed differences in thermodynamic feasibility among different temperatures (**Table B in Data S2**). The central metabolic reactions, glyceraldehyde-3-phosphate dehydrogenase (GAPD), fumarase (FUM), and phosphate acetyltransferase (PTAr), were thermodynamically constrained to different directions among the different temperatures. While the GAPD reaction was constrained to the 1,3-bisphosphoglycerate (1,3 BPG) producing direction under 15 °C and 20 °C, it was constrained to the opposite direction under 4 °C (**S2 Fig**). Similarly, the phosphate acetyltransferase reaction (PTAr) was

constrained to the production of acetyl-phosphate (AcP) under 15 °C and 20 °C but was constrained to the production of acetyl-CoA (AcCoA) under 4 °C, leading to the utilization of distinct pathways in energy generation and production of precursor metabolites (Fig **2**). The fumarase (FUM) reaction, in contrast, had similar constraints under 4 °C and 15 °C permitting the production of malate from fumarate, while it was constrained to the opposite direction under 20 °C (**S3 Fig**). Other reactions were constrained to one direction under certain temperatures while being unconstrained at the others. For example, the glycolysis reactions, phosphoglycerate kinase (PGK), phosphoglycerate mutase (PGM), enolase (ENO), and pyruvate kinase (PYK), were thermodynamically constrained under 15 °C and 20 °C to the final production of pyruvate (PYR) from the pathway, while these reactions were thermodynamically unconstrained under 4 °C (**S2 Fig**).

Variability in metabolic fluxes between temperatures

A quantitative comparison of all metabolic fluxes in the 4 °C, 15 °C, and 20 °C simulations was performed with the flux values normalized by the biomass yield in each corresponding condition (**Table C in Data S2**). To assess the overall variability of the metabolic fluxes, flux ranges were measured by calculating the differences between the maximum and minimum feasible fluxes of each reaction under each simulation condition (**Materials and Methods**). The analyses revealed 88 reactions that were present in all three temperature-dependent models and carried variable fluxes in at least one of the three simulations. Interestingly, the 4 °C model had significantly higher flux variability than the 15 °C or 20 °C model based on a pairwise Wilcoxon

Rank Sum test, indicating potentially higher metabolic flexibility of WP2 under the 4 °C condition. In contrast, a low variability of metabolic fluxes was observed in the 15 °C and 20 °C models, and the flux ranges showed no significant difference between the two temperatures (**S4 Fig**). Another 93 reactions that had invariable fluxes in all three temperatures and had non-zero fluxes in at least one temperature, showed differences in the value of normalized metabolic fluxes among different temperatures. The N-Acetyl-D-Glucosamine (GlcNac) catabolism, PPP, and ACKr had higher biomass normalized fluxes in the 4 °C and 20 °C models than the 15 °C model. The citrate synthase (CS) and aconitase (ACONT) reactions of the TCA cycle carried higher normalized fluxes in the 4 °C and 15 °C models than the 20 °C model. A precursor reaction of the ED pathway, glucose-6-phosphate isomerase (PGI), had a higher normalized flux in the 4 °C model than either 15 °C or 20 °C models (**Table C in Data S2**).

As was documented for other known *Shewanella* species, WP2 lacks a complete Embden-Meyerhof-Parnas glycolytic pathway because an essential gene, encoding the 6-phosphofructokinase function, is missing in its genome [28]. The payoff phase of glycolysis and the gluconeogenesis pathway, however, are encoded in the WP2 genome. Hence, WP2 carries the metabolic potential of converting G3P to PEP via the GAPD, PGK, PGM, and ENO reactions, as well as the potential of producing fructose-6-phosphate (F6P) from G3P via the fructose-bisphosphate aldolase (FBA) and the fructose bisphosphatase (FBP) reactions. Additionally, the Entner-Doudoroff (ED) pathway and the pentose phosphate pathway (PPP) are also

encoded in the WP2 genome and could be used as alternative paths of carbon utilization.

The comparison of metabolic fluxes in the carbon metabolism pathways of WP2 revealed a remodeling of central metabolic processes in the acclimation to different temperatures (**Fig 2**). Specifically, the ED pathway was exclusively used in the 4 °C condition but carried no flux in the 15°C and 20°C conditions. In contrast, the payoff phase of glycolysis was active under 15°C and 20°C but was inactivated in the 4 °C model due to thermodynamic infeasibility of the GAPD reaction. This resulted in the dependency of the 4 °C model on phosphoenolpyruvate synthase (PPS), an ATP-consuming reaction required for the production of PEP, an essential compound and a precursor of downstream reactions. Next, the non-oxidative PPP was used in all three temperatures in a direction opposite to the canonical PPP, carrying higher fluxes at 4 °C and 20 °C and lower fluxes at 15 °C. Finally, the FBA and FBP reactions of gluconeogenesis carried twice the flux in the 4 °C than the 20 °C simulation, while they were not used in the 15 °C simulation (**Fig 2 and S3 Fig**).

Additional variations of metabolic fluxes were observed in substrate-level phosphorylation reactions. While the acetate kinase reaction (ACKr) was identified as an important mechanism of ATP production in WP2 under all three temperature conditions, its upstream reaction, PTAr, was utilized differently in the different temperatures (**Fig 2**). Under 4 °C, PTAr contributed to the conversion of AcP, which was generated from the non-oxidative PPP, to AcCoA, a precursor of the TCA cycle. Under 15 °C and 20 °C, PTAr was utilized in the opposite direction, converting the

AcCoA produced from the payoff phase of glycolysis into AcP and subsequently driving substrate-level phosphorylation via ACKr.

The utilization of the tricarboxylic acid (TCA) cycle reactions was also different among the three temperatures (**Fig 2 and S3 Fig**). Under 4 °C and 15 °C, the glyoxylate shunt was utilized by activating the isocitrate lyase (ICL) reaction that converts isocitrate to succinate. The succinate was subsequently converted to succinyl-CoA (SucCoA), an important metabolic precursor, and to fumarate and malate, leading back to the production of PYR via the malic enzyme (ME2) reaction. The glyoxylate shunt was not utilized in the 20 °C model. Instead, metabolic flux was directed from oxaloacetate (Oaa) to the production of succinate. Like many other *Shewanella* species, WP2 was characterized by the utilization of a partial TCA cycle. Despite variations in the mechanism of succinate production, the production of alpha-keto-glutarate (AKG) recruited the same pathway in all three temperatures, where Oaa and AcCoA acted as precursors for the production of AKG (**Fig 2**).

Temperature-dependent changes in carbon use efficiency and energy costs of biosynthesis

The remodeling of metabolic fluxes was further reflected in the calculation of global parameters that measure the carbon and energy efficiency of WP2 metabolism under different temperature conditions (**Materials and Methods**). Specifically, an over two times higher carbon use efficiency (CUE) was observed in the 15 °C model than the 4 °C or 20 °C models (**Figure 3A**). Such differences in CUE were largely attributed to the high efficiency of the 15 °C model in coupling ATP generation and the production

of biosynthesis precursors through the payoff phase of glycolysis. Although the 20 °C model similarly used the glycolysis pathway for ATP and biosynthesis precursor production, it had a higher ATP demand resulting in higher flux through the ACKr reaction, leading to potential carbon loss through the increased production of acetate. In contrast, the payoff phase of glycolysis was blocked in the 4 °C model due to thermodynamic infeasibility of the GAPD reaction. As a result, the process of ATP generation relied primarily on having higher flux through the ACKr reaction and higher acetate production (**Table C in Data S2**).

In line with the CUE measurements, the energy efficiency of WP2 was evaluated based on the combined measurements of ATP production and ATP consumption fluxes (**Materials and Methods**). The 20 °C model demonstrated a similar ATP production efficiency to the 15 °C model (**Figure 3B**), reflecting the shared capacity of utilizing the payoff phase of glycolysis, an efficient energy production and precursor biosynthesis pathway, under both temperature conditions. The ATP cost of biomass production, however, was higher in the 20 °C model than in the 15 °C model (**Figure 3C**), reflecting a higher ATP demand and the potential carbon loss via the increased production of acetate in 20 °C. The 4 °C model, in contrast, had lower ATP production efficiency (**Figure 3B**) and higher ATP cost in biomass production (**Figure 3C**) than the 15 °C model.

Overall, a global remodeling of metabolic fluxes in WP2 was revealed through the simulation of thermodynamically constrained models under supraoptimal (20°C) and suboptimal (4°C) temperatures as compared to the optimal (15°C) temperature. While the optimal temperature demonstrated the highest efficiency in CUE, ATP

production, and biomass production, the acclimation to suboptimal and supraoptimal temperatures resulted in varied remodeling of metabolic fluxes, with the former driven by changes in thermodynamic feasibility in the central metabolism and the later driven by the increased demand of ATP in biomass production.

Differential gene expression of WP2 across different temperatures and growth phases

A comparison of the gene expression profiles across the early exponential, late exponential, and stationary phases of WP3 growth further elucidated the different metabolic responses of the organism under the supraoptimal and suboptimal temperatures (**Data S3**). When WP2 was acclimated to the suboptimal temperature (4 °C) as compared to the optimal temperature (15 °C), genes encoding the ATP synthase (ATPS4r), pyruvate dehydrogenase (PDH), pyruvate formate lyase (PFL), and cytochrome c oxidase (CYOO2) reactions were significantly downregulated in the early and/or late exponential phases, genes encoding the NADH dehydrogenase reaction (NADH11/NADH13) were significantly downregulated in the stationary phase, while genes encoding the CS, ICL, malate synthase (MALS), and the purine allantoinase (ALLTN), and OHCU decarboxylase (5HPUDICDCs) reactions were significantly upregulated during the late exponential phase (**Fig 4, Tables A, B, and C in Data S3**). In contrast, the acclimation to the supraoptimal temperature (20 °C) was characterized by the upregulation of NADH dehydrogenase and the downregulation of genes encoding the XPK, PFL, and PYK reactions during late exponential phase (**Fig 4, Table E in Data S3**). These regulatory changes were largely consistent with the

simulation of metabolic fluxes. The PFL reaction carried higher fluxes under 15 °C than the suboptimal or supraoptimal temperature, and had a higher flux in the upstream glycolytic pathway relative to the 4 °C. In parallel, the ATP synthase reaction carried flux in the ATP-driven proton pumping direction at 15 °C but was inactive in either of the other two temperatures, indicating the potential abundance in ATP production at the optimal temperature. The TCA cycle reactions, CS and ICL, carried higher biomass normalized fluxes under 4 °C compared to 15 °C, indicating a higher reliance on these reactions during suboptimal conditions. Finally, the NADH dehydrogenase reaction carried a higher flux under 20 °C, indicating a potentially higher cost in redox balancing than either of the other temperatures.

In addition to the differential expression of metabolic genes, the comparison of transcriptomes highlighted regulatory variations in environmental responses, secretion systems, and motility (**Fig 4**). Signs of stress were observed at both the suboptimal and supraoptimal temperatures during early exponential phase, as the cultures were going through the initial period of acclimation to the different temperatures. At 4 °C, a possible stress response was observed through the significant upregulation of a putative cold shock protein, transposes and integrases), and TonB receptor functions in early exponential phase (**Fig 4, Tables A and H in Data S3**). At 20 °C, a possible heat shock response was indicated through the upregulation of a putative heat shock protein relative to 15 °C (**Figure 4, Table F in Data S3**), the upregulation of GroES chaperone genes, DNA damage repair genes, and redox stress-related genes relative to 4 °C (**Table G in Data S3**) and the upregulation of group II intron reverse transcriptases was observed during late exponential phase relative to both other

temperatures (**Figure 4, Tables E and H in Data S3**). Multiple genes related to the secretion systems were also differentially regulated. Specifically, a putative type III secretion system was significantly downregulated at 4 °C during late exponential phase, while a type VI secretion system was significantly downregulated at 20 °C throughout all growth phases (**Figure 4, Tables A, B, C, G, H, and I in Data S3**). Multiple flagellar proteins and the sigma factor *fliA*, a transcriptional regulator of the flagellar complex, were upregulated in the 4 °C condition during early exponential phase but downregulated in contrast to the 15 °C and 20 °C conditions during stationary phase (**Figure 5, Table A, G, and I in Data S3**). Overall, the changes in expression of both the metabolic and non-metabolic genes between the temperatures further highlighted the different responses of WP2 to different conditions and provided a broader context to the metabolic remodeling seen in the temperature-dependent models.

Discussion

Genome-scale metabolic modeling has been applied to a variety of different biological problems, but the incorporation of complex environmental factors like pH, pressure, or temperature into GEMs remains challenging. In this study, a thermodynamically and transcriptomically constrained GEM of *Shewanella psychrophila* WP2 was developed and used to simulate growth in optimal and non-optimal temperatures. The *Shewanella* genus has been studied through a variety of experimental and computational approaches because of their environmental and metabolic diversity. Multiple genome-scale models have been developed and applied to study metabolism in the *Shewanella*

genus including four models of strains from the broadly adapted Group 2 clade of the *Shewanella [27,56]* and two models from the deep-sea, low-temperature adapted Group 1[36,57] (**Fig 5**). The WP2 GEM represents a previously unmodeled clade within the Group 1 *Shewanella* and provides a platform to further investigate the complex adaptations to low-temperature that are present in the Group 1 *Shewanella*. An integrated modeling approach that combined transcriptomic and thermodynamic constraints was used to investigate temperature acclimation in WP2, resulting in predictions of metabolic phenotypes that broadly agreed with what was observed in transcriptomic analysis and provided context to the metabolic changes that occurred during growth at different temperatures. Growth at the optimal growth temperature of WP2, 15 °C, was characterized by a streamlined metabolism geared toward the efficient utilization of nutrients to produce energy and biomass. WP2's growth at the supraoptimal temperature of 20 °C showed a metabolic network that used similar pathways as the optimal condition but was less efficient at using cellular energy to produce biomass. Lastly, growth at the suboptimal, but environmentally relevant temperature of 4 °C was characterized by the lower efficiency production of energy and biomass caused by the rerouting of metabolic fluxes to overcome changes in the thermodynamic feasibility of central metabolic pathways.

The application of the integrated modeling approach to simulate WP2 growth at suboptimal, optimal, and supraoptimal temperatures predicted broad differences in metabolic pathway utilization between different temperatures. Due to the lack of the 6-phosphofructokinase enzyme, the Embden-Meyerhof-Parnas (EMP) glycolytic pathway is incomplete in *S. psychrophila* WP2 and other *Shewanella* strains leaving

the Entner-Doudoroff (ED) and Pentose phosphate pathway as the only routes available for sugar catabolism [28]. These two pathways were utilized in different ways between the three temperatures. The 4 °C model was predicted to use a combination of the ED pathway and Pentose phosphate pathway to catabolize N-acetyl-D-Glucosamine to glyceraldehyde 3-phosphate, acetyl-phosphate, and pyruvate. In contrast the 15 °C and 20 °C models predicted that just the pentose phosphate pathway would be utilized to produce glyceraldehyde 3-phosphate and acetyl phosphate from N-acetyl-D-glucosamine. The result of these pathway utilization differences is changes in the production of glyceraldehyde 3-phosphate and acetyl-phosphate that can then be used to generate energy through substrate level phosphorylation reactions.

Changes in the reaction thermodynamics between the three temperatures result in a broad remodeling of metabolic fluxes, which alters how energy and biosynthetic precursors are produced in each temperature. In the 20 °C and 15 °C models' energy in the form of ATP is produced through the reactions of the payoff phase of glycolysis and through the production of acetate. The utilization of the payoff phase reactions of glycolysis also allows the models for these two temperatures to produce phosphoenolpyruvate, an essential biosynthetic precursor, through the same set of reactions. Because of the lower temperature, the glyceraldehyde 3-phosphate dehydrogenase reaction (GAPD) was predicted to become thermodynamically unfavorable compared to the 15 °C and 20 °C conditions. This resulted in the 4 °C model not utilizing these payoff phase reactions, and instead rerouting fluxes and relying primarily on the acetate production pathway for its production of ATP. The

lower efficiency of this metabolic strategy is seen in the decrease in the amount of ATP produced per unit of GlcNac in the 4 °C model compared to the other two temperatures. Coupled with the lowered capacity to efficiently produce ATP at 4 °C is a corresponding shift toward the utilization of energy consuming reactions to produce phosphoenolpyruvate. To overcome the lack of production of phosphoenolpyruvate from the payoff phase reactions of glycolysis, the 4 °C model utilized the phosphoenolpyruvate synthase (PPS) reaction to produce phosphoenolpyruvate from pyruvate, which consumes ATP and contributes to the lower ATP consumed per biomass efficiency of the 4 °C model. The downregulation of genes involved in the payoff phase of glycolysis has been observed in multiple strains of psychrophilic bacteria including *Pseudoalteromonas haloplanktis* TAC125 [14], *Psychrobacter sp.* PAMC 21119 [58], and *Sphingopyxis alaskensis* [13][59][13]can lead to psychrophilic organisms having to maintain high concentrations of ATP in order to keep certain reactions favorable [25]

The 4 °C model had a much higher reliance on the acetate production pathway than the other two temperatures. This was a result of the model not being able to produce energy through the glycolytic substrate-level phosphorylation reactions, and instead needing to produce nearly all of its ATP through acetate production. This increase in flux through the acetate production pathway has been linked in *Shewanella oneidensis* MR-1 to an increased reliance on substrate-level phosphorylation during both aerobic and anaerobic growth [60–62], indicating that this feature may be a central part of *Shewanella* metabolism. These changes in the production of acetate coupled with the lack of energy being produced from the substrate level

phosphorylation reactions of the glycolytic pathways, contributes to the changes in efficiency seen in at the suboptimal temperature. At 4 °C the reliance on acetate production as the only route of ATP production is reflected in the lower ATP production efficiency and lower CUE relative to the 15 °C model. Unlike the 4 °C model, the 20 °C model is not predicted to have a lower ATP production efficiency than the 15 °C model and uses many of the same pathways to produce energy as the 15 °C model. Despite this similar ability to produce ATP to the 15 °C model, the CUE is lowest in the 20 °C model and the ATP cost to produce biomass is the highest among the three temperatures. Where the differences in these efficiency metrics at 4 °C can be explained by shifts in pathway utilization, the differences in 20 °C are instead based on the higher maintenance cost that is estimated at the supraoptimal temperature. This higher maintenance requirement requires the 20 °C model to divert more carbon through the acetate production pathway to produce more ATP, as can be seen through the higher normalized flux through the acetate kinase reaction at 20 °C. This extra ATP that is produced does not get used in the 20 °C model in biomass producing pathways, but instead just goes toward the non-growth associated maintenance. In total the differences between the temperatures are a result of multiple factors that end up resulting in changes in efficiency and pathway utilization in the models.

In addition to the broad changes observed in metabolic efficiency between temperatures, altered utilization of the TCA cycle was also observed between temperatures. Shewanella strains have been previously observed to utilize partial TCA cycles in both aerobic and anaerobic conditions, primarily relying on this pathway for the production of metabolic precursors [60,62–64], and this feature was observed in

the WP2 model and transcriptomes as well. All three temperature-dependent models predicted a partial utilization of the TCA cycle, and the genes for citrate synthase, isocitrate lyase, and malate synthase were all upregulated at 4 °C compared to the other two temperatures. Psychrophilic bacteria have had displayed a variety of changes in this pathway in response to low temperatures, with many strains showing a general decrease in the expression of TCA cycle genes [13,14,58], and some marine strains showing increased expression of portions of the TCA cycle, especially in the reactions that convert citrate to alpha-ketoglutarate [13,14,65] and the reactions that make up the glyoxylate shunt [59]. The utilization of a partial TCA cycle, similar to other *Shewanella* combined with the differential expression of genes in this pathway, highlight the importance of the TCA cycle within *Shewanella* metabolism and hint at broader roles that this pathway may have during acclimation to different conditions.

A comparison of gene expression between the three temperatures provided additional insights into the responses of WP2 at each temperature and helped contextualize the model predictions. The downregulation of genes related to energy metabolism like the subunits of NADH dehydrogenase and cytochrome oxidase at 4 °C is a common feature of other psychrophiles during low temperature growth [9,15,66,67], and are often indications of a transition toward a metabolic strategy that is geared toward maintaining slower growth [13–15,58,66]. These broad changes in metabolic gene expression were coupled with signs of a possible stress response including the expression of cold shock proteins, phage shock proteins, and mobile genetic elements. Taken together with the model predictions, this indicates that WP2 likely goes through a stress response during low-temperature acclimation but is able to

remodel how its metabolic pathways are used to overcome thermodynamic changes and shift its growth strategy. The 20 °C model primarily predicts a lower efficiency metabolic strategy due to the diversion of energy away from growth and toward maintenance costs. This model prediction is accompanied by various signs of stress in the 20 °C transcriptomes especially when compared to the low temperature condition. The induction of a stress response to the high temperature growth helps explain the predicted changes in efficiency seen at 20 °C and is likely reflective of the inability of WP2 to efficiently survive near the upper limit of its growth supporting temperature range.

Overall the metabolic response of WP2 to low-temperature growth showed some consistent trends with other psychrophiles, including the downregulation of portions of the central carbon metabolism [13,14,58] and the upregulation of specific amino acid metabolic pathways [9,15,66,67]. The WP2 metabolic pathways also showed hallmark characteristics of *Shewanella* metabolism that are not always consistent with other psychrophilic bacteria, including a heavy reliance on acetate production for the generation of ATP [60–62], the utilization of an incomplete TCA cycle for the production of metabolic precursors [60,62,63], and low reliance on oxidative phosphorylation during growth [60,61]. The integrated view of WP2 metabolism provided by the model predictions and transcriptomic analysis in these different temperatures demonstrates the diversity in metabolic changes that occur during acclimation to different conditions. The changes in WP2 demonstrated that the small shifts in pathway utilization observed between the temperatures can lead to large impacts on WP2's growth efficiency, providing additional context to these

observations. These kinds of approaches highlight the benefits of accounting for more than just stoichiometric constraints in a GEM and promise to allow for the simulation of increasingly complex metabolic phenotypes.

MATERIALS AND METHODS

WP2 Growth Experiments

Inoculation of three biological replicates for each growth temperature (4°C, 15°C, and 20°C) were performed in 150 mL of fresh LMO-812 media [36] with 1mL of inoculum obtained from exponential growth culture at the optimal temperature (15°C) in the 2216 Marine Medium (Difco). The cultures were grown with 5 mM GlcNac as the sole carbon source under aerobic conditions at different temperatures with shaking, and an initial OD600 of 0.002 was measured for each inoculation. Turbidity was monitored throughout the growth phases of the cultures, and the OD600 values were converted to gram dry weight values for each culture using a previously established relationship between OD and dry weight biomass in *Shewanella [56]*. Growth rates were calculated based on the periods of exponential growth for each temperature condition (**S5 Fig**).

Transcriptome sampling and Differential Expression Analysis

Samples for transcriptome sequencing were taken from the early exponential, late exponential, and stationary phases for each replicate in the 4°C, 15°C, and 20°C cultures (**S5 Fig**). Two biological replicates were prepared from each of the targeted growth phases for each temperature, where 2 mL of samples were taken from each

replicate, centrifuged at 12000 times gravity for 2 minutes, and the cell pellet was used for the application of RNA extraction and sequencing using services provided by the Sangon Biotech in Shanghai, China. Total RNA was extracted from the cell pellets and cleaned using the Ribo-off rRNA depletion kit. cDNA libraries were prepared using the VAHTS Stranded mRNA-seq V2 Library Prep kit for Illumina. Paired-end sequencing was performed on the HiSeq X Ten system generating 2 x 150 bp reads.

Raw transcriptome reads were quality filtered using Trimmomatic version 0.33 [68] to remove (1) any leading or lagging bases with quality scores less than 20, (2) any Illumina adapters, with a 5 bp sliding window filtering and a quality score of 20 or higher, and (3) any sequences shorter than 50 bp. The trimmed reads, both paired and unpaired, were then mapped to the WP2 genome using BBMap version 38.81 [68], with all default settings except for requiring a minimum identity for mapping of 90%. The mapped reads were then used to generate count tables of the number of transcripts that map to each gene using the featureCounts program version 1.6.3 [69] with default settings. Differential expression of genes among different growth phases and across different temperature conditions was identified using Deseq2 version 1.22.2 [70]. Genes were considered to be differentially expressed if the log fold change between conditions was greater than 2 or less than -2 and if the adjusted p-value for the differential expression of the gene was less than $1x10^{-3}$. Temperature-dependent models were constructed based on the transcripts per million (TPM) values using the equation: $TPM = 10^6 * \frac{reads\ mapped\ to\ gene\ /\ gene\ length}{\sum_{all\ genes}\ (reads\ mapped\ to\ gene\ /\ gene\ length)}$[71,72].

Genome-scale Metabolic Reconstruction

A genome-scale model was constructed for WP2 based on ortholog mapping and manual curations (**Table C in Data S1**). A draft model was first created using the *psammotate* function provided in the PSAMM software package version 1.1 [73]. Five template models were used for the application of the *psammotate* approach, including models of *Shewanella piezotolerans* WP3 [36], *Shewanella oneidensis* MR1 [56], *Shewanella* sp. MR4, *Shewanella sp.* W3-18-1, and *Shewanella denitrificans* OS217 [27]. Following the initial reconstruction, manual curations were performed by combining literature information, reference databases, and identification of functional domains. A biomass objective function for WP2 was constructed following standard procedures [43] combining experimentally measured composition of macromolecular components [26,41,74] and inferred values from other *Shewanella* strains [27,36,56] (**Table D in Data S1**). The complete WP2 GEM was validated through comparison to previously reported growth phenotypes for WP2 on the utilization of carbon sources and electron acceptors (**Table C in Data S1**).

Identification of Thermodynamic Constraints

Standard Gibbs free energy change of reaction ($\Delta_r G'^{\circ}$) were calculated for reactions in the WP2 model under the standard conditions of 25°C and a pH 7 using The Group Contribution python package [52] (**Table E in Data S1**). In order to run the Group Contribution approach on individual reactions in the WP2 model, all metabolites participating in a reaction were represented in one of two forms: (1) identifiers in the Thermodynamics of Enzyme-Catalyzed Reactions Database (TECRdb)[75], which provides thermodynamic data for a collection of enzyme-catalyzed reactions; (2)

metabolite structure represented as Simplified Molecular-Input Line-Entry System (SMILES) strings (**Table C in Data S1**), which can be used to derive information related to metabolite properties for the $\Delta_r G'^{\circ}$ calculation. Metabolites in the WP2 model were first mapped to the TECRdb based on their names and formulas, and when a mapping is not available, metabolite structural information was collected from the Pubchem Database [76] in the form of the canonical SMILES strings. When SMILES strings were not available in the Pubchem database, for example, for chitin, eicosapentaenoic acid (EPA), 3-hydroxy-11-methyldodecanoic acid, 11-octadecenoic acid, and the fatty-acyl ACP compounds, metabolites structures were manually drawn using the MarvinSketch application version 19.11 (ChemAxon, https://www.chemaxon.com) and exported using the SMILES export function. The biomass objective function, macromolecular biosynthesis reactions, and several reactions in the cell wall biosynthesis pathway were not mapped with $\Delta_r G^{\circ}$ calculations due to the complexity of the metabolites involved.

Reconstruction of Temperature-dependent Models

Temperature-dependent models were reconstructed from the WP2 model using the PSAMM implementation of the GIMME algorithm, which creates context-specific metabolic networks based on gene expression data [46]. The transcriptome of each replicate from the 4°C, 15°C, and 20°C conditions was used as input data for running the PSAMM *gimme* (version 1.1), along with the complete genome-scale metabolic reconstruction of WP2. A gene expression threshold of no less than 35 TPM was applied, and the biomass objective constraints were set based on the experimentally

measured growth rate in each temperature (**S5 Fig**). The temperature-dependent models were then constructed based on a union of the metabolic functions that were either actively expressed or required for biomass productions in the replicate models. The resulting metabolic reactions in each temperature-dependent model were classified into two categories: Expressed, indicating reactions catalyzed by genes with higher expressions than the TPM threshold applied in PSAMM *gimme* in either replicate of a temperature; Used_Below, indicating reactions essential for the production of biomass but associated with gene subunits of relatively low expression (i.e., below the TPM threshold) in both replicates. Reactions associated with genes with low expressions and were not essential for biomass generation in a given temperature condition were not included in the model of that specific temperature (**Table B in Data S1**).

Metabolic simulations with temperature-dependent, thermodynamically constrained models

Using the temperature-dependent models, thermodynamics-based metabolic flux analysis [50,51] was performed using the *tmfa* function implemented in PSAMM (version 1.1). The PSAMM *tmfa* implementation takes as input a configuration file that references the $\Delta_r G'^{\circ}$estimations as described in a prior section (**Table E in Data S1**), a list of reactions excluded from the $\Delta_r G'^{\circ}$calculation due to the high complexity of the involved metabolite's structures (**Table F in Data S1**), a list of transport reactions mapped to parameters (i.e., net charge and net protons transported from outside to inside of the cell) that can be used to calculate energy associated with

electrochemical potential and pH gradient across the cell membrane (**Table G in Data S1**), and definitions of metabolite concentrations and exchange constraints (**Tables H and I in Data S1**). By default, all metabolites were constrained to be within a range of 1e-5 to 0.02 mol/L following prior studies [50,77]. All compounds present in the LMO-812 media were constrained by setting the upper bound of their concentrations according to the media composition. If the concentration of a compound was lower than the default lower bound (1e-5 mol/L) in the media, then the lower bound of its concentration was set to two orders of magnitude lower than its upper bound to allow for the potential fluctuation of compound concentrations. Following prior conventions [50], the concentrations of two metabolites, n-carbamoyl-L-aspartate and (S)-dihydroorotate, were expanded with a range from 1e-6 to 0.05 mol/L, to enable thermodynamic feasibility in an essential dihydroorotase (DHORTS) reaction (**Table H in Data S1**). The exchange flux constraints for the TMFA simulation were formulated based on the experimental media and to allow the diffusion of metabolic products. The exchange constraints of small molecules and metal ions in the media were set as the default upper and lower bounds of the model, and the uptake bound of oxygen was set according to the solubility of oxygen in liquid media under different temperatures (**Table I in Data S1**). An ATP maintenance equation, representing an ATP-consuming non-growth-related maintenance cost to the cell, was introduced to each temperature-dependent model and was constrained for each temperature condition by specifically fitting the computationally predicted biomass production rates to the experimentally measured growth rates (**S5 Fig**). The ATP maintenance constraint was determined for each temperature via a robustness analysis, where the

ATP maintenance fluxes were constrained to successively increasing values while the biomass yields were profiled. An intersection between the experimentally measured and the computationally simulated biomass was identified for each temperature condition, and the ATP maintenance constraints were pinpointed based on a linear fitting over data points immediately surrounding the experimentally measured biomass (**S6 Fig**).

To probe for the utilization of metabolic pathways under different temperature, ranges of feasible values were predicted for the Gibbs free energy of reactions ($\Delta_r G'$), metabolite concentrations, and metabolic fluxes while constraining the temperature-specific parameters. For example, the biomass production was constrained based on the experimentally measured growth rate in each temperature, the temperature parameter in the $\Delta_r G'$estimation was based on the different temperatures in Kelvin, and the oxygen exchange flux was constrained based on the solubility of oxygen at a given temperature. For the direct comparison of pathway utilizations across the different temperatures, individual reaction fluxes were normalized by the biomass flux of each simulation (**Table C in Data S2**). An overview of the flux variability was achieved by calculating the range between maximum and minimum fluxes of each reaction, and subsequently comparing the overall distribution of temperature variability among the temperature-dependent models. Statistical significance was estimated based on a pairwise Wilcoxon rank sum test using the 'pairwise.wilcox.test' function in R with a significance threshold of p-value less than 0.05. The carbon use efficiency (CUE) was calculated for each simulation using the equation $CUE = \frac{(Carbon\ atoms\ consumed - Carbon\ atoms\ secreted)}{Carbon\ atoms\ consumed}$following an existing approach[19],

where all the carbon-containing exchange compounds were grouped into lists of consumed or produced metabolites based on the direction of their exchange fluxes in a simulation, their corresponding fluxes were scaled based on the number of carbon atoms in each compound, and sums of the scaled fluxes were taken for the list of consumed and produced metabolites, respectively, to obtain the carbon atoms consumed and the carbon atoms secreted parameters in the CUE equation. To calculate the total amount of ATP produced or consumed in a model simulation, the metabolic flux of each reaction that involved ATP was multiplied by the stoichiometry of ATP in that reaction, resulting in normalized fluxes where positive values indicated the production of ATP and negative values indicated the consumption of ATP. The ATP production per unit of carbon source was calculated through dividing the sum of all normalized ATP-producing fluxes by the exchange flux of the carbon source (i.e., GlcNac). The ATP consumed per biomass gram dry weight (gDW) was calculated through dividing the sum of all normalized ATP-consuming fluxes by the biomass flux, excluding the ATP maintenance flux.

Phylogenetic Positioning of WP2

Orthologs were identified among WP2, and 44 additional complete genomes of the *Shewanella* genus based on the identification of bidirectional best BLAST hits, as documented in prior studies [36,78]. Five *Gammaproteobacteria* were included as outgroups for the phylogenomic reconstruction (*Pseudoalteromonas haloplanktis*, *Colwellia psychrerythraea*, *Psychromonas ingrahamii*, *Photobacterium profundum*, and *Moritella viscosa*). Conserved single-copy genes (CSCGs) were identified based

on the ortholog mapping. A multiple sequence alignment was built for the encoded protein sequences of each CSCG using MUSCLE version 3.8.31 [79]. The individual alignments were then concatenated as the input for phylogenetic reconstruction using RAxML version 8.2.3 [80] with the JTT substitution model and GAMMA model of rate heterogeneity. Support values were estimated by running 100 bootstrapping replicates. The phylogenomic reconstruction was visualized using iTOL [81], where clades containing multiple strains of the same species were shown in a collapsed view.

Data and Software Availability

Modeling approaches implemented in this study are accessible through the open source PSAMM software, release v1.1 and are freely available in a git repository: https://github.com/zhanglab/psamm. The WP2 GEM along with all input data for the TMFA simulations are available on GitHub at the following address: https://github.com/zhanglab/GEM-iWP2.

Competing Interests: The authors have declared that no competing interests exist.

Funding Information

The metabolic modeling was supported by the National Science Foundation under Grant No. 1553211, and a fellowship to KDT from the RI NSF EPSCoR Cooperative Agreement #EPS-1004057. The experimental work was supported by the National Natural Science Foundation of China (Grant No. 31290232). Any opinions, findings,

and conclusions or recommendations expressed in this material are those of the author(s) and do not necessarily reflect the views of the funders.

References

1. DeLong JP, Gibert JP, Luhring TM, Bachman G, Reed B, Neyer A, et al. The combined effects of reactant kinetics and enzyme stability explain the temperature dependence of metabolic rates. Ecol Evol. 2017;7: 3940–3950.

2. Romero-Romero ML, Inglés-Prieto A, Ibarra-Molero B, Sanchez-Ruiz JM. Highly anomalous energetics of protein cold denaturation linked to folding-unfolding kinetics. PLoS One. 2011;6: e23050.

3. Lepock JR, Frey HE, Inniss WE. Thermal analysis of bacteria by differential scanning calorimetry: relationship of protein denaturation in situ to maximum growth temperature. Biochim Biophys Acta. 1990;1055: 19–26.

4. Eriksson S, Hurme R, Rhen M. Low--temperature sensors in bacteria. Philos Trans R Soc Lond B Biol Sci. 2002;357: 887–893.

5. Ermolenko DN, Makhatadze GI. Bacterial cold-shock proteins. Cell Mol Life Sci. 2002;59: 1902–1913.

6. Gao H, Wang Y, Liu X, Yan T, Wu L, Alm E, et al. Global transcriptome analysis of the heat shock response of Shewanella oneidensis. J Bacteriol. 2004;186: 7796–7803.

7. Li S, Xiao X, Sun P, Wang F. Screening of genes regulated by cold shock in Shewanella piezotolerans WP3 and time course expression of cold-regulated genes. Arch Microbiol. 2008;189: 549–556.

8. Piette F, Leprince P, Feller G. Is there a cold shock response in the Antarctic psychrophile Pseudoalteromonas haloplanktis? Extremophiles. 2012;16: 681–683.

9. Wang F, Xiao X, Ou H-Y, Gai Y, Wang F. Role and regulation of fatty acid biosynthesis in the response of Shewanella piezotolerans WP3 to different temperatures and pressures. J Bacteriol. 2009;191: 2574–2584.

10. Phadtare S, Alsina J, Inouye M. Cold-shock response and cold-shock proteins. Curr Opin Microbiol. 1999;2: 175–180.

11. Raymond-Bouchard I, Whyte LG. From Transcriptomes to Metatranscriptomes: Cold Adaptation and Active Metabolisms of Psychrophiles from Cold Environments. In: Margesin R, editor. Psychrophiles: From Biodiversity to Biotechnology. Cham: Springer International Publishing; 2017. pp. 437–457.

12. Hébraud M, Potier P. Cold shock response and low temperature adaptation in psychrotrophic bacteria. J Mol Microbiol Biotechnol. 1999;1: 211–219.

13. Ting L, Williams TJ, Cowley MJ, Lauro FM, Guilhaus M, Raftery MJ, et al. Cold adaptation in the marine bacterium, Sphingopyxis alaskensis, assessed using quantitative proteomics. Environ Microbiol. 2010;12: 2658–2676.

14. Piette F, D'Amico S, Mazzucchelli G, Danchin A, Leprince P, Feller G. Life in the cold: a proteomic study of cold-repressed proteins in the antarctic bacterium pseudoalteromonas haloplanktis TAC125. Appl Environ Microbiol. 2011;77: 3881–3883.

15. Raymond-Bouchard I, Tremblay J, Altshuler I, Greer CW, Whyte LG. Comparative Transcriptomics of Cold Growth and Adaptive Features of a Eury- and Steno-Psychrophile. Frontiers in Microbiology. 2018. doi:10.3389/fmicb.2018.01565

16. De Maayer P, Anderson D, Cary C, Cowan DA. Some like it cold: understanding the survival strategies of psychrophiles. EMBO Rep. 2014;15: 508–517.

17. McCallum KL, Heikkila JJ, Inniss WE. Temperature-dependent pattern of heat shock protein synthesis in psychrophilic and psychrotrophic microorganisms. Can J Microbiol. 1986;32: 516–521.

18. Hakeda Y, Fukunaga N. Effect of Temperature Stress on Adenylate Pools and Energy Charge in a Psychrophilic Bacterium, Vibrio sp. ABE-1. Plant Cell Physiol. 1983;24: 849–856.

19. Saifuddin M, Bhatnagar JM, Segrè D, Finzi AC. Microbial carbon use efficiency predicted from genome-scale metabolic models. Nat Commun. 2019;10: 3568.

20. Steinweg JM, Plante AF, Conant RT, Paul EA, Tanaka DL. Patterns of substrate utilization during long-term incubations at different temperatures. Soil Biol Biochem. 2008;40: 2722–2728.

21. Laiz L, Gonzalez-Delvalle M, Hermosin B, Ortiz-Martinez A, Saiz-Jimenez C. Isolation of Cave Bacteria and Substrate Utilization at Different Temperatures. Geomicrobiology Journal. 2003. pp. 479–489. doi:10.1080/713851125

22. Pold G, Domeignoz-Horta LA, Morrison EW, Frey SD, Sistla SA, DeAngelis KM. Carbon Use Efficiency and Its Temperature Sensitivity Covary in Soil Bacteria. MBio. 2020;11. doi:10.1128/mBio.02293-19

23. Malik AA, Puissant J, Buckeridge KM, Goodall T, Jehmlich N, Chowdhury S, et al. Land use driven change in soil pH affects microbial carbon cycling processes. Nature Communications. 2018. doi:10.1038/s41467-018-05980-1

24. Blagodatskaya E, Blagodatsky S, Anderson T-H, Kuzyakov Y. Microbial growth and carbon use efficiency in the rhizosphere and root-free soil. PLoS One. 2014;9: e93282.

25. Amato P, Christner BC. Energy metabolism response to low-temperature and frozen conditions in Psychrobacter cryohalolentis. Appl Environ Microbiol. 2009;75: 711–718.

26. Xiao X, Wang P, Zeng X, Bartlett DH, Wang F. Shewanella psychrophila sp. nov. and Shewanella piezotolerans sp. nov., isolated from west Pacific deep-sea sediment. Int J Syst Evol Microbiol. 2007;57: 60–65.

27. Ong WK, Vu TT, Lovendahl KN, Llull JM, Serres MH, Romine MF, et al. Comparisons

of Shewanella strains based on genome annotations, modeling, and experiments. BMC Syst Biol. 2014;8: 31.

28. Rodionov DA, Yang C, Li X, Rodionova IA, Wang Y, Obraztsova AY, et al. Genomic encyclopedia of sugar utilization pathways in the Shewanella genus. BMC Genomics. 2010;11: 494.

29. Kato C, Nogi Y. Correlation between phylogenetic structure and function: examples from deep-sea Shewanella. FEMS Microbiol Ecol. 2001;35: 223–230.

30. Park S, Chen S, Lee J-S, Kim W, Yoon J-H. Description of Shewanella salipaludis sp. nov., isolated from a salt marsh. FEMS Microbiol Lett. 2020;367. doi:10.1093/femsle/fnaa121

31. Park S, Kim IK, Kim W, Yoon J-H. Shewanella insulae sp. nov., isolated from a tidal flat. Int J Syst Evol Microbiol. 2020;70: 3872–3877.

32. Namirimu T, Park M-J, Yang S-H, Zo Y-G, Kwon KK. Parashewanella tropica sp. nov., a mesophilic bacterium isolated from a marine sponge from Chuuk lagoon, Federated States of Micronesia, and emended description of the genus Parashewanella. International Journal of Systematic and Evolutionary Microbiology. 2019. pp. 3256–3261. doi:10.1099/ijsem.0.003617

33. Marritt SJ, Lowe TG, Bye J, McMillan DGG, Shi L, Fredrickson J, et al. A functional description of CymA, an electron-transfer hub supporting anaerobic respiratory flexibility in Shewanella. Biochem J. 2012;444: 465–474.

34. Li F, Li Y, Sun L, Chen X, An X, Yin C, et al. Modular Engineering Intracellular NADH Regeneration Boosts Extracellular Electron Transfer of Shewanella oneidensis MR-1. ACS Synth Biol. 2018;7: 885–895.

35. Leung KM, Wanger G, El-Naggar MY, Gorby Y, Southam G, Lau WM, et al. Shewanella oneidensis MR-1 bacterial nanowires exhibit p-type, tunable electronic behavior. Nano Lett. 2013;13: 2407–2411.

36. Dufault-Thompson K, Jian H, Cheng R, Li J, Wang F, Zhang Y. A Genome-Scale Model of Shewanella piezotolerans Simulates Mechanisms of Metabolic Diversity and Energy Conservation. mSystems. 2017;2. doi:10.1128/mSystems.00165-16

37. Yang X-W, He Y, Xu J, Xiao X, Wang F-P. The regulatory role of ferric uptake regulator (Fur) during anaerobic respiration of Shewanella piezotolerans WP3. PLoS One. 2013;8: e75588.

38. Wang F, Wang J, Jian H, Zhang B, Wang F, Yu J, et al. Environmental adaptation: Genomic analysis of the piezotolerant and psychrotolerant deep-sea iron reducing bacterium Shewanella piezotolerans WP3. Journal of Biotechnology. 2008. pp. S542–S543. doi:10.1016/j.jbiotec.2008.07.1275

39. Yamada M, Nakasone K, Tamegai H, Kato C, Usami R, Horikoshi K. Pressure Regulation of Soluble Cytochromesc in a Deep-Sea Piezophilic Bacterium,Shewanella violacea. Journal of Bacteriology. 2000. pp. 2945–2952. doi:10.1128/jb.182.10.2945-2952.2000

40. Xiong L, Jian H, Xiao X. Deep-Sea Bacterium Shewanella piezotolerans WP3 Has Two Dimethyl Sulfoxide Reductases in Distinct Subcellular Locations. Appl Environ Microbiol. 2017;83. doi:10.1128/AEM.01262-17

41. Wang F, Wang P, Chen M, Xiao X. Isolation of extremophiles with the detection and retrieval of Shewanella strains in deep-sea sediments from the west Pacific. Extremophiles. 2004;8: 165–168.

42. Orth JD, Thiele I, Palsson BØ. What is flux balance analysis? Nat Biotechnol. 2010;28: 245.

43. Feist AM, Palsson BO. The biomass objective function. Curr Opin Microbiol. 2010;13: 344–349.

44. Colijn C, Brandes A, Zucker J, Lun DS, Weiner B, Farhat MR, et al. Interpreting expression data with metabolic flux models: predicting Mycobacterium tuberculosis mycolic acid production. PLoS Comput Biol. 2009;5: e1000489.

45. Mao Z, Ma H. iMTBGO: An Algorithm for Integrating Metabolic Networks with Transcriptomes Based on Gene Ontology Analysis. Curr Genomics. 2019;20: 252–259.

46. Becker SA, Palsson BO. Context-specific metabolic networks are consistent with experiments. PLoS Comput Biol. 2008;4: e1000082.

47. Agren R, Bordel S, Mardinoglu A, Pornputtapong N, Nookaew I, Nielsen J. Reconstruction of genome-scale active metabolic networks for 69 human cell types and 16 cancer types using INIT. PLoS Comput Biol. 2012;8: e1002518.

48. Joshi CJ, Schinn S-M, Richelle A, Shamie I, O'Rourke EJ, Lewis NE. StanDep: Capturing transcriptomic variability improves context-specific metabolic models. PLoS Comput Biol. 2020;16: e1007764.

49. Chang RL, Andrews K, Kim D, Li Z, Godzik A, Palsson BO. Structural systems biology evaluation of metabolic thermotolerance in Escherichia coli. Science. 2013;340: 1220–1223.

50. Henry CS, Broadbelt LJ, Hatzimanikatis V. Thermodynamics-based metabolic flux analysis. Biophys J. 2007;92: 1792–1805.

51. Hamilton JJ, Dwivedi V, Reed JL. Quantitative assessment of thermodynamic constraints on the solution space of genome-scale metabolic models. Biophys J. 2013;105: 512–522.

52. Du B, Zhang Z, Grubner S, Yurkovich JT, Palsson BO, Zielinski DC. Temperature-Dependent Estimation of Gibbs Energies Using an Updated Group-Contribution Method. Biophys J. 2018;114: 2691–2702.

53. Noor E, Haraldsdóttir HS, Milo R, Fleming RMT. Consistent estimation of Gibbs energy using component contributions. PLoS Comput Biol. 2013;9: e1003098.

54. Flamholz A, Noor E, Bar-Even A, Milo R. eQuilibrator--the biochemical thermodynamics calculator. Nucleic Acids Res. 2012;40: D770–5.

55. Henry CS, Jankowski MD, Broadbelt LJ, Hatzimanikatis V. Genome-scale

thermodynamic analysis of Escherichia coli metabolism. Biophys J. 2006;90: 1453–1461.

56. Pinchuk GE, Hill EA, Geydebrekht OV, De Ingeniis J, Zhang X, Osterman A, et al. Constraint-based model of Shewanella oneidensis MR-1 metabolism: a tool for data analysis and hypothesis generation. PLoS Comput Biol. 2010;6: e1000822.

57. Xu Z, Guo J, Yue Y, Meng J, Sun X. IN SILICO GENOME-SCALE RECONSTRUCTION AND ANALYSIS OF THE SHEWANELLA LOIHICA PV-4 METABOLIC NETWORK. J Biol Syst. 2018;26: 373–397.

58. Koh HY, Park H, Lee JH, Han SJ, Sohn YC, Lee SG. Proteomic and transcriptomic investigations on cold-responsive properties of the psychrophilic Antarctic bacteriumPsychrobactersp. PAMC 21119 at subzero temperatures. Environmental Microbiology. 2017. pp. 628–644. doi:10.1111/1462-2920.13578

59. Czajka JJ, Abernathy MH, Benites VT, Baidoo EEK, Deming JW, Tang YJ. Model metabolic strategy for heterotrophic bacteria in the cold ocean based on Colwellia psychrerythraea 34H. Proc Natl Acad Sci U S A. 2018;115: 12507–12512.

60. Pinchuk GE, Geydebrekht OV, Hill EA, Reed JL, Konopka AE, Beliaev AS, et al. Pyruvate and lactate metabolism by Shewanella oneidensis MR-1 under fermentation, oxygen limitation, and fumarate respiration conditions. Appl Environ Microbiol. 2011;77: 8234–8240.

61. Hunt KA, Flynn JM, Naranjo B, Shikhare ID, Gralnick JA. Substrate-level phosphorylation is the primary source of energy conservation during anaerobic respiration of Shewanella oneidensis strain MR-1. J Bacteriol. 2010;192: 3345–3351.

62. Tang YJ, Martin HG, Dehal PS, Deutschbauer A, Llora X, Meadows A, et al. Metabolic flux analysis of Shewanella spp. reveals evolutionary robustness in central carbon metabolism. Biotechnol Bioeng. 2009;102: 1161–1169.

63. Brutinel ED, Gralnick JA. Anomalies of the anaerobic tricarboxylic acid cycle in S hewanella oneidensis revealed by T n-seq. Mol Microbiol. 2012;86: 273–283.

64. Tang YJ, Hwang JS, Wemmer DE, Keasling JD. Shewanella oneidensis MR-1 fluxome under various oxygen conditions. Appl Environ Microbiol. 2007;73: 718–729.

65. Piette F, D'Amico S, Struvay C, Mazzucchelli G, Renaut J, Tutino ML, et al. Proteomics of life at low temperatures: trigger factor is the primary chaperone in the Antarctic bacterium Pseudoalteromonas haloplanktis TAC125. Mol Microbiol. 2010;76: 120–132.

66. Bergholz PW, Bakermans C, Tiedje JM. Psychrobacter arcticus 273-4 uses resource efficiency and molecular motion adaptations for subzero temperature growth. J Bacteriol. 2009;191: 2340–2352.

67. Koh HY, Park H, Lee JH, Han SJ. Proteomic and transcriptomic investigations on cold-responsive properties of the psychrophilic Antarctic bacterium Psychrobacter sp. PAMC 21119 at subzero …. Environmentalist. 2017. Available: https://sfamjournals.onlinelibrary.wiley.com/doi/abs/10.1111/1462-2920.13578

68. Bushnell B. BBMap: a fast, accurate, splice-aware aligner. Lawrence Berkeley National

Lab.(LBNL), Berkeley, CA (United States); 2014. Available: https://www.osti.gov/biblio/1241166

69. Liao Y, Smyth GK, Shi W. featureCounts: an efficient general purpose program for assigning sequence reads to genomic features. Bioinformatics. 2014;30: 923–930.

70. Love MI, Huber W, Anders S. Moderated estimation of fold change and dispersion for RNA-seq data with DESeq2. Genome Biol. 2014;15: 550.

71. Zhao S, Ye Z, Stanton R. Misuse of RPKM or TPM normalization when comparing across samples and sequencing protocols. RNA. 2020;26: 903–909.

72. Wagner GP, Kin K, Lynch VJ. Measurement of mRNA abundance using RNA-seq data: RPKM measure is inconsistent among samples. Theory Biosci. 2012;131: 281–285.

73. Steffensen JL, Dufault-Thompson K, Zhang Y. PSAMM: A Portable System for the Analysis of Metabolic Models. PLoS Comput Biol. 2016;12: e1004732.

74. Xu G, Jian H, Xiao X, Wang F. Complete genome sequence of Shewanella psychrophila WP2, a deep-sea bacterium isolated from west Pacific sediment. Mar Genomics. 2017;35: 19–21.

75. Goldberg RN, Tewari YB, Bhat TN. Thermodynamics of enzyme-catalyzed reactions--a database for quantitative biochemistry. Bioinformatics. 2004. pp. 2874–2877. doi:10.1093/bioinformatics/bth314

76. Kim S, Thiessen PA, Bolton EE, Chen J, Fu G, Gindulyte A, et al. PubChem Substance and Compound databases. Nucleic Acids Res. 2016;44: D1202–13.

77. Albe KR, Butler MH, Wright BE. Cellular concentrations of enzymes and their substrates. J Theor Biol. 1990;143: 163–195.

78. Zhang Y, Sievert SM. Pan-genome analyses identify lineage- and niche-specific markers of evolution and adaptation in Epsilonproteobacteria. Front Microbiol. 2014;5: 110.

79. Edgar RC. MUSCLE: multiple sequence alignment with high accuracy and high throughput. Nucleic Acids Res. 2004;32: 1792–1797.

80. Stamatakis A. RAxML version 8: a tool for phylogenetic analysis and post-analysis of large phylogenies. Bioinformatics. 2014;30: 1312–1313.

81. Letunic I, Bork P. Interactive Tree Of Life (iTOL) v4: recent updates and new developments. Nucleic Acids Res. 2019;47: W256–W259.

Figures for Manuscript II

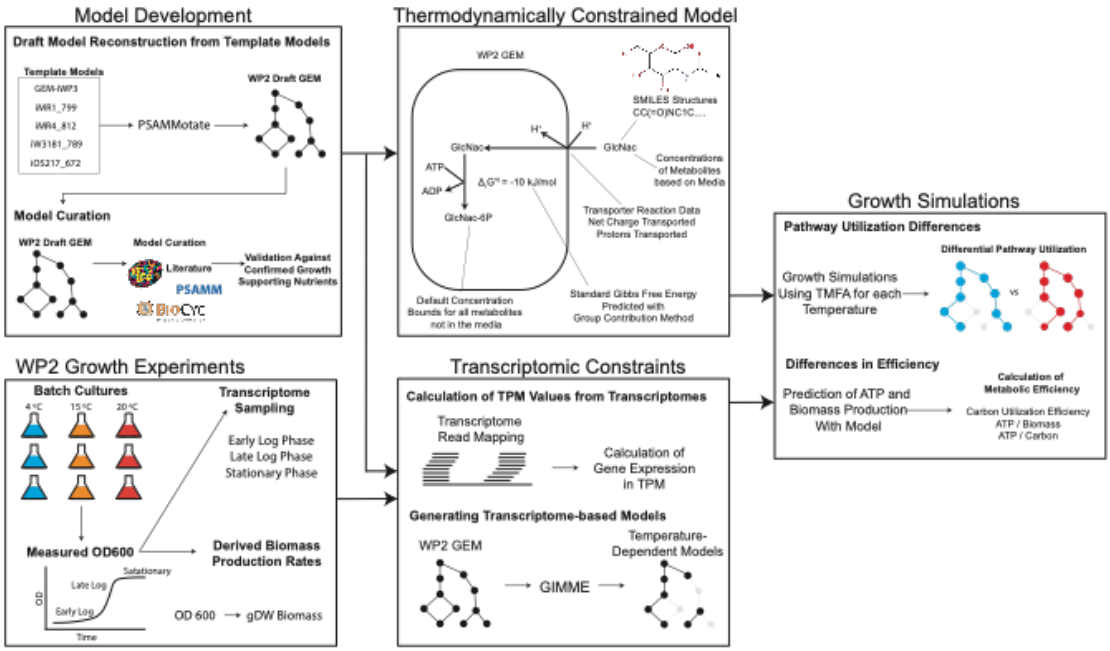

Fig 1: Modeling development and simulation pipeline showing the steps involved in generating the integrated temperature-dependent models and performing simulations for growth at each temperature.

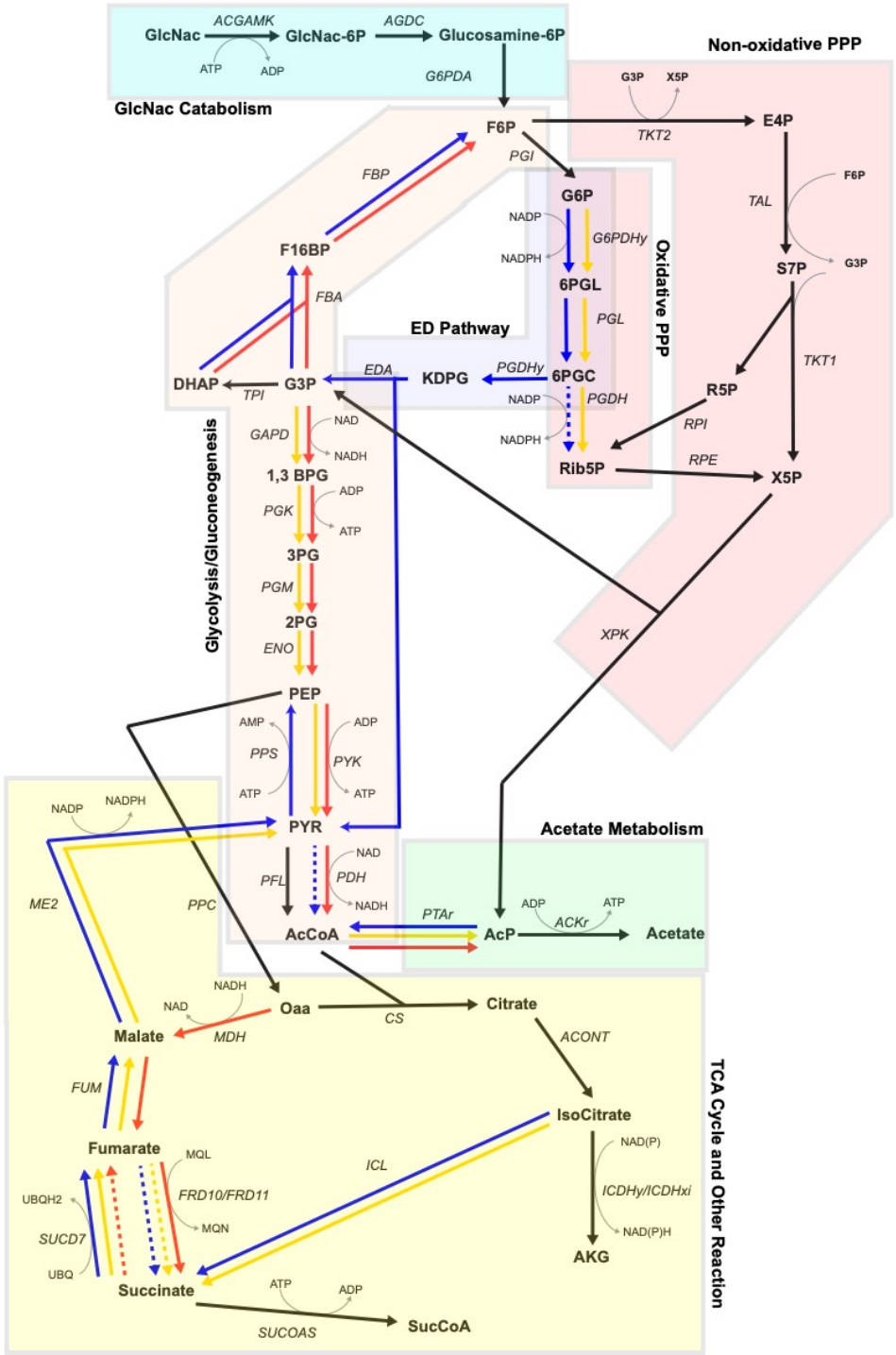

Fig 2: Pathway diagram showing the direction of fluxes through metabolic reactions in the different temperature simulations. Solid lines indicate that the flux of the reaction is always in the same direction, while dashed lines indicate that the reaction flux is variable and can be zero. Black lines represent all three temperatures, blue represents 4 °C, yellow represents 15 °C, and red represents 20 °C. Pathways are indicated by shaded boxes around groups of reactions.

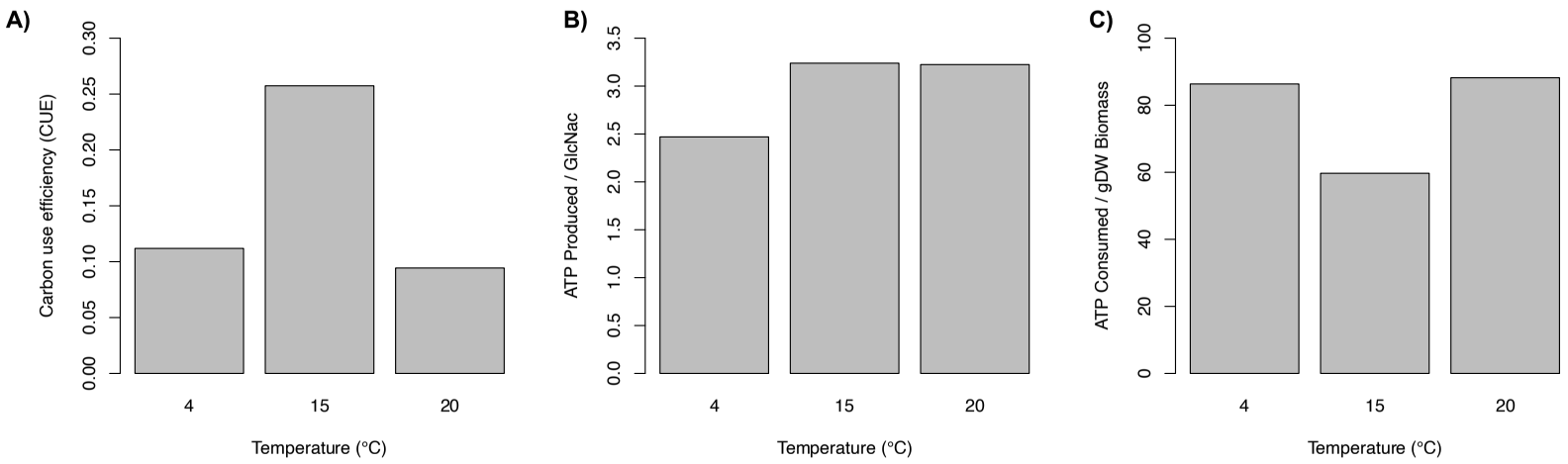

Fig 3: A) Carbon utilization efficiency for the 4, 15, and 20 °C simulations. B) Maximum ATP produced per mmol of carbon source utilized. C) ATP cost (mmol) required to produce 1 gDW of biomass.

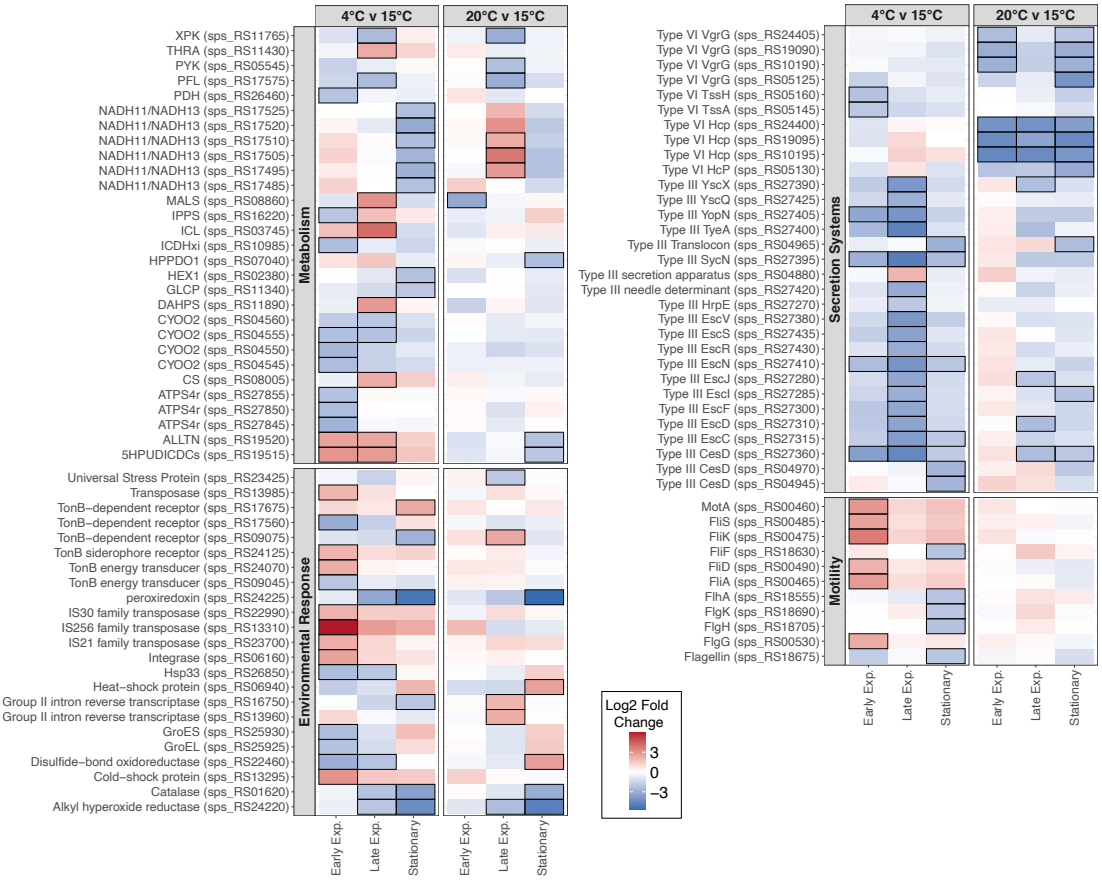

Fig 4: Heatmap showing selected significantly differentially expressed genes between temperatures. Comparisons are shown for the 4 °C and 20 °C conditions relative to the 15 °C condition, with red indicating that the gene was more highly expressed in that temperature relative to 15 °C and blue indicating that the gene was lowly expressed relative to the 15 °C condition. Comparisons are shown between the temperatures for the early exponential phase, late exponential phase, and stationary phase transcriptomes. Comparisons that were significant are highlighted with a black outline in the heatmap.

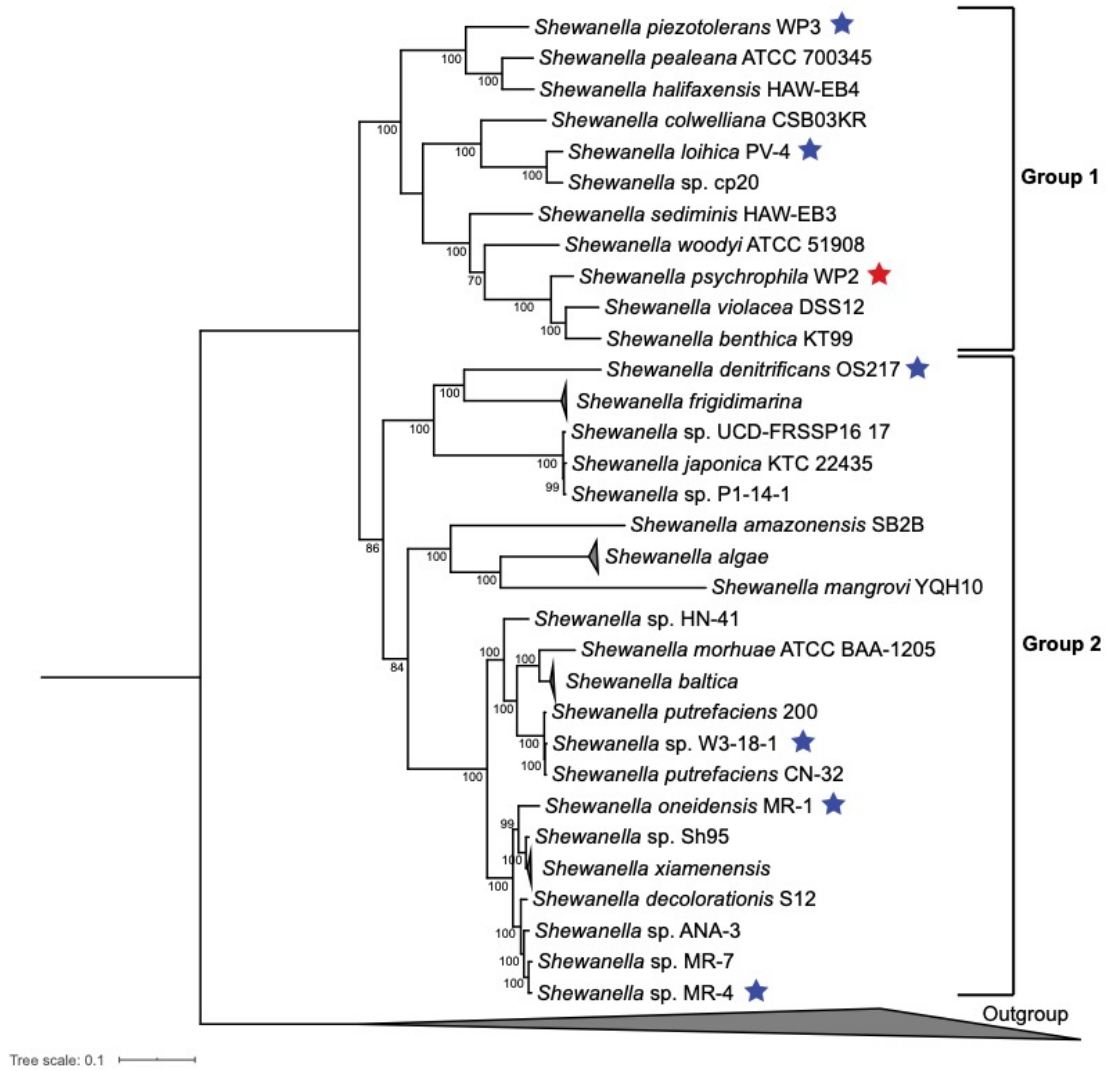

Fig 5: Phylogenetic tree of the Shewanella genus. Clades with multiple strains of the same species are collapsed into shaded triangles. Bootstrapping values greater than 70 are shown on the tree. Blue stars indicate strains with previously published GEMs. The red star marks S. psychrophila WP2.

Supplemental Figures for Manuscript II

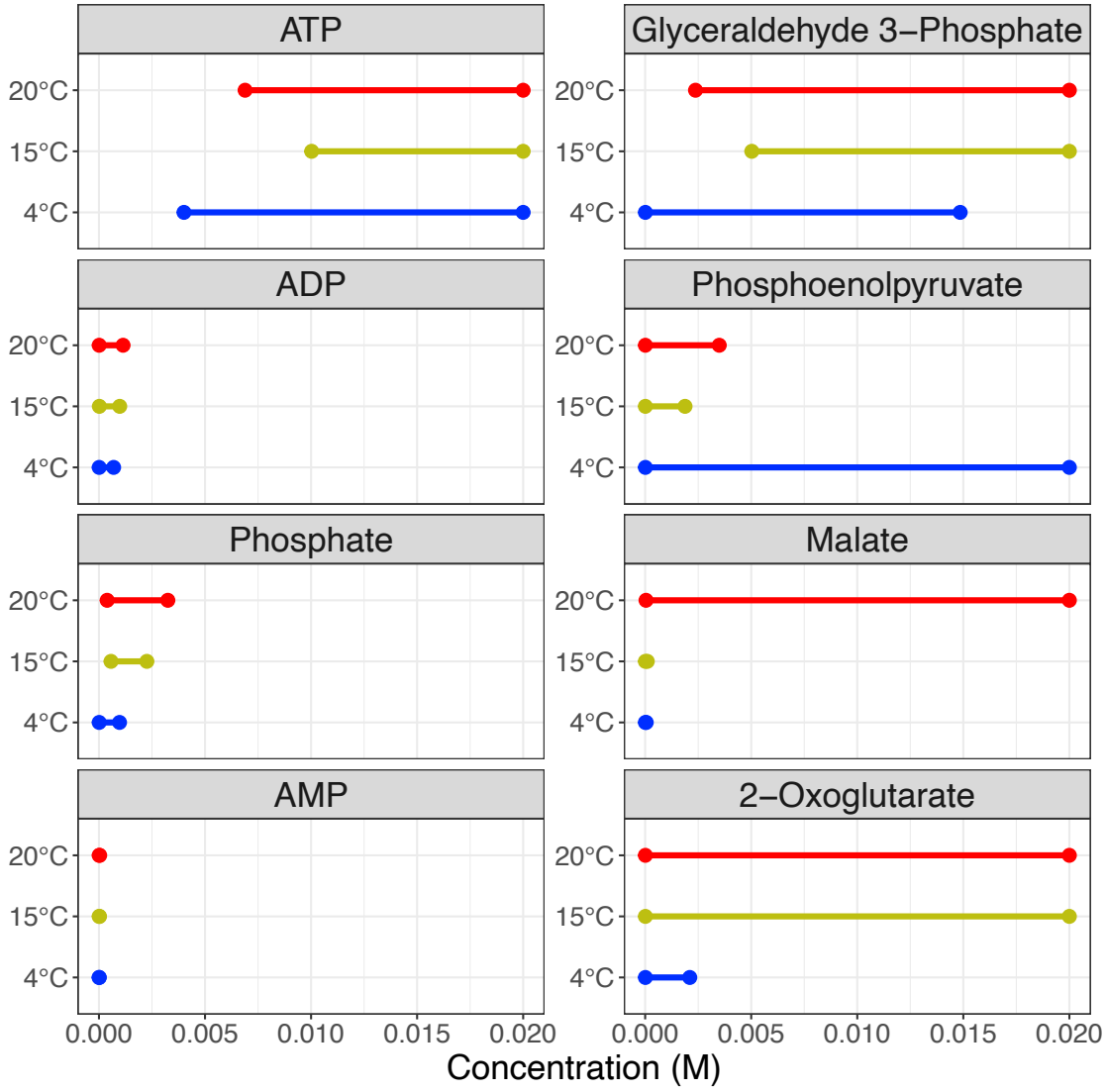

S1 Fig: Plots of feasible ranges the concentrations of selected metabolites involved in central metabolic processes. Ranges based on the 4 °C temperature-dependent model are shown in blue, the ranges from the 15 °C model are shown in yellow, and the ranges from the 20 °C model are shown in red.

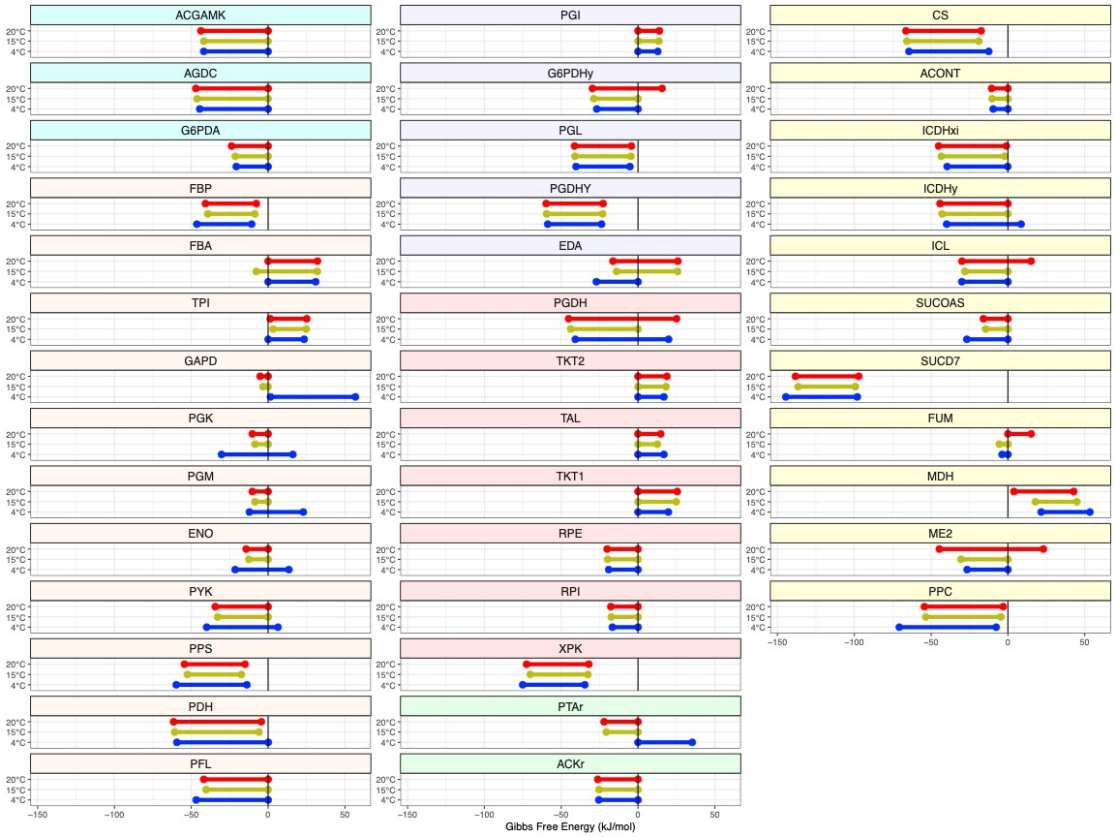

S2 Fig: Plots of feasible ranges for the $\Delta_r G'$ of reactions in the central carbon metabolism pathways based on TMFA simulations for the temperature dependent models. Ranges based on the 4 °C temperature-dependent model are shown in blue, the ranges from the 15 °C model are shown in yellow, and the ranges from the 20 °C model are shown in red. N-acetyl-D-glucosamine metabolism reactions are shown with a blue background, glycolytic and gluconeogenic reactions with orange, Entner-Doudoroff reactions with purple, pentose phosphate reactions with red, acetate production reactions with green, and TCA cycle reactions with yellow.

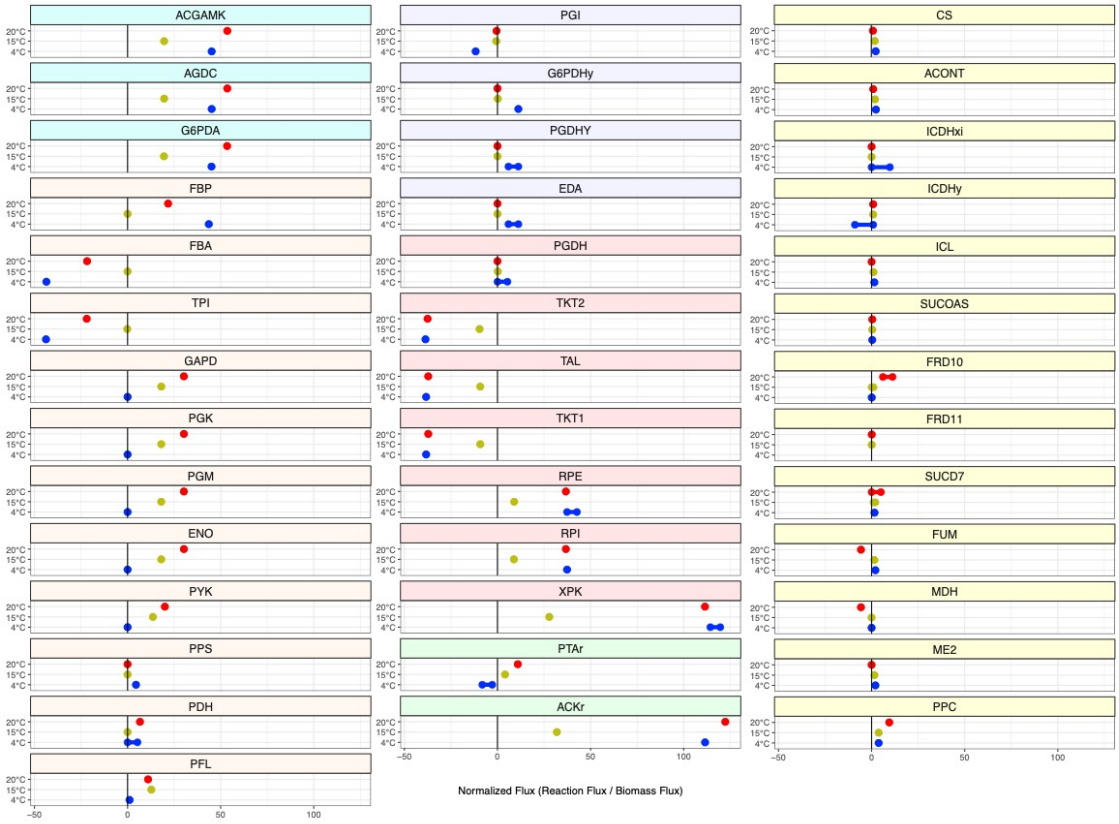

S3 Fig: Plots of feasible ranges the fluxes of reactions involved in central carbon metabolism pathways based on TMFA simulations for the temperature dependent models. Ranges based on the 4 °C temperature-dependent model are shown in blue, the ranges from the 15 °C model are shown in yellow, and the ranges from the 20 °C model are shown in red. N-acetyl-D-glucosamine metabolism reactions are shown with a blue background, glycolytic and gluconeogenic reactions with orange, Entner-Doudoroff reactions with purple, pentose phosphate reactions with red, acetate production reactions with green, and TCA cycle reactions with yellow.

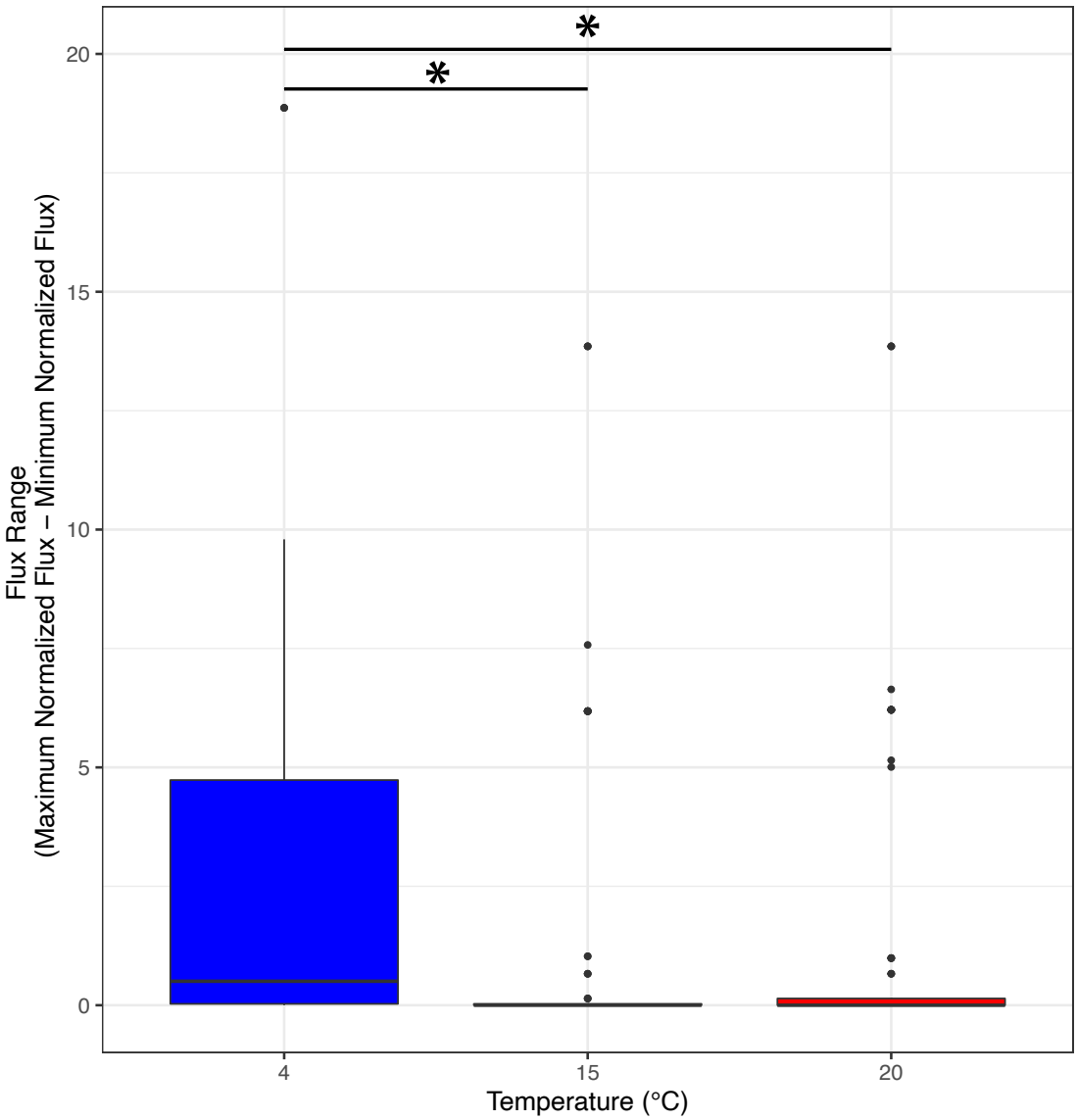

S4 Fig: Boxplots showing the distribution of normalized flux ranges from the 4 °C, 15 °C, and 20 °C model simulations for 88 reactions that were present in all three temperature-dependent models and had a variable flux in at least one simulation. Significant differences in the distributions of flux ranges based on a pairwise Wilcoxon Rank Sum test are indicated by the asterisks and bars above the plots.

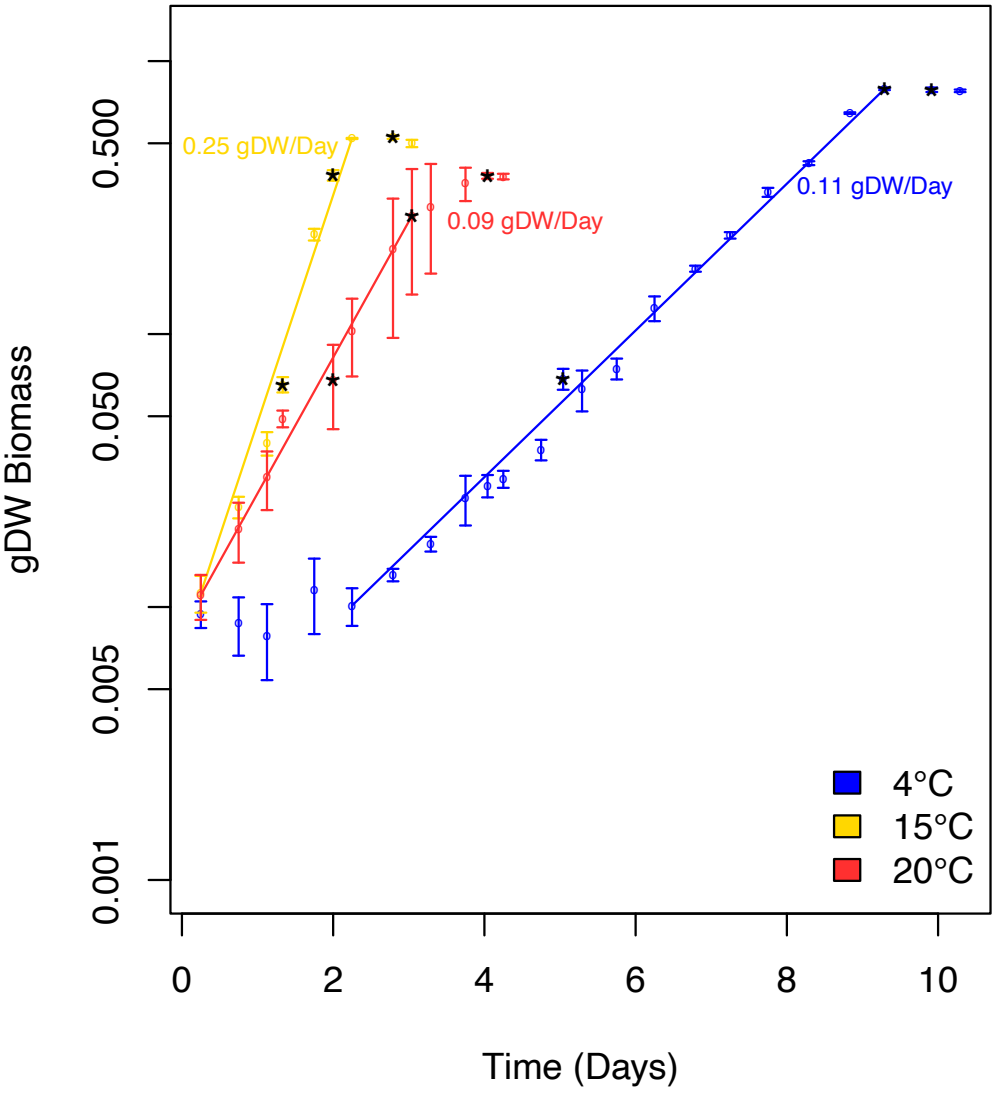

S5 Fig: Growth curves for WP2 growth experiments at 4 (blue), 15 (yellow), and 20 (red) °C. Asterisks indicate timepoints where RNA-Seq samples were taken. The solid lines indicate the region of the exponential growth over the growth curve.

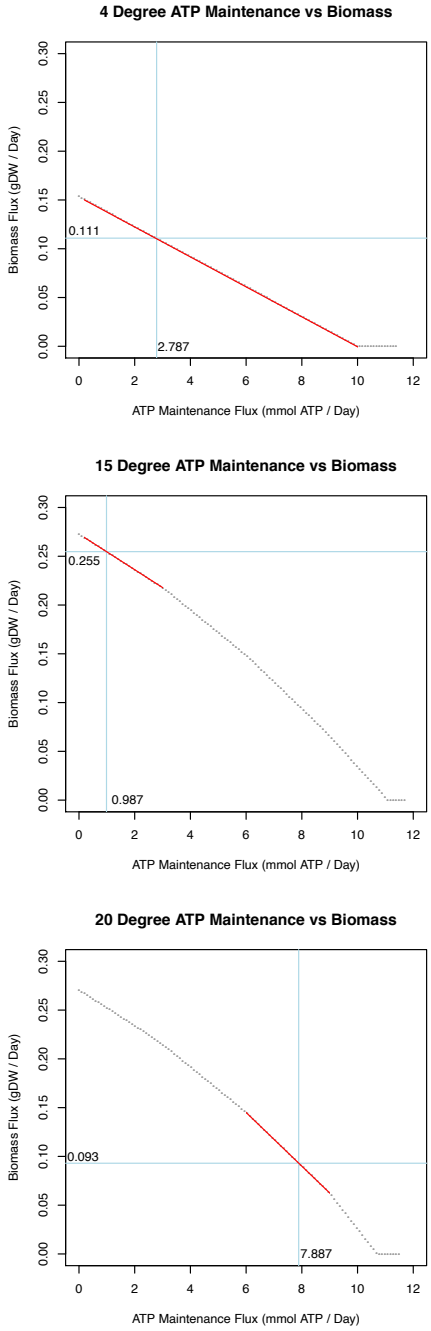

S6 Fig: Scatter plots showing the ATP maintenance reaction flux vs the biomass flux for each of the three temperature subset models. The x-axis shows the flux through the ATP maintenance reaction, with higher values increased hydrolysis of ATP. The target biomass flux is indicated by a horizontal blue line and the required ATP maintenance flux to achieve this biomass is shown as a vertical blue line. The linear region used to identify the required ATP maintenance to reach the target biomass flux is indicated by a red solid line.

Manuscript III

Publication Status: Formatted for submission to Nature Communications

Title: Investigation of the Structure of Element Transfer Networks within Metabolism

Keith Dufault-Thompson[1], Christopher Powers[1], Ying Zhang[1#]

Author Affiliations:

1. Department of Cell and Molecular Biology, College of the Environment and Life Sciences, University of Rhode Island, 120 Flagg Rd., Kingston, 02881 RI, USA

Corresponding Author:

#Ying Zhang, University of Rhode Island, yingzhang@uri.edu

ABSTRACT

Previous analyses of metabolic networks have provided insights into the organization and robustness of metabolism, but these analyses have been affected by the methods used to represent the networks. In this study, metabolic networks were generated based on the annotations of prokaryotic genomes in the KEGG database using previously established methods and a new application of the FindPrimaryPairs algorithm. A comparison of the different network representations revealed significant differences in network structure and scale-free properties, depending on the representation. Element-based subsetting of the FindPrimaryPairs networks demonstrated the separate influence of carbon, nitrogen, and phosphorus metabolism within the overall network and highlighted the scale-free properties of the phosphorus metabolism. These properties were further investigated through reaction deletions in three published genome-scale model-based networks, revealing that while the core functions required for growth do not have a scale-free organization, the overall networks do. This study highlights the utility of the FindPrimaryPairs function in representing metabolic networks and demonstrates the need for further network analyses utilizing this type of network representation.

INTRODUCTION

Metabolism dictates how organisms respond to their environment, interact with other organisms, and adapt to new conditions. The study of the metabolism of microorganisms has provided a wealth of information about metabolic pathways and the physiology of growth. While metabolism has classically been studied through *in*

vivo culturing-based methods, the advancement of genome sequencing technology has led to an increase in the availability of genetic information, even for organisms that are not isolated in pure cultures. This genomic information has allowed for the prediction of what metabolic functions could be present in an organism based on its gene content. The widespread availability of genomic data and the rapid increase in the number of available genomes has led to the development of extensive metabolic databases like KEGG and MetaCyc, which include metabolic predictions for thousands of organisms from all three domains of life [1,2]. The availability of these metabolic predictions allowed metabolism to be studied in many novel ways such as through the development of *in silico* representations of an organism's metabolism called Genome-Scale Models (GEMs) [3–6] and the analysis of metabolism as a mathematical network [7–9]. In particular, the application of graph theory to study metabolism as a mathematical network has led to many new insights related to the evolution and flexibility of metabolism [7–9].

Graph theory has proven to be a valuable method for the analysis of a variety of natural and artificial systems [10–14], but its application to metabolism remains challenging. The field of Graph theory involves the study of graphs, or networks, which represent connections (edges) between nodes (objects). In the application of graph theory to metabolism, these networks typically consist of a set of metabolites, which are the nodes, connected by metabolic reactions, which are the edges [15–17]. These connections are typically based on the stoichiometry of the metabolites in each reaction, where all substrates will be connected through edges to all products in a reaction. While the analysis of these metabolic networks has provided some insights

into network structure and organization [7–9,18], the application of these methods has often been hampered by the ability to represent the metabolism in an accurate and meaningful way. Multiple studies have identified that metabolic networks tend to be highly centralized, have very short distances between metabolites, and to be dominated by highly connected metabolites like protons, water, ATP, and NADH [18–21]. These metabolites tend to be involved in many reactions as byproducts or as currency metabolites, where they participate only as cofactors related to the transfer of electrons or protons [20]. The outsized influence of these currency metabolites and small molecules has made it difficult to examine many properties of metabolic networks and many studies have started to handle them through filtering and removal of these types of nodes from the network entirely [9,22]. The removal of these nodes has resulted in much less densely connected networks with highly modular structures revealing network topologies that had previously been missed when currency metabolites were present in the networks [18,23,24]. The differences seen in network topology when using these different network representations highlights the importance of not only what metabolic pathways and reactions are included in a network, but also how they are represented.

An alternative to stoichiometry based metabolic network representations is to represent connections between metabolites based on the conserved chemical structures that are shared between substrates and products in reactions. In this kind of network representation, connections are only formed between a substrate and product if they share elements, meaning that the resulting network is representative of the actual biochemical transformations that occur in metabolic pathways [21]. This approach has

resulted in dramatically different network representations compared to the stoichiometry-based approaches, where the metabolic networks had longer path lengths and were less clustered around currency metabolites, but the application of these methods relied on the availability of detailed metabolite structural information which has limited their broader application [21,25]. The recent development of the MapMaker [26] and FindPrimaryPairs [27] algorithms has allowed for the efficient prediction of the shared structures between substrates and products in metabolic reactions through the use of reaction stoichiometry and metabolite formulas, but these algorithms have not been extensively applied in the study of metabolic networks. Furthermore, a thorough comparison of metabolic networks generated using stoichiometry-based approaches to networks based on reactant/product pair predictions is lacking and is needed to fully understand the benefits and drawbacks of different network representation methods.

A major implication of the differences between network representation methods is the effects that they could have on the analysis of global network organization and structure. Two major structural properties that have been analyzed in metabolic networks have been scale-free and small-world properties. Small-world networks are characterized by having clusters of tightly connected nodes with links between the clusters [28,29]. This structure leads to the small world networks having a short mean path length, meaning that the distance between any two nodes is relatively small, and leads to these kinds of networks being robust to deletions of nodes or edges [7,30,31]. Metabolic networks have been described as generally having small-world properties which have implications for the evolutionary history and robustness of

metabolic pathways [7,8,32,33]. In addition to having small-world properties, metabolic networks have also been described as having scale-free properties though these claims have varied across studied [8,32,34,35]. Scale-free networks are characterized by having degree distributions that follow a power-law distribution where a few nodes have many connections, while most of the nodes have only a few connections [34,36,37]. While some analyses of metabolic networks have found scale-free properties [34,36,37], others have claimed that these properties are artifacts that arise due to the presence of currency metabolites and small molecules in the metabolic network representations [38,39]. Small-world and scale-free properties have been suggested to have biological meaning related to the evolution of metabolic pathways [32,40], the robustness of organisms to mutation [41,42], and the adaptability of organisms to different environments [43]. The differences between network representation methods make it difficult to fully understand these network properties and draw biologically meaningful conclusions from them.

In this study the effects of different network representation methods on metabolic network structure were analyzed, revealing the large effect that network construction approaches can have on network properties. Three network representation methods were used to generate metabolic networks based on the KEGG and MetaCyc databases, with two of the representations being based on previously used methods that rely on reaction stoichiometry, and one newly developed representation based on reactant/product pair predictions using the recently developed FindPrimaryPairs algorithm. The comparison of network descriptive statistics between different network representations demonstrated the large influence of small molecules and currency

metabolites on network structure corroborating what had been observed in previous studies. An analysis of small-world properties revealed that these properties were almost always present regardless of network representation method. In contrast the analysis of scale-free properties in metabolism suggested that the scale-free properties seen in metabolic networks largely come from the transfer of phosphorus groups in substrate level phosphorylation reactions. Lastly the robustness of the small-world and scale-free properties of metabolic networks were examined through random deletion experiments done with published GEMs. These simulations demonstrated that the maintenance of essential functions required for growth had a heavy influence on the scale-free properties of metabolism. Overall, this analysis highlights the importance of network representation methods on the structure and analysis of metabolic networks. The application of the FindPrimary pairs algorithm allows for the efficient generation of element transfer-based networks, which allows for the examination of underlying metabolic structures that is not possible with stoichiometry-based network-representations. The further investigation of these networks and their properties promises to expand our understanding of the evolution and function of metabolism in different organisms.

RESULTS

Network Representations

Metabolic networks representing organisms in the domains Bacteria and Archaea were generated based on genome annotations from the KEGG database using three network representation methods, with two methods replicating previous studies and one based

on the application of a recently developed algorithm (**Fig. 1**). First, an All-Pairs (AP) network representation was developed to replicate a common type of network representation used in prior studies [8,15,44], where each metabolite was included as a node and edges were used to connect all substrates to all products in each reaction (**Fig. 1A**). Second, an All-Pairs Filtered (AP-filtered) network representation was developed to replicate another commonly used network representation [9,18,44,45], where the network was made by removing nodes representing 'currency metabolites' (**Supplemental Table S1**), which are metabolites of high turnover and are involved in diverse metabolic processes [18,24], and their associated edges from the corresponding AP network (**Fig. 1B**). Lastly, a new, FindPrimaryPairs (FPP) network representation, was developed based on the application of the recently developed FPP algorithm that identifies element-transferring reactant-product pairs from genome-scale metabolic reconstructions [27]. In the FPP network, an edge was introduced for a substrate-product pair only if transferring of elements was predicted in the pair based on the FPP algorithm (**Fig. 1C**). Additional modifications of the network representations involved the subsetting of metabolic networks based on the composition of elements in the metabolites. For example, carbon-based networks were constructed from the AP, AP-filtered, and FPP networks by keeping only the carbon-containing metabolites and their associated edges (**Fig. 1D-F**). Other element-based networks were constructed similarly for the nitrogen- or phosphorus-containing metabolites. A total of 3799 bacterial and 240 archaeal metabolic networks were built based on genome annotations in the Kyoto Encyclopedia of Genes and Genomes (KEGG) database [1]. The network representations were derived for each organism based on the AP, AP-

filtered, and FPP definitions and the carbon, nitrogen-, and phosphorus-based networks corresponding to each definition (**Materials and Methods**).

Effects of Network Representations on Network Topology

An overview of the distribution of node degrees revealed potential variations in network topology (**Fig. 2**). The AP-filtered network is the most distinct among the three all-element representations due to the removal of currency metabolites in the network. The FPP network showed a similar profile to the AP network in the node distributions, with a slightly higher fraction of nodes ranked as the 10% least connected due to the removal of edges that do not contribute to element transfer. Highly connected nodes with degrees ranked in the top 5% of each network were identified, and the most frequently occurring high degree nodes were summarized for each representation (**Supplemental Table S2**). As expected, the AP networks were characterized by the high connectivity of common cofactors and small molecules known as the currency metabolites. For example, water, protons, phosphate, ATP, and adenosine diphosphate (ADP) were among the top 5% nodes of highest degrees for over 99% of the AP networks analyzed. The FPP networks similarly ranked many currency metabolites as the most highly connected nodes, as seen in the AP networks, but the average degree of the top connected nodes was scaled down due to the requirement of element-transferring edges. In contrast, the AP-filtered networks ranked some of the common precursor metabolites (e.g., glutamate, adenosine monophosphate (AMP), pyruvate) as the highest connected nodes, reflecting the removal of currency metabolites seen in the AP networks (**Supplemental Table S2**).

Descriptive statistics summarizing the network structure and organization were calculated for each of the element-based varieties of the FPP, AP, and AP-filtered networks (**Supplemental Text S1**). The median values of the descriptive statistics across the KEGG networks were compared between the FPP, AP, and AP-filtered all-elements networks (**Supplemental Table S3**). The median number of nodes was similar between the FPP and AP networks, 713 nodes, and 714 nodes, respectively, but due to the filtering that was applied, the AP-filtered networks tended to be smaller (median of 608 nodes). The median number of edges was very different between the three network representations with the AP networks having the most edges (2102), the FPP networks having less (1489), and the AP-filtered networks having the fewest edges (1024), but it is notable that the number of edges was highly variable for each of the network representations. The average path length and diameter for the AP-filtered networks both tended to be higher than in the FPP and AP networks, which were similar to each other.

In addition to the all-elements networks, the descriptive statistics were also compared between the carbon, nitrogen, and sulfur networks (**Supplemental Table S4-6**). The trends between these different element-filtered networks were consistent between the three network representations. The carbon networks tended to be the largest in terms of the median number of nodes and edges, with the nitrogen networks being in the middle, and the phosphorus networks having the fewest nodes and edges. The average path lengths were generally shortest for the phosphorus networks and longest in the carbon networks. The networks' density followed the opposite trend where the density was highest for the phosphorus networks and lowest for the carbon

networks. Notably, when compared to the all-elements networks, the element subset FPP networks tended to have much larger diameters, while the AP and AP-filtered networks had similar diameters between the all-elements and element subset networks. The analysis of the descriptive statistics between the network types and elements highlighted the broad differences in these networks, but to assess differences in the overall organization of the networks, additional analysis of the small-world and scale-free properties of the networks was performed.

Influence of network representation, database, and taxonomy on network metrics

With the availability of sequenced genomes, multiple databases centered around annotation of metabolic pathways have been developed. Each database has its own conventions and may represent similar pathways in different ways which could lead to differences in the metabolic networks that are derived from them. To address possible biases introduced from using the KEGG database as the source of data for the analysis of the network types, an additional set of metabolic networks was generated using the MetaCyc database. Networks were generated for an overlapping set of 2931 organisms that were present in both the KEGG and MetaCyc databases and the influence of the databases (KEGG or MetaCyc), taxonomic rank at the phylum level (32 different phyla), and network representation were assessed (FPP, AP, or AP-filtered) was assessed using through a multi-way ANOVA (**Supplemental Table S7**). The effect sizes, representing the amount of variance explained by a factor, of each of these factors were calculated (**Materials and Methods**) for each of the analyzed network metrics, showing vastly different trends for each factor (**Supplemental Table S8**). The

network representation explained greater than 79% of the variance for the average degree, degree assortativity, closeness centrality, diameter, and average path length, while the other two factors both explained only small fractions of the variance. For 3 of the metrics, density, transitivity, and betweenness centrality, the network's phylum explained a plurality of the variance. In contrast to network representation, which tended to explain a very high fraction of the variance, phylum tended to explain a lower percent of the variance (between 25.4% and 49.3%), and the three statistics that were driven by phylum had high fractions of unexplained variance. The differences between phyla were further examined for the all-elements FPP network representations, highlighting that the differences between phyla were only present for a few of the metrics, while many metrics were largely consistent across all of the phyla (**Supplemental Figure S1**). In contrast to the other two factors, the database had very little influence on the network statistics, only explaining at most 7.3% of the variance for the betweenness centrality of the networks. Overall, the comparison of database, taxonomy, and network representation, highlights that the network representations are a dominant factor in driving differences between many of the network metrics analyzed.

In addition to the broad comparison between the KEGG and MetaCyc databases, a set of 13 organisms which also had well-curated GEMs were chosen to compare between the databases and the GEM derived networks (**Supplemental Table S9**). For 12 of the organisms, only one model was used in the comparison, but for *E. coli* K-12 MG1655 three versions of the GEM that are commonly used in other analyses were included (iJR904[46], iAF1260[47], iJ01366[48]). The summary statistics were

calculated and compared between the models revealing that while there were some differences present between networks generated from each of the three sources, the broader trends appeared to be largely consistent regardless of network sources (**Supplemental Figure S2**). In particular, the size of the networks generated from the GEMs and databases were fairly similar, except for in the cases of some of the more extensively studied organisms (*E. coli* K-12 MG1655 and *S. typhimurium* LT2). The differences in the reaction content between the database derived networks and GEM derived networks were examined in more depth for the iJO1366 *E. coli* model. This comparison revealed that 82% of the reactions that were present in the iJO1366 GEM but not in the KEGG based network were involved in pathways related to lipid metabolism, cell wall metabolism, and transport across membranes. These pathways tend to be less curated and are represented as generic processes in many reaction databases leading to their lack of inclusion in the database derived networks.

Small-worldness and scale-free measures of metabolic networks

To look at differences in the overall organization of the networks, the small-worldness of the networks was compared between the different network representations and elements, revealing the prevalence of small-world properties in all of the network types. The small-worldness of networks was determined through the comparison of the average path lengths between nodes and clustering coefficient of a network to random networks of the same size, following a previously established protocol [28]. An analysis of the all-elements networks revealed that greater than 95% of the networks in all three network representations had small world properties (**Supplemental Table S10**).

Similarly, almost all of the carbon, nitrogen, and phosphorus networks were observed to have small-world properties (**Supplemental Table S10**). The ubiquity of these properties across all network representations and elements, suggests that this property could be a universal feature of metabolism.

The scale-free properties of the different network representations and element subsets were assessed by categorizing the networks into different groups based on how strong the evidence was that they had scale-free properties, with networks being classified into the following categories in order of increasing evidence that their degree distributions followed a power law: not scale free, weakest, weak, strong, strongest (**Materials and Methods**). For the AP networks between 28.8% and 52.7% of the networks from the four different element-based networks had strong evidence of scale-free properties (**Fig. 3A**). The AP-filtered networks had a higher percentage of networks with strong evidence of scale-free properties ranging between 42.5% and 69.2% across the different network representations (**Fig. 3B**). The FPP networks had the largest differences between the four element networks, with the all-element transfers showing 48.5% of the network with scale-free properties, both the nitrogen and carbon networks with only 7.0% and 16.9% with evidence of scale-free properties, and the phosphorus network having 87.4% of the networks showing scale-free properties (**Fig. 3C**).

Robustness of metabolic networks to random and non-random reaction deletions

The robustness of the small world and scale-free properties of carbon, nitrogen, and phosphorus transfer networks were examined through a set of deletion simulations

done on GEMs of *E. coli* K-12 MG1655 (iJR904)[46], *T. maritima* MSB8 (iTZ479)[49], and *S. piezotolerans* WP3 (GEM-iWP3)[50]. The three-element networks consistently showed small-world properties for all three models for the starting GEM based networks (**Fig. 4A**). The networks maintained these properties through the reaction deletion simulations when the models were required to maintain biomass production and when no biomass constraint was applied. In contrast to the GEM based networks, while a majority of the analogous random networks and rewired networks started off having small-world properties, the small world properties were not maintained when edges were deleted from these networks for either the carbon or nitrogen networks. The exception to this was the phosphorus graphs, which tended to maintain some small-world properties for a majority of the random and rewired networks.

The scale-free properties of the networks were also examined over the course of the deletion simulations (**Fig. 4B**). The starting GEM based networks had similar trends to the previously analyzed KEGG networks, where the Carbon and nitrogen networks for all three models did not have scale-free properties, while the phosphorus networks had strong-scale free properties. The trends for the carbon and phosphorus networks were consistent between all three GEM networks, with none of the starting models having any scale-free properties and the final models after deletions of reactions or edges only having a small percent of the networks having scale-free properties. The phosphorus networks all started out as scale-free, but this property's robustness was variable among the different deletion simulations. When reactions were randomly deleted from the GEM networks without requiring the models to produce biomass flux, the models kept their scale-free properties in a majority of the

final networks. This was not the case when reactions were deleted while requiring that biomass production was maintained. In these deletion simulations, only 1.5% of the final GEM-iWP3 networks, 4.8% of the iJR904 networks, and 3.6% of the final iTZ479 networks had strong evidence of scale-free properties. The rewired phosphorus networks all started off being scale-free and did maintain these properties throughout the edge deletions, while the random networks were not scale-free for the starting networks or final networks.

DISCUSSION

Metabolism has been investigated through many different lenses, including both experimental and theoretical approaches. Advances in genomics have led to the widespread ability to sequence the genomes of almost any organism from any environment, providing a wealth of data to analyze and help in the prediction of what these organisms might be doing in their environments. The annotation of these genomes and the collection of metabolic data databases and highlight curated GEMs has provided yet another opportunity to analyze metabolism from a different perspective, as a mathematical network. The application of graph theory to different problems has provided insights into the structure and function of manmade and natural systems, including metabolic networks [29,34,35]. But these analyses have been hampered by the methods that have been used to represent metabolism as a network.

An analysis of metabolic networks, consisting of a set of metabolites (nodes) connected by edges (reactions partial reactions), highlighted how large of an effect different network representation methods can have on the networks' structure and how

they are interpreted. Two previously used network representations were used as a comparison for a new type of network representation, applying a recently developed reactant-product pair prediction algorithm, FindPrimaryPairs. The AP network representation was generated by connecting all substrates in a reaction to all products of that reaction, resulting in very densely connected networks dominated by extremely high degree currency metabolites and small molecules. These currency metabolites and small molecules are present as cofactors in many reactions across the metabolism, meaning that the connections formed by them link together very distant and sometimes unrelated portions of the metabolism. Even from a visual inspection of these networks, the influence of these heavily connected hub metabolites can be seen (**Supplemental Figure S3**). The AP-Filtered network representation seeks to remove these hub metabolites' influence by arbitrarily filtering out certain compounds. While this representation does result in less densely connected networks with longer linear pathways, the impact of those currency metabolites is completely lost in these networks (**Supplemental Figure S3**). While these hub metabolites are mostly involved in the reactions where they play roles as cofactors, they do all have roles as the primary parts of reactions in some subsystems. For example, ATP, while primarily acting as a phosphorus donor in many reactions, can also be involved as a metabolite in nucleotide biosynthesis and salvage[51].

The FPP algorithm was applied to generate a new kind of network representation that naturally dealt with currency metabolites' influence without having to apply arbitrary filtering to remove them. The metabolite networks that were generated using the FPP network representation tended to have longer path lengths and

larger diameters than the AP networks, and while they still contained currency metabolites as relatively high degree nodes, these metabolites did not have the same centralizing influence on the network structure (**Supplemental Figure S3**). The use of the FPP network representation also allows for the separation of different element networks within the metabolism that show the flows of important elements like carbon, nitrogen, and phosphorus. Element-based filtering can be applied to the metabolites in AP or AP-Filtered networks, resulting in slight differences between the subset networks. But even with this filtering, because the edges in the networks can't be filtered in the same way, it is difficult to disentangle the influence of different elements on the overall structure of the metabolism. In the FPP networks, all of the edges represent connections between substrates and products through shared elements. This lets the filtering be applied to both the edges and the nodes in the networks, leading to distinctly different element subset networks where the influence of different processes can be analyzed in more detail.

Almost all of the KEGG networks analyzed had small-world properties regardless of the representation or element subset. While the threshold used to test for small-world properties was relatively generous, the fact that almost all of the networks had these properties and that the properties were robust to random deletions in the GEMs indicates that small-worldness is likely an inherent feature of metabolism. On the other hand, the scale-freeness of the networks was highly variable between network representation and element subsets. The AP and AP-Filtered networks only had small variations between the element subsets, indicating that the application of an element-based metabolite filtering was not sufficient to differentiate the influence of

different elements in these networks. In contrast, the filtering by element for the FPP networks resulted in vastly different networks for the carbon, nitrogen, and phosphorus metabolism, with the phosphorus networks being almost all scale-free across the KEGG database, while the carbon and nitrogen had very few scale-free networks. The phosphorus networks were scale-free due to the presence of very high degree nodes like phosphate, ATP, and ADP forming central hubs that connected to relatively linear pathways extending out from these hubs (**Supplemental Figure S3**). Unlike the small-worldness of the networks, the scale-free structure of the metabolism was not maintained in the GEM networks during the deletion simulations while maintaining growth. The final networks produced from the GEMs in the growth maintaining deletion simulations can be thought of as only containing the core metabolic functions that are required for growth. The loss of the scale-free properties in these core metabolic networks shows that while the core functions needed for growth might not be organized in a scale-free manner, these properties may arise from the addition of alternative metabolic pathways that utilize common cofactors like ATP.

These analyses taken together demonstrate the major influence that different network representations can have on the structure of the metabolic network. A comparison between the KEGG networks used in this study and networks derived from GEMs and the MetaCyc database shows that network representation has a disproportionate effect on the network structure compared to the source database, highlighting the dramatic effects that these representation choices can have. Interestingly, it was found that some of the network metrics analyzed were heavily influenced by the taxonomy of the organism that they were based on. While these

phyla driven differences are difficult to analyze in the context of multiple network representations, they do warrant further study with a focus on the application of FPP and the association of additional taxonomic and ecological information about the organisms. Given the large impact of network representation on model statistics and the benefits of FPP in mitigating the impact of currency metabolism while keeping them in the network, applying the FPP algorithm to metabolic analysis could provide novel and valuable insights into the evolution and organization of metabolism. The further study of these networks using the FPP algorithm promises to provide a new way to view and interpret metabolic pathways and understand the flow of essential elements like carbon, nitrogen, and phosphorus within a broader metabolic context.

METHODS

Generating Organism Specific Reaction Databases from KEGG and MetaCyc

The entire KEGG database [1] was downloaded and converted to a YAML formatted reaction database (downloaded on 2017-07-03). The database was first filtered to remove any compounds that had undefined or variable formulas, including metabolites that represent generic electron acceptors and donors and metabolites with undefined formula like variable fatty acids of undefined length, resulting in the removal of 2,514 compounds out of the total of 18,048 compounds in the initial database. The reactions in the database were then filtered to remove any reactions that had either undefined stoichiometry or compounds of undefined or variable formula, resulting in the removal of 2,643 reactions out of a total of 10,584 reactions in the initial database. This filtered KEGG reaction database was then subset to make organism-specific reaction sets

based on the KEGG orthology annotations for each organism. These annotations consist of a mapping of genes to KEGG orthology numbers. These KEGG orthology numbers were then mapped to KEGG reaction IDs to generate the association between genes and reactions for each organism. This mapping was done for the entire set of 4190 complete prokaryotic genomes included in the 2017-07-03 version of the KEGG database.

The preparation of the MetaCyc database [2] followed a similar procedure as the KEGG database. First, the entire MetaCyc database was downloaded (downloaded on 2016-07-13), and the SBML formatted reaction database was converted to the YAML format. The compounds in this database were then filtered to remove any compounds that had undefined or variable formulas resulting in the removal of 1,946 compounds out of the original 13,018 compounds. The reaction database was then filtered to remove any reactions that included these compounds or had variable stoichiometries resulting in the removal of 3,035 reactions out of the original 15,924 reactions. Organism specific mappings were obtained by extracting the gene to reaction associations for the 7,597 organisms included in the database from the organism-specific Systems Biology Markup Language (SBML) reaction databases provided in MetaCyc.

Generating AP, AP-filtered, and FPP networks

The organism-specific databases of metabolites and reactions were represented in YAML format and used for the construction of networks following definitions of the AP, AP-filtered, and FPP representations. The AP networks were produced by

enumerating all reactants and products and creating edges between each reactant-product pair in each metabolic reaction. The AP-filtered networks were created by removing all the previously identified currency metabolites (**Supplemental Table S1**) and their associated edges from the corresponding AP networks. The FPP networks were created by including all metabolites in the AP network, while trimming the edges to only keep a set of predicted element-transferring reactant-product pairs using the 'fpp' algorithm implemented in the 'primarypairs' function of the PSAMM software (version 1.0)[27]. By default, the all-element networks were created following each representation, where all metabolites were included regardless of the element-composition of the metabolites. To create carbon-, nitrogen-, and phosphorus-specific networks, the AP and AP-filtered networks were trimmed by removing any metabolites and their associated edges if the metabolites do not include the element of interest. Besides filtering metabolites based on their element compositions, the FPP networks were further trimmed to remove any edges that were not predicted to involve the transfer of the target element.

Three sets of AP, AP-filtered, and FPP networks were constructed based on different sources of genome annotations: (1) KEGG, (2) MetaCyc, (3) expert-curated GEMs in literature (**Supplemental Table S9**). Graph operations and visualizations of each network were created with the igraph python package[52]. Parallel edges that connect the same pair of nodes were combined to a single edge in the final graph. The largest connected component (LCC) was identified for each network by identifying the subgraph that contained the largest number of nodes using the 'decompose' function in igraph and this LCC was used for all downstream analyses of network properties. All-

element networks obtained from KEGG and MetaCyc annotations sources were filtered based on the percentage of nodes incorporated in the LCC, and the threshold was selected based on the overall distribution of the percentage of nodes in LCC, as seen among all networks reconstructed from KEGG or MetaCyc, respectively.

Network descriptors statistics

Network descriptors were calculated using the 'python-igraph' package version 0.8.2 and the 'poweRlaw' R package version 0.70.6 (**Supplemental Text S1**). The organism-specific reconstructions were first mapped between the KEGG and MetaCyc databases based on the strain level NCBI taxonomy identifiers, followed by a filtering step that removed networks in phyla that had less than four species in the dataset. This resulted in a set of 2,931 organisms from 32 distinct phyla that were independently annotated by both the KEGG and the MetaCyc databases. The relative effect sizes of network representation (e.g. AP, AP-filtered, or FPP), annotation database (e.g. KEGG or MetaCyc), and taxonomic classification on the different network descriptors were assessed by calculating the eta-squared statistics, which estimates the fraction of total variance explained by each factor in the analysis[53], following a multi-way ANOVA. Logarithmic transformations were applied to any models demonstrating heteroscedasticity (**Supplemental Table S7**).

Comparisons of network representations and databases using ANOVA

The effects of network, database, and taxonomic distribution were assessed through a multi-way ANOVA for the KEGG and MetaCyc database. First the overlapping set of

organisms between KEGG and MetaCyc were filtered to only include phyla that had at least four species in them, resulting in a set of 2931 organisms from 32 different phyla. The effects of phylum and network representations (FPP, AP, AP-filtered), and source database on the network descriptive statistics were analyzed using a multi-way ANOVA. Logarithmic transformations were applied to any models demonstrating heteroscedasticity (**Supplemental Table S7**). Due to the large number of organisms in the analysis, all of the comparisons were seen to be significant. To provide context to what was driving these differences, the relative effect sizes of phyla and network representations were analyzed by calculating the eta-squared statistics, which estimates the fraction of total variance explained by each factor in the analysis[53].

Power law fitting and calculation of small world properties

The network degree distributions for the carbon, nitrogen, and phosphorus KEGG networks were fit to a power-law distribution using the poweRlaw package (version 0.70.6) in R[54]. The distribution parameters including the exponent of the power law curve and a data cutoff value to determine which nodes were in the tail of the distribution ("x_{min}") were estimated using the "estimate_pars" function, and a goodness of fit test was done performing 1000 bootstrapping simulations using the "bootstrap_p" function to assess the likelihood that the distribution followed a power-law. The quality of the fitting of the data to a power-law distribution was then compared to the fitting of the data with log-normal, exponential, and Poisson distributions using the "compare_distributions" function within the poweRlaw package. Networks were assessed to be scale-free or not based on previously

established thresholds related to the power-law fitting parameters and comparisons to other distribution fittings[55]. Networks were classified as weakest scale-free if they the power-law fitting was not rejected during a goodness of fit test, weak scale-free if they also had greater than or equal to 50 nodes in the tail of the distribution, strong if they had exponent values between 2 and 3, and strongest if they met the qualifications of all the other categories and the power-law fitting was the best fit of the four distributions that were tested, following the previously established criteria[55].

The small-world properties of the networks were quantified by calculating the network small-worldness, S, based on a previously established method[28]. First, 1000 Erdős-Rényi random networks with the same number of nodes and edges as the original network were generated using the "erdos_renyi_game" function in the iGraph python package[52]. The average clustering coefficient and average mean shortest path lengths from these 1000 random graphs were calculated and compared to the clustering coefficient and mean path length of the original network using the formula: $S = \frac{(Clustering\ Coef\ Original\ /\ Avg\ Clustering\ Coef\ Random)}{(mean\ path\ length\ Original\ /\ Avg\ mean\ path\ length\ Random)}$. Networks were considered to have small world properties if their value of S was greater than 1 and to not have small world properties if S was less than 1.

GEM reaction deletion simulations

Three GEMs were used to assess the effects of reaction deletions on the structure and properties of their metabolic networks. The three models analyzed were of the organisms *E. coli* K-12 MG1655 (iJR904)[46], *T. maritima* MSB8 (iTZ479)[49], and *S. piezotolerans* WP3 (GEM-iWP3)[50]. First new exchange constraints were set up for all

three models that allowed for the free uptake of all carbohydrates, vitamins, and small molecules, but prevented the uptake of amino acids, nucleotides, and their derivatives (**Supplemental Tables S11-13**). Using these exchange constraints, random reaction deletion simulations were performed for each of the three models using the 'randomsparse' command as implemented in PSAMM. Using this function, 1000 random minimal reaction networks were generated while requiring that the biomass flux for the model be maintained as greater than or equal to 20% of the maximum biomass flux for that model. A second set of 1000 simulations were done for each model where reactions were randomly deleted from the GEM without applying any biomass constraint. The number of reactions deleted from each model was based on the median number of reactions deleted in the previous 'randomsparse' simulation done while maintaining the biomass at greater than 20% of the maximum value.

Two additional sets of deletions were also done on artificial networks to serve as comparisons to the GEM based deletions. One thousand random networks with the same number of edges and nodes as the GEM networks were generated using the Erdős-Rényi game function in the igraph python package for each of the three models. The median number of edges deleted in the 20% biomass 'randomsparse' simulations was calculated for each model, and the same number of edges were deleted from the generated random graphs. The second set of artificial networks were generated by taking the original GEM networks and rewiring the edges in the network 10,000 times. The rewired networks maintain the same degree distribution as the original networks but end up having a different set of edges. One thousand deletion simulations were done on these networks for each GEM, where the number of edges deleted from the

network was the same as the median number of edges deleted in the 20% 'randomsparse' simulations. All four of these deletion simulations were done for the carbon, nitrogen, and phosphorus FPP networks for each of the three GEMs. The calculation of the small-worldness and fitting of the degree distributions to a power-law was done for all of the starting and final networks from the deletion simulations.

ACKNOWLEDGEMENTS

This work was supported by the National Science Foundation under Grant No. 1553211. Any opinions, findings, and conclusions or recommendations expressed in this material are those of the author(s) and do not necessarily reflect the views of the funders.

AUTHOR CONTRIBUTIONS

K.D.T and Y.Z planned the research, interpreted the results, and wrote the manuscript. K.D.T performed the analyses. C.P. and K.D.T carried out the statistical analyses.

REFERENCES

1. Kanehisa, M. & Goto, S. KEGG: kyoto encyclopedia of genes and genomes. *Nucleic Acids Res.* **28**, 27–30 (2000).
2. Caspi, R. *et al.* The MetaCyc database of metabolic pathways and enzymes and the BioCyc collection of Pathway/Genome Databases. *Nucleic Acids Res.* **42**, D459–71 (2014).
3. Zhang, C. & Hua, Q. Applications of Genome-Scale Metabolic Models in Biotechnology and Systems Medicine. *Front. Physiol.* **6**, 413 (2015).

4. Kim, T. Y., Sohn, S. B., Kim, Y. B., Kim, W. J. & Lee, S. Y. Recent advances in reconstruction and applications of genome-scale metabolic models. *Curr. Opin. Biotechnol.* **23**, 617–623 (2012).
5. Dufault-Thompson, K., Steffensen, J. L. & Zhang, Y. Using PSAMM for the Curation and Analysis of Genome-Scale Metabolic Models. *Methods in Molecular Biology* 131–150 (2018) doi:10.1007/978-1-4939-7528-0_6.
6. Lopes, H. & Rocha, I. Genome-scale modeling of yeast: chronology, applications and critical perspectives. *FEMS Yeast Res.* **17**, (2017).
7. Zhang, Z. & Zhang, J. A big world inside small-world networks. *PLoS One* **4**, e5686 (2009).
8. Rodríguez-Caso, C. & Montañez, R. Topology of Metabolic Reaction Networks. *Encyclopedia of Systems Biology* 2185–2188 (2013) doi:10.1007/978-1-4419-9863-7_1175.
9. Croes, D., Couche, F., Wodak, S. J. & van Helden, J. Metabolic PathFinding: inferring relevant pathways in biochemical networks. *Nucleic Acids Res.* **33**, W326–30 (2005).
10. Marina, T. I. *et al.* Architecture of marine food webs: To be or not be a 'small-world'. *PLoS One* **13**, e0198217 (2018).
11. Frainay, C. & Jourdan, F. Computational methods to identify metabolic sub-networks based on metabolomic profiles. *Brief. Bioinform.* **18**, 43–56 (2017).
12. Urban, D. L., Minor, E. S., Treml, E. A. & Schick, R. S. Graph models of habitat mosaics. *Ecol. Lett.* **12**, 260–273 (2009).
13. Zou, X., Yang, J. & Zhang, J. Microblog sentiment analysis using social and

topic context. *PLoS One* **13**, e0191163 (2018).

14. Walker, R. *et al.* Modeling spatial decisions with graph theory: logging roads and forest fragmentation in the Brazilian Amazon. *Ecol. Appl.* **23**, 239–254 (2013).
15. van Helden, J., Wernisch, L., Gilbert, D. & Wodak, S. J. Graph-based analysis of metabolic networks. *Ernst Schering Res. Found. Workshop* 245–274 (2002).
16. Rodríguez, A. & Infante, D. Network models in the study of metabolism. *Electron. J. Biotechnol.* **12**, 11–12 (2009).
17. Chalancon, G., Kruse, K. & Madan Babu, M. Metabolic Networks, Structure and Dynamics. *Encyclopedia of Systems Biology* 1263–1267 (2013) doi:10.1007/978-1-4419-9863-7_561.
18. Huss, M. & Holme, P. Currency and commodity metabolites: their identification and relation to the modularity of metabolic networks. *IET Syst. Biol.* **1**, 280–285 (2007).
19. Samal, A. & Martin, O. C. Randomizing genome-scale metabolic networks. *PLoS One* **6**, e22295 (2011).
20. Holme, P. & Huss, M. Substance graphs are optimal simple-graph representations of metabolism. *Chinese Science Bulletin* vol. 55 3161–3168 (2010).
21. Arita, M. The metabolic world of Escherichia coli is not small. *Proc. Natl. Acad. Sci. U. S. A.* **101**, 1543–1547 (2004).
22. Oyelade, J. *et al.* Computational Identification of Metabolic Pathways of Plasmodium falciparum using the -Shortest Path Algorithm. *Int. J. Genomics Proteomics* **2019**, (2019).
23. Ma, H.-W., Zhao, X.-M., Yuan, Y.-J. & Zeng, A.-P. Decomposition of metabolic

network into functional modules based on the global connectivity structure of reaction graph. *Bioinformatics* **20**, 1870–1876 (2004).

24. Holme, P. Signatures of Currency Vertices. *J. Phys. Soc. Jpn.* **78**, 034801 (2009).
25. Barupal, D. K. *et al.* MetaMapp: mapping and visualizing metabolomic data by integrating information from biochemical pathways and chemical and mass spectral similarity. *BMC Bioinformatics* **13**, 99 (2012).
26. Tervo, C. J. & Reed, J. L. MapMaker and PathTracer for tracking carbon in genome-scale metabolic models. *Biotechnol. J.* **11**, 648–661 (2016).
27. Steffensen, J. L., Dufault-Thompson, K. & Zhang, Y. FindPrimaryPairs: An efficient algorithm for predicting element-transferring reactant/product pairs in metabolic networks. *PLoS One* **13**, e0192891 (2018).
28. Humphries, M. D. & Gurney, K. Network 'Small-World-Ness': A Quantitative Method for Determining Canonical Network Equivalence. *PLoS ONE* vol. 3 e0002051 (2008).
29. Telesford, Q. K., Joyce, K. E., Hayasaka, S., Burdette, J. H. & Laurienti, P. J. The ubiquity of small-world networks. *Brain Connect.* **1**, 367–375 (2011).
30. Gong, Y. & Zhang, Z. Global Robustness and Identifiability of Random, Scale-Free, and Small-World Networks. *Ann. N. Y. Acad. Sci.* **1158**, 82–92 (2009).
31. Goodarzinick, A., Niry, M. D., Valizadeh, A. & Perc, M. Robustness of functional networks at criticality against structural defects. *Phys Rev E* **98**, 022312 (2018).
32. Wagner, A. & Fell, D. A. The small world inside large metabolic networks. *Proc. Biol. Sci.* **268**, 1803–1810 (2001).

33. Waller, T. C., Berg, J. A., Lex, A., Chapman, B. E. & Rutter, J. Compartment and hub definitions tune metabolic networks for metabolomic interpretations. *Gigascience* **9**, (2020).

34. Jeong, H., Tombor, B., Albert, R., Oltvai, Z. N. & Barabási, A. L. The large-scale organization of metabolic networks. *Nature* **407**, 651–654 (2000).

35. Albert, R. Scale-free networks in cell biology. *J. Cell Sci.* **118**, 4947–4957 (2005).

36. Barabási, A.-L. & PÃ3sfai, M. *Network Science*. (Cambridge University Press, 2016).

37. Bollobás, B. & Riordan, O. Robustness and Vulnerability of Scale-Free Random Graphs. *Internet Math.* **1**, 1–35 (2004).

38. Tanaka, R. Scale-rich metabolic networks. *Phys. Rev. Lett.* **94**, 168101 (2005).

39. Tanaka, R. & Doyle, J. Scale-rich metabolic networks: background and introduction. *arXiv [q-bio.MN]* (2004).

40. Pang, T. Y. & Maslov, S. A toolbox model of evolution of metabolic pathways on networks of arbitrary topology. *PLoS Comput. Biol.* **7**, e1001137 (2011).

41. Grigorov, M. G. Global properties of biological networks. *Drug Discov. Today* **10**, 365–372 (2005).

42. Peng, G.-S., Tan, S.-Y., Wu, J. & Holme, P. Trade-offs between robustness and small-world effect in complex networks. *Sci. Rep.* **6**, 37317 (2016).

43. Papp, B., Teusink, B. & Notebaart, R. A. A critical view of metabolic network adaptations. *HFSP J.* **3**, 24–35 (2009).

44. Zhao, J., Yu, H., Luo, J., Cao, Z. W. & Li, Y. Complex networks theory for

analyzing metabolic networks. *Chin. Sci. Bull.* **51**, 1529–1537 (2006).

45. Ma, H. & Zeng, A.-P. Reconstruction of metabolic networks from genome data and analysis of their global structure for various organisms. *Bioinformatics* **19**, 270–277 (2003).
46. Reed, J. L., Vo, T. D., Schilling, C. H. & Palsson, B. O. An expanded genome-scale model of Escherichia coli K-12 (iJR904 GSM/GPR). *Genome Biol.* **4**, R54 (2003).
47. Feist, A. M. *et al.* A genome-scale metabolic reconstruction for Escherichia coli K-12 MG1655 that accounts for 1260 ORFs and thermodynamic information. *Mol. Syst. Biol.* **3**, 121 (2007).
48. Orth, J. D. *et al.* A comprehensive genome-scale reconstruction of Escherichia coli metabolism--2011. *Mol. Syst. Biol.* **7**, 535 (2011).
49. Zhang, Y. *et al.* Three-dimensional structural view of the central metabolic network of Thermotoga maritima. *Science* **325**, 1544–1549 (2009).
50. Dufault-Thompson, K. *et al.* A Genome-Scale Model of Shewanella piezotolerans Simulates Mechanisms of Metabolic Diversity and Energy Conservation. *mSystems* **2**, (2017).
51. Liechti, G. & Goldberg, J. B. Helicobacter pylori relies primarily on the purine salvage pathway for purine nucleotide biosynthesis. *J. Bacteriol.* **194**, 839–854 (2012).
52. Csardi, G., Nepusz, T. & Others. The igraph software package for complex network research. *InterJournal, Complex Systems* **1695**, 1–9 (2006).
53. Cohen, J. Eta-squared and partial eta-squared in fixed factor ANOVA designs.

Educ. Psychol. Meas. (1973).

54. Gillespie, C. S. Fitting heavy tailed distributions: the poweRlaw package. *arXiv [stat.CO]* (2014).

55. Broido, A. D. & Clauset, A. Scale-free networks are rare. *Nat. Commun.* **10**, 1017 (2019).

Figures for Manuscript III

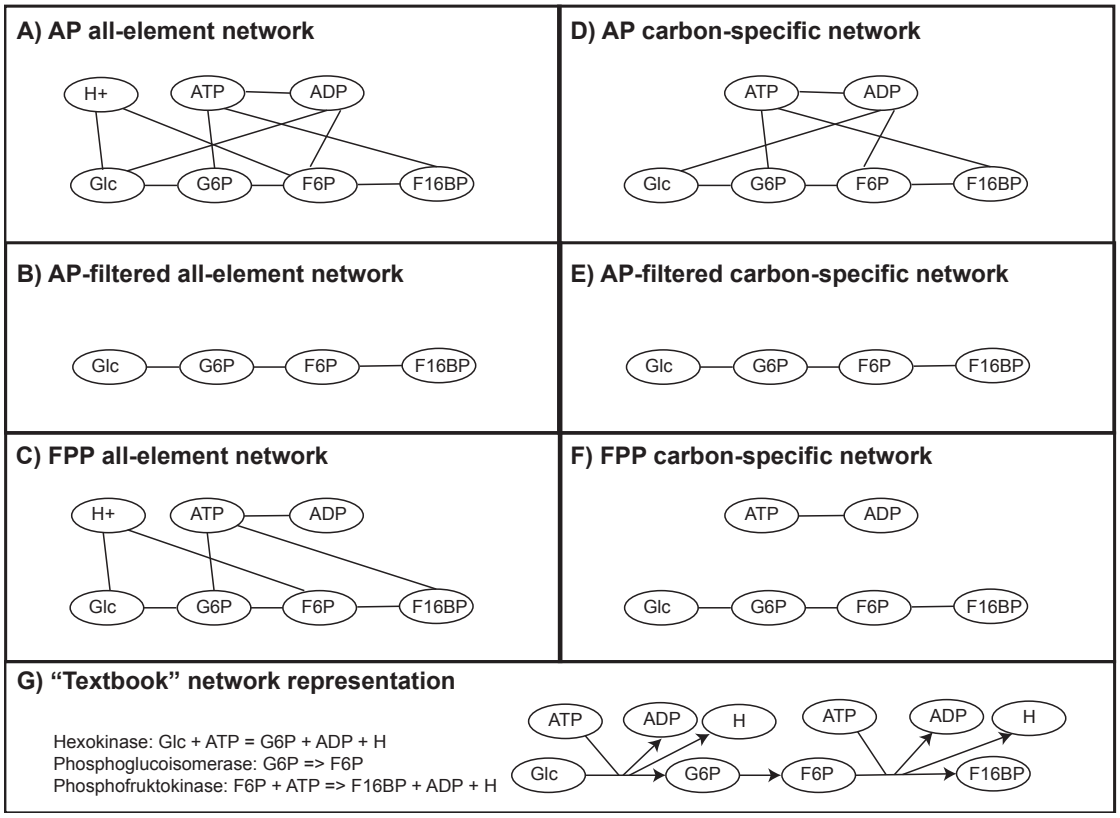

Fig. 1: Graphical representation of different network representations. All-element networks are shown for the AP (A), AP-filtered (B), and FPP (C) network representations. Carbon-based networks are shown for the AP (D), AP-filtered (E), and FPP (F) network representations. A classic 'textbook' network representation with the reaction equations used to make the networks are shown in panel G.

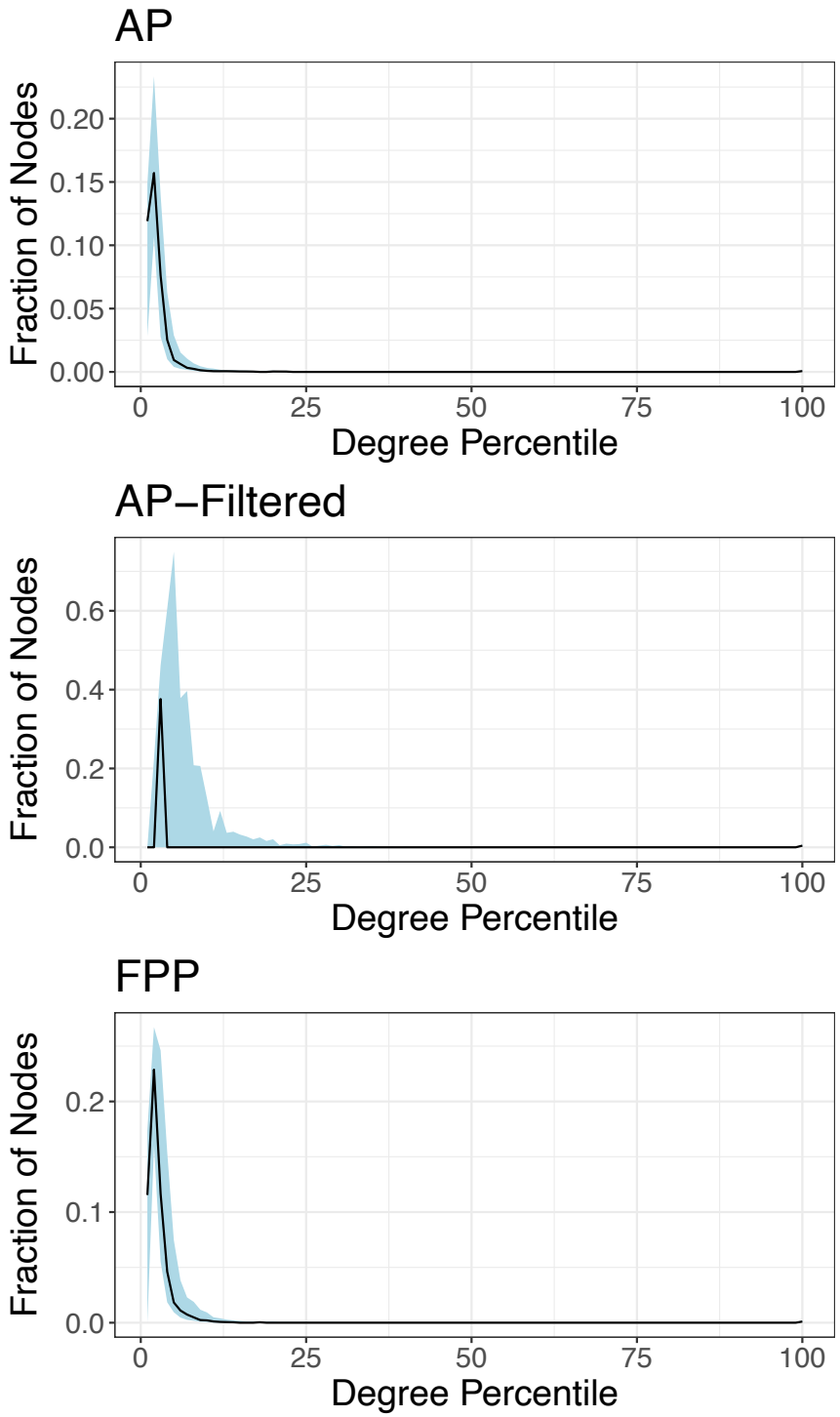

Fig. 2: Summarized degree distributions for all KEGG derived all-elements networks. The black line shows the median across all organisms, while the blue shaded regions indicate the 25th to 75th percentiles.

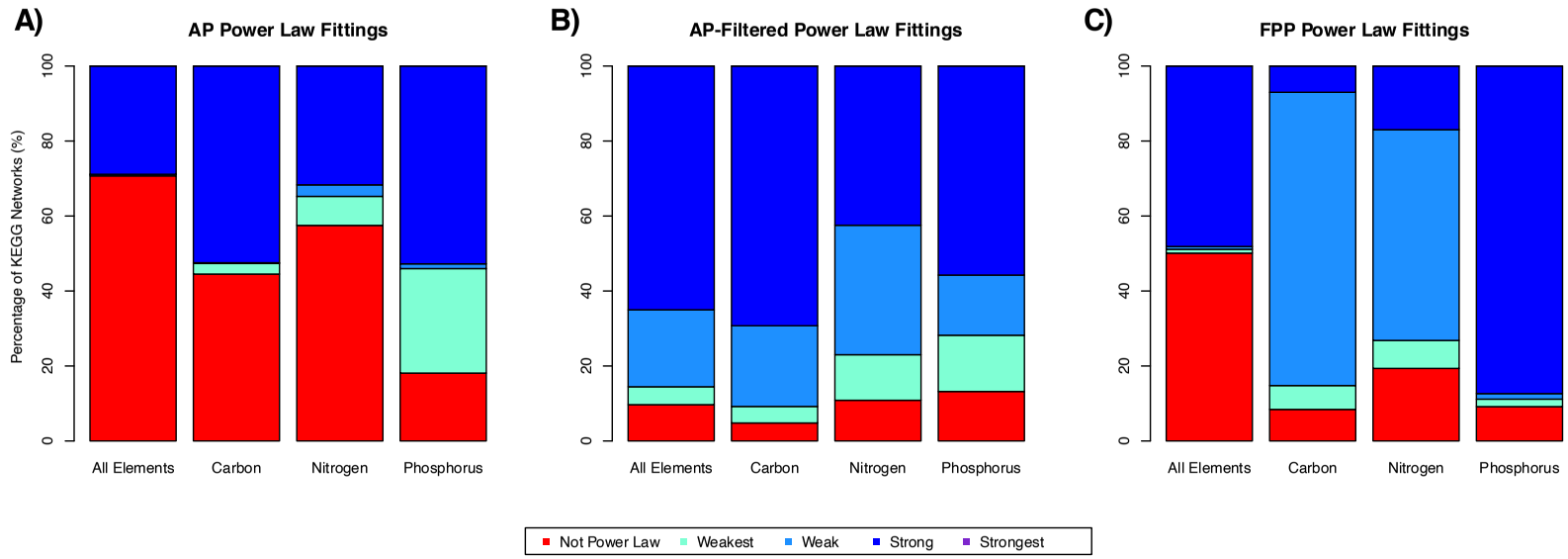

Fig. 3: Bar plots showing the fractions of KEGG networks having each category of scale-free evidence for the all-elements, carbon, nitrogen, and phosphorus filtered versions of the FPP (A), AP (B), and AP-Filtered (C).

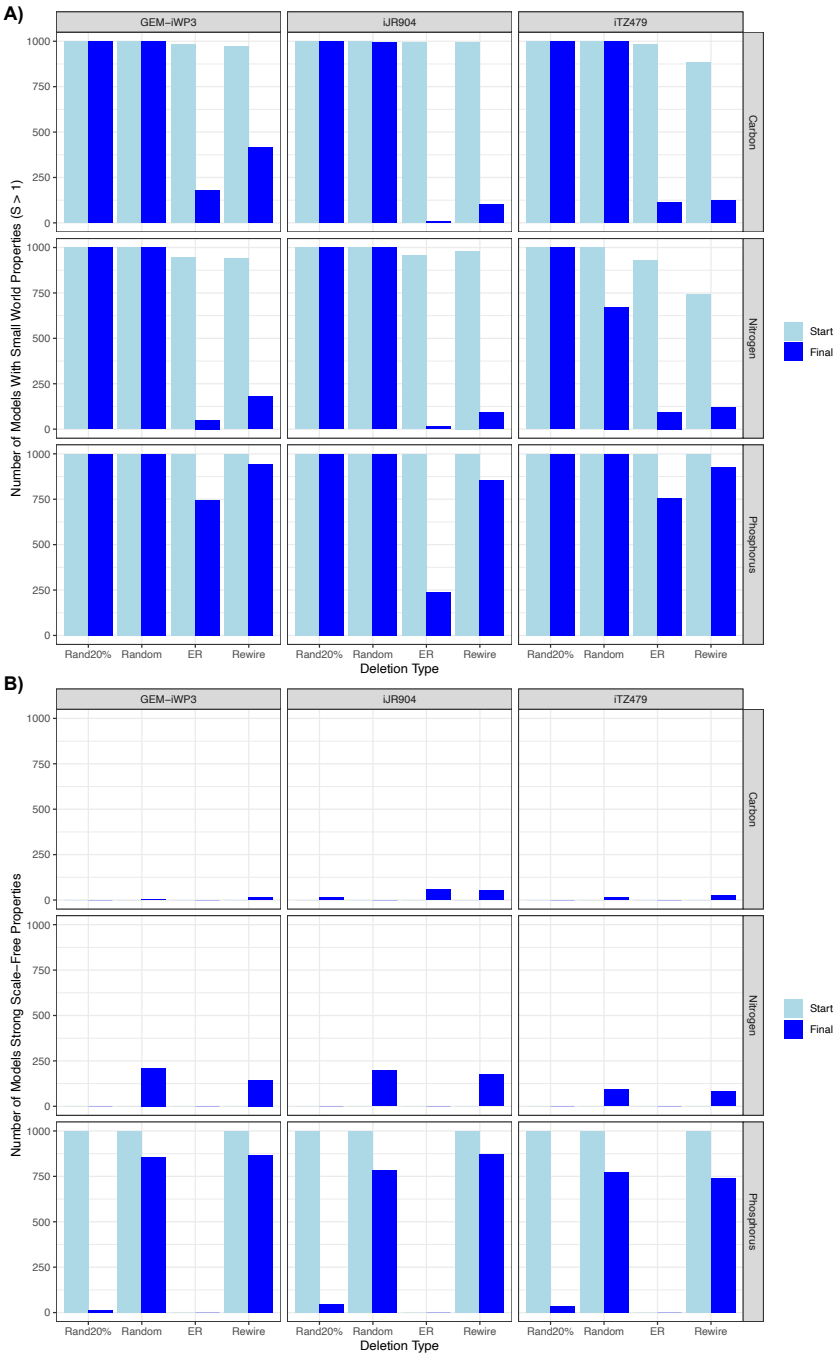

Fig. 4: A) Bar plots showing the number of networks with small-world properties before deletions (light blue) and after deletions have finished (dark blue). B) Bar plots showing the number of networks with strong or strongest evidence of scale-free properties before (light blue) and after (dark blue) deletions.

Supplemental Text for Manuscript III

Supplemental Text S1: Description of network descriptors and analysis process

All network statistics were calculated using the 'python-igraph'[1] package version 0.8.2 and 'poweRlaw'[2] R package version 0.70.6. Networks were read into the program as edge lists and converted into iGraph graph objects. These networks were then simplified to remove any multi-edges that were present in the graphs. The graphs were then subset to only keep the nodes that were present in the largest connected component of the network. All subsequent analysis was performed using this largest connected component. Various igraph functions were then used to calculate the network metrics for each network. These metrics and how they were calculated are described in the following sections.

Number of Nodes and Edges:

The number of nodes and edges in the networks were counted based on the largest connected component of each network by using the 'len' function in python to find the number of nodes and edges contained in the 'igraph.graph' object.

Average Degree:

The average degree was calculated by summing all of the degrees of all nodes in the network and dividing that value by the total number of nodes. The degrees of the nodes in each network were found using the 'graph.degree' function in igraph.

Density:

The density of the network is a measure of how many edges are present in the network compared to the total number of edges that would be present if all nodes were connected to all other nodes. Higher values indicate that more edges are present in the

network, while lower values indicate that the network is more sparsely connected. The density of the networks was calculated using the ‘graph.density’ function in igraph.

Transitivity:

Transitivity is a measure of the likelihood that two nodes that have a mutual connection to a third node also share a connection with each other, forming a triangle. Higher values mean that more triangles exist in the network. This metric was calculated using the ‘graph.transitivty_undirected’ function in igraph.

Degree Assortativity:

Assortativity is a measure that quantifies how connected nodes with similar properties are in the network. In the case of degree assortativity, this measure is related to how likely nodes of similar degrees are to be connected to each other. Low values mean that the network is disassortative, indicating that many nodes of high degree are connected to low degree nodes. Higher values indicate that nodes of similar degrees are connected to each other. This was calculated using the ‘graph.assortativity_degree’ function in igraph.

Average Betweenness Centrality:

The betweenness centrality of a node is a measure of how many shortest paths in the network pass through the node. The average betweenness centrality of the graph was calculated by averaging the betweenness centrality of all nodes across the network. This betweenness of each node was calculated using the ‘graph.betweenness’ function in igraph.

Average Closeness Centrality:

The closeness centrality of a node is a measure of how close each node is to the other nodes in the network. Lower values indicate that the nodes are more distant from each other, while higher values indicate that the nodes are all less distant from each other. The average value was calculated by taking the average of the closeness of all the nodes. The closeness of each node was calculated using the 'graph.closeness' function in igraph.

Diameter:

The diameter of a network is the length of the longest shortest path between any two nodes in the network. The diameter of the networks was calculated using the 'graph.diameter' function in igraph.

Average Shortest Path Length:

The average shortest path length is a measure of the average length of all the shortest paths in the network. This measure was calculated using the 'graph.average_path_length' function in igraph.

Small Worldness:

The small worldness of each network was quantified following the methods detailed in Humphries and Gurney 2008 [3]. First the transitivity and mean shortest path lengths of the network were calculated using the 'graph.transitivty_undirected' and 'graph.average_path_length' length functions in igraph. Then 1000 random networks with the same number of nodes and edges as the original network were generated using the 'igraph.GraphBase.Erdos_Renyi' function in igrah.

Power Law Fitting:

Power law fitting was done on the network degree distributions using the 'poweRlaw' R package [2]. The degree distributions were fit to a power law distribution using the 'displ' and 'estimate_xmin' function and the strength of the fitting was assessed using the 'bootstrap_p' function. Fitting to a log normal distribution was done using the 'dislnorm' and 'estimate_xmin' functions. Fitting to an exponential distribution was done using the 'disexp' and 'estimate_xmin' functions. Fitting to a poisson distribution was done using the 'dispois' and estimate_xmin' functions. Comparisons of the fittings to different types of distributions was done using the 'compare_distributions' function to assess if the power law fitting was better than the other distributions.

References

1. Csardi, G., Nepusz, T. & Others. The igraph software package for complex network research. *InterJournal, Complex Systems* **1695**, 1–9 (2006).
2. Gillespie, C. S. Fitting heavy tailed distributions: the poweRlaw package. *arXiv [stat.CO]* (2014).
3. Humphries, M. D. & Gurney, K. Network 'Small-World-Ness': A Quantitative Method for Determining Canonical Network Equivalence. *PLoS ONE* vol. 3 e0002051 (2008).

Supplemental Figures for Manuscript III

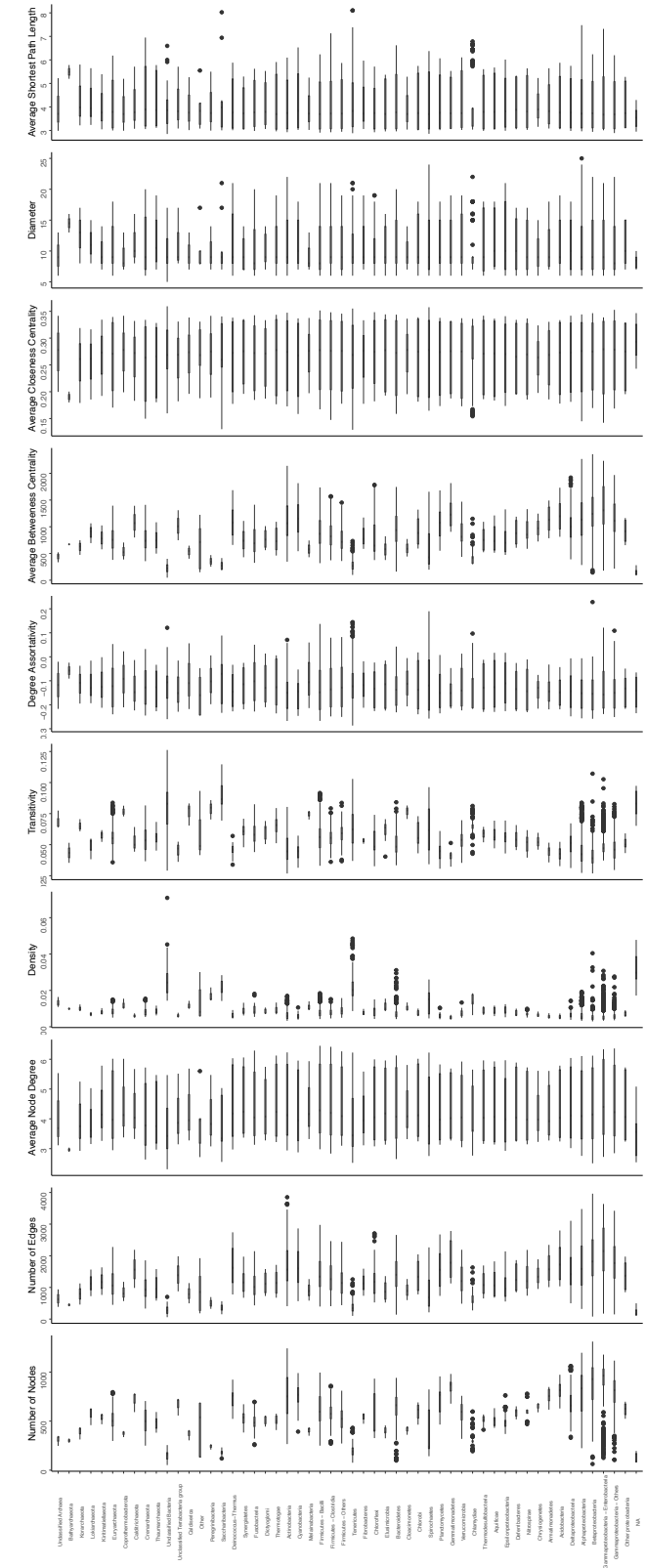

Supplemental Figure S1: Boxplots showing differences in network metrics across 55 taxonomic groups in the KEGG database. Outliers are indicated as black dots.

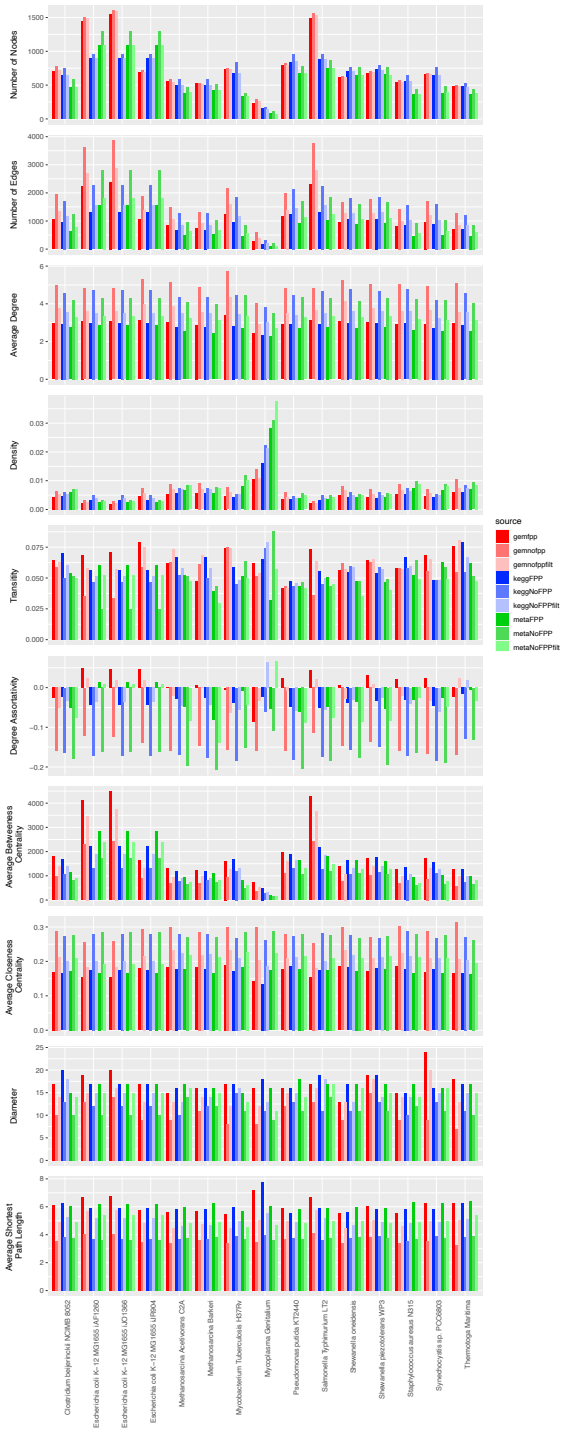

Supplemental Figure S2: Bar plots showing differences in network metrics between networks generated from KEGG, MetaCyc, and published GEMs of 13 organisms.

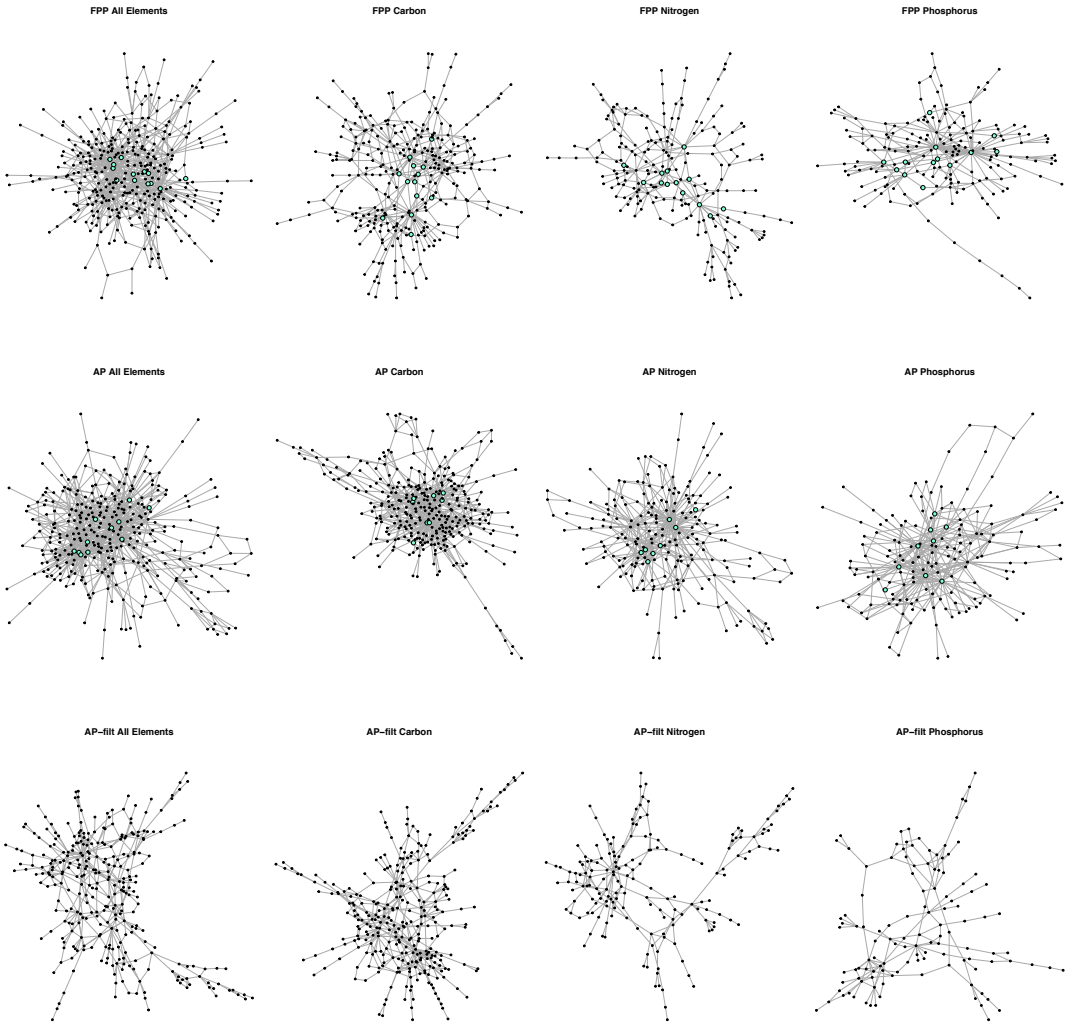

Supplemental Figure S3: Visualizations of the *Buchnera aphidicola* APS metabolic network from KEGG. Visualizations were done for each of the 3 network representations (FPP, AP, AP-Filtered) and 4 element subsets (all-elements, carbon, nitrogen, and phosphorus). Nodes representing common currency metabolites and small molecules are colored cyan in the FPP and AP networks.

Conclusions

Metabolism is central to life, dictating organisms' ability to grow, compete with other organisms, and survive in different environments. The increasing availability of genomic data has led to advancements in new ways to study metabolism, even in organisms that were previously difficult to work with. This dissertation highlights the application of metabolic modeling to investigate metabolism in non-model organisms and the further use of these methods to study the structure of metabolism across the prokaryotic tree of life.

The development of a Genome-scale model (GEM) of metabolism for *Shewanella piezotolerans* WP3 provided the first model of a *Shewanella* strain from the deep-sea clade of this genus. This model provided a platform to study energy conservation mechanisms within this traditionally challenging study of deep-sea bacteria. The WP3 GEM was used to simulate energy metabolism in WP3, showing a reliance on substrate-level phosphorylation, combined with utilization of external electron acceptors during anaerobic growth. This feature was shared with other well-studied *Shewanella*, indicating that these mechanisms may be a conserved growth strategy in the genus. Further simulations highlighted the ability of ATP synthase to act as a proton balancing mechanism depending on the availability of reducing equivalents within the model. The metabolic flexibility demonstrated with this GEM shows the importance of metabolic flexibility as a part of WP3's adaptation to the variable conditions of the deep-sea.

The study of deep-sea metabolism was continued through the development of a GEM for another deep-sea *Shewanella* strain, *Shewanella psychrophila* WP2. Unlike

WP3, which is psychrotolerant, WP2 is a psychrophilic strain. This low-temperature adaptation in WP2 was investigated through a combination of transcriptomics and the application of transcriptome and thermodynamic data into the GEM. Broad metabolic changes characterized the growth of WP2 at sub-optimal, optimal, and supra-optimal growth temperatures. The differential expression of genes within central carbon pathways in WP2 was contextualized by the use of thermodynamics-based metabolic flux analysis. These simulations revealed that changes in the flux through central metabolic pathways led to global changes in WP2's efficiency in producing biomass and energy. The metabolic shifts and utilization of lower efficiency growth strategies in WP2 were similar to previously reported growth trends in other psychrophiles. The investigations of the metabolism of WP2 and WP3 through a combination of experimental and modeling methods led to a broader understanding of metabolism in the *Shewanella* genus. These studies highlight the importance of metabolic flexibility within the *Shewanella* genus and demonstrate the critical roles that conserved metabolic strategies play in these organisms' ability to survive in extreme environments.

Both the WP2 and WP3 models demonstrated the utility of GEMs for investigating specific metabolic mechanisms and features within single organisms. The analysis of metabolism was then extended to look at common metabolic functions across all prokaryotes. This analysis utilized the mathematical field of graph theory to examine the structure and organization of metabolism when it is represented as a mathematical network. This analysis focused on the methods used to represent metabolic networks and highlighted the application of the FindPrimaryPairs algorithm

to generate a new kind type of metabolic network. This new type of network had the benefit of not requiring arbitrary filtering and allowing for the filtering of the network to show different element transfer networks. The further analyses of these network structures revealed distinct differences in the organization of carbon, nitrogen, and phosphorus metabolism and can contribute to the broader understanding of how these networks have evolved.

The work described in this dissertation highlights the complexity of metabolism. The application of multiple methods in studying metabolic processes will be critical to future research in this field. The future integration of techniques like genomes scale modeling and network analysis combined with sequencing and growth experiments will allow for the exploration of increasingly complex systems. While any one of these methods will not provide a full context on its own, each of these methods can enhance each other and lead to new and exciting conclusions.

Appendix I: GEM Reconstruction and Simulation Methods

INTRODUCTION

GEnome-scale Models of Metabolism have been increasing in popularity and utility since the start of their development. Modern models are made for a variety of organisms and can be used to simulate many aspects of metabolism and growth, but early models were much more limited in what they represented and could be used for. The comprehensive GEMs currently being developed have their origins in the modeling and reconstruction of specific pathways or cells with simple metabolic functions [1–3]. These early pathway reconstructions proved to be useful in predicting metabolic phenotypes, and eventually, they were expanded to become representations of the full metabolism of organisms. The first true GEM that represented metabolism at a whole-genome scale was published in 2000 and was based on *Escherichia coli* K-12 [4]. This early *E. coli* model, iJE660, only included functions encoded by 660 of the 4391 protein-coding genes in the *E. coli* K-12 genome. However, even with its relatively small size, this model was still used to predict gene deletion phenotypes and broad metabolic growth phenotypes [4]. Over the two following decades, GEMs have been more broadly developed to include more metabolic pathways and to represent organisms from all three domains of life [5,6]. The creation of new GEMs has corresponded with an expansion of simulation methods that can be used with the models. These methods range from the fundamental Flux Balance Analysis, where the flow of metabolites through a network is simulated based on stoichiometric constraints [7], to more complex simulations that account for thermodynamics [8] and growth over time [9]. The increased availability of genome data and the improvements that are

being made in gene annotation pipelines have made GEMs a more useful and available tool that can contribute to a wide range of different research projects.

COMPONENTS OF A GEM

GEMs are representations of the metabolism of an organism based on that organism's annotated genome. As representations of metabolism, these models primarily contain data related to metabolites and metabolic reactions, but they also include additional information related to the setting up simulations like artificial reactions, reaction flux limits, and exchange conditions representing growth media [10].

Reactions

The reactions in a GEM consists of metabolic reaction equations and the associated metadata for that reaction. The reaction equation is similar to what would be seen in a textbook representation of a metabolic function, consisting of a series of metabolite IDs with some form of an equal's sign representing the separation of the products and reactants (Figure 1A). These equations represent metabolic processes that occur in a cell either catalyzed by enzymes or occurring through spontaneous processes. GEMs for many organisms will represent different cellular locations like the extracellular space, cytosol, periplasm, and for eukaryotes different organelles. To specify where reactions occur in the modeled cell, the reaction equations will often contain some specified reaction ID alongside the metabolites to designate where the metabolic reaction occurs. Reactions are often associated with additional data that allows the GEM to be used as an annotation reference as well as a simulation tool. The

other data can include reaction names, enzyme commission numbers, gene associations, and literature references.

Metabolites

The metabolites in GEMs are what make the reaction equations are made up from. Each metabolite in the model is often involved in multiple reactions. Similar to the reactions, metabolites in GEMs are typically associated with additional information (Figure 1B). Metabolites can be associated with biochemical data like formulas, ionic charges, and molecular masses. The metabolites' properties can be used to ensure that the reaction equations in the GEM are balanced in terms of conserving charge and mass in the reaction equations. GEMs often include additional metadata like metabolite names and database IDs and the metabolites' biochemical properties.

Artificial Reactions

The reactions and metabolites in a GEM are mostly based on biochemical data and the current understanding of enzymatic processes in a cell. Still, there are some processes related to growth that have to be represented through artificial reactions. These reactions often represent larger-scale processes related to growth, like DNA synthesis and protein synthesis, that can't necessarily be represented by single enzyme associated reactions. To overcome the challenge of representing these parts of growth in a model, the overall processes are often condensed down into summary reactions (Figure 2A). For example, DNA synthesis involves multiple steps catalyzed by different enzymes and is an iterative process, where bases get added to a growing

DNA strand successively. In the context of a GEM, this process, along with all of its energy requirements, is summarized into a condensed reaction representing the cost of DNA synthesis in terms of the amount of each base and the amount of energy in the form of ATP. These artificial growth reactions are typically normalized to represent the synthesis of 1 gDW of the product. This normalization is then used when the products of these reactions are combined into an overall biomass reaction equation (Figure 2B). This biomass reaction is formulated based on measured or estimated compositions of the dry weight of an organism. For example, if the protein made up 50% of the cells' dry weight, then the biomass reaction would reflect this by having the synthesized protein be 50% of the reaction. The final formulation of the biomass reaction represents the production of 1 gDW of biomass, which allows for easier comparisons of model simulation results to experimental results [11,12].

Simulation Settings

In addition to the biology-related GEM features like reactions and metabolites, some additional features are included in GEMs related to setting up simulations with the GEM. The first of these features is limits on reaction fluxes. These limits can be set up to force reactions to be used in the model or force them only to be used in specific ways. Flux limits like this are typically simulation specific and can be used to constrain the model better to replicate experimental conditions. A prevalent example of reaction limits in the model involves forcing flux through an artificial ATP maintenance reaction. This type of maintenance reaction is used to represent the non-growth associated maintenance energy in a cell, and reaction limits are used to force a certain amount of ATP to be hydrolyzed in the model to replicate this cost [12–14].

The other part of GEMs related to simulation settings is the exchange settings. These exchange settings are analogous to a growth media, and they are used to define what nutrients are available and can be produced in the simulation. Like the limits, these exchange settings are typically conditioned specific and can be changed depending on the type of experiment replicated with the model.

Overall, GEMs are a collection of information related to setting up metabolic simulations and the annotations of metabolic functions in an organism. With the development of more GEMs from diverse groups of organisms, they have started to shift from being primarily used to perform simulations of growth to now being useful annotation resources that can be used to bring together genomic, biochemical, and physiological data [6,15,16].

GETTING FROM A GENOME TO A GEM

Early GEMs were based mainly on experimental data. They leveraged the extensive research history of model organisms, which is why they were mostly based around well-known pathways and well-studied microorganisms like *E. coli [4,17]*. This process involved manual curation of metabolic functions and the gradual expansion of the models from one pathway to another based on experimental verification of the functions. Unfortunately, this process is impossible for many organisms due to the limited experimental history of many non-model organisms. This challenge has been highlighted by the growth in environmental sequencing methods, where it is now possible to obtain nearly complete genomes of organisms from environmental samples, even when it is not possible to isolate them in pure cultures

[18,19]. To overcome these limitations, there have been concurrent advancements in gene annotation methods [20–22] and the development of extensive gene orthology and metabolic pathway databases [23–26]. These tools have made it possible to develop GEMs for almost any organism that has an available genome.

Gene-Protein-Reaction Associations

The central concept in the development of a GEM is the gene-protein-reaction (GPR) association. This GPR concept is made from the idea that a gene present in an organism can be predicted, then translated to a protein sequence, analyzed, and then, based on the putative function, assigned a metabolic function [27,28]. The process of developing a GEM consists of generating these GPR associations for as many genes as possible in an organism's genome. This overall process is often aided by the use of automated tools and databases, followed by extensive manual curation.

Gene and Protein Analysis

The starting point for a new GEM is a genome sequence. The first step to generate the GPR associations for a new GEM involves predicted the open reading frames from the genomes and translating those ORFs to putative protein sequences. Various tools have been developed to do this task that can account for alternative codon usage in different phyla and utilize previously annotated genomes as templates, including GeneMark and Prodigal [29,30]. The bulk of the analysis is then done on the protein sequence associated with a gene. This sequence can be analyzed using a variety of tools that contribute different pieces of evidence about a gene's potential functions. Sequence homology searches are a typical first step with protein sequence

analysis. Tools like BLAST can be used to search for similar sequences in online databases or in other organisms' genomes [20]. These similar sequences may provide evidence of the functions of the new genes through their annotation or through published studies. In addition to these broad sequence similarity searches, more specific gene orthology predictions can be performed to try to group the new sequence into groups of potentially related orthologs using databases like COG, EggNOG, or KEGG [23,26,31]. The next steps typically consist of performing protein domain analysis on the predicted protein sequence. Tools like Pfam, ScanProsite, and TMHMM can be used to predict protein structural domains and compare them to well-annotated reference proteins [21,22,32]. The presence of certain domains in a protein can be strong indications of what types of substrates that protein might bind to or what enzymatic activity that protein might have (protein domain analysis to function annotation). Additional evidence can also be brought into the gene annotation process from previous studies and from direct experimental evidence of gene function, but these two pieces of evidence are only available for certain organisms. All of the evidence from these different processes are used together to make a determination of what type of enzyme this gene might encode for.

Reaction Association

Once a prediction about what enzyme the gene encodes is made, the next step is to associate that enzyme with a metabolic reaction to complete the GPR association. This process relies on two major sources of information, previously published GEMs and metabolic pathway databases. Previously published GEMs are often used as a starting point for new models either as a reference or if the organisms are closely

related as a template for generating a draft set of reactions for a new GEM [33–35]. No GEM is going to be a perfect match for a new organism through, and there will likely be holes that need to be filled in with new reactions. This process is done through referencing metabolic pathway databases like KEGG and MetaCyc and other resources that include enzyme functional data like BRENDA [23,24,36]. These reactions can be collected into an overall set of metabolic reactions for the GEM and assembled into a complete GEM in one of the various formats used by the different modeling software such as the YAML format [5,10], SBML format [37], or JSON format [25].

SIMULATION METHODS

The purpose of developing GEMs is to use them to perform simulations of the growth of the organism. The fundamental method for doing this is to translate the model into a set of linear constraints and use a type of mathematics called linear programming to maximize the flux through the biomass reaction. This method is called Flux Balance Analysis (FBA) and forms the basis for almost all other modeling methods developed [7,38].

The Stoichiometric Matrix

Reactions in a GEM are typically stored as text, where reaction equations are written out using metabolite IDs and stoichiometry. Before any simulations are done with the GEM, these reactions are converted to a matrix called the stoichiometric matrix. In this matrix, the rows represent metabolites, the columns represent reactions, and the values represent the stoichiometry of a given metabolite in a reaction [38]. As most metabolic reactions only contain a small number of unique metabolites, the

stoichiometric matrix is typically sparse. This matrix forms the basic structure of most constraint-based simulation methods.

Fluxes

Reaction fluxes are what is solved for in most modeling methods. These fluxes obtained from metabolic simulations represent the activity of each reaction in the GEM and can be related to measurable flux values that can be obtained through experimental methods through the scaling of the uptake and production rates in the model[11,38,39]. These fluxes are represented as a vector where each value in the vector corresponds to the flux through a single reaction. The result of an FBA simulation is a flux vector that has been solved for, where one value in the flux vector has been maximized.

Steady State Assumption

The steady-state assumption is the last fundamental component of setting up a stoichiometric modeling problem. This assumption means that in the modeling problem, the amount of any metabolite that is produced must be equal to the amount of that metabolite that is consumed. This means that there cannot be any accumulation of metabolites in the model or any consumption of non-produced metabolites.

Maximization of an Objective Function Flux through Linear Programming

The final step in stoichiometric modeling is the conversion of the stoichiometric matrix along with other model constraints to a linear programming problem. This process involves converting the stoichiometric matrix and flux vector into a series of linear equations based on the values in the stoichiometric matrix. The

steady-state assumption allows for the formulation of linear constraints in the problem, where each linear constraint represents the overall consumption and production of metabolites through multiple reactions. In addition to the linear constraints based on the stoichiometric matrix, many models also include additional constraints that are added to the model to limit flux ranges to reasonable values, establish which nutrients are available or can be produced, or to force certain reactions to carry specific fluxes [7].

FBA Variations and Other Simulation Methods

Many additional modeling methods have been developed using the basic FBA framework and expanding it. Some of these methods, like Flux Variability Analysis (FVA), have been developed to explore the inherent variability that results from solving large linear programming problems [7,40]. Other methods like Thermodynamics-based metabolic flux analysis [8] and Metabolic Adjustment by Differential Expression [41] focus on expanding the basic FBA framework through the incorporation of thermodynamic and transcriptomic data respectively. Regardless of the type of simulation, most of the constraint-based analysis approaches utilize the same basic formulation of the stoichiometric constraints as FBA does.

REFERENCES

1. Lee ID, Palsson BO. A Macintosh software package for simulation of human red blood cell metabolism. Comput Methods Programs Biomed. 1992;38: 195–226.
2. Varma A, Boesch BW, Palsson BO. Stoichiometric interpretation of Escherichia coli glucose catabolism under various oxygenation rates. Appl Environ Microbiol. 1993;59: 2465–2473.

3. Varma A, Palsson BO. Stoichiometric flux balance models quantitatively predict growth and metabolic by-product secretion in wild-type Escherichia coli W3110. Appl Environ Microbiol. 1994;60: 3724–3731.

4. Edwards JS, Palsson BO. The Escherichia coli MG1655 in silico metabolic genotype: its definition, characteristics, and capabilities. Proc Natl Acad Sci U S A. 2000;97: 5528–5533.

5. Steffensen JL, Dufault-Thompson K, Zhang Y. PSAMM: A Portable System for the Analysis of Metabolic Models. PLoS Comput Biol. 2016;12: e1004732.

6. Kim WJ, Kim HU, Lee SY. Current state and applications of microbial genome-scale metabolic models. Current Opinion in Systems Biology. 2017;2: 10–18.

7. Orth JD, Thiele I, Palsson BØ. What is flux balance analysis? Nat Biotechnol. 2010;28: 245.

8. Henry CS, Broadbelt LJ, Hatzimanikatis V. Thermodynamics-based metabolic flux analysis. Biophys J. 2007;92: 1792–1805.

9. Mahadevan R, Edwards JS, Doyle FJ 3rd. Dynamic flux balance analysis of diauxic growth in Escherichia coli. Biophys J. 2002;83: 1331–1340.

10. Dufault-Thompson K, Steffensen JL, Zhang Y. Using PSAMM for the Curation and Analysis of Genome-Scale Metabolic Models. Methods in Molecular Biology. 2018. pp. 131–150. doi:10.1007/978-1-4939-7528-0_6

11. Feist AM, Palsson BO. The biomass objective function. Curr Opin Microbiol. 2010;13: 344–349.

12. Pinchuk GE, Hill EA, Geydebrekht OV, De Ingeniis J, Zhang X, Osterman A, et al. Constraint-based model of Shewanella oneidensis MR-1 metabolism: a tool for data analysis and hypothesis generation. PLoS Comput Biol. 2010;6: e1000822.

13. Cheung CYM, Williams TCR, Poolman MG, Fell DA, Ratcliffe RG, Sweetlove LJ. A method for accounting for maintenance costs in flux balance analysis improves the prediction of plant cell metabolic phenotypes under stress conditions. Plant J. 2013;75: 1050–1061.

14. Lachance J-C, Lloyd CJ, Monk JM, Yang L, Sastry AV, Seif Y, et al. BOFdat: Generating biomass objective functions for genome-scale metabolic models from experimental data. PLoS Comput Biol. 2019;15: e1006971.

15. Mardinoglu A, Agren R, Kampf C, Asplund A, Nookaew I, Jacobson P, et al. Integration of clinical data with a genome-scale metabolic model of the human adipocyte. Mol Syst Biol. 2013;9: 649.

16. Oberhardt MA, Palsson BØ, Papin JA. Applications of genome-scale metabolic reconstructions. Mol Syst Biol. 2009;5: 320.

17. Reed JL, Vo TD, Schilling CH, Palsson BO. An expanded genome-scale model of Escherichia coli K-12 (iJR904 GSM/GPR). Genome Biol. 2003;4: R54.

18. Parks DH, Rinke C, Chuvochina M, Chaumeil P-A, Woodcroft BJ, Evans PN, et al. Recovery of nearly 8,000 metagenome-assembled genomes substantially expands the tree of life. Nat Microbiol. 2017;2: 1533–1542.

19. Xu J. Invited review: microbial ecology in the age of genomics and metagenomics: concepts, tools, and recent advances. Mol Ecol. 2006;15: 1713–1731.

20. Altschul SF, Gish W, Miller W, Myers EW, Lipman DJ. Basic local alignment search tool. J Mol Biol. 1990;215: 403–410.

21. Bateman A, Coin L, Durbin R, Finn RD, Hollich V, Griffiths-Jones S, et al. The Pfam protein families database. Nucleic Acids Res. 2004;32: D138–41.

22. De Castro E, Sigrist CJA, Gattiker A, Bulliard V, Langendijk-Genevaux PS, Gasteiger E, et al. ScanProsite: detection of PROSITE signature matches and ProRule-associated functional and structural residues in proteins. Nucleic Acids Res. 2006;34: W362–W365.

23. Kanehisa M, Goto S. KEGG: kyoto encyclopedia of genes and genomes. Nucleic Acids Res. 2000;28: 27–30.

24. Caspi R, Altman T, Billington R, Dreher K, Foerster H, Fulcher CA, et al. The MetaCyc database of metabolic pathways and enzymes and the BioCyc collection of Pathway/Genome Databases. Nucleic Acids Res. 2014;42: D459–71.

25. Norsigian CJ, Pusarla N, McConn JL, Yurkovich JT, Dräger A, Palsson BO, et al. BiGG Models 2020: multi-strain genome-scale models and expansion across the phylogenetic tree. Nucleic Acids Res. 2020;48: D402–D406.

26. Huerta-Cepas J, Szklarczyk D, Heller D, Hernández-Plaza A, Forslund SK, Cook H, et al. eggNOG 5.0: a hierarchical, functionally and phylogenetically annotated orthology resource based on 5090 organisms and 2502 viruses. Nucleic Acids Res. 2019;47: D309–D314.

27. Machado D, Herrgård MJ, Rocha I. Stoichiometric Representation of Gene–Protein–Reaction Associations Leverages Constraint-Based Analysis from Reaction to Gene-Level Phenotype Prediction. PLoS Comput Biol. 2016;12: e1005140.

28. Cardoso J, Vilaça P, Soares S, Rocha M. An Algorithm to Assemble Gene-Protein-Reaction Associations for Genome-Scale Metabolic Model Reconstruction. Pattern Recognition in Bioinformatics. Springer Berlin Heidelberg; 2012. pp. 118–128.

29. Borodovsky M, McIninch J. GENMARK: Parallel gene recognition for both DNA strands. Comput Chem. 1993;17: 123–133.

30. Hyatt D, Chen G-L, Locascio PF, Land ML, Larimer FW, Hauser LJ. Prodigal: prokaryotic gene recognition and translation initiation site identification. BMC Bioinformatics. 2010;11: 119.

31. Tatusov RL, Galperin MY, Natale DA, Koonin EV. The COG database: a tool for genome-scale analysis of protein functions and evolution. Nucleic Acids Res. 2000;28: 33–36.

32. Krogh A, Larsson B, von Heijne G, Sonnhammer EL. Predicting transmembrane protein topology with a hidden Markov model: application to complete genomes. J Mol Biol. 2001;305: 567–580.

33. Dufault-Thompson K, Jian H, Cheng R, Li J, Wang F, Zhang Y. A Genome-Scale Model of Shewanella piezotolerans Simulates Mechanisms of Metabolic Diversity and Energy Conservation. mSystems. 2017;2. doi:10.1128/mSystems.00165-16

34. Ong WK, Vu TT, Lovendahl KN, Llull JM, Serres MH, Romine MF, et al. Comparisons of Shewanella strains based on genome annotations, modeling, and experiments. BMC Syst Biol. 2014;8: 31.

35. Machado D, Andrejev S, Tramontano M, Patil KR. Fast automated reconstruction of genome-scale metabolic models for microbial species and communities. Nucleic Acids Res. 2018;46: 7542–7553.

36. Schomburg I, Chang A, Ebeling C, Gremse M, Heldt C, Huhn G, et al. BRENDA, the enzyme database: updates and major new developments. Nucleic Acids Res. 2004;32: D431–3.

37. Olivier BG, Bergmann FT. SBML Level 3 Package: Flux Balance Constraints version 2. J Integr Bioinform. 2018;15. doi:10.1515/jib-2017-0082

38. Maarleveld TR, Khandelwal RA, Olivier BG, Teusink B, Bruggeman FJ. Basic concepts and principles of stoichiometric modeling of metabolic networks. Biotechnol J. 2013;8: 997–1008.

39. Raman K, Chandra N. Flux balance analysis of biological systems: applications and challenges. Brief Bioinform. 2009;10: 435–449.

40. Gudmundsson S, Thiele I. Computationally efficient flux variability analysis. BMC Bioinformatics. 2010. doi:10.1186/1471-2105-11-489

41. Jensen PA, Papin JA. Functional integration of a metabolic network model and expression data without arbitrary thresholding. Bioinformatics. 2011;27: 541–547.

Appendix I Figures

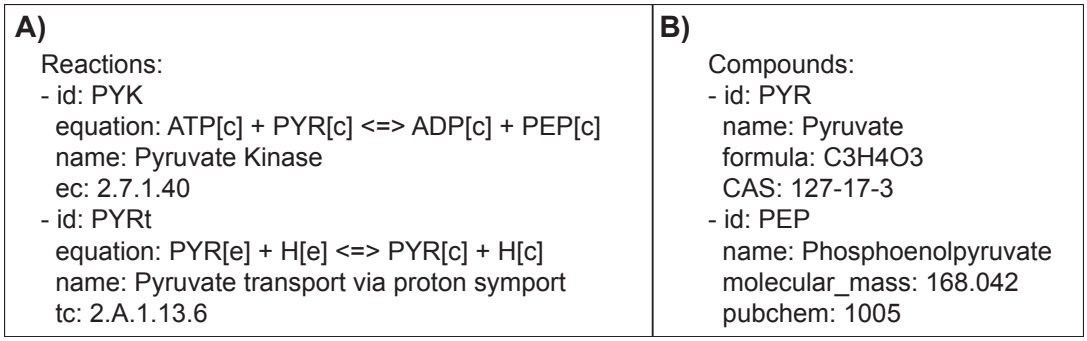

Figure 1: Example representations of metabolic reactions (A) and metabolites (B) in a GEM.

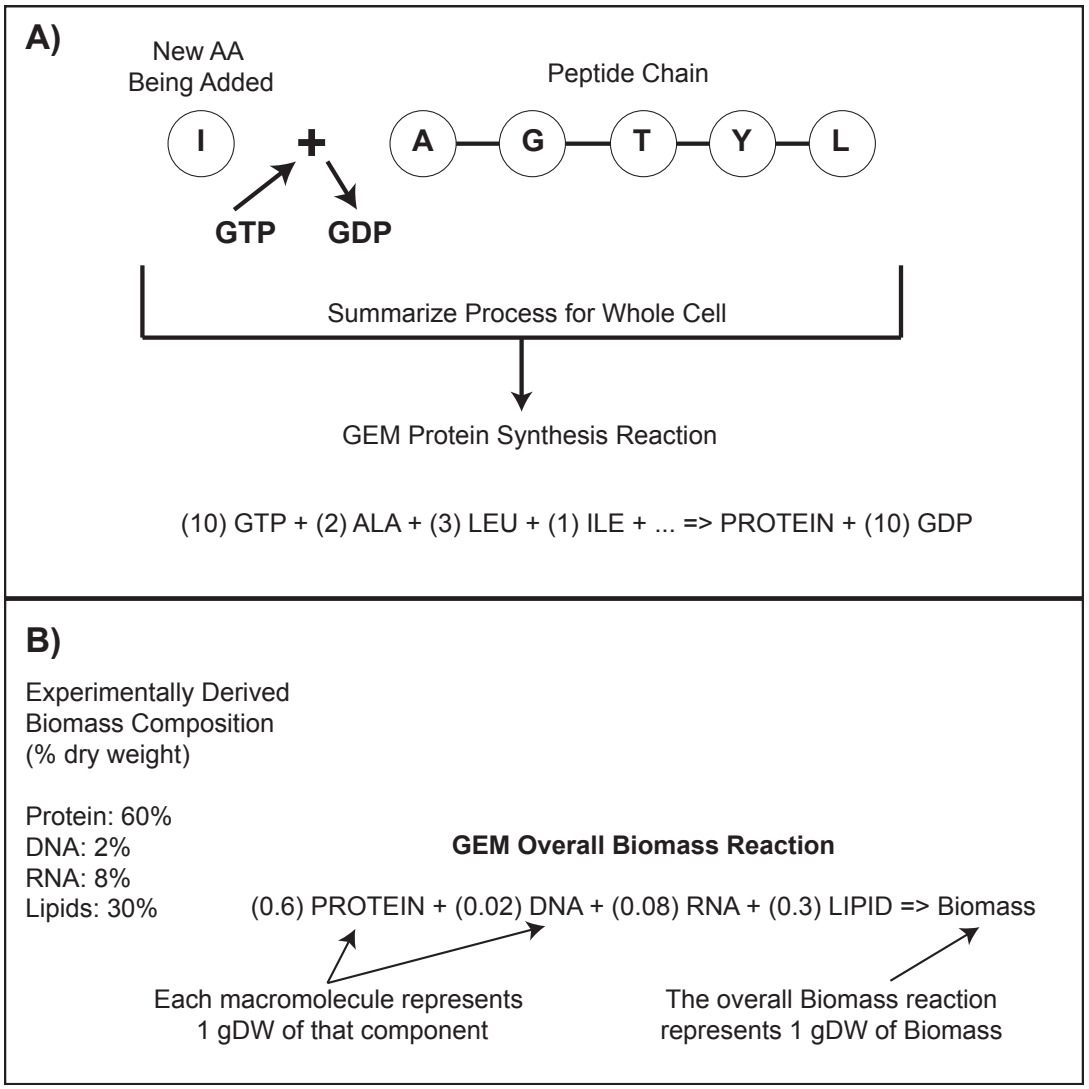

Figure 2: Schematic representation of a macromolecule synthesis reaction (A) and the overall biomass reaction of a GEM (B).

Appendix II: Supplemental Tables for Manuscript I

Supplemental Table S1. Stoichiometry of the biomass compounds involved in the biomass synthesis equation of the WP3 GEM.

Compound_ ID	Stoichiometry	Compound_ Name	Molecular Weight (g/mol)	Weight (g/gDW)
cpd_12dag3p	0.000078	1,2-Diacyl-sn-glycerol 3-phosphate	645.2608	5.033034E-05
cpd_12dgr	0.139174	1,2-Diacylglycerol	567.2988	7.895324E-02
cpd_5mthf	0.050000	5-Methyltetrahydrofolate	458.4620	2.292310E-02
cpd_accoa	0.000050	Acetyl-CoA	805.5480	4.027740E-05
cpd_amp	0.001000	AMP	345.2160	3.452160E-04
cpd_coa	0.000006	CoenzymeA	763.5120	4.581072E-06
cpd_dna	0.001819	DNA	30792.5160	5.601159E-02
cpd_fad	0.000050	FAD	783.5480	3.917740E-05
cpd_lps_Core	0.011270	LPS	3052.1980	3.439675E-02
cpd_nad	0.002150	NAD	662.4280	1.424220E-03
cpd_nadh	0.000050	NADH	663.4360	3.317180E-05
cpd_nadp	0.000130	NADP	740.3900	9.625070E-05
cpd_nadph	0.000400	NADPH	741.3980	2.965592E-04
cpd_pe	0.078517	Phosphatidylethanolamine	690.3468	5.420396E-02
cpd_peptx	0.031434	Peptidoglycan subunit crosslinked	899.8900	2.828714E-02
cpd_pgly	0.022716	Phosphatidylglycerol	720.3468	1.636340E-02
cpd_protein	0.000551	Protein	1083383.9340	5.969445E-01
cpd_rna	0.000003	RNA	32013.8140	9.604144E-05
cpd_succoa	0.000003	Succinyl-CoA	862.5760	2.587728E-06
cpd_udpg	0.003000	UDP-Glucose	564.2860	1.692858E-03

cpd_glycogen	0.472431	Glycogen	162.1400	7.659996E-02
cpd_ptrc	0.035000	Putrescine	90.1720	3.156020E-03
cpd_spmd	0.007000	Spermidine	148.2760	1.037932E-03
cpd_k	0.169185	K+	38.9637	6.592084E-03
cpd_nh4	0.011279	NH4	18.0390	2.034622E-04
cpd_mg2	0.007519	Mg2+	23.9850	1.803515E-04
cpd_ca2	0.004512	Ca2+	39.9626	1.802956E-04
cpd_fe2	0.006767	Fe2+	55.9349	3.785345E-04
cpd_cu2	0.012698	Cu2+	63.5460	8.069333E-04
cpd_mn2	0.012698	Mn2+	54.9380	6.976254E-04
cpd_mobd	0.012698	Molybdate	159.9400	2.030984E-03
cpd_cobalt2	0.012698	Co2+	58.9332	7.483581E-04
cpd_cl	0.019048	Chloride	34.9689	6.660743E-04
cpd_so4	0.015873	SO4	96.0620	1.524794E-03
cpd_pydx5p	0.000223	Pyridoxal 5'-phosphate	245.1270	5.474503E-05
cpd_pheme	0.000223	Protoheme	690.6269	1.542400E-04
cpd_udcpdp	0.000055	Undecaprenyl diphosphate	924.2580	5.116008E-05
cpd_chor	0.000223	Chorismate	224.1680	5.006419E-05
cpd_amet	0.000223	S-Adenosyl-L-methionine	399.4520	8.921095E-05
cpd_ribflv	0.000223	Riboflavin	376.3690	8.405574E-05
cpd_sheme	0.000223	Siroheme	908.6969	2.026394E-04
cpd_ubq8h2	0.000223	Ubiquinol-8	729.1430	1.625989E-04
cpd_mqn7	0.000223	Menaquinone 7	719.1510	1.603707E-04
cpd_cobamcoa	0.000223	Cobamide coenzyme	1579.5818	3.522467E-04
cpd_thmpp	0.000223	Thiamine diphosphate	422.2950	9.417179E-05
cpd_btn	0.000002	Biotin	244.3100	4.886200E-07

Supplemental Table S2. Stoichiometry of the fatty acid components in the lipid biosynthesis equation of the WP3 GEM. The stoichiometry of unsaturated, saturated, and branch-chain fatty acids were calibrated based on experimental measurements of the WP3 fatty acid composition at 20°C and 0.1 MPa (Wang et al., 2009).

Compound_ID	Type	Stoichiometry
fa11ACP	Iso-C17:0	0.2210
fa13ACP	Iso-C13:0	0.0649
fa1ACP	Iso-C14:0	0.2040
fa3ACP	iso-C15:0	0.0759
fa6ACP	Iso-C16:0	0.2550
hdeACP	n-C16:1	0.1346
hpdACP	n-C17:0	0.0510
hpdeACP	C17:1	0.4250
ocdACP	n-C18:0	0.0340
octeACP	n-C18:1	0.0434
palmACP	n-C16:0A	0.2210
pdACP	n-C15:0	0.0340
pdeACP	C15:1	0.2040
epa	20:5	0.0321

Supplemental Table S3. Basal constraints for metabolic simulations performed in the WP3 and MR-1 models (Materials and Methods). Compound ID/Name: the identifiers/names of extracellular compounds with defined exchange reactions, which were used to simulate the availability of nutrients and the removal of metabolic byproducts. The compound identifiers were shown for both the WP3 and MR-1 models. Lower/Upper Bound: basal constraints for the lower and upper bounds of exchange reaction fluxes. Negative lower bounds would indicate compounds provided as nutrient sources to the model, and a lower bound of zero would indicate a compound that could only be released as a metabolic byproduct but not acquired from the environment. Type: classification of the exchange compounds. Growth supporting in WP3: the growth supporting carbon sources and terminal electron acceptors were marked as TRUE in this column.

Compound ID	Compound Name	Lower Bound	Upper Bound	Type	Growth Supporting
cpd_h[e]	H+	-1000	1000	Basal media	-
cpd_h2o[e]	H2O	-1000	1000	Basal media	-
cpd_na1[e]	Sodium	0	1000	Basal media	-
cpd_ca2[e]	Calcium	-1000	1000	Basal salt media	-
cpd_cl[e]	Chloride	-1000	1000	Basal salt media	-
cpd_k[e]	K+	-1000	1000	Basal salt media	-
cpd_mg2[e]	Mg	-1000	1000	Basal salt media	-
cpd_nh4[e]	Ammonium	-1000	1000	Basal salt media	-
cpd_pi[e]	Phosphate	-1000	1000	Basal salt media	-
cpd_so4[e]	Sulfate	-1000	1000	Basal salt media	-
cpd_ac[e]	Acetate	0	1000	Carbon source	TRUE
cpd_acgam[e]	N-Acetyl-D-glucosamine	0	1000	Carbon source	TRUE
cpd_adn[e]	Adenosine	0	1000	Carbon source	TRUE
cpd_ala-D[e]	D-Alanine	0	1000	Carbon source	TRUE
cpd_ala-L[e]	L-Alanine	0	1000	Carbon source	TRUE
cpd_asp-L[e]	L-Aspartate	0	1000	Carbon source	TRUE
cpd_bgl[e]	Cellobiose	0	1000	Carbon source	TRUE
cpd_chitin[e]	Chitin	0	1000	Carbon source	TRUE
cpd_cytd[e]	Cytidine	0	1000	Carbon source	TRUE
cpd_dad-2[e]	Deoxyadenosine	0	1000	Carbon source	TRUE
cpd_damp[e]	dAMP	0	1000	Carbon source	TRUE
cpd_dcmp[e]	dCMP	0	1000	Carbon source	TRUE
cpd_dcyt[e]	Deoxycytidine	0	1000	Carbon source	TRUE
cpd_dna[e]	DNA	0	1000	Carbon source	TRUE
cpd_dodca[e]	Dodecanoic acid	0	1000	Carbon source	TRUE

cpd_duri[e]	Deoxyuridine	0	1000	Carbon source	TRUE
cpd_for[e]	Formate	0	1000	Carbon source	TRUE
cpd_fum[e]	Fumarate	0	1000	Carbon source	TRUE
cpd_gal[e]	D-Galactose	0	1000	Carbon source	TRUE
cpd_galactan[e]	Galactan	0	1000	Carbon Source	TRUE
cpd_glc-D[e]	D-Glucose	0	1000	Carbon source	TRUE
cpd_glu-L[e]	L-Glutamate	0	1000	Carbon source	TRUE
cpd_gly-asp-L[e]	Glycyl-L-aspartic acid	0	1000	Carbon source	TRUE
cpd_gly-glu-L[e]	Glycyl-L-glutamic acid	0	1000	Carbon source	TRUE
cpd_gly[e]	Glycine	0	1000	Carbon source	TRUE
cpd_glyc-R[e]	(R)-Glycerate	0	1000	Carbon source	TRUE
cpd_glyc[e]	Glycerol	0	1000	Carbon source	TRUE
cpd_hdca[e]	hexadecanoate (n-C16:0)	0	1000	Carbon source	TRUE
cpd_ile-L[e]	L-Isoleucine	0	1000	Carbon source	TRUE
cpd_lac-D[e]	D-Lactate	0	1000	Carbon source	TRUE
cpd_lac-L[e]	L-Lactate	0	1000	Carbon source	TRUE
cpd_lami[e]	laminarin	0	1000	Carbon source	TRUE
cpd_leu-L[e]	L-Leucine	0	1000	Carbon source	TRUE
cpd_mal-L[e]	L-Malate	0	1000	Carbon source	TRUE
cpd_malt[e]	Maltose	0	1000	Carbon source	TRUE
cpd_malthp[e]	Maltoheptaose	0	1000	Carbon source	TRUE
cpd_malthx[e]	Maltohexaose	0	1000	Carbon source	TRUE
cpd_maltpt[e]	Maltopentaose	0	1000	Carbon source	TRUE
cpd_malttr[e]	Maltotriose	0	1000	Carbon source	TRUE
cpd_maltttr[e]	Maltotetraose	0	1000	Carbon source	TRUE
cpd_ocdca[e]	Octadecanoate (n-C18:0)	0	1000	Carbon source	TRUE
cpd_panose[e]	Panose	0	1000	Carbon Source	TRUE
cpd_ppa[e]	Propionate	0	1000	Carbon source	TRUE
cpd_pro-L[e]	L-Proline	0	1000	Carbon source	TRUE
cpd_ptrc[e]	Putrescine	0	1000	Carbon source	TRUE
cpd_pyr[e]	Pyruvate	0	1000	Carbon source	TRUE
cpd_ser-L[e]	L-Serine	0	1000	Carbon source	TRUE
cpd_succ[e]	Succinate	0	1000	Carbon source	TRUE
cpd_thr-L[e]	L-Threonine	0	1000	Carbon source	TRUE
cpd_ttdca[e]	tetradecanoate (C14:0)	0	1000	Carbon source	TRUE
cpd_tyr-L[e]	L-Tyrosine	0	1000	Carbon source	TRUE

cpd_uri[e]	Uridine	0	1000	Carbon source	TRUE
cpd_val-L[e]	L-Valine	0	1000	Carbon source	TRUE
cpd_dgmp[e]	dGMP	0	1000	Carbon source	FALSE
cpd_dgsn[e]	Deoxyguanosine	0	1000	Carbon source	FALSE
cpd_dtmp[e]	dTMP	0	1000	Carbon source	FALSE
cpd_glyclt[e]	Glycolate	0	1000	Carbon source	FALSE
cpd_indole[e]	Indole	0	1000	Carbon source	FALSE
cpd_lys-L[e]	L-Lysine	0	1000	Carbon source	FALSE
cpd_met-L[e]	L-Methionine	0	1000	Carbon source	FALSE
cpd_thymd[e]	Thymidine	0	1000	Carbon source	FALSE
cpd_trp-L[e]	L-Tryptophan	0	1000	Carbon source	FALSE
cpd_ura[e]	Uracil	0	1000	Carbon source	FALSE
cpd_xan[e]	Xanthine	0	1000	Carbon source	FALSE
cpd_cro4[e]	chromate	0	1000	Electron acceptor	TRUE
cpd_dmso[e]	Dimethyl sulfoxide	0	1000	Electron acceptor	TRUE
cpd_fe3[e]	Fe3+	0	1000	Electron acceptor	TRUE
cpd_h2o2[e]	Hydrogen peroxide	0	1000	Electron acceptor	TRUE
cpd_mn4o[e]	Manganese(IV) oxide	0	1000	Electron acceptor	TRUE
cpd_no2[e]	Nitrite	0	1000	Electron acceptor	TRUE
cpd_no3[e]	Nitrate	0	1000	Electron acceptor	TRUE
cpd_o2[e]	O2	0	1000	Electron acceptor	TRUE
cpd_tmao[e]	Trimethylamine N-oxide	0	1000	Electron acceptor	TRUE
cpd_tsul[e]	Thiosulfate	0	1000	Electron acceptor	TRUE
cpd_tttnt[e]	tetrathionate	0	1000	Electron acceptor	TRUE
cpd_urnyl[e]	Uranyl	0	1000	Electron acceptor	TRUE
cpd_cobalt3[e]	Co3+	0	1000	Electron acceptor	FALSE
cpd_co2[e]	CO2	0	1000	Metabolic byproduct	-
cpd_CrOH3[e]	Cr(OH)3	0	1000	Metabolic byproduct	-
cpd_dms[e]	Dimethyl sulfide	0	1000	Metabolic byproduct	-
cpd_h2s[e]	Hydrogen sulfide	0	1000	Metabolic byproduct	-
cpd_so3[e]	Sulfite	0	1000	Metabolic byproduct	-
cpd_tma[e]	Trimethylamine	0	1000	Metabolic byproduct	-
cpd_urdio[e]	Uranium dioxide	0	1000	Metabolic byproduct	-

cpd_urea[e]	Urea	0	1000	Metabolic byproduct	-
cpd_cobalt2[e]	Co2+	-1000	1000	Trace element	-
cpd_cu2[e]	Cu2+	-1000	1000	Trace element	-
cpd_fe2[e]	Fe2+	-1000	1000	Trace element	-
cpd_mn2[e]	Mn2+	-1000	1000	Trace element	-
cpd_mobd[e]	Molybdate	-1000	1000	Trace element	-
cpd_pmcoa[e]	Pimeloyl-CoA	-1000	1000	Vitamin precursor	-
cpd_cbl1[e]	Cob(I)alamin	-1000	1000	Vitamin solution	-

Supplemental Table S4. Maximum and minimum flux values obtained from flux variability analysis (FVA) corresponding to the simulation condition in Figure 4D. FVA was performed in the WP3 wild type model and the Δ*pta*, Δ*ackA*, and Δ*pta*Δ*ackA* mutant models with biomass production set to its maximum (Materials and Methods). Numbers in this table indicated raw values of the minimum and maximum fluxes before they were normalized by the biomass flux.

REACTION ID	WT		DPTA		DACK		DPTA/DACK	
	Lower	Upper	Lower	Upper	Lower	Upper	Lower	Upper
ATPS4R	1.723547	1.723547	0.462743	0.586943	0.201432	0.201432	0.201432	0.201432
FDH	10.046548	10.046548	6.302506	6.488806	2.662379	18.064684	2.662379	18.064684
NDH	7.109320	7.109320	9.918376	9.918376	2.526106	75.846249	2.526106	75.846249
PTAR	6.353348	6.353348	0.000000	0.000000	0.000000	0.000000	0.000000	0.000000
ACKR	12.445169	12.445169	12.972714	13.034814	0.000000	0.000000	0.000000	0.000000
PYK	6.257749	6.257749	6.184985	6.309184	3.286322	8.420424	3.286322	8.420424
XPK	6.091821	6.091821	12.972714	13.034814	0.000000	0.000000	0.000000	0.000000
CORE_BIOMASS	0.537444	0.537444	0.521138	0.521138	0.226851	0.226851	0.226851	0.226851

Appendix III: Data S1 for Manuscript II

Data S1 Table A: Comparison of overall WP2 GEM grow/no-growth predictions to experimentally confirmed growth supporting nutrients.

Table A: Comparison of overall WP2 GEM grow/no-growth predictions to experimentally confirmed growth supporting nutrients.			
Nutrient Condition	**Experimentally Confirmed Growth**	**Model Predicted Growth**	**Literature Support (PMID)**
Aerobic Conditions			
Acetate + O2	NG	G	17220442
Cellobiose + O2	NG	NG	17220442
Citrate + O2	G	G	17220442
D-Galactose + O2	NG	NG	17220442
D-Glucose + O2	NG	NG	17220442
Maltose + O2	NG	NG	17220442
N-acetyl-D-Glucosamine + O2	G	G	17220442
Sucrose + O2	G	G	17220442
D-Trehalose + O2	G	G	17220442
Anaerobic Conditions			
Lactate + Irone 3+	NG	NG	17220442
Lactate + TMAO	G	G	17220442
Lactate + DMSO	G	G	17220442
Lactate + Fumarate	NG	G	17220442
Lactate + Nitrate	G	G	17220442
Lactate + Nitrite	NG	NG	17220442

Data S1 Table B: Table showing differences between 4, 15 and 20 temperature-dependent models. The reactions are marked as being Expressed, if they were included in the model and all associated genes were above the expression threshold. Used below if they were kept in the final model so that biomass could be produced but were associated with genes that fell below the expression threshold. Below if they were associated with genes below the expression threshold and were not kept in the final model.

Reaction	Subsystem	in 4C Model	in 15C Model	in 20C Model	Reaction Name	Genes
ALAD_L	Alanine and Aspartate Metabolism	Expressed	Expressed	Expressed	L-alanine dehydrogenase	sps_RS05300
ALAGLYX	Alanine and Aspartate Metabolism	Expressed	Expressed	Expressed	Alanine-glyoxylate transaminase	sps_RS15405
ALAR	Alanine and Aspartate Metabolism	Used_Below	Used_Below	Expressed	alanine racemase	sps_RS25455
ALATA_L	Alanine and Aspartate Metabolism	Expressed	Expressed	Expressed	L-alanine transaminase	sps_RS03805
ALATRS	Alanine and Aspartate Metabolism	Expressed	Expressed	Expressed	Alanyl-tRNA synthetase	sps_RS20190
AMAA	Alanine and Aspartate Metabolism	Expressed	Expressed	Expressed	N-acetylmuramoyl-L-alanine amidase	sps_RS25025
ASNN	Alanine and Aspartate Metabolism	Expressed	Below	Expressed	L-asparaginase	sps_RS06280 or sps_RS03935

ASNS1	Alanine and Aspartate Metabolism	Expressed	Expressed	Expressed	asparagine synthase (glutamine-hydrolysing)	sps_RS02360
ASNTRS	Alanine and Aspartate Metabolism	Expressed	Expressed	Expressed	Asparaginyl-tRNA synthetase	sps_RS03690
ASP1DC	Alanine and Aspartate Metabolism	Expressed	Expressed	Expressed	aspartate 1-decarboxylase	Gap
ASPTA1	Alanine and Aspartate Metabolism	Expressed	Expressed	Expressed	aspartate transaminase	sps_RS04490 or sps_RS03990
ASPTRS	Alanine and Aspartate Metabolism	Expressed	Expressed	Expressed	Aspartyl-tRNA synthetase	sps_RS05760
A5PISO	Alternate Carbon Metabolism	Used_Below	Used_Below	Used_Below	arabinose-5-phosphate isomerase	sps_RS25600
ACCOAL	Alternate Carbon Metabolism	Used_Below	Below	Below	acetate-CoA ligase (ADP-forming)	sps_RS10210 and sps_RS02570
ACGAMK	Alternate Carbon Metabolism	Expressed	Expressed	Expressed	N-acetylglucosamine kinase	sps_RS11615
AEPPAT	Alternate Carbon Metabolism	Below	Below	Below	2-aminoethylphosphonate---pyruvate transaminase	sps_RS20360

AGDC	Alternate Carbon Metabolism	Expressed	Expressed	Expressed	N-acetylglucosamine-6-phosphate deacetylase	sps_RS11610
ALCD2x	Alternate Carbon Metabolism	Expressed	Expressed	Expressed	alcohol dehydrogenase (ethanol: NAD)	sps_RS03765
ALDD2x	Alternate Carbon Metabolism	Expressed	Expressed	Below	aldehyde dehydrogenase (acetaldehyde, NAD)	sps_RS01610
AMALT1	Alternate Carbon Metabolism	Expressed	Expressed	Expressed	Amylomaltase (maltotriose)	sps_RS11355
AMALT2	Alternate Carbon Metabolism	Expressed	Expressed	Expressed	Amylomaltase (maltotetraose)	sps_RS11355
AMALT3	Alternate Carbon Metabolism	Expressed	Expressed	Expressed	Amylomaltase (maltopentaose)	sps_RS11355
AMALT4	Alternate Carbon Metabolism	Expressed	Expressed	Expressed	Amylomaltase (maltohexaose)	sps_RS11355
BUTSUCCCOA	Alternate Carbon Metabolism	Expressed	Expressed	Expressed	Succinyl-CoA:butyrate-CoA transferase	sps_RS10260 and sps_RS10265
CHITINS	Alternate Carbon Metabolism	Below	Below	Below	chitinase	sps_RS12690
DNA_CUT	Alternate Carbon Metabolism	Below	Below	Below	DNA Hydrolase	sps_RS14030 or sps_RS07515
DRBK	Alternate Carbon	Expressed	Expressed	Expressed	Deoxyribokinase	sps_RS13530

	Metabolism					
DRPA	Alternate Carbon Metabolism	Expressed	Expressed	Expressed	deoxyribose-phosphate aldolase	sps_RS20880
FAO4	Alternate Carbon Metabolism	Expressed	Expressed	Expressed	Fatty acid oxidation (dodecanoate:ubiquinone) and swp_0034 and swp_0035)	(sps_RS06355 and sps_RS05895 and sps_RS00295 and sps_RS00300) or (sps_RS05895 and sps_RS23935 and sps_RS00295 and sps_RS00300)
FAO5	Alternate Carbon Metabolism	Expressed	Expressed	Expressed	Fatty acid oxidation (tetradecanoate:ubiquinone) and swp_0034 and swp_0035)	(sps_RS06355 and sps_RS05895 and sps_RS00295 and sps_RS00300) or (sps_RS05895 and sps_RS23935 and sps_RS00295 and sps_RS00300)
FAO6	Alternate Carbon Metabolism	Expressed	Expressed	Expressed	Fatty acid oxidation (hexadecanoate:ubiquinone) and swp_0034 and swp_0035)	(sps_RS06355 and sps_RS05895 and sps_RS00295 and sps_RS00300) or

						(sps_RS05895 and sps_RS23935 and sps_RS00295 and sps_RS00300)
FAO7	Alternate Carbon Metabolism	Expressed	Expressed	Expressed	Fatty acid oxidation (octadecanoate:ubiquinone) and swp_0034 and swp_0035)	(sps_RS06355 and sps_RS05895 and sps_RS00295 and sps_RS00300) or (sps_RS05895 and sps_RS23935 and sps_RS00295 and sps_RS00300)
FMNRDDMBZ	Alternate Carbon Metabolism	Below	Below	Below	5,6-dimethylbenzimidazole synthase	sps_RS01325
G3PD2	Alternate Carbon Metabolism	Expressed	Expressed	Expressed	glycerol-3-phosphate dehydrogenase (NADP)	sps_RS27670
G6PDA	Alternate Carbon Metabolism	Expressed	Expressed	Expressed	glucosamine-6-phosphate deaminase	sps_RS24130
GAL1PURI	Alternate Carbon Metabolism	Below	Below	Expressed	galactose-1-phosphate uridylyltransferase	sps_RS03510
GALACN	Alternate Carbon Metabolism	Below	Below	Below	Beta-galactosidase	sps_RS14390

GALKr	Alternate Carbon Metabolism	Expressed	Expressed	Expressed	galactokinase	sps_RS14400
GALU	Alternate Carbon Metabolism	Expressed	Expressed	Expressed	UTP-glucose-1-phosphate uridylyltransferase	sps_RS18075
GBEZ	Alternate Carbon Metabolism	Expressed	Expressed	Expressed	1,4-alpha-glucan branching enzyme	sps_RS11350
GLCGSD	Alternate Carbon Metabolism	Expressed	Below	Below	glucan 1,4-alpha-glucosidase	sps_RS03490
GLYCKb	Alternate Carbon Metabolism	Below	Below	Below	glycerate kinase	sps_RS09490
GLYK	Alternate Carbon Metabolism	Expressed	Expressed	Expressed	glycerol kinase	sps_RS16190
HMGDx	Alternate Carbon Metabolism	Expressed	Expressed	Expressed	S-(hydroxymethyl)glutathione dehydrogenase	sps_RS21145
HMGSs	Alternate Carbon Metabolism	Expressed	Below	Expressed	S-(hydroxymethyl)glutathione synthase	sps_RS24790 or sps_RS07340
HOXPRx	Alternate Carbon Metabolism	Expressed	Below	Below	2-hydroxy-3-oxopropionate reductase (NAD)	sps_RS06690
HPYRRx	Alternate Carbon Metabolism	Expressed	Expressed	Expressed	Hydroxypyruvate reductase	sps_RS22825

HPYRRy	Alternate Carbon Metabolism	Expressed	Expressed	Expressed	Hydroxypyruvate reductase	sps_RS22825
HXAD	Alternate Carbon Metabolism	Expressed	Expressed	Expressed	Hexosaminidase	sps_RS11620 or sps_RS08120
MCITD	Alternate Carbon Metabolism	Expressed	Below	Expressed	2-methylcitrate dehydratase	sps_RS09950
MCITS	Alternate Carbon Metabolism	Expressed	Expressed	Expressed	2-methylcitrate synthase	sps_RS09955
MEAMP1_GLU-ASP	Alternate Carbon Metabolism	Expressed	Expressed	Expressed	Dipeptide hydrolase	sps_RS10485 or sps_RS09500
MEAMP1_GLY-ASP	Alternate Carbon Metabolism	Expressed	Expressed	Expressed	methionyl aminopeptidase	sps_RS10485 or sps_RS09500
MEAMP1_GLY-GLU	Alternate Carbon Metabolism	Expressed	Expressed	Expressed	methionyl aminopeptidase	sps_RS10485 or sps_RS09500
MICITH	Alternate Carbon Metabolism	Expressed	Expressed	Expressed	2-methylisocitrate hydratase	sps_RS26425
MICITL	Alternate Carbon Metabolism	Expressed	Expressed	Expressed	methylisocitrate lyase	sps_RS09960
MLTAM	Alternate Carbon Metabolism	Below	Below	Below	Alpha-Amylase (maltotetraose)	sps_RS03475
MLTG1e	Alternate Carbon Metabolism	Below	Below	Below	glucoamylase (maltotriose)	sps_RS03280

MLTG2e	Alternate Carbon Metabolism	Below	Below	Below	glucoamylase (maltotetraose)	sps_RS03280
MLTG3e	Alternate Carbon Metabolism	Below	Below	Below	glucoamylase (maltopentaose)	sps_RS03280
MLTG4e	Alternate Carbon Metabolism	Below	Below	Below	glucoamylase (maltohexaose)	sps_RS03280
MLTG5e	Alternate Carbon Metabolism	Below	Below	Below	glucoamylase (maltoheptaose)	sps_RS03280
MLTS	Alternate Carbon Metabolism	Expressed	Below	Below	maltase	sps_RS03490
MLTSp	Alternate Carbon Metabolism	Expressed	Expressed	Expressed	maltase (periplasmic), Alpha glucosidase	sps_RS03315
OBTFL	Alternate Carbon Metabolism	Expressed	Expressed	Expressed	2-Oxobutanoate formate lyase	sps_RS17580 and sps_RS17575
PGLYCP	Alternate Carbon Metabolism	Expressed	Expressed	Expressed	phosphoglycolate phosphatase	sps_RS26595
PGMT	Alternate Carbon Metabolism	Expressed	Expressed	Expressed	phosphoglucomutase	sps_RS03845
PMANM	Alternate Carbon Metabolism	Expressed	Below	Expressed	phosphomannomutase	sps_RS09635 or sps_RS16065
PPM	Alternate Carbon Metabolism	Expressed	Expressed	Used_Below	phosphopentomutase	sps_RS20870

PPM2	Alternate Carbon Metabolism	Expressed	Expressed	Used_Below	phosphopentomutase (deoxyribose)	sps_RS20870
PULLNASE	Alternate Carbon Metabolism	Below	Below	Below	Neopullulanase	sps_RS03480
RBK	Alternate Carbon Metabolism	Expressed	Expressed	Expressed	ribokinase	sps_RS13530
SFGTH	Alternate Carbon Metabolism	Expressed	Expressed	Expressed	S-Formylglutathione hydralase	sps_RS21140
SPA	Alternate Carbon Metabolism	Expressed	Expressed	Expressed	serine-pyruvate aminotransferase,	sps_RS15405
UDPG4E	Alternate Carbon Metabolism	Expressed	Expressed	Expressed	UDPglucose 4-epimerase	sps_RS18080
UDPHEXURI	Alternate Carbon Metabolism	Below	Below	Expressed	UDP-glucose-hexose-1-phosphate uridylyltransferase	sps_RS03510
ICL	Anaplerotic Reactions	Expressed	Expressed	Expressed	isocitrate lyase	sps_RS03745
MALS	Anaplerotic Reactions	Expressed	Expressed	Expressed	malate synthase	sps_RS18985 or sps_RS03755 or sps_RS08860
ME2	Anaplerotic Reactions	Expressed	Expressed	Expressed	malic enzyme (NADP)	sps_RS21805 or sps_RS26375
PPC	Anaplerotic Reactions	Expressed	Expressed	Expressed	phosphoenolpyruvate	sps_RS26695

					carboxylase	
PPCK	Anaplerotic Reactions	Expressed	Expressed	Expressed	phosphoenolpyruvate carboxykinase	sps_RS26860
ABTA	Arginine and Proline Metabolism	Expressed	Expressed	Expressed	4-aminobutyrate transaminase	sps_RS13900
ACGK	Arginine and Proline Metabolism	Expressed	Expressed	Expressed	acetylglutamate kinase	sps_RS26680
ACGS	Arginine and Proline Metabolism	Expressed	Expressed	Expressed	N-acetylglutamate synthase	sps_RS16260
ACODA	Arginine and Proline Metabolism	Expressed	Expressed	Expressed	acetylornithine deacetylase	sps_RS26690
ACOTA	Arginine and Proline Metabolism	Expressed	Expressed	Expressed	acetylornithine transaminase	sps_RS24950
ADMDC	Arginine and Proline Metabolism	Expressed	Expressed	Expressed	Adenosylmethionine decarboxylase	sps_RS06620
AGMAHYD	Arginine and Proline Metabolism	Expressed	Expressed	Expressed	Agmatine ureohydrolase	sps_RS06615
AGPR	Arginine and Proline Metabolism	Expressed	Expressed	Expressed	N-acetyl-g-glutamyl-phosphate reductase	sps_RS26685
AMPTASEPG	Arginine and Proline Metabolism	Expressed	Below	Expressed	Aminopeptidase (pro-gly)	sps_RS02885

ARGDC	Arginine and Proline Metabolism	Expressed	Expressed	Expressed	arginine decarboxylase	sps_RS06625
ARGSL	Arginine and Proline Metabolism	Expressed	Expressed	Expressed	argininosuccinate lyase	sps_RS26665
ARGSS	Arginine and Proline Metabolism	Expressed	Expressed	Expressed	argininosuccinate synthase	sps_RS26670
ARGTRS	Arginine and Proline Metabolism	Expressed	Expressed	Expressed	Arginyl-tRNA synthetase	sps_RS26400
AST	Arginine and Proline Metabolism	Expressed	Expressed	Expressed	Arginine succinyltransferase	sps_RS24945
CBPS	Arginine and Proline Metabolism	Expressed	Expressed	Expressed	carbamoyl-phosphate synthase (glutamine-hydrolysing)	sps_RS21035 and sps_RS21030
G5SD	Arginine and Proline Metabolism	Expressed	Expressed	Expressed	glutamate-5-semialdehyde dehydrogenase	sps_RS21110
GGLUGABDH	Arginine and Proline Metabolism	Expressed	Expressed	Expressed	gammaglutamyl-gamma-aminobutyraldehyde dehydrogenase	sps_RS13905
GGLUGABH	Arginine and Proline Metabolism	Expressed	Expressed	Expressed	gammaglutamyl-gamma-aminobutyrate hydrolase	sps_RS12585

GGLUPTO	Arginine and Proline Metabolism	Below	Below	Below	gammaglutamyl putrescine oxidase	sps_RS12555
GGLUPTS	Arginine and Proline Metabolism	Expressed	Expressed	Expressed	gammaglutamyl putrescine synthetase	sps_RS12580
GLU5K	Arginine and Proline Metabolism	Expressed	Expressed	Expressed	glutamate 5-kinase	sps_RS21115
MTAN	Arginine and Proline Metabolism	Expressed	Expressed	Expressed	methylthioadenosine nucleosidase	sps_RS12090
OCBT	Arginine and Proline Metabolism	Expressed	Expressed	Expressed	ornithine carbamoyltransferase	sps_RS26675
ORNCD	Arginine and Proline Metabolism	Expressed	Used_Below	Expressed	ornithine cyclodeaminase	sps_RS21700 or sps_RS23625 or sps_RS05420
P5CD	Arginine and Proline Metabolism	Expressed	Expressed	Expressed	1-pyrroline-5-carboxylate dehydrogenase	sps_RS24730
P5CR	Arginine and Proline Metabolism	Expressed	Expressed	Expressed	pyrroline-5-carboxylate reductase	sps_RS11505
PRO1q	Arginine and Proline Metabolism	Expressed	Expressed	Expressed	proline oxidase	sps_RS24730
PROTRS	Arginine and Proline Metabolism	Expressed	Expressed	Expressed	Prolyl-tRNA synthetase	sps_RS10345

SADH	Arginine and Proline Metabolism	Expressed	Expressed	Expressed	Succinylarginine dihydrolase	sps_RS08145
SGDS	Arginine and Proline Metabolism	Expressed	Expressed	Expressed	Succinylglutamate desuccinylase	sps_RS03855
SGSAD	Arginine and Proline Metabolism	Expressed	Expressed	Expressed	Succinylglutamic semialdehyde dehydrogenase	sps_RS24940
SOTA	Arginine and Proline Metabolism	Expressed	Expressed	Expressed	Succinylornithine transaminase	sps_RS24950
SPMS	Arginine and Proline Metabolism	Used_Below	Used_Below	Expressed	spermidine synthase	sps_RS24680
SPRS	Arginine and Proline Metabolism	Below	Below	Expressed	spermine synthase	sps_RS24680
SSALx	Arginine and Proline Metabolism	Expressed	Expressed	Expressed	succinate-semialdehyde dehydrogenase (NAD)	sps_RS12605
Biomass_WP2	Biomass	Expressed	Expressed	Expressed	biomass 1gDW	Biomass
DNA_SYNTHESIS	Biomass	Expressed	Expressed	Expressed	DNA synthesis 1g	Biomass
GLYCOGEN_SYNTHESIS	Biomass	Expressed	Expressed	Expressed	Glycogen Synthesis WP2 (1g)	Biomass
LIPID_SYNTHESIS	Biomass	Expressed	Expressed	Expressed	Phospholipid Synthesis WP2 (1g)	Biomass

LPS_SYNTHESIS	Biomass	Expressed	Expressed	Expressed	LPS synthesis WP2 (1g)	Biomass
PASYN_WP2	Biomass	Expressed	Expressed	Expressed	Lipid Synthesis WP2 (1g)	Biomass
PEPTIDO_SYNTHESIS	Biomass	Expressed	Expressed	Expressed	peptidoglycan 1gDW	Biomass
PROT_SYNTHESIS	Biomass	Expressed	Expressed	Expressed	Protein synthesis 1g	Biomass
RNA_SYNTHESIS	Biomass	Expressed	Expressed	Expressed	RNA synthesis 1g	Biomass
TRACE_ELEMENTS	Biomass	Expressed	Expressed	Expressed	Trace Element Synthesis WP2 (1g)	Biomass
AACPS10	Cell Envelope Biosynthesis	Expressed	Below	Expressed	acyl-[acyl-carrier-protein] synthetase (n-C14:0)	sps_RS26765 and sps_RS06710
AACPS11	Cell Envelope Biosynthesis	Expressed	Below	Expressed	acyl-[acyl-carrier-protein] synthetase (n-C15:0)	sps_RS26765 and sps_RS06710
AACPS12	Cell Envelope Biosynthesis	Expressed	Below	Expressed	acyl-[acyl-carrier-protein] synthetase (n-C16:0)	sps_RS26765 and sps_RS06710
AACPS13	Cell Envelope Biosynthesis	Expressed	Below	Expressed	acyl-[acyl-carrier-protein] synthetase (n-C17:0)	sps_RS26765 and sps_RS06710
AACPS14	Cell Envelope Biosynthesis	Expressed	Below	Expressed	acyl-[acyl-carrier-protein] synthetase (n-C15:1)	sps_RS26765 and sps_RS06710
AACPS15	Cell Envelope	Expressed	Below	Expressed	acyl-[acyl-carrier-	sps_RS26765 and

	Biosynthesis				protein] synthetase (n-C17:1)	sps_RS06710
AACPS16	Cell Envelope Biosynthesis	Expressed	Below	Expressed	acyl-[acyl-carrier-protein] synthetase (n-C18:1)	sps_RS26765 and sps_RS06710
AACPS3	Cell Envelope Biosynthesis	Expressed	Below	Expressed	acyl-[acyl-carrier-protein] synthetase (n-C16:0)	sps_RS26765 and sps_RS06710
AACPS4	Cell Envelope Biosynthesis	Expressed	Below	Expressed	acyl-[acyl-carrier-protein] synthetase (n-C16:1)	sps_RS26765 and sps_RS06710
AACPS5	Cell Envelope Biosynthesis	Expressed	Below	Expressed	acyl-[acyl-carrier-protein] synthetase (n-C18:1)	sps_RS26765 and sps_RS06710
AACPS6	Cell Envelope Biosynthesis	Expressed	Below	Expressed	acyl-[acyl-carrier-protein] synthetase (n-C15:0)	sps_RS26765 and sps_RS06710
AACPS7	Cell Envelope Biosynthesis	Expressed	Below	Expressed	acyl-[acyl-carrier-protein] synthetase (n-C17:0)	sps_RS26765 and sps_RS06710
AACPS8	Cell Envelope Biosynthesis	Expressed	Below	Expressed	acyl-[acyl-carrier-protein] synthetase (n-C18:0)	sps_RS26765 and sps_RS06710
AACPS9	Cell Envelope Biosynthesis	Expressed	Below	Expressed	acyl-[acyl-carrier-protein] synthetase (n-C13:0)	sps_RS26765 and sps_RS06710
AACPSFA130OH	Cell Envelope	Expressed	Below	Expressed	acyl-[acyl-carrier-protein]	sps_RS26765 and

	Biosynthesis				synthetase (n-C14:0)	sps_RS06710
AACPSFA1718	Cell Envelope Biosynthesis	Expressed	Below	Expressed	acyl-[acyl-carrier-protein] synthetase (n-C14:0)	sps_RS26765 and sps_RS06710
AACPSFA1817	Cell Envelope Biosynthesis	Expressed	Below	Expressed	acyl-[acyl-carrier-protein] synthetase (n-C14:0)	sps_RS26765 and sps_RS06710
ACNAMS	Cell Envelope Biosynthesis	Expressed	Expressed	Expressed	N-acetylneuraminate synthase	sps_RS18415
ALAALA	Cell Envelope Biosynthesis	Expressed	Expressed	Expressed	D-alanine-D-alanine ligase (reversible)	sps_RS06170 or sps_RS21595
CDPG46D	Cell Envelope Biosynthesis	Expressed	Expressed	Expressed	CDP-glucose 4,6-dehydratase	sps_RS18335
CKDOAS	Cell Envelope Biosynthesis	Expressed	Expressed	Expressed	CMP-8-amino-3,8-dideoxy-D-manno-oct-2-ulosonic acid synthase	Gap
DAGK	Cell Envelope Biosynthesis	Expressed	Below	Expressed	diacylglycerol kinase	sps_RS06795
DASYN	Cell Envelope Biosynthesis	Used_Below	Used_Below	Used_Below	phosphatidate cytidylyltransferase	sps_RS10455
DMOCT	Cell Envelope Biosynthesis	Expressed	Expressed	Expressed	3-deoxy-manno-octulosonate	sps_RS03170

					cytidylyltransferase	
EDTXS5	Cell Envelope Biosynthesis	Used_Below	Used_Below	Expressed	Endotoxin Synthesis (lauroyl transferase)	sps_RS13825 and sps_RS06710
EDTXS6	Cell Envelope Biosynthesis	Used_Below	Expressed	Expressed	Endotoxin Synthesis (myristoyl transferase)	sps_RS06545 and sps_RS06710
G1PACT	Cell Envelope Biosynthesis	Expressed	Expressed	Expressed	glucosamine-1-phosphate N-acetyltransferase	sps_RS27830
G1PCT	Cell Envelope Biosynthesis	Expressed	Expressed	Below	glucose-1-phosphate cytidylyltransferase	sps_RS18340
G1PTMT	Cell Envelope Biosynthesis	Expressed	Below	Expressed	glucose-1-phosphate thymidylyltransferase	sps_RS18200
GF6PTA	Cell Envelope Biosynthesis	Below	Below	Below	glutamine-fructose-6-phosphate transaminase	sps_RS27815
GLUR	Cell Envelope Biosynthesis	Expressed	Expressed	Expressed	glutamate racemase	sps_RS26735
GMHEPAT	Cell Envelope Biosynthesis	Expressed	Expressed	Expressed	D-glycero-D-manno-hepose 1-phosphate adenyltransferase	sps_RS00805
GMHEPK	Cell Envelope Biosynthesis	Expressed	Expressed	Expressed	D-glycero-D-manno-heptose 7-phosphate kinase	sps_RS00805

GMHEPPA	Cell Envelope Biosynthesis	Expressed	Expressed	Expressed	D-glycero-D-manno-heptose 1,7-bisphosphate phosphatase	sps_RS16660
GPDDA2	Cell Envelope Biosynthesis	Expressed	Expressed	Expressed	Glycerophosphodiester phosphodiesterase (Glycerophosphoethanolamine)	sps_RS25085
GPDDA4	Cell Envelope Biosynthesis	Expressed	Expressed	Expressed	Glycerophosphodiester phosphodiesterase (Glycerophosphoglycerol)	sps_RS25085
KDOPP	Cell Envelope Biosynthesis	Expressed	Expressed	Expressed	3-deoxy-manno-octulosonate-8-phosphatase	sps_RS25605
KDOPS	Cell Envelope Biosynthesis	Expressed	Expressed	Expressed	2-dehydro-3-deoxy-phosphooctonate aldolase	sps_RS21375
LPADSS	Cell Envelope Biosynthesis	Expressed	Expressed	Expressed	Lipid A disaccaride synthase	sps_RS10415
LPSSYN_core	Cell Envelope Biosynthesis	Used_Below	Expressed	Expressed	LPS synthesis (general)	sps_RS00730
MAN1PT2	Cell Envelope	Expressed	Expressed	Expressed	mannose-1-phosphate	sps_RS16060

	Biosynthesis				guanylyltransferase (GDP)	
MI1PP	Cell Envelope Biosynthesis	Expressed	Expressed	Expressed	myo-inositol 1-phosphatase	sps_RS17735
MOAT3	Cell Envelope Biosynthesis	Used_Below	Used_Below	Used_Below	8-amino 3,8-dideoxy-D-manno-octulosonic acid transferase	sps_RS00725
PAP	Cell Envelope Biosynthesis	Used_Below	Used_Below	Used_Below	phosphatidic acid phosphatase	sps_RS15375
PAPPT3	Cell Envelope Biosynthesis	Used_Below	Expressed	Expressed	phospho-N-acetylmuramoyl-pentapeptide-transferase (meso-2,6-diaminopimelate)	sps_RS16150
PEPTIDOXe	Cell Envelope Biosynthesis	Expressed	Expressed	Expressed	Peptidoglyan subunit crosslinking reaction	Gap
PGAMT	Cell Envelope Biosynthesis	Used_Below	Expressed	Expressed	phosphoglucosamine mutase	sps_RS20975
PGPPH	Cell Envelope Biosynthesis	Used_Below	Used_Below	Used_Below	Phosphatidylglycerophosphate phosphohydrolase	sps_RS15375 or sps_RS20310
PGSA	Cell Envelope Biosynthesis	Used_Below	Used_Below	Used_Below	CDPdiacylglycerol:sn-glycerol-3-phosphate	sps_RS02985

					3-phosphatidyltransferase	
PPTGSe	Cell Envelope Biosynthesis	Expressed	Expressed	Expressed	Peptidoglycan subunit synthesis	Gap
PSD	Cell Envelope Biosynthesis	Expressed	Expressed	Expressed	Phosphatidylserine decarboxylase	sps_RS25070
PSSA	Cell Envelope Biosynthesis	Expressed	Expressed	Expressed	CDPdiacylglycerol-serine O-phosphatidyltransferase	sps_RS04060 or sps_RS21655
S7PI	Cell Envelope Biosynthesis	Expressed	Expressed	Expressed	sedoheptulose 7-phosphate isomerase	sps_RS26565 or sps_RS17375
TDP3AAAT	Cell Envelope Biosynthesis	Expressed	Expressed	Expressed	dTDP-3-amino-3,6-dideoxy-alpha-D-galactopyranose transaminase	sps_RS18350
TDPDRE	Cell Envelope Biosynthesis	Expressed	Expressed	Expressed	dTDP-4-dehydrorhamnose 3,5-epimerase	sps_RS00745
TDPDRR	Cell Envelope Biosynthesis	Expressed	Expressed	Expressed	dTDP-4-dehydrorhamnose reductase	sps_RS00735 or sps_RS14745
TDPGDH	Cell Envelope Biosynthesis	Expressed	Expressed	Expressed	dTDPglucose 4,6-dehydratase	sps_RS18385
TDSK	Cell Envelope Biosynthesis	Used_Below	Used_Below	Used_Below	Tetraacyldisaccharide 4'kinase	sps_RS08055

U23GAAT	Cell Envelope Biosynthesis	Expressed	Expressed	Expressed	UDP-3-O-(3-hydroxymyristoyl)glucosamine acyltransferase	sps_RS10430 and sps_RS06710
UAAGDS	Cell Envelope Biosynthesis	Expressed	Expressed	Expressed	UDP-N-acetylmuramoyl-L-alanyl-D-glutamyl-meso-2,6-diaminopimelate synthetase	sps_RS16160
UAGAAT	Cell Envelope Biosynthesis	Expressed	Expressed	Expressed	UDP-N-acetylglucosamine acyltransferase	sps_RS10420 and sps_RS06710
UAGCVT	Cell Envelope Biosynthesis	Expressed	Expressed	Expressed	UDP-N-acetylglucosamine 1-carboxyvinyltransferase	sps_RS25560
UAGDP	Cell Envelope Biosynthesis	Expressed	Expressed	Expressed	UDP-N-acetylglucosamine diphosphorylase	sps_RS27830
UAGPT3	Cell Envelope Biosynthesis	Expressed	Expressed	Expressed	UDP-N-acetylglucosamine-N-acetylmuramyl-(pentapeptide)pyrophosphoryl-undecaprenol N-acetylglucosamine transferase	sps_RS16135

UAMAGS	Cell Envelope Biosynthesis	Expressed	Expressed	Expressed	UDP-N-acetylmuramoyl-L-alanyl-D-glutamate synthetase	sps_RS16145
UAMAS	Cell Envelope Biosynthesis	Expressed	Expressed	Expressed	UDP-N-acetylmuramoyl-L-alanine synthetase	sps_RS16130
UAPGR	Cell Envelope Biosynthesis	Expressed	Used_Below	Used_Below	UDP-N-acetylenolpyruvoylglucosamine reductase	sps_RS01705
UDCPDP	Cell Envelope Biosynthesis	Used_Below	Used_Below	Expressed	undecaprenyl-diphosphatase	sps_RS12505
UGMDDS	Cell Envelope Biosynthesis	Expressed	Expressed	Expressed	UDP-N-acetylmuramoyl-L-alanyl-D-glutamyl-meso-2,6-diaminopimeloyl-D-alanyl-D-alanine synthetase	sps_RS16155
UHGADA	Cell Envelope Biosynthesis	Expressed	Expressed	Expressed	UDP-3-0-acyl N-acetylglucosamine deacetylase	sps_RS16110
USHD	Cell Envelope Biosynthesis	Expressed	Expressed	Expressed	UDP-sugar hydrolase	sps_RS09265
ACONT	Citrate Cycle (TCA)	Expressed	Expressed	Expressed	aconitase	sps_RS26425

AKGD	Citrate Cycle (TCA)	Expressed	Expressed	Expressed	2-oxoglutarate dehydrogenase	sps_RS26455 and sps_RS07975 and sps_RS07980
CS	Citrate Cycle (TCA)	Expressed	Expressed	Expressed	citrate synthase	sps_RS08005
FUM	Citrate Cycle (TCA)	Expressed	Expressed	Expressed	fumarase	sps_RS03715
ICDHxi	Citrate Cycle (TCA)	Expressed	Expressed	Expressed	isocitrate dehydrogenase (NAD)	sps_RS10985
ICDHy	Citrate Cycle (TCA)	Expressed	Expressed	Expressed	isocitrate dehydrogenase (NADP)	sps_RS02755
MDH	Citrate Cycle (TCA)	Expressed	Expressed	Expressed	malate dehydrogenase	sps_RS13275
SUCD7	Citrate Cycle (TCA)	Expressed	Expressed	Expressed	Succinate Dehydrogenase	sps_RS07985 and sps_RS07995 and sps_RS07990 and sps_RS08000
SUCOAS	Citrate Cycle (TCA)	Expressed	Expressed	Expressed	succinyl-CoA synthetase (ADP-forming)	sps_RS07965 and sps_RS07970
2MAHMP	Cofactor and Prosthetic Group Biosynthesis	Used_Below	Used_Below	Used_Below	2-Methyl-4-amino-5-hydroxymethylpyrimidine diphosphatase	sps_RS02745
4HBTE	Cofactor and Prosthetic	Expressed	Below	Expressed	4-hydroxybenzoyl-CoA	sps_RS20600

	Group Biosynthesis				thioesterase	
5DOAN	Cofactor and Prosthetic Group Biosynthesis	Expressed	Expressed	Expressed	5'-deoxyadenosine nuclosidase	sps_RS12090
ACBIPGT	Cofactor and Prosthetic Group Biosynthesis	Expressed	Below	Below	Adenosyl cobainamide GTP transferase	sps_RS23545
ACPS1	Cofactor and Prosthetic Group Biosynthesis	Expressed	Expressed	Expressed	acyl-carrier protein synthase	sps_RS11945 and sps_RS06710
ACPSc	Cofactor and Prosthetic Group Biosynthesis	Expressed	Expressed	Expressed	[acyl-carrier-protein] phosphodiesterase	sps_RS17800 and sps_RS06710
ADCL	Cofactor and Prosthetic Group Biosynthesis	Expressed	Expressed	Expressed	4-amino-4-deoxychorismate lyase	sps_RS06845 or sps_RS06840
ADCOBAK	Cofactor and Prosthetic Group Biosynthesis	Expressed	Below	Below	Adenosyl cobinamide kinase	sps_RS23545
ADCOBAS	Cofactor and Prosthetic Group Biosynthesis	Below	Below	Below	adenosylcobinamide-phosphate synthase	sps_RS12095

ADCOBHEXS	Cofactor and Prosthetic Group Biosynthesis	Below	Below	Below	adenosylcobyric acid synthase	sps_RS23540
ADCS	Cofactor and Prosthetic Group Biosynthesis	Used_Below	Used_Below	Used_Below	4-amino-4-deoxychorismate synthase	sps_RS03710 and sps_RS24965
ALATA_D2	Cofactor and Prosthetic Group Biosynthesis	Expressed	Expressed	Expressed	D-alanine transaminase	sps_RS20350 or sps_RS11430
ALATA_L2	Cofactor and Prosthetic Group Biosynthesis	Expressed	Expressed	Expressed	alanine transaminase	sps_RS20350 or sps_RS11430
AMAOT	Cofactor and Prosthetic Group Biosynthesis	Used_Below	Used_Below	Expressed	adenosylmethionine-8-amino-7-oxononanoate transaminase	sps_RS07865
AMMQT7_2	Cofactor and Prosthetic Group Biosynthesis	Expressed	Expressed	Expressed	S-adenosylmethione:2-demthylmenaquinone methyltransferase (menaquinone 7)	sps_RS15015
AMPMS2	Cofactor and Prosthetic Group Biosynthesis	Expressed	Used_Below	Expressed	4-amino-2-methyl-5-phosphomethylpyrimidine synthetase	sps_RS05845

AOXS	Cofactor and Prosthetic Group Biosynthesis	Used_Below	Used_Below	Expressed	8-amino-7-oxononanoate synthase	sps_RS07855
APRAUR	Cofactor and Prosthetic Group Biosynthesis	Expressed	Expressed	Expressed	5-amino-6-(5-phosphoribosylamino) uracil reductase	sps_RS20340
ASPO3	Cofactor and Prosthetic Group Biosynthesis	Expressed	Expressed	Expressed	L-aspartate oxidase	sps_RS12000
ASPO5	Cofactor and Prosthetic Group Biosynthesis	Expressed	Expressed	Expressed	L-aspartate oxidase	sps_RS12000
ASPO6	Cofactor and Prosthetic Group Biosynthesis	Expressed	Expressed	Expressed	L-aspartate oxidase	sps_RS12000
ASPO8	Cofactor and Prosthetic Group Biosynthesis	Expressed	Expressed	Expressed	L-aspartate oxidase	sps_RS12000
ASPO9	Cofactor and Prosthetic Group Biosynthesis	Expressed	Expressed	Expressed	L-aspartate oxidase	sps_RS12000
BTS4	Cofactor and Prosthetic Group	Expressed	Expressed	Expressed	biotin synthase condensed reaction	sps_RS07860 and sps_RS17715

	Biosynthesis					
CBIAT	Cofactor and Prosthetic Group Biosynthesis	Below	Below	Below	Cobinamide adenyltransferase	sps_RS23535
CBLAT	Cofactor and Prosthetic Group Biosynthesis	Used_Below	Used_Below	Used_Below	cob(I)alamin adenosyltransferase	sps_RS23535
CDPMEK	Cofactor and Prosthetic Group Biosynthesis	Expressed	Expressed	Expressed	4-(cytidine 5'-diphospho)-2-C-methyl-D-erythritol kinase	sps_RS21425
CHOLDH1	Cofactor and Prosthetic Group Biosynthesis	Expressed	Below	Below	choline dehydrogenase	sps_RS17440
CHOLDH2	Cofactor and Prosthetic Group Biosynthesis	Expressed	Below	Below	choline dehydrogenase	sps_RS17440
CHOLDH3	Cofactor and Prosthetic Group Biosynthesis	Expressed	Below	Below	choline dehydrogenase	sps_RS17440
CHOLDH4	Cofactor and Prosthetic Group Biosynthesis	Expressed	Below	Below	choline dehydrogenase	sps_RS17440

CHOLDH5	Cofactor and Prosthetic Group Biosynthesis	Expressed	Below	Below	choline dehydrogenase	sps_RS17440
CHRPL	Cofactor and Prosthetic Group Biosynthesis	Used_Below	Used_Below	Used_Below	chorismate pyruvate lyase	sps_RS27220
COBPS	Cofactor and Prosthetic Group Biosynthesis	Below	Below	Below	cobalamin-5'-phosphate synthase	sps_RS23550
CPPPGO	Cofactor and Prosthetic Group Biosynthesis	Expressed	Expressed	Expressed	coproporphyrinogen oxidase	sps_RS00400
CPPPGOAN	Cofactor and Prosthetic Group Biosynthesis	Expressed	Expressed	Expressed	Oxygen Independent coproporphyrinogen-III oxidase	sps_RS00660 or sps_RS27115
DB4PS	Cofactor and Prosthetic Group Biosynthesis	Expressed	Expressed	Expressed	3,4-Dihydroxy-2-butanone-4-phosphate synthase	sps_RS20330 or sps_RS26910
DBTSr	Cofactor and Prosthetic Group Biosynthesis	Expressed	Expressed	Expressed	dethiobiotin synthase	sps_RS07845
DHFR	Cofactor and Prosthetic	Expressed	Used_Below	Used_Below	dihydrofolate reductase	sps_RS13240

	Group Biosynthesis					
DHFS	Cofactor and Prosthetic Group Biosynthesis	Expressed	Expressed	Expressed	dihydrofolate synthase	sps_RS08600
DHNAOT7	Cofactor and Prosthetic Group Biosynthesis	Expressed	Expressed	Expressed	1,4-dihydroxy-2-naphthoate octaprenyltransferase	sps_RS10130
DHNPA	Cofactor and Prosthetic Group Biosynthesis	Expressed	Used_Below	Used_Below	dihydroneopterin aldolase	sps_RS12515
DHPPDA2	Cofactor and Prosthetic Group Biosynthesis	Expressed	Expressed	Expressed	diaminohydroxyphosphoribosylaminopyrimidine deaminase	sps_RS20340
DHPRx	Cofactor and Prosthetic Group Biosynthesis	Expressed	Expressed	Expressed	dihydropteridine reductase	sps_RS22440
DHPS3	Cofactor and Prosthetic Group Biosynthesis	Used_Below	Expressed	Expressed	dihydropteroate synthase	sps_RS20980
DHPTPE	Cofactor and Prosthetic Group Biosynthesis	Expressed	Expressed	Expressed	Dihydroneopterin triphosphate 2'-epimerase	sps_RS17620

DMATT	Cofactor and Prosthetic Group Biosynthesis	Expressed	Expressed	Expressed	dimethylallyltranstransferase	sps_RS11035
DMPPS	Cofactor and Prosthetic Group Biosynthesis	Expressed	Expressed	Expressed	1-hydroxy-2-methyl-2-(E)-butenyl 4-diphosphate reductase (dmpp)	sps_RS11705
DMQMT	Cofactor and Prosthetic Group Biosynthesis	Expressed	Expressed	Expressed	3-Dimethylubiquinonol 3-methyltransferase	sps_RS03975
DNMPPA	Cofactor and Prosthetic Group Biosynthesis	Expressed	Expressed	Expressed	Dihydroneopterin monophosphate dephosphorylase	Gap
DNTPPA	Cofactor and Prosthetic Group Biosynthesis	Expressed	Expressed	Expressed	Dihydroneopterin triphosphate pyrophosphatase	Gap
DPCOAK	Cofactor and Prosthetic Group Biosynthesis	Expressed	Expressed	Expressed	dephospho-CoA kinase	sps_RS26510
DPR	Cofactor and Prosthetic Group Biosynthesis	Expressed	Expressed	Expressed	2-dehydropantoate 2-reductase	sps_RS15440 or sps_RS21335
DXPRI	Cofactor and Prosthetic	Expressed	Expressed	Expressed	1-deoxy-D-xylulose-5-	sps_RS10450

	Group Biosynthesis				phosphate reductoisomerase	
DXPS	Cofactor and Prosthetic Group Biosynthesis	Expressed	Expressed	Expressed	1-deoxy-D-xylulose 5-phosphate synthase	sps_RS11040
E4PD	Cofactor and Prosthetic Group Biosynthesis	Expressed	Expressed	Expressed	Erythrose 4-phosphate dehydrogenase	sps_RS12990
FCLT	Cofactor and Prosthetic Group Biosynthesis	Expressed	Expressed	Expressed	Heme B synthesis reaction	sps_RS08165
FMNAT	Cofactor and Prosthetic Group Biosynthesis	Expressed	Expressed	Expressed	FMN adenylyltransferase	sps_RS11725
FMNRx	Cofactor and Prosthetic Group Biosynthesis	Expressed	Expressed	Expressed	FMN reductase (NADH dependent)	sps_RS15800
FRTT	Cofactor and Prosthetic Group Biosynthesis	Expressed	Expressed	Expressed	farnesyltranstransferase	sps_RS13270
G1SATi	Cofactor and Prosthetic Group Biosynthesis	Expressed	Expressed	Expressed	glutamate-1-semialdehyde aminotransferase	sps_RS12460 or sps_RS22475

GGTT	Cofactor and Prosthetic Group Biosynthesis	Expressed	Expressed	Expressed	geranylgeranyltranstransferase	sps_RS13270
GLUCYSL	Cofactor and Prosthetic Group Biosynthesis	Expressed	Expressed	Expressed	glutamate-cysteine ligase	sps_RS20075
GRTT	Cofactor and Prosthetic Group Biosynthesis	Expressed	Expressed	Expressed	geranyltranstransferase	sps_RS11035
GTHRD	Cofactor and Prosthetic Group Biosynthesis	Expressed	Expressed	Expressed	glutathione-disulfide reductase	sps_RS00900
GTHS	Cofactor and Prosthetic Group Biosynthesis	Expressed	Expressed	Expressed	glutathione synthase	sps_RS14275
GTPCI	Cofactor and Prosthetic Group Biosynthesis	Expressed	Expressed	Expressed	GTP cyclohydrolase I	sps_RS16300
GTPCII	Cofactor and Prosthetic Group Biosynthesis	Expressed	Expressed	Expressed	GTP cyclohydrolase II	sps_RS20330 or sps_RS08895
HBZOPT	Cofactor and Prosthetic Group	Expressed	Expressed	Expressed	4-hydroxybenzoate	sps_RS15480

	Biosynthesis				octaprenyltransferase	
HEMEOS	Cofactor and Prosthetic Group Biosynthesis	Expressed	Expressed	Expressed	Heme O synthase	sps_RS01260 or sps_RS27785
HEPTT	Cofactor and Prosthetic Group Biosynthesis	Expressed	Expressed	Expressed	trans-heptaprenyltranstransferase	sps_RS13270
HEXTT	Cofactor and Prosthetic Group Biosynthesis	Expressed	Expressed	Expressed	trans-hexaprenyltranstransferase	sps_RS13270
HMBS	Cofactor and Prosthetic Group Biosynthesis	Expressed	Expressed	Expressed	hydroxymethylbilane synthase	sps_RS15205
HPPK	Cofactor and Prosthetic Group Biosynthesis	Expressed	Expressed	Expressed	2-amino-4-hydroxy-6-hydroxymethyldihydropteridine diphosphokinase	sps_RS12510 or sps_RS24490
HTHBPD	Cofactor and Prosthetic Group Biosynthesis	Expressed	Expressed	Expressed	4a-hydroxytetrahydrobiopterin dehydratase	sps_RS18065
ICHORSi	Cofactor and Prosthetic Group Biosynthesis	Expressed	Expressed	Expressed	Isochorismate Synthase	sps_RS00880

IPDPS	Cofactor and Prosthetic Group Biosynthesis	Expressed	Expressed	Expressed	1-hydroxy-2-methyl-2-(E)-butenyl 4-diphosphate reductase (ipdp)	sps_RS11705
MECDPDH	Cofactor and Prosthetic Group Biosynthesis	Expressed	Expressed	Expressed	2C-methyl-D-erythritol 2,4 cyclodiphosphate dehydratase	sps_RS18905 and sps_RS03820
MECDPS	Cofactor and Prosthetic Group Biosynthesis	Expressed	Used_Below	Used_Below	2-C-methyl-D-erythritol 2,4-cyclodiphosphate synthase	sps_RS20235
MEPCT	Cofactor and Prosthetic Group Biosynthesis	Used_Below	Used_Below	Used_Below	2-C-methyl-D-erythritol 4-phosphate cytidylyltransferase	sps_RS20240
MOHMT	Cofactor and Prosthetic Group Biosynthesis	Expressed	Expressed	Expressed	3-methyl-2-oxobutanoate hydroxymethyltransferase	sps_RS24495
NADK	Cofactor and Prosthetic Group Biosynthesis	Expressed	Expressed	Expressed	NAD kinase	sps_RS11050 or sps_RS08730
NADS1	Cofactor and Prosthetic Group	Expressed	Used_Below	Used_Below	NAD synthase (nh4)	sps_RS02135

	Biosynthesis					
NMNAT	Cofactor and Prosthetic Group Biosynthesis	Below	Below	Below	nicotinamide-nucleotide adenylyltransferase	sps_RS21560
NNAT	Cofactor and Prosthetic Group Biosynthesis	Used_Below	Used_Below	Used_Below	nicotinate-nucleotide adenylyltransferase	sps_RS21560
NNDMBRT	Cofactor and Prosthetic Group Biosynthesis	Below	Below	Below	nicotinate-nucleotide-dimethylbenzimidazole phosphoribosyltransferase	sps_RS23555
NNDPR	Cofactor and Prosthetic Group Biosynthesis	Expressed	Expressed	Expressed	nicotinate-nucleotide diphosphorylase (carboxylating)	sps_RS26485
NPHS	Cofactor and Prosthetic Group Biosynthesis	Expressed	Expressed	Expressed	naphthoate synthase	sps_RS27755
OHPBAT	Cofactor and Prosthetic Group Biosynthesis	Expressed	Expressed	Expressed	O-Phospho-4-hydroxy-L-threonine:2-oxoglutarate aminotransferase	sps_RS03985
OHPHM	Cofactor and	Expressed	Expressed	Expressed	3-demethylu	sps_RS03975

	Prosthetic Group Biosynthesis				biquinol 3-O-methyltransferase	
OMBZLM	Cofactor and Prosthetic Group Biosynthesis	Expressed	Expressed	Expressed	2-Octaprenyl-6-methoxy-benzoquinol methylase	sps_RS15015
OMMBLHX	Cofactor and Prosthetic Group Biosynthesis	Expressed	Expressed	Expressed	2-Octaprenyl-3-methyl-6-methoxy-1,4-benzoquinol hydroxylase	sps_RS21500
OMMBLHXAN	Cofactor and Prosthetic Group Biosynthesis	Expressed	Expressed	Expressed	2-Octaprenyl-3-methyl-6-methoxy-1,4-benzoquinol hydroxylase Anaerobic	Gap
OMPHHX	Cofactor and Prosthetic Group Biosynthesis	Expressed	Expressed	Expressed	2-octaprenyl-6-methoxyphenol hydroxylase	sps_RS23850
OMPHHXAN	Cofactor and Prosthetic Group Biosynthesis	Expressed	Expressed	Expressed	2-octaprenyl-6-methoxyphenol hydroxylas	Gap

					e Anaerobic	
OPHBDC	Cofactor and Prosthetic Group Biosynthesis	Expressed	Expressed	Expressed	3-octaprenyl-4-hydroxybenzoate carboxy-lyase	sps_RS24535 or sps_RS15795
OPHHX	Cofactor and Prosthetic Group Biosynthesis	Expressed	Expressed	Expressed	2-Octaprenylphenol hydroxylase	sps_RS15025
OPHHXAN	Cofactor and Prosthetic Group Biosynthesis	Expressed	Expressed	Expressed	2-Octaprenylphenol hydroxylase Anaerobic	Gap
OXGDC2	Cofactor and Prosthetic Group Biosynthesis	Expressed	Expressed	Expressed	2-oxoglutarate decarboxylase	sps_RS01485
PANTS	Cofactor and Prosthetic Group Biosynthesis	Expressed	Expressed	Expressed	pantothenate synthase	sps_RS24500
PDX5PO	Cofactor and Prosthetic Group Biosynthesis	Expressed	Expressed	Expressed	pyridoxine 5'-phosphate oxidase	sps_RS06610
PDX5PS	Cofactor and Prosthetic Group Biosynthesis	Expressed	Expressed	Expressed	Pyridoxine 5'-phosphate synthase	sps_RS11950 and sps_RS22860

PERD	Cofactor and Prosthetic Group Biosynthesis	Expressed	Expressed	Expressed	Erythronate 4-phosphate (4per) dehydrogenase	sps_RS08620
PMDPHT	Cofactor and Prosthetic Group Biosynthesis	Expressed	Expressed	Expressed	pyrimidine phosphatase	Gap
PMPK	Cofactor and Prosthetic Group Biosynthesis	Below	Below	Below	phosphomethylpyrimidine kinase	sps_RS05840
PNTK	Cofactor and Prosthetic Group Biosynthesis	Expressed	Expressed	Expressed	pantothenate kinase	sps_RS01715
PPBNGS	Cofactor and Prosthetic Group Biosynthesis	Expressed	Expressed	Expressed	porphobilinogen synthase	sps_RS15060
PPCDC	Cofactor and Prosthetic Group Biosynthesis	Expressed	Expressed	Expressed	phosphopantothenoylcysteine decarboxylase	sps_RS16280
PPNCL	Cofactor and Prosthetic Group Biosynthesis	Expressed	Expressed	Expressed	phosphopantothenate-cysteine ligase	sps_RS16280
PPPGFUM	Cofactor and Prosthetic Group	Expressed	Expressed	Expressed	protoporphyrinogen synthesis anaerobic	sps_RS00330 or sps_RS00320 or

	Biosynthesis					sps_RS13700
PPPGMEN	Cofactor and Prosthetic Group Biosynthesis	Expressed	Expressed	Expressed	protoporphyrinogen synthesis anaerobic	sps_RS00330 or sps_RS00320 or sps_RS13700
PPPGNO3	Cofactor and Prosthetic Group Biosynthesis	Expressed	Expressed	Expressed	protoporphyrinogen synthesis anaerobic	sps_RS00330 or sps_RS00320 or sps_RS13700
PPPGO	Cofactor and Prosthetic Group Biosynthesis	Expressed	Expressed	Expressed	protoporphyrinogen oxidase	sps_RS00330 or sps_RS00320 or sps_RS13700
PPTT	Cofactor and Prosthetic Group Biosynthesis	Expressed	Expressed	Expressed	trans-pentaprenyltranstransferase	sps_RS13270
PTPATi	Cofactor and Prosthetic Group Biosynthesis	Expressed	Expressed	Expressed	pantetheine-phosphate adenylyltransferase	sps_RS00810
PYAM5PO	Cofactor and Prosthetic Group Biosynthesis	Expressed	Expressed	Expressed	pyridoxamine-phosphate oxidase	sps_RS06610
PYDXL5PSYN	Cofactor and Prosthetic Group Biosynthesis	Expressed	Expressed	Expressed	Pyridoxal 5'-phosphate synthase	Gap
QULNS	Cofactor and	Expressed	Expressed	Expressed	quinolinate synthase	sps_RS03875

	Prosthetic Group Biosynthesis					
RBFK	Cofactor and Prosthetic Group Biosynthesis	Expressed	Expressed	Expressed	riboflavin kinase	sps_RS11725
RBFSa	Cofactor and Prosthetic Group Biosynthesis	Expressed	Used_Below	Expressed	6,7-dimethyl-8-ribitylluma zine synthase	sps_RS05345 and sps_RS20325
RBFSb	Cofactor and Prosthetic Group Biosynthesis	Expressed	Expressed	Expressed	riboflavin synthase	sps_RS20335
RBZP	Cofactor and Prosthetic Group Biosynthesis	Below	Below	Below	alpha-ribazole-5-phosphatase	sps_RS23570
SHCHCS2	Cofactor and Prosthetic Group Biosynthesis	Expressed	Expressed	Expressed	2-succinyl-6-hydroxy-2,4-cyclohexadiene 1-carboxylate synthase	sps_RS01485 or sps_RS01480
SHCHD2	Cofactor and Prosthetic Group Biosynthesis	Expressed	Expressed	Expressed	sirohydrochlorin dehydrogenase (NAD)	sps_RS17765
SHCHF	Cofactor and Prosthetic Group	Expressed	Expressed	Expressed	sirohydrochlorin ferrochetalase	sps_RS17765

	Biosynthesis					
SUCBZL	Cofactor and Prosthetic Group Biosynthesis	Used_Below	Used_Below	Used_Below	o-succinylbenzoate-CoA ligase	sps_RS01470
SUCBZS	Cofactor and Prosthetic Group Biosynthesis	Used_Below	Used_Below	Used_Below	O-succinylbenzoate-CoA synthase	sps_RS01475
TDP	Cofactor and Prosthetic Group Biosynthesis	Below	Below	Below	Thiamin pyrophosphatase	sps_RS02745
THZPSN	Cofactor and Prosthetic Group Biosynthesis	Used_Below	Used_Below	Used_Below	thiazole phosphate synthesis	sps_RS17715 and sps_RS05835 and sps_RS05825 and sps_RS05830 and sps_RS11015 and sps_RS05820
TMPKr	Cofactor and Prosthetic Group Biosynthesis	Expressed	Used_Below	Used_Below	thiamine-phosphate kinase	sps_RS20315
TMPPP	Cofactor and Prosthetic Group Biosynthesis	Used_Below	Used_Below	Used_Below	thiamine-phosphate diphosphorylase	sps_RS05840
UDCPDPS	Cofactor and	Used_Below	Used_Below	Used_Below	Undecaprenyl	sps_RS10460

	Prosthetic Group Biosynthesis				diphosphate synthase	
UPP3MT	Cofactor and Prosthetic Group Biosynthesis	Expressed	Expressed	Expressed	uroporphyrinogen methyltransferase	sps_RS15215 or sps_RS13735
UPP3S	Cofactor and Prosthetic Group Biosynthesis	Expressed	Expressed	Expressed	uroporphyrinogen-III synthase	sps_RS15210
UPPDC1	Cofactor and Prosthetic Group Biosynthesis	Expressed	Expressed	Expressed	uroporphyrinogen decarboxylase (uroporphyrinogen III)	sps_RS15715
ADSK	Cysteine Metabolism	Expressed	Expressed	Expressed	adenylyl-sulfate kinase	sps_RS18215
AMPTASECG	Cysteine Metabolism	Expressed	Below	Expressed	Aminopeptidase (cys-gly)	sps_RS02885
ASPTA4	Cysteine Metabolism	Expressed	Expressed	Expressed	aspartate transaminase	sps_RS04490 or sps_RS03990
BPNT	Cysteine Metabolism	Expressed	Expressed	Expressed	3',5'-bisphosphate nucleotidase	sps_RS26770
CYSS	Cysteine Metabolism	Expressed	Expressed	Expressed	cysteine synthase	sps_RS17470 or sps_RS03160 or sps_RS05610

CYSTL	Cysteine Metabolism	Expressed	Expressed	Expressed	cystathionine b-lyase	sps_RS02815
CYSTRS	Cysteine Metabolism	Expressed	Expressed	Expressed	Cysteinyl-tRNA synthetase	sps_RS09255
PAPSR	Cysteine Metabolism	Expressed	Expressed	Expressed	phosphoadenylyl-sulfate reductase (thioredoxin)	sps_RS13780
SADT2	Cysteine Metabolism	Expressed	Expressed	Expressed	sulfate adenylyltransferase	sps_RS18225 and sps_RS18235
SLCYSS	Cysteine Metabolism	Expressed	Expressed	Expressed	O-acetyl-L-serine sulfhydrylase	sps_RS14565
SULR	Cysteine Metabolism	Expressed	Expressed	Expressed	sulfite reductase (NADPH2)	sps_RS13785 and sps_RS13790
ARSRD2	Energy Metabolism	Below	Below	Below	arsenate reductase (glutaredoxin)	sps_RS02560 and sps_RS03080
ATPS4r	Energy Metabolism	Expressed	Expressed	Expressed	ATP synthase (four protons for one ATP) and swp_5161	sps_RS27845 and sps_RS27850 and sps_RS27855 and sps_RS27860 and sps_RS27865 and sps_RS27870 and sps_RS27875 and sps_RS27885 and sps_RS27880

CYCPOe	Energy Metabolism	Expressed	Below	Below	cytochrome-c peroxidase	sps_RS07025 or sps_RS24825
CYOO2	Energy Metabolism	Expressed	Expressed	Expressed	cytochrome-c oxidase (2 protons translocated) and swp_2572)	(sps_RS01285 and sps_RS01295 and sps_RS01300) or (sps_RS04545 and sps_RS04550 and sps_RS04555 and sps_RS04560)
CYOR7	Energy Metabolism	Expressed	Expressed	Expressed	cytochrome-c reductase (ubiquinol 8: 4 protons translocated)	sps_RS24990 and sps_RS24980 and sps_RS24985
CYTBD	Energy Metabolism	Expressed	Expressed	Expressed	cytochrome oxidase bd (ubiquinol-8: 2 protons)	sps_RS18840 and sps_RS18835
CYTBO3_4	Energy Metabolism	Below	Below	Below	cytochrome bo3 ubiquinol oxidase	sps_RS27800 and sps_RS27795 and sps_RS27790 and sps_RS27805 and sps_RS00035
FDH10	Energy Metabolism	Expressed	Expressed	Expressed	Formate Dehydrogenase (methylme	(sps_RS27125 and sps_RS27130 and

					naquinone-7: 1 protons)	sps_RS27120 and sps_RS27195) or (sps_RS27155 and sps_RS27160 and sps_RS27165 and sps_RS27195)
FDH9	Energy Metabolism	Expressed	Expressed	Expressed	Formate Dehydrogenase (menaquinone-7: 1 protons)	(sps_RS27125 and sps_RS27130 and sps_RS27120 and sps_RS27195) or (sps_RS27155 and sps_RS27160 and sps_RS27165 and sps_RS27195)
FNOR	Energy Metabolism	Expressed	Expressed	Expressed	ferredoxin-NADP reductase	sps_RS22515 and sps_RS03820
FRD10	Energy Metabolism	Used_Below	Expressed	Expressed	succinate dehydrogenase (menaquinol 7:0 proton)	sps_RS15135 and sps_RS15130 and sps_RS15140 and sps_RS15145
FRD11	Energy Metabolism	Below	Expressed	Expressed	succinate dehydrogenase (methylmenaquinol 7: 0proton)	sps_RS15135 and sps_RS15130 and sps_RS15140 and

						sps_RS15145
FRD8	Energy Metabolism	Below	Below	Below	succinate dehydrogenase (menaquinol 7:0 proton)	sps_RS01395 and sps_RS24315
FRD9	Energy Metabolism	Below	Below	Below	succinate dehydrogenase (methylmenaquinol 7:0proton)	sps_RS01395 and sps_RS24315
G3PD4	Energy Metabolism	Expressed	Below	Expressed	glycerol-3-phosphate dehydrogenase (menaquinone 7)	sps_RS24175
G3PD8	Energy Metabolism	Expressed	Below	Expressed	glycerol-3-phosphate dehydrogenase (methylmenaquinone 7)	sps_RS24175
GSHPO	Energy Metabolism	Expressed	Below	Below	glutathione peroxidase	sps_RS11315
NADH11	Energy Metabolism	Below	Used_Below	Used_Below	NADH dehydrogenase (ubiquinone-8 and 4 protons)	sps_RS17485 and sps_RS17490 and sps_RS17495 and sps_RS17500 and sps_RS17505 and sps_RS17510 and sps_RS17515 and sps_RS17520 and

						sps_RS17525 and sps_RS17530 and (sps_RS02420 or sps_RS02430) and sps_RS17540 and sps_RS17545
NADH12	Energy Metabolism	Expressed	Expressed	Expressed	NADH dehydrogenase (ubiquinone-8)	sps_RS06415
NADH13	Energy Metabolism	Below	Used_Below	Used_Below	NADH dehydrogenase (menaquinone-7 and 4 protons)	sps_RS17485 and sps_RS17490 and sps_RS17495 and sps_RS17500 and sps_RS17505 and sps_RS17510 and sps_RS17515 and sps_RS17520 and sps_RS17525 and sps_RS17530 and (sps_RS02420 or sps_RS02430) and sps_RS17540 and sps_RS17545

NADH14	Energy Metabolism	Expressed	Expressed	Expressed	NADH dehydrogenase (methylmenaquinone 7 & no proton)	sps_RS06415
NADH16	Energy Metabolism	Below	Below	Below	NADH dehydrogenase (methylmenaquinone-7 and 4 protons)	sps_RS17485 and sps_RS17490 and sps_RS17495 and sps_RS17500 and sps_RS17505 and sps_RS17510 and sps_RS17515 and sps_RS17520 and sps_RS17525 and sps_RS17530 and (sps_RS02420 or sps_RS02430) and sps_RS17540 and sps_RS17545
NADH4	Energy Metabolism	Expressed	Expressed	Expressed	NADH dehydrogenase (Menaquinone 7 & no proton)	sps_RS06415
NH4HNADOR	Energy Metabolism	Below	Below	Below	ammonium-hydroxide: NAD+	sps_RS07795 and sps_RS07800

					oxidoreductase	
NH4HNADPOR	Energy Metabolism	Below	Below	Below	ammonium-hydroxide:NADP+ oxidoreductase	sps_RS07795 and sps_RS07800
NODOx	Energy Metabolism	Expressed	Expressed	Expressed	nitric oxide dioxygenase	sps_RS13200
NODOy	Energy Metabolism	Expressed	Expressed	Expressed	nitric oxide dioxygenase	sps_RS13200
NTR4	Energy Metabolism	Expressed	Expressed	Expressed	nitrate reductase	((sps_RS14135 and sps_RS14140) or (sps_RS06205 and sps_RS06200)) and sps_RS06195
NTR5	Energy Metabolism	Expressed	Expressed	Expressed	nitrate reductase (methylmenaquinone-7)	((sps_RS14135 and sps_RS14140) or (sps_RS06205 and sps_RS06200)) and sps_RS06195
THD2	Energy Metabolism	Expressed	Expressed	Expressed	NAD(P) transhydrogenase	sps_RS16890 and sps_RS16885
THD5	Energy Metabolism	Expressed	Expressed	Expressed	NAD transhydrogenase	sps_RS16890 and sps_RS16885
TRDR	Energy Metabolism	Expressed	Expressed	Expressed	thioredoxin reductase (NADPH)	sps_RS05305

UQOR	Energy Metabolism	Expressed	Expressed	Expressed	NADH-Ubiquinone Oxidoreductase (Na+ translocating)	(sps_RS21215 and sps_RS21220 and sps_RS21200 and sps_RS21210 and sps_RS21205 and sps_RS21225) or (sps_RS11130 and sps_RS11125 and sps_RS11105 and sps_RS11120 and sps_RS11115 and sps_RS11110)
ACCOAC	Fatty Acid Synthesis	Used_Below	Used_Below	Used_Below	acetyl-CoA carboxylase	sps_RS14240 and sps_RS14940 and sps_RS14945
ACMAT1	Fatty Acid Synthesis	Expressed	Expressed	Expressed	Acyl-[acyl-carrier-protein]:malonyl-[acyl-carrier-protein] C-acyltransferase (decarboxylating)	(sps_RS08695 and sps_RS06710) or (sps_RS06705 and sps_RS06710)
ACOATA	Fatty Acid Synthesis	Expressed	Expressed	Expressed	Acetyl-CoA ACP transacylase	(sps_RS09695 and sps_RS06710) or

						(sps_RS16795 and sps_RS06710)
AGPEPHOS	Fatty Acid Synthesis	Below	Below	Below	Lysophospholipase	sps_RS00650
C120SN	Fatty Acid Synthesis	Expressed	Expressed	Expressed	Fatty acid biosynthesis (n-C12:0) and swp_3510 and swp_3256) or (swp_2802 and swp_3121 and swp_3045 and swp_3256) or (swp_3045 and swp_3510 and swp_3042 and swp_3256)	(sps_RS02955 and sps_RS06715 and sps_RS06705 and sps_RS09190 and sps_RS06710) or (sps_RS06715 and sps_RS08695 and sps_RS10425 and sps_RS09190 and sps_RS06710) or (sps_RS02955 and sps_RS08695 and sps_RS06715 and sps_RS09190 and sps_RS06710) or (sps_RS06715 and sps_RS10425 and sps_RS06705 and sps_RS09190 and sps_RS06710)

C130ISN	Fatty Acid Synthesis	Expressed	Expressed	Expressed	b-ketoacyl synthetase (Iso-C13:0) and swp_3510 and swp_3256) or (swp_2802 and swp_3121 and swp_3045 and swp_3256) or (swp_3045 and swp_3510 and swp_3042 and swp_3256)	(sps_RS02955 and sps_RS06715 and sps_RS06705 and sps_RS09190 and sps_RS06710) or (sps_RS06715 and sps_RS08695 and sps_RS10425 and sps_RS09190 and sps_RS06710) or (sps_RS02955 and sps_RS08695 and sps_RS06715 and sps_RS09190 and sps_RS06710) or (sps_RS06715 and sps_RS10425 and sps_RS06705 and sps_RS09190 and sps_RS06710)
C130OHISN	Fatty Acid Synthesis	Used_Below	Expressed	Expressed	b-ketoacyl synthetase (Iso-C13:0) and swp_3510 and	sps_RS02955 and sps_RS08695 and sps_RS06715 and

					swp_3256) or (swp_2802 and swp_3121 and swp_3045 and swp_3256) or (swp_3045 and swp_3510 and swp_3042 and swp_3256)	sps_RS10425 and sps_RS06705 and sps_RS09190 and sps_RS06710
C140ISN	Fatty Acid Synthesis	Expressed	Expressed	Expressed	b-ketoacyl synthetase (Iso-C14:0) and swp_3510 and swp_3256) or (swp_2802 and swp_3121 and swp_3045 and swp_3256) or (swp_3045 and swp_3510 and swp_3042 and swp_3256)	(sps_RS02955 and sps_RS06715 and sps_RS06705 and sps_RS09190 and sps_RS06710) or (sps_RS06715 and sps_RS08695 and sps_RS10425 and sps_RS09190 and sps_RS06710) or (sps_RS02955 and sps_RS08695 and sps_RS06715 and sps_RS09190 and sps_RS067

						10) or (sps_RS06715 and sps_RS10425 and sps_RS06705 and sps_RS09190 and sps_RS06710)
C140SN	Fatty Acid Synthesis	Expressed	Expressed	Expressed	Fatty acid biosynthesis (n-C14:0) and swp_3510 and swp_3256) or (swp_2802 and swp_3121 and swp_3045 and swp_3256) or (swp_3045 and swp_3510 and swp_3042 and swp_3256)	(sps_RS02955 and sps_RS06715 and sps_RS06705 and sps_RS09190 and sps_RS06710) or (sps_RS06715 and sps_RS08695 and sps_RS10425 and sps_RS09190 and sps_RS06710) or (sps_RS02955 and sps_RS08695 and sps_RS06715 and sps_RS09190 and sps_RS06710) or (sps_RS06715 and sps_RS10425 and sps_RS067

						05 and sps_RS09190 and sps_RS06710)
C150ISN	Fatty Acid Synthesis	Expressed	Expressed	Expressed	b-ketoacyl synthetase (Iso-C15:0) and swp_3510 and swp_3256) or (swp_2802 and swp_3121 and swp_3045 and swp_3256) or (swp_3045 and swp_3510 and swp_3042 and swp_3256)	(sps_RS02955 and sps_RS06715 and sps_RS06705 and sps_RS09190 and sps_RS06710) or (sps_RS06715 and sps_RS08695 and sps_RS10425 and sps_RS09190 and sps_RS06710) or (sps_RS02955 and sps_RS08695 and sps_RS06715 and sps_RS09190 and sps_RS06710) or (sps_RS06715 and sps_RS10425 and sps_RS06705 and sps_RS09190 and sps_RS06710)

C150SN	Fatty Acid Synthesis	Expressed	Expressed	Expressed	b-ketoacyl synthetase (C15:0) and swp_3510 and swp_3256) or (swp_2802 and swp_3121 and swp_3045 and swp_3256) or (swp_3045 and swp_3510 and swp_3042 and swp_3256)	(sps_RS02955 and sps_RS06715 and sps_RS06705 and sps_RS09190 and sps_RS06710) or (sps_RS06715 and sps_RS08695 and sps_RS10425 and sps_RS09190 and sps_RS06710) or (sps_RS02955 and sps_RS08695 and sps_RS06715 and sps_RS09190 and sps_RS06710) or (sps_RS06715 and sps_RS10425 and sps_RS06705 and sps_RS09190 and sps_RS06710)
C151SN	Fatty Acid Synthesis	Below	Expressed	Expressed	Fatty acid biosynthesis (n-C15:1)	(sps_RS02955 and sps_RS08695 and sps_RS06715 and

						sps_RS10425 and sps_RS06710) and (sps_RS06705 and sps_RS09190 and sps_RS06710)
C160ISN	Fatty Acid Synthesis	Expressed	Expressed	Expressed	b-ketoacyl synthetase (Iso-C16:0) and swp_3510 and swp_3256) or (swp_2802 and swp_3121 and swp_3045 and swp_3256) or (swp_3045 and swp_3510 and swp_3042 and swp_3256)	(sps_RS02955 and sps_RS06715 and sps_RS06705 and sps_RS09190 and sps_RS06710) or (sps_RS06715 and sps_RS08695 and sps_RS10425 and sps_RS09190 and sps_RS06710) or (sps_RS02955 and sps_RS08695 and sps_RS06715 and sps_RS09190 and sps_RS06710) or (sps_RS06715 and sps_RS10425 and sps_RS06705 and

						sps_RS09190 and sps_RS06710)
C160SN	Fatty Acid Synthesis	Expressed	Expressed	Expressed	Fatty acid biosynthesis (n-C16:0) and swp_3510 and swp_3256) or (swp_2802 and swp_3121 and swp_3045 and swp_3256) or (swp_3045 and swp_3510 and swp_3042 and swp_3256)	(sps_RS02955 and sps_RS06715 and sps_RS06705 and sps_RS09190 and sps_RS06710) or (sps_RS06715 and sps_RS08695 and sps_RS10425 and sps_RS09190 and sps_RS06710) or (sps_RS02955 and sps_RS08695 and sps_RS06715 and sps_RS09190 and sps_RS06710) or (sps_RS06715 and sps_RS10425 and sps_RS06705 and sps_RS09190 and sps_RS06710)

C161SN	Fatty Acid Synthesis	Used_Below	Expressed	Expressed	Fatty acid biosynthesis (n-C16:1)	sps_RS02955 and sps_RS08695 and sps_RS06715 and sps_RS10425 and sps_RS09190 and sps_RS06710
C170ISN	Fatty Acid Synthesis	Expressed	Expressed	Expressed	b-ketoacyl synthetase (Iso-C17:0) and swp_3510 and swp_3256) or (swp_2802 and swp_3121 and swp_3045 and swp_3256) or (swp_3045 and swp_3510 and swp_3042 and swp_3256)	(sps_RS02955 and sps_RS06715 and sps_RS06705 and sps_RS09190 and sps_RS06710) or (sps_RS06715 and sps_RS08695 and sps_RS10425 and sps_RS09190 and sps_RS06710) or (sps_RS02955 and sps_RS08695 and sps_RS06715 and sps_RS09190 and sps_RS06710) or (sps_RS06715 and sps_RS10425 and

						sps_RS06705 and sps_RS09190 and sps_RS06710)
C170SN	Fatty Acid Synthesis	Expressed	Expressed	Expressed	b-ketoacyl synthetase (C17:0) and swp_3510 and swp_3256) or (swp_2802 and swp_3121 and swp_3045 and swp_3256) or (swp_3045 and swp_3510 and swp_3042 and swp_3256)	(sps_RS02955 and sps_RS06715 and sps_RS06705 and sps_RS09190 and sps_RS06710 and sps_RS06710) or (sps_RS06715 and sps_RS08695 and sps_RS10425 and sps_RS09190 and sps_RS06710) or (sps_RS02955 and sps_RS08695 and sps_RS06715 and sps_RS09190 and sps_RS06710) or (sps_RS06715 and sps_RS10425 and sps_RS06705 and sps_RS09190 and

						sps_RS06710)
C171n8SN	Fatty Acid Synthesis	Used_Below	Expressed	Expressed	b-ketoacyl synthetase (C17:1)	sps_RS02955 and sps_RS08695 and sps_RS06715 and sps_RS10425 and sps_RS06705 and sps_RS09190 and sps_RS06710
C171SN	Fatty Acid Synthesis	Below	Expressed	Expressed	b-ketoacyl synthetase (C17:1)	sps_RS02955 and sps_RS08695 and sps_RS06715 and sps_RS10425 and sps_RS06705 and sps_RS09190 and sps_RS06710
C180SN	Fatty Acid Synthesis	Expressed	Expressed	Expressed	Fatty acid biosynthesis (n-C18:0) and swp_3510 and swp_3256) or (swp_2802 and swp_3121 and swp_3045 and swp_3256) or	(sps_RS02955 and sps_RS06715 and sps_RS06705 and sps_RS09190 and sps_RS06710) or (sps_RS06715 and sps_RS08695 and sps_RS10425 and

					(swp_3045 and swp_3510 and swp_3042 and swp_3256)	sps_RS09190 and sps_RS06710) or (sps_RS02955 and sps_RS08695 and sps_RS06715 and sps_RS09190 and sps_RS06710) or (sps_RS06715 and sps_RS10425 and sps_RS06705 and sps_RS09190 and sps_RS06710)
C181n7SN	Fatty Acid Synthesis	Used_Below	Expressed	Expressed	Fatty acid biosynthesis (n-C18:1)	sps_RS02955 and sps_RS08695 and sps_RS06715 and sps_RS10425 and sps_RS06705 and sps_RS09190 and sps_RS06710
C181SN	Fatty Acid Synthesis	Below	Expressed	Expressed	Fatty acid biosynthesis (n-C18:1)	sps_RS02955 and sps_RS08695 and sps_RS06715 and sps_RS10425 and

						sps_RS06705 and sps_RS09190 and sps_RS06710
C205SN	Fatty Acid Synthesis	Expressed	Expressed	Expressed	EPA synthesis condensed reaction	sps_RS10750 and sps_RS10740
C50SN	Fatty Acid Synthesis	Expressed	Expressed	Expressed	Fatty acid biosynthesis (n-C5:0) and swp_3045 and swp_3256) or (swp_2802 and swp_3045 and swp_3047 and swp_3256) or (swp_3045 and swp_3510 and swp_3047 and swp_3256) or (swp_3256 and swp_2802 and swp_1980 and swp_3045) or (swp_3045 and swp_3510 and	(sps_RS09695 and sps_RS06715 and sps_RS10425 and sps_RS09190 and sps_RS06710) or (sps_RS09695 and sps_RS02955 and sps_RS06715 and sps_RS09190 and sps_RS06710) or (sps_RS09190 and sps_RS02955 and sps_RS16795 and sps_RS06715 and sps_RS06710) or (sps_RS06715 and sps_RS10425 and sps_RS16795 and

					swp_1980 and swp_3256)	sps_RS09190 and sps_RS06710)
C60ISN	Fatty Acid Synthesis	Expressed	Expressed	Expressed	b-ketoacyl synthetase (Iso-C6:0) and swp_3045 and swp_3256) or (swp_2802 and swp_3045 and swp_3047 and swp_3256) or (swp_3045 and swp_3510 and swp_3047 and swp_3256) or (swp_3256 and swp_2802 and swp_1980 and swp_3045) or (swp_3045 and swp_3510 and swp_1980 and swp_3256)	(sps_RS09695 and sps_RS06715 and sps_RS10425 and sps_RS09190 and sps_RS06710) or (sps_RS09695 and sps_RS02955 and sps_RS06715 and sps_RS09190 and sps_RS06710) or (sps_RS09190 and sps_RS02955 and sps_RS16795 and sps_RS06715 and sps_RS06710) or (sps_RS06715 and sps_RS10425 and sps_RS16795 and sps_RS09190 and sps_RS06710)
C70ISN	Fatty Acid Synthesis	Expressed	Expressed	Expressed	b-ketoacyl synthetase	(sps_RS09695 and

					(Iso-C7:0) and swp_3045 and swp_3256) or (swp_2802 and swp_3045 and swp_3047 and swp_3256) or (swp_3045 and swp_3510 and swp_3047 and swp_3256) or (swp_3256 and swp_2802 and swp_1980 and swp_3045) or (swp_3045 and swp_3510 and swp_1980 and swp_3256)	sps_RS06715 and sps_RS10425 and sps_RS09190 and sps_RS06710) or (sps_RS09695 and sps_RS02955 and sps_RS06715 and sps_RS09190 and sps_RS06710) or (sps_RS09190 and sps_RS02955 and sps_RS16795 and sps_RS06715 and sps_RS06710) or (sps_RS06715 and sps_RS10425 and sps_RS16795 and sps_RS09190 and sps_RS06710)
KAS15	Fatty Acid Synthesis	Expressed	Expressed	Expressed	b-ketoacyl synthase	sps_RS09695 or sps_RS16795 and sps_RS06710
KAS16	Fatty Acid Synthesis	Expressed	Expressed	Expressed	3-hydroxy-myristoyl-	(sps_RS06715 and

					ACP synthesis	sps_RS08695 and sps_RS06710) or (sps_RS06715 and sps_RS06705 and sps_RS06710)
MACPD	Fatty Acid Synthesis	Expressed	Expressed	Expressed	Malonyl-ACP decarboxylase	sps_RS08695
MCOATA	Fatty Acid Synthesis	Expressed	Expressed	Expressed	Malonyl-CoA-ACP transacylase	sps_RS06720 and sps_RS06710
FMETTRS	Folate Metabolism	Expressed	Expressed	Expressed	Methionyl-tRNA formyltransferase	sps_RS00360
FTHFD	Folate Metabolism	Expressed	Expressed	Expressed	formyltetrahydrofolate deformylase	sps_RS10520
FTHFL	Folate Metabolism	Expressed	Expressed	Expressed	formate-tetrahydrofolate ligase	sps_RS26070
GCALDD	Folate Metabolism	Expressed	Expressed	Expressed	Glycolaldehyde dehydrogenase	Gap
GLYCL	Folate Metabolism	Expressed	Expressed	Expressed	Glycine Cleavage System	sps_RS23840 and sps_RS26455 and sps_RS23830 and sps_RS23835
GLYCLTDXR	Folate Metabolism	Expressed	Expressed	Expressed	Glycolate dehydrogenase (NAD)	sps_RS22825

MTHFC	Folate Metabolism	Expressed	Expressed	Expressed	methenyltetrahydrofolate cyclohydrolase	sps_RS09250
MTHFD	Folate Metabolism	Expressed	Expressed	Expressed	methylenetetrahydrofolate dehydrogenase (NADP)	sps_RS09250
MTHFR2	Folate Metabolism	Expressed	Expressed	Expressed	5,10-methylenetetrahydrofolate reductase (NADH)	sps_RS14555
GLNS	Glutamate Metabolism	Expressed	Expressed	Expressed	glutamine synthetase	sps_RS16570 or sps_RS06400 or sps_RS12580
GLNTRS	Glutamate Metabolism	Expressed	Expressed	Expressed	Glutaminyl-tRNA synthetase	sps_RS09285
GLUDx	Glutamate Metabolism	Expressed	Expressed	Expressed	glutamate dehydrogenase (NAD)	sps_RS02915
GLUN	Glutamate Metabolism	Below	Below	Expressed	glutaminase	sps_RS11545
GLUSy	Glutamate Metabolism	Expressed	Expressed	Expressed	glutamate synthase (NADPH)	sps_RS12080 and sps_RS12085 and sps_RS07955
GLUTRR	Glutamate Metabolism	Expressed	Expressed	Expressed	glutamyl-tRNA reductase	sps_RS21415
GLUTRS	Glutamate Metabolism	Expressed	Expressed	Expressed	Glutamyl-tRNA synthetase	sps_RS17980

BETALDHx	Glycine and Serine Metabolism	Below	Below	Below	betaine-aldehyde dehydrogenase	sps_RS17435
BETALDHy	Glycine and Serine Metabolism	Below	Below	Below	betaine-aldehyde dehydrogenase	sps_RS17435
GHMT	Glycine and Serine Metabolism	Expressed	Expressed	Expressed	glycine hydroxymethyltransferase	sps_RS20350
GLYAT	Glycine and Serine Metabolism	Expressed	Expressed	Expressed	glycine C-acetyltransferase	sps_RS00715
GLYTRS	Glycine and Serine Metabolism	Expressed	Expressed	Expressed	Glycyl-tRNA synthetase	sps_RS00255 and sps_RS00250
PGCD	Glycine and Serine Metabolism	Expressed	Expressed	Expressed	phosphoglycerate dehydrogenase	sps_RS14045
PSERT	Glycine and Serine Metabolism	Expressed	Expressed	Expressed	phosphoserine transaminase	sps_RS03985
PSP_L	Glycine and Serine Metabolism	Expressed	Used_Below	Expressed	phosphoserine phosphatase (L-serine)	sps_RS20855
SERAT	Glycine and Serine Metabolism	Expressed	Expressed	Expressed	serine O-acetyltransferase	sps_RS17725 or sps_RS15460
SERD_D	Glycine and Serine Metabolism	Below	Below	Below	D-serine deaminase	sps_RS20430
SERD_L	Glycine and Serine Metabolism	Expressed	Expressed	Expressed	L-serine deaminase	sps_RS08125 or sps_RS13050

SERGLYX	Glycine and Serine Metabolism	Expressed	Expressed	Expressed	Serine-glyoxylate transaminase	sps_RS15405
SERTRS	Glycine and Serine Metabolism	Expressed	Expressed	Expressed	Seryl-tRNA synthetase	sps_RS05270
THRD	Glycine and Serine Metabolism	Expressed	Expressed	Expressed	L-threonine dehydrogenase (w/ AOBUTDs)	sps_RS00710
ADPRDP	Glycolysis/ Gluconeogenesis	Below	Below	Below	ADP ribose diphosphotase	sps_RS25140 and sps_RS26775
ENO	Glycolysis/ Gluconeogenesis	Expressed	Expressed	Expressed	enolase	sps_RS20250
FBA	Glycolysis/ Gluconeogenesis	Expressed	Expressed	Expressed	fructose-bisphosphate aldolase	sps_RS12980
FBP	Glycolysis/ Gluconeogenesis	Expressed	Expressed	Expressed	fructose-bisphosphatase	sps_RS24310
GAPD	Glycolysis/ Gluconeogenesis	Expressed	Expressed	Expressed	glyceraldehyde-3-phosphate dehydrogenase (NAD)	sps_RS04450 or sps_RS26180 or sps_RS04460 or sps_RS20735
GLCP	Glycolysis/ Gluconeogenesis	Below	Expressed	Expressed	glycogen phosphorylase	sps_RS11340 or sps_RS11345
GLCS1	Glycolysis/ Gluconeogenesis	Used_Below	Expressed	Expressed	glycogen synthase (ADPGlc)	sps_RS11330
GLGC	Glycolysis/ Gluconeogenesis	Expressed	Expressed	Expressed	glucose-1-phosphate adenylyltransferase	sps_RS11335

HEX1	Glycolysis/ Gluconeogenesis	Expressed	Expressed	Expressed	hexokinase	sps_RS18105
PDH	Glycolysis/ Gluconeogenesis	Expressed	Expressed	Expressed	pyruvate dehydrogenase	sps_RS26460 and sps_RS26465 and sps_RS26455
PGI	Glycolysis/ Gluconeogenesis	Expressed	Expressed	Expressed	glucose-6-phosphate isomerase	sps_RS11780
PGK	Glycolysis/ Gluconeogenesis	Expressed	Expressed	Expressed	phosphoglycerate kinase	sps_RS12985
PGM	Glycolysis/ Gluconeogenesis	Expressed	Expressed	Expressed	phosphoglycerate mutase	sps_RS27685
PPS	Glycolysis/ Gluconeogenesis	Expressed	Expressed	Expressed	phosphoenolpyruvate synthase	sps_RS02625
PYK	Glycolysis/ Gluconeogenesis	Expressed	Expressed	Expressed	pyruvate kinase	sps_RS05545
TPI	Glycolysis/ Gluconeogenesis	Expressed	Expressed	Expressed	triose-phosphate isomerase	sps_RS20970
ATPPRT	Histidine Metabolism	Expressed	Expressed	Expressed	ATP phosphoribosyltransferase	sps_RS06490
FGLU	Histidine Metabolism	Expressed	Expressed	Expressed	formimidoylglutamase	sps_RS15010
HISD1	Histidine Metabolism	Expressed	Expressed	Expressed	Histadine Ammonia Lyase	sps_RS27480
HISTD	Histidine Metabolism	Expressed	Expressed	Expressed	histidinol dehydrogenase	sps_RS06495
HISTP	Histidine Metabolism	Expressed	Expressed	Expressed	histidinol-phosphatase	sps_RS06505
HISTRS	Histidine Metabolism	Expressed	Expressed	Expressed	Histidyl-tRNA synthetase	sps_RS18900

HSTPT	Histidine Metabolism	Expressed	Expressed	Expressed	histidinol-phosphate transaminase	sps_RS06500
IG3PS	Histidine Metabolism	Expressed	Expressed	Expressed	Imidazole-glycerol-3-phosphate synthase	sps_RS06520 and sps_RS06510
IGPDH	Histidine Metabolism	Expressed	Expressed	Expressed	imidazoleglycerol-phosphate dehydratase	sps_RS06505
IZPN	Histidine Metabolism	Expressed	Expressed	Expressed	imidazolonepropionase	sps_RS27495
PRAMPC	Histidine Metabolism	Expressed	Expressed	Expressed	phosphoribosyl-AMP cyclohydrolase	sps_RS06525
PRATPP	Histidine Metabolism	Expressed	Expressed	Expressed	phosphoribosyl-ATP pyrophosphatase	sps_RS06525
PRMICIi	Histidine Metabolism	Expressed	Expressed	Expressed	1-(5-phosphoribosyl)-5-[(5-phosphoribosylamino)methylideneamino)imidazole-4-carboxamide isomerase (irreversible)	sps_RS06515
PRPPS	Histidine Metabolism	Expressed	Expressed	Expressed	phosphoribosylpyrophosphate synthetase	sps_RS21430
URCN	Histidine Metabolism	Expressed	Expressed	Expressed	urocanase	sps_RS27485

AHCYSNS	Methionine Metabolism	Expressed	Expressed	Expressed	adenosylhomocysteine nucleosidase	sps_RS12090
DKMPPD3	Methionine Metabolism	Expressed	Expressed	Expressed	2,3-diketo-5-methylthio-1-phosphopentane degradation reaction	Gap
HSST	Methionine Metabolism	Expressed	Expressed	Expressed	homoserine O-succinyltransferase	sps_RS10075
MDRPD	Methionine Metabolism	Expressed	Expressed	Expressed	5-Methylthio-5-deoxy-D-ribulose 1-phosphate dehydratase	Gap
METAT	Methionine Metabolism	Expressed	Expressed	Expressed	methionine adenosyltransferase	sps_RS13000
METGL	Methionine Metabolism	Expressed	Below	Expressed	methionine g-lyase	sps_RS09130
METS	Methionine Metabolism	Expressed	Expressed	Expressed	tetrahydrofolate methyltransferase	sps_RS23585 or sps_RS22050
METTRS	Methionine Metabolism	Expressed	Expressed	Expressed	Methionyl-tRNA synthetase	sps_RS06815
MTHPTGHM	Methionine Metabolism	Expressed	Below	Below	5-methyltetrahydropteroyltriglutamate---homocyste	sps_RS22050

					ine S-methyltransferase	
MTRI	Methionine Metabolism	Expressed	Expressed	Expressed	5-methylthioribose-1-phosphate isomerase	Gap
MTRK	Methionine Metabolism	Expressed	Expressed	Expressed	5-methylthioribose kinase	Gap
RHCCE	Methionine Metabolism	Expressed	Expressed	Expressed	S-ribosylhomocysteine cleavage enzyme	sps_RS21230
SHSL1	Methionine Metabolism	Expressed	Expressed	Expressed	O-succinylhomoserine lyase (L-cysteine)	sps_RS14565
UNK3	Methionine Metabolism	Expressed	Expressed	Expressed	2-keto-4-methylthiobutyrate transamination	Gap
5HPUDICDCr	Purine and Pyrimidine Metabolism	Expressed	Expressed	Expressed	OHCU Decarboxylase (spontaneous)	spontaneous
5HPUDICDCs	Purine and Pyrimidine Metabolism	Expressed	Below	Below	OHCU Decarboxylase	sps_RS05465
ALLNRAC	Purine and Pyrimidine Metabolism	Expressed	Expressed	Expressed	Allantoin Racemase	Gap
ALLTC	Purine and Pyrimidine Metabolism	Expressed	Below	Below	Allantoicase	sps_RS05470
ALLTN	Purine and Pyrimidine	Expressed	Expressed	Expressed	Allantoinase	Gap

	Metabolism					
HIUH	Purine and Pyrimidine Metabolism	Below	Below	Below	hydroxyisourate hydrolase	sps_RS05460
URDGLY	Purine and Pyrimidine Metabolism	Below	Below	Below	Ureidoglycolate lyase	sps_RS05455
URHYDROX	Purine and Pyrimidine Metabolism	Expressed	Expressed	Expressed	Urate Hydroxylase	sps_RS05480 and sps_RS05485
ADA	Nucleotide Salvage Pathways	Expressed	Expressed	Expressed	Adenosine deaminase	sps_RS21850
ADK1	Nucleotide Salvage Pathways	Expressed	Expressed	Expressed	adenylate kinase	sps_RS08170
ADK3	Nucleotide Salvage Pathways	Expressed	Expressed	Expressed	guanylate kinase (aMP:gTP)	sps_RS08170
ADK4	Nucleotide Salvage Pathways	Expressed	Expressed	Expressed	adentylate kinase (ITP)	sps_RS08170
ADNCYC	Nucleotide Salvage Pathways	Expressed	Expressed	Expressed	adenylate cyclase	sps_RS15865 or sps_RS12055 or sps_RS15200 or sps_RS24710
ADNK1	Nucleotide Salvage Pathways	Expressed	Expressed	Expressed	adenosine kinase	sps_RS08170
ADPT	Nucleotide Salvage Pathways	Expressed	Expressed	Expressed	adenine phosphoribosyltransferase	sps_RS08200
AP4AH	Nucleotide Salvage Pathways	Below	Below	Below	bis(5'-nucleosyl)-tetraphosphatase	sps_RS22875

AP5AH	Nucleotide Salvage Pathways	Below	Below	Below	Ap5A hydrolase	sps_RS22875
CYTD	Nucleotide Salvage Pathways	Expressed	Expressed	Expressed	cytidine deaminase	sps_RS06685
CYTDH	Nucleotide Salvage Pathways	Expressed	Expressed	Expressed	Cytodine Hydrolase	sps_RS09820
CYTDK1	Nucleotide Salvage Pathways	Expressed	Expressed	Expressed	cytidine kinase (ATP)	sps_RS06850
CYTDK2	Nucleotide Salvage Pathways	Expressed	Expressed	Expressed	cytidine kinase (GTP)	sps_RS06850
CYTDK3	Nucleotide Salvage Pathways	Expressed	Expressed	Expressed	cytidine kinase (ITP)	sps_RS06850
CYTK1	Nucleotide Salvage Pathways	Expressed	Expressed	Expressed	cytidylate kinase (CMP)	sps_RS04000
CYTK2	Nucleotide Salvage Pathways	Expressed	Expressed	Expressed	cytidylate kinase (dCMP)	sps_RS04000
DADA	Nucleotide Salvage Pathways	Expressed	Expressed	Expressed	deoxyadenosine deaminase	sps_RS21850
DADK	Nucleotide Salvage Pathways	Expressed	Expressed	Expressed	deoxyadenylate kinase	sps_RS08170
DCYTD	Nucleotide Salvage Pathways	Expressed	Expressed	Expressed	deoxycytidine deaminase	sps_RS06685
DGK1	Nucleotide Salvage Pathways	Expressed	Expressed	Expressed	deoxyguanylate kinase (dGMP:ATP)	sps_RS16355
DTMPK	Nucleotide Salvage Pathways	Used_Below	Used_Below	Used_Below	dTMP kinase	sps_RS06835
DURIK1	Nucleotide Salvage Pathways	Expressed	Expressed	Expressed	deoxyuridine kinase (ATP:Deoxyuridine)	sps_RS10290

DURIPP	Nucleotide Salvage Pathways	Expressed	Expressed	Expressed	purine-nucleoside phosphatase (deoxyuridine)	sps_RS20875
DUTPDP	Nucleotide Salvage Pathways	Expressed	Expressed	Expressed	dUTP diphosphatase	sps_RS16285
GK1	Nucleotide Salvage Pathways	Expressed	Expressed	Expressed	guanylate kinase (GMP:ATP)	sps_RS16355
GP4GH	Nucleotide Salvage Pathways	Below	Below	Below	Gp4G hydrolase	sps_RS22875
GSNK	Nucleotide Salvage Pathways	Expressed	Expressed	Expressed	guanosine kinase	sps_RS08160
GTPDPK	Nucleotide Salvage Pathways	Expressed	Expressed	Expressed	GTP diphospho kinase	sps_RS20265
GUAD	Nucleotide Salvage Pathways	Expressed	Used_Below	Used_Below	Guanine deaminase	sps_RS05450
GUAPRT	Nucleotide Salvage Pathways	Expressed	Expressed	Expressed	guanine phosphoribosyltransferase	sps_RS24530 or sps_RS12840
HXPRT	Nucleotide Salvage Pathways	Expressed	Expressed	Expressed	hypoxanthine phosphoribosyltransferase (Hypoxanthine)	sps_RS24530 or sps_RS12840
INSK	Nucleotide Salvage Pathways	Expressed	Expressed	Expressed	inosine kinase	sps_RS08160
NDPK1	Nucleotide Salvage Pathways	Expressed	Expressed	Expressed	nucleoside-diphosphate kinase (ATP:GDP)	sps_RS17680

NDPK2	Nucleotide Salvage Pathways	Expressed	Expressed	Expressed	nucleoside-diphosphate kinase (ATP:UDP)	sps_RS17680
NDPK3	Nucleotide Salvage Pathways	Expressed	Expressed	Expressed	nucleoside-diphosphate kinase (ATP:CDP)	sps_RS17680
NDPK4	Nucleotide Salvage Pathways	Expressed	Expressed	Expressed	nucleoside-diphosphate kinase (ATP:dTDP)	sps_RS17680
NDPK5	Nucleotide Salvage Pathways	Expressed	Expressed	Expressed	nucleoside-diphosphate kinase (ATP:dGDP)	sps_RS17680
NDPK6	Nucleotide Salvage Pathways	Expressed	Expressed	Expressed	nucleoside-diphosphate kinase (ATP:dUDP)	sps_RS17680
NDPK7	Nucleotide Salvage Pathways	Expressed	Expressed	Expressed	nucleoside-diphosphate kinase (ATP:dCDP)	sps_RS17680
NDPK8	Nucleotide Salvage Pathways	Expressed	Expressed	Expressed	nucleoside-diphosphate kinase (ATP:dADP)	sps_RS17680
NTD1	Nucleotide Salvage Pathways	Expressed	Expressed	Expressed	5'-nucleotidase (dUMP)	sps_RS06945 or sps_RS15745 or

						sps_RS03795
NTD10	Nucleotide Salvage Pathways	Expressed	Expressed	Expressed	5'-nucleotidase (XMP)	sps_RS06945
NTD11	Nucleotide Salvage Pathways	Expressed	Expressed	Expressed	5'-nucleotidase (IMP)	sps_RS06945 or sps_RS26780
NTD12	Nucleotide Salvage Pathways	Expressed	Below	Below	5' nucleotidase (dIMP)	sps_RS03795
NTD2	Nucleotide Salvage Pathways	Expressed	Expressed	Expressed	5'-nucleotidase (UMP)	sps_RS06945 or sps_RS15745
NTD3	Nucleotide Salvage Pathways	Expressed	Expressed	Expressed	5'-nucleotidase (dCMP)	sps_RS06945 or sps_RS03795
NTD3_P	Nucleotide Salvage Pathways	Expressed	Expressed	Expressed	5' Nucleotidase (dCMP)	sps_RS06945 or sps_RS03795
NTD4	Nucleotide Salvage Pathways	Expressed	Expressed	Expressed	5'-nucleotidase (CMP)	sps_RS06945
NTD5	Nucleotide Salvage Pathways	Expressed	Expressed	Expressed	5'-nucleotidase (dTMP)	sps_RS06945 or sps_RS15745 or sps_RS03795
NTD5_P	Nucleotide Salvage Pathways	Expressed	Expressed	Expressed	5' Nucleotidase (dTMP)	sps_RS06945 or sps_RS15745 or sps_RS03795
NTD6	Nucleotide Salvage Pathways	Expressed	Expressed	Expressed	5'-nucleotidase (dAMP)	sps_RS06945 or sps_RS03795
NTD6_P	Nucleotide Salvage Pathways	Expressed	Expressed	Expressed	5' Nucleotidase (dAMP)	sps_RS06945 or

						sps_RS03795
NTD7	Nucleotide Salvage Pathways	Expressed	Expressed	Expressed	5'-nucleotidase (AMP)	sps_RS06945
NTD8	Nucleotide Salvage Pathways	Expressed	Expressed	Expressed	5'-nucleotidase (dGMP)	sps_RS06945 or sps_RS03795
NTD8_P	Nucleotide Salvage Pathways	Expressed	Expressed	Expressed	5' Nucleotidase (dGMP)	sps_RS06945 or sps_RS03795
NTD9	Nucleotide Salvage Pathways	Expressed	Expressed	Expressed	5'-nucleotidase (GMP)	sps_RS06945 or sps_RS26780
NTPP1	Nucleotide Salvage Pathways	Below	Below	Below	Nucleoside triphosphate pyrophosphorylase (dgtp)	sps_RS20260
NTPP10	Nucleotide Salvage Pathways	Expressed	Below	Expressed	Nucleoside triphosphate pyrophosphorylase (dITP)	sps_RS11520
NTPP11	Nucleotide Salvage Pathways	Expressed	Below	Expressed	Nucleoside triphosphate pyrophosphorylase (xtp)	sps_RS11520
NTPP2	Nucleotide Salvage Pathways	Below	Below	Below	Nucleoside triphosphate pyrophosphorylase (gtp)	sps_RS20260
NTPP3	Nucleotide Salvage Pathways	Below	Below	Below	dCTP diphosphatase	sps_RS20260

NTPP4	Nucleotide Salvage Pathways	Below	Below	Below	Nucleoside triphosphate pyrophosphorylase (ctp)	sps_RS20260
NTPP5	Nucleotide Salvage Pathways	Below	Below	Below	Nucleoside triphosphate pyrophosphorylase (datp)	sps_RS20260
NTPP6	Nucleotide Salvage Pathways	Below	Below	Below	Nucleoside triphosphate pyrophosphorylase (atp)	sps_RS20260
NTPP7	Nucleotide Salvage Pathways	Below	Below	Below	Nucleoside triphosphate pyrophosphorylase (dttp)	sps_RS20260
NTPP8	Nucleotide Salvage Pathways	Below	Below	Below	Nucleoside triphosphate pyrophosphorylase (utp)	sps_RS20260
NTPP9	Nucleotide Salvage Pathways	Expressed	Below	Expressed	Nucleoside triphosphate pyrophosphorylase (ITP)	sps_RS11520
PUNP1	Nucleotide Salvage Pathways	Expressed	Expressed	Expressed	purine-nucleoside phosphorylase (Adenosine)	sps_RS20440 or sps_RS20865
PUNP2	Nucleotide Salvage Pathways	Expressed	Expressed	Expressed	purine-nucleoside phosphorylase	sps_RS20440 or sps_RS20865

					(Deoxyadenosine)	
PUNP3	Nucleotide Salvage Pathways	Expressed	Expressed	Expressed	purine-nucleoside phosphorylase (Guanosine)	sps_RS20440 or sps_RS20865
PUNP4	Nucleotide Salvage Pathways	Expressed	Expressed	Expressed	purine-nucleoside phosphorylase (Deoxyguanosine)	sps_RS20440 or sps_RS20865
PUNP5	Nucleotide Salvage Pathways	Expressed	Expressed	Expressed	purine-nucleoside phosphorylase (Inosine)	sps_RS20440 or sps_RS20865
PUNP6	Nucleotide Salvage Pathways	Expressed	Expressed	Expressed	purine-nucleoside phosphorylase (Deoxyinosine)	sps_RS20440 or sps_RS20865
PUNP7	Nucleotide Salvage Pathways	Expressed	Expressed	Expressed	purine-nucleoside phosphorylase (Xanthosine)	sps_RS20440 or sps_RS20865
PYNP2	Nucleotide Salvage Pathways	Expressed	Expressed	Expressed	pyrimidine-nucleoside phosphorylase (uracil)	sps_RS15525
RNDR1	Nucleotide Salvage Pathways	Expressed	Expressed	Expressed	ribonucleoside-diphosphate reductase (ADP)	sps_RS03955 and sps_RS03965 and sps_RS03820
RNDR2	Nucleotide Salvage Pathways	Expressed	Expressed	Expressed	ribonucleoside-diphosphat	sps_RS03955 and sps_RS03965 and

					e reductase (GDP)	sps_RS03820
RNDR3	Nucleotide Salvage Pathways	Expressed	Expressed	Expressed	ribonucleoside-diphosphate reductase (CDP)	sps_RS03955 and sps_RS03965 and sps_RS03820
RNDR4	Nucleotide Salvage Pathways	Expressed	Expressed	Expressed	ribonucleoside-diphosphate reductase (UDP)	sps_RS03955 and sps_RS03965 and sps_RS03820
RNTR1	Nucleotide Salvage Pathways	Expressed	Expressed	Expressed	ribonucleoside-triphosphate reductase (ATP)	sps_RS08910 and sps_RS03820
RNTR2	Nucleotide Salvage Pathways	Expressed	Expressed	Expressed	ribonucleoside-triphosphate reductase (GTP)	sps_RS08910 and sps_RS03820
RNTR3	Nucleotide Salvage Pathways	Expressed	Expressed	Expressed	ribonucleoside-triphosphate reductase (CTP)	sps_RS08910 and sps_RS03820
RNTR4	Nucleotide Salvage Pathways	Expressed	Expressed	Expressed	ribonucleoside-triphosphate reductase (UTP)	sps_RS08910 and sps_RS03820
TMDK1	Nucleotide Salvage Pathways	Expressed	Expressed	Expressed	thymidine kinase (ATP:thymidine)	sps_RS10290
TMDPP	Nucleotide Salvage Pathways	Expressed	Expressed	Expressed	thymidine phosphorylase	sps_RS20875
TMDS	Nucleotide Salvage Pathways	Expressed	Expressed	Expressed	thymidylate synthase	sps_RS12030

UMPK	Nucleotide Salvage Pathways	Expressed	Used_Below	Used_Below	UMP kinase	sps_RS10470
UPPRT	Nucleotide Salvage Pathways	Expressed	Expressed	Expressed	uracil phosphoribosyltransferase	sps_RS02460
URIDK2	Nucleotide Salvage Pathways	Used_Below	Used_Below	Used_Below	uridylate kinase (dUMP)	sps_RS06835
URIK1	Nucleotide Salvage Pathways	Expressed	Expressed	Expressed	uridine kinase (ATP:Uridine)	sps_RS06850
URIK2	Nucleotide Salvage Pathways	Expressed	Expressed	Expressed	uridine kinase (GTP:Uridine)	sps_RS06850
URIK3	Nucleotide Salvage Pathways	Expressed	Expressed	Expressed	uridine kinase (ITP:Uridine)	sps_RS06850
EDA	Pentose Phosphate Pathway	Expressed	Expressed	Expressed	2-dehydro-3-deoxy-phosphogluconate aldolase	sps_RS05520
G6PDHy	Pentose Phosphate Pathway	Expressed	Expressed	Expressed	glucose 6-phosphate dehydrogenase	sps_RS05535
PGDH	Pentose Phosphate Pathway	Expressed	Expressed	Expressed	phosphogluconate dehydrogenase	sps_RS10205
PGDHY	Pentose Phosphate Pathway	Expressed	Expressed	Expressed	phosphogluconate dehydratase	sps_RS05525
PGL	Pentose Phosphate Pathway	Expressed	Expressed	Expressed	6-phosphogluconolactonase	sps_RS05530
PRKIN	Pentose Phosphate Pathway	Expressed	Expressed	Expressed	Phosphoribulokinase	sps_RS24905

RPE	Pentose Phosphate Pathway	Expressed	Expressed	Expressed	ribulose 5-phosphate 3-epimerase	sps_RS26600
RPI	Pentose Phosphate Pathway	Expressed	Expressed	Expressed	ribose-5-phosphate isomerase	sps_RS12880
TAL	Pentose Phosphate Pathway	Expressed	Expressed	Expressed	transaldolase	sps_RS11775
TKT1	Pentose Phosphate Pathway	Expressed	Expressed	Expressed	transketolase	sps_RS12995
TKT2	Pentose Phosphate Pathway	Expressed	Expressed	Expressed	transketolase	sps_RS12995
XPK	Pentose Phosphate Pathway	Expressed	Expressed	Expressed	Xylulose-5-phosphate phosphoketolase	sps_RS11765
ADHMCYSSYN	Purine and Pyrimidine Metabolism	Expressed	Expressed	Expressed	adenosylhomocysteinase	Gap
ADSL1r	Purine and Pyrimidine Metabolism	Expressed	Expressed	Expressed	adenylsuccinate lyase	sps_RS02730
ADSL2r	Purine and Pyrimidine Metabolism	Expressed	Expressed	Expressed	adenylosuccinate lyase	sps_RS02730
ADSS	Purine and Pyrimidine Metabolism	Expressed	Expressed	Expressed	adenylosuccinate synthetase	sps_RS25520 or sps_RS04270
AICART	Purine and Pyrimidine Metabolism	Expressed	Expressed	Expressed	phosphoribosylaminoimidazolecarboxamide formyltransferase	sps_RS15675
AIRC2	Purine and Pyrimidine	Expressed	Expressed	Expressed	phosphoribosylaminoimidazole	Gap

	Metabolism				carboxylase	
AIRC3	Purine and Pyrimidine Metabolism	Expressed	Expressed	Expressed	phosphoribosylaminoimidazole carboxylase (mutase rxn)	sps_RS20035
ASPCT	Purine and Pyrimidine Metabolism	Expressed	Expressed	Expressed	aspartate carbamoyltransferase	sps_RS19135 or sps_RS19130
CampHydrolyase	Purine and Pyrimidine Metabolism	Expressed	Expressed	Expressed	Camp Hydrolase	sps_RS25130
CSND	Purine and Pyrimidine Metabolism	Expressed	Expressed	Expressed	Cytosine deaminase	sps_RS06225
CTPS2	Purine and Pyrimidine Metabolism	Expressed	Expressed	Expressed	CTP synthase (glutamine)	sps_RS20255
DHORD2	Purine and Pyrimidine Metabolism	Expressed	Expressed	Expressed	dihydoorotic acid dehydrogenase (quinone8)	sps_RS02920
DHORD4i	Purine and Pyrimidine Metabolism	Expressed	Expressed	Expressed	dihydroorotate dehydrogenase	sps_RS02920
DHORD8	Purine and Pyrimidine Metabolism	Expressed	Expressed	Expressed	dihydroorotate dehydrogenase	sps_RS02920
DHORTS	Purine and Pyrimidine Metabolism	Expressed	Expressed	Expressed	dihydroorotase	sps_RS22305
EPPP2	Purine and Pyrimidine Metabolism	Expressed	Expressed	Expressed	guanosine pentaphosphatase	sps_RS15105

G35DP	Purine and Pyrimidine Metabolism	Expressed	Expressed	Expressed	guanosine-3',5'-bis(diphosphate) 3'-diphosphatase	sps_RS16365
GARFT	Purine and Pyrimidine Metabolism	Expressed	Expressed	Expressed	phosphoribosylglycinamide formyltransferase	sps_RS02450
GLUPRT	Purine and Pyrimidine Metabolism	Expressed	Expressed	Expressed	glutamine phosphoribosyldiphosphate amidotransferase	sps_RS08585
GMPS2	Purine and Pyrimidine Metabolism	Below	Below	Below	GMP synthase (glutamine-hydrolysing)	sps_RS18865 and sps_RS18860 and sps_RS25850
IMPC	Purine and Pyrimidine Metabolism	Expressed	Expressed	Expressed	IMP cyclohydrolase	sps_RS15675
IMPD	Purine and Pyrimidine Metabolism	Expressed	Expressed	Expressed	IMP dehydrogenase	sps_RS18865
OMPDC	Purine and Pyrimidine Metabolism	Expressed	Expressed	Expressed	orotidine-5'-phosphate decarboxylase	sps_RS04025
ORPT	Purine and Pyrimidine Metabolism	Expressed	Expressed	Expressed	orotate phosphoribosyltransferase	sps_RS16305
PRAGS	Purine and Pyrimidine Metabolism	Expressed	Expressed	Expressed	phosphoribosylglycinamide synthetase	sps_RS15680
PRAIS	Purine and Pyrimidine	Expressed	Expressed	Expressed	phosphoribosylaminoi	sps_RS02455

	Metabolism				midazole synthetase	
PRASCS	Purine and Pyrimidine Metabolism	Expressed	Expressed	Expressed	phosphoribosylaminoimidazolesuccinocarboxamide synthase	sps_RS06535
PRFGS	Purine and Pyrimidine Metabolism	Expressed	Expressed	Expressed	phosphoribosylformylglycinamidine synthase	sps_RS18845
PSUDS	Purine and Pyrimidine Metabolism	Expressed	Expressed	Expressed	pseudouridylate synthase	sps_RS08605 and sps_RS06755 and sps_RS08255 and sps_RS21680
URIH	Purine and Pyrimidine Metabolism	Expressed	Expressed	Expressed	uridine hydrolase	sps_RS09820
XAND	Purine and Pyrimidine Metabolism	Expressed	Expressed	Expressed	xanthine dehydrogenase	sps_RS04460
ACALDi	Pyruvate Metabolism	Expressed	Expressed	Expressed	acetaldehyde dehydrogenase (acetylating)	sps_RS03765
ACKr	Pyruvate Metabolism	Expressed	Expressed	Expressed	acetate kinase	sps_RS17590
ACS	Pyruvate Metabolism	Expressed	Expressed	Expressed	acetyl-CoA synthetase	sps_RS02570
LDH_Dir	Pyruvate Metabolism	Expressed	Expressed	Expressed	D-lactate dehydrogenase	sps_RS24240

OAADC	Pyruvate Metabolism	Expressed	Expressed	Expressed	oxaloacetate decarboxylase	sps_RS20135 and sps_RS20130 and sps_RS20125
PFL	Pyruvate Metabolism	Expressed	Expressed	Expressed	Formate C-acetyltransferase	sps_RS17575
PTAr	Pyruvate Metabolism	Expressed	Expressed	Expressed	phosphotransacetylase	sps_RS17595
ASAD	Threonine and Lysine Metabolism	Expressed	Expressed	Expressed	aspartate-semialdehyde dehydrogenase	sps_RS08615
ASPK	Threonine and Lysine Metabolism	Expressed	Expressed	Expressed	aspartate kinase	sps_RS11825 or sps_RS14560 or sps_RS24290
DAPDC	Threonine and Lysine Metabolism	Expressed	Expressed	Expressed	diaminopimelate decarboxylase	sps_RS15190 or sps_RS27560
DAPE	Threonine and Lysine Metabolism	Expressed	Expressed	Expressed	diaminopimelate epimerase	sps_RS15185
DHDPRy	Threonine and Lysine Metabolism	Expressed	Expressed	Expressed	dihydrodipicolinate reductase (NADPH)	sps_RS21040
DHDPS	Threonine and Lysine Metabolism	Expressed	Expressed	Expressed	dihydrodipicolinate synthase	sps_RS03120
HSDy	Threonine and Lysine Metabolism	Expressed	Expressed	Expressed	homoserine dehydrogenase (NADPH)	sps_RS11825 or sps_RS14560
HSK	Threonine and Lysine	Expressed	Expressed	Expressed	homoserine kinase	sps_RS11820

	Metabolism					
LYSTRS	Threonine and Lysine Metabolism	Expressed	Expressed	Expressed	Lysyl-tRNA synthetase	sps_RS24155
SDPDS	Threonine and Lysine Metabolism	Expressed	Expressed	Expressed	succinyl-diaminopimelate desuccinylase	sps_RS03210
SDPTA	Threonine and Lysine Metabolism	Expressed	Expressed	Expressed	succinyldiaminopimelate transaminase	sps_RS24950
THDPS	Threonine and Lysine Metabolism	Expressed	Expressed	Expressed	tetrahydropicolinate succinylase	sps_RS10495
THRA	Threonine and Lysine Metabolism	Expressed	Expressed	Expressed	threonine aldolase	sps_RS20350 or sps_RS11430
THRLAD	Threonine and Lysine Metabolism	Expressed	Expressed	Expressed	L-allo-threonine aldolase	sps_RS11430
THRS	Threonine and Lysine Metabolism	Expressed	Expressed	Expressed	threonine synthase	sps_RS11815
THRTRS	Threonine and Lysine Metabolism	Expressed	Expressed	Expressed	Threonyl-tRNA synthetase	sps_RS05325
ACACt2	Transport, Extracellular	Below	Below	Below	Acetoacetate transport via proton symport	sps_RS06295
ACGAt2	Transport, Extracellular	Expressed	Expressed	Expressed	N-Acetyl-D-glucosamine transport	sps_RS11600

					via proton symport	
ACt6	Transport, Extracellular	Used_Below	Used_Below	Used_Below	acetate transport in/out via proton symport	sps_RS16925
ADNt2	Transport, Extracellular	Expressed	Expressed	Expressed	adenosine transport in via proton symport	sps_RS20890
ALA_Dt4	Transport, Extracellular	Expressed	Expressed	Expressed	D-Alanine-Sodium symporter	sps_RS26165 or sps_RS24365 or sps_RS11760
ALAt4	Transport, Extracellular	Expressed	Expressed	Expressed	Alanine-Sodium symporter	sps_RS26165 or sps_RS24365 or sps_RS11760
ARBABC	Transport, Extracellular	Below	Below	Expressed	L-arabinose transport via ABC system	sps_RS13535 and sps_RS13545 and sps_RS13540
ARSt1	Transport, Extracellular	Below	Below	Below	arsenite transporter via uniport	sps_RS26185
ASPt2	Transport, Extracellular	Expressed	Expressed	Expressed	L-Aspartate transport	sps_RS08155
BUT_T	Transport, Extracellular	Below	Below	Below	butyrate symporter	sps_RS06295
CBL1abc	Transport, Extracellular	Used_Below	Used_Below	Used_Below	Cob(1)alamin transport via ABC system	sps_RS23565 and sps_RS23560 and sps_RS23525

CHOLt4	Transport, Extracellular	Expressed	Expressed	Expressed	choline-sodium symporter	sps_RS17445 or sps_RS11405 or sps_RS09720
CITT7	Transport, Extracellular	Below	Below	Below	Citrate transport via succinate antiport	sps_RS21775 and sps_RS21770 and sps_RS21780
Clt	Transport, Extracellular	Expressed	Used_Below	Expressed	chloride ion transport	sps_RS12415
CO2t	Transport, Extracellular	Expressed	Expressed	Expressed	CO2 transport out via diffusion	Diffusion
COBALTt3	Transport, Extracellular	Expressed	Expressed	Expressed	cobalt transport out via proton antiporter	sps_RS21525
COBALTt5	Transport, Extracellular	Expressed	Expressed	Expressed	cobalt transport in/out via permease (no H+)	sps_RS02045
CRO4t6	Transport, Extracellular	Below	Below	Below	chromate transport in/out via proton symport	sps_RS24170
CSNt2	Transport, Extracellular	Expressed	Expressed	Expressed	cytosine transport via proton symport	sps_RS06220
CU2t	Transport, Extracellular	Expressed	Expressed	Expressed	Copper ABC transport	Gap
Cut1	Transport, Extracellular	Below	Below	Below	Copper export via ATPase	sps_RS10010

CYTDt2	Transport, Extracellular	Expressed	Expressed	Expressed	cytidine transport in via proton symport	sps_RS20890
D-LACt2	Transport, Extracellular	Below	Below	Below	D-lactate transport via proton symport	sps_RS08480
DADNt2	Transport, Extracellular	Expressed	Expressed	Expressed	deoxyadenosine transport in via proton symport	sps_RS20890
DCYTt2	Transport, Extracellular	Expressed	Expressed	Expressed	deoxycytidine transport in via proton symport	sps_RS20890
DIPEPabc10	Transport, Extracellular	Below	Below	Below	Dipeptide transport via ABC system (gly-glu)	sps_RS09165 and sps_RS09175 and sps_RS09170 and sps_RS09185 and sps_RS09180
DIPEPabc13	Transport, Extracellular	Below	Below	Below	Dipeptide transport via ABC system (gly-asp)	sps_RS09165 and sps_RS09175 and sps_RS09170 and sps_RS09185 and sps_RS09180
DURIt2	Transport, Extracellular	Expressed	Expressed	Expressed	deoxyuridine transport in via proton symport	sps_RS20890
FE2abc	Transport, Extracellular	Expressed	Expressed	Expressed	iron (II) transport	sps_RS09290

					via ABC system	
FE3abc	Transport, Extracellular	Below	Below	Below	iron (III) transport via ABC system	sps_RS22495 and sps_RS22500 and sps_RS22505
FORt	Transport, Extracellular	Expressed	Expressed	Expressed	formate transport	sps_RS17570
FUMt4_2	Transport, Extracellular	Below	Below	Below	fumarate via sodium symport	sps_RS16580
GLUt2	Transport, Extracellular	Expressed	Expressed	Expressed	L-glutamate transport in via proton symport	sps_RS08155 or sps_RS24335
GLUt4i	Transport, Extracellular	Expressed	Expressed	Expressed	Na+/glutamate symport	sps_RS26985
GLYBt4	Transport, Extracellular	Expressed	Expressed	Expressed	betaine-sodium symporter	sps_RS17445 or sps_RS11405 or sps_RS09720
GLYC_T	Transport, Extracellular	Expressed	Expressed	Expressed	Glycerol Transport	sps_RS12390
GLYCLTt2r	Transport, Extracellular	Below	Below	Below	glycolate transport via proton symport, reversible	sps_RS08480
GLYCRt2	Transport, Extracellular	Below	Below	Expressed	D-glycerate transport (proton symport)	sps_RS09485
GLYt4	Transport, Extracellular	Expressed	Expressed	Expressed	glycine reversible transport via sodium symport	sps_RS24365 or sps_RS11760 or

						sps_RS26165
GTHRDabc	Transport, Extracellular	Below	Below	Below	Glutathione export via ABC system	sps_RS24745 and sps_RS24740
H2Ot5	Transport, Extracellular	Expressed	Expressed	Expressed	H2O transport via Diffusion	sps_RS12390
HGT	Transport, Extracellular	Below	Below	Below	mercury transport	sps_RS20655 or sps_RS20650
HOMt2	Transport, Extracellular	Below	Below	Below	homoserine transport via proton symport	sps_RS17385
ILEt4	Transport, Extracellular	Expressed	Expressed	Expressed	Na+/Isoleucine-L symporter	sps_RS12925
INDOLEt2	Transport, Extracellular	Below	Below	Expressed	Indole transport via proton symport, reversible	sps_RS01320
Kt2i	Transport, Extracellular	Expressed	Expressed	Expressed	potassium irreversible transport via proton symporter	sps_RS00345 or sps_RS00315 or sps_RS03370 or sps_RS03365
Kt3	Transport, Extracellular	Expressed	Expressed	Expressed	potassium transport out via proton antiport	sps_RS19925 or sps_RS14380 or sps_RS10390
L-LACt2	Transport, Extracellular	Below	Below	Below	L-lactate reversible transport via proton symport	sps_RS08480

LEUt4	Transport, Extracellular	Expressed	Expressed	Expressed	Na+/Leucine-L symporter	sps_RS12925
LYSt3	Transport, Extracellular	Below	Expressed	Below	L-lysine transport out via proton antiport	sps_RS03105
MET-LABC	Transport, Extracellular	Expressed	Expressed	Expressed	L-Methionine Transport via ABC system	Gap
MGt3	Transport, Extracellular	Expressed	Expressed	Expressed	magnesium transport out via proton antiporter	sps_RS21525
MGt5	Transport, Extracellular	Expressed	Expressed	Expressed	magnesium transport in/out via permease (no H+)	sps_RS02045 or sps_RS25650
MNabc	Transport, Extracellular	Expressed	Used_Below	Used_Below	Manganese Transporter	sps_RS26045 and sps_RS26040
MOBDabc	Transport, Extracellular	Used_Below	Used_Below	Used_Below	molybdate transport via ABC system	sps_RS27030 and sps_RS27035 and sps_RS27040
NAabcO	Transport, Extracellular	Expressed	Below	Below	sodium transport out via ABC system	sps_RS27630 or sps_RS27625
NAt3	Transport, Extracellular	Expressed	Expressed	Expressed	sodium transport out via proton antiport	sps_RS06305 or sps_RS05900 or sps_RS12470 or sps_RS13880

NAt3_2	Transport, Extracellular	Expressed	Expressed	Expressed	sodium proton antiporter (H:NA is 2)	sps_RS12025
NAt9	Transport, Extracellular	Expressed	Used_Below	Expressed	sodium transport in/out via calcium antiport	sps_RS16390 or sps_RS25595
NH4t	Transport, Extracellular	Used_Below	Used_Below	Used_Below	ammonium transport	sps_RS22570
NIt3	Transport, Extracellular	Expressed	Expressed	Expressed	nickel transport in/out via proton antiporter	sps_RS21525
NMNP	Transport, Extracellular	Below	Below	Below	NMN permease	sps_RS07685
NO3T7	Transport, Extracellular	Below	Below	Below	nitrite transporter	sps_RS07790
O2t	Transport, Extracellular	Expressed	Expressed	Expressed	O2 transport in via diffusion	Diffusion
OMP_AC	Transport, Extracellular	Expressed	Expressed	Expressed	Acetate transport to periplasm (ompF, ompC, or oprF)	sps_RS10915 or sps_RS14350 or sps_RS14345 or sps_RS11360 or sps_RS24395 or sps_RS11770
OMP_ACGAM	Transport, Extracellular	Expressed	Expressed	Expressed	N-Acetyl-D-glucosamine transport to periplasm	sps_RS11650

OMP_ADN	Transport, Extracellular	Expressed	Expressed	Below	Adenosine transport to periplasm (tsx)	sps_RS20885
OMP_ALA-D	Transport, Extracellular	Expressed	Expressed	Expressed	D-Alanine transport to periplasm (ompF, ompC, or oprF)	sps_RS10915 or sps_RS14350 or sps_RS14345 or sps_RS11360 or sps_RS24395 or sps_RS11770
OMP_ALA-L	Transport, Extracellular	Expressed	Expressed	Expressed	L-Alanine transport to periplasm (ompF, ompC, or oprF)	sps_RS10915 or sps_RS14350 or sps_RS14345 or sps_RS11360 or sps_RS24395 or sps_RS11770
OMP_ASP-L	Transport, Extracellular	Expressed	Expressed	Expressed	L-Aspartate transport to periplasm (ompF, ompC, or oprF)	sps_RS10915 or sps_RS14350 or sps_RS14345 or sps_RS11360 or sps_RS24395 or sps_RS11770
OMP_BGL	Transport, Extracellular	Below	Below	Below	cellobiose transport to periplasm	sps_RS19750
OMP_CA2	Transport, Extracellular	Expressed	Expressed	Expressed	Calcium transport to periplasm	sps_RS10915 or sps_RS143

					(ompF, ompC, or oprF)	50 or sps_RS14345 or sps_RS11360 or sps_RS24395 or sps_RS11770
OMP_CBL1	Transport, Extracellular	Expressed	Expressed	Expressed	Cob(I)alamin transport to periplasm (btuB)	Gap
OMP_CHITOB	Transport, Extracellular	Expressed	Expressed	Expressed	chitobiose transport to periplasm	sps_RS11650
OMP_CHOL	Transport, Extracellular	Expressed	Expressed	Expressed	choline transport to periplasm (ompF, ompC, or oprF)	sps_RS10915 or sps_RS14350 or sps_RS14345 or sps_RS11360 or sps_RS24395 or sps_RS11770
OMP_CL	Transport, Extracellular	Expressed	Expressed	Expressed	Chloride transport to periplasm (ompF, ompC, or oprF)	sps_RS10915 or sps_RS14350 or sps_RS14345 or sps_RS11360 or sps_RS24395 or sps_RS11770
OMP_CO2	Transport, Extracellular	Expressed	Expressed	Expressed	CO2 transport to periplasm (ompF,	sps_RS10915 or sps_RS14350 or sps_RS143

					ompC, or oprF)	45 or sps_RS11360 or sps_RS24395 or sps_RS11770
OMP_COBALT2	Transport, Extracellular	Expressed	Expressed	Expressed	Co2+ transport to periplasm (ompF, ompC, or oprF)	sps_RS10915 or sps_RS14350 or sps_RS14345 or sps_RS11360 or sps_RS24395 or sps_RS11770
OMP_CU2	Transport, Extracellular	Expressed	Expressed	Expressed	Cu2+ transport to periplasm (ompF, ompC, or oprF)	sps_RS10915 or sps_RS14350 or sps_RS14345 or sps_RS11360 or sps_RS24395 or sps_RS11770
OMP_CYTD	Transport, Extracellular	Expressed	Expressed	Below	Cytidine transport to periplasm (tsx)	sps_RS20885
OMP_DAD-2	Transport, Extracellular	Expressed	Expressed	Below	Deoxyadenosine transport to periplasm (tsx)	sps_RS20885
OMP_DAMP	Transport, Extracellular	Expressed	Expressed	Below	dAMP transport to periplasm (tsx)	sps_RS20885

OMP_DCMP	Transport, Extracellular	Expressed	Expressed	Below	dCMP transport to periplasm (tsx)	sps_RS20885
OMP_DCYT	Transport, Extracellular	Expressed	Expressed	Below	Deoxycytidine transport to periplasm (tsx)	sps_RS20885
OMP_DGMP	Transport, Extracellular	Expressed	Expressed	Below	dGMP transport to periplasm (tsx)	sps_RS20885
OMP_DGSN	Transport, Extracellular	Expressed	Expressed	Below	Deoxyguanosine transport to periplasm (tsx)	sps_RS20885
OMP_DMS	Transport, Extracellular	Expressed	Expressed	Expressed	Dimethyl sulfide transport to periplasm (ompF, ompC, or oprF)	sps_RS10915 or sps_RS14350 or sps_RS14345 or sps_RS11360 or sps_RS24395 or sps_RS11770
OMP_DMSO	Transport, Extracellular	Expressed	Expressed	Expressed	Dimethyl sulfoxide transport to periplasm (ompF, ompC, or oprF)	sps_RS10915 or sps_RS14350 or sps_RS14345 or sps_RS11360 or sps_RS24395 or sps_RS11770
OMP_DODCA	Transport, Extracellular	Expressed	Expressed	Expressed	Dodecanoic acid transport to periplasm	sps_RS16200 or sps_RS08835

OMP_DTMP	Transport, Extracellular	Expressed	Expressed	Below	dTMP transport to periplasm (tsx)	sps_RS20885
OMP_DURI	Transport, Extracellular	Expressed	Expressed	Below	Deoxyuridine transport to periplasm (tsx)	sps_RS20885
OMP_FE2	Transport, Extracellular	Expressed	Expressed	Expressed	Fe2+ transport to periplasm (ompF, ompC, or oprF)	sps_RS10915 or sps_RS14350 or sps_RS14345 or sps_RS11360 or sps_RS24395 or sps_RS11770
OMP_FOR	Transport, Extracellular	Expressed	Expressed	Expressed	Formate transport to periplasm (ompF, ompC, or oprF)	sps_RS10915 or sps_RS14350 or sps_RS14345 or sps_RS11360 or sps_RS24395 or sps_RS11770
OMP_FUM	Transport, Extracellular	Expressed	Expressed	Expressed	Fumarate transport to periplasm (ompF, ompC, or oprF)	sps_RS10915 or sps_RS14350 or sps_RS14345 or sps_RS11360 or sps_RS24395 or sps_RS11770

OMP_GAL	Transport, Extracellular	Below	Below	Below	D-Galactose transport to periplasm (oprB)	sps_RS07370
OMP_GALTAN	Transport, Extracellular	Below	Below	Below	Galactan transport to periplasm (oprB)	sps_RS07370
OMP_GLC-D	Transport, Extracellular	Below	Below	Below	D-Glucose transport to periplasm (oprB)	sps_RS07370
OMP_GLU-L	Transport, Extracellular	Expressed	Expressed	Expressed	L-Glutamate transport to periplasm (ompF, ompC, or oprF)	sps_RS10915 or sps_RS14350 or sps_RS14345 or sps_RS11360 or sps_RS24395 or sps_RS11770
OMP_GLY	Transport, Extracellular	Expressed	Expressed	Expressed	Glycine transport to periplasm (ompF, ompC, or oprF)	sps_RS10915 or sps_RS14350 or sps_RS14345 or sps_RS11360 or sps_RS24395 or sps_RS11770
OMP_GLY-ASP-L	Transport, Extracellular	Expressed	Expressed	Expressed	glycyl-L-aspartic acid transport to periplasm (ompF, ompC, or oprF)	sps_RS10915 or sps_RS14350 or sps_RS14345 or sps_RS11360 or sps_RS243

						95 or sps_RS11770
OMP_GLY-GLU-L	Transport, Extracellular	Expressed	Expressed	Expressed	glycyl-L-glutamic acid transport to periplasm (ompF, ompC, or oprF)	sps_RS10915 or sps_RS14350 or sps_RS14345 or sps_RS11360 or sps_RS24395 or sps_RS11770
OMP_GLYB	Transport, Extracellular	Expressed	Expressed	Expressed	Glycine betaine transport to periplasm (ompF, ompC, or oprF)	sps_RS10915 or sps_RS14350 or sps_RS14345 or sps_RS11360 or sps_RS24395 or sps_RS11770
OMP_GLYC	Transport, Extracellular	Below	Below	Below	Glycerol transport to periplasm (oprB)	sps_RS07370
OMP_GLYC-R	Transport, Extracellular	Below	Below	Below	(R)-Glycerate transport to periplasm (oprB)	sps_RS07370
OMP_GLYCLT	Transport, Extracellular	Expressed	Expressed	Expressed	Glycolate transport to periplasm (ompF, ompC, or oprF)	sps_RS10915 or sps_RS14350 or sps_RS14345 or sps_RS11360 or sps_RS24395 or

						sps_RS11770
OMP_GTHRD	Transport, Extracellular	Expressed	Expressed	Expressed	Reduced glutathione transport to periplasm (ompF, ompC, or oprF)	sps_RS10915 or sps_RS14350 or sps_RS14345 or sps_RS11360 or sps_RS24395 or sps_RS11770
OMP_H	Transport, Extracellular	Expressed	Expressed	Expressed	H+ transport to periplasm (ompF, ompC, or oprF)	sps_RS10915 or sps_RS14350 or sps_RS14345 or sps_RS11360 or sps_RS24395 or sps_RS11770
OMP_H2	Transport, Extracellular	Expressed	Expressed	Expressed	H2 transport to periplasm (ompF, ompC, or oprF)	sps_RS10915 or sps_RS14350 or sps_RS14345 or sps_RS11360 or sps_RS24395 or sps_RS11770
OMP_H2O	Transport, Extracellular	Expressed	Expressed	Expressed	H2O transport to periplasm (ompF, ompC, or oprF)	sps_RS10915 or sps_RS14350 or sps_RS14345 or sps_RS11360 or

						sps_RS24395 or sps_RS11770 or sps_RS08935
OMP_H2O2	Transport, Extracellular	Expressed	Expressed	Expressed	Hydrogen peroxide transport to periplasm (ompF, ompC, or oprF)	sps_RS10915 or sps_RS14350 or sps_RS14345 or sps_RS11360 or sps_RS24395 or sps_RS11770
OMP_H2S	Transport, Extracellular	Expressed	Expressed	Expressed	Hydrogen sulfide transport to periplasm (ompF, ompC, or oprF)	sps_RS10915 or sps_RS14350 or sps_RS14345 or sps_RS11360 or sps_RS24395 or sps_RS11770
OMP_HDCA	Transport, Extracellular	Expressed	Expressed	Expressed	hexadecanoate (n-C16:0) transport to periplasm	sps_RS16200 or sps_RS08835
OMP_ILE-L	Transport, Extracellular	Expressed	Expressed	Expressed	L-Isoleucine transport to periplasm (ompF, ompC, or oprF)	sps_RS10915 or sps_RS14350 or sps_RS14345 or sps_RS11360 or sps_RS24395 or

						sps_RS11770
OMP_INDOLE	Transport, Extracellular	Expressed	Expressed	Expressed	Indole transport to periplasm (ompF, ompC, or oprF)	sps_RS10915 or sps_RS14350 or sps_RS14345 or sps_RS11360 or sps_RS24395 or sps_RS11770
OMP_INOSHP	Transport, Extracellular	Expressed	Expressed	Expressed	myo-Inositol hexakisphosphate transport to periplasm (ompF, ompC, or oprF)	sps_RS10915 or sps_RS14350 or sps_RS14345 or sps_RS11360 or sps_RS24395 or sps_RS11770
OMP_INOSPP1	Transport, Extracellular	Expressed	Expressed	Expressed	1D-myo-inositol 1 transport to periplasm (ompF, ompC, or oprF)	sps_RS10915 or sps_RS14350 or sps_RS14345 or sps_RS11360 or sps_RS24395 or sps_RS11770
OMP_K	Transport, Extracellular	Expressed	Expressed	Expressed	K+ transport to periplasm (ompF, ompC, or oprF)	sps_RS10915 or sps_RS14350 or sps_RS14345 or sps_RS11360 or

						sps_RS24395 or sps_RS11770
OMP_LAC-D	Transport, Extracellular	Expressed	Expressed	Expressed	D-Lactate transport to periplasm (ompF, ompC, or oprF)	sps_RS10915 or sps_RS14350 or sps_RS14345 or sps_RS11360 or sps_RS24395 or sps_RS11770
OMP_LAC-L	Transport, Extracellular	Expressed	Expressed	Expressed	L-Lactate transport to periplasm (ompF, ompC, or oprF)	sps_RS10915 or sps_RS14350 or sps_RS14345 or sps_RS11360 or sps_RS24395 or sps_RS11770
OMP_LEU-L	Transport, Extracellular	Expressed	Expressed	Expressed	L-Leucine transport to periplasm (ompF, ompC, or oprF)	sps_RS10915 or sps_RS14350 or sps_RS14345 or sps_RS11360 or sps_RS24395 or sps_RS11770
OMP_LYS-L	Transport, Extracellular	Expressed	Expressed	Expressed	L-Lysine transport to periplasm (ompF, ompC, or oprF)	sps_RS10915 or sps_RS14350 or sps_RS14345 or

						sps_RS11360 or sps_RS24395 or sps_RS11770
OMP_MAL-L	Transport, Extracellular	Expressed	Expressed	Expressed	L-Malate transport to periplasm (ompF, ompC, or oprF)	sps_RS10915 or sps_RS14350 or sps_RS14345 or sps_RS11360 or sps_RS24395 or sps_RS11770
OMP_MALT	Transport, Extracellular	Below	Below	Below	Maltose transport to periplasm (lamB or ompMal2)	sps_RS03485
OMP_MALTHP	Transport, Extracellular	Below	Below	Below	Maltoheptaose transport to periplasm (lamB or ompMal2)	sps_RS03485
OMP_MALTTTR	Transport, Extracellular	Below	Below	Below	Maltotetraose transport to periplasm (lamB or ompMal2)	sps_RS03485
OMP_MET-L	Transport, Extracellular	Expressed	Expressed	Expressed	L-Methionine transport to periplasm (ompF, ompC, or oprF)	sps_RS10915 or sps_RS14350 or sps_RS14345 or sps_RS11360 or sps_RS24395 or

						sps_RS11770
OMP_MG2	Transport, Extracellular	Expressed	Expressed	Expressed	Mg transport to periplasm (ompF, ompC, or oprF)	sps_RS10915 or sps_RS14350 or sps_RS14345 or sps_RS11360 or sps_RS24395 or sps_RS11770
OMP_MN2	Transport, Extracellular	Expressed	Expressed	Expressed	Mn2+ transport to periplasm (ompF, ompC, or oprF)	sps_RS10915 or sps_RS14350 or sps_RS14345 or sps_RS11360 or sps_RS24395 or sps_RS11770
OMP_MOBD	Transport, Extracellular	Expressed	Expressed	Expressed	Molybdate transport to periplasm (ompF, ompC, or oprF)	sps_RS10915 or sps_RS14350 or sps_RS14345 or sps_RS11360 or sps_RS24395 or sps_RS11770
OMP_na1	Transport, Extracellular	Expressed	Expressed	Expressed	Sodium transport to periplasm (ompF, ompC, or oprF)	sps_RS10915 or sps_RS14350 or sps_RS14345 or sps_RS11360 or

						sps_RS24395 or sps_RS11770
OMP_NH4	Transport, Extracellular	Expressed	Expressed	Expressed	Ammonium transport to periplasm (ompF, ompC, or oprF)	sps_RS10915 or sps_RS14350 or sps_RS14345 or sps_RS11360 or sps_RS24395 or sps_RS11770
OMP_NMN	Transport, Extracellular	Expressed	Expressed	Expressed	NMN transport to periplasm (ompF, ompC, or oprF)	sps_RS10915 or sps_RS14350 or sps_RS14345 or sps_RS11360 or sps_RS24395 or sps_RS11770
OMP_NO2	Transport, Extracellular	Expressed	Expressed	Expressed	Nitrite transport to periplasm (ompF, ompC, or oprF)	sps_RS10915 or sps_RS14350 or sps_RS14345 or sps_RS11360 or sps_RS24395 or sps_RS11770
OMP_NO3	Transport, Extracellular	Expressed	Expressed	Expressed	Nitrate transport to periplasm (ompF, ompC, or oprF)	sps_RS10915 or sps_RS14350 or sps_RS14345 or

						sps_RS11360 or sps_RS24395 or sps_RS11770
OMP_O2	Transport, Extracellular	Expressed	Expressed	Expressed	O2 transport to periplasm (ompF, ompC, or oprF)	sps_RS10915 or sps_RS14350 or sps_RS14345 or sps_RS11360 or sps_RS24395 or sps_RS11770
OMP_OCDCA	Transport, Extracellular	Expressed	Expressed	Expressed	octadecanoate (n-C18:0) transport to periplasm	sps_RS16200 or sps_RS08835
OMP_PI	Transport, Extracellular	Used_Below	Used_Below	Used_Below	Phosphate transport to periplasm (oprP)	sps_RS21785
OMP_PMCOA	Transport, Extracellular	Expressed	Expressed	Expressed	Pimeloyl-CoA transport to periplasm (ompF, ompC, or oprF)	sps_RS10915 or sps_RS14350 or sps_RS14345 or sps_RS11360 or sps_RS24395 or sps_RS11770
OMP_PPA	Transport, Extracellular	Expressed	Expressed	Expressed	Propionate transport to periplasm (ompF, ompC, or oprF)	sps_RS10915 or sps_RS14350 or sps_RS14345 or sps_RS113

						60 or sps_RS24395 or sps_RS11770
OMP_PRO-L	Transport, Extracellular	Expressed	Expressed	Expressed	L-Proline transport to periplasm (ompF, ompC, or oprF)	sps_RS10915 or sps_RS14350 or sps_RS14345 or sps_RS11360 or sps_RS24395 or sps_RS11770
OMP_PTRC	Transport, Extracellular	Expressed	Expressed	Expressed	Putrescine transport to periplasm (ompF, ompC, or oprF)	sps_RS10915 or sps_RS14350 or sps_RS14345 or sps_RS11360 or sps_RS24395 or sps_RS11770
OMP_PYR	Transport, Extracellular	Expressed	Expressed	Expressed	Pyruvate transport to periplasm (ompF, ompC, or oprF)	sps_RS10915 or sps_RS14350 or sps_RS14345 or sps_RS11360 or sps_RS24395 or sps_RS11770
OMP_SER-L	Transport, Extracellular	Expressed	Expressed	Expressed	L-Serine transport to periplasm (ompF,	sps_RS10915 or sps_RS14350 or sps_RS143

					ompC, or oprF)	45 or sps_RS11360 or sps_RS24395 or sps_RS11770
OMP_SO3	Transport, Extracellular	Expressed	Expressed	Expressed	Sulfite transport to periplasm (ompF, ompC, or oprF)	sps_RS10915 or sps_RS14350 or sps_RS14345 or sps_RS11360 or sps_RS24395 or sps_RS11770
OMP_SO4	Transport, Extracellular	Expressed	Expressed	Expressed	Sulfate transport to periplasm (ompF, ompC, or oprF)	sps_RS10915 or sps_RS14350 or sps_RS14345 or sps_RS11360 or sps_RS24395 or sps_RS11770
OMP_SUCC	Transport, Extracellular	Expressed	Expressed	Expressed	Succinate transport to periplasm (ompF, ompC, or oprF)	sps_RS10915 or sps_RS14350 or sps_RS14345 or sps_RS11360 or sps_RS24395 or sps_RS11770
OMP_THR-L	Transport, Extracellular	Expressed	Expressed	Expressed	L-Threonine transport to	sps_RS10915 or sps_RS143

					periplasm (ompF, ompC, or oprF)	50 or sps_RS14345 or sps_RS11360 or sps_RS24395 or sps_RS11770
OMP_THYMD	Transport, Extracellular	Expressed	Expressed	Below	Thymidine transport to periplasm (tsx)	sps_RS20885
OMP_TMA	Transport, Extracellular	Expressed	Expressed	Expressed	Trimethylamine transport to periplasm (ompF, ompC, or oprF)	sps_RS10915 or sps_RS14350 or sps_RS14345 or sps_RS11360 or sps_RS24395 or sps_RS11770
OMP_TMAO	Transport, Extracellular	Expressed	Expressed	Expressed	Trimethylamine N-oxide transport to periplasm (ompF, ompC, or oprF)	sps_RS10915 or sps_RS14350 or sps_RS14345 or sps_RS11360 or sps_RS24395 or sps_RS11770
OMP_TRP-L	Transport, Extracellular	Expressed	Expressed	Expressed	L-Tryptophan transport to periplasm (ompF, ompC, or oprF)	sps_RS10915 or sps_RS14350 or sps_RS14345 or sps_RS11360 or sps_RS243

						95 or sps_RS11770
OMP_TSUL	Transport, Extracellular	Expressed	Expressed	Expressed	Thiosulfate transport to periplasm (ompF, ompC, or oprF)	sps_RS10915 or sps_RS14350 or sps_RS14345 or sps_RS11360 or sps_RS24395 or sps_RS11770
OMP_TTDCA	Transport, Extracellular	Expressed	Expressed	Expressed	tetradecanoate (C14:0) transport to periplasm	sps_RS16200 or sps_RS08835
OMP_TTTNT	Transport, Extracellular	Expressed	Expressed	Expressed	tetrathionate transport to periplasm (ompF, ompC, or oprF)	sps_RS10915 or sps_RS14350 or sps_RS14345 or sps_RS11360 or sps_RS24395 or sps_RS11770
OMP_TYR-L	Transport, Extracellular	Expressed	Expressed	Expressed	L-Tyrosine transport to periplasm (ompF, ompC, or oprF)	sps_RS10915 or sps_RS14350 or sps_RS14345 or sps_RS11360 or sps_RS24395 or sps_RS11770

OMP_URA	Transport, Extracellular	Expressed	Expressed	Expressed	Uracil transport to periplasm (ompF, ompC, or oprF)	sps_RS10915 or sps_RS14350 or sps_RS14345 or sps_RS11360 or sps_RS24395 or sps_RS11770
OMP_UREA	Transport, Extracellular	Expressed	Expressed	Expressed	Urea transport to periplasm (ompF, ompC, or oprF)	sps_RS10915 or sps_RS14350 or sps_RS14345 or sps_RS11360 or sps_RS24395 or sps_RS11770
OMP_URI	Transport, Extracellular	Expressed	Expressed	Below	Uridine transport to periplasm (tsx)	sps_RS20885
OMP_VAL-L	Transport, Extracellular	Expressed	Expressed	Expressed	L-Valine transport to periplasm (ompF, ompC, or oprF)	sps_RS10915 or sps_RS14350 or sps_RS14345 or sps_RS11360 or sps_RS24395 or sps_RS11770
OMP_XAN	Transport, Extracellular	Expressed	Expressed	Below	Xanthine transport to periplasm (tsx)	sps_RS20885

PHEMEabc	Transport, Extracellular	Expressed	Expressed	Below	Protoheme transport via ABC	sps_RS01955 and sps_RS01960 and sps_RS01945
PHNabc	Transport, Extracellular	Below	Below	Below	phosphonate transport via ABC system	sps_RS02085 and sps_RS02090 and sps_RS02080
PIabc	Transport, Extracellular	Expressed	Below	Below	phosphate transport via ABC system and swp_5141 and swp_5140)	(sps_RS10900 and sps_RS09735 and sps_RS09730 and sps_RS09740) or (sps_RS27780 and sps_RS27775 and sps_RS27770 and sps_RS27765)
PIt6	Transport, Extracellular	Expressed	Expressed	Expressed	phosphate transport in/out via proton symporter	sps_RS24720
PMCOAt	Transport, Extracellular	Expressed	Expressed	Expressed	Pimeloyl-CoA Transport	Gap
PPAtNa	Transport, Extracellular	Expressed	Expressed	Expressed	Propionate Transporter	sps_RS08830
PROt4	Transport, Extracellular	Expressed	Expressed	Expressed	L-proline via sodium symport	sps_RS08830
PTRCabc	Transport, Extracellular	Below	Below	Below	putrescine transport via ABC system	sps_RS12575 and sps_RS12570 and

						sps_RS12565 and sps_RS12560
PYRt2	Transport, Extracellular	Expressed	Expressed	Expressed	pyruvate reversible transport via proton symport	Gap
RIBabc	Transport, Extracellular	Below	Below	Expressed	D-Ribose transport via ABC	sps_RS13535 and sps_RS13545 and sps_RS13540
SERt4	Transport, Extracellular	Expressed	Expressed	Expressed	serine/threonine:Na+ symporter, SstT	sps_RS17900
SERt6	Transport, Extracellular	Expressed	Expressed	Expressed	L-serine transport in/out via proton symport	sps_RS13055
SO4t2	Transport, Extracellular	Used_Below	Used_Below	Used_Below	sulfate transport in via proton symport	sps_RS06765
SUCCt4	Transport, Extracellular	Below	Below	Below	succinate via sodium symport	sps_RS16580
SUCCtex	Transport, Extracellular	Expressed	Expressed	Expressed	Succinate antiport	Gap
THMabc	Transport, Extracellular	Below	Below	Below	thiamin transport via ABC system	sps_RS07685
THMDt2	Transport, Extracellular	Expressed	Expressed	Expressed	thymidine transport in via proton symport	sps_RS20890
THRHT	Transport, Extracellular	Below	Used_Below	Used_Below	L-Threonine Transport	sps_RS17385

THRt3	Transport, Extracellular	Expressed	Below	Expressed	L-threonine transport out via proton antiport	sps_RS02125
THRt4	Transport, Extracellular	Expressed	Expressed	Expressed	serine/threonine:Na+ symporter, SstT	sps_RS17900
TRPt6	Transport, Extracellular	Below	Expressed	Expressed	L-tryptophan transport in/out via proton symport	sps_RS01320 or sps_RS14005
TYRt6	Transport, Extracellular	Below	Expressed	Expressed	L-tyrosine transport in/out via proton symport	sps_RS14005
URAt6	Transport, Extracellular	Expressed	Expressed	Expressed	uracil transport in/out via proton symport	sps_RS03055 or sps_RS21120 or sps_RS20730
UreaExp	Transport, Extracellular	Expressed	Expressed	Expressed	Urea Diffusion	Diffusion
URIt2	Transport, Extracellular	Expressed	Expressed	Expressed	uridine transport in via proton symport	sps_RS20890
VALt4	Transport, Extracellular	Expressed	Expressed	Expressed	Na+/Valine-L symporter	sps_RS12925
WO4abc	Transport, Extracellular	Expressed	Expressed	Expressed	tungstate transporter	sps_RS00855 and sps_RS00850 and sps_RS00845
XANt	Transport, Extracellular	Expressed	Expressed	Expressed	Xanthine Transporter	sps_RS21120 or sps_RS207

						30 or sps_RS03055
ANPRT	Tyrosine, Tryptophan, and Phenylalanine Metabolism	Expressed	Expressed	Expressed	anthranilate phosphoribosyltransferase	sps_RS08290
ANS1	Tyrosine, Tryptophan, and Phenylalanine Metabolism	Expressed	Expressed	Expressed	anthranilate synthase	sps_RS08280 and sps_RS08285
CHORM	Tyrosine, Tryptophan, and Phenylalanine Metabolism	Expressed	Expressed	Expressed	chorismate mutase	sps_RS11860 and sps_RS11885
CHORS	Tyrosine, Tryptophan, and Phenylalanine Metabolism	Expressed	Expressed	Expressed	chorismate synthase	sps_RS08740
DAHPS	Tyrosine, Tryptophan, and Phenylalanine Metabolism	Expressed	Expressed	Expressed	3-deoxy-D-arabino-heptulosonate 7-phosphate synthetase	sps_RS11860 or sps_RS22545 or sps_RS02615 or sps_RS11890
DHQD1	Tyrosine, Tryptophan, and Phenylalanine Metabolism	Expressed	Used_Below	Expressed	3-dehydroquinate dehydratase	sps_RS14935

DHQS	Tyrosine, Tryptophan, and Phenylalanine Metabolism	Expressed	Expressed	Expressed	3-dehydroquinate synthase	sps_RS26625
FUMACA	Tyrosine, Tryptophan, and Phenylalanine Metabolism	Expressed	Expressed	Expressed	fumarylacetoacetase	sps_RS18055
HPPDO1	Tyrosine, Tryptophan, and Phenylalanine Metabolism	Expressed	Below	Below	4-hydroxyphenylpyruvate dioxygenase	sps_RS07040
IGPS	Tyrosine, Tryptophan, and Phenylalanine Metabolism	Expressed	Expressed	Expressed	indole-3-glycerol-phosphate synthase	sps_RS08295
MLACI	Tyrosine, Tryptophan, and Phenylalanine Metabolism	Expressed	Below	Below	maleylacetoacetate isomerase	sps_RS18050
PHE4MO	Tyrosine, Tryptophan, and Phenylalanine Metabolism	Expressed	Below	Below	phenylalanine 4-monooxygenase	sps_RS18070
PHEAL	Tyrosine, Tryptophan, and Phenylalan	Expressed	Expressed	Expressed	phenylalanine ammonia-lyase	sps_RS16460

	ine Metabolism					
PHETA1	Tyrosine, Tryptophan, and Phenylalanine Metabolism	Expressed	Expressed	Expressed	phenylalanine transaminase	sps_RS04490 or sps_RS03990
PHETRS	Tyrosine, Tryptophan, and Phenylalanine Metabolism	Expressed	Expressed	Expressed	Phenylalanyl-tRNA synthetase	sps_RS06560 and sps_RS06555
PPND	Tyrosine, Tryptophan, and Phenylalanine Metabolism	Expressed	Expressed	Expressed	prephenate dehydrogenase	sps_RS11885
PPNDH	Tyrosine, Tryptophan, and Phenylalanine Metabolism	Expressed	Expressed	Expressed	prephenate dehydratase	sps_RS11860
PRAIi	Tyrosine, Tryptophan, and Phenylalanine Metabolism	Expressed	Expressed	Expressed	phosphoribosylanthranilate isomerase (irreversible)	sps_RS08295
PSCVT	Tyrosine, Tryptophan, and Phenylalanine Metabolism	Expressed	Expressed	Expressed	3-phosphoshikimate 1-carboxyvinyltransferase	sps_RS03995

SHK3D	Tyrosine, Tryptophan, and Phenylalanine Metabolism	Expressed	Expressed	Expressed	shikimate dehydrogenase	sps_RS00410
SHKK	Tyrosine, Tryptophan, and Phenylalanine Metabolism	Expressed	Expressed	Expressed	shikimate kinase	sps_RS26630
TRPOR	Tyrosine, Tryptophan, and Phenylalanine Metabolism	Expressed	Expressed	Expressed	tryptophan 7-halogenase	sps_RS11640
TRPS2	Tyrosine, Tryptophan, and Phenylalanine Metabolism	Expressed	Expressed	Expressed	tryptophan synthase (indole)	sps_RS08300
TRPS3	Tyrosine, Tryptophan, and Phenylalanine Metabolism	Expressed	Expressed	Expressed	tryptophan synthase (indoleglycerol phosphate)	sps_RS08305
TRPTRS	Tyrosine, Tryptophan, and Phenylalanine Metabolism	Expressed	Expressed	Expressed	Tryptophanyl-tRNA synthetase	sps_RS26590
TYRTA	Tyrosine, Tryptophan, and Phenylalan	Expressed	Expressed	Expressed	tyrosine transaminase	sps_RS04490 or sps_RS03990

	ine Metabolism					
TYRTRS	Tyrosine, Tryptophan, and Phenylalanine Metabolism	Expressed	Expressed	Expressed	Tyrosyl-tRNA synthetase	sps_RS12360
4HBASink	Unassigned	Expressed	Expressed	Expressed	4HBA compound Sink	Sink
5DRIB_Sink	Unassigned	Expressed	Expressed	Expressed	5DRIB compound Sink	Sink
AMOB_Sink	Unassigned	Expressed	Expressed	Expressed	AMOB compound Sink	Sink
CAT	Unassigned	Expressed	Expressed	Expressed	catalase	sps_RS01620 or sps_RS08500 or sps_RS14015
CLAT	Unassigned	Below	Below	Below	chloramphenicol acetyltransferase	sps_RS04265
CONFALDD	Unassigned	Expressed	Below	Expressed	Coniferyl-aldehyde dehydrogenase	sps_RS23440
GLYOX	Unassigned	Expressed	Expressed	Expressed	hydroxyacylglutathione hydrolase	sps_RS05945
Growth	Unassigned	Expressed	Expressed	Expressed	Biomass Compound Sink	Biomass
GTHRDH	Unassigned	Expressed	Expressed	Expressed	Glutathione hydralase (periplasmic)	sps_RS07055
HCO3E	Unassigned	Expressed	Expressed	Expressed	carbonate dehydratas	sps_RS03185

					e (HCO3 equilibration reaction)	
LGTHL	Unassigned	Below	Below	Below	lactoylglutathione lyase	sps_RS05705
PPA	Unassigned	Expressed	Expressed	Expressed	inorganic diphosphatase	sps_RS04825
SELNPS	Unassigned	Expressed	Expressed	Expressed	Selenophosphate synthase	sps_RS26755
SOD	Unassigned	Expressed	Expressed	Expressed	superoxide dismutase	sps_RS03045
TSULST	Unassigned	Expressed	Below	Expressed	thiosulfate sulfurtransferase	sps_RS00705
ACACCB	Valine, Leucine, and Isoleucine Metabolism	Expressed	Expressed	Expressed	acetyl-CoA C-acetyltransferase	sps_RS10060
ACACCT	Valine, Leucine, and Isoleucine Metabolism	Expressed	Expressed	Expressed	acetyl-CoA:acetoacetyl-CoA transferase	sps_RS10260 and sps_RS10265
ACACT10R	Valine, Leucine, and Isoleucine Metabolism	Expressed	Expressed	Expressed	acetyl-CoA C-acyltransferase (2-Methyl-3-acetoacetyl-CoA)	sps_RS00295
ACHBS	Valine, Leucine, and Isoleucine Metabolism	Expressed	Expressed	Expressed	2-aceto-2-hydroxybutanoate synthase	(sps_RS15435 and sps_RS15430) or (sps_RS06935 and sps_RS06930)

ACLS	Valine, Leucine, and Isoleucine Metabolism	Expressed	Expressed	Expressed	acetolactate synthase (Also catalyzes ACHBS)	(sps_RS15435 and sps_RS15430) or (sps_RS06935 and sps_RS06930)
ACOAD10	Valine, Leucine, and Isoleucine Metabolism	Expressed	Expressed	Expressed	acyl-CoA dehydrogenase (2-methylbutanoyl-CoA)	sps_RS00300
ACOAD8	Valine, Leucine, and Isoleucine Metabolism	Below	Below	Expressed	acyl-CoA dehydrogenase (isovaleryl-CoA)	sps_RS10230
ACOAD9	Valine, Leucine, and Isoleucine Metabolism	Expressed	Expressed	Expressed	acyl-CoA dehydrogenase (isobutyryl-CoA)	sps_RS00300
AHAI	Valine, Leucine, and Isoleucine Metabolism	Expressed	Expressed	Expressed	acetohydroxy acid isomeroreductase	sps_RS15440
DHAD1	Valine, Leucine, and Isoleucine Metabolism	Expressed	Expressed	Expressed	dihydroxy-acid dehydratase (2,3-dihydroxy-3-methylbutanoate)	sps_RS15420
DHAD2	Valine, Leucine, and Isoleucine Metabolism	Expressed	Expressed	Expressed	Dihydroxy-acid dehydratase (2,3-dihydroxy-3-	sps_RS15420

					methylpentanoate)	
ECOAH2C	Valine, Leucine, and Isoleucine Metabolism	Expressed	Expressed	Expressed	enoyl-CoA hydratase, bacterial	sps_RS10040 or sps_RS00300
ECOAH9	Valine, Leucine, and Isoleucine Metabolism	Expressed	Expressed	Expressed	2-Methylprop-2-enoyl-CoA (2-Methylbut-2-enoyl-CoA)	sps_RS10040 or sps_RS00300
HACD8	Valine, Leucine, and Isoleucine Metabolism	Expressed	Expressed	Expressed	3-hydroxyacyl-CoA dehydrogenase (2-Methylacetoacetyl-CoA)	sps_RS05895
HACOADr	Valine, Leucine, and Isoleucine Metabolism	Expressed	Used_Below	Expressed	3-hydroxyacyl-CoA dehydrogenase	sps_RS10035
HIBHR	Valine, Leucine, and Isoleucine Metabolism	Expressed	Expressed	Expressed	3-hydroxyisobutyryl-CoA hydrolase	sps_RS00295
HMGL	Valine, Leucine, and Isoleucine Metabolism	Expressed	Below	Below	hydroxymethylglutaryl-CoA lyase	sps_RS10255
ILEDH2	Valine, Leucine, and Isoleucine	Expressed	Expressed	Expressed	isoleucine dehydrogenase	sps_RS02655

	Metabolism					
ILETA	Valine, Leucine, and Isoleucine Metabolism	Expressed	Expressed	Expressed	isoleucine transaminase	sps_RS15930
ILETRS	Valine, Leucine, and Isoleucine Metabolism	Expressed	Expressed	Expressed	Isoleucyl-tRNA synthetase	sps_RS11720
IPMD	Valine, Leucine, and Isoleucine Metabolism	Expressed	Expressed	Expressed	3-isopropylmalate dehydrogenase	sps_RS16215
IPPMIa	Valine, Leucine, and Isoleucine Metabolism	Expressed	Expressed	Expressed	3-isopropylmalate dehydratase	sps_RS16205 and sps_RS16210
IPPMIb	Valine, Leucine, and Isoleucine Metabolism	Expressed	Expressed	Expressed	2-isopropylmalate hydratase	sps_RS16205 and sps_RS16210
IPPS	Valine, Leucine, and Isoleucine Metabolism	Expressed	Expressed	Expressed	2-isopropylmalate synthase	sps_RS16220
KARA2i	Valine, Leucine, and Isoleucine Metabolism	Expressed	Expressed	Expressed	ketol-acid reductoisomerase (2-Aceto-2-hydroxybutanoate)	sps_RS15440

LEUTA	Valine, Leucine, and Isoleucine Metabolism	Expressed	Expressed	Expressed	leucine transaminase	sps_RS15930 or sps_RS15425
LEUTRS	Valine, Leucine, and Isoleucine Metabolism	Expressed	Expressed	Expressed	Leucyl-tRNA synthetase	sps_RS21545
LLEUDr	Valine, Leucine, and Isoleucine Metabolism	Expressed	Expressed	Expressed	L-leucine dehydrogenase	sps_RS02655
MCCC	Valine, Leucine, and Isoleucine Metabolism	Below	Below	Below	methylcrotonoyl-CoA carboxylase	sps_RS10235 and sps_RS10245
MGCH	Valine, Leucine, and Isoleucine Metabolism	Expressed	Below	Below	methylglutaconyl-CoA hydratase	sps_RS10240
MMSDHir	Valine, Leucine, and Isoleucine Metabolism	Expressed	Used_Below	Expressed	methylmalonate-semialdehyde dehydrogenase (acylating)	sps_RS10055
OIVD1i	Valine, Leucine, and Isoleucine Metabolism	Expressed	Expressed	Expressed	2-oxoisovalerate dehydrogenase (acylating; 4-methyl-2-	sps_RS03865 and sps_RS03870 and sps_RS03860 and sps_RS26455

					oxopentaoate)	
OIVD2	Valine, Leucine, and Isoleucine Metabolism	Expressed	Expressed	Expressed	2-oxoisovalerate dehydrogenase (acylating; 3-methyl-2-oxobutanoate)	sps_RS03865 and sps_RS03870 and sps_RS03860 and sps_RS26455
OIVD3	Valine, Leucine, and Isoleucine Metabolism	Expressed	Expressed	Expressed	2-oxoisovalerate dehydrogenase (acylating; 3-methyl-2-oxopentanoate)	sps_RS03865 and sps_RS03870 and sps_RS03860 and sps_RS26455
OMCDC	Valine, Leucine, and Isoleucine Metabolism	Expressed	Expressed	Expressed	2-Oxo-4-methyl-3-carboxypentanoate decarboxylation	sps_RS16215
THRD_L	Valine, Leucine, and Isoleucine Metabolism	Expressed	Expressed	Expressed	L-threonine deaminase	sps_RS15415
VALALAMOB	Valine, Leucine, and Isoleucine Metabolism	Expressed	Expressed	Expressed	Valine Pyruvate Transaminase	sps_RS08985
VALDHr	Valine, Leucine, and Isoleucine Metabolism	Expressed	Expressed	Expressed	valine dehydrogenase	sps_RS02655

VALTA	Valine, Leucine, and Isoleucine Metabolism	Expressed	Expressed	Expressed	valine transaminase	sps_RS15930
VALTRS	Valine, Leucine, and Isoleucine Metabolism	Expressed	Expressed	Expressed	Valyl-tRNA synthetase	sps_RS22650
DMSOR3e	Energy Metabolism	Expressed	Expressed	Expressed	Dimethyl sulfoxide reductase (Menaquinol 7)	sps_RS06195
DMSOR4e	Energy Metabolism	Expressed	Expressed	Expressed	Dimethyl sulfoxide reductase (methylmenaquinol 7)	sps_RS06195
TMAOR3e	Energy Metabolism	Expressed	Expressed	Expressed	Trimethylamine N-oxide reductase (ubiquinol 8)	sps_RS06195 or sps_RS01395
OMP_TREH	Transport, Extracellular	Below	Below	Below	Trehalose transport to periplasm (oprB)	sps_RS07370
TRE6PP	Alternate Carbon Metabolism	Expressed	Expressed	Expressed	Trehalose Phosphotase	Gap
TREHtex	Transport, Extracellular	Expressed	Expressed	Expressed	Trehalose Transport vis PTS	Gap
TREH	Alternate Carbon Metabolism	Expressed	Expressed	Expressed	Trehalase	sps_RS27235
SUCRPTS	Transport, Extracellular	Expressed	Expressed	Expressed	Sucrose transport	Gap

					via PTS system	
FFSD	Alternate Carbon Metabolism	Expressed	Expressed	Expressed	beta-fructofuranosidase	Gap
SUCP	Alternate Carbon Metabolism	Expressed	Expressed	Expressed	Sucrose phosphorylase	Gap
FRUK	Alternate Carbon Metabolism	Expressed	Expressed	Expressed	fructokinase	sps_RS18105
OMP_SUCR	Transport, Extracellular	Below	Below	Below	Sucrose transport to periplasm (oprB)	sps_RS07370
OMP_CIT	Transport, Extracellular	Expressed	Expressed	Expressed	citrate transport to periplasm (ompF, ompC, or oprF)	sps_RS10915 or sps_RS14350 or sps_RS14345 or sps_RS11360 or sps_RS24395 or sps_RS11770

Data S1 Table C: Metabolite Structural Information. Table contains metabolite names, formulas, and charges from the model. SMILES strings are provided for the metabolites along with an indication of the source of the structure. Additionally, a mapping to the TECRdb database used by the Group Contribution package is included.

ID	Name	Kegg ID	Charge	Formula	SMILES	Structure Source
cpd_10fthf	10-Formyltetrahydrofolate	C00234	-2	C20H21N7O7	C1C(NC2=C(N1)N=C(NC2=O)N)CN(C=O)C3=CC=C(C=C3)C(=O)NC(CCC(=O)O)C(=O)O	Pubchem
cpd_12dag3p	1,2-Diacyl-sn-glycerol 3-phosphate	C00416	-2	C5H5O8PR2	[H]C(=O)OCC(COP(O)(O)=O)OC([H])=O	Manually Drawn
cpd_12dgr	1,2-Diacylglycerol	C00641	0	C5H6O5R2	[H]C(=O)OCC(CO)OC([H])=O	Manually Drawn
cpd_13dpg	3-Phospho-D-glyceroyl phosphate	C00236	-4	C3H4O10P2	C(C(C(=O)OP(=O)(O)O)O)OP(=O)(O)O	Manually Drawn
cpd_1ap2ol	1-Aminopropan-2-ol	C05771	1	C3H10NO	CC(CN)O	Pubchem
cpd_1pyr5c	1-Pyrroline-5-carboxylate	C03912	-1	C5H6NO2	C1CC(N=C1)C(=O)O	Pubchem
cpd_23dhdp	2,3-Dihydrodipicolinate	C03340	-2	C7H5NO4	C1C=CC(=NC1C(=O)[O-])C(=O)[O-]	Pubchem
cpd_23dhmb	(R)-2,3-Dihydroxy-3-	C04272	-1	C5H9O4	CC(C)(C(C(=O)O)O)O	Pubchem

	methylbutanoate					
cpd_23dhmp	(R)-2,3-Dihydroxy-3-methylpentanoate	C06007	-1	C6H11O4	CCC(C)(C(C(=O)O)O)O	Pubchem
cpd_25aics	(S)-2-[5-Amino-1-(5-phospho-D-ribosyl)imidazole-4-carboxamido]succinate	C04823	-4	C13H15N4O12P	C1=NC(=C(N1C2C(C(C(O2)COP(=O)(O)O)O)O)N)C(=O)NC(CC(=O)O)C(=O)O	Pubchem
cpd_25dhpp	2,5-Diamino-6-hydroxy-4-(5'-phosphoribosylamino)-pyrimidine	C01304	-2	C9H14N5O8P	C(C1C(C(C(O1)NC2=C(C(=O)NC(=N2)N)N)O)O)OP(=O)(O)O	Pubchem
cpd_26dap-LL	LL-2,6-Diaminoheptanedioate	C00666	0	C7H14N2O4	C(CC(C(=O)O)N)CC(C(=O)O)N	Pubchem
cpd_26dap-M	meso-2,6-Diaminoheptanedioate	C00680	0	C7H14N2O4	C(CC(C(=O)O)N)CC(C(=O)O)N	Pubchem
cpd_2aep	2-Aminoethylphosphonate	C03557	-2	C2H6NO3P	C(CP(=O)(O)O)N	Pubchem
cpd_2ahbut	(S)-2-Aceto-2-hydroxybutanoate	C06006	-1	C6H9O4	CCC(C(=O)C)(C(=O)O)O	Pubchem
cpd_2ahhmd	2-Amino-4-hydroxy-6-hydroxymethyl-7,8-	C04807	-3	C7H8N5O8P2	C1C(=NC2=C(N1)N=C(NC2=O)N)COP(	Pubchem

	dihydropteridine diphosphate				=O)(O)OP(=O)(O)O	
cpd_2ahhmp	2-Amino-4-hydroxy-6-hydroxymethyl-7,8-dihydropteridine	C01300	0	C7H9N5O2	C1C(=NC2=C(N1)N=C(NC2=O)N)CO	Pubchem
cpd_2aobut	L-2-Amino-3-oxobutanoate	C03508	0	C4H7NO3	CC(=O)C(C(=O)O)N	Pubchem
cpd_2cpr5p	1-(2-Carboxyphenylamino)-1-deoxy-D-ribulose 5-phosphate	C01302	-3	C12H13NO9P	C1=CC=C(C(=C1)C(=O)O)NCC(=O)[C@@H]([C@@H](COP(=O)(O)O)O)O	Pubchem
cpd_2dda7p	2-Dehydro-3-deoxy-D-arabino-heptonate 7-phosphate	C04691	-3	C7H10O10P	C(C(C(C(C(COP(=O)(O)O)O)O)O)O)C(=O)C(=O)O	Pubchem
cpd_2ddg6p	2-Dehydro-3-deoxy-D-gluconate 6-phosphate	C04442	-3	C6H8O9P	C(C(C(C(COP(=O)(O)O)O)O)O)C(=O)C(=O)O	Pubchem
cpd_2dhp	2-Dehydropantoate	C00966	-1	C6H9O4	CC(C)(CO)C(=O)C(=O)O	Pubchem
cpd_2dmmq7	2-Demethylmenaquinone 7	NA	0	C45H62O2	CC(=CCCC(=CCCC(=CCCC(=CCCC(=CCCC(=CCC	Pubchem

					1=CC(=O)C2=CC=CC=C2C1=O)C)C)C)C)C)C	
cpd_2dr1p	2-Deoxy-D-ribose 1-phosphate	C00672	-2	C5H9O7P	C1C(C(OC1OP(=O)(O)O)CO)O	Pubchem
cpd_2dr5p	2-Deoxy-D-ribose 5-phosphate	C00673	-2	C5H9O7P	C1C(C(OC1O)COP(=O)(O)O)O	Pubchem
cpd_2h3opp	2-Hydroxy-3-oxopropanoate	C01146	-1	C3H3O4	C(=O)C(C(=O)O)O	Pubchem
cpd_2ippm	2-Isopropylmaleate	C02631	-2	C7H8O4	CC(C)C(=CC(=O)O)C(=O)O	Pubchem
cpd_2kmb	2-keto-4-methylthiobutyrate	C01180	-1	C5H7O3S	CSCCC(=O)C(=O)O	Pubchem
cpd_2maacoa	2-Methylacetoacetyl-CoA	C03344	-4	C26H38N7O18P3S	CC(C(=O)C)C(=O)SCCNC(=O)CCNC(=O)C(C(C)(C)COP(=O)(O)OP(=O)(O)OCC1C(C(C(O1)N2C=NC3=C2N=CN=C3N)O)OP(=O)(O)O)O	Pubchem
cpd_2mahmp	2-Methyl-4-amino-5-hydroxymethylpyrimidine diphosphate	C04752	-3	C6H8N3O7P2	CC1=NC=C(C(=N1)N)COP(=O)([O-])OP(=O)([O-])[O-]	Pubchem
cpd_2mb2coa	2-Methylbut-	C03345	-4	C26H38N7O17P3S	CC=C(C)C(=O)SCCNC(=O)CC	Pubchem

	2-enoyl-CoA				NC(=O)C(C(C)(C)COP(=O)([O-])OP(=O)([O-])OCC1C(C(C(O1)N2C=NC3=C2N=CN=C3N)O)OP(=O)([O-])[O-])O	
cpd_2mbcoa	2-Methylbutanoyl-CoA	C01033	-4	C26H40N7O17P3S	CCC(C)C(=O)SCCNC(=O)CCNC(=O)C(C(C)(C)COP(=O)(O)OP(=O)(O)OCC1C(C(C(O1)N2C=NC3=C2N=CN=C3N)O)OP(=O)(O)O)O	Pubchem
cpd_2mcacn	cis-2-Methylaconitate	C04225	-3	C7H5O6	CC(=C(CC(=O)O)C(=O)O)C(=O)O	Pubchem
cpd_2mcit	2-Hydroxybutane-1,2,3-tricarboxylate	C02225	-3	C7H7O7	CC(C(=O)[O-])C(CC(=O)[O-])(C(=O)[O-])O	Pubchem
cpd_2me4p	2-C-methyl-D-erythritol 4-phosphate	C11434	-2	C5H11O7P	CC(CO)(C(COP(=O)(O)O)O)O	Pubchem
cpd_2mecdp	2-C-methyl-D-erythritol 2,4-	C11453	-2	C5H10O9P2	CC1(C(COP(=O)(OP(=O)(O1)O)O)O)CO	Pubchem

	cyclodiphosphate					
cpd_2mp2coa	2-Methylprop-2-enoyl-CoA	C03460	-4	C25H36N7O17P3S	CC(=C)C(=O)SCCNC(=O)CCNC(=O)C(C(C)(C)COP(=O)(O)OP(=O)(O)OCC1C(C(C(O1)N2C=NC3=C2N=CN=C3N)O)OP(=O)(O)O)O	Pubchem
cpd_2obut	2-Oxobutanoate	C00109	-1	C4H5O3	CCC(=O)C(=O)O	Pubchem
cpd_2ohph	2-Octaprenyl-6-hydroxyphenol	C05811	0	C46H70O2	CC(=CCCC(=CCCC(=CCCC(=CCCC(=CCCC(=CCCC1=C(C(=CC=C1)O)O)C)C)C)C)C)C)C	Pubchem
cpd_2ombzl	2-Octaprenyl-6-methoxy-1,4-benzoquinol	C05813	0	C47H72O3	CC(=CCCC(=CCCC(=CCCC(=CCCC(=CCCC(=CCCC1=CC(=CC(=C1O)OC)O)C)C)C)C)C)C)C	Pubchem
cpd_2omhmbl	2-Octaprenyl-3-methyl-5-hydroxy-	C05815	0	C48H74O4	CC1=C(C(=C(C(=C1O)O)OC)O)CC=C(C)	Pubchem

	6-methoxy-1,4-benzoquinol				CCC=C(C)CCC=C(C)CCC=C(C)CCC=C(C)CCC=C(C)CCC=C(C)CCC=C(C)C	
cpd_2ommbl	2-Octaprenyl-3-methyl-6-methoxy-1,4-benzoquinol	C05814	0	C48H74O3	CC1=C(C(=C(C=C1O)OC)O)CC=C(C)CCC=C(C)CCC=C(C)CCC=C(C)CCC=C(C)CCC=C(C)CCC=C(C)C	Pubchem
cpd_2omph	2-Octaprenyl-6-methoxyphenol	C05812	0	C47H72O2	CC(=CCCC(=CCCC(=CCCC(=CCCC(=CCC=CC=CC(=CCCC(=CCC1=C(C(=CC=C1)OC)O)C)C)C)C)C)C)C)C	Pubchem
cpd_2oph	2-Octaprenylphenol	C05810	0	C46H70O	CC(=CCCC(=CCCC(=CCCC(=CCCC(=CCC=CC=CC(=CCCC(=CCC1=CC=CC=C1O)C)C)C)C)C)C)C)C	Pubchem
cpd_2p4c2me	2-phospho-4-(cytidine 5'-diphospho)-2-C-	C11436	-4	C14H22N3O17P3	CC(CO)(C(COP(=O)(O)OP(=O)(O)OCC1C(C(C(O1)	Pubchem

	methyl-D-erythritol				N2C=CC(=NC2=O)N)O)O)OP(=O)(O)O	
cpd_2pg	D-Glycerate 2-phosphate	C00631	-3	C3H4O7P	C(C(C(=O)O)OP(=O)(O)O)O	Pubchem
cpd_2pglyc	2-Phosphoglycolate	C00988	-3	C2H2O6P	C(C(=O)O)OP(=O)(O)O	Pubchem
cpd_2shchc	2-Succinyl-6-hydroxy-2,4-cyclohexadiene-1-carboxylate	C05817	-2	C11H10O6	C1=CC(C(C(=C1)C(=O)CCC(=O)O)C(=O)O)O	Pubchem
cpd_34hpp	3-(4-Hydroxyphenyl)pyruvate	C01179	-1	C9H7O4	C1=CC(=CC=C1CC(=O)C(=O)O)O	Pubchem
cpd_3c2hmp	3-Carboxy-2-hydroxy-4-methylpentanoate	C04411	-2	C7H10O5	CC(C)C(C(C(=O)O)O)C(=O)O	Pubchem
cpd_3c3hmp	3-Carboxy-3-hydroxy-4-methylpentanoate	C02504	-2	C7H10O5	CC(C)C(CC(=O)O)(C(=O)O)O	Pubchem
cpd_3c4mop	3-Carboxy-4-methyl-2-oxopentanoate	C04236	-2	C7H8O5	CC(C)C(C(=O)C(=O)O)C(=O)O	Pubchem
cpd_3dhq	3-Dehydroquinate	C00944	-1	C7H9O6	C1C(C(C(=O)CC1(C(=O)O)O)O)O	Pubchem

cpd_3dhsk	3-Dehydroshikimate	C02637	-1	C7H7O5	C1C(C(C(=O)C=C1C(=O)O)O)O	Pubchem
cpd_3hmbcoa	(2S,3S)-3-Hydroxy-2-methylbutanoyl-CoA	C04405	-4	C26H40N7O18P3S	CC(C(C)O)C(=O)SCCNC(=O)CCNC(=O)C(C(C)(C)COP(=O)(O)OP(=O)(O)OCC1C(C(C(O1)N2C=NC3=C2N=CN=C3N)O)OP(=O)(O)O)O	Pubchem
cpd_3hmp	3-Hydroxy-2-methylpropanoate	C01188	-1	C4H7O3	CC(CO)C(=O)[O-]	Pubchem
cpd_3ig3p	C'-(3-Indolyl)-glycerol 3-phosphate	C03506	-2	C11H12NO6P	C1=CC=C2C(=C1)C(=CN2)C(C(COP(=O)(O)O)O)O	Pubchem
cpd_3mb2coa	3-Methylbut-2-enoyl-CoA	C03069	-4	C26H38N7O17P3S	CC(=CC(=O)SCCNC(=O)CCNC(=O)C(C(C)(C)COP(=O)(O)OP(=O)(O)OCC1C(C(C(O1)N2C=NC3=C2N=CN=C3N)O)OP(=O)(O)O)C	Pubchem
cpd_3mgcoa	3-Methylglutaconyl-CoA	C03231	-5	C27H37N7O19P3S	CC(=CC(=O)SCCNC(=O)CCNC(=O)C(C	Pubchem

					(C)(C)COP(=O)(O)OP(=O)(O)OCC1C(C(C(O1)N2C=NC3=C2N=CN=C3N)O)OP(=O)(O)O)O)CC(=O)O	
cpd_3mob	3-Methyl-2-oxobutanoate	C00141	-1	C5H7O3	CC(C)C(=O)C(=O)O	Pubchem
cpd_3mop	(S)-3-Methyl-2-oxopentanoate	C00671	-1	C6H9O3	CCC(C)C(=O)C(=O)O	Pubchem
cpd_3ophb	3-Octaprenyl-4-hydroxybenzoate	C05809	-1	C47H69O3	CC(=CCCC(=CCCC(=CCCC(=CCCC(=CCCC(=CCCC(=CCCC1=C(C=CC(=C1)C(=O)O)O)C)C)C)C)C)C)C	Pubchem
cpd_3pg	3-Phospho-D-glycerate	C00197	-3	C3H4O7P	C(C(C(=O)O)O)OP(=O)(O)O	Pubchem
cpd_3php	3-Phosphohydroxypyruvate	C03232	-3	C3H2O7P	C(C(=O)C(=O)O)OP(=O)(O)O	Pubchem
cpd_3psme	5-O-(1-Carboxyvinyl)-3-phosphoshikimate	C01269	-4	C10H9O10P	C=C(C(=O)O)OC1CC(=CC(C1O)OP(=O)(O)O)C(=O)O	Pubchem

cpd_4abut	4-Aminobutanoate	C00334	0	C4H9NO2	C(CC(=O)O)CN	Pubchem
cpd_4abz	4-Aminobenzoate	C00568	-1	C7H6NO2	C1=CC(=CC=C1C(=O)[O-])N	Pubchem
cpd_4adcho	4-amino-4-deoxychorismate	C11355	-1	C10H10NO5	C=C(C(=O)[O-])OC1C=C(C=CC1[NH3+])C(=O)[O-]	Pubchem
cpd_4ampm	4-Amino-2-methyl-5-phosphomethylpyrimidine	C04556	-2	C6H8N3O4P	CC1=NC=C(C(=N1)N)COP(=O)(O)O	Pubchem
cpd_4c2me	4-(cytidine 5'-diphospho)-2-C-methyl-D-erythritol	C11435	-2	C14H23N3O14P2	CC(CO)(C(COP(=O)(O)OP(=O)(O)OCC1C(C(C(O1)N2C=CC(=NC2=O)N)O)O)O)O	Pubchem
cpd_4fumacac	4-Fumarylacetoacetate	C01061	-2	C8H6O6	C(C(=O)CC(=O)[O-])C(=O)C=CC(=O)[O-]	Pubchem
cpd_4hba	4-Hydroxy-benzyl alcohol	C17467	0	C7H8O2	C1=CC(=CC=C1CO)O	Pubchem
cpd_4hbcoa	4-Hydroxybenzoyl-CoA	C02949	-4	C28H36N7O18P3S	CC(C)(COP(=O)(O)OP(=O)(O)OCC1C(C(C(O1)N2C=NC3=C2N=CN=C3N)O)OP(=O)(O)O)C(C(=O)N	Pubchem

					CCC(=O)NCCSC(=O)C4=CC=C(C=C4)O)O	
cpd_4hbz	4-Hydroxybenzoate	C00156	-1	C7H5O3	C1=CC(=CC=C1C(=O)O)[O-]	Pubchem
cpd_4izp	4-Imidazolone-5-propanoate	C03680	-1	C6H7N2O3	C1=NC(C(=O)N1)CCC(=O)O	Pubchem
cpd_4mlacac	4-Maleylacetoacetate	C01036	-2	C8H6O6	C(C(=O)CC(=O)O)C(=O)C=CC(=O)O	Pubchem
cpd_4mop	4-Methyl-2-oxopentanoate	C00233	-1	C6H9O3	CC(C)CC(=O)C(=O)O	Pubchem
cpd_4mpetz	4-Methyl-5-(2-phosphoethyl)-thiazole	C04327	-2	C6H8NO4PS	CC1=C(SC=N1)CCOP(=O)(O)O	Pubchem
cpd_4pasp	4-Phospho-L-aspartate	C03082	-2	C4H6NO7P	C(C(C(=O)O)N)C(=O)OP(=O)(O)O	Pubchem
cpd_4per	4-Phospho-D-erythronate	C03393	-3	C4H6O8P	C(C(C(C(=O)O)O)O)OP(=O)(O)O	Pubchem
cpd_4ppan	D-4'-Phosphopantothenate	C03492	-3	C9H15NO8P	CC(C)(COP(=O)([O-])[O-])C(C(=O)NCCC(=O)[O-])O	Pubchem
cpd_4ppcys	N-((R)-4-Phosphopantothenoyl)-L-cysteine	C04352	-3	C12H20N2O9PS	CC(C)(COP(=O)(O)O)C(C(=O)NCCC(=O)NC(CS)C(=O)O)O	Pubchem

cpd_4r5au	4-(1-D-Ribitylamino)-5-aminouracil	C04732	0	C9H16N4O6	C(C(C(C(CO)O)O)O)NC1=C(C(=O)NC(=O)N1)N	Pubchem
cpd_5678thh	(6R)-6-(L-erythro-1,2-Dihydroxypropyl)-5,6,7,8-tetrahydro-4a-hydropterin	C00386	0	C9H14N4O3	CC(C(C1CN=C2C(N1)(C(=O)NC(=N2)N)O)O)O	Pubchem
cpd_5aizc	5-amino-1-(5-phospho-D-ribosyl)imidazole-4-carboxylate	C04751	-3	C9H11N3O9P	C1=NC(=C(N1C2C(C(C(O2)COP(=O)(O)O)O)O)O)N)C(=O)O	Pubchem
cpd_5aop	5-Amino-4-oxopentanoate	C00430	0	C5H9NO3	C(CC(=O)O)C(=O)CN	Pubchem
cpd_5aprbu	5-Amino-6-(5'-phosphoribitylamino)uracil	C04454	-2	C9H15N4O9P	C(C(C(C(COP(=O)(O)O)O)O)O)NC1=C(C(=O)NC(=O)N1)N	Pubchem
cpd_5apru	5-Amino-6-(5'-phosphoribosylamino)uracil	C01268	-2	C9H13N4O9P	C(C1C(C(C(O1)NC2=C(C(=O)NC(=O)N2)N)O)O)OP(=O)(O)O	Pubchem
cpd_5caiz	5-phosphoribosyl-5-carboxyaminoimidazole	C15667	-3	C9H11N3O9P	C1=C(N(C=N1)C2C(C(C(O2)COP(=O)(O)O)O)O)NC(=O)O	Pubchem

cpd_5drib	5-Deoxy-D-ribose	NA	0	C5H10O4	CC(C(C(C=O)O)O)O	Pubchem
cpd_5hiu	5-Hydroxyisourate	C11821	0	C5H4N4O4	C12=NC(=O)NC1(C(=O)NC(=O)N2)O	Pubchem
cpd_5mdr1p	5-Methylthio-5-deoxy-D-ribose 1-phosphate	C04188	-2	C6H11O7PS	CSCC1C(C(C(O1)OP(=O)(O)O)O)O	Pubchem
cpd_5mdru1p	5-Methylthio-5-deoxy-D-ribulose 1-phosphate	C04582	-2	C6H11O7PS	CSCC(C(C(=O)COP(=O)(O)O)O)O	Pubchem
cpd_5mta	5-Methylthioadenosine	C00170	0	C11H15N5O3S	CSCC1C(C(C(O1)N2C=NC3=C2N=CN=C3N)O)O	Pubchem
cpd_5mthf	5-Methyltetrahydrofolate	C00440	-1	C20H24N7O6	CN1C(CNC2=C1C(=O)NC(=N2)N)CNC3=CC=C(C=C3)C(=O)NC(CCC(=O)O)C(=O)O	Pubchem
cpd_5mthglu	5-Methyltetrahydropteroyltri-L-glutamate	C04489	0	C30H39N9O12	CN1C(CNC2=C1C(=O)NC(=N2)N)CNC3=CC=C(C=C3)C(=O)NC(CCC(=O)NC(CCC(=O)NC(CCC(=O)O)C(=O)O)C(=O)O)C(=O)O	Pubchem

cpd_5mtr	5-Methylthio-D-ribose	C03089	0	C6H12O4S	CSCC1C(C(C(O1)O)O)O	Pubchem
cpd_5prdmbz	N1-(5-Phospho-alpha-D-ribosyl)-5,6-dimethylbenzimidazole	C04778	-2	C14H17N2O7P	CC1=CC2=C(C=C1C)N(C=N2)C3C(C(C(O3)COP(=O)(O)O)O)O	Pubchem
cpd_6pgc	6-Phospho-D-gluconate	C00345	-3	C6H10O10P	C(C(C(C(C(C(=O)O)O)O)O)O)OP(=O)(O)O	Pubchem
cpd_6pgl	6-phospho-D-glucono-1,5-lactone	C01236	-2	C6H9O9P	C(C1C(C(C(C(=O)O1)O)O)O)OP(=O)(O)O	Pubchem
cpd_78dhp	(6R)-6-(L-erythro-1,2-Dihydroxypropyl)-7,8-dihydro-6H-pterin	C00268	0	C9H12N4O2	CC(C(C1CN=C2C(=N1)C(=O)NC(=N2)N)O)O	Pubchem
cpd_7cltrp	7-Chloro-L-tryptophan	C19687	-1	C11H10N2O2Cl	C1=CC2=C(C(=C1)Cl)NC=C2CC(C(=O)O)N	Pubchem
cpd_8aonn	8-Amino-7-oxononanoate	C01092	0	C9H17NO3	CC(C(=O)CCCCCC(=O)[O-])N	Pubchem
cpd_aacoa	Acetoacetyl-CoA	C00332	-4	C25H36N7O18P3S	CC(=O)CC(=O)SCCNC(=O)CCNC(=O)C(C(C)(C)COP(=O)(O)OP(=O)(O)OCC1	Pubchem

					C(C(C(O1)N2C=NC3=C2N=CN=C3N)O)OP(=O)(O)O)O	
cpd_ac	Acetate	C00033	-1	C2H3O2	CC(=O)[O-]	Pubchem
cpd_acac	Acetoacetate	C00164	-1	C4H5O3	CC(=O)CC(=O)[O-]	Pubchem
cpd_acald	Acetaldehyde	C00084	0	C2H4O	CC=O	Pubchem
cpd_accoa	Acetyl-CoA	C00024	-4	C23H34N7O17P3S	CC(=O)SCCNC(=O)CCNC(=O)C(C(C)(C)COP(=O)(O)OP(=O)(O)OCC1C(C(C(O1)N2C=NC3=C2N=CN=C3N)O)OP(=O)(O)O)O	Pubchem
cpd_acg5p	N-Acetyl-L-glutamyl 5-phosphate	C04133	-3	C7H9NO8P	CC(=O)NC(CCC(=O)OP(=O)(O)O)C(=O)O	Pubchem
cpd_acg5sa	N-Acetyl-L-glutamate 5-semialdehyde	C01250	-1	C7H10NO4	CC(=O)NC(CCC=O)C(=O)O	Pubchem
cpd_acgam	N-Acetyl-D-glucosamine	C00140	0	C8H15NO6	CC(=O)NC1C(C(C(OC1O)CO)O)O	Pubchem
cpd_acgam1p	N-Acetyl-D-glucosamine 1-phosphate	C04256	-2	C8H14NO9P	CC(=O)NC1C(C(C(OC1OP(=O)(O)O)CO)O)O	Pubchem

cpd_acgam6p	N-Acetyl-D-glucosamine 6-phosphate	C00357	-2	C8H14NO9P	CC(=O)NC1C(C(C(OC1O)COP(=O)(O)O)O)O	Pubchem
cpd_acglu	N-Acetyl-L-glutamate	C00624	-2	C7H9NO5	CC(=O)NC(CCC(=O)O)C(=O)O	Pubchem
cpd_acmam	N-Acetyl-D-muramoate	C02713	-1	C11H18NO8	CC(C(=O)O)OC1C(C(OC(C1O)CO)O)NC(=O)C	Pubchem
cpd_acmama	N-Acetyl-D-muramoyl-L-alanine	C02999	-1	C14H23N2O9	CC(C(=O)O)NC(=O)C(C)OC1C(C(OC(C1O)CO)O)NC(=O)C	Pubchem
cpd_acmana	N-Acetyl-D-mannosamine	C00645	0	C8H15NO6	CC(=O)NC1C(C(C(OC1O)CO)O)O	Pubchem
cpd_acnam	N-Acetylneuraminate	C00270	-1	C11H18NO9	CC(=O)NC1C(CC(OC1C(C(CO)O)O)(C(=O)O)O)O	Pubchem
cpd_acorn	N2-Acetyl-L-ornithine	C00437	0	C7H14N2O3	CC(=O)NC(CCCN)C(=O)O	Pubchem
cpd_acser	O-Acetyl-L-serine	C00979	0	C5H9NO4	CC(=O)OCC(C(=O)O)N	Pubchem
cpd_actp	Acetyl phosphate	C00227	-2	C2H3O5P	CC(=O)OP(=O)(O)O	Pubchem
cpd_adcoba	Adenosyl cobinamide	C06508	1	C58H84CoN16O11	CC1=C2C(C(C([N-]2)C3(C(C(C(=N3)C(=C4C(C(C(=N4)C=C5C(C(C1=N5)CCC(=O)N)(C)C)	Pubchem

					CCC(=O)N)(C)CC(=O)N)C)CC(=O)N)(C)CC(=O)N)C)CC(=O)N)(C)CCC(=O)NCC(C)O.[CH2-]C1C(C(C(O1)N2C=NC3=C2N=CN=C3N)O)O.[Co]	
cpd_adcobap	Adenosylcobinamide phosphate	C06509	-1	C58H83CoN16O14P	CC1=C2C(C(C([N-]2)C3(C(C(C(=N3)C(=C4C(C(C(=N4)C=C5C(C(C1=N5)CCC(=O)N)(C)C)CCC(=O)N)(C)CC(=O)N)C)CC(=O)N)(C)CC(=O)N)C)CC(=O)N)(C)CCC(=O)NCC(C)OP(=O)(O)O.[CH2-]C1C(C(C(O1)N2C=NC3=C2N=CN=C3N)O)O.[Co]	Pubchem
cpd_adcobdam	Adenosylcobyrinate diamide	C06506	-4	C55H68CoN11O15	CC1=C2C(C(C([N-]2)C3(C(C(C(=N3)C(=C4C(C(C(=N4)C=C	Pubchem

					5C(C(C1=N5)CCC(=O)O)(C)C)CCC(=O)O)(C)CC(=O)N)C)CC(=O)O)(C)CC(=O)N)C)CC(=O)O)(C)CCC(=O)O.[CH2-]C1C(C(C(O1)N2C=NC3=C2N=CN=C3N)O)O.[Co+3]	
cpd_adcobhex	adenosyl-cobyric acid	C06507	0	C55H76CoN15O11	CC1=C2C(C(C([N-]2)C3(C(C(C(=N3)C(=C4C(C(C(=N4)C=C5C(C(C1=N5)CCC(=O)N)(C)C)CCC(=O)N)(C)CC(=O)N)C)CC(=O)N)(C)CC(=O)N)C)CC(=O)N)(C)CCC(=O)O.[CH2-]C1C(C(C(O1)N2C=NC3=C2N=CN=C3N)O)O.[Co]	Pubchem
cpd_ade	Adenine	C00147	0	C5H5N5	C1=NC2=C(N1)C(=NC=N2)N	Pubchem
cpd_adgcoba	Adenosine-GDP-	C06510	-1	C68H95CoN21O21P2	CC1=C2C(C(C([N-	Pubchem

	cobinamide				]2)C3(C(C(C(=N3)C(=C4C(C(C(=N4)C=C5C(C(C1=N5)CCC(=O)N)(C)C)CCC(=O)N)(C)CC(=O)N)C)CCC(=O)N)(C)CC(=O)N)C)CC(=O)N)(C)CCC(=O)NCC(C)OP(=O)(O)OP(=O)(O)OCC6C(C(C(O6)N7C=NC8=C7N=C(NC8=O)N)O)O.[CH2-]C1C(C(C(O1)N2C=NC3=C2N=CN=C3N)O)O.[Co]	
cpd_adn	Adenosine	C00212	0	C10H13N5O4	C1=NC2=C(C(=N1)N)N=CN2C3C(C(C(O3)CO)O)O	Pubchem
cpd_adp	ADP	C00008	-3	C10H12N5O10P2	C1=NC2=C(C(=N1)N)N=CN2C3C(C(C(O3)COP(=O)(O)OP(=O)(O)O)O)O	Pubchem
cpd_adpglc	ADPglucose	C00498	-2	C16H23N5O15P2	C1=NC2=C(C(=N1)N)N=CN2	Pubchem

					C3C(C(C(C(O3)COP(=O)(O)OP(=O)(O)OC4C(C(C(C(O4)CO)O)O)O)O)O	
cpd_adphep-DD	ADP-D-glycero-D-manno-heptose	C06397	-2	C17H25N5O16P2	C1=NC2=C(C(=N1)N)N=CN2C3C(C(C(C(O3)COP(=O)(O)OP(=O)(O)OC4C(C(C(C(O4)C(CO)O)O)O)O)O)O	Pubchem
cpd_adprib	ADP Ribose	C00301	-2	C15H21N5O14P2	C1=NC2=C(C(=N1)N)N=CN2C3C(C(C(C(O3)COP(=O)(O)OP(=O)(O)OCC(C(C(C(=O)O)O)O)O)O	Pubchem
cpd_agm	Agmatine	C00179	2	C5H16N4	C(CCN=C(N)N)CN	Pubchem
cpd_agpe	acyl-glycerophosphoethanolamine	C04438	-1	C6H13NO7PR	[H]C(=O)OC[C@@H](O)COP(O)(=O)OCCN	Pubchem
cpd_ahcys	S-Adenosyl-L-homocysteine	C00021	0	C14H20N6O5S	C1=NC2=C(C(=N1)N)N=CN2C3C(C(C(O3)CSCCC(C(=O)O)N)O)O	Pubchem
cpd_ahdt	2-Amino-4-hydroxy-6-(erythro-1,2,3-	C04895	-4	C9H12N5O13P3	C1C(=NC2=C(N1)N=C(NC2=O)N)C(C(	Pubchem

	trihydroxypropyl)dihydropteridine triphosphate				COP(=O)(O)OP(=O)(O)OP(=O)(O)O)O)O	
cpd_aicar	5-Amino-1-(5-Phospho-D-ribosyl)imidazole-4-carboxamide	C04677	-2	C9H13N4O8P	C1=NC(=C(N1C2C(C(C(O2)COP(=O)(O)O)O)O)N)C(=O)N	Pubchem
cpd_air	5-amino-1-(5-phospho-D-ribosyl)imidazole	C03373	-2	C8H12N3O7P	C1=C(N(C=N1)C2C(C(C(O2)COP(=O)(O)O)O)O)N	Pubchem
cpd_akg	2-Oxoglutarate	C00026	-2	C5H4O5	C(CC(=O)O)C(=O)C(=O)O	Pubchem
cpd_ala-B	beta-Alanine	C00099	0	C3H7NO2	C(CN)C(=O)O	Pubchem
cpd_ala-D	D-Alanine	C00133	0	C3H7NO2	CC(C(=O)O)N	Pubchem
cpd_ala-L	L-Alanine	C00041	0	C3H7NO2	CC(C(=O)O)N	Pubchem
cpd_alaala	D-Alanyl-D-alanine	C00993	0	C6H12N2O3	CC(C(=O)NC(C)C(=O)O)N	Pubchem
cpd_alac-S	(S)-2-Acetolactate	C06010	-1	C5H7O4	CC(=O)C(C)(C(=O)O)O	Pubchem
cpd_alltn-R	R-Allantoin	C02348	0	C4H6N4O3	C1(C(=O)NC(=O)N1)NC(=O)N	Pubchem
cpd_alltn-S	S-Allantoin	C02350	0	C4H6N4O3	C1(C(=O)NC(=O)N1)NC(=O)N	Pubchem
cpd_alltt	Allantoate	C00499	0	C4H8N4O4	C(C(=O)[O-])(NC(=O)N)NC(=O)N	Pubchem

cpd_amet	S-Adenosyl-L-methionine	C00019	1	C15H23N6O5S	C[S+](CCC(C(=O)[O-])N)CC1C(C(C(O1)N2C=NC3=C2N=CN=C3N)O)O	Pubchem
cpd_ametam	S-Adenosylmethioninamine	C01137	2	C14H24N6O3S	C[S+](CCCN)CC1C(C(C(O1)N2C=NC3=C2N=CN=C3N)O)O	Pubchem
cpd_amob	S-Adenosyl-4-methylthio-2-oxobutanoate	C04425	0	C15H19N5O6S	C[S+](CCC(=O)C(=O)O)CC1C(C(C(O1)N2C=NC3=C2N=CN=C3N)O)O	Pubchem
cpd_amp	AMP	C00020	-2	C10H12N5O7P	C1=NC2=C(C(=N1)N)N=CN2C3C(C(C(O3)COP(=O)(O)O)O)O	Pubchem
cpd_anth	Anthranilate	C00108	-1	C7H6NO2	C1=CC=C(C(=C1)C(=O)O)N	Pubchem
cpd_ap4a	P1,P4-Bis(5'-adenosyl) tetraphosphate	C01260	-4	C20H24N10O19P4	C1=NC2=C(C(=N1)N)N=CN2C3C(C(C(O3)COP(=O)(O)OP(=O)(O)OP(=O)(O)OP(=O)(O)OCC4C(C(C(O4)N5C=NC6=C5N=CN=C6N)O)O)O)O	Pubchem

cpd_ap5a	P1,P5-Bis(5'-adenosyl) pentaphosphate	C04058	-5	C20H24N10O22P5	C1=NC2=C(C(=N1)N)N=CN2C3C(C(C(O3)COP(=O)(O)OP(=O)(O)OP(=O)(O)OP(=O)(O)OP(=O)(O)OCC4C(C(C(O4)N5C=NC6=C5N=CN=C6N)O)O)O)O	Pubchem
cpd_aps	Adenosine 5'-phosphosulfate	C00224	-2	C10H12N5O10PS	C1=NC2=C(C(=N1)N)N=CN2C3C(C(C(O3)COP(=O)(O)OS(=O)(=O)O)O)O	Pubchem
cpd_ara5p	D-Arabinose 5-phosphate	C01112	-2	C5H9O8P	C(C(C(C(C(=O)O)O)O)OP(=O)(O)O	Pubchem
cpd_arab-L	L-Arabinose	C00259	0	C5H10O5	C1C(C(C(C(O1)O)O)O)O	Pubchem
cpd_arg-L	L-Arginine	C00062	1	C6H15N4O2	C(CC(C(=O)O)N)CN=C(N)N	Pubchem
cpd_argsuc	N(omega)-(L-Arginino)succinate	C03406	-1	C10H17N4O6	C(CC(C(=O)O)N)CN=C(N)NC(CC(=O)O)C(=O)O	Pubchem
cpd_arsna	Arsenate	C01478	-2	AsHO4	O[As](=O)(O)O	Pubchem
cpd_arsni2	arsenite	C06697	0	AsH3O3	[O-][As]([O-])[O-]	Pubchem

cpd_asn-L	L-Asparagine	C00152	0	C4H8N2O3	C(C(C(=O)O)N)C(=O)N	Pubchem
cpd_asp-L	L-Aspartate	C00049	-1	C4H6NO4	C(C(C(=O)O)N)C(=O)O	Pubchem
cpd_aspsa	L-Aspartate 4-semialdehyde	C00441	0	C4H7NO3	C(C=O)C(C(=O)[O-])[NH3+]	Pubchem
cpd_atp	ATP	C00002	-4	C10H12N5O13P3	C1=NC2=C(C(=N1)N)N=CN2C3C(C(C(O3)COP(=O)(O)OP(=O)(O)OP(=O)(O)O)O)O	Pubchem
cpd_betald	Betaine aldehyde	C00576	1	C5H12NO	C[N+](C)(C)CC=O	Pubchem
cpd_bgl	cellobiose	C00185	0	C12H22O11	C(C1C(C(C(C(O1)OC2C(OC(C(C2O)O)O)CO)O)O)O)O	Pubchem
cpd_btcoa	Butanoyl-CoA	C00136	-4	C25H38N7O17P3S	CCCC(=O)SCCNC(=O)CCNC(=O)C(C(C)(C)COP(=O)(O)OP(=O)(O)OCC1C(C(C(O1)N2C=NC3=C2N=CN=C3N)O)OP(=O)(O)O)O	Pubchem
cpd_btn	Biotin	C00120	-1	C10H15N2O3S	C1C2C(C(S1)CCCCC(=O)O)NC(=O)N2	Pubchem

cpd_but	Butyrate	C00246	-1	C4H7O2	CCCC(=O)O	Pubchem
cpd_ca2	Calcium	C00076	2	Ca	[Ca]	Pubchem
cpd_camp	cAMP	C00575	-1	C10H11N5O6P	C1C2C(C(C(O2)N3C=NC4=C3N=CN=C4N)O)OP(=O)(O1)O	Pubchem
cpd_cbasp	N-Carbamoyl-L-aspartate	C00438	-2	C5H6N2O5	C(C(C(=O)O)NC(=O)N)C(=O)O	Pubchem
cpd_cbi	Cobinamide	C05774	0	C48H72CoN11O8	CC1=C2C(C(C([N-]2)C3(C(C(C(=N3)C(=C4C(C(C(=N4)C=C5C(C(C1=N5)CCC(=O)N)(C)C)CCC(=O)N)(C)CC(=O)N)C)CC(=O)N)(C)CC(=O)N)C)CC(=O)N)(C)CCC(=O)NCC(C)O.[Co+3]	Pubchem
cpd_cbl1	Cob(I)alamin	C00853	-1	C62H88CoN13O14P	CC1=CC2=C(C=C1C)N(C=N2)C3C(C(C(O3)CO)OP(=O)(O)OC(C)CNC(=O)CCC4(C(C5C6(C(C(C(=N6)C(=C7C(C(C(=N7)C=C8C(C(C(=N8)C(=	Pubchem

					C4[N-]5)C)CCC(=O)N)(C)C)CCC(=O)N)(C)CC(=O)N)CCC(=O)N)(C)CC(=O)N)C)CC(=O)N)C)O.[Co]	
cpd_cbp	Carbamoyl phosphate	C00169	-2	CH2NO5P	C(=O)(N)OP(=O)(O)O	Pubchem
cpd_cdp	CDP	C00112	-3	C9H12N3O11P2	C1=CN(C(=O)N=C1N)C2C(C(C(O2)COP(=O)(O)OP(=O)(O)O)O)O	Pubchem
cpd_cdp4d6dg	CDP-4-dehydro-6-deoxy-D-glucose	C01219	-2	C15H21N3O15P2	CC1C(=O)C(C(C(O1)OP(=O)(O)OP(=O)(O)OCC2C(C(C(O2)N3C=CC(=NC3=O)N)O)O)O)O	Pubchem
cpd_cdpdag	CDPdiacylglycerol	C00269	-2	C14H17N3O15P2R2	[H]C(=O)OC[C@H](COP(O)(=O)OP(O)(=O)OC[C@H]1O[C@H]([C@H](O)[C@@H]1O)N1C=CC(N)=NC1=O)OC([H])=O	Pubchem
cpd_cdpg	CDP-glucose	C00501	-2	C15H23N3O16P2	C1=CN(C(=O)N=C1	Pubchem

					N)C2C(C(C(O2)COP(=O)(O)OP(=O)(O)OC3C(C(C(C(O3)CO)O)O)O)O)O	
cpd_ch4s	Methanethiol	C00409	0	CH4S	CS	Pubchem
cpd_chitob	Chitobiose	C01674	0	C16H28N2O11	CC(=O)NC1C(C(C(OC1O)CO)OC2C(C(C(C(O2)CO)O)O)O)NC(=O)C)O	Pubchem
cpd_chol	choline	C00114	1	C5H14NO	C[N+](C)(C)CCO	Pubchem
cpd_chor	Chorismate	C00251	-2	C10H8O6	C=C(C(=O)O)OC1C=C(C=CC1O)C(=O)O	Pubchem
cpd_cinnm	trans-Cinnamate	C00423	-1	C9H7O2	C1=CC=C(C=C1)C=CC(=O)O	Pubchem
cpd_cit	Citrate	C00158	-3	C6H5O7	C(C(=O)O)C(CC(=O)O)(C(=O)O)O	Pubchem
cpd_citr-L	L-Citrulline	C00327	0	C6H13N3O3	C(CC(C(=O)O)N)CNC(=O)N	Pubchem
cpd_ckdo	CMP-3-deoxy-D-manno-octulosonate	C04121	-2	C17H24N3O15P	C1C(C(C(OC1(C(=O)O)OP(=O)(O)OCC2C(C(C(O2)N3C=CC(=NC3=O)N)O)O)C(CO)O)O)O	Pubchem
cpd_ckdo8n	CMP-8-amino-3,8-dideoxy-D-manno-	C21334	-1	C17H26N4O14P	C1C(C(C(OC1(C(=O)[O-])OP(=O)([	Pubchem

	oct-2-ulosonic acid				O-])OCC2C(C(C(O2)N3C=CC(=NC3=O)N)O)O)C(C[NH3+])O)O)O	
cpd_cl	Chloride	C00698	-1	Cl	[Cl-]	Pubchem
cpd_cm	Chloramphenicol	C00918	0	C11H12Cl2N2O5	C1=CC(=CC=C1C(C(CO)NC(=O)C(Cl)Cl)O)[N+](=O)[O-]	Pubchem
cpd_cmac	Chloramphenicol 3-acetate	C03601	0	C13H14Cl2N2O6	CC(=O)OCC(C(C1=CC=C(C=C1)[N+](=O)[O-])O)NC(=O)C(Cl)Cl	Pubchem
cpd_cmp	CMP	C00055	-2	C9H12N3O8P	C1=CN(C(=O)N=C1N)C2C(C(C(O2)COP(=O)(O)O)O)O	Pubchem
cpd_co2	CO2	C00011	0	CO2	C(=O)=O	Pubchem
cpd_coa	Coenzyme A	C00010	-4	C21H32N7O16P3S	CC(C)(COP(=O)(O)OP(=O)(O)OCC1C(C(C(O1)N2C=NC3=C2N=CN=C3N)O)OP(=O)(O)O)C(C(=O)NCCC(=O)NCCS)O	Pubchem
cpd_cobalt2	Co2+	C00175	2	Co	[Co+2]	Pubchem
cpd_cobalt3	Co3+	C19171	3	Co	[Co+3]	Pubchem

cpd_cobamcoa	Cobamide coenzyme	C00194	0	C72H100CoN18O17P	CC1=CC2=C(C=C1C)N(C=N2)C3C(C(C(O3)CO)OP(=O)([O-])OC(C)CNC(=O)CCC4(C(C5C6(C(C(C(=N6)C(=C7C(C(C(=N7)C=C8C(C(C(=N8)C(=C4[N-]5)C)CCC(=O)N)(C)C)CCC(=O)N)(C)CC(=O)N)C)CCC(=O)N)(C)CC(=O)N)C)O.[CH2-]C1C(C(C(O1)N2C=NC3=C2N=CN=C3N)O)O.[Co+3]	Pubchem
cpd_coniferaldd	Coniferaldehyde	C02666	0	C10H10O3	COC1=C(C=CC(=C1)C=CC=O)O	Pubchem
cpd_cpppg3	Coproporphyrinogen III	C03263	-4	C36H40N4O8	CC1=C2CC3=C(C(=C(N3)CC4=C(C(=C(N4)CC5=C(C(=C(N5)CC(=C1CCC(=O)O)N2)C)CCC(=O)O)	Pubchem

					C)CCC(=O)O)CCC(=O)O)C	
cpd_cro4	chromate	NA	-2	CrO4	[O-][Cr](=O)(=O)[O-]	Pubchem
cpd_CrOH3	Cr(OH)3	NA	0	CrO3H3	[OH-].[OH-].[OH-].[Cr+3]	Pubchem
cpd_csn	Cytosine	C00380	0	C4H5N3O	C1=C(NC(=O)N=C1)N	Pubchem
cpd_ctp	CTP	C00063	-4	C9H12N3O14P3	C1=CN(C(=O)N=C1N)C2C(C(C(O2)COP(=O)(O)OP(=O)(O)OP(=O)(O)O)O)O	Pubchem
cpd_cu2	Cu2+	C00070	2	Cu	[Cu+2]	Pubchem
cpd_cyan	cyanide	C01326	0	HCN	C#N	Pubchem
cpd_cys-gly	Cystyl-Glycine	C01419	0	C5H10N2O3S	C(C(C(=O)NCC(=O)O)N)S	Pubchem
cpd_cys-L	L-Cysteine	C00097	0	C3H7NO2S	C(C(C(=O)O)N)S	Pubchem
cpd_cysth-L	L-Cystathionine	C02291	0	C7H14N2O4S	C(CSCC(C(=O)O)N)C(C(=O)O)N	Pubchem
cpd_cytd	Cytidine	C00475	0	C9H13N3O5	C1=CN(C(=O)N=C1N)C2C(C(C(O2)CO)O)O	Pubchem
cpd_dad-2	Deoxyadenosine	C00559	0	C10H13N5O3	C1C(C(OC1N2C=NC3=C2N=CN=C3N)CO)O	Pubchem
cpd_dad-5	5'-Deoxyadenosine	C05198	0	C10H13N5O3	CC1C(C(C(O1)N2C=NC3=C2N	Pubchem

					=CN=C3N)O)O	
cpd_dadp	dADP	C00206	-3	C10H12N5O9P2	C1C(C(OC1N2C=NC3=C2N=CN=C3N)COP(=O)(O)OP(=O)(O)O)O	Pubchem
cpd_damp	dAMP	C00360	-2	C10H12N5O6P	C1C(C(OC1N2C=NC3=C2N=CN=C3N)COP(=O)(O)O)O	Pubchem
cpd_dann	7,8-Diaminononanoate	C01037	1	C9H21N2O2	CC(C(CCCCCC(=O)O)N)N	Pubchem
cpd_datp	dATP	C00131	-4	C10H12N5O12P3	C1C(C(OC1N2C=NC3=C2N=CN=C3N)COP(=O)(O)OP(=O)(O)OP(=O)(O)O)O	Pubchem
cpd_db4p	3,4-dihydroxy-2-butanone 4-phosphate	C15556	-2	C4H7O6P	CC(=O)C(COP(=O)(O)O)O	Pubchem
cpd_dcamp	N6-(1,2-Dicarboxyethyl)-AMP	C03794	-4	C14H14N5O11P	C1=NC2=C(C(=N1)NC(CC(=O)O)C(=O)O)N=CN2C3C(C(C(O3)COP(=O)(O)O)O)O	Pubchem
cpd_dcdp	dCDP	C00705	-3	C9H12N3O10P2	C1C(C(OC1N2C=CC(=NC2=O)N)COP(=O)(O)OP(	Pubchem

					=O)(O)O)O	
cpd_dcmp	dCMP	C00239	-2	C9H12N3O7P	C1C(C(OC1N2C=CC(=NC2=O)N)COP(=O)(O)O)O	Pubchem
cpd_dctp	dCTP	C00458	-4	C9H12N3O13P3	C1C(C(OC1N2C=CC(=NC2=O)N)COP(=O)(O)OP(=O)(O)OP(=O)(O)O)O	Pubchem
cpd_dcyt	Deoxycytidine	C00881	0	C9H13N3O4	C1C(C(OC1N2C=CC(=NC2=O)N)CO)O	Pubchem
cpd_dgdp	dGDP	C00361	-3	C10H12N5O10P2	C1C(C(OC1N2C=NC3=C2N=C(NC3=O)N)COP(=O)(O)OP(=O)(O)O)O	Pubchem
cpd_dgmp	dGMP	C00362	-2	C10H12N5O7P	C1C(C(OC1N2C=NC3=C2N=C(NC3=O)N)COP(=O)(O)O)O	Pubchem
cpd_dgsn	Deoxyguanosine	C00330	0	C10H13N5O4	C1C(C(OC1N2C=NC3=C2N=C(NC3=O)N)CO)O	Pubchem
cpd_dgtp	dGTP	C00286	-4	C10H12N5O13P3	C1C(C(OC1N2C=NC3=C2N=C(NC3=O)N)COP(=O)(O)OP(=O)(O)OP(=O)(O)O)O	Pubchem

cpd_dhap	Dihydroxyacetone phosphate	C00111	-2	C3H5O6P	C(C(=O)COP(=O)(O)O)O	Pubchem
cpd_dhbpt	6,7-Dihydrobiopterin	C00268	0	C9H13N5O3	CC(C(C1CN=C2C(=N1)C(=O)NC(=N2)N)O)O	Pubchem
cpd_dhf	7,8-Dihydrofolate	C00415	-2	C19H19N7O6	C1C(=NC2=C(N1)N=C(NC2=O)N)CNC3=CC=C(C=C3)C(=O)NC(CCC(=O)O)C(=O)O	Pubchem
cpd_dhmptp	Dihydromonapterin-triphosphate	C21094	-4	C9H12N5O13P3	C1C(=NC2=C(N1)N=C(NC2=O)N)C(C(COP(=O)(O)OP(=O)(O)OP(=O)(O)O)O)O	Pubchem
cpd_dhna	1,4-Dihydroxy-2-naphthoate	C03657	-1	C11H7O4	C1=CC=C2C(=C1)C(=CC(=C2O)C(=O)O)O	Pubchem
cpd_dhnpt	2-Amino-4-hydroxy-6-(D-erythro-1,2,3-trihydroxypropyl)-7,8-dihydropteridine	C04874	0	C9H13N5O4	C1C(=NC2=C(N1)N=C(NC2=O)N)C(C(CO)O)O	Pubchem
cpd_dhor-S	(S)-Dihydroorotate	C00337	-1	C5H5N2O4	C1C(NC(=O)NC1=O)C(=O)O	Pubchem
cpd_dhpmp	Dihydroneopterin	C05925	-2	C9H12N5O7P	C1C(=NC2=C(N1)N=C(NC2=	Pubchem

	monophosphate				O)N)C(C(CO)OP(=O)(O)O)O	
cpd_dhpt	Dihydropteroate	C00921	-1	C14H13N6O3	C1C(=NC2=C(N1)N=C(NC2=O)N)CNC3=CC=C(C=C3)C(=O)O	Pubchem
cpd_dhptd	4,5-dihydroxy-2,3-pentanedione	C11838	0	C5H8O4	CC(=O)C(=O)C(CO)O	Pubchem
cpd_dialu	Dialuric Acid	NA	0	C4H4N2O4	C1(C(=O)NC(=O)NC1=O)O	Pubchem
cpd_dimp	dIMP	C06196	-2	C10H11N4O7P	C1C(C(OC1N2C=NC3=C2N=CNC3=O)COP(=O)(O)O)O	Pubchem
cpd_din	Deoxyinosine	C05512	0	C10H12N4O4	C1C(C(OC1N2C=NC3=C2N=CNC3=O)CO)O	Pubchem
cpd_ditp	dITP	C01345	-4	C10H11N4O13P3	C1C(C(OC1N2C=NC3=C2N=CNC3=O)COP(=O)(O)OP(=O)(O)OP(=O)(O)O)O	Pubchem
cpd_dkmpp	2,3-diketo5-methylthio-1-phosphopentane	C15650	-2	C6H9O6PS	CSCCC(=O)C(=O)COP(=O)(O)O	Pubchem
cpd_dmbzid	5,6-Dimethylb	C03114	0	C9H10N2	CC1=CC2=C(C=C1C)N=CN2	Pubchem

	enzimidazole					
cpd_dmlz	6,7-Dimethyl-8-(1-D-ribityl)lumazine	C04332	0	C13H18N4O6	CC1=C(N(C2=NC(=O)NC(=O)C2=N1)CC(C(C(CO)O)O)O)C	Pubchem
cpd_dmpp	Dimethylallyl diphosphate	C00235	-3	C5H9O7P2	CC(=CCOP(=O)(O)OP(=O)(O)O)C	Pubchem
cpd_dms	Dimethyl sulfide	C00580	0	C2H6S	CSC	Pubchem
cpd_dmso	Dimethyl sulfoxide	C11143	0	C2H6OS	CS(=O)C	Pubchem
cpd_dnad	Deamino-NAD+	C00857	-2	C21H24N6O15P2	C1=CC(=C[N+](=C1)C2C(C(C(O2)COP(=O)(O)OP(=O)(O)OCC3C(C(C(O3)N4C=NC5=C4N=CN=C5N)O)O)O)O)C(=O)O	Pubchem
cpd_dodca	Dodecanoic acid	C02679	-1	C12H23O2	CCCCCCCCCCCC(=O)[O-]	Pubchem
cpd_dodcan	Dodecanoic acid (neutral)	C02679	0	C12H24O2	CCCCCCCCCCCC(=O)O	Pubchem
cpd_dpcoa	Dephospho-CoA	C00882	-2	C21H33N7O13P2S	CC(C)(COP(=O)(O)OP(=O)(O)OCC1C(C(C(O1)N2C=NC3=C2N=CN=C3N)O)O)C(C(=O)NCCC(=O)NCCS)O	Pubchem

cpd_drib	Deoxyribose	C01801	0	C5H10O4	C(C=O)C(C(CO)O)O	Pubchem
cpd_dtbt	Dethiobiotin	C01909	-1	C10H17N2O3	CC1C(NC(=O)N1)CCCCCC(=O)O	Pubchem
cpd_dtdp	dTDP	C00363	-3	C10H13N2O11P2	CC1=CN(C(=O)NC1=O)C2CC(C(O2)COP(=O)(O)OP(=O)(O)O)O	Pubchem
cpd_dtdp3adgalp	dTDP-3-amino-3,6-dideoxy-alpha-D-galactopyranose	C19947	-2	C16H25N3O14P2	CC1C(C(C(C(O1)OP(=O)(O)OP(=O)(O)OCC2C(CC(O2)N3C=C(C(=O)NC3=O)C)O)O)N)O	Pubchem
cpd_dtdp3ddgalp	dTDP-3-dehydro-6-deoxy-alpha-D-galactopyranose	C19960	-2	C16H22N2O15P2	CC1C(C(=O)C(C(O1)OP(=O)(O)OP(=O)(O)OCC2C(CC(O2)N3C=C(C(=O)NC3=O)C)O)O)O	Pubchem
cpd_dtdp6dm	dTDP-6-deoxy-L-mannose	C03319	-2	C16H24N2O15P2	CC1C(C(C(C(O1)OP(=O)(O)OP(=O)(O)OCC2C(CC(O2)N3C=C(C(=O)NC3=O)C)O)O)O)O	Pubchem
cpd_dtdpddg	dTDP-4-dehydro-6-deoxy-D-glucose	C11907	-2	C16H22N2O15P2	CC1C(=O)C(C(C(O1)OP(=O)(O)OP(=O)(O)OCC2C	Pubchem

					(CC(O2)N3C=C(C(=O)NC3=O)C)O)O)O	
cpd_dtdpddm	dTDP-4-dehydro-6-deoxy-L-mannose	C00688	-2	C16H22N2O15P2	CC1C(=O)C(C(C(O1)OP(=O)(O)OP(=O)(O)OCC2C(CC(O2)N3C=C(C(=O)NC3=O)C)O)O)O	Pubchem
cpd_dtdpglc	dTDPglucose	C00842	-2	C16H24N2O16P2	CC1=CN(C(=O)NC1=O)C2CC(C(O2)COP(=O)(O)OP(=O)(O)OC3C(C(C(C(O3)CO)O)O)O)O	Pubchem
cpd_dtmp	dTMP	C00364	-2	C10H13N2O8P	CC1=CN(C(=O)NC1=O)C2CC(C(O2)COP(=O)(O)O)O	Pubchem
cpd_dttp	dTTP	C00459	-4	C10H13N2O14P3	CC1=CN(C(=O)NC1=O)C2CC(C(O2)COP(=O)(O)OP(=O)(O)OP(=O)(O)O)O	Pubchem
cpd_dudp	dUDP	C01346	-3	C9H11N2O11P2	C1C(C(OC1N2C=CC(=O)NC2=O)COP(=O)(O)OP(=O)(O)O)O	Pubchem
cpd_dump	dUMP	C00365	-2	C9H11N2O8P	C1C(C(OC1N2C=CC(=O)NC2=	Pubchem

					O)COP(=O)(O)O)O	
cpd_duri	Deoxyuridine	C00526	0	C9H12N2O5	C1C(C(OC1N2C=CC(=O)NC2=O)CO)O	Pubchem
cpd_dutp	dUTP	C00460	-4	C9H11N2O14P3	C1C(C(OC1N2C=CC(=O)NC2=O)COP(=O)(O)OP(=O)(O)OP(=O)(O)O)O	Pubchem
cpd_dxyl5p	1-deoxy-D-xylulose 5-phosphate	C11437	-2	C5H9O7P	CC(=O)C(C(COP(=O)(O)O)O)O	Pubchem
cpd_e4p	D-Erythrose 4-phosphate	C00279	-2	C4H7O7P	C(C(C(C(C=O)O)O)OP(=O)(O)O	Pubchem
cpd_eig3p	D-erythro-1-(Imidazol-4-yl)glycerol 3-phosphate	C04666	-2	C6H9N2O6P	C1=C(NC=N1)C(C(COP(=O)(O)O)O)O	Pubchem
cpd_etha	Ethanolamine	C00189	1	C2H8NO	C(CO)N	Pubchem
cpd_etoh	Ethanol	C00469	0	C2H6O	CCO	Pubchem
cpd_f6p	D-Fructose 6-phosphate	C00085	-2	C6H11O9P	C(C1C(C(C(O1)(CO)O)O)O)OP(=O)(O)O	Pubchem
cpd_fa1	Fatty acid (Iso-C14:0)	C06424	-1	C14H27O2	CC(C)CCCCCCCCCC(=O)O	Pubchem
cpd_fa11	Fatty acid (Iso-C17:0)	C16995	-1	C17H33O2	CC(C)CCCCCCCCCCCCC(=O)O	Pubchem

cpd_fa13	Iso-C13:0	NA	-1	C13H25O2	CC(C)CCCCCCCCC(=O)O	Pubchem
cpd_fa171n8	9E-Heptadecenoic acid	C16536	-1	C17H31O2	CCCCCCCC=CCCCCCCCC(=O)O	Pubchem
cpd_fa181n7	C18:1omega7	NA	-1	C18H33O2	CCCCCCC=CCCCCCCCCCC(=O)O	Pubchem
cpd_fa3	Fatty acid (Iso-C15:0)	C16537	-1	C15H29O2	CC(C)CCCCCCCCCCC(=O)O	Pubchem
cpd_fa6	Fatty acid (iso-C16:0)	C00249	-1	C16H31O2	CC(C)CCCCCCCCCCCC(=O)O	Pubchem
cpd_fad	FAD	C00016	-2	C27H31N9O15P2	CC1=CC2=C(C=C1C)N(C3=NC(=O)NC(=O)C3=N2)CC(C(C(COP(=O)(O)OP(=O)(O)OCC4C(C(C(O4)N5C=NC6=C5N=CN=C6N)O)O)O)O)O	Pubchem
cpd_fadh2	FADH2	C01352	-2	C27H33N9O15P2	CC1=CC2=C(C=C1C)N(C3=C(N2)C(=O)NC(=O)N3)CC(C(C(COP(=O)(O)OP(=O)(O)OCC4C(C(C(O4)N5C=NC6=C5N=CN	Pubchem

					=C6N)O)O)O)O	
cpd_fald	Formaldehyde	C00067	0	CH2O	C=O	Pubchem
cpd_fdp	D-Fructose 1,6-bisphosphate	C00354	-4	C6H10O12P2	C(C1C(C(C(O1)(COP(=O)(O)O)O)O)O)OP(=O)(O)O	Pubchem
cpd_fe2	Fe2+	C14818	2	Fe	[Fe+2]	Pubchem
cpd_fe3	Fe3+	C14819	3	Fe	[Fe+3]	Pubchem
cpd_fgam	N2-Formyl-N1-(5-phospho-D-ribosyl)glycinamide	C04376	-2	C8H13N2O9P	C(C1C(C(C(O1)NC(=O)CNC=O)O)O)OP(=O)(O)O	Pubchem
cpd_fglut-S	S-Formylglutathione	C01031	-1	C11H16N3O7S	C(CC(=O)NC(CSC=O)C(=O)NCC(=O)O)C(C(=O)O)N	Pubchem
cpd_ficytcc	Ferricytochrome c	C00125	3	C42H50FeN8O6S2	CC1=C(C2=CC3=NC(=CC4=NC(=CC5=C(C(=C([N-]5)C=C1[N-]2)C)CCC(=O)O)C(=C4C)CCC(=O)O)C(=C3C=C)C)C.[Fe+5]	Pubchem
cpd_fmn	flavin mononucleotide	C00061	-2	C17H19N4O9P	CC1=CC2=C(C=C1C)N(C3=NC(=O)NC(=O)C3=N2)CC(C(C(COP(=O)(	Pubchem

					O)O)O)O)O	
cpd_fmnRD	flavin mononucleotide reduced	C01847	-2	C17H21N4O9P	CC1=CC2=C(C=C1C)N(C3=C(N2)C(=O)NC(=O)N3)CC(C(C(COP(=O)([O-])[O-])O)O)O	Pubchem
cpd_focytcc	Ferrocytochrome c	C00126	2	C42H50FeN8O6S2	CC1=C(C2=NC1=CC3=C(C(=C([N-]3)C=C4C(=C(C(=N4)C=C5C(=C(C(=C2)[N-]5)C=C)C)C)CCC(=O)O)CCC(=O)O)C)C.[Fe+2]	Pubchem
cpd_for	Formate	C00058	-1	CH1O2	C(=O)[O-]	Pubchem
cpd_forglu	N-Formimidoyl-L-glutamate	C00439	-1	C6H9N2O4	C(CC(=O)O)C(C(=O)O)N=CN	Pubchem
cpd_fpram	2-(Formamido)-N1-(5-phospho-D-ribosyl)acetamidine	C04640	-2	C8H14N3O8P	C(C1C(C(C(O1)N=C(CNC=O)N)O)O)OP(=O)(O)O	Pubchem
cpd_fprica	5-Formamido-1-(5-phospho-D-ribosyl)imidazole-4-carboxamide	C04734	-2	C10H13N4O9P	C1=NC(=C(N1C2C(C(C(O2)COP(=O)(O)O)O)O)NC=O)C(=O)N	Pubchem

cpd_frdp	Farnesyl diphosphate	C00448	-3	C15H25O7P2	CC(=CCCC(=CCCC(=CCOP(=O)(O)OP(=O)(O)O)C)C)C	Pubchem
cpd_frlt	Ferulate	C01494	-1	C10H9O4	COC1=C(C=CC(=C1)C=CC(=O)O)O	Pubchem
cpd_frmd	Formamide	C00488	0	CH3NO	C(=O)N	Pubchem
cpd_fum	Fumarate	C00122	-2	C4H2O4	C(=CC(=O)[O-])C(=O)[O-]	Pubchem
cpd_g1p	D-Glucose 1-phosphate	C00103	-2	C6H11O9P	C(C1C(C(C(C(O1)OP(=O)(O)O)O)O)O)O	Pubchem
cpd_g3p	Glyceraldehyde 3-phosphate	C00661	-2	C3H5O6P	C(C(C=O)O)OP(=O)(O)O	Pubchem
cpd_g3pe	sn-Glycero-3-phosphoethanolamine	C01233	0	C5H14NO6P	C(COP(=O)(O)OCC(CO)O)N	Pubchem
cpd_g3pg	Glycerophosphoglycerol	C03274	-1	C6H14O8P	C(C(COP(=O)(O)OCC(CO)O)O)O	Pubchem
cpd_g6p	D-Glucose 6-phosphate	C00092	-2	C6H11O9P	C(C(C(C(C(C=O)O)O)O)O)OP(=O)(O)O	Pubchem
cpd_gal	D-Galactose	C00124	0	C6H12O6	C(C1C(C(C(C(O1)O)O)O)O)O	Pubchem
cpd_gal1p	alpha-D-Galactose 1-phosphate	C00446	-2	C6H11O9P	C(C1C(C(C(C(O1)OP(=O)(O)O)O)O)O)O	Pubchem

cpd_galactan	Galactan	C05796	0	C12H22O11	C(C1C(C(C(C(C(O1)OC2C(OC(C(C2O)O)O)CO)O)O)O)O)O	Pubchem
cpd_gam1p	D-Glucosamine 1-phosphate	C06156	-1	C6H13NO8P	C(C1C(C(C(C(O1)OP(=O)(O)O)N)O)O)O	Pubchem
cpd_gam6p	D-Glucosamine 6-phosphate	C00352	-1	C6H13NO8P	C(C1C(C(C(C(O1)O)N)O)O)OP(=O)(O)O	Pubchem
cpd_gar	N1-(5-Phospho-D-ribosyl)glycinamide	C03838	-1	C7H14N2O8P	C(C1C(C(C(O1)NC(=O)CN)O)O)OP(=O)(O)O	Pubchem
cpd_gcald	Glycolaldehyde	C00266	0	C2H4O2	C(C=O)O	Pubchem
cpd_gdp	GDP	C00035	-3	C10H12N5O11P2	C1=NC2=C(N1C3C(C(C(O3)COP(=O)(O)OP(=O)(O)O)O)O)N=C(NC2=O)N	Pubchem
cpd_gdpdp	Guanosine 3',5'-bis(diphosphate)	C01228	-6	C10H11N5O17P4	C1=NC2=C(N1C3C(C(C(O3)COP(=O)(O)OP(=O)(O)O)OP(=O)(O)OP(=O)(O)O)O)N=C(NC2=O)N	Pubchem
cpd_gdpmann	GDP-mannose	C00096	-2	C16H23N5O16P2	C1=NC2=C(N1C3C(C(C(O3)COP(=O)(O)OP(=O)(	Pubchem

					O)OC4C(C(C(C(O4)CO)O)O)O)O)N=C(NC2=O)N	
cpd_gdptp	Guanosine 3'-diphosphate 5'-triphosphate	C04494	-7	C10H11N5O20P5	C1=NC2=C(N1C3C(C(C(O3)COP(=O)(O)OP(=O)(O)OP(=O)(O)O)OP(=O)(O)OP(=O)(O)O)O)N=C(NC2=O)N	Pubchem
cpd_ggdp	Geranylgeranyl diphosphate	C00353	-3	C20H33O7P2	CC(=CCCC(=CCCC(=CCCC(=CCOP(=O)(O)OP(=O)(O)O)C)C)C)C	Pubchem
cpd_gglutaba	gammaglutamyl-gamma-aminobutyraldehyde	C15700	0	C9H16N2O4	C(CC=O)CNC(=O)CCC(C(=O)O)N	Pubchem
cpd_gglutabt	gammaglutamyl-gamma-aminobutyrate	C15767	-1	C9H15N2O5	C(CC(=O)O)CNC(=O)CCC(C(=O)O)N	Pubchem
cpd_glupturc	gammaglutamyl putrescine	C15699	1	C9H20N3O3	C(CCNC(=O)CCC(C(=O)O)N)CN	Pubchem
cpd_glc-D	D-Glucose	C00031	0	C6H12O6	C(C1C(C(C(C(O1)O)O)O)O)O	Pubchem
cpd_gln-L	L-Glutamine	C00064	0	C5H10N2O3	C(CC(=O)N)C(C(=O)O)N	Pubchem
cpd_glu-asp-L	glutamyl-L-aspartic acid	NA	-2	C9H12N2O7	C(CC(=O)O)C(C(=O)NC(CC(=	Pubchem

					O)O)C(=O)O)N	
cpd_glu-D	D-Glutamate	C00217	-1	C5H8NO4	C(CC(=O)O)C(C(=O)O)N	Pubchem
cpd_glu-L	L-Glutamate	C00025	-1	C5H8NO4	C(CC(=O)O)C(C(=O)O)N	Pubchem
cpd_glu1sa	L-Glutamate 1-semialdehyde	C03741	0	C5H9NO3	C(CC(=O)O)C(C=O)N	Pubchem
cpd_glu5p	L-Glutamate 5-phosphate	C03287	-2	C5H8NO7P	C(CC(=O)OP(=O)(O)O)C(C(=O)O)N	Pubchem
cpd_glu5sa	L-Glutamate 5-semialdehyde	C01165	0	C5H9NO3	C(CC(C(=O)O)N)C=O	Pubchem
cpd_glucys	gamma-L-Glutamyl-L-cysteine	C00669	-1	C8H13N2O5S	C(CC(=O)NC(CS)C(=O)O)C(C(=O)O)N	Pubchem
cpd_glx	Glyoxylate	C00048	-1	C2H1O3	C(=O)C(=O)O	Pubchem
cpd_gly	Glycine	C00037	0	C2H5NO2	C(C(=O)O)N	Pubchem
cpd_gly-asp-L	glycyl-L-aspartic acid	NA	-1	C6H9N2O5	C(C(C(=O)O)NC(=O)CN)C(=O)O	Pubchem
cpd_gly-glu-L	glycyl-L-glutamic acid	NA	-1	C7H11N2O5	C(CC(=O)O)C(C(=O)O)NC(=O)CN	Pubchem
cpd_glyb	Glycine betaine	C00719	0	C5H11NO2	C[N+](C)(C)CC(=O)[O-]	Pubchem
cpd_glyc	Glycerol	C00116	0	C3H8O3	C(C(CO)O)O	Pubchem
cpd_glyc-R	(R)-Glycerate	C00258	-1	C3H5O4	C(C(C(=O)O)O)O	Pubchem

cpd_glyc3p	sn-Glycerol 3-phosphate	C00093	-2	C3H7O6P	C(C(COP(=O)(O)O)O)O	Pubchem
cpd_glyclt	Glycolate	C00160	-1	C2H3O3	C(C(=O)O)O	Pubchem
cpd_glycogen	glycogen	C00182	0	C24H42O21	C(C1C(C(C(C(O1)OCC2C(C(C(C(O2)OC3C(OC(C(C3O)O)O)CO)O)O)OC4C(C(C(C(O4)CO)O)O)O)O)O)O)O	Pubchem
cpd_gmh17bp	D-Glycero-D-manno-heptose 1,7-bisphosphate	C19879	-4	C7H12O13P2	C(C(C1C(C(C(C(O1)OP(=O)(O)O)O)O)O)O)OP(=O)(O)O	Pubchem
cpd_gmh1p	D-Glycero-D-manno-heptose 1-phosphate	C07838	-2	C7H13O10P	C(C(C1C(C(C(C(O1)OP(=O)(O)O)O)O)O)O)O	Pubchem
cpd_gmh7p	D-Glycero-D-manno-heptose 7-phosphate	C19882	-2	C7H13O10P	C(C(C(C1C(C(C(C(O1)O)O)O)O)O)O)OP(=O)(O)O	Pubchem
cpd_gmp	GMP	C00144	-2	C10H12N5O8P	C1=NC2=C(N1C3C(C(C(O3)COP(=O)(O)O)O)O)N=C(NC2=O)N	Pubchem
cpd_gp4g	P1,P4-Bis(5'-guanosyl) tetraphosphate	C01261	-4	C20H24N10O21P4	C1=NC2=C(N1C3C(C(C(O3)COP(=O)(O)OP(=O)(O)OP(=O)	Pubchem

					(O)OP(=O)(O)OCC4C(C(C(O4)N5C=NC6=C5N=C(NC6=O)N)O)O)O)O)N=C(NC2=O)N	
cpd_grdp	Geranyl diphosphate	C00341	-3	C10H17O7P2	CC(=CCCC(=CCOP(=O)(O)OP(=O)(O)O)C)C	Pubchem
cpd_gsn	Guanosine	C00387	0	C10H13N5O5	C1=NC2=C(N1C3C(C(C(O3)CO)O)O)N=C(NC2=O)N	Pubchem
cpd_gthox	Oxidized glutathione	C00127	-2	C20H30N6O12S2	C(CC(=O)NC(CSSCC(C(=O)NCC(=O)O)NC(=O)CCC(C(=O)O)N)C(=O)NCC(=O)O)C(C(=O)O)N	Pubchem
cpd_gthrd	Reduced glutathione	C00051	-1	C10H16N3O6S	C(CC(=O)NC(CS)C(=O)NCC(=O)O)C(C(=O)O)N	Pubchem
cpd_gtp	GTP	C00044	-4	C10H12N5O14P3	C1=NC2=C(N1C3C(C(C(O3)COP(=O)(O)OP(=O)(O)OP(=O)(O)O)O)O)O)N=C(NC2=O)N	Pubchem
cpd_gua	Guanine	C00242	0	C5H5N5O	C1=NC2=C(N1)C(=	Pubchem

					O)NC(=N2)N	
cpd_h	H+	C00080	1	H	[H]	Pubchem
cpd_h2	H2	C00282	0	H2	[HH]	Pubchem
cpd_h2mb4p	1-hydroxy-2-methyl-2-(E)-butenyl 4-diphosphate	C11811	-3	C5H9O8P2	CC(=CCOP(=O)([O-])OP(=O)([O-])[O-])CO	Pubchem
cpd_h2o	H2O	C00001	0	H2O	O	Pubchem
cpd_h2o2	Hydrogen peroxide	C00027	0	H2O2	OO	Pubchem
cpd_h2s	Hydrogen sulfide	C00283	-1	HS	S	Pubchem
cpd_hco3	Bicarbonate	C00288	-1	CHO3	C(=O)(O)[O-]	Pubchem
cpd_hcys-L	L-Homocysteine	C00155	0	C4H9NO2S	C(CS)C(C(=O)O)N	Pubchem
cpd_hdca	hexadecanoate (n-C16:0)	C00249	-1	C16H31O2	CCCCCCCCCCCCCCCC(=O)O	Pubchem
cpd_hdcan	hexadecanoate (n-C16:0) (neutral)	C00249	0	C16H32O2	CCCCCCCCCCCCCCCC(=O)O	Pubchem
cpd_hdcea	hexadecenoate (n-C16:1)	C08362	-1	C16H29O2	CCCCCCC=CCCCCCCCC(=O)O	Pubchem
cpd_hemeO	Heme O	C15672	-2	C49H56FeN4O5	CC1=C(C2=CC3=NC(=CC4=C(C(=C([N-]4)C=C5C(=C(C(=N5)C=C1[N-]2)C=C)C)C(CCC=C(C)CCC=C(C)CCC=C(C)C)O)C)C(=C3CC	Pubchem

					C(=O)O)C)CCC(=O)O.[Fe+2]	
cpd_hepdp	all-trans-Heptaprenyl diphosphate	C04216	-3	C35H57O7P2	CC(=CCCC(=CCCC(=CCCC(=CCCC(=CCCC(=CCOP(=O)(O)OP(=O)(O)C)C)C)C)C)C)C	Pubchem
cpd_hexdp	all-trans-Hexaprenyl diphosphate	C01230	-3	C30H49O7P2	CC(=CCCC(=CCCC(=CCCC(=CCCC(=CCOP(=O)(O)OP(=O)(O)C)C)C)C)C)C	Pubchem
cpd_hg2	Mercury (charged +2)	C00703	2	Hg	[Hg+2]	Pubchem
cpd_hgentis	Homogentisate	C00544	-1	C8H7O4	C1=CC(=C(C=C1O)CC(=O)O)O	Pubchem
cpd_hibcoa	3-Hydroxyisobutyryl-CoA	C04047	-3	C25H39N7O18P3S	CC(CO)C(=O)SCCNC(=O)CCNC(=O)C(C(C)(C)COP(=O)(O)OP(=O)(O)OCC1C(C(C(O1)N2C=NC3=C2N=CN=C3N)O)OP(=O)(O)O)O	Pubchem
cpd_his-L	L-Histidine	C00135	0	C6H9N3O2	C1=C(NC=N1)CC(C(=O)O)N	Pubchem

cpd_hisp	L-Histidinol phosphate	C01100	-1	C6H11N3O4P	C1=C(NC=N1)CC(COP(=O)(O)O)N	Pubchem
cpd_histd	L-Histidinol	C00860	1	C6H12N3O	C1=C(NC=N1)CC(CO)N	Pubchem
cpd_hmbil	Hydroxymethylbilane	C01024	-8	C40H38N4O17	C1=C(C(=C(N1)CC2=C(C(=C(N2)CC3=C(C(=C(N3)CC4=C(C(=C(N4)CO)CC(=O)O)CCC(=O)O)CC(=O)O)CCC(=O)O)CC(=O)O)CC(=O)O)CCC(=O)O	Pubchem
cpd_hmgcoa	Hydroxymethylglutaryl-CoA	C00356	-5	C27H39N7O20P3S	CC(C)(COP(=O)(O)OP(=O)(O)OCC1C(C(C(O1)N2C=NC3=C2N=CN=C3N)O)OP(=O)(O)O)C(C(=O)NCCC(=O)NCCSC(=O)CC(C)(CC(=O)O)O)O	Pubchem
cpd_hmglut-S	S-(Hydroxymethyl)glutathione	C14180	-1	C11H18N3O7S	C(CC(=O)NC(CSCO)C(=O)NCC(=O)O)C(C(=O)O)N	Pubchem

cpd_hom-L	L-Homoserine	C00263	0	C4H9NO3	C(CO)C(C(=O)O)N	Pubchem
cpd_hpdca	heptadecanoate (n-C17:0)	C16995	-1	C17H33O2	CCCCCCCCCCCCCCCC(=O)[O-]	Pubchem
cpd_hpde	heptadecenoate (n-C17:1)	NA	-1	C17H31O2	CCCCCCC=CCCCCCCCC(=O)[O-]	Pubchem
cpd_hpyr	Hydroxypyruvate	C00168	-1	C3H3O4	C(C(=O)C(=O)O)O	Pubchem
cpd_hxan	Hypoxanthine	C00262	0	C5H4N4O	C1=NC2=C(N1)C(=O)NC=N2	Pubchem
cpd_iasp	Iminoaspartate	C05840	-2	C4H3NO4	C(C(=N)C(=O)O)C(=O)O	Pubchem
cpd_ibcoa	Isobutyryl-CoA	C00630	-4	C25H38N7O17P3S	CC(C)C(=O)SCCNC(=O)CCNC(=O)C(C(C)(C)COP(=O)(O)OP(=O)(O)OCC1C(C(C(O1)N2C=NC3=C2N=CN=C3N)O)OP(=O)(O)O)O	Pubchem
cpd_ichor	Isochorismate	C00885	-2	C10H8O6	C=C(C(=O)O)OC1C=CC=C(C1O)C(=O)O	Pubchem
cpd_icit	Isocitrate	C00311	-3	C6H5O7	C(C(C(C(=O)O)O)C(=O)O)C(=O)O	Pubchem
cpd_idp	IDP	C00104	-3	C10H11N4O11P2	C1=NC2=C(C(=O)N1)N=CN2C3C(C(C(O3)COP(=	Pubchem

					O)(O)OP(=O)(O)O)O)O	
cpd_ile-L	L-Isoleucine	C00407	0	C6H13NO2	CCC(C)C(C(=O)O)N	Pubchem
cpd_imp	IMP	C00130	-2	C10H11N4O8P	C1=NC2=C(C(=O)N1)N=CN2C3C(C(C(O3)COP(=O)(O)O)O)O	Pubchem
cpd_indole	Indole	C00463	0	C8H7N	C1=CC=C2C(=C1)C=CN2	Pubchem
cpd_inosh p	myo-Inositol hexakisphosphate	C01204	-12	C6H6O24P6	C1(C(C(C(C(C1OP(=O)(O)O)OP(=O)(O)O)OP(=O)(O)O)OP(=O)(O)O)OP(=O)(O)O)OP(=O)(O)O	Pubchem
cpd_inosp p1	1D-myo-inositol 1,3,4,5,6-pentakisphosphate	C01284	-10	C6H7O21P5	C1(C(C(C(C(C1OP(=O)(O)O)OP(=O)(O)O)OP(=O)(O)O)OP(=O)(O)O)OP(=O)(O)O)O	Pubchem
cpd_inost	myo-Inositol	C00137	0	C6H12O6	C1(C(C(C(C(C1O)O)O)O)O)O	Pubchem
cpd_ins	Inosine	C00294	0	C10H12N4O5	C1=NC2=C(C(=O)N1)N=CN2C3C(C(C(O3)CO)O)O	Pubchem
cpd_ipdp	Isopentenyl	C00129	-3	C5H9O7P2	CC(=C)CCOP(=O)(O	Pubchem

	diphosphate				)OP(=O)(O)O	
cpd_itp	ITP	C00081	-4	C10H11N4O14P3	C1=NC2=C(C(=O)N1)N=CN2C3C(C(C(O3)COP(=O)(O)OP(=O)(O)OP(=O)(O)O)O)O	Pubchem
cpd_ivcoa	Isovaleryl-CoA	C02939	-4	C26H40N7O17P3S	CC(C)CC(=O)SCCNC(=O)CCNC(=O)C(C(C)(C)COP(=O)(O)OP(=O)(O)OCC1C(C(C(O1)N2C=NC3=C2N=CN=C3N)O)OP(=O)(O)O)O	Pubchem
cpd_k	K+	C00238	1	K	[K+]	Pubchem
cpd_kdo	3-Deoxy-D-manno-2-octulosonate	C21063	-1	C8H13O8	C(C(C(C(C(CO)O)O)O)O)C(=O)C(=O)O	Pubchem
cpd_kdo8p	3-Deoxy-D-manno-octulosonate 8-phosphate	C04478	-3	C8H12O11P	C(C(C(C(C(COP(=O)(O)O)O)O)O)O)C(=O)C(=O)O	Pubchem
cpd_lac-D	D-Lactate	C00256	-1	C3H5O3	CC(C(=O)O)O	Pubchem
cpd_lac-L	L-Lactate	C00186	-1	C3H5O3	CC(C(=O)O)O	Pubchem
cpd_lami	laminarin	C00771	0	C24H42O21	OC[C@H]1O[C@@H](O[C@H]2[C@H](O)[C@@H](CO)O[	Pubchem

					C@@H](O[C@H]3[C@H](O)[C@@H](CO)O[C@@H](O[C@@H]4[C@@H](O)[C@@H](O)O[C@H](CO)[C@H4O)[C@@H3O)[C@@H2O)[C@H](O)[C@@H](O)[C@@H]1O	
cpd_leu-L	L-Leucine	C00123	0	C6H13NO2	CC(C)CC(C(=O)O)N	Pubchem
cpd_lgt-S	(R)-S-Lactoylglutathione	C03451	-1	C13H20N3O8S	CC(C(=O)SCC(C(=O)NCC(=O)O)NC(=O)CCC(C(=O)O)N)O	Pubchem
cpd_lipidA	2,3-Bis(3-hydroxytetradecanoyl)-D-glucosaminyl-1,6-beta-D-2,3-bis(3-hydroxytetradecanoyl)-beta-D-glucosaminyl 1-phosphate	C04919	-4	C68H126N2O23P2	CCCCCCCCCCCCC(CC(=O)NC1C(C(C(OC1OCC2C(C(C(C(O2)OP(=O)(O)O)NC(=O)CC(CCCCCCCCCCC)O)OC(=O)CC(CCCCCCCCCCC)O)O)CO)O)OC(=O)CC(CCCCCCCCCCC)O)O	Pubchem

cpd_lipidAds	Lipid A Disaccharide	C04932	-2	C68H127N2O20P	CCCCCCCCCCCCC(CC(=O)NC1C(C(C(OC1OCC2C(C(C(C(O2)OP(=O)(O)O)NC(=O)CC(CCCCCCCCCCC)O)OC(=O)CC(CCCCCCCCCCCCC)O)O)CO)O)OC(=O)CC(CCCCCCCCCCCCC)O)O	Pubchem
cpd_lipidX	2,3-Bis(3-hydroxytetradecanoyl)-beta-D-glucosaminyl 1-phosphate	C04824	-2	C34H64NO12P	CCCCCCCCCCCCC(CC(=O)NC1C(C(C(OC1OP(=O)(O)O)CO)O)OC(=O)CC(CCCCCCCCCCC)O)O	Pubchem
cpd_lys-L	L-Lysine	C00047	1	C6H15N2O2	C(CCN)CC(C(=O)O)N	Pubchem
cpd_mal-L	L-Malate	C00149	-2	C4H4O5	C(C(C(=O)O)O)C(=O)O	Pubchem
cpd_malcoa	Malonyl-CoA	C00083	-5	C24H33N7O19P3S	CC(C)(COP(=O)(O)OP(=O)(O)OCC1C(C(C(O1)N2C=NC3=C2N=CN=C3N)O)OP(=O)(O)O)C(C(=O)NCCC(=O)	Pubchem

					NCCSC(=O)CC(=O)O)O	
cpd_malt	Maltose	C00208	0	C12H22O11	C(C1C(C(C(C(O1)OC2C(OC(C(C2O)O)O)CO)O)O)O)O	Pubchem
cpd_malthp	Maltoheptaose	C06216	0	C42H72O36	C(C1C(C(C(C(O1)OC2C(OC(C(C2O)O)OC3C(OC(C(C3O)O)OC4C(OC(C(C4O)O)OC5C(OC(C(C5O)O)OC6C(OC(C(C6O)O)OC7C(OC(C(C7O)O)O)CO)CO)CO)CO)CO)CO)O)O)O)O	Pubchem
cpd_malthx	Maltohexaose	C01936	0	C36H62O31	C(C1C(C(C(C(O1)OC2C(OC(C(C2O)O)OC3C(OC(C(C3O)O)OC4C(OC(C(C4O)O)OC5C(OC(C(C5O)O)OC6C(OC(C(C6O)O)O)CO)CO)CO)CO)CO)O)O)O)O	Pubchem
cpd_maltpt	Maltopentaose	NA	0	C30H52O26	C(C1C(C(C(C(O1)OC2C(OC(C(C2O)O)O	Pubchem

					C3C(OC(C(C3O)O)O C4C(OC(C(C4O)O)O C5C(OC(C(C5O)O)O)CO)CO)CO)CO)O)O)O	
cpd_malttr	Maltotriose	C01835	0	C18H32O16	C(C1C(C(C(C(O1)O C2C(OC(C(C2O)O)O C3C(OC(C(C3O)O)O)CO)CO)O)O)O)O	Pubchem
cpd_malttttr	Maltotetraose	C02052	0	C24H42O21	C(C1C(C(C(C(O1)O C2C(OC(C(C2O)O)O C3C(OC(C(C3O)O)O C4C(OC(C(C4O)O)O)CO)CO)CO)O)O)O)O)O	Pubchem
cpd_man1p	D-Mannose 1-phosphate	C00636	-2	C6H11O9P	C(C1C(C(C(C(O1)OP(=O)(O)O)O)O)O)O)O	Pubchem
cpd_man6p	D-Mannose 6-phosphate	C00275	-2	C6H11O9P	C(C1C(C(C(C(O1)O)O)O)O)O)OP(=O)(O)O	Pubchem
cpd_mercppyr	Mercaptopyruvate	C00957	-1	C3H3O3S	C(C(=O)C(=O)O)S	Pubchem
cpd_met-L	L-Methionine	C00073	0	C5H11NO2S	CSCCC(C(=O)O)N	Pubchem
cpd_methf	5,10-Methenylte	C00445	-1	C20H20N7O6	C1C2CN(C=[N+]2C3=C(N1)N	Pubchem

	trahydrofolate				=C(NC3=O)N)C4=CC=C(C=C4)C(=O)NC(CCC(=O)O)C(=O)O	
cpd_mg2	Mg	C00305	2	Mg	[Mg+2]	Pubchem
cpd_mi1p-D	1D-myo-Inositol 1-phosphate	C01177	-2	C6H11O9P	C1(C(C(C(C(C1O)O)OP(=O)(O)O)O)O)O	Pubchem
cpd_micit	Methylisocitrate	C04593	-3	C7H7O7	CC(C(CC(=O)[O-])C(=O)[O-])(C(=O)[O-])O	Pubchem
cpd_mlthf	5,10-Methylenetetrahydrofolate	C00143	-2	C20H21N7O6	C1C2CN(CN2C3=C(N1)N=C(NC3=O)N)C4=CC=C(C=C4)C(=O)NC(CCC(=O)O)C(=O)O	Pubchem
cpd_mmalsa	(S)-Methylmalonate semialdehyde	C06002	-1	C4H5O3	CC(C=O)C(=O)O	Pubchem
cpd_mmql7	methymenaquinol 7	NA	0	C47H68O2	CC1=CC=CC2=C1C(=O)C(=C(C2=O)CC=C(C)CCC=C(C)CCC=C(C)CCC=C(C)CCC=C(C)CCC=C(C)C)C	Pubchem
cpd_mmqn7	methylmenaquinone 7	NA	0	C47H66O2	CC1=CC=CC2=C1C(=O)C(=C(	Pubchem

					C2=O)CC=C(C)CCC=C(C)CCC=C(C)CCC=C(C)CCC=C(C)CCC=C(C)C)C	
cpd_mn2	Mn2+	C19610	2	Mn	[Mn+2]	Pubchem
cpd_mn4o	Manganese (IV) oxide	C21744	0	MnO2	O=[Mn]=O	Pubchem
cpd_mobd	Molybdate	C06232	-2	MoO4	[O-][Mo](=O)(=O)[O-]	Pubchem
cpd_mql7	Menaquinol 7	NA	0	C46H66O2	CC1=C(C2=CC=CC=C2C(=C1CC=C(C)CCC=C(C)CCC=C(C)CCC=C(C)CCC=C(C)CCC=C(C)CCC=C(C)C)O)O	Pubchem
cpd_mqn7	Menaquinone 7	NA	0	C46H64O2	CC1=C(C(=O)C2=CC=CC=C2C1=O)CC=C(C)CCC=C(C)CCC=C(C)CCC=C(C)CCC=C(C)CCC=C(C)CCC=C(C)C	Pubchem
cpd_mthgxl	Methylglyoxal	C00546	0	C3H4O2	CC(=O)C=O	Pubchem
cpd_na1	Sodium	C01330	1	Na	[Na]	Pubchem
cpd_nac	Nicotinate	C00253	-1	C6H4NO2	C1=CC(=CN=C1)C(=O)[O-]	Pubchem
cpd_nad	Nicotinamide adenine dinucleotide	C00003	-1	C21H26N7O14P2	C1=CC(=C[N+](=C1)C2C(C(C(O2)COP	Pubchem

					(=O)([O-])OP(=O)(O)OCC3C(C(C(O3)N4C=NC5=C4N=CN=C5N)O)O)O)C(=O)N	
cpd_nadh	Nicotinamide adenine dinucleotide - reduced	C00004	-2	C21H27N7O14P2	C1C=CN(C=C1C(=O)N)C2C(C(C(O2)COP(=O)(O)OP(=O)(O)OCC3C(C(C(O3)N4C=NC5=C4N=CN=C5N)O)O)O)O	Pubchem
cpd_nadp	Nicotinamide adenine dinucleotide phosphate	C00006	-3	C21H25N7O17P3	C1=CC(=C[N+](=C1)C2C(C(C(O2)COP(=O)(O)OP(=O)(O)OCC3C(C(C(O3)N4C=NC5=C4N=CN=C5N)OP(=O)(O)O)O)O)O)C(=O)N	Pubchem
cpd_nadph	Nicotinamide adenine dinucleotide phosphate - reduced	C00005	-4	C21H26N7O17P3	C1C=CN(C=C1C(=O)N)C2C(C(C(O2)COP(=O)(O)OP(=O)(O)OCC3C(C(C(O3)N4C=NC5=C4N=CN=C5N)OP(	Pubchem

					=O)(O)O)O)O)O	
cpd_nh4	Ammonium	C00014	1	H4N	N	Pubchem
cpd_ni2	Ni2+	C19609	2	Ni	[Ni+2]	Pubchem
cpd_nicrnt	Nicotinate D-ribonucleotide	C01185	-2	C11H12NO9P	C1=CC(=C[N+](=C1)C2C(C(C(O2)COP(=O)(O)O)O)O)C(=O)O	Pubchem
cpd_nmn	NMN	C00455	-1	C11H14N2O8P	C1=CC(=C[N+](=C1)C2C(C(C(O2)COP(=O)(O)[O-])O)O)C(=O)N	Pubchem
cpd_no	Nitric oxide	C00533	0	NO	[N]=O	Pubchem
cpd_no2	Nitrite	C00088	-1	NO2	N(=O)[O-]	Pubchem
cpd_no3	Nitrate	C00244	-1	NO3	[N+](=O)([O-])[O-]	Pubchem
cpd_o2	O2	C00007	0	O2	O=O	Pubchem
cpd_o2-	Superoxide	C00704	-1	O2	[O-][O]	Pubchem
cpd_oaa	Oxaloacetate	C00036	-2	C4H2O5	C(C(=O)C(=O)O)C(=O)O	Pubchem
cpd_ocdca	octadecanoate (n-C18:0)	NA	-1	C18H35O2	CCCCCCCCCCCCCCCCCC(=O)[O-]	Pubchem
cpd_ocdcan	octadecanoate (n-C18:0) neutral	NA	0	C18H36O2	CCCCCCCCCCCCCCCCCC(=O)O	Pubchem
cpd_ocdcea	octadecenoate (n-C18:1)	C00712	-1	C18H33O2	CCCCCCCCC=CCCCCCCCC(=O)[O-]	Pubchem
cpd_octdp	all-trans-Octaprenyl	C04146	-3	C40H65O7P2	CC(=CCCC(=CCCC(=CCCC(=	Pubchem

	diphosphate				CCCC(=CCCC(=CCCC(=CCCC(=CCOP(=O)(O)OP(=O)(O)O)C)C)C)C)C)C)C	
cpd_ohcu	5-Hydroxy-2-oxo-4-ureido-2,5-dihydro-1H-imidazole-5-carboxylate	C12248	0	C5H6N4O5	C1(=NC(=O)NC1(C(=O)O)O)NC(=O)N	Pubchem
cpd_ohpb	2-Oxo-3-hydroxy-4-phosphobutanoate	C06054	-3	C4H4O8P	C(C(C(=O)C(=O)O)O)OP(=O)(O)O	Pubchem
cpd_orn-L	L-Ornithine	C00077	1	C5H13N2O2	C(CC(C(=O)O)N)CN	Pubchem
cpd_orot	Orotate	C00295	-1	C5H3N2O4	C1=C(NC(=O)NC1=O)C(=O)[O-]	Pubchem
cpd_orot5p	Orotidine 5'-phosphate	C01103	-3	C10H10N2O11P	C1=C(N(C(=O)NC1=O)C2C(C(C(O2)COP(=O)(O)O)O)O)C(=O)O	Pubchem
cpd_pan4p	Pantetheine 4'-phosphate	C01134	-2	C11H21N2O7PS	CC(C)(COP(=O)(O)O)C(C(=O)NCCC(=O)NCCS)O	Pubchem
cpd_panose	Panose	C00713	0	C18H32O16	C(C1C(C(C(C(O1)OCC2C(C(C(C(O2)OC(C(CO)O)	Pubchem

					C(C(C=O)O)O)O)O)O)O)O)O	
cpd_pant-R	(R)-Pantoate	C00522	-1	C6H11O4	CC(C)(CO)C(C(=O)[O-])O	Pubchem
cpd_pap	Adenosine 3',5'-bisphosphate	C00054	-4	C10H11N5O10P2	C1=NC2=C(C(=N1)N)N=CN2C3C(C(C(O3)COP(=O)(O)O)OP(=O)(O)O)O	Pubchem
cpd_paps	3'-Phosphoadenylyl sulfate	C00053	-4	C10H11N5O13P2S	C1=NC2=C(C(=N1)N)N=CN2C3C(C(C(O3)COP(=O)(O)OS(=O)(=O)O)OP(=O)(O)O)O	Pubchem
cpd_pde	pentadecenoate (n-C15:1)	C17676	-1	C15H27O2	CCCCCCCCCCCCCC=CC(=O)O	Pubchem
cpd_pdx5p	Pyridoxine 5'-phosphate	C00627	-2	C8H10NO6P	CC1=NC=C(C(=C1O)CO)COP(=O)(O)O	Pubchem
cpd_pe	Phosphatidylethanolamine	C00350	0	C7H12NO8PR2	[H]C(=O)OCC(COP(O)(=O)OCCN)OC([H])=O	Pubchem
cpd_pendp	all-trans-Pentaprenyl diphosphate	C04217	-3	C25H41O7P2	CC(=CCCC(=CCCC(=CCCC(=CCCC(=CCOP(=O)(O)OP(=O)(O)O)C)C)C)C)C	Pubchem

cpd_pep	Phosphoenolpyruvate	C00074	-3	C3H2O6P	C=C(C(=O)O)OP(=O)(O)O	Pubchem
cpd_pgly	Phosphatidylglycerol	C00344	-1	C8H12O10PR2	[H]C(=O)OC[C@H](COP(O)(=O)OC[C@@H](O)COP(O)(O)=O)OC([H])=O	Pubchem
cpd_pglyp	Phosphatidylglycerophosphate	C03892	-3	C8H11O13P2R2	[H]C(=O)OC[C@H](COP(O)(=O)OC[C@@H](O)COP(O)(O)=O)OC([H])=O	Pubchem
cpd_phe-L	L-Phenylalanine	C00079	0	C9H11NO2	C1=CC=C(C=C1)CC(C(=O)O)N	Pubchem
cpd_pheme	Protoheme	C00032	-1	C34H31FeN4O4	CC1=C(C2=CC3=C(C(=C([N-]3)C=C4C(=C(C(=N4)C=C5C(=C(C(=N5)C=C1[N-]2)C=C)C)C=C)C)CCC(=O)O)CCC(=O)O.[Fe+2]	Pubchem
cpd_phn	phosphonate	C06701	-2	HO3P	OP(O)O	Pubchem
cpd_phnacald	Phosphonoacetaldehyde	C03167	-2	C2H3O4P	C(C=O)P(=O)(O)O	Pubchem
cpd_phom	O-Phospho-L-homoserine	C01102	-2	C4H8NO6P	C(COP(=O)(O)O)C(C(=O)O)N	Pubchem

cpd_phpyr	Phenylpyruvate	C00166	-1	C9H7O3	C1=CC=C(C=C1)CC(=O)C(=O)O	Pubchem
cpd_phthr	O-Phospho-4-hydroxy-L-threonine	C06055	-2	C4H8NO7P	C(C(C(C(=O)O)N)O)OP(=O)(O)O	Pubchem
cpd_pi	Phosphate	C00009	-2	HO4P	[O-]P(=O)([O-])[O-]	Pubchem
cpd_pmcoa	Pimeloyl-CoA	C01063	-5	C28H41N7O19P3S	CC(C)(COP(=O)(O)OP(=O)(O)OCC1C(C(C(O1)N2C=NC3=C2N=CN=C3N)O)OP(=O)(O)O)C(C(=O)NCCC(=O)NCCSC(=O)CCCCCC(=O)O)O	Pubchem
cpd_pnto-R	(R)-Pantothenate	C00864	-1	C9H16NO5	CC(C)(CO)C(C(=O)NCCC(=O)O)O	Pubchem
cpd_ppa	Propionate	C00163	-1	C3H5O2	CCC(=O)[O-]	Pubchem
cpd_ppbng	Porphobilinogen	C00931	-1	C10H13N2O4	C1=C(C(=C(N1)CN)CC(=O)O)CCC(=O)O	Pubchem
cpd_ppcoa	Propanoyl-CoA	C00100	-4	C24H36N7O17P3S	CCC(=O)SCCNC(=O)CCNC(=O)C(C(C)(C)COP(=O)(O)OP(=O)(O)OCC1C(C(C(O1)N2C=N	Pubchem

					C3=C2N=CN=C3N)O)OP(=O)(O)O)O	
cpd_pphn	Prephenate	C00254	-2	C10H8O6	C1=CC(C=CC1O)(CC(=O)C(=O)O)C(=O)O	Pubchem
cpd_ppi	Diphosphate	C00013	-3	HO7P2	[O-]P(=O)([O-])OP(=O)([O-])[O-]	Pubchem
cpd_ppp9	Protoporphyrin	C02191	-2	C34H32N4O4	CC1=C(C2=CC3=C(C(=C(N3)C=C4C(=C(C(=N4)C=C5C(=C(C(=N5)C=C1N2)C)CCC(=O)O)CCC(=O)O)C)C=C)C)C=C	Pubchem
cpd_pppg9	Protoporphyrinogen IX	C01079	-2	C34H38N4O4	CC1=C2CC3=C(C(=C(N3)CC4=C(C(=C(N4)CC5=C(C(=C(N5)CC(=C1CCC(=O)O)O)N2)CCC(=O)O)C)C=C)C)C=C	Pubchem
cpd_pram	5-Phospho-beta-D-ribosylamine	C03090	-1	C5H11NO7P	C(C1C(C(C(O1)N)O)O)OP(=O)(O)O	Pubchem
cpd_pran	N-(5-Phospho-D-	C04302	-3	C12H13NO9P	C1=CC=C(C(=C1)C(=O)O)NC2C(C(C(O2)	Pubchem

	ribosyl)anthranilate				COP(=O)(O)O)O)O	
cpd_prbamp	1-(5-Phosphoribosyl)-AMP	C02741	-4	C15H19N5O14P2	C1=NC2=C(N1C3C(C(C(O3)COP(=O)(O)O)O)O)N=CN(C2=N)C4C(C(C(O4)COP(=O)(O)O)O)O	Pubchem
cpd_prbatp	1-(5-Phosphoribosyl)-ATP	C02739	-6	C15H19N5O20P4	C1=NC2=C(N1C3C(C(C(O3)COP(=O)(O)OP(=O)(O)OP(=O)(O)O)O)O)N=CN(C2=N)C4C(C(C(O4)COP(=O)(O)O)O)O	Pubchem
cpd_prfp	1-(5-Phosphoribosyl)-5-[(5-phosphoribosylamino)methylideneamino]imidazole-4-carboxamide	C04896	-3	C15H22N5O15P2	C1=NC(=C(N1C2C(C(C(O2)COP(=O)(O)O)O)O)O)NC=NC3C(C(C(O3)COP(=O)(O)O)O)O)C(=O)N	Pubchem
cpd_prlp	5-[(5-phospho-1-deoxyribulos-1-ylamino)methylideneamino]-1-(5-phosphoribosyl)imidazole-4-	C04916	-3	C15H22N5O15P2	C1=NC(=C(N1C2C(C(C(O2)COP(=O)(O)O)O)O)O)NC=NCC(=O)C(C(COP(=O)(O)O)O)O)C(=O)N	Pubchem

	carboxamide					
cpd_pro-gly	Proly-glycine	NA	0	C7H12N2O3	C1CC(NC1)C(=O)NCC(=O)O	Pubchem
cpd_pro-L	L-Proline	C00148	0	C5H9NO2	C1CC(NC1)C(=O)O	Pubchem
cpd_prpp	5-Phospho-alpha-D-ribose 1-diphosphate	C00119	-5	C5H8O14P3	C(C1C(C(C(O1)OP(=O)(O)OP(=O)(O)O)O)O)OP(=O)(O)O	Pubchem
cpd_ps	Phosphatidylserine	C02737	-1	C8H11NO10PR2	[H]C(=O)OCC(COP(O)(=O)OC[C@H](N)C(O)=O)OC([H])=O	Pubchem
cpd_psd5p	Pseudouridine 5'-phosphate	C01168	-2	C9H11N2O9P	C1=C(C(=O)NC(=O)N1)C2C(C(C(O2)COP(=O)(O)O)O)O	Pubchem
cpd_pser-L	O-Phospho-L-serine	C01005	-2	C3H6NO6P	C(C(C(=O)O)N)OP(=O)(O)O	Pubchem
cpd_ptdca	pentadecanoate (n-C15:0)	NA	-1	C15H29O2	CCCCCCCCCCCCCCC(=O)[O-]	Pubchem
cpd_ptrc	Putrescine	C00134	2	C4H14N2	C(CCN)CN	Pubchem
cpd_pyam5p	Pyridoxamine 5'-phosphate	C00647	-2	C8H11N2O5P	CC1=NC=C(C(=C1O)CN)COP(=O)(O)O	Pubchem
cpd_pydx5p	Pyridoxal 5'-phosphate	C00018	-3	C8H7NO6P	CC1=NC=C(C(=C1O)C=O)COP(=O)(O)O	Pubchem
cpd_pyr	Pyruvate	C00022	-1	C3H3O3	CC(=O)C(=O)[O-]	Pubchem

cpd_quln	Quinolinate	C03722	-2	C7H3NO4	C1=CC(=C(N=C1)C(=O)O)C(=O)O	Pubchem
cpd_r1p	alpha-D-Ribose 1-phosphate	C00620	-2	C5H9O8P	C(C1C(C(C(O1)OP(=O)(O)O)O)O)O	Pubchem
cpd_r5p	alpha-D-Ribose 5-phosphate	C03736	-2	C5H9O8P	C(C1C(C(C(O1)O)O)O)OP(=O)(O)O	Pubchem
cpd_rb15bp	D-Ribulose 1,5-bisphosphate	C01182	-4	C5H8O11P2	C(C(C(C(=O)COP(=O)(O)O)O)O)OP(=O)(O)O	Pubchem
cpd_rdmbzi	N1-(alpha-D-ribosyl)-5,6-dimethylbenzimidazole	C05775	0	C14H18N2O4	CC1=CC2=C(C=C1C)N(C=N2)C3C(C(C(O3)CO)O)O	Pubchem
cpd_rhcys	S-Ribosyl-L-homocysteine	C03539	0	C9H17NO6S	C(CSCC1C(C(C(O1)O)O)O)C(C(=O)O)N	Pubchem
cpd_rib-d	D-Ribose	C00121	0	C5H10O5	C1C(C(C(C(O1)O)O)O)O	Pubchem
cpd_ribflv	Riboflavin	C00255	0	C17H20N4O6	CC1=CC2=C(C=C1C)N(C3=NC(=O)NC(=O)C3=N2)CC(C(C(CO)O)O)O	Pubchem
cpd_ru5p-D	D-Ribulose 5-phosphate	C00199	-2	C5H9O8P	C(C(C(C(=O)CO)O)O)OP(=O)(O)O	Pubchem
cpd_s7p	Sedoheptulose 7-phosphate	C05382	-2	C7H13O10P	C(C(C(C(C(C(=O)CO)O)O)O)O)OP(=O)(O)O	Pubchem

cpd_sbzcoa	O-Succinylbenzoyl-CoA	C03160	-5	C32H39N7O20P3S	CC(C)(COP(=O)([O-])OP(=O)([O-])OCC1C(C(C(O1)N2C=NC3=C2N=CN=C3N)O)OP(=O)([O-])[O-])C(C(=O)NCCC(=O)NCCSC(=O)CCC(=O)C4=CC=CC=C4C(=O)[O-])O	Pubchem
cpd_seln	Selenide	C01528	-1	HSe	[SeH2]	Pubchem
cpd_selnp	Selenophosphate	C05172	-1	H2O3PSe	OP(=[Se])(O)O	Pubchem
cpd_ser-D	D-Serine	C00740	0	C3H7NO3	C(C(C(=O)O)N)O	Pubchem
cpd_ser-L	L-Serine	C00065	0	C3H7NO3	C(C(C(=O)O)N)O	Pubchem
cpd_shcl	dihydrosirohydrochlorin	C02463	-8	C42H40N4O16	CC1(C(C2=CC3=NC(=CC4=C(C(=C(N4)CC5=C(C(=C(N5)C=C1N2)CC(=O)O)CCC(=O)O)CCC(=O)O)CC(=O)O)C(C3(C)CC(=O)O)CCC(=O)O)CCC(=O)O)CCC(=O)O)CC(=O)O	Pubchem
cpd_sheme	Siroheme	C00748	-8	C42H36FeN4O16	CC1(C(C2=CC3=NC(=CC4=C(	Pubchem

					C(=C([N-]4)C=C5C(C(C(=N5)C=C1[N-]2)CCC(=O)O)(C)CC(=O)O)CC(=O)O)CCC(=O)O)C(=C3CC(=O)O)CCC(=O)O)CCC(=O)O)CC(=O)O.[Fe+2]	
cpd_skm	Shikimate	C00493	-1	C7H9O5	C1C(C(C(C(C=C1C(=O)O)O)O)O)O	Pubchem
cpd_skm5p	Shikimate 5-phosphate	C03175	-3	C7H8O8P	C1C(C(C(C(C=C1C(=O)O)OP(=O)(O)O)O)O)O	Pubchem
cpd_sl26da	N-Succinyl-LL-2,6-diaminoheptanedioate	C04421	-2	C11H16N2O7	C(CC(C(=O)O)N)CC(C(=O)O)NC(=O)CCC(=O)O	Pubchem
cpd_sl2a6o	N-Succinyl-2-L-amino-6-oxoheptanedioate	C04462	-3	C11H12NO8	C(CC(C(=O)O)NC(=O)CCC(=O)O)CC(=O)C(=O)O	Pubchem
cpd_slcys	S-Sulfo-L-cysteine	C05824	-1	C3H6NO5S2	C(C(C(=O)O)N)SS(=O)(=O)O	Pubchem
cpd_so3	Sulfite	C00094	-2	O3S	[O-]S(=O)[O-]	Pubchem
cpd_so4	Sulfate	C00059	-2	O4S	[O-]S(=O)(=O)[O-]	Pubchem
cpd_spmd	Spermidine	C00315	3	C7H22N3	C(CCNCCCN)CN	Pubchem

cpd_sprm	Spermine	C00750	4	C10H30N4	C(CCNCCCN)CNCCCN	Pubchem
cpd_srch	sirohydrochlorin	C05778	-8	C42H38N4O16	CC1(C(C2=NC1=CC3=NC(=CC4=C(C(=C(N4)C=C5C(=C(C(=C2)N5)CC(=O)O)CCC(=O)O)CC(=O)O)C(C3CCC(=O)O)(C)CC(=O)O)CCC(=O)O)CC(=O)O	Pubchem
cpd_ssaltpp	Succinate semialdehyde-thiamin diphosphate anion	C05381	-2	C16H22N4O10P2S	CC1=C(SC(=[N+]1CC2=CN=C(N=C2N)C)C(CCC(=O)O)O)CCOP(=O)(O)OP(=O)(O)O	Pubchem
cpd_sucarg	N2-Succinyl-L-arginine	C03296	-1	C10H17N4O5	C(CC(C(=O)O)NC(=O)CCC(=O)O)CN=C(N)N	Pubchem
cpd_sucbz	o-Succinylbenzoate	C02730	-2	C11H8O5	C1=CC=C(C(=C1)C(=O)CCC(=O)O)C(=O)O	Pubchem
cpd_succ	Succinate	C00042	-2	C4H4O4	C(CC(=O)[O-])C(=O)[O-]	Pubchem
cpd_succoa	Succinyl-CoA	C00091	-5	C25H35N7O19P3S	CC(C)(COP(=O)(O)OP(=O)(O	Pubchem

					)OCC1C(C(C(O1)N2C=NC3=C2N=CN=C3N)O)OP(=O)(O)O)C(C(=O)NCCC(=O)NCCSC(=O)CCC(=O)O)O	
cpd_sucglu	N2-Succinyl-L-glutamate	C05931	-3	C9H10NO7	C(CC(=O)O)C(C(=O)O)NC(=O)CCC(=O)O	Pubchem
cpd_sucgsa	N2-Succinyl-L-glutamate 5-semialdehyde	C05932	-2	C9H11NO6	C(CC(C(=O)O)NC(=O)CCC(=O)O)C=O	Pubchem
cpd_suchms	O-Succinyl-L-homoserine	C01118	-1	C8H12NO6	C(COC(=O)CCC(=O)O)C(C(=O)O)N	Pubchem
cpd_sucorn	N2-Succinyl-L-ornithine	C03415	-1	C9H15N2O5	C(CC(C(=O)O)NC(=O)CCC(=O)O)CN	Pubchem
cpd_sucsal	Succinic semialdehyde	C00232	-1	C4H5O3	C(CC(=O)O)C=O	Pubchem
cpd_tcynt	Thiocyanate	C01755	-1	CNS	C(#N)[S-]	Pubchem
cpd_thbpt	Tetrahydrobiopterin	C00272	0	C9H15N5O3	CC(C(C1CNC2=C(N1)C(=O)NC(=N2)N)O)O	Pubchem
cpd_thdp	2,3,4,5-Tetrahydrodipicolinate	C03972	-2	C7H7NO4	C1CC(N=C(C1)C(=O)O)C(=O)O	Pubchem

cpd_thf	5,6,7,8-Tetrahydrofolate	C00101	-2	C19H21N7O6	C1C(NC2=C(N1)N=C(NC2=O)N)CNC3=CC=C(C=C3)C(=O)NC(CCC(=O)O)C(=O)O	Pubchem
cpd_thglu	Tetrahydropteroyltri-L-glutamate	C04144	0	C29H37N9O12	C1C(NC2=C(N1)N=C(NC2=O)N)CNC3=CC=C(C=C3)C(=O)NC(CCC(=O)NC(CCC(=O)NC(CCC(=O)O)C(=O)O)C(=O)O)C(=O)O	Pubchem
cpd_thm	Thiamin	C00378	1	C12H17N4OS	CC1=C(SC=[N+]1CC2=CN=C(N=C2N)C)CCO	Pubchem
cpd_thmmp	Thiamin monophosphate	C01081	-1	C12H16N4O4PS	CC1=C(SC=[N+]1CC2=CN=C(N=C2N)C)CCOP(=O)(O)O	Pubchem
cpd_thmpp	Thiamine diphosphate	C00068	-2	C12H16N4O7P2S	CC1=C(SC=[N+]1CC2=CN=C(N=C2N)C)CCOP(=O)(O)OP(=O)(O)O	Pubchem
cpd_thr-L	L-Threonine	C00188	0	C4H9NO3	CC(C(C(=O)O)N)O	Pubchem
cpd_thr-LA	L-Allo-threonine	C05519	0	C4H9NO3	CC(C(C(=O)O)N)O	Pubchem

cpd_thym	Thymine	C00178	0	C5H6N2O2	CC1=CNC(=O)NC1=O	Pubchem
cpd_thymd	Thymidine	C00214	0	C10H14N2O5	CC1=CN(C(=O)NC1=O)C2CC(C(O2)CO)O	Pubchem
cpd_tma	Trimethylamine	C00565	1	C3H10N	CN(C)C	Pubchem
cpd_tmao	Trimethylamine N-oxide	C01104	0	C3H9NO	C[N+](C)(C)[O-]	Pubchem
cpd_trp-L	L-Tryptophan	C00078	0	C11H12N2O2	C1=CC=C2C(=C1)C(=CN2)CC(C(=O)O)N	Pubchem
cpd_tsul	Thiosulfate	C00320	-2	O3S2	[O-]S(=O)(=S)[O-]	Pubchem
cpd_ttdcan	tetradecanoate (C14:0) (neutral)	C06424	0	C14H28O2	CCCCCCCCCCCCCC(=O)O	Pubchem
cpd_tttnt	tetrathionate	C02084	-2	O6S4	[O-]S(=O)(=O)SSS(=O)(=O)[O-]	Pubchem
cpd_tyr-L	L-Tyrosine	C00082	0	C9H11NO3	C1=CC(=CC=C1CC(C(=O)O)N)O	Pubchem
cpd_u23ga	UDP-2,3-bis(3-hydroxytetradecanoyl)glucosamine	C04652	-2	C43H75N3O20P2	CCCCCCCCCCCC(CC(=O)NC1C(C(C(OC1OP(=O)(O)OP(=O)(O)OCC2C(C(C(O2)N3C=CC(=O)NC3=O)O)O)CO)O)OC(=O)CC(CCCCCC	Pubchem

					CCCC)O)O	
cpd_u3aga	UDP-3-O-(3-hydroxytetradecanoyl)-N-acetylglucosamine	C04738	-2	C31H51N3O19P2	CCCCCCCCCCCCCC(CC(=O)OC1C(C(OC(C1O)CO)OP(=O)([O-])OP(=O)([O-])OCC2C(C(C(O2)N3C=CC(=O)NC3=O)O)O)NC(=O)C)O	Pubchem
cpd_u3hga	UDP-3-O-(3-hydroxytetradecanoyl)-D-glucosamine	C06022	-1	C29H50N3O18P2	CCCCCCCCCCCCCC(CC(=O)OC1C(C(OC(C1O)CO)OP(=O)(O)OP(=O)(O)OCC2C(C(C(O2)N3C=CC(=O)NC3=O)O)O)N)O	Pubchem
cpd_uaagmda	Undecaprenyl-diphospho-N-acetylmuramoyl-(N-acetylglucosamine)-L-alanyl-D-glutamyl-meso-2,6-diaminopimeloyl-D-alanyl-D-alanine	C05898	-4	C95H152N8O28P2	CC(C(=O)NC(CCC(=O)NC(CCCC(C(=O)O)N)C(=O)NC(C)C(=O)NC(C)C(=O)O)C(=O)O)NC(=O)C(C)OC1C(C(OC(C1OC2C(C(C(C(O2)CO)O)O)O)NC(=O)C)CO)O	Pubchem

					P(=O)(O)OP(=O)(O)OCC=C(C)CCC=C(C)CCC=C(C)CCC=C(C)CCC=C(C)CCC=C(C)CCC=C(C)CCC=C(C)CCC=C(C)CCC=C(C)C)NC(=O)C	
cpd_uaccg	UDP-N-acetyl-3-O-(1-carboxyvinyl)-D-glucosamine	C04631	-3	C20H26N3O19P2	CC(=O)NC1C(C(C(OC1OP(=O)(O)OP(=O)(O)OCC2C(C(C(O2)N3C=CC(=O)NC3=O)O)O)CO)O)OC(=C)C(=O)O	Pubchem
cpd_uacgam	UDP-N-acetyl-D-glucosamine	C00043	-2	C17H25N3O17P2	CC(=O)NC1C(C(C(OC1OP(=O)(O)OP(=O)(O)OCC2C(C(C(O2)N3C=CC(=O)NC3=O)O)O)CO)O)O	Pubchem
cpd_uagmda	Undecaprenyl-diphospho-N-acetylmuramoyl-L-alanyl-D-glutamyl-meso-2,6-	C05897	-4	C87H139N7O23P2	CC(C(=O)NC(CCC(=O)NC(CCCC(C(=O)O)N)C(=O)NC(C)C(=O)NC(C)C(=O)O)C(=O)O)	Pubchem

	diaminopimeloyl-D-alanyl-D-alanine				NC(=O)C(C)OC1C(C(OC(C1O)CO)OP(=O)(O)OP(=O)(O)OCC=C(C)CCC=C(C)CCC=C(C)CCC=C(C)CCC=C(C)CCC=C(C)CCC=C(C)CCC=C(C)CCC=C(C)CCC=C(C)C)NC(=O)C	
cpd_uama	UDP-N-acetylmuramoyl-L-alanine	C01212	-3	C23H33N4O20P2	CC(C(=O)O)NC(=O)C(C)OC1C(C(OC(C1O)CO)OP(=O)(O)OP(=O)(O)OCC2C(C(C(O2)N3C=CC(=O)NC3=O)O)O)NC(=O)C	Pubchem
cpd_uamag	UDP-N-acetylmuramoyl-L-alanyl-D-glutamate	C00692	-4	C28H39N5O23P2	CC(C(=O)NC(CCC(=O)O)C(=O)O)NC(=O)C(C)OC1C(C(OC(C1O)CO)OP(=O)(O)OP(=O)(O)OCC2C(C(C(O2)N3C=CC(=O)NC3=O)O)O)NC(=O)C	Pubchem

cpd_uamr	UDP-N-acetylmuramate	C01050	-3	C20H28N3O19P2	CC(C(=O)O)OC1C(C(OC(C1O)CO)OP(=O)(O)OP(=O)(O)OCC2C(C(C(O2)N3C=CC(=O)NC3=O)O)O)NC(=O)C	Pubchem
cpd_ubq8	Ubiquinone-8	C17569	0	C49H74O4	CC1=C(C(=O)C(=C(C1=O)OC)OC)CC=C(C)CCC=C(C)CCC=C(C)CCC=C(C)CCC=C(C)CCC=C(C)CCC=C(C)C	Pubchem
cpd_ubq8h2	Ubiquinol-8	C00390	0	C49H76O4	CC1=C(C(=C(C(=C1O)OC)OC)O)CC=C(C)CCC=C(C)CCC=C(C)CCC=C(C)CCC=C(C)CCC=C(C)CCC=C(C)C	Pubchem
cpd_udcdp	Undecaprenyl diphosphate	C04574	-3	C55H89O7P2	CC(=CCCC(=CCCC(=CCCC(=CCCC(=CCCC(=CCCC(=CCCC(=CCOP(=O)(O)OP(=O)	Pubchem

					(O)O)C)C)C)C)C)C)C)C)C)C)C)C	
cpd_udcpp	Undecaprenyl phosphate	C00348	-2	C55H89O4P	CC(=CCCC(=CCCC(=CCCC(=CCCC(=CCCC(=CCCC(=CCCC(=CCCC(=CCOP(=O)(O)O)C)C)C)C)C)C)C)C)C)C)C	Pubchem
cpd_udp	UDP	C00015	-3	C9H11N2O12P2	C1=CN(C(=O)NC1=O)C2C(C(C(O2)COP(=O)(O)OP(=O)(O)O)O)O	Pubchem
cpd_udpg	UDPglucose	C00029	-2	C15H22N2O17P2	C1=CN(C(=O)NC1=O)C2C(C(C(O2)COP(=O)(O)OP(=O)(O)OC3C(C(C(C(O3)CO)O)O)O)O)O	Pubchem
cpd_udpgal	UDPgalactose	C00052	-2	C15H22N2O17P2	C1=CN(C(=O)NC1=O)C2C(C(C(O2)COP(=O)(O)OP(=O)(O)OC3C(C(C(C(O3)CO)O)O)O)O)O	Pubchem

cpd_ugmd	UDP-N-acetylmuramoyl-L-alanyl-D-gamma-glutamyl-meso-2,6-diaminopimelate	C20886	-4	C35H51N7O26P2	CC(C(=O)NC(CCC(=O)NC(CCCC(C(=O)O)N)C(=O)O)C(=O)O)NC(=O)C(C)OC1C(C(OC(C1O)CO)OP(=O)(O)OP(=O)(O)OCC2C(C(C(O2)N3C=CC(=O)NC3=O)O)O)NC(=O)C	Pubchem
cpd_ugmda	UDP-N-acetylmuramoyl-L-alanyl-D-glutamyl-meso-2,6-diaminopimeloyl-D-alanyl-D-alanine	C04882	-4	C41H61N9O28P2	CC(C(=O)NC(CCC(=O)NC(CCCC(C(=O)O)N)C(=O)NC(C)C(=O)NC(C)C(=O)O)C(=O)O)NC(=O)C(C)OC1C(C(OC(C1O)CO)OP(=O)(O)OP(=O)(O)OCC2C(C(C(O2)N3C=CC(=O)NC3=O)O)O)NC(=O)C	Pubchem
cpd_ump	UMP	C00105	-2	C9H11N2O9P	C1=CN(C(=O)NC1=O)C2C(C(C(O2)COP(=O)(O)O)O)O	Pubchem
cpd_uppg3	Uroporphyrinogen III	C01051	-8	C40H36N4O16	C1C2=C(C(=C(N2)C	Pubchem

					C3=C(C(=C(N3)CC4=C(C(=C(N4)CC5=C(C(=C1N5)CCC(=O)O)CC(=O)O)CC(=O)O)CCC(=O)O)CC(=O)O)CCC(=O)O)CCC(=O)O	
cpd_ura	Uracil	C00106	0	C4H4N2O2	C1=CNC(=O)NC1=O	Pubchem
cpd_urate	urate	C00366	0	C5H4N4O3	C12=C(NC(=O)N1)NC(=O)NC2=O	Pubchem
cpd_urcan	Urocanate	C00785	-1	C6H5N2O2	C1=C(NC=N1)C=CC(=O)O	Pubchem
cpd_urdglyc	(S)-Ureidoglycolate	C00603	0	C3H6N2O4	C(C(=O)O)(NC(=O)N)O	Pubchem
cpd_urdio	Uranium dioxide	NA	0	UO2	O=[U]=O	Pubchem
cpd_urea	Urea	C00086	0	CH4N2O	C(=O)(N)N	Pubchem
cpd_uri	Uridine	C00299	0	C9H12N2O6	C1=CN(C(=O)NC1=O)C2C(C(C(O2)CO)O)O	Pubchem
cpd_urnyl	Uranyl	NA	2	UO2	O=[U+2]=O	Pubchem
cpd_utp	UTP	C00075	-4	C9H11N2O15P3	C1=CN(C(=O)NC1=O)C2C(C(C(O2)COP(=O)(O)OP(=O)(O)OP(=O)(O)O)O)O	Pubchem

cpd_val-L	L-Valine	C00183	0	C5H11NO2	CC(C)C(C(=O)O)N	Pubchem
cpd_wo4	tungstate	C20679	-2	WO4	[O-][W](=O)(=O)[O-]	Pubchem
cpd_xan	Xanthine	C00385	0	C5H4N4O2	C1=NC2=C(N1)C(=O)NC(=O)N2	Pubchem
cpd_xmp	Xanthosine 5'-phosphate	C00655	-2	C10H11N4O9P	C1=NC2=C(N1C3C(C(C(O3)COP(=O)([O-])[O-])O)O)NC(=O)NC2=O	Pubchem
cpd_xtp	XTP	C00700	-4	C10H11N4O15P3	C1=NC2=C(N1C3C(C(C(O3)COP(=O)(O)OP(=O)(O)OP(=O)(O)O)O)O)NC(=O)NC2=O	Pubchem
cpd_xtsn	Xanthosine	C01762	0	C10H12N4O6	C1=NC2=C(N1C3C(C(C(O3)CO)O)O)NC(=O)NC2=O	Pubchem
cpd_xu5p-D	D-Xylulose 5-phosphate	C00231	-2	C5H9O8P	C(C(C(C(=O)CO)O)O)OP(=O)(O)O	Pubchem
cpd_trehalose	Trehalose	C01083	0	C12H22O11	C(C1C(C(C(C(O1)OC2C(C(C(C(O2)CO)O)O)O)O)O)O)O	Pubchem
cpd_trehalose6p	Trehalose 6-Phosphate	C00689	0	C12H23O14P	C(C1C(C(C(C(O1)OC2C(C(C(C(O2)COP	Pubchem

					(=O)(O)O)O)O)O)O)O)O	
cpd_sucr	Sucrose	C00089	0	C12H22O11	C(C1C(C(C(C(O1)OC2(C(C(C(O2)CO)O)O)CO)O)O)O)O	Pubchem
cpd_suc6p	Sucrose 6-Phosphate	C16688	-2	C12H21O14P	C(C1C(C(C(C(O1)OC2(C(C(C(O2)COP(=O)(O)O)O)O)CO)O)O)O)O	Pubchem

Data S1 Table D: Tables detailing the composition of each biomass component and the overall biomass reaction in the WP2 GEM.

Biomass Objective Function *Shewanella psychrophila* WP2 Requirements for the production of 1g dry weight of Biomass (gDW Cellular Biomass)				
Overall				
		Weight Percentage (% gDW)	Stoichiometry in Biomass Reaction	Data Source
1 gDW DNA	cpd_dna_macro	5	0.05	Inferred from other *Shewanella* models
1 gDW RNA	cpd_rna_macro	9	0.09	Inferred from other *Shewanella* models
1 gDW Protein	cpd_protein_macro	52.8	0.528	Inferred from other *Shewanella* models
1 gDW Lipid	cpd_lipid_macro	17.5	0.175	Inferred from other *Shewanella* models
1 gDW Peptidoglycan	cpd_peptidoglycan_macro	2.5	0.025	Inferred from other *Shewanella* models
1 gDW LPS	cpd_lps_macro	3.4	0.034	Inferred from other *Shewanella* models
1 gDW Carbohydrate	cpd_carbohydrate_macro	7.7	0.077	Inferred from other *Shewanella* models
1 gDW Trace Elements	cpd_trace_macro	2.1	0.021	Inferred from other *Shewanella* models

DNA Requirements for the production of 1g dry weight of DNA (gDW DNA)

dNTP	Composition (p, mmol/mmol)	cpd ID	MW (g/mol)	p*MW (g/mol)	(p/sum g/mmol)	Stoichiometry (mmol/gDW DNA)
dATP	0.2215	cpd_datp	491.1816	108.7967244	0.454872	
dTTP	0.2215	cpd_dttp	482.1683	106.8002785	0.454872	
dGTP	0.2785	cpd_dgtp	507.181	141.2499085	0.571927	
dCTP	0.2785	cpd_dctp	467.1569	130.1031967	0.571927	
			Molecular weight of DNA in S. psyhcorphila model:	486.950108	2.053598	4.107196

RNA Requirements for the production of 1g dry weight of RNA (gDW RNA)						
DTP	Count in the genome cds	Mol Composition (p, mol/mol)	cpd ID	MW (g/mol)	p*MW (g/mol RNA)	Stoichiometry (mmol/gDW RNA)
ATP	1492316	0.2786591714	cpd_atp	507.181	141.3306372	0.557645
UTP	1428293	0.2667041993	cpd_utp	484.1411	129.1224644	0.533721
GTP	1283649	0.2396949216	cpd_gtp	523.1804	125.403685	0.479671
CTP	1151087	0.2149417078	cpd_ctp	483.1563	103.8504402	0.430135
				Molecular weight of RNA in S. psyhcorphila model:	499.7072268	2.001172

Protein Requirements for the production of 1g dry weight of Protein (gDW Protein)									
Amino Acid	cpd	cpd	Count in genome	Mol composition (P,	MW (g/mol)	P*MW (g/mol total aa)	aa-trna KEGG ID	trna(aa) KEGG ID	Stoichiometry of aa (mmol/

				mol/mol)					gDW pro)
Alanine	**ala**	**A**	144451	0.08441242	89.0932	7.52057225	cpd_alatrna	cpd_trnaala	0.655475
Arginine	**arg**	**R**	73450	0.04292177	174.201	7.47701447	cpd_argtrna	cpd_trnaarg	0.333294
Asparagine	**asn**	**N**	73303	0.04283586	132.1179	5.65938434	cpd_asntrna	cpd_trnaasn	0.332627
Aspartate	**asp**	**D**	97093	0.05673796	133.1027	7.55197534	cpd_asptrna	cpd_trnaasp	0.440579
Cysteine	**cys**	**C**	17453	0.01019896	121.1582	1.23568757	cpd_cystrna	cpd_trnacys	0.079196
Glutamine	**gln**	**Q**	77088	0.04504769	146.1445	6.58347259	cpd_gltrna	cpd_trnagln	0.349802
Glutamate	**glu**	**E**	103719	0.06060997	147.1293	8.91750306	cpd_glutrna	cpd_trnaglu	0.470646
Glycine	**gly**	**G**	118198	0.06907103	75.0666	5.18492706	cpd_glytrna	cpd_trnagly	0.536347
Histidine	**his**	**H**	36885	0.02155438	155.1546	3.34426144	cpd_histrna	cpd_trnahis	0.167373
Isoleucine	**ile**	**I**	112022	0.06546197	131.1729	8.58683702	cpd_iletrna	cpd_trnaile	0.508322
Leucine	**leu**	**L**	181128	0.10584525	131.1729	13.8840283	cpd_leutrna	cpd_trnaleu	0.821905
Lysine	**lys**	**K**	91276	0.05333869	146.1876	7.79745565	cpd_lystrna	cpd_trnalys	0.414183
Methionine	**met**	**M**	44992	0.02629185	149.2113	3.92304049	cpd_mettrna	cpd_trnamet	0.20416
Phenylalanine	**phe**	**F**	69651	0.04070175	165.1891	6.72348624	cpd_phetrna	cpd_trnaphe	0.316055
Proline	**pro**	**P**	64889	0.037919	115.1305	4.36563326	cpd_protrna	cpd_trnapro	0.294447
Serine	**ser**	**S**	124943	0.07301258	105.0926	7.67308208	cpd_sertrna	cpd_trnaser	0.566954
Threonine	**thr**	**T**	93554	0.05466988	119.1192	6.51223264	cpd_thrtrna	cpd_trnathr	0.42452
Tryptophan	**trp**	**W**	20613	0.01204556	204.2252	2.46000682	cpd_trptrna	cpd_trnatrp	0.093536
Tyrosine	**tyr**	**Y**	52874	0.03089783	181.1885	5.59833102	cpd_tyrtrna	cpd_trnatyr	0.239926
Valine	**val**	**V**	113671	0.0664256	117.1463	7.78151277	cpd_valtrna	cpd_trnaval	0.515805
					Molecular	128.780444			7.765152

					weight of Protein in S. psyhcorphila model:				

Lipids								
Requirements for the production of 1g dry weight of Lipid (gDW Lipid)								
Fatty acid	**WP2T 10C (Wang, 2007) % composition**	**Fatty Acid ID**	Fatty Acid ACP ID	Mol composition (P, mol/mol)	**Formula**	MW (g/mol)	P*MW (g/mol total aa)	**Stoichiometry of aa (mmol/gDW pro)**
12:00	5.9	cpd_dodca	cpd_ddcaACP	0.059	C12H24O2	200.32	11.81888	0.239054
iso-13 : 0	7.3	cpd_fa13	cpd_fa13ACP	0.073	C13H25O2	213.34	15.57382	0.295778
14:00	7.9	cpd_ttdca	cpd_myrsACP	0.079	C14H27O2	227.36	17.96144	0.320089
iso-13 : 0 3-OH	1.8	cpd_fa130OH3	cpd_fa130OH3ACP	0.018	C13H25O3	229.33	4.12794	0.072932
iso-15 : 0	4	cpd_fa3	cpd_fa3ACP	0.04	C15H30O2	242.4	9.696	0.16207
16 : 1ω7c	38.2	cpd_hdcea	cpd_hdeACP	0.382	C16H30O2	254.41	97.18462	1.547771
16:00	12.7	cpd_hdca	cpd_palmACP	0.127	C16H32O2	256.42	32.56534	0.514573
17 : 1ω8c	1.6	cpd_fa171n8	cpd_fa171n8ACP	0.016	C17H31O2	267.43	4.27888	0.064828
18 : 1ω7t	9.4	cpd_fa181n7	cpd_fa181n7ACP	0.094	C18H33O2	281.45	26.4563	0.380865
18:00	2	cpd_ocdca	cpd_ocdACP	0.02	C18H35O2	283.47	5.6694	0.081035
20 : 5ω3	7.1	cpd_epaapo	cpd_epa	0.071	C20H30O2	302.45	21.47395	0.287675
			Molecular weight of Lipids	0.979			246.80657	3.96667

			in S. psyhcorphila model:					

Cell Wall				
Requirements for the production of 1 gDW of peptidoglycan or 1 gDW of LPS				
Metabolite	Metabolite ID	Molecular Weight g/mol	mol/g	mmol/g
Peptidoglycan	cpd_peptx	901.87	0.001108807256	1.108807256
LPS	cpd_lps_Core[c	2849.04	0.000350995423	0.350995423

Carbohydrates				
Requirements for the production of 1 gDW of carbohydrate				
Metabolite	Metabolite ID	Molecular Weight g/mol	mol/g	mmol/g
Glycogen 1 gDW	|cpd_glycogen[c]|	666.58	0.001500195025	1.500195025

Trace Elements						
Requiremnets for the production of 1g dry weight of trace elements						
Metabolite	Metabolite ID	iJO1366 Stoichiometry (mmol/gDW of cell)	g/mol Molecular weight	g/gDW of cell	g/g of solute pool	mmol/g of Solutes
Biotin	cpd_btn[c]	2.00E-06	244.31	4.89E-07	2.63E-05	0.00
Succinyl-CoA	cpd_succoa[c]	9.80E-05	867.61	8.50E-05	4.58E-03	0.01
CoA	cpd_coa[c]	0.000168	767.53	0.00012894504	6.95E-03	0.01
Acetyl-CoA	cpd_accoa[c]	0.000279	809.57	0.00022587003	1.22E-02	0.02
FAD+	cpd_fad[c]	0.000223	785.55	0.00017517765	9.44E-03	0.01
NADH	cpd_nadh[c]	4.50E-05	665.44	2.99E-05	1.61E-03	0.00
Undecaprenyl diphosphate	cpd_udcpdp[c]	5.50E-05	927.26	5.10E-05	2.75E-03	0.00

NADP+	cpd_nadp[c]	0.000112	745.42	0.00008348704	4.50E-03	0.01
Cobamide coenzyme	cpd_cobamcoa[c]	0.000223	1579.58	0.00035224634	1.90E-02	0.01
Menaquinone 7	cpd_mqn7[c]	0.000223	649	0.000144727	7.80E-03	0.01
Siroheme	cpd_sheme[c]	0.000223	916.66	0.00020441518	1.10E-02	0.01
Thiamine diphosphate	cpd_thmpp[c]	0.000223	425.31	0.00009484413	5.11E-03	0.01
Ubiquinol-8	cpd_ubq8h2[c]	0.000223	729.12	0.00016259376	8.76E-03	0.01
S-Adenosyl-L-methionine	cpd_amet[c]	0.000223	398.44	0.00008885212	4.79E-03	0.01
Chorismate	cpd_chor[c]	0.000223	226.18	0.00005043814	2.72E-03	0.01
Protoheme	cpd_pheme[c]	0.000223	616.49	0.00013747727	7.41E-03	0.01
Pyridoxal 5'phosphate	cpd_pydx5p[c]	0.000223	247.14	0.00005511222	2.97E-03	0.01
Riboflavin	cpd_ribflv[c]	0.000223	376.36	0.00008392828	4.52E-03	0.01
NADPH	cpd_nadph[c]	0.000335	745.42	0.0002497157	1.35E-02	0.02
AMP	cpd_amp[c]	0.001	347.22	0.000347222	1.87E-02	0.05
NAD	cpd_nad[c]	0.001787	664.43	0.00118733641	6.40E-02	0.10
UDP-Glucose	cpd_udpg[c]	0.003	566.3	0.0016989	9.16E-02	0.16
Calcium 2+	cpd_ca2[c]	0.004952	40.08	0.00019847616	1.07E-02	0.27
Iron 2+	cpd_fe2[c]	0.006388	55.85	0.0003567698	1.92E-02	0.34
Spermidine	cpd_spmd[c]	0.006744	145.25	0.00097956	5.28E-02	0.36
Magnesium 2+	cpd_mg2[c]	0.008253	24.31	0.00020063043	1.08E-02	0.45
Ammonium	cpd_nh4[c]	0.012379	18.04	0.00022331716	1.20E-02	0.67

Cobalt 2+	cpd_cobalt2[c]	2.40E-05	58.93	1.41E-06	7.62E-05	0.00
Copper 2+	cpd_cu2[c]	0.000674	63.55	0.0000428327	2.31E-03	0.04
Manganese 2+	cpd_mn2[c]	0.000658	54.94	0.00003615052	1.95E-03	0.04
Molybdate	cpd_mobd[c]	7.00E-06	161.95	1.13E-06	6.11E-05	0.00
Sulfate	cpd_so4[c]	0.004126	98.08	0.00040467808	2.18E-02	0.22
Chlorine	cpd_cl[c]	0.004952	35.45	0.0001755484	9.46E-03	0.27
Putrescine	cpd_ptrc[c]	0.03327	88.15	0.0029327505	1.58E-01	1.79
5-Methyltetrahydrofolate	cpd_5mthf[c]	0.000223	459.45	0.00010245735	5.52E-03	0.01
Potassium	cpd_k[c]	0.18569	39.1	0.007260479	3.91E-01	10.00
		Molecular weight of Trace Elements in S. psyhcorphila model:	1.86E-02	1.00E+00	14.95	

Data S1 Table E: Standard Gibbs Free Energy predictions for reactions in the WP2 GEM based on the Group Contribution method. Values are provided in kJ/mol.

Reaction ID	Standard Gibbs Free Energy (kJ/mol)
2MAHMP	-32.3319
4HBTE	-20.3735
5DOAN	3.1817
5HPUDICDCs	-56.4442
A5PISO	-2.5059
AACPS10	39.8926
AACPS11	32.3752
AACPS12	24.8578
AACPS13	17.3404
AACPS14	-38.1024
AACPS15	-53.1317
AACPS16	55.2334
AACPS3	25.1638
AACPS4	-45.6153
AACPS5	-60.6501
AACPS6	32.6812
AACPS7	17.6464
AACPS8	10.1290
AACPS9	47.4101
AACPSFA130OH	206.5742
AACPSFA1718	-53.1325
AACPSFA1817	-60.6512
ABTA	8.0322
ACACCB	-27.0104
ACACCT	7.1852
ACACT10R	-27.0958
ACACt2	0.0000
ACALDi	-20.9198
ACBIPGT	1072.9123
ACCOAC	-600.8426
ACCOAL	5.7673
ACGAMK	-10.0797
ACGAt2	0.0000
ACGK	23.2061
ACGS	-22.6163

ACHBS	-37.5569
ACKr	-14.1282
ACLS	-42.5482
ACMAT1	12.2573
ACNAMS	-65.3855
ACOAD10	42.5546
ACOAD8	42.5546
ACOAD9	51.7576
ACOATA	-4.0389
ACODA	-7.6529
ACONT	7.9076
ACOTA	-6.8947
ACS	-10.5274
ACt6	0.0000
ADA	-21.2807
ADCL	-89.9053
ADCOBAK	829.5900
ADCOBAS	-84.0023
ADCOBHEXS	-789.5845
ADCS	-16.6873
ADHMCYSSYN	35.4788
ADK1	-1.5889
ADK3	-1.6941
ADK4	0.6524
ADMDC	-386.9345
ADNCYC	-29.8265
ADNK1	-9.1420
ADNt2	0.0000
ADPRDP	-3.3598
ADPT	-16.3867
ADSK	-47.4721
ADSL1r	43.6293
ADSL2r	36.1607
ADSS	-28.2548
AEPPAT	-4.9380
AGDC	-3.6537
AGMAHYD	-51.3623
AGPEPHOS	-262.4762
AGPR	11.2357

AHAI	-11.9988
AHCYSNS	-16.6547
AICART	9.2504
AIRC2	-590.3691
AIRC3	31.1116
AKGD	-29.0756
ALAALA	-32.1185
ALAD_L	36.9584
ALAGLYX	-2.1955
ALAR	0.1480
ALATA_D2	5.8161
ALATA_L	0.4930
ALATA_L2	5.9641
ALA_Dt4	0.0000
ALAt4	0.0000
ALCD2x	22.5188
ALDD2x	-52.9600
ALLNRAC	0.0000
ALLTC	40.7525
ALLTN	-19.3822
AMAA	6.6165
AMALT1	21.8932
AMALT2	-49.2133
AMALT3	-4.0235
AMALT4	-23.2966
AMAOT	-0.6370
AMMQT7_2	-22.5975
AMPMS2	-174.5798
AMPTASECG	14.8248
AMPTASEPG	30.7607
ANPRT	-57.4517
ANS1	-106.5955
AOXS	13.5538
AP4AH	7.3520
AP5AH	-4481.7856
APRAUR	-17.4027
ARBABC	-28.4564
ARGDC	1.3864
ARGSL	10.2505

ARGSS	-0.7817
ARSRD2	-167.6156
ARSt1	0.0000
ASAD	4.8180
ASNN	-12.7136
ASNS1	-43.9536
ASP1DC	-17.0629
ASPCT	-21.5122
ASPK	18.4267
ASPO3	-137.0836
ASPO5	-21.1030
ASPO6	49.6899
ASPO8	47.0520
ASPO9	-15.0478
ASPTA1	2.9241
ASPTA4	-21.4896
ASPt2	0.0000
AST	-9.9090
ATPPRT	-94.9959
ATPS4r	28.4564
BETALDHx	-36.6929
BETALDHy	-35.4461
BPNT	-1.8987
BTS4	-213.7232
BUTSUCCCOA	-5.5095
BUT_T	0.0000
C120SN	-242.8593
C130ISN	-234.2998
C130OHISN	-11.7990
C140ISN	-312.3998
C140SN	-320.9593
C150ISN	-312.3998
C150SN	-390.4997
C151SN	-344.5762
C160ISN	-390.4997
C160SN	-399.0592
C161SN	-419.5231
C170ISN	-390.4997
C170SN	-468.5997

C171SN	-422.6762
C171n8SN	-422.6760
C180SN	-477.1592
C181SN	-497.6230
C181n7SN	-497.6229
C205SN	-132.5571
C50SN	66.3874
C60ISN	58.5640
C70ISN	51.0466
CAT	-469.5288
CBIAT	-564.2452
CBL1abc	-28.4564
CBLAT	-564.2452
CBPS	-612.6891
CDPG46D	-104.9434
CDPMEK	-8.9890
CHITINS	4.2064
CHOLDH1	12.8478
CHOLDH2	25.7139
CHOLDH3	26.9607
CHOLDH4	28.3864
CHOLDH5	-33.7134
CHOLt4	0.0000
CHORM	-44.6970
CHORS	-54.2881
CHRPL	-113.3597
CITT7	0.0000
CKDOAS	20.8014
CLAT	-17.4929
CO2t	0.0000
COBALTt3	0.0000
COBALTt5	0.0000
COBPS	-1074.7693
CONFALDD	-35.1930
CPPPGO	-370.9605
CRO4t6	0.0000
CS	-37.2457
CSND	-25.8642
CSNt2	0.0000

CTPS2	-17.1322
CU2t	-28.4564
CYCPOe	-404.7802
CYOO2	-170.0158
CYOR7	122.0250
CYSS	-56.3647
CYSTL	6.7668
CYTBD	-47.9908
CYTBO3_4	-47.9908
CYTD	-18.7127
CYTDH	3.0113
CYTDK1	-19.0820
CYTDK2	-19.1872
CYTDK3	-16.8407
CYTDt2	0.0000
CYTK1	3.4455
CYTK2	1.4770
CampHydrolyase	-12.7410
Clt	0.0000
Cut1	-28.4564
D-LACt2	0.0000
DADA	-17.7245
DADK	6.2712
DADNt2	0.0000
DAGK	-13.5785
DAHPS	-73.4702
DAPDC	-50.4450
DAPE	-0.6778
DASYN	-46.8030
DB4PS	-81.2807
DBTSr	-15.7897
DCYTD	-16.9033
DCYTt2	0.0000
DGALCT	0.0000
DGK1	0.7299
DHAD1	-42.9287
DHAD2	-42.9285
DHDPRy	-22.8764
DHDPS	-115.6186

DHFR	-25.3220
DHFS	-14.8557
DHNAOT7	-79.3129
DHNPA	-0.7509
DHORD2	-167.3374
DHORD4i	16.7982
DHORD8	-45.3016
DHORTS	-6.2540
DHPPDA2	26.2786
DHPRx	36.5043
DHPS3	-56.1496
DHPTPE	0.0000
DHQD1	-5.0321
DHQS	-124.8859
DIPEPabc10	-28.4564
DIPEPabc13	-28.4564
DKMPPD3	-66.2517
DMATT	-94.2693
DMOCT	-33.6612
DMPPS	-64.0817
DMQMT	-8.8454
DNMPPA	-18.7088
DNTPPA	-42.4220
DPCOAK	0.7018
DPR	-18.3304
DRBK	-16.8977
DRPA	21.6257
DTMPK	2.6577
DURIK1	-14.8571
DURIPP	14.1772
DURIt2	0.0000
DUTPDP	-59.1159
DXPRI	-15.8021
DXPS	-31.9101
E4PD	-38.9570
ECOAH2C	14.6247
ECOAH9	19.5288
EDA	16.9469
ENO	-3.9803

EPPP2	-24.7655
FAO4	-702.5430
FAO5	-837.9614
FAO6	-973.3797
FAO7	-1108.7980
FBA	23.1470
FBP	-12.2367
FCLT	3.0275
FDH10	-77.2869
FDH9	-15.1871
FE2abc	-28.4564
FE3abc	-28.4564
FGLU	-23.4058
FMNAT	796.4044
FMNRDDMBZ	-1824.7386
FMNRx	-17.0620
FORt	0.0000
FRD8	-68.1550
FRD9	-6.0552
FRTT	-91.9688
FTHFD	-23.0424
FTHFL	-5.4140
FUM	-3.3554
FUMACA	-51.9912
FUMt4_2	0.0000
G1PACT	-27.3289
G1PCT	-4.7267
G1PTMT	-1.3619
G1SATi	-9.3218
G35DP	-14.0308
G3PD2	28.4300
G3PD4	29.8556
G3PD8	-32.2442
G5SD	-13.6007
G6PDA	0.9313
G6PDHy	-4.1033
GAL1PURI	-7.4941
GALACN	7.2636
GALKr	-8.7593

GALU	-0.7036
GAPD	6.0739
GARFT	-8.2601
GBEZ	-26.5267
GCALDD	-70.7548
GF6PTA	-15.0310
GGLUGABDH	-36.6869
GGLUGABH	-10.6130
GGLUPTO	38.6237
GGLUPTS	-27.7762
GGTT	-91.9688
GHMT	-5.0624
GK1	-0.1999
GLCGSD	-1.9298
GLCP	63.3489
GLCS1	-76.1704
GLCt2	0.0000
GLGC	-12.4946
GLNS	-14.3568
GLU5K	30.0557
GLUCYSL	-38.2558
GLUDx	36.4654
GLUN	-14.0997
GLUPRT	-57.3985
GLUR	-1.0762
GLUSy	-51.8119
GLUt2	0.0000
GLUt4i	0.0000
GLYAT	29.0015
GLYBt4	0.0000
GLYCKb	-9.9458
GLYCL	17.0517
GLYCLTDXR	45.6904
GLYCLTt2r	0.0000
GLYCRt2	0.0000
GLYC_T	0.0000
GLYK	-20.2955
GLYOX	-25.4406
GLYt4	0.0000

GMHEPAT	-42.1009
GMHEPK	-11.8633
GMHEPPA	-10.1508
GMPS2	-69.9399
GP4GH	5.0237
GPDDA2	-38.3594
GPDDA4	-51.6379
GRTT	-91.9688
GSHPO	-452.3002
GSNK	-13.4399
GTHRD	13.1651
GTHRDH	8.8653
GTHRDabc	-28.4564
GTHS	-42.3471
GTPCI	-84.3269
GTPCII	-92.0689
GTPDPK	-32.3329
GUAD	23.7965
GUAPRT	-26.0846
HACD8	10.7512
HACOADr	-202.8887
HBZOPT	-91.2717
HCO3E	588.7135
HEMEOS	-81.2580
HEPTT	-91.9688
HEX1	-19.3379
HEXTT	-91.9688
HGT	0.0000
HIBHR	-22.4541
HISD1	4.3577
HISTD	-33.5316
HISTP	-14.8854
HIUH	-9.9416
HMBS	-139.9223
HMGDx	-3.7793
HMGL	-16.7829
HMGSs	-21.4948
HOMt2	0.0000
HOXPRx	33.1499

HPPDO1	-489.5702
HPPK	-14.8273
HPYRRx	-31.1897
HPYRRy	-32.4366
HSDy	22.6015
HSK	-11.4997
HSST	-20.4990
HSTPT	7.7854
HTHBPD	-149.8202
HXAD	-2.9286
HXPRT	-25.2301
ICDHxi	0.2701
ICDHy	1.5169
ICHORSi	0.9690
ICL	6.1298
IG3PS	-77.5508
IGPDH	-47.9232
IGPS	-55.0300
ILEDH2	24.4992
ILETA	-11.9662
ILEt4	0.0000
IMPC	3.2423
IMPD	10.5638
INDOLEt2	0.0000
INSK	-18.1939
IPDPS	-59.4799
IPMD	10.7808
IPPMIa	-19.5025
IPPMIb	11.0961
IPPS	-22.4440
IZPN	20.3024
KARA2i	-11.9989
KAS15	8.2185
KAS16	144.4009
KDOPP	-12.4409
KDOPS	-64.8318
Kt2i	0.0000
Kt3	0.0000
L-LACt2	0.0000

LDH_Dir	-24.3489
LEUTA	-0.4372
LEUt4	0.0000
LGTHL	-24.3634
LLEUDr	36.0281
LPADSS	-2.2201
LYSt3	0.0000
MACPD	-18.5655
MALS	-29.2374
MALTt	0.0000
MAN1PT2	7.5288
MCCC	-604.6988
MCITD	-17.6248
MCITS	-42.9960
MCOATA	-1.8008
MDH	29.1413
MDRPD	-51.3109
ME2	9.0084
MEAMP1_GLU-ASP	1.5276
MEAMP1_GLY-ASP	5.1335
MEAMP1_GLY-GLU	-1.3250
MECDPDH	-1925.8360
MECDPS	1853.4811
MEPCT	-46.7152
MET-LABC	-28.4564
METAT	51.0181
METGL	188.0958
METS	-181.8689
MGCH	11.1261
MGt3	0.0000
MGt5	0.0000
MI1PP	-34.8893
MICITH	17.6236
MICITL	14.1583
MLACI	0.0000
MLTAM	-14.4523
MLTG1e	7.4409
MLTG2e	-36.5597
MLTG3e	34.5468

MLTG4e	-10.6430
MLTG5e	8.6301
MLTSp	-14.6665
MMSDHir	184.9999
MNabc	-28.4564
MOBDabc	-28.4564
MOHMT	0.5373
MTAN	-6.3914
MTHFC	-7.0021
MTHFD	9.8392
MTHFR2	-41.5579
MTHPTGHM	-201.8188
MTRI	-1.2217
MTRK	-11.3016
NADH12	-181.4631
NADH16	-59.4273
NADH4	2.6725
NADK	-8.9524
NADS1	48.3246
NAabcO	-28.4564
NAt3	0.0000
NAt3_2	0.0000
NAt9	0.0000
NDPK1	0.1052
NDPK2	-2.9123
NDPK3	10.2079
NDPK4	10.7254
NDPK5	0.9827
NDPK6	7.3017
NDPK7	9.7270
NDPK8	8.3746
NH4HNADOR	-465.9219
NH4HNADPOR	-469.6624
NH4t	0.0000
NIt3	0.0000
NMNAT	0.8877
NNAT	-42.3829
NNDMBRT	-41.3487
NNDPR	-13.0579

NO3T7	0.0000
NODOx	-93.4530
NODOy	-94.6999
NPHS	-58.4858
NTD1	-13.5994
NTD10	0.2256
NTD11	-10.2625
NTD12	-27.6919
NTD2	-14.9848
NTD3_P	-17.2631
NTD4	-9.3745
NTD5_P	-10.1953
NTD6_P	-15.4962
NTD7	-19.3144
NTD8_P	-28.0640
NTD9	-15.0166
NTPP1	-45.8690
NTPP10	-48.3402
NTPP11	-48.3575
NTPP2	-44.0618
NTPP3	-55.3604
NTPP4	-57.8098
NTPP5	-58.8022
NTPP6	-42.5675
NTPP7	-57.5395
NTPP8	-45.4883
NTPP9	-31.0115
NTR4	-182.7447
NTR5	-120.6449
O2t	0.0000
OAADC	-21.3797
OBTFL	-13.2330
OCBT	-25.1184
OHPBAT	15.6051
OHPHM	-8.8293
OIVD1i	-31.2086
OIVD2	-25.5321
OIVD3	-25.5320
OMBZLM	3.1963

OMCDC	-10.7660
OMMBLHX	-213.6298
OMMBLHXAN	-41.0887
OMPDC	3.1964
OMPHHX	-213.6306
OMPHHXAN	-41.0894
OMP_AC	0.0000
OMP_ACGAM	0.0000
OMP_ADN	0.0000
OMP_ALA-D	0.0000
OMP_ALA-L	0.0000
OMP_ASP-L	0.0000
OMP_BGL	0.0000
OMP_CA2	0.0000
OMP_CBL1	0.0000
OMP_CHITOB	0.0000
OMP_CHOL	0.0000
OMP_CL	0.0000
OMP_CO2	0.0000
OMP_COBALT2	0.0000
OMP_CU2	0.0000
OMP_CYTD	0.0000
OMP_DAD-2	0.0000
OMP_DAMP	0.0000
OMP_DCMP	0.0000
OMP_DCYT	0.0000
OMP_DGMP	0.0000
OMP_DGSN	0.0000
OMP_DMS	0.0000
OMP_DMSO	0.0000
OMP_DODCA	0.0000
OMP_DTMP	0.0000
OMP_DURI	0.0000
OMP_FE2	0.0000
OMP_FOR	0.0000
OMP_FUM	0.0000
OMP_GAL	0.0000
OMP_GALTAN	0.0000
OMP_GLC-D	0.0000

OMP_GLU-L	0.0000
OMP_GLY	0.0000
OMP_GLY-ASP-L	0.0000
OMP_GLY-GLU-L	0.0000
OMP_GLYB	0.0000
OMP_GLYC	0.0000
OMP_GLYC-R	0.0000
OMP_GLYCLT	0.0000
OMP_GTHRD	0.0000
OMP_H2	0.0000
OMP_H2O2	0.0000
OMP_H2S	0.0000
OMP_HDCA	0.0000
OMP_ILE-L	0.0000
OMP_INDOLE	0.0000
OMP_INOSHP	0.0000
OMP_INOSPP1	0.0000
OMP_K	0.0000
OMP_LAC-D	0.0000
OMP_LAC-L	0.0000
OMP_LEU-L	0.0000
OMP_LYS-L	0.0000
OMP_MAL-L	0.0000
OMP_MALT	0.0000
OMP_MALTHP	0.0000
OMP_MALTTTR	0.0000
OMP_MET-L	0.0000
OMP_MG2	0.0000
OMP_MN2	0.0000
OMP_MOBD	0.0000
OMP_NH4	0.0000
OMP_NMN	0.0000
OMP_NO2	0.0000
OMP_NO3	0.0000
OMP_O2	0.0000
OMP_OCDCA	0.0000
OMP_PI	0.0000
OMP_PMCOA	0.0000
OMP_PPA	0.0000

OMP_PRO-L	0.0000
OMP_PTRC	0.0000
OMP_PYR	0.0000
OMP_SER-L	0.0000
OMP_SO3	0.0000
OMP_SO4	0.0000
OMP_SUCC	0.0000
OMP_THR-L	0.0000
OMP_THYMD	0.0000
OMP_TMA	0.0000
OMP_TMAO	0.0000
OMP_TRP-L	0.0000
OMP_TSUL	0.0000
OMP_TTDCA	0.0000
OMP_TTTNT	0.0000
OMP_TYR-L	0.0000
OMP_URA	0.0000
OMP_UREA	0.0000
OMP_URI	0.0000
OMP_VAL-L	0.0000
OMP_XAN	0.0000
OMP_na1	0.0000
OPHBDC	-11.1587
OPHHX	-213.6356
OPHHXAN	-41.0945
ORNCD	-27.3416
ORPT	53.0230
OXGDC2	-26.5042
P5CD	-35.5741
P5CR	-50.2885
PANTS	-46.9966
PAP	-14.8779
PAPPT3	12.3438
PASYN_WP2	-4337.7399
PDH	-39.9381
PDX5PO	19.9222
PDX5PS	-245.3944
PERD	10.8037
PFL	-22.0785

PGAMT	-3.1968
PGCD	33.6222
PGDH	8.4651
PGDHY	-41.2653
PGI	2.5440
PGK	-18.9302
PGL	-22.8106
PGLYCP	-39.4018
PGM	5.3631
PGMT	-7.2012
PGPPH	-12.4368
PGSA	25.4994
PHE4MO	-442.9088
PHEAL	-3.2282
PHEMEabc	-28.4564
PHETA1	-0.4583
PHNabc	-28.4564
PIabc	-28.4564
PIt6	0.0000
PMANM	-5.7616
PMCOAt	0.0000
PMDPHT	-14.6176
PMPK	3.8755
PNTK	-17.3954
PPA	-12.7564
PPAtNa	0.0000
PPBNGS	-106.7508
PPC	-35.7028
PPCDC	-15.4095
PPCK	7.2463
PPM	-8.4638
PPM2	-3.7316
PPNCL	-56.7092
PPND	-81.8141
PPNDH	-88.7499
PPPGFUM	-137.4842
PPPGMEN	66.9810
PPPGNO3	-481.2531
PPPGO	-629.3985

PPS	1.7586
PPTT	-91.9688
PRAGS	-34.8275
PRAIS	-42.6920
PRAIi	-5.3714
PRAMPC	24.2280
PRASCS	-43.6532
PRATPP	-44.1557
PRFGS	21.2756
PRKIN	-15.2390
PRMICIi	-5.3453
PRO1q	-132.4215
PROt4	0.0000
PRPPS	-6.3433
PSCVT	-36.1614
PSD	-17.6453
PSERT	-10.4317
PSP_L	-9.0827
PSSA	7.9993
PSUDS	-34.1782
PTAr	10.5445
PTPATi	-62.2738
PTRCabc	-28.4564
PULLNASE	32.7481
PUNP1	7.9407
PUNP2	14.7310
PUNP3	13.3408
PUNP4	20.9876
PUNP5	7.7323
PUNP6	10.9663
PUNP7	8.6224
PYAM5PO	36.3047
PYDXL5PSYN	-321.3548
PYK	-28.6261
PYNP2	5.7115
PYRt2	0.0000
QULNS	-225.3764
RBFK	1340.6846
RBFSa	-135.0046

RBFSb	-30.0783
RBK	-27.0685
RBZP	-15.0572
RHCCE	-15.0514
RIBabc	-28.4564
RPE	-2.3946
RPI	0.8296
S7PI	9.0014
SADH	-82.8720
SADT2	13.0909
SDPDS	15.9013
SDPTA	-0.2408
SELNPS	796.6392
SERAT	-6.7919
SERD_D	-29.5449
SERD_L	-33.3421
SERGLYX	1.2458
SERt4	0.0000
SERt6	0.0000
SFGTH	-23.4579
SGDS	1.5712
SGSAD	-40.3701
SHCHCS2	-63.9442
SHCHD2	-11.7941
SHCHF	3.0258
SHK3D	-43.7709
SHKK	-2.9934
SHSL1	-65.4309
SLCYSS	-635.1769
SO4t2	0.0000
SOD	98.9507
SOTA	-5.5894
SPA	3.4413
SPMS	388.8698
SPRS	387.6919
SSALx	-41.7819
SUCBZL	-25.2725
SUCBZS	-54.9104
SUCCt4	0.0000

SUCCtex	0.0000
SUCD7	-115.9806
SUCOAS	-1.9778
SULR	654.5751
TAL	0.0878
TDP	-33.5401
TDP3AAAT	33.6580
TDPDRE	0.0000
TDPDRR	12.6029
TDPGDH	-80.1348
TDSK	868.9786
THD2	1.2469
THD5	-1.2469
THDPS	27.7727
THMDt2	0.0000
THMabc	-28.4564
THRA	3.4249
THRD	11.5065
THRD_L	-31.1538
THRHT	0.0000
THRLAD	1.0904
THRS	-21.0875
THRt3	0.0000
THRt4	0.0000
THZPSN	-238.8132
TKT1	-3.0475
TKT2	-9.2771
TMDK1	-18.2612
TMDPP	13.1461
TMDS	-54.1168
TMPKr	5.0836
TMPPP	-20.6844
TPI	6.6057
TRPOR	-414.2907
TRPS2	-54.5276
TRPS3	-27.3530
TRPt6	0.0000
TSULST	49.7466
TYRTA	-46.0259

TYRt6	0.0000
U23GAAT	-252.9035
UAAGDS	-38.5493
UAGAAT	-245.0629
UAGCVT	-44.0353
UAGDP	-31.1016
UAGPT3	-4.9579
UAMAGS	-34.9903
UAMAS	-35.0729
UAPGR	-53.0046
UDCPDP	-31.6685
UDCPDPS	-735.7502
UDPG4E	3.3284
UDPHEXURI	-6.7905
UGMDDS	-38.3237
UHGADA	-3.9573
UMPK	4.2442
UNK3	-156.3544
UPP3MT	161.8946
UPP3S	-242.5116
UPPDC1	-42.4884
UPPRT	-18.4871
UQOR	-181.4631
URAt6	0.0000
URCN	-5.8493
URDGLY	-31.8912
URHYDROX	-359.3361
URIDK2	7.6578
URIH	-4.1402
URIK1	-13.4717
URIK2	-13.5769
URIK3	-11.2304
URIt2	0.0000
USHD	-3.1930
UreaExp	0.0000
VALALAMOB	-5.5474
VALDHr	31.4110
VALTA	-5.0544
VALt4	0.0000

WO4abc	-28.4564
XAND	-50.2096
XANt	0.0000
XPK	-58.5356
FFSD	-22.3563
FRUK	-17.7598
SUCP	0.9948
SUCRPTS	-54.7209
TRE6PP	-15.8962
TREH	-6.2194
TREHtex	-44.6792
OMP_SUCR	0.0000
OMP_CIT	0.0000
OMP_TREH	0.0000

Data S1 Table F: List of all reactions contained in the WP2 GEM that were excluded from the thermodynamic constraints.

TMAOR3e
DMSOR4e
DMSOR3e
2MAHMP
4HBASink
5DRIB_Sink
5HPUDICDCr
ACBIPGT
ACPS1
ACPSc
ADCOBAK
ALATRS
AMOB_Sink
ARGTRS
ASNTRS
ASPTRS
ATPM
Biomass_WP2
CBLAT
CPPPGOAN
CYSTRS
DNA_CUT
DNA_SYNTHESIS
EDTXS5
EDTXS6
FCLT
FMETTRS
FMNAT
FNOR
FRD10
FRD11
GLNTRS
GLUTRR
GLUTRS
GLYCLTDXR
GLYCOGEN_SYNTHESIS

GLYD
GLYTRS
Growth
H2Ot5
HCO3E
HISTRS
ILETRS
IPPMIa
KAS16
LEUTRS
LIPID_SYNTHESIS
LPS_SYNTHESIS
LPSSYN_core
LYSTRS
MECDPDH
MECDPS
METTRS
MLTS
MOAT3
NADH11
NADH13
NADH14
NMNP
NTD3
NTD5
NTD6
NTD8
OMP_H
OMP_H2O
PAPSR
PASYN_WP2
PEPTIDO_SYNTHESIS
PEPTIDOXe
PHETRS
PPTGSe
PRAMPC
PROT_SYNTHESIS
PROTRS
RBFK

RNA_SYNTHESIS
RNDR1
RNDR2
RNDR3
RNDR4
RNTR1
RNTR2
RNTR3
RNTR4
SELNPS
SERTRS
SHCHF
SPMS
SULR
TDSK
THRTRS
TRACE_ELEMENTS
TRDR
TRPTRS
TYRTA
TYRTRS
UPP3MT
VALTRS

Data S1 Table G: Net number of protons and net charge transported from outside of the cell to inside of the cell for each transport reaction in the WP2 GEM.

Reaction ID	Net Charge Transported (out to in)	Net Protons Transporterd (out to in)
ACACt2	1	1
ACGALT2	1	1
ACGAt2	1	1
ACt6	1	1
ADNt2	1	1
AKGt6	1	1
ALA_Dt4	1	0
ALAt4	1	0
ARBABC	0	0
ARGABC	0	0
ARGabc	0	0
ARSTATPASE	3	0
ARSt	1	1
ARSt1	-3	0
ASNt2	1	1
ASPt2	1	1
ASPt2_3	3	3
ATPS4r	3	3
BGLP	1	1
BGLP2	1	0
BUT_T	1	1
CAT4I	-1	1
CBL1abc	-3	0
CH4SXPORT	0	0
CHOLt4	2	0
CO2t	0	0
COBALTabc	2	0
COBALTt3	-1	1
COBALTt5	2	2
CRO4t6	-1	1
CSNt2	1	1
CU2t	2	0
CYOO2	-2	-2
CYOR7	-4	-4
CYSt2	1	1

CYTBD	-2	-2
CYTBO3_4	-4	-4
CYTDt2	1	1
Clt	-1	0
Cut1	-2	0
D-LACt2	1	1
DADNt2	1	1
DCYTt2	1	1
DGALCT	1	0
DGSNt2	1	1
DIPEPABC15	-2	0
DIPEPabc10	-1	
DIPEPabc13	-1	0
DODCAt2	0	1
DURIt2	1	1
ETOHT1	0	0
FE2abc	2	0
FE3abc	3	0
FORt	0	0
FRMDT	0	0
FUMT2_2	2	2
FUMt4	3	3
FUMt4_2	1	0
G3PGABC	0	0
GLCPTS	0	0
GLCt2	1	1
GLNT2	1	1
GLUt2	1	1
GLUt4i	1	0
GLYBt4	1	0
GLYCLTt2r	1	1
GLYCRt2	1	1
GLYC_T	0	0
GLYt4	1	0
GSNT	0	0
GTHRDabc	0	0
GUAT	0	0
H2Ot5	0	0
HDCAT2	0	-1

HGT	2	0
HIST2R	1	1
HOMt2	1	1
HYXNT	0	0
ILEt4	1	0
INDOLEt2	1	1
INST2	1	1
Kt2i	2	1
Kt3	0	1
L-LACt2	1	1
LEU_ABC	0	0
LEUt4	1	0
LYSt3	1	1
MALT2_2	2	2
MALTt	1	1
MALt2_3	3	3
MET-LABC	0	0
MGt3	-1	1
MGt5	2	0
MNabc	2	2
MOBDabc	0	0
NADH11	-4	-4
NADH13	-4	-4
NADH16	-4	-4
NAabcO	-1	0
NAt3	0	1
NAt3_2	1	2
NAt9	-1	0
NH4t	0	0
NIt3	-1	1
NMNP	0	0
NO3T7	0	0
NOT2	1	1
O2t	0	0
OCDCAT2	0	1
PHEMEabc	0	0
PHET2R	1	1
PHNabc	0	0
PIabc	0	0

PIt6	1	1
PMCOAt	0	0
PPAT2	1	1
PPAtNa	1	0
PRO_LABC	0	0
PROt4	1	0
PTRCORNT7	0	0
PTRCT2	1	1
PTRCabc	0	0
PYRt2	1	1
SABC	0	0
SERt4	1	0
SERt6	1	1
SO4T4	1	0
SO4t2	1	1
SUCCT2_2	2	2
SUCCt2_3	3	3
SUCCt4	1	0
SUCCtex	1	1
SUCFUMtdc	0	0
SUCRPTS	0	0
SULabc	0	0
THD2	2	2
THMDt2	1	1
THMabc	1	0
THRHT	1	1
THRt3	1	1
THRt4	1	0
THYMT6	1	1
TRPt6	1	1
TSULABC	-1	0
TTDCAT2	0	1
TYRt6	1	1
UQOR	-2	0
URAt6	1	1
URIt2	1	1
UreaExp	0	0
VALt4	1	1
WO4abc	0	0

XANt	0	0

Data S1 Table H: Non-default concentration bounds used in the WP2 TMFA simulations. Concentrations are based on the LMO-812 media composition for all compounds except cpd_cbasp and cpd_dhor-S which were modified based on previous literature (Materials and Methods).

Metabolite ID	Lower Concentration Bound (M)	Upper Concentration Bound (M)
cpd_cbasp[c]	1.00E-06	5.00E-02
cpd_dhor-S[c]	1.00E-06	5.00E-02
cpd_4abz[e]	5.46E-08	5.46E-06
cpd_4abz[p]	5.46E-08	5.46E-06
cpd_4abz[c]	5.46E-08	5.46E-06
cpd_btn[e]	2.43E-08	2.43E-06
cpd_btn[p]	2.43E-08	2.43E-06
cpd_btn[c]	2.43E-08	2.43E-06
cpd_ca2[e]	1.00E-05	1.55E-01
cpd_ca2[p]	1.00E-05	1.55E-01
cpd_ca2[c]	1.00E-05	1.55E-01
cpd_cl[e]	1.00E-05	2.82E+00
cpd_cl[p]	1.00E-05	2.82E+00
cpd_cl[c]	1.00E-05	2.82E+00
cpd_cobalt2[e]	2.46E-07	2.46E-05
cpd_cobalt2[p]	2.46E-07	2.46E-05
cpd_cobalt2[c]	2.46E-07	2.46E-05
cpd_cu2[e]	1.34E-08	1.34E-06
cpd_cu2[p]	1.34E-08	1.34E-06
cpd_cu2[c]	1.34E-08	1.34E-06
cpd_adcoba[e]	6.75E-07	6.75E-05
cpd_adcoba[p]	6.75E-07	6.75E-05
cpd_adcoba[c]	6.75E-07	6.75E-05
cpd_fe2[e]	1.00E-05	3.18E-04
cpd_fe2[p]	1.00E-05	3.18E-04
cpd_fe2[c]	1.00E-05	3.18E-04
cpd_k[e]	1.00E-05	5.07E-02
cpd_k[p]	1.00E-05	5.07E-02
cpd_k[c]	1.00E-05	5.07E-02
cpd_mobd[e]	7.38E-08	7.38E-06
cpd_mobd[p]	7.38E-08	7.38E-06
cpd_mobd[c]	7.38E-08	7.38E-06
cpd_na1[e]	1.00E-05	2.79E+00

cpd_na1[p]	1.00E-05	2.79E+00
cpd_na1[c]	1.00E-05	2.79E+00
cpd_nh4[e]	1.00E-05	1.60E-02
cpd_nh4[p]	1.00E-05	1.60E-02
cpd_nh4[c]	1.00E-05	1.60E-02
cpd_ni2[e]	3.10E-08	3.10E-06
cpd_ni2[p]	3.10E-08	3.10E-06
cpd_ni2[c]	3.10E-08	3.10E-06
cpd_nac[e]	1.23E-07	1.23E-05
cpd_nac[p]	1.23E-07	1.23E-05
cpd_nac[c]	1.23E-07	1.23E-05
cpd_pnto-R[e]	1.19E-07	1.19E-05
cpd_pnto-R[p]	1.19E-07	1.19E-05
cpd_pnto-R[c]	1.19E-07	1.19E-05
cpd_pi[e]	1.00E-05	1.36E-02
cpd_pi[p]	1.00E-05	1.36E-02
cpd_pi[c]	1.00E-05	1.36E-02
cpd_so4[e]	1.00E-05	5.66E-01
cpd_so4[p]	1.00E-05	5.66E-01
cpd_so4[c]	1.00E-05	5.66E-01
cpd_thm[e]	3.36E-07	3.36E-05
cpd_thm[p]	3.36E-07	3.36E-05
cpd_thm[c]	3.36E-07	3.36E-05
cpd_acgam[e]	1.00E-05	5.00E-03
cpd_acgam[p]	1.00E-05	5.00E-03
cpd_acgam[c]	1.00E-05	5.00E-03
cpd_o2[e]	1.00E-05	0.00032952 (4C) , 0.00025746 (15C), 0.00023388 (20C)
cpd_o2[p]	1.00E-05	0.00032952 (4C) , 0.00025746 (15C), 0.00023388 (20C)
cpd_o2[c]	1.00E-05	0.00032952 (4C) , 0.00025746 (15C), 0.00023388 (20C)

Data S1 Table I: Exchange Constraints used for the temperature-dependent model simulations based on the LMO-812 media.

Compound ID	Compound Name	Lower Limit	Upper Limit
cpd_na1[e]	Sodium	-1000	1000
cpd_pro-L[e]	L-Proline	0	1000
cpd_h2o2[e]	Hydrogen peroxide	0	1000
cpd_damp[e]	dAMP	0	1000
cpd_dcmp[e]	dCMP	0	1000
cpd_dgmp[e]	dGMP	0	1000
cpd_dtmp[e]	dTMP	0	1000
cpd_met-L[e]	L-Methionine	0	1000
cpd_adn[e]	Adenosine	0	1000
cpd_dad-2[e]	Deoxyadenosine	0	1000
cpd_dgsn[e]	Deoxyguanosine	0	1000
cpd_glyc-R[e]	(R)-Glycerate	0	1000
cpd_indole[e]	Indole	0	1000
cpd_ura[e]	Uracil	0	1000
cpd_CrOH3[e]	Cr(OH)3	0	1000
cpd_ac[e]	Acetate	0	1000
cpd_acgam[e]	N-Acetyl-D-glucosamine	-5	1000
cpd_ala-D[e]	D-Alanine	0	1000
cpd_ala-L[e]	L-Alanine	0	1000
cpd_asp-L[e]	L-Aspartate	0	1000
cpd_bgl[e]	cellobiose	0	1000
cpd_ca2[e]	Calcium	-1000	1000
cpd_cl[e]	Chloride	-1000	1000
cpd_co2[e]	CO2	0	1000
cpd_cobalt3[e]	Co3+	0	1000
cpd_cobalt2[e]	Co2+	-1000	1000
cpd_cro4[e]	chromate	0	1000
cpd_cu2[e]	Cu2+	-1000	1000
cpd_cytd[e]	Cytidine	0	1000
cpd_dcyt[e]	Deoxycytidine	0	1000
cpd_dms[e]	Dimethyl sulfide	0	1000
cpd_dmso[e]	Dimethyl sulfoxide	0	1000
cpd_dna[e]	Dimethyl sulfoxide	0	1000
cpd_dodcan[e]	Dodecanoic acid (neutral)	0	1000

cpd_duri[e]	Deoxyuridine	0	1000
cpd_fe2[e]	Fe2+	-1000	1000
cpd_fe3[e]	Fe3+	0	1000
cpd_for[e]	Formate	0	1000
cpd_fum[e]	Fumarate	0	1000
cpd_galactan[e]	Galactan	0	1000
cpd_gal[e]	D-Galactose	0	1000
cpd_glc-D[e]	D-Glucose	0	1000
cpd_glu-L[e]	L-Glutamate	0	1000
cpd_gly[e]	glycyl-L-glutamic acid	0	1000
cpd_gly-asp-L[e]	glycyl-L-aspartic acid	0	1000
cpd_gly-glu-L[e]	glycyl-L-glutamic acid	0	1000
cpd_glyc[e]	(R)-Glycerate	0	1000
cpd_glyclt[e]	Glycolate	0	1000
cpd_h[e]	H+	-1000	1000
cpd_h2o[e]	H2O	-1000	1000
cpd_h2s[e]	Hydrogen sulfide	0	1000
cpd_hdcan[e]	hexadecanoate (n-C16:0) (neutral)	0	1000
cpd_ile-L[e]	L-Isoleucine	0	1000
cpd_k[e]	K+	-1000	1000
cpd_lac-D[e]	D-Lactate	0	1000
cpd_lac-L[e]	L-Lactate	0	1000
cpd_lami[e]	laminarin	0	1000
cpd_leu-L[e]	L-Leucine	0	1000
cpd_mal-L[e]	L-Malate	0	1000
cpd_panose[e]	Panose	0	1000
cpd_malt[e]	Maltose	0	1000
cpd_malthp[e]	Maltoheptaose	0	1000
cpd_malthx[e]	Maltohexaose	0	1000
cpd_maltpt[e]	Maltopentaose	0	1000
cpd_malttr[e]	Maltotriose	0	1000
cpd_maltttr[e]	Maltotetraose	0	1000
cpd_mg2[e]	Mg	-1000	1000
cpd_mn2[e]	Mn2+	-1000	1000
cpd_mn4o[e]	Manganese(IV) oxide	0	1000

cpd_nh4[e]	Ammonium	-5.6	1000
cpd_no2[e]	Nitrite	0	1000
cpd_no3[e]	Nitrate	0	1000
cpd_o2[e]	Oxygen	-0.32952261 (4C), -0.25745959 (15C), -0.23387845 (20C)	1000
cpd_ocdcan[e]	octadecanoate (n-C18:0) neutral	0	1000
cpd_pi[e]	Phosphate	-0.7	1000
cpd_pmcoa[e]	Pimeloyl-CoA	-1000	1000
cpd_ptrc[e]	Putrescine	0	1000
cpd_pyr[e]	Pyruvate	0	1000
cpd_ser-L[e]	L-Serine	0	1000
cpd_so3[e]	Sulfite	0	1000
cpd_so4[e]	Sulfate	-9.8	1000
cpd_succ[e]	Succinate	0	1000
cpd_thr-L[e]	L-Threonine	0	1000
cpd_tma[e]	Trimethylamine	0	1000
cpd_tmao[e]	Trimethylamine N-oxide	0	1000
cpd_tsul[e]	Thiosulfate	0	1000
cpd_ttdcan[e]	tetradecanoate (C14:0) (neutral)	0	1000
cpd_tttnt[e]	tetrathionate	0	1000
cpd_tyr-L[e]	L-Tyrosine	0	1000
cpd_urdio[e]	Uranium dioxide	0	1000
cpd_uri[e]	Uridine	0	1000
cpd_urnyl[e]	Uranyl	0	1000
cpd_val-L[e]	L-Valine	0	1000
cpd_thymd[e]	Thymidine	0	1000
cpd_mobd[e]	Molybdate	-1000	1000
cpd_cbl1[e]	Cob(I)alamin	-1000	1000
cpd_ppa[e]	Propionate	0	1000
cpd_urea[e]	Urea	0	1000
cpd_chitin[e]	Methanethiol	0	1000
cpd_lys-L[e]	L-Lysine	0	1000
cpd_trp-L[e]	L-Tryptophan	0	1000
cpd_xan[e]	Xanthine	0	1000
cpd_etoh[e]	Ethanol	0	1000
cpd_akg[e]	2-Oxoglutarate	0	1000

cpd_gln-L[e]	L-Glutamine	0	1000
cpd_asn-L[e]	L-Asparagine	0	1000
cpd_ins[e]	Inosine	0	1000
cpd_thym[e]	Thymine	0	1000
cpd_hxan[e]	Hypoxanthine	0	1000

Appendix IV Data S2 for Manuscript II

Data S2 Table A Metabolite concentration ranges from TMFA simulations.

Metabolite ID	Lower Bound 4	Upper Bound 4	Range 4	Lower Bound 15	Upper Bound 15	Range 15	Lower Bound 20	Upper Bound 20	Range 20
Biomass[c]	1.00E-05	0.02	0.01999	1.00E-05	0.02	0.01999	1.00E-05	0.02	0.01999
cpd_10fthf[c]	0.0002087677907	0.02	0.01979123221	0.0001859027951	0.02	0.01981409721	0.0001768629373	0.02	0.01982313706
cpd_12dag3p[c]	1.00E-05	0.02	0.01999	1.00E-05	0.02	0.01999	1.00E-05	0.02	0.01999
cpd_12dgr[c]	1.00E-05	0.02	0.01999	1.00E-05	0.02	0.01999	1.00E-05	0.02	0.01999
cpd_13dpg[c]	1.00E-05	0.02	0.01999	1.00E-05	3.98E-05	2.98E-05	1.00E-05	8.43E-05	7.43E-05
cpd_1pyr5c[c]	1.00E-05	0.02	0.01999	1.00E-05	0.02	0.01999	1.00E-05	0.02	0.01999
cpd_23dhdp[c]	1.00E-05	0.02	0.01999	1.00E-05	0.02	0.01999	1.00E-05	0.02	0.01999
cpd_23dhmb[c]	1.00E-05	0.02	0.01999	1.00E-05	0.02	0.01999	1.00E-05	0.02	0.01999
cpd_23dhmp[c]	1.00E-05	0.02	0.01999	1.00E-05	0.02	0.01999	1.00E-05	0.02	0.01999
cpd_25aics[c]	0.0006532782848	0.02	0.01934672172	0.0003588680821	0.02	0.01964113192	0.0002774170274	0.02	0.01972258297
cpd_25dhpp[c]	0.0028719315 99	0.02	0.0171280684	0.0023309650 44	0.02	0.0176690349 6	0.0009127681899	0.02	0.0190872318 1
cpd_26dap-LL[c]	1.00E-05	0.02	0.01999	1.00E-05	0.02	0.01999	1.00E-05	0.02	0.01999
cpd_26dap-M[c]	1.00E-05	0.02	0.01999	1.00E-05	0.02	0.01999	1.00E-05	0.02	0.01999
cpd_2ahbut[c]	1.00E-05	0.02	0.01999	1.00E-05	0.02	0.01999	1.00E-05	0.02	0.01999

cpd_2ahhmd[c]	1.00E-05	0.02	0.01999	1.00E-05	0.02	0.01999	1.00E-05	0.02	0.01999
cpd_2ahhmp[c]	1.00E-05	0.02	0.01999	1.00E-05	0.02	0.01999	1.00E-05	0.02	0.01999
cpd_2aobut[c]	1.00E-05	0.02	0.01999	1.00E-05	0.02	0.01999	1.00E-05	0.02	0.01999
cpd_2cpr5p[c]	1.00E-05	0.02	0.01999	1.00E-05	0.02	0.01999	1.00E-05	0.02	0.01999
cpd_2dda7p[c]	1.00E-05	0.02	0.01999	1.00E-05	0.02	0.01999	1.00E-05	0.02	0.01999
cpd_2ddg6p[c]	1.00E-05	0.02	0.01999	1.00E-05	0.02	0.01999	1.00E-05	0.02	0.01999
cpd_2dhp[c]	1.00E-05	0.02	0.01999	1.00E-05	0.02	0.01999	1.00E-05	0.02	0.01999
cpd_2dmmq7[c]	1.00E-05	0.02	0.01999	1.00E-05	0.02	0.01999	1.00E-05	0.02	0.01999
cpd_2dr1p[c]	1.00E-05	0.00412976794	0.00411976794	1.00E-05	0.02	0.01999	1.00E-05	0.02	0.01999
cpd_2dr5p[c]	1.35E-05	0.02	0.019986534	1.00E-05	0.02	0.01999	1.00E-05	0.02	0.01999
cpd_2h3opp[c]	1.00E-05	0.02	0.01999	NA	NA	NA	NA	NA	NA
cpd_2ippm[c]	1.00E-05	0.02	0.01999	1.00E-05	0.02	0.01999	1.00E-05	0.02	0.01999
cpd_2kmb[c]	1.00E-05	0.02	0.01999	1.00E-05	0.02	0.01999	1.00E-05	0.02	0.01999
cpd_2maaco a[c]	1.00E-05	0.02	0.01999	1.00E-05	0.02	0.01999	1.00E-05	0.02	0.01999
cpd_2mahmp[c]	1.00E-05	0.02	0.01999	1.00E-05	0.02	0.01999	1.00E-05	0.02	0.01999
cpd_2mb2coa[c]	1.00E-05	0.02	0.01999	1.00E-05	0.02	0.01999	1.00E-05	0.02	0.01999

cpd_2mbcoa[c]	1.00E-05	0.02	0.01999	1.00E-05	0.02	0.01999	1.00E-05	0.02	0.01999
cpd_2mcacn[c]	1.00E-05	0.02	0.01999	1.00E-05	0.02	0.01999	1.00E-05	0.02	0.01999
cpd_2mcit[c]	1.00E-05	0.02	0.01999	1.00E-05	0.02	0.01999	1.00E-05	0.02	0.01999
cpd_2me4p[c]	1.00E-05	0.02	0.01999	1.00E-05	0.02	0.01999	1.00E-05	0.02	0.01999
cpd_2mecdp[c]	1.00E-05	0.02	0.01999	1.00E-05	0.02	0.01999	1.00E-05	0.02	0.01999
cpd_2mp2coa[c]	1.00E-05	0.02	0.01999	1.00E-05	0.02	0.01999	1.00E-05	0.02	0.01999
cpd_2obut[c]	1.00E-05	0.02	0.01999	1.00E-05	0.02	0.01999	1.00E-05	0.02	0.01999
cpd_2ohph[c]	1.00E-05	0.02	0.01999	1.00E-05	0.02	0.01999	1.00E-05	0.02	0.01999
cpd_2ombzl[c]	2.01E-05	0.02	0.01997994865	0.00025763892 67	0.02	0.01974236107	9.24E-05	0.02	0.01990763471
cpd_2omhmbl[c]	1.00E-05	0.02	0.01999	1.00E-05	0.02	0.01999	1.00E-05	0.02	0.01999
cpd_2ommbl[c]	1.00E-05	0.00997439255 9	0.00996439255 9	1.00E-05	0.00077628020 94	0.00076628020 94	1.00E-05	0.00216531550 4	0.00215531550 4
cpd_2omph[c]	1.00E-05	0.02	0.01999	1.00E-05	0.02	0.01999	1.00E-05	0.02	0.01999
cpd_2oph[c]	1.00E-05	0.02	0.01999	1.00E-05	0.02	0.01999	1.00E-05	0.02	0.01999
cpd_2p4c2me[c]	1.00E-05	0.02	0.01999	1.00E-05	0.02	0.01999	1.00E-05	0.02	0.01999
cpd_2pg[c]	1.00E-05	0.02	0.01999	1.00E-05	0.00035690535 04	0.00034690535 04	1.00E-05	0.00068245950 55	0.00067245950 55
cpd_2pglyc[c]	1.00E-05	0.02	0.01999	1.00E-05	0.02	0.01999	1.00E-05	0.02	0.01999

cpd_2shchc[c]	1.00E-05	0.02	0.01999	1.00E-05	0.02	0.01999	1.00E-05	0.02	0.01999
cpd_34hpp[c]	1.00E-05	0.02	0.01999	1.00E-05	0.02	0.01999	1.00E-05	0.02	0.01999
cpd_3c2hmp[c]	0.00021561853 43	0.02	0.01978438147	8.10E-05	0.02	0.01991900762	5.32E-05	0.02	0.01994682566
cpd_3c3hmp[c]	1.00E-05	0.02	0.01999	1.00E-05	0.02	0.01999	1.00E-05	0.02	0.01999
cpd_3c4mop[c]	1.00E-05	0.00092756404 55	0.00091756404 55	1.00E-05	0.00246936824	0.00245936824	1.00E-05	0.00376121251 2	0.00375121251 2
cpd_3dhq[c]	1.00E-05	0.02	0.01999	1.00E-05	0.02	0.01999	1.00E-05	0.02	0.01999
cpd_3dhsk[c]	1.00E-05	0.02	0.01999	1.00E-05	0.02	0.01999	1.00E-05	0.02	0.01999
cpd_3hmbcoa[c]	1.00E-05	0.02	0.01999	1.00E-05	0.02	0.01999	1.00E-05	0.02	0.01999
cpd_3hmp[c]	1.00E-05	0.02	0.01999	1.00E-05	0.02	0.01999	1.00E-05	0.02	0.01999
cpd_3htdACP[c]	1.00E-05	0.02	0.01999	1.00E-05	0.02	0.01999	1.00E-05	0.02	0.01999
cpd_3ig3p[c]	1.00E-05	0.02	0.01999	1.00E-05	0.02	0.01999	1.00E-05	0.02	0.01999
cpd_3mb2coa[c]	NA	NA	NA	NA	NA	NA	1.00E-05	0.02	0.01999
cpd_3mgcoa[c]	1.00E-05	0.02	0.01999	NA	NA	NA	NA	NA	NA
cpd_3mob[c]	1.00E-05	0.02	0.01999	1.00E-05	0.02	0.01999	1.00E-05	0.02	0.01999
cpd_3mop[c]	1.00E-05	0.02	0.01999	1.00E-05	0.02	0.01999	1.00E-05	0.02	0.01999
cpd_3ophb[c]	1.00E-05	0.02	0.01999	1.00E-05	0.02	0.01999	1.00E-05	0.02	0.01999
cpd_3pg[c]	1.00E-05	0.02	0.01999	9.38E-05	0.00334757104 9	0.00325377668 5	9.03E-05	0.00616129600 4	0.00607101524 8

cpd_3php[c]	1.00E-05	0.02	0.01999	1.00E-05	0.02	0.01999	1.00E-05	0.02	0.01999
cpd_3psme[c]	1.00E-05	0.02	0.01999	1.00E-05	0.02	0.01999	1.00E-05	0.02	0.01999
cpd_4abut[c]	1.00E-05	0.02	0.01999	1.00E-05	0.02	0.01999	1.00E-05	0.02	0.01999
cpd_4abz[c]	5.46E-08	5.46E-06	5.41E-06	5.46E-08	5.46E-06	5.41E-06	5.46E-08	5.46E-06	5.41E-06
cpd_4adcho[c]	1.00E-05	0.02	0.01999	1.00E-05	0.02	0.01999	1.00E-05	0.02	0.01999
cpd_4ampm[c]	1.00E-05	0.02	0.01999	1.00E-05	0.02	0.01999	1.00E-05	0.02	0.01999
cpd_4c2me[c]	1.00E-05	0.02	0.01999	1.00E-05	0.02	0.01999	1.00E-05	0.02	0.01999
cpd_4fumacac[c]	1.00E-05	0.02	0.01999	1.00E-05	0.02	0.01999	1.00E-05	0.02	0.01999
cpd_4hba[c]	1.00E-05	0.02	0.01999	1.00E-05	0.02	0.01999	1.00E-05	0.02	0.01999
cpd_4hbcoa[c]	1.00E-05	0.02	0.01999	NA	NA	NA	1.00E-05	0.02	0.01999
cpd_4hbz[c]	1.00E-05	0.02	0.01999	1.00E-05	0.02	0.01999	1.00E-05	0.02	0.01999
cpd_4izp[c]	1.00E-05	0.02	0.01999	1.00E-05	0.02	0.01999	1.00E-05	0.02	0.01999
cpd_4mlacac[c]	1.00E-05	0.02	0.01999	NA	NA	NA	NA	NA	NA
cpd_4mop[c]	1.00E-05	0.02	0.01999	1.00E-05	0.02	0.01999	1.00E-05	0.02	0.01999
cpd_4mpetz[c]	1.00E-05	0.02	0.01999	1.00E-05	0.02	0.01999	1.00E-05	0.02	0.01999
cpd_4pasp[c]	1.00E-05	0.013466189974	0.013456189974	1.00E-05	0.010467506755	0.010457506755	1.00E-05	0.02	0.01999
cpd_4per[c]	0.00021777014 76	0.02	0.01978222985	1.00E-05	0.02	0.01999	1.00E-05	0.02	0.01999
cpd_4ppan[c]	1.00E-05	0.02	0.01999	1.00E-05	0.02	0.01999	1.00E-05	0.02	0.01999

cpd_4ppcys[c]	1.00E-05	0.02	0.01999	1.00E-05	0.02	0.01999	1.00E-05	0.02	0.01999
cpd_4r5au[c]	1.00E-05	0.02	0.01999	1.00E-05	0.02	0.01999	1.00E-05	0.02	0.01999
cpd_5678thh[c]	1.00E-05	0.02	0.01999	1.00E-05	0.02	0.01999	1.00E-05	0.02	0.01999
cpd_5aizc[c]	1.00E-05	0.02	0.01999	1.00E-05	0.02	0.01999	1.00E-05	0.02	0.01999
cpd_5aop[c]	1.00E-05	0.02	0.01999	1.00E-05	0.02	0.01999	1.00E-05	0.02	0.01999
cpd_5aprbu[c]	1.00E-05	0.02	0.01999	1.00E-05	0.02	0.01999	1.00E-05	0.02	0.01999
cpd_5apru[c]	1.00E-05	6.96E-05	5.96E-05	1.00E-05	8.58E-05	7.58E-05	1.00E-05	0.0002191136832	0.0002091136832
cpd_5caiz[c]	1.00E-05	0.02	0.01999	1.00E-05	0.02	0.01999	1.00E-05	0.02	0.01999
cpd_5drib[c]	1.00E-05	0.02	0.01999	1.00E-05	0.02	0.01999	1.00E-05	0.02	0.01999
cpd_5hiu[c]	1.00E-05	0.02	0.01999	1.00E-05	0.02	0.01999	1.00E-05	0.02	0.01999
cpd_5mdr1p[c]	1.00E-05	0.02	0.01999	1.00E-05	0.02	0.01999	1.00E-05	0.02	0.01999
cpd_5mdru1p[c]	1.00E-05	0.02	0.01999	1.00E-05	0.02	0.01999	1.00E-05	0.02	0.01999
cpd_5mta[c]	1.00E-05	0.02	0.01999	1.00E-05	0.02	0.01999	1.00E-05	0.02	0.01999
cpd_5mthf[c]	1.00E-05	0.02	0.01999	1.00E-05	0.02	0.01999	1.00E-05	0.02	0.01999
cpd_5mthglu[c]	1.00E-05	0.02	0.01999	NA	NA	NA	NA	NA	NA
cpd_5mtr[c]	1.00E-05	0.02	0.01999	1.00E-05	0.02	0.01999	1.00E-05	0.02	0.01999
cpd_6pgc[c]	1.00E-05	0.02	0.01999	1.00E-05	0.02	0.01999	1.00E-05	0.02	0.01999
cpd_6pgl[c]	1.00E-05	0.02	0.01999	1.00E-05	0.02	0.01999	1.00E-05	0.02	0.01999
cpd_78dhp[c]	1.00E-05	0.02	0.01999	1.00E-05	0.02	0.01999	1.00E-05	0.02	0.01999

cpd_7cltrp[c]	1.00E-05	0.02	0.01999	1.00E-05	0.02	0.01999	1.00E-05	0.02	0.01999
cpd_8aonn[c]	1.00E-05	0.02	0.01999	1.00E-05	0.02	0.01999	1.00E-05	0.02	0.01999
cpd_aacoa[c]	1.00E-05	0.02	0.01999	1.00E-05	0.02	0.01999	1.00E-05	0.02	0.01999
cpd_ac[c]	1.00E-05	0.02	0.019989999999	1.00E-05	0.02	0.01999	1.00E-05	0.02	0.01999
cpd_ac[e]	1.00E-05	0.019999973996	0.019989973996	1.00E-05	0.019999991665	0.019989991665	1.00E-05	0.019999991779	0.019989991779
cpd_ac[p]	1.00E-05	0.019999982664	0.019989982664	1.00E-05	0.02	0.01999	1.00E-05	0.02	0.01999
cpd_acac[c]	1.00E-05	0.02	0.01999	1.00E-05	0.02	0.01999	1.00E-05	0.02	0.01999
cpd_acACP[c]	1.00E-05	0.02	0.01999	1.00E-05	0.02	0.01999	1.00E-05	0.02	0.01999
cpd_acald[c]	0.00011310904 07	0.02	0.019886890 96	1.00E-05	0.02	0.01999	1.00E-05	0.02	0.01999
cpd_accoa[c]	1.00E-05	0.02	0.01999	1.00E-05	0.02	0.01999	1.00E-05	0.02	0.01999
cpd_acg5p[c]	1.00E-05	0.001692311022	0.001682311022	1.00E-05	0.001423852477	0.001413852477	1.00E-05	0.002932164113	0.002922164113
cpd_acg5sa[c]	1.00E-05	0.02	0.01999	1.00E-05	0.02	0.01999	1.00E-05	0.02	0.01999
cpd_acgam[c]	1.00E-05	0.005	0.00499	1.00E-05	0.005	0.00499	1.00E-05	0.005	0.00499
cpd_acgam[e]	1.00E-05	0.005	0.004989999996	1.00E-05	0.005	0.004989999996	1.00E-05	0.005	0.004989999996
cpd_acgam[p]	1.00E-05	0.004999978 3	0.004989997 83	1.00E-05	0.004999979 13	0.004989997 913	1.00E-05	0.004999979 49	0.004989997 949
cpd_acgam1p[c]	1.00E-05	0.02	0.01999	1.00E-05	0.02	0.01999	1.00E-05	0.02	0.01999
cpd_acgam6p[c]	1.00E-05	0.02	0.01999	1.00E-05	0.02	0.01999	1.00E-05	0.02	0.01999

cpd_acglu[c]	0.0001181815857	0.02	0.01988181841	0.0001404639899	0.02	0.01985953601	6.82E-05	0.02	0.01993179099
cpd_acmam[c]	1.00E-05	0.02	0.01999	1.00E-05	0.02	0.01999	1.00E-05	0.02	0.01999
cpd_acmama[c]	1.00E-05	0.02	0.01999	1.00E-05	0.02	0.01999	1.00E-05	0.02	0.01999
cpd_acmana[c]	1.00E-05	0.02	0.01999	1.00E-05	0.02	0.01999	1.00E-05	0.02	0.01999
cpd_acnam[c]	1.00E-05	0.02	0.01999	1.00E-05	0.02	0.01999	1.00E-05	0.02	0.01999
cpd_acorn[c]	1.00E-05	0.02	0.01999	1.00E-05	0.02	0.01999	1.00E-05	0.02	0.01999
cpd_ACP[c]	1.00E-05	0.02	0.01999	1.00E-05	0.02	0.01999	1.00E-05	0.02	0.01999
cpd_acser[c]	1.00E-05	0.02	0.01999	1.00E-05	0.02	0.01999	1.00E-05	0.02	0.01999
cpd_actACP[c]	1.00E-05	0.02	0.01999	1.00E-05	0.02	0.01999	1.00E-05	0.02	0.01999
cpd_actp[c]	1.00E-05	0.02	0.01999	1.00E-05	0.02	0.01999	1.00E-05	0.02	0.01999
cpd_adcoba[c]	6.75E-07	6.75E-05	6.68E-05	NA	NA	NA	NA	NA	NA
cpd_adcobap[c]	1.00E-05	0.02	0.01999	NA	NA	NA	NA	NA	NA
cpd_ade[c]	1.00E-05	0.02	0.01999	1.00E-05	0.02	0.01999	1.00E-05	0.02	0.01999
cpd_adgcoba[c]	1.00E-05	0.02	0.01999	NA	NA	NA	NA	NA	NA
cpd_adn[c]	1.00E-05	0.00041157289 08	0.00040157289 08	1.00E-05	0.00074080541 22	0.00073080541 22	1.00E-05	0.00095366880 61	0.00094366880 61
cpd_adn[e]	1.00E-05	0.02	0.01999	1.00E-05	0.02	0.01999	1.00E-05	0.02	0.01999
cpd_adn[p]	1.00E-05	0.02	0.01999	1.00E-05	0.02	0.01999	1.00E-05	0.02	0.01999

cpd_adp[c]	1.00E-05	0.00069090995 49	0.00068090995 49	1.75E-05	0.00097871021 4	0.00096125301 02	1.00E-05	0.00113669599 1	0.00112669599 1
cpd_adpglc[c]	1.00E-05	0.02	0.01999	1.00E-05	0.02	0.01999	1.00E-05	0.02	0.01999
cpd_adphep-DD[c]	1.00E-05	0.02	0.01999	1.00E-05	0.02	0.01999	1.00E-05	0.02	0.01999
cpd_agm[c]	1.00E-05	0.02	0.01999	1.00E-05	0.02	0.01999	1.00E-05	0.02	0.01999
cpd_ahcys[c]	0.00048594065 47	0.02	0.01951405935	0.00026997642 93	0.02	0.01973002357	0.00020971641 17	0.02	0.01979028359
cpd_ahdt[c]	1.00E-05	0.02	0.01999	1.00E-05	0.02	0.01999	1.00E-05	0.02	0.01999
cpd_aicar[c]	1.00E-05	0.00030614824 45	0.00029614824 45	1.00E-05	0.00055730785 22	0.00054730785 22	1.00E-05	0.00072093628 1	0.00071093628 1
cpd_air[c]	1.00E-05	0.02	0.01999	1.00E-05	0.02	0.01999	1.00E-05	0.02	0.01999
cpd_akg[c]	1.00E-05	0.00210386499	0.00209386499	1.00E-05	0.02	0.01999	1.00E-05	0.02	0.01999
cpd_akg[e]	1.00E-05	0.02	0.01999	1.00E-05	0.02	0.01999	1.00E-05	0.02	0.01999
cpd_ala-B[c]	1.00E-05	0.02	0.01999	1.00E-05	0.02	0.01999	1.00E-05	0.02	0.01999
cpd_ala-D[c]	1.00E-05	0.01875568 25	0.01874568 25	1.00E-05	0.01880173091	0.01879173091	1.00E-05	0.01882155431	0.01881155431
cpd_ala-D[e]	1.00E-05	0.02	0.01999	1.00E-05	0.02	0.01999	1.00E-05	0.01999999179	0.01998999179
cpd_ala-D[p]	1.00E-05	0.02	0.01999	1.00E-05	0.02	0.01999	1.00E-05	0.02	0.01999
cpd_ala-L[c]	1.07E-05	0.02	0.01998933657	1.06E-05	0.02	0.01998936269	1.06E-05	0.02	0.01998937389
cpd_ala-L[e]	1.00E-05	0.02	0.01999	1.00E-05	0.02	0.01999	1.00E-05	0.02	0.01999
cpd_ala-L[p]	1.00E-05	0.02	0.01999	1.00E-05	0.02	0.01999	1.00E-05	0.02	0.01999

cpd_alaala[c]	1.00E-05	0.02	0.01999	1.00E-05	0.02	0.01999	1.00E-05	0.02	0.01999
cpd_alac-S[c]	1.00E-05	0.02	0.01999	1.00E-05	0.02	0.01999	1.00E-05	0.02	0.01999
cpd_alatrna[c]	1.00E-05	0.02	0.01999	1.00E-05	0.02	0.01999	1.00E-05	0.02	0.01999
cpd_alltn-R[c]	1.00E-05	0.02	0.01999	1.00E-05	0.02	0.01999	1.00E-05	0.02	0.01999
cpd_alltn-S[c]	1.00E-05	0.02	0.01999	1.00E-05	0.02	0.01999	1.00E-05	0.02	0.01999
cpd_alltt[c]	1.00E-05	0.02	0.01999	1.00E-05	0.02	0.01999	1.00E-05	0.02	0.01999
cpd_amet[c]	1.00E-05	0.00097013265 28	0.00096013265 28	1.00E-05	3.98E-05	2.98E-05	1.00E-05	8.43E-05	7.43E-05
cpd_ametam[c]	1.00E-05	0.02	0.01999	1.00E-05	0.02	0.01999	1.00E-05	0.02	0.01999
cpd_amob[c]	1.00E-05	0.02	0.01999	1.00E-05	0.02	0.01999	1.00E-05	0.02	0.01999
cpd_amp[c]	1.00E-05	1.20E-05	1.98E-06	1.00E-05	2.47E-05	1.47E-05	1.00E-05	3.37E-05	2.37E-05
cpd_anth[c]	1.00E-05	0.02	0.01999	1.00E-05	0.02	0.01999	1.00E-05	0.02	0.01999
cpd_apoACP[c]	1.00E-05	0.02	0.01999	1.00E-05	0.02	0.01999	1.00E-05	0.02	0.01999
cpd_aps[c]	1.00E-05	0.02	0.01999	1.00E-05	0.02	0.01999	1.00E-05	0.02	0.01999
cpd_ara5p[c]	1.00E-05	0.02	0.01999	1.00E-05	0.02	0.01999	1.00E-05	0.02	0.01999
cpd_arab-L[c]	NA	NA	NA	NA	NA	NA	1.00E-05	0.02	0.01999
cpd_arab-L[p]	NA	NA	NA	NA	NA	NA	1.00E-05	0.02	0.01999
cpd_arg-L[c]	1.00E-05	0.02	0.01999	1.00E-05	0.02	0.01999	1.00E-05	0.02	0.01999
cpd_argsuc[c]	1.00E-05	0.02	0.01999	1.00E-05	0.02	0.01999	1.00E-05	0.02	0.01999
cpd_argtrna[c]	1.00E-05	0.02	0.01999	1.00E-05	0.02	0.01999	1.00E-05	0.02	0.01999

cpd_asn-L[c]	1.00E-05	0.02	0.01999	1.00E-05	0.02	0.01999	1.00E-05	0.02	0.01999
cpd_asn-L[e]	1.00E-05	0.02	0.01999	1.00E-05	0.02	0.01999	1.00E-05	0.02	0.01999
cpd_asntrna[c]	1.00E-05	0.02	0.01999	1.00E-05	0.02	0.01999	1.00E-05	0.02	0.01999
cpd_asp-L[c]	1.49E-05	0.02	0.019985147999	1.91E-05	0.02	0.019980893225	1.00E-05	0.02	0.01999
cpd_asp-L[e]	1.00E-05	0.02	0.01999	1.00E-05	0.02	0.01999	1.00E-05	0.02	0.01999
cpd_asp-L[p]	1.00E-05	0.02	0.01999	1.00E-05	0.02	0.01999	1.00E-05	0.02	0.01999
cpd_aspsa[c]	1.00E-05	0.02	0.01999	1.00E-05	0.02	0.01999	1.00E-05	0.02	0.01999
cpd_asptrna[c]	1.00E-05	0.02	0.01999	1.00E-05	0.02	0.01999	1.00E-05	0.02	0.01999
cpd_atp[c]	0.004007682356	0.02	0.015992317644	0.010027094601	0.02	0.009972905392	0.006889879235	0.02	0.013110120767
cpd_betald[c]	1.00E-05	0.02	0.01999	NA	NA	NA	NA	NA	NA
cpd_bgl[e]	1.00E-05	0.02	0.01999	1.00E-05	0.02	0.01999	1.00E-05	0.02	0.01999
cpd_btcoa[c]	1.00E-05	0.02	0.01999	1.00E-05	0.02	0.01999	1.00E-05	0.02	0.01999
cpd_btn[c]	2.43E-08	2.43E-06	2.41E-06	2.43E-08	2.43E-06	2.41E-06	2.43E-08	2.43E-06	2.41E-06
cpd_but[c]	1.00E-05	0.02	0.01999	1.00E-05	0.02	0.01999	1.00E-05	0.02	0.01999
cpd_ca2[c]	1.00E-05	0.154752988	0.154742988	1.00E-05	0.154752988	0.154742988	1.00E-05	0.154752988	0.154742988
cpd_ca2[e]	1.00E-05	0.154752988	0.154742988	1.00E-05	0.154752988	0.154742988	1.00E-05	0.154752988	0.154742988
cpd_ca2[p]	1.00E-05	0.154752920	8 0.154742920	1.00E-05	0.154752923	4 0.154742923	1.00E-05	0.154752924	5 0.154742924
cpd_camp[c]	1.00E-05	0.02	0.01999	1.00E-05	0.02	0.01999	1.00E-05	0.02	0.01999
cpd_carbohyd	1.00E-05	0.02	0.01999	1.00E-05	0.02	0.01999	1.00E-05	0.02	0.01999

rate_macro[c]									
cpd_cbasp[c]	1.51E-05	0.05	0.0499849106 3	1.36E-05	0.05	0.0499863957 1	1.30E-05	0.05	0.0499869881 3
cpd_cbl1[c]	1.00E-05	0.02	0.0199 9	1.00E-05	0.02	0.0199 9	1.00E-05	0.02	0.0199 9
cpd_cbl1[e]	1.00E-05	0.02	0.0199 9	1.00E-05	0.02	0.0199 9	1.00E-05	0.02	0.0199 9
cpd_cbl1[p]	1.00E-05	0.0199999913 2	0.0199899913 2	1.00E-05	0.0199999916 5	0.0199899916 5	1.00E-05	0.0199999917 9	0.0199899917 9
cpd_cbp[c]	1.00E-05	0.02	0.0199 9	1.00E-05	0.02	0.0199 9	1.00E-05	0.02	0.0199 9
cpd_cdp[c]	1.00E-05	0.02	0.0199 9	1.00E-05	0.02	0.0199 9	1.00E-05	0.02	0.0199 9
cpd_cdp4d6dg[c]	1.00E-05	0.02	0.0199 9	1.00E-05	0.02	0.0199 9	1.00E-05	0.02	0.0199 9
cpd_cdpdag[c]	0.0003197212782	0.02	0.0196802787 2	0.0002095618 253	0.02	0.0197904381 7	0.0001747724 501	0.02	0.0198252275 5
cpd_cdpg[c]	1.00E-05	0.02	0.0199 9	1.00E-05	0.02	0.0199 9	1.00E-05	0.02	0.0199 9
cpd_ch4s[c]	1.00E-05	0.02	0.0199 9	NA	NA	NA	1.00E-05	0.02	0.0199 9
cpd_chitin[e]	1.00E-05	0.02	0.0199 9	1.00E-05	0.02	0.0199 9	1.00E-05	0.02	0.0199 9
cpd_chitob[e]	1.00E-05	0.02	0.0199 9	1.00E-05	0.02	0.0199 9	1.00E-05	0.02	0.0199 9
cpd_chitob[p]	1.00E-05	0.02	0.0199 9	1.00E-05	0.02	0.0199 9	1.00E-05	0.02	0.0199 9
cpd_chol[c]	1.00E-05	0.02	0.0199 9	1.00E-05	0.02	0.0199 9	1.00E-05	0.02	0.0199 9
cpd_chol[e]	1.00E-05	0.02	0.0199 9	1.00E-05	0.02	0.0199 9	1.00E-05	0.02	0.0199 9
cpd_chol[p]	1.00E-05	0.02	0.0199 9	1.00E-05	0.02	0.0199 9	1.00E-05	0.02	0.0199 9
cpd_chor[c]	1.52E-05	0.02	0.0199847725 9	1.50E-05	0.02	0.0199850150 8	1.49E-05	0.02	0.0199851181
cpd_cinnm[c]	1.00E-05	0.02	0.0199 9	1.00E-05	0.02	0.0199 9	1.00E-05	0.02	0.0199 9

cpd_cit[c]	0.0003092576375	0.02	0.01969074236	0.0002712864511	0.02	0.01972871355	0.0002564362	0.02	0.01974356377
cpd_cit[e]	1.00E-05	0.02	0.01999	1.00E-05	0.02	0.01999	1.00E-05	0.02	0.01999
cpd_cit[p]	1.00E-05	0.02	0.01999	1.00E-05	0.02	0.01999	1.00E-05	0.02	0.01999
cpd_citr-L[c]	1.00E-05	0.02	0.01999	1.00E-05	0.02	0.01999	1.00E-05	0.02	0.01999
cpd_ckdo[c]	1.00E-05	0.02	0.01999	1.00E-05	0.02	0.01999	1.00E-05	0.02	0.01999
cpd_ckdo8n[c]	1.00E-05	0.02	0.01999	1.00E-05	0.02	0.01999	1.00E-05	0.02	0.01999
cpd_cl[c]	1.00E-05	0.7797 78977	0.7797 68977	1.00E-05	0.8255 972559	0.8255 872559	1.00E-05	0.8459 146659	0.8459 046659
cpd_cl[e]	3.62E-05	2.8244 35219	2.8243 98998	3.42E-05	2.8244 35219	2.8244 01008	3.34E-05	2.8244 35219	2.8244 0183
cpd_cl[p]	3.62E-05	2.8244 33993	2.8243 97772	3.42E-05	2.8244 3404	2.8243 99829	3.34E-05	2.8244 3406	2.8244 00671
cpd_cmp[c]	1.00E-05	0.0006 255448 532	0.0006 155448 532	1.00E-05	0.0009 543722 944	0.0009 443722 944	1.00E-05	0.0011 443451 18	0.0011 343451 18
cpd_co2[c]	1.00E-05	0.02	0.0199 8999999	1.00E-05	0.02	0.0199 8999999	1.00E-05	0.02	0.01999
cpd_co2[e]	1.00E-05	0.0199 9998264	0.0199 8998264	1.00E-05	0.0199 999833	0.0199 899833	1.00E-05	0.02	0.01999
cpd_co2[p]	1.00E-05	0.0199 9999132	0.0199 8999132	1.00E-05	0.0199 9999165	0.0199 8999165	1.00E-05	0.02	0.01999
cpd_coa[c]	1.00E-05	0.0002 332534 765	0.0002 232534 765	1.00E-05	0.0003 695239 856	0.0003 595239 856	1.00E-05	0.0004 503085 914	0.0004 403085 914
cpd_cobalt2[c]	2.46E-07	2.46E-05	2.43E-05	2.46E-07	2.46E-05	2.43E-05	2.46E-07	2.46E-05	2.43E-05
cpd_cobalt2[e]	2.46E-07	2.46E-05	2.43E-05	2.46E-07	2.46E-05	2.43E-05	2.46E-07	2.46E-05	2.43E-05

cpd_cobalt2[p]	2.46E-07	2.46E-05	2.43E-05	2.46E-07	2.46E-05	2.43E-05	2.46E-07	2.46E-05	2.43E-05
cpd_cobalt3[e]	1.00E-05	0.02	0.01999	1.00E-05	0.02	0.01999	1.00E-05	0.02	0.01999
cpd_cobamcoa[c]	1.00E-05	0.02	0.01999	1.00E-05	0.02	0.01999	1.00E-05	0.02	0.01999
cpd_confald[c]	1.00E-05	0.02	0.01999	NA	NA	NA	1.00E-05	0.02	0.01999
cpd_cpppg3[c]	1.00E-05	0.02	0.01999	1.00E-05	0.02	0.01999	1.00E-05	0.02	0.01999
cpd_cro4[e]	1.00E-05	0.02	0.01999	1.00E-05	0.02	0.01999	1.00E-05	0.02	0.01999
cpd_CrOH3[e]	1.00E-05	0.02	0.01999	1.00E-05	0.02	0.01999	1.00E-05	0.02	0.01999
cpd_csn[c]	1.00E-05	0.02	0.01999	1.00E-05	0.02	0.01999	1.00E-05	0.02	0.01999
cpd_csn[p]	1.00E-05	0.02	0.01999	1.00E-05	0.02	0.01999	1.00E-05	0.02	0.01999
cpd_ctp[c]	1.00E-05	0.02	0.01999	1.00E-05	0.02	0.01999	1.00E-05	0.02	0.01999
cpd_cu2[c]	1.00E-05	0.02	0.01999	1.00E-05	0.02	0.01999	1.00E-05	0.02	0.01999
cpd_cu2[e]	1.00E-05	0.02	0.01999	1.00E-05	0.02	0.01999	1.00E-05	0.02	0.01999
cpd_cu2[p]	1.00E-05	0.019999991332	0.019989991332	1.00E-05	0.019999991665	0.019989991665	1.00E-05	0.019999991779	0.019989991779
cpd_cyan[c]	1.00E-05	0.02	0.01999	NA	NA	NA	1.00E-05	0.02	0.01999
cpd_cys-gly[c]	1.00E-05	0.02	0.01999	NA	NA	NA	1.00E-05	0.02	0.01999
cpd_cys-gly[p]	1.00E-05	0.02	0.01999	1.00E-05	0.02	0.01999	1.00E-05	0.02	0.01999
cpd_cys-L[c]	1.00E-05	0.02	0.01999	1.00E-05	0.02	0.01999	1.00E-05	0.02	0.01999
cpd_cysth-L[c]	1.00E-05	0.02	0.01999	1.00E-05	0.02	0.01999	1.00E-05	0.02	0.01999
cpd_cystrna[c]	1.00E-05	0.02	0.01999	1.00E-05	0.02	0.01999	1.00E-05	0.02	0.01999

cpd_cytd[c]	1.00E-05	0.02	0.01999	1.00E-05	0.02	0.01999	1.00E-05	0.02	0.01999
cpd_cytd[e]	1.00E-05	0.02	0.01999	1.00E-05	0.02	0.01999	1.00E-05	0.02	0.01999
cpd_cytd[p]	1.00E-05	0.02	0.01999	1.00E-05	0.02	0.01999	1.00E-05	0.02	0.01999
cpd_dad-2[c]	1.00E-05	0.020000000001	0.019990000001	1.00E-05	0.02	0.01999	1.00E-05	0.02	0.01999
cpd_dad-2[e]	1.00E-05	0.02	0.01999	1.00E-05	0.02	0.01999	1.00E-05	0.02	0.01999
cpd_dad-2[p]	1.00E-05	0.02	0.01999	1.00E-05	0.02	0.01999	1.00E-05	0.02	0.01999
cpd_dad-5[c]	1.00E-05	0.02	0.01999	1.00E-05	0.02	0.01999	1.00E-05	0.02	0.01999
cpd_dadp[c]	1.00E-05	0.02	0.01999	1.00E-05	0.02	0.01999	1.00E-05	0.02	0.01999
cpd_damp[c]	1.00E-05	0.02	0.01999	1.00E-05	0.02	0.01999	1.00E-05	0.02	0.01999
cpd_damp[e]	1.00E-05	0.02	0.01999	1.00E-05	0.02	0.01999	1.00E-05	0.02	0.01999
cpd_damp[p]	1.00E-05	0.02	0.01999	1.00E-05	0.02	0.01999	1.00E-05	0.02	0.01999
cpd_dann[c]	1.00E-05	0.02	0.01999	1.00E-05	0.02	0.01999	1.00E-05	0.02	0.01999
cpd_datp[c]	1.00E-05	0.02	0.01999	1.00E-05	0.02	0.01999	1.00E-05	0.02	0.01999
cpd_db4p[c]	1.00E-05	0.02	0.01999	1.00E-05	0.02	0.01999	1.00E-05	0.02	0.01999
cpd_dcamp[c]	0.016698375333	0.02	0.003301624668	0.008105451903	0.02	0.011894548097	0.005941337483	0.02	0.014058662522
cpd_dcdp[c]	1.00E-05	0.02	0.01999	1.00E-05	0.02	0.01999	1.00E-05	0.02	0.01999
cpd_dcmp[c]	1.00E-05	0.02	0.01999	1.00E-05	0.02	0.01999	1.00E-05	0.02	0.01999
cpd_dcmp[e]	1.00E-05	0.02	0.01999	1.00E-05	0.02	0.01999	1.00E-05	0.02	0.01999
cpd_dcmp[p]	1.00E-05	0.02	0.01999	1.00E-05	0.02	0.01999	1.00E-05	0.02	0.01999
cpd_dctp[c]	1.00E-05	0.02	0.01999	1.00E-05	0.02	0.01999	1.00E-05	0.02	0.01999

cpd_dcyt[c]	1.00E-05	0.02	0.01999	1.00E-05	0.02	0.01999	1.00E-05	0.02	0.01999
cpd_dcyt[e]	1.00E-05	0.02	0.01999	1.00E-05	0.02	0.01999	1.00E-05	0.02	0.01999
cpd_dcyt[p]	1.00E-05	0.02	0.01999	1.00E-05	0.02	0.01999	1.00E-05	0.02	0.01999
cpd_ddcaACP[c]	1.00E-05	0.02	0.01999	1.00E-05	0.02	0.01999	1.00E-05	0.02	0.01999
cpd_dgdp[c]	1.00E-05	0.02	0.01999	1.00E-05	0.02	0.01999	1.00E-05	0.02	0.01999
cpd_dgmp[c]	1.00E-05	0.02	0.01999	1.00E-05	0.02	0.01999	1.00E-05	0.02	0.01999
cpd_dgmp[e]	1.00E-05	0.02	0.01999	1.00E-05	0.02	0.01999	1.00E-05	0.02	0.01999
cpd_dgmp[p]	1.00E-05	0.02	0.01999	1.00E-05	0.02	0.01999	1.00E-05	0.02	0.01999
cpd_dgsn[c]	1.00E-05	0.02	0.01999	1.00E-05	0.02	0.01999	1.00E-05	0.02	0.01999
cpd_dgsn[e]	1.00E-05	0.02	0.01999	1.00E-05	0.02	0.01999	1.00E-05	0.02	0.01999
cpd_dgsn[p]	1.00E-05	0.02	0.01999	1.00E-05	0.02	0.01999	1.00E-05	0.02	0.01999
cpd_dgtp[c]	1.00E-05	0.02	0.01999	1.00E-05	0.02	0.01999	1.00E-05	0.02	0.01999
cpd_dhap[c]	1.00E-05	0.02	0.01999	1.00E-05	0.02	0.01999	1.00E-05	0.02	0.01999
cpd_dhbpt[c]	1.00E-05	0.02	0.01999	1.00E-05	0.02	0.01999	1.00E-05	0.02	0.01999
cpd_dhf[c]	1.00E-05	0.02	0.01999	1.00E-05	0.02	0.01999	1.00E-05	0.02	0.01999
cpd_dhmptp[c]	1.00E-05	0.02	0.01999	1.00E-05	0.02	0.01999	1.00E-05	0.02	0.01999
cpd_dhna[c]	1.00E-05	0.02	0.01999	1.00E-05	0.02	0.01999	1.00E-05	0.02	0.01999
cpd_dhnpt[c]	1.00E-05	0.02	0.01999	1.00E-05	0.02	0.01999	1.00E-05	0.02	0.01999
cpd_dhor-S[c]	1.00E-06	0.00331359145	0.00331259145	1.00E-06	0.00367531995	0.00367431995	1.00E-06	0.00384264559	0.00384164559
cpd_dhpmp[c]	1.00E-05	0.02	0.01999	1.00E-05	0.02	0.01999	1.00E-05	0.02	0.01999

cpd_dhpt[c]	1.00E-05	0.02	0.01999	1.00E-05	0.02	0.01999	1.00E-05	0.02	0.01999
cpd_dhptd[c]	1.00E-05	0.02	0.01999	1.00E-05	0.02	0.01999	1.00E-05	0.02	0.01999
cpd_dimp[c]	1.00E-05	0.02	0.01999	NA	NA	NA	1.00E-05	0.02	0.01999
cpd_din[c]	1.00E-05	0.02	0.01999	1.00E-05	0.02	0.01999	1.00E-05	0.02	0.01999
cpd_ditp[c]	1.00E-05	0.02	0.01999	NA	NA	NA	1.00E-05	0.02	0.01999
cpd_dkmpp[c]	1.00E-05	0.02	0.01999	1.00E-05	0.02	0.01999	1.00E-05	0.02	0.01999
cpd_dmlz[c]	1.00E-05	0.02	0.01999	1.00E-05	0.02	0.01999	1.00E-05	0.02	0.01999
cpd_dmpp[c]	1.00E-05	0.02	0.01999	1.00E-05	0.02	0.01999	1.00E-05	0.02	0.01999
cpd_dms[e]	1.00E-05	0.02	0.01999	1.00E-05	0.02	0.01999	1.00E-05	0.02	0.01999
cpd_dms[p]	1.00E-05	0.02	0.01999	1.00E-05	0.02	0.01999	1.00E-05	0.02	0.01999
cpd_dmso[e]	1.00E-05	0.02	0.01999	1.00E-05	0.02	0.01999	1.00E-05	0.02	0.01999
cpd_dmso[p]	1.00E-05	0.02	0.01999	1.00E-05	0.02	0.01999	1.00E-05	0.02	0.01999
cpd_dna_macro[c]	1.00E-05	0.02	0.01999	1.00E-05	0.02	0.01999	1.00E-05	0.02	0.01999
cpd_dna[e]	1.00E-05	0.02	0.01999	1.00E-05	0.02	0.01999	1.00E-05	0.02	0.01999
cpd_dnad[c]	0.004007682356	0.02	0.01599231764	0.005027131315	0.02	0.01497286869	0.002373521794	0.02	0.017626478211
cpd_dodca[c]	1.00E-05	0.02	0.01999	NA	NA	NA	1.00E-05	0.02	0.01999
cpd_dodcan[e]	1.00E-05	0.02	0.01999	1.00E-05	0.02	0.01999	1.00E-05	0.02	0.01999
cpd_dodcan[p]	1.00E-05	0.02	0.01999	1.00E-05	0.02	0.01999	1.00E-05	0.02	0.01999
cpd_dpcoa[c]	1.00E-05	0.02	0.01999	1.00E-05	0.02	0.01999	1.00E-05	0.02	0.01999
cpd_drib[c]	1.00E-05	0.02	0.01999	1.00E-05	0.02	0.01999	1.00E-05	0.02	0.01999

cpd_dtbt[c]	1.00E-05	0.02	0.01999	1.00E-05	0.02	0.01999	1.00E-05	0.02	0.01999
cpd_dtdp[c]	1.00E-05	0.02	0.01999	1.00E-05	0.02	0.01999	1.00E-05	0.02	0.01999
cpd_dtdp3adgalp[c]	1.00E-05	0.02	0.01999	1.00E-05	0.02	0.01999	1.00E-05	0.02	0.01999
cpd_dtdp3ddgalp[c]	1.00E-05	0.02	0.01999	1.00E-05	0.02	0.01999	1.00E-05	0.02	0.01999
cpd_dtdp6dm[c]	1.00E-05	0.02	0.01999	1.00E-05	0.02	0.01999	1.00E-05	0.02	0.01999
cpd_dtdpddg[c]	1.00E-05	0.02	0.01999	1.00E-05	0.02	0.01999	1.00E-05	0.02	0.01999
cpd_dtdpddm[c]	1.00E-05	0.02	0.01999	1.00E-05	0.02	0.01999	1.00E-05	0.02	0.01999
cpd_dtdpglc[c]	1.00E-05	0.02	0.01999	1.00E-05	0.02	0.01999	1.00E-05	0.02	0.01999
cpd_dtmp[c]	1.00E-05	0.02	0.01999	1.00E-05	0.02	0.01999	1.00E-05	0.02	0.01999
cpd_dtmp[e]	1.00E-05	0.02	0.01999	1.00E-05	0.02	0.01999	1.00E-05	0.02	0.01999
cpd_dtmp[p]	1.00E-05	0.02	0.01999	1.00E-05	0.02	0.01999	1.00E-05	0.02	0.01999
cpd_dttp[c]	1.00E-05	0.02	0.01999	1.00E-05	0.02	0.01999	1.00E-05	0.02	0.01999
cpd_dudp[c]	1.00E-05	0.02	0.01999	1.00E-05	0.02	0.01999	1.00E-05	0.02	0.01999
cpd_dump[c]	1.00E-05	0.02	0.01999	1.00E-05	0.02	0.01999	1.00E-05	0.02	0.01999
cpd_duri[c]	1.00E-05	0.02	0.01999	1.00E-05	0.02	0.01999	1.00E-05	0.02	0.01999
cpd_duri[e]	1.00E-05	0.02	0.01999	1.00E-05	0.02	0.01999	1.00E-05	0.02	0.01999
cpd_duri[p]	1.00E-05	0.02	0.01999	1.00E-05	0.02	0.01999	1.00E-05	0.02	0.01999
cpd_dutp[c]	1.00E-05	0.02	0.01999	1.00E-05	0.02	0.01999	1.00E-05	0.02	0.01999

cpd_dxyl5p[c]	1.00E-05	0.02	0.01999	1.00E-05	0.02	0.01999	1.00E-05	0.02	0.01999
cpd_e4p[c]	1.00E-05	0.02	0.01999	0.00010377335517	0.02	0.01989622665	4.60E-05	0.02	0.01995401675
cpd_eig3p[c]	1.00E-05	0.02	0.01999	1.00E-05	0.02	0.01999	1.00E-05	0.02	0.01999
cpd_epa[c]	1.00E-05	0.02	0.01999	1.00E-05	0.02	0.01999	1.00E-05	0.02	0.01999
cpd_etha[c]	1.00E-05	0.02	0.01999	1.00E-05	0.02	0.01999	1.00E-05	0.02	0.01999
cpd_etoh[c]	1.00E-05	0.02	0.01999	1.00E-05	0.02	0.01999	1.00E-05	0.02	0.01999
cpd_etoh[e]	1.00E-05	0.02	0.01999	1.00E-05	0.02	0.01999	1.00E-05	0.02	0.01999
cpd_f6p[c]	0.00051781517736	0.02	0.019482184838	0.00044538634870	0.02	0.019554613665	0.00041746094890	0.02	0.019582539055
cpd_fa1[c]	1.00E-05	0.02	0.01999	NA	NA	NA	1.00E-05	0.02	0.01999
cpd_fa11[c]	1.00E-05	0.02	0.01999	NA	NA	NA	1.00E-05	0.02	0.01999
cpd_fa11ACP[c]	1.00E-05	0.02	0.01999	1.00E-05	0.02	0.01999	1.00E-05	0.02	0.01999
cpd_fa13[c]	1.00E-05	0.02	0.01999	NA	NA	NA	1.00E-05	0.02	0.01999
cpd_fa130OH3[c]	1.00E-05	0.02	0.01999	NA	NA	NA	1.00E-05	0.02	0.01999
cpd_fa130OH3ACP[c]	1.00E-05	0.02	0.01999	1.00E-05	0.02	0.01999	1.00E-05	0.02	0.01999
cpd_fa13ACP[c]	1.00E-05	0.02	0.01999	1.00E-05	0.02	0.01999	1.00E-05	0.02	0.01999
cpd_fa14ACP[c]	1.00E-05	0.02	0.01999	1.00E-05	0.02	0.01999	1.00E-05	0.02	0.01999
cpd_fa171n8[c]	1.00E-05	0.02	0.01999	NA	NA	NA	1.00E-05	0.02	0.01999

cpd_fa171n8ACP[c]	1.00E-05	0.02	0.01999	1.00E-05	0.02	0.01999	1.00E-05	0.02	0.01999
cpd_fa181n7[c]	1.00E-05	0.02	0.01999	NA	NA	NA	1.00E-05	0.02	0.01999
cpd_fa181n7ACP[c]	1.00E-05	0.02	0.01999	1.00E-05	0.02	0.01999	1.00E-05	0.02	0.01999
cpd_fa1ACP[c]	1.00E-05	0.02	0.01999	1.00E-05	0.02	0.01999	1.00E-05	0.02	0.01999
cpd_fa3[c]	1.00E-05	0.02	0.01999	NA	NA	NA	1.00E-05	0.02	0.01999
cpd_fa3ACP[c]	1.00E-05	0.02	0.01999	1.00E-05	0.02	0.01999	1.00E-05	0.02	0.01999
cpd_fa6[c]	1.00E-05	0.02	0.01999	NA	NA	NA	1.00E-05	0.02	0.01999
cpd_fa6ACP[c]	1.00E-05	0.02	0.01999	1.00E-05	0.02	0.01999	1.00E-05	0.02	0.01999
cpd_fa7ACP[c]	1.00E-05	0.02	0.01999	1.00E-05	0.02	0.01999	1.00E-05	0.02	0.01999
cpd_fa8ACP[c]	1.00E-05	0.02	0.01999	1.00E-05	0.02	0.01999	1.00E-05	0.02	0.01999
cpd_fad[c]	1.00E-05	0.02	0.01999	1.00E-05	0.02	0.01999	1.00E-05	0.02	0.01999
cpd_fadh2[c]	1.00E-05	0.02	0.01999	1.00E-05	0.02	0.01999	1.00E-05	0.02	0.01999
cpd_fald[c]	1.00E-05	0.02	0.01999	NA	NA	NA	1.00E-05	0.02	0.01999
cpd_fdp[c]	1.00E-05	0.02	0.01999	1.00E-05	0.02	0.01999	1.00E-05	0.02	0.01999
cpd_fdxo-4:2[c]	1.00E-05	0.02	0.01999	1.00E-05	0.02	0.01999	1.00E-05	0.02	0.01999
cpd_fdxr-4:2[c]	1.00E-05	0.02	0.01999	1.00E-05	0.02	0.01999	1.00E-05	0.02	0.01999

cpd_fe2[c]	1.00E-05	0.000317736	0.000307736	1.00E-05	0.000317736	0.000307736	1.00E-05	0.000317736	0.000307736
cpd_fe2[e]	1.00E-05	0.000317736	0.0003077359957	1.00E-05	0.000317736	0.0003077359958	1.00E-05	0.000317736	0.0003077359959
cpd_fe2[p]	1.00E-05	0.0003177358621	0.0003077358621	1.00E-05	0.0003177358674	0.0003077358674	1.00E-05	0.0003177358696	0.0003077358696
cpd_fe3[e]	1.00E-05	0.02	0.01999	1.00E-05	0.02	0.01999	1.00E-05	0.02	0.01999
cpd_fgam[c]	1.00E-05	0.02	0.01999	1.00E-05	0.02	0.01999	1.00E-05	0.02	0.01999
cpd_fglut-S[c]	1.00E-05	0.02	0.01999	1.00E-05	0.02	0.01999	1.00E-05	0.02	0.01999
cpd_ficytcc[c]	1.00E-05	0.02	0.01999	1.00E-05	0.02	0.01999	1.00E-05	0.02	0.01999
cpd_fmettrna[c]	1.00E-05	0.02	0.01999	1.00E-05	0.02	0.01999	1.00E-05	0.02	0.01999
cpd_fmn[c]	1.00E-05	0.02	0.01999	1.00E-05	0.02	0.01999	1.00E-05	0.02	0.01999
cpd_fmnRD[c]	1.00E-05	0.02	0.01999	1.00E-05	0.02	0.01999	1.00E-05	0.02	0.01999
cpd_focytcc[c]	1.00E-05	0.02	0.01999	1.00E-05	0.02	0.01999	1.00E-05	0.02	0.01999
cpd_for[c]	1.00E-05	0.02	0.01999	1.00E-05	0.02	0.019899999999	1.00E-05	0.02	0.019899999999
cpd_for[e]	1.00E-05	0.02	0.01999	1.00E-05	0.019999833	0.019899833	1.00E-05	0.019999835	0.019899835
cpd_for[p]	1.00E-05	0.02	0.01999	1.00E-05	0.0199999165	0.0199899165	1.00E-05	0.0199999179	0.0199899179
cpd_forglu[c]	1.00E-05	0.02	0.01999	1.00E-05	0.02	0.01999	1.00E-05	0.02	0.01999
cpd_fpram[c]	1.00E-05	0.02	0.01999	1.00E-05	0.02	0.01999	1.00E-05	0.02	0.01999
cpd_fprica[c]	4.81E-05	0.0110552575	0.0110072037	1.91E-05	0.02	0.0199808850	1.29E-05	0.02	0.0199871374
cpd_frdp[c]	1.00E-05	0.02	0.01999	1.00E-05	0.02	0.01999	1.00E-05	0.02	0.01999

cpd_frlt[c]	1.00E-05	0.02	0.01999	NA	NA	NA	1.00E-05	0.02	0.01999
cpd_frmd[c]	1.00E-05	0.02	0.01999	1.00E-05	0.02	0.01999	1.00E-05	0.02	0.01999
cpd_fru[c]	1.00E-05	0.02	0.01999	1.00E-05	0.02	0.01999	1.00E-05	0.02	0.01999
cpd_fum[c]	1.00E-05	1.20E-05	1.98E-06	1.00E-05	2.47E-05	1.47E-05	1.00E-05	3.37E-05	2.37E-05
cpd_fum[e]	1.00E-05	0.02	0.01999	1.00E-05	0.02	0.01999	1.00E-05	0.02	0.01999
cpd_fum[p]	1.00E-05	0.02	0.01999	1.00E-05	0.02	0.01999	1.00E-05	0.02	0.01999
cpd_g1p[c]	1.00E-05	0.000878718793	0.000868718793	1.00E-05	0.000990055794	0.000980055794	1.00E-05	0.001042135561	0.001032135561
cpd_g3p[c]	1.00E-05	0.014852562801	0.014842562801	0.005027131315	0.02	0.014972868691	0.002373521794	0.02	0.017626478201
cpd_g3pe[c]	1.00E-05	0.02	0.01999	1.00E-05	0.02	0.01999	1.00E-05	0.02	0.01999
cpd_g3pg[c]	1.00E-05	0.02	0.01999	1.00E-05	0.02	0.01999	1.00E-05	0.02	0.01999
cpd_g6p[c]	0.000227604099	0.02	0.01972395900	0.000202008817	0.02	0.019797991183	0.000191913612	0.02	0.019808086391
cpd_gal[c]	1.00E-05	0.02	0.01999	1.00E-05	0.02	0.01999	1.00E-05	0.02	0.01999
cpd_gal[e]	1.00E-05	0.02	0.01999	1.00E-05	0.02	0.01999	1.00E-05	0.02	0.01999
cpd_gal1p[c]	1.00E-05	0.02	0.01999	1.00E-05	0.02	0.01999	1.00E-05	0.02	0.01999
cpd_galactan[e]	1.00E-05	0.02	0.01999	1.00E-05	0.02	0.01999	1.00E-05	0.02	0.01999
cpd_gam1p[c]	1.00E-05	0.004995086207	0.004985086207	1.00E-05	0.005266749533	0.005256749533	1.00E-05	0.005387986113	0.005377986113
cpd_gam6p[c]	4.00E-05	0.02	0.019959960655	3.80E-05	0.02	0.019962025911	3.71E-05	0.02	0.019962880388
cpd_gar[c]	1.00E-05	0.02	0.01999	1.00E-05	0.02	0.01999	1.00E-05	0.02	0.01999

cpd_gcald[c]	1.00E-05	0.02	0.01999	1.00E-05	0.02	0.01999	1.00E-05	0.02	0.01999
cpd_gdp[c]	1.00E-05	0.02	0.01999	1.00E-05	0.02	0.01999	1.00E-05	0.02	0.01999
cpd_gdpdp[c]	1.00E-05	0.02	0.01999	1.00E-05	0.02	0.01999	1.00E-05	0.02	0.01999
cpd_gdpmann[c]	1.00E-05	0.02	0.01999	1.00E-05	0.02	0.01999	1.00E-05	0.02	0.01999
cpd_gdptp[c]	1.00E-05	0.02	0.01999	1.00E-05	0.02	0.01999	1.00E-05	0.02	0.01999
cpd_ggdp[c]	1.00E-05	0.02	0.01999	1.00E-05	0.02	0.01999	1.00E-05	0.02	0.01999
cpd_ggluaba[c]	1.00E-05	0.02	0.01999	1.00E-05	0.02	0.01999	1.00E-05	0.02	0.01999
cpd_ggluabt[c]	1.00E-05	0.02	0.01999	1.00E-05	0.02	0.01999	1.00E-05	0.02	0.01999
cpd_ggluptrc[c]	1.00E-05	0.02	0.01999	1.00E-05	0.02	0.01999	1.00E-05	0.02	0.01999
cpd_glc-D[c]	1.00E-05	0.02	0.01999	1.00E-05	0.02	0.01999	1.00E-05	0.02	0.01999
cpd_glc-D[e]	1.00E-05	0.02	0.01999	1.00E-05	0.02	0.01999	1.00E-05	0.02	0.01999
cpd_glc-D[p]	1.00E-05	0.02	0.01999	1.00E-05	0.02	0.01999	1.00E-05	0.02	0.01999
cpd_gln-L[c]	1.00E-05	0.02	0.01999	1.00E-05	0.02	0.01999	1.00E-05	0.02	0.01999
cpd_gln-L[e]	1.00E-05	0.02	0.01999	1.00E-05	0.02	0.01999	1.00E-05	0.02	0.01999
cpd_glntrna[c]	1.00E-05	0.02	0.01999	1.00E-05	0.02	0.01999	1.00E-05	0.02	0.01999
cpd_glu-asp-L[c]	1.00E-05	0.02	0.01999	1.00E-05	0.02	0.01999	1.00E-05	0.02	0.01999
cpd_glu-D[c]	1.00E-05	0.012537122006	0.012527122006	1.00E-05	0.012762650667	0.012752650667	1.00E-05	0.012860810666	0.012850810666

cpd_glu-L[c]	9.51E-05	0.02	0.0199049368 7	1.57E-05	0.02	0.0199843292 8	1.56E-05	0.02	0.0199844488 8
cpd_glu-L[e]	1.00E-05	0.02	0.01999	1.00E-05	0.02	0.01999	1.00E-05	0.02	0.01999
cpd_glu-L[p]	1.00E-05	0.02	0.01999	1.00E-05	0.02	0.01999	1.00E-05	0.02	0.01999
cpd_glu1sa[c]	1.00E-05	0.02	0.01999	1.00E-05	0.02	0.01999	1.00E-05	0.02	0.01999
cpd_glu5p[c]	1.00E-05	0.02	0.01999	1.00E-05	0.02	0.01999	1.00E-05	0.02	0.01999
cpd_glu5sa[c]	1.00E-05	0.02	0.01999	1.00E-05	0.02	0.01999	1.00E-05	0.02	0.01999
cpd_glucys[c]	1.00E-05	0.02	0.01999	1.00E-05	0.02	0.01999	1.00E-05	0.02	0.01999
cpd_glutrna[c]	1.00E-05	0.02	0.01999	1.00E-05	0.02	0.01999	1.00E-05	0.02	0.01999
cpd_glx[c]	1.00E-05	0.02	0.01999	1.00E-05	0.02	0.01999	1.00E-05	0.02	0.01999
cpd_gly-asp-L[c]	1.00E-05	0.02	0.01999	1.00E-05	0.02	0.01999	1.00E-05	0.02	0.01999
cpd_gly-asp-L[e]	1.00E-05	0.02	0.01999	1.00E-05	0.02	0.01999	1.00E-05	0.02	0.01999
cpd_gly-asp-L[p]	1.00E-05	0.02	0.01999	1.00E-05	0.02	0.01999	1.00E-05	0.02	0.01999
cpd_gly-glu-L[c]	1.00E-05	0.02	0.01999	1.00E-05	0.02	0.01999	1.00E-05	0.02	0.01999
cpd_gly-glu-L[e]	1.00E-05	0.02	0.01999	1.00E-05	0.02	0.01999	1.00E-05	0.02	0.01999
cpd_gly-glu-L[p]	1.00E-05	0.02	0.01999	1.00E-05	0.02	0.01999	1.00E-05	0.02	0.01999
cpd_gly[c]	0.0001131090407	0.02	0.0198868909 6	1.00E-05	0.02	0.01999	1.00E-05	0.02	0.01999
cpd_gly[e]	1.00E-05	0.02	0.01999	1.00E-05	0.02	0.01999	1.00E-05	0.02	0.01999

cpd_gly[p]	1.00E-05	0.02	0.01999	1.00E-05	0.02	0.01999	1.00E-05	0.02	0.01999
cpd_glyb[c]	1.00E-05	0.02	0.01999	1.00E-05	0.02	0.01999	1.00E-05	0.02	0.01999
cpd_glyb[e]	1.00E-05	0.02	0.01999	1.00E-05	0.02	0.01999	1.00E-05	0.02	0.01999
cpd_glyb[p]	1.00E-05	0.02	0.01999	1.00E-05	0.02	0.01999	1.00E-05	0.02	0.01999
cpd_glyc-R[c]	1.00E-05	0.02	0.01999	1.00E-05	0.02	0.01999	1.00E-05	0.02	0.01999
cpd_glyc-R[e]	1.00E-05	0.02	0.01999	1.00E-05	0.02	0.01999	1.00E-05	0.02	0.01999
cpd_glyc-R[p]	NA	NA	NA	NA	NA	NA	1.00E-05	0.02	0.01999
cpd_glyc[c]	1.00E-05	0.02	0.01999	1.00E-05	0.02	0.01999	1.00E-05	0.02	0.01999
cpd_glyc[e]	1.00E-05	0.02	0.01999	1.00E-05	0.02	0.01999	1.00E-05	0.02	0.01999
cpd_glyc[p]	1.00E-05	0.02	0.01999	1.00E-05	0.02	0.01999	1.00E-05	0.02	0.01999
cpd_glyc3p[c]	0.00031972127 82	0.02	0.01968027872	0.00020956182 53	0.02	0.01979043817	0.00017477245 01	0.02	0.01982522755
cpd_glyclt[c]	1.00E-05	0.02	0.01999	1.00E-05	0.02	0.01999	1.00E-05	0.02	0.01999
cpd_glyclt[e]	1.00E-05	0.02	0.01999	1.00E-05	0.02	0.01999	1.00E-05	0.02	0.01999
cpd_glyclt[p]	1.00E-05	0.02	0.01999	1.00E-05	0.02	0.01999	1.00E-05	0.02	0.01999
cpd_glycogen[c]	1.00E-05	0.02	0.01999	1.00E-05	0.02	0.01999	1.00E-05	0.02	0.01999
cpd_glytrna[c]	1.00E-05	0.02	0.01999	1.00E-05	0.02	0.01999	1.00E-05	0.02	0.01999
cpd_gmh17bp[c]	1.00E-05	0.02	0.01999	1.00E-05	0.02	0.01999	1.00E-05	0.02	0.01999
cpd_gmh1p[c]	1.00E-05	0.02	0.01999	1.00E-05	0.02	0.01999	1.00E-05	0.02	0.01999

cpd_gmh7p[c]	1.00E-05	0.0004023114491	0.0003923114491	1.00E-05	0.0004670079777	0.0004570079777	1.00E-05	0.0004979145976	0.0004879145976
cpd_gmp[c]	1.00E-05	0.02	0.01999	1.00E-05	0.02	0.01999	1.00E-05	0.02	0.01999
cpd_grdp[c]	1.00E-05	0.02	0.01999	1.00E-05	0.02	0.01999	1.00E-05	0.02	0.01999
cpd_gsn[c]	1.00E-05	0.02	0.01999	1.00E-05	0.02	0.01999	1.00E-05	0.02	0.01999
cpd_gthox[c]	1.00E-05	0.02	0.01999	1.00E-05	0.02	0.01999	1.00E-05	0.02	0.01999
cpd_gthrd[c]	1.00E-05	0.02	0.01999	1.00E-05	0.02	0.01999	1.00E-05	0.02	0.01999
cpd_gthrd[e]	1.00E-05	0.02	0.01999	1.00E-05	0.02	0.01999	1.00E-05	0.02	0.01999
cpd_gthrd[p]	1.00E-05	0.02	0.01999	1.00E-05	0.02	0.01999	1.00E-05	0.02	0.01999
cpd_gtp[c]	1.00E-05	0.02	0.01999	1.00E-05	0.02	0.01999	1.00E-05	0.02	0.01999
cpd_gua[c]	1.00E-05	0.02	0.01999	1.00E-05	0.02	0.01999	1.00E-05	0.02	0.01999
cpd_h2[e]	1.00E-05	0.02	0.01999	1.00E-05	0.02	0.01999	1.00E-05	0.02	0.01999
cpd_h2[p]	1.00E-05	0.02	0.01999	1.00E-05	0.02	0.01999	1.00E-05	0.02	0.01999
cpd_h2mb4p[c]	1.00E-05	0.02	0.01999	1.00E-05	0.02	0.01999	1.00E-05	0.02	0.01999
cpd_h2o2[c]	1.00E-05	0.0001159414127	0.0001059414127	1.00E-05	0.02	0.01999	1.00E-05	0.02	0.01999
cpd_h2o2[e]	1.00E-05	0.02	0.01999	1.00E-05	0.02	0.01999	1.00E-05	0.02	0.01999
cpd_h2o2[p]	1.00E-05	0.02	0.01999	1.00E-05	0.02	0.01999	1.00E-05	0.02	0.01999
cpd_h2s[c]	1.00E-05	0.02	0.01999	1.00E-05	0.02	0.01999	1.00E-05	0.02	0.01999
cpd_h2s[e]	1.00E-05	0.02	0.01999	1.00E-05	0.02	0.01999	1.00E-05	0.02	0.01999
cpd_h2s[p]	1.00E-05	0.02	0.01999	1.00E-05	0.02	0.01999	1.00E-05	0.02	0.01999
cpd_hco3[c]	1.00E-05	0.02	0.01999	1.00E-05	0.02	0.01999	1.00E-05	0.02	0.01999

cpd_hcys-L[c]	1.00E-05	0.00041157289 08	0.00040157289 08	1.00E-05	0.00074080541 22	0.00073080541 22	1.00E-05	0.00095366880 61	0.00094366880 61
cpd_hdca[c]	1.00E-05	0.02	0.01999	NA	NA	NA	1.00E-05	0.02	0.01999
cpd_hdcan[e]	1.00E-05	0.02	0.01999	1.00E-05	0.02	0.01999	1.00E-05	0.02	0.01999
cpd_hdcan[p]	1.00E-05	0.02	0.01999	1.00E-05	0.02	0.01999	1.00E-05	0.02	0.01999
cpd_hdcea[c]	1.00E-05	0.02	0.01999	NA	NA	NA	1.00E-05	0.02	0.01999
cpd_hdeACP[c]	1.00E-05	0.02	0.01999	1.00E-05	0.02	0.01999	1.00E-05	0.02	0.01999
cpd_hemeO[c]	1.00E-05	0.02	0.01999	1.00E-05	0.02	0.01999	1.00E-05	0.02	0.01999
cpd_hepdp[c]	1.00E-05	0.02	0.01999	1.00E-05	0.02	0.01999	1.00E-05	0.02	0.01999
cpd_hexdp[c]	1.00E-05	0.02	0.01999	1.00E-05	0.02	0.01999	1.00E-05	0.02	0.01999
cpd_hgentis[c]	1.00E-05	0.02	0.01999	NA	NA	NA	NA	NA	NA
cpd_hibcoa[c]	1.00E-05	0.02	0.01999	1.00E-05	0.02	0.01999	1.00E-05	0.02	0.01999
cpd_his-L[c]	1.00E-05	0.02	0.01999	1.00E-05	0.02	0.01999	1.00E-05	0.02	0.01999
cpd_hisp[c]	1.00E-05	0.02	0.01999	1.00E-05	0.02	0.01999	1.00E-05	0.02	0.01999
cpd_histd[c]	1.00E-05	0.02	0.01999	1.00E-05	0.02	0.01999	1.00E-05	0.02	0.01999
cpd_histrna[c]	1.00E-05	0.02	0.01999	1.00E-05	0.02	0.01999	1.00E-05	0.02	0.01999
cpd_hmbil[c]	1.00E-05	0.02	0.01999	1.00E-05	0.02	0.01999	1.00E-05	0.02	0.01999
cpd_hmgcoa[c]	1.00E-05	0.02	0.01999	NA	NA	NA	NA	NA	NA
cpd_hmglut-S[c]	1.00E-05	0.02	0.01999	1.00E-05	0.02	0.01999	1.00E-05	0.02	0.01999
cpd_hom-L[c]	1.00E-05	0.02	0.01999	1.00E-05	0.02	0.01999	1.00E-05	0.02	0.01999

cpd_hpdACP[c]	1.00E-05	0.02	0.01999	1.00E-05	0.02	0.01999	1.00E-05	0.02	0.01999
cpd_hpdca[c]	1.00E-05	0.02	0.01999	NA	NA	NA	1.00E-05	0.02	0.01999
cpd_hpde[c]	1.00E-05	0.02	0.01999	NA	NA	NA	1.00E-05	0.02	0.01999
cpd_hpdeACP[c]	1.00E-05	0.02	0.01999	1.00E-05	0.02	0.01999	1.00E-05	0.02	0.01999
cpd_hpyr[c]	1.00E-05	0.02	0.01999	1.00E-05	0.02	0.01999	1.00E-05	0.02	0.01999
cpd_hxan[c]	1.00E-05	0.02	0.01999	1.00E-05	0.02	0.01999	1.00E-05	0.02	0.01999
cpd_hxan[e]	1.00E-05	0.02	0.01999	1.00E-05	0.02	0.01999	1.00E-05	0.02	0.01999
cpd_iasp[c]	1.00E-05	0.02	0.01999	1.00E-05	0.02	0.01999	1.00E-05	0.02	0.01999
cpd_ibcoa[c]	1.00E-05	0.02	0.01999	1.00E-05	0.02	0.01999	1.00E-05	0.02	0.01999
cpd_ichor[c]	1.00E-05	0.013134208226	0.013124208226	1.00E-05	0.013346751344	0.013336751344	1.00E-05	0.013439142227	0.013429142227
cpd_icit[c]	1.00E-05	0.000646709978 2	0.000636709978 2	1.00E-05	0.000737228118 8	0.000727228118 8	1.00E-05	0.000779920984 1	0.000769920984 1
cpd_idp[c]	1.00E-05	0.02	0.01999	1.00E-05	0.02	0.01999	1.00E-05	0.02	0.01999
cpd_ile-L[c]	1.00E-05	0.02	0.01999	1.00E-05	0.02	0.01999	1.00E-05	0.02	0.01999
cpd_ile-L[e]	1.00E-05	0.02	0.01999	1.00E-05	0.02	0.01999	1.00E-05	0.02	0.01999
cpd_ile-L[p]	1.00E-05	0.02	0.01999	1.00E-05	0.02	0.01999	1.00E-05	0.02	0.01999
cpd_iletrna[c]	1.00E-05	0.02	0.01999	1.00E-05	0.02	0.01999	1.00E-05	0.02	0.01999
cpd_imacp[c]	1.00E-05	0.02	0.01999	1.00E-05	0.02	0.01999	1.00E-05	0.02	0.01999
cpd_imp[c]	0.000196239587 1	0.02	0.019803760 41	7.40E-05	0.02	0.019926021 42	4.86E-05	0.02	0.019951355 37
cpd_indole[c]	1.00E-05	0.02	0.01999	1.00E-05	0.02	0.01999	1.00E-05	0.02	0.01999

cpd_indole[e]	1.00E-05	0.02	0.01999	1.00E-05	0.02	0.01999	1.00E-05	0.019999999179	0.019989999179
cpd_indole[p]	1.00E-05	0.02	0.01999	1.00E-05	0.02	0.01999	1.00E-05	0.02	0.01999
cpd_inoshp[e]	1.00E-05	0.02	0.01999	1.00E-05	0.02	0.01999	1.00E-05	0.02	0.01999
cpd_inoshp[p]	1.00E-05	0.02	0.01999	1.00E-05	0.02	0.01999	1.00E-05	0.02	0.01999
cpd_inospp1[e]	1.00E-05	0.02	0.01999	1.00E-05	0.02	0.01999	1.00E-05	0.02	0.01999
cpd_inospp1[p]	1.00E-05	0.02	0.01999	1.00E-05	0.02	0.01999	1.00E-05	0.02	0.01999
cpd_inost[c]	1.00E-05	0.02	0.01999	1.00E-05	0.02	0.01999	1.00E-05	0.02	0.01999
cpd_ins[c]	1.00E-05	0.02	0.01999	1.00E-05	0.02	0.01999	1.00E-05	0.02	0.01999
cpd_ins[e]	1.00E-05	0.02	0.01999	1.00E-05	0.02	0.01999	1.00E-05	0.02	0.01999
cpd_ipdp[c]	1.00E-05	0.02	0.01999	1.00E-05	0.02	0.01999	1.00E-05	0.02	0.01999
cpd_itp[c]	1.00E-05	0.02	0.01999	1.00E-05	0.02	0.01999	1.00E-05	0.02	0.01999
cpd_ivcoa[c]	1.00E-05	0.02	0.01999	1.00E-05	0.02	0.01999	1.00E-05	0.02	0.01999
cpd_k[c]	1.00E-05	0.050681275	0.050671275	1.00E-05	0.050681275	0.050671275	1.00E-05	0.050681275	0.050671275
cpd_k[e]	1.00E-05	0.050681275	0.050671275	1.00E-05	0.050681275	0.050671275	1.00E-05	0.050681275	0.050671275
cpd_k[p]	1.00E-05	0.0506812530 1	0.0506712530 1	1.00E-05	0.0506812538 5	0.0506712538 5	1.00E-05	0.0506812542 1	0.0506712542 1
cpd_kdo[c]	1.00E-05	0.02	0.01999	1.00E-05	0.02	0.01999	1.00E-05	0.02	0.01999
cpd_kdo8nlipa[c]	1.00E-05	0.02	0.01999	1.00E-05	0.02	0.01999	1.00E-05	0.02	0.01999
cpd_kdo8nlipid4[c]	1.00E-05	0.02	0.01999	1.00E-05	0.02	0.01999	1.00E-05	0.02	0.01999

cpd_kdo8nlipid4L[c]	1.00E-05	0.02	0.01999	1.00E-05	0.02	0.01999	1.00E-05	0.02	0.01999
cpd_kdo8p[c]	1.00E-05	0.02	0.01999	1.00E-05	0.02	0.01999	1.00E-05	0.02	0.01999
cpd_lac-D[c]	1.00E-05	0.02	0.01999	1.00E-05	0.02	0.01999	1.00E-05	0.02	0.01999
cpd_lac-D[e]	1.00E-05	0.02	0.01999	1.00E-05	0.02	0.01999	1.00E-05	0.02	0.01999
cpd_lac-D[p]	1.00E-05	0.02	0.01999	1.00E-05	0.02	0.01999	1.00E-05	0.02	0.01999
cpd_lac-L[e]	1.00E-05	0.02	0.01999	1.00E-05	0.02	0.01999	1.00E-05	0.02	0.01999
cpd_lac-L[p]	1.00E-05	0.02	0.01999	1.00E-05	0.02	0.01999	1.00E-05	0.02	0.01999
cpd_lami[e]	1.00E-05	0.02	0.01999	1.00E-05	0.02	0.01999	1.00E-05	0.02	0.01999
cpd_leu-L[c]	1.00E-05	0.02	0.01999	1.00E-05	0.02	0.01999	1.00E-05	0.02	0.01999
cpd_leu-L[e]	1.00E-05	0.02	0.01999	1.00E-05	0.02	0.01999	1.00E-05	0.02	0.01999
cpd_leu-L[p]	1.00E-05	0.02	0.01999	1.00E-05	0.02	0.01999	1.00E-05	0.02	0.01999
cpd_leutrna[c]	1.00E-05	0.02	0.01999	1.00E-05	0.02	0.01999	1.00E-05	0.02	0.01999
cpd_lgt-S[c]	1.00E-05	0.02	0.01999	1.00E-05	0.02	0.01999	1.00E-05	0.02	0.01999
cpd_lipid_macro[c]	1.00E-05	0.02	0.01999	1.00E-05	0.02	0.01999	1.00E-05	0.02	0.01999
cpd_lipidA[c]	1.00E-05	0.02	0.01999	1.00E-05	0.02	0.01999	1.00E-05	0.02	0.01999
cpd_lipidAds[c]	1.00E-05	0.02	0.01999	1.00E-05	0.02	0.01999	1.00E-05	0.02	0.01999
cpd_lipidX[c]	1.00E-05	0.02	0.01999	1.00E-05	0.02	0.01999	1.00E-05	0.02	0.01999
cpd_lps_Core[c]	1.00E-05	0.02	0.01999	1.00E-05	0.02	0.01999	1.00E-05	0.02	0.01999

cpd_lps_macro[c]	1.00E-05	0.02	0.01999	1.00E-05	0.02	0.01999	1.00E-05	0.02	0.01999
cpd_lys-L[c]	1.00E-05	0.02	0.01999	1.00E-05	0.02	0.01999	1.00E-05	0.02	0.01999
cpd_lys-L[e]	1.00E-05	0.02	0.01999	1.00E-05	0.02	0.01999	1.00E-05	0.02	0.01999
cpd_lys-L[p]	1.00E-05	0.02	0.01999	1.00E-05	0.02	0.01999	1.00E-05	0.02	0.01999
cpd_lystrna[c]	1.00E-05	0.02	0.01999	1.00E-05	0.02	0.01999	1.00E-05	0.02	0.01999
cpd_mal-L[c]	1.00E-05	5.14E-05	4.14E-05	1.00E-05	0.00010011257 38	9.01E-05	3.96E-05	0.02	0.019960384 78
cpd_mal-L[e]	1.00E-05	0.02	0.01999	1.00E-05	0.02	0.01999	1.00E-05	0.02	0.01999
cpd_mal-L[p]	1.00E-05	0.02	0.01999	1.00E-05	0.02	0.01999	1.00E-05	0.02	0.01999
cpd_malACP[c]	1.00E-05	0.02	0.01999	1.00E-05	0.02	0.01999	1.00E-05	0.02	0.01999
cpd_malcoa[c]	1.00E-05	0.02	0.01999	1.00E-05	0.02	0.01999	1.00E-05	0.02	0.01999
cpd_malt[c]	1.00E-05	0.02	0.01999	1.00E-05	0.02	0.01999	1.00E-05	0.02	0.01999
cpd_malt[e]	1.00E-05	0.02	0.01999	1.00E-05	0.02	0.01999	1.00E-05	0.02	0.01999
cpd_malt[p]	1.00E-05	0.02	0.01999	1.00E-05	0.02	0.01999	1.00E-05	0.02	0.01999
cpd_malthp[c]	1.00E-05	0.02	0.01999	1.00E-05	0.02	0.01999	1.00E-05	0.02	0.01999
cpd_malthp[e]	1.00E-05	0.02	0.01999	1.00E-05	0.02	0.01999	1.00E-05	0.02	0.01999
cpd_malthx[c]	1.00E-05	0.02	0.01999	1.00E-05	0.02	0.01999	1.00E-05	0.02	0.01999
cpd_malthx[e]	1.00E-05	0.02	0.01999	1.00E-05	0.02	0.01999	1.00E-05	0.02	0.01999
cpd_maltpt[c]	1.00E-05	0.02	0.01999	1.00E-05	0.02	0.01999	1.00E-05	0.02	0.01999

cpd_maltpt[e]	1.00E-05	0.02	0.01999	1.00E-05	0.02	0.01999	1.00E-05	0.02	0.01999
cpd_malttr[c]	1.00E-05	0.02	0.01999	1.00E-05	0.02	0.01999	1.00E-05	0.02	0.01999
cpd_malttr[e]	1.00E-05	0.02	0.01999	1.00E-05	0.02	0.01999	1.00E-05	0.02	0.01999
cpd_maltttr[c]	1.00E-05	0.02	0.01999	1.00E-05	0.02	0.01999	1.00E-05	0.02	0.01999
cpd_maltttr[e]	1.00E-05	0.02	0.01999	1.00E-05	0.02	0.01999	1.00E-05	0.02	0.01999
cpd_man1p[c]	1.00E-05	0.02	0.01999	1.00E-05	0.02	0.01999	1.00E-05	0.02	0.01999
cpd_man6p[c]	1.00E-05	0.02	0.01999	NA	NA	NA	1.00E-05	0.02	0.01999
cpd_mercppyr[c]	1.00E-05	0.02	0.01999	1.00E-05	0.02	0.01999	1.00E-05	0.02	0.01999
cpd_met-L[c]	0.00020615737739	0.02	0.019793842623	0.005027131315	0.02	0.014972868689	0.002373521794	0.02	0.017626478211
cpd_met-L[e]	1.00E-05	0.02	0.01999	1.00E-05	0.02	0.01999	1.00E-05	0.02	0.01999
cpd_met-L[p]	1.00E-05	0.02	0.01999	1.00E-05	0.02	0.01999	1.00E-05	0.02	0.01999
cpd_methf[c]	1.00E-05	0.00095800218 68	0.00094800218 68	1.00E-05	0.00107583105 4	0.00106583105 4	1.00E-05	0.00113081917	0.00112081917
cpd_mettrna[c]	1.00E-05	0.02	0.01999	1.00E-05	0.02	0.01999	1.00E-05	0.02	0.01999
cpd_mg2[c]	1.00E-05	0.00152443945 6	0.00151443945 6	1.00E-05	0.00170884866 4	0.00169884866 4	1.00E-05	0.00179399085 4	0.00178399085 4
cpd_mg2[e]	0.00013119576 46	0.02	0.019868804 24	0.00011703786 54	0.02	0.019882962 13	0.00011483288 5	0.02	0.019888516 71
cpd_mg2[p]	0.00013119570 76	0.01999999132	0.019868795 61	0.00011703781 66	0.01999999165	0.019882953 84	0.00011483284 28	0.01999999179	0.019888508 55
cpd_mi1p-D[c]	1.00E-05	0.02	0.01999	1.00E-05	0.02	0.01999	1.00E-05	0.02	0.01999

cpd_micit[c]	1.00E-05	0.02	0.01999	1.00E-05	0.02	0.01999	1.00E-05	0.02	0.01999
cpd_mlthf[c]	1.00E-05	0.02	0.01999	1.00E-05	0.02	0.01999	1.00E-05	0.02	0.01999
cpd_mmalsa[c]	1.00E-05	0.02	0.01999	1.00E-05	0.02	0.01999	1.00E-05	0.02	0.01999
cpd_mmql7[c]	1.00E-05	0.02	0.01999	1.00E-05	0.02	0.01999	1.00E-05	0.02	0.01999
cpd_mmqn7[c]	1.00E-05	0.02	0.01999	1.00E-05	0.02	0.01999	1.00E-05	0.02	0.01999
cpd_mn2[c]	1.00E-05	0.02	0.01999	1.00E-05	0.02	0.01999	1.00E-05	0.02	0.01999
cpd_mn2[e]	1.00E-05	0.02	0.01999	1.00E-05	0.02	0.01999	1.00E-05	0.02	0.01999
cpd_mn2[p]	1.00E-05	0.019999991332	0.019989991332	1.00E-05	0.019999991665	0.019989991665	1.00E-05	0.019999991779	0.019989991779
cpd_mn4o[e]	1.00E-05	0.02	0.01999	1.00E-05	0.02	0.01999	1.00E-05	0.02	0.01999
cpd_mobd[c]	7.38E-08	7.38E-06	7.31E-06	7.38E-08	7.38E-06	7.31E-06	7.38E-08	7.38E-06	7.31E-06
cpd_mobd[e]	7.38E-08	7.38E-06	7.31E-06	7.38E-08	7.38E-06	7.31E-06	7.38E-08	7.38E-06	7.31E-06
cpd_mobd[p]	7.38E-08	7.38E-06	7.31E-06	7.38E-08	7.38E-06	7.31E-06	7.38E-08	7.38E-06	7.31E-06
cpd_mql7[c]	1.00E-05	0.02	0.01999	1.00E-05	0.02	0.01999	1.00E-05	0.02	0.01999
cpd_mqn7[c]	1.00E-05	0.02	0.01999	1.00E-05	0.02	0.01999	1.00E-05	0.02	0.01999
cpd_myrsACP[c]	1.00E-05	0.02	0.01999	1.00E-05	0.02	0.01999	1.00E-05	0.02	0.01999
cpd_na1[c]	1.00E-05	2.785791739	2.785781739	1.00E-05	2.785791739	2.785781739	1.00E-05	2.785791739	2.785781739
cpd_na1[e]	1.00E-05	2.785791739	2.785781739	1.00E-05	2.785791739	2.785781739	1.00E-05	2.785791739	2.785781739
cpd_na1[p]	1.00E-05	2.785791739	2.785781739	1.00E-05	2.785791739	2.785781739	1.00E-05	2.785791739	2.785781739
cpd_nad[c]	1.00E-05	4.99E-05	3.99E-05	2.79E-05	0.0001111257514	8.32E-05	1.86E-05	0.0001567561763	0.0001381529663

cpd_nadh[c]	1.00E-05	0.00091839952 46	0.00090839952 46	1.00E-05	3.98E-05	2.98E-05	1.00E-05	8.43E-05	7.43E-05
cpd_nadp[c]	1.00E-05	0.02	0.01999	1.00E-05	0.02	0.01999	1.00E-05	0.02	0.01999
cpd_nadph[c]	1.00E-05	0.02	0.01999	1.00E-05	0.02	0.01999	1.00E-05	0.02	0.01999
cpd_nh4[c]	0.00320275298 1	0.015983068	0.01278031502	0.00401744908 3	0.015983068	0.01196561892	0.00189680801 1	0.015983068	0.01408625999
cpd_nh4[e]	1.00E-05	0.01598305413	0.01597305413	1.00E-05	0.01598305466	0.01597305466	1.00E-05	0.01598305489	0.01597305489
cpd_nh4[p]	1.00E-05	0.01598306107	0.01597306106	1.00E-05	0.01598306133	0.01597306133	1.00E-05	0.01598306144	0.01597306144
cpd_ni2[c]	3.10E-08	3.10E-06	3.07E-06	3.10E-08	3.10E-06	3.07E-06	3.10E-08	3.10E-06	3.07E-06
cpd_ni2[p]	3.10E-08	3.10E-06	3.07E-06	3.10E-08	3.10E-06	3.07E-06	3.10E-08	3.10E-06	3.07E-06
cpd_nicrnt[c]	1.00E-05	0.02	0.01999	1.00E-05	0.02	0.01999	1.00E-05	0.02	0.01999
cpd_nmn[e]	1.00E-05	0.02	0.01999	1.00E-05	0.02	0.01999	1.00E-05	0.02	0.01999
cpd_nmn[p]	1.00E-05	0.02	0.01999	1.00E-05	0.02	0.01999	1.00E-05	0.02	0.01999
cpd_no[c]	1.00E-05	0.02	0.01999	1.00E-05	0.02	0.01999	1.00E-05	0.02	0.01999
cpd_no2[c]	1.00E-05	0.02	0.01999	1.00E-05	0.02	0.01999	1.00E-05	0.02	0.01999
cpd_no2[e]	1.00E-05	0.02	0.01999	1.00E-05	0.02	0.01999	1.00E-05	0.02	0.01999
cpd_no2[p]	1.00E-05	0.02	0.01999	1.00E-05	0.02	0.01999	1.00E-05	0.02	0.01999
cpd_no3[c]	1.00E-05	0.02	0.01999	1.00E-05	0.02	0.01999	1.00E-05	0.02	0.01999
cpd_no3[e]	1.00E-05	0.02	0.01999	1.00E-05	0.02	0.01999	1.00E-05	0.02	0.01999
cpd_no3[p]	1.00E-05	0.02	0.01999	1.00E-05	0.02	0.01999	1.00E-05	0.02	0.01999
cpd_o2-[c]	1.00E-05	0.02	0.01999	1.00E-05	0.02	0.01999	1.00E-05	0.02	0.01999

cpd_o2[c]	2.84E-05	0.000329519714	0.000301098487 6	1.00E-05	0.000257459785 1	0.000247459785 1	1.00E-05	0.000233879808 1	0.000223879808 1
cpd_o2[e]	2.84E-05	0.00032952	0.000301098749	1.00E-05	0.00025746	0.000247459917	1.00E-05	0.00023388	0.000223879918
cpd_o2[p]	2.84E-05	0.000329519857	0.000301098618 3	1.00E-05	0.000257459892 5	0.000247459888 4	1.00E-05	0.000233879904	0.000223879899 9
cpd_oaa[c]	1.00E-05	0.02	0.01999	1.00E-05	0.02	0.01999	1.00E-05	0.02	0.01999
cpd_ocdACP[c]	1.00E-05	0.02	0.01999	1.00E-05	0.02	0.01999	1.00E-05	0.02	0.01999
cpd_ocdca[c]	1.00E-05	0.02	0.01999	NA	NA	NA	1.00E-05	0.02	0.01999
cpd_ocdcan[e]	1.00E-05	0.02	0.01999	1.00E-05	0.02	0.01999	1.00E-05	0.02	0.01999
cpd_ocdcan[p]	1.00E-05	0.02	0.01999	1.00E-05	0.02	0.01999	1.00E-05	0.02	0.01999
cpd_ocdcea[c]	1.00E-05	0.02	0.01999	NA	NA	NA	1.00E-05	0.02	0.01999
cpd_octdp[c]	1.00E-05	0.02	0.01999	1.00E-05	0.02	0.01999	1.00E-05	0.02	0.01999
cpd_octeACP[c]	1.00E-05	0.02	0.01999	1.00E-05	0.02	0.01999	1.00E-05	0.02	0.01999
cpd_ohcu[c]	1.00E-05	0.02	0.01999	1.00E-05	0.02	0.01999	1.00E-05	0.02	0.01999
cpd_ohpb[c]	1.00E-05	0.000918399524 7	0.000908399524 7	1.00E-05	0.02	0.01999	1.00E-05	0.02	0.01999
cpd_orn-L[c]	1.00E-05	0.02	0.01999	1.00E-05	0.02	0.01999	1.00E-05	0.02	0.01999
cpd_orot[c]	1.00E-05	0.02	0.01999	1.00E-05	0.02	0.01999	1.00E-05	0.02	0.01999
cpd_orot5p[c]	1.00E-05	0.02	0.01999	1.00E-05	0.02	0.01999	1.00E-05	0.02	0.01999
cpd_palmACP[c]	1.00E-05	0.02	0.01999	1.00E-05	0.02	0.01999	1.00E-05	0.02	0.01999
cpd_pan4p[c]	1.00E-05	0.02	0.01999	1.00E-05	0.02	0.01999	1.00E-05	0.02	0.01999

cpd_panose[e]	1.00E-05	0.02	0.01999	1.00E-05	0.02	0.01999	1.00E-05	0.02	0.01999
cpd_pant-R[c]	1.00E-05	0.02	0.01999	1.00E-05	0.02	0.01999	1.00E-05	0.02	0.01999
cpd_pap[c]	1.00E-05	0.02	0.01999	1.00E-05	0.02	0.01999	1.00E-05	0.02	0.01999
cpd_paps[c]	1.00E-05	0.02	0.01999	1.00E-05	0.02	0.01999	1.00E-05	0.02	0.01999
cpd_pdACP[c]	1.00E-05	0.02	0.01999	1.00E-05	0.02	0.01999	1.00E-05	0.02	0.01999
cpd_pde[c]	1.00E-05	0.02	0.01999	NA	NA	NA	1.00E-05	0.02	0.01999
cpd_pdeACP[c]	1.00E-05	0.02	0.01999	1.00E-05	0.02	0.01999	1.00E-05	0.02	0.01999
cpd_pdx5p[c]	0.001725009169	0.02	0.018274990883	1.00E-05	0.02	0.01999	1.00E-05	0.02	0.01999
cpd_pe[c]	1.00E-05	0.02	0.01999	1.00E-05	0.02	0.01999	1.00E-05	0.02	0.01999
cpd_pendp[c]	1.00E-05	0.02	0.01999	1.00E-05	0.02	0.01999	1.00E-05	0.02	0.01999
cpd_pep[c]	1.00E-05	0.02	0.01999	1.00E-05	0.001879633997	0.001869633997	1.00E-05	0.003493740941	0.003483740941
cpd_peptido[p]	1.00E-05	0.02	0.01999	1.00E-05	0.02	0.01999	1.00E-05	0.02	0.01999
cpd_peptidoglycan_macro[p]	1.00E-05	0.02	0.01999	1.00E-05	0.02	0.01999	1.00E-05	0.02	0.01999
cpd_peptx[p]	1.00E-05	0.02	0.01999	1.00E-05	0.02	0.01999	1.00E-05	0.02	0.01999
cpd_pgly[c]	1.00E-05	0.02	0.01999	1.00E-05	0.02	0.01999	1.00E-05	0.02	0.01999
cpd_pglyp[c]	1.00E-05	0.000625544853 2	0.000615544853 2	1.00E-05	0.000954372294 4	0.000944372294 4	1.00E-05	0.001144345118	0.001134345118
cpd_phe-L[c]	1.00E-05	0.02	0.01999	1.00E-05	0.02	0.01999	1.00E-05	0.02	0.01999

cpd_pheme[c]	1.00E-05	0.02	0.01999	1.00E-05	0.02	0.01999	1.00E-05	0.02	0.01999
cpd_pheme[p]	1.00E-05	0.02	0.01999	1.00E-05	0.02	0.01999	NA	NA	NA
cpd_phetrna[c]	1.00E-05	0.02	0.01999	1.00E-05	0.02	0.01999	1.00E-05	0.02	0.01999
cpd_phom[c]	1.00E-05	0.02	0.01999	1.00E-05	0.02	0.01999	1.00E-05	0.02	0.01999
cpd_phpyr[c]	1.00E-05	0.02	0.01999	1.00E-05	0.02	0.01999	1.00E-05	0.02	0.01999
cpd_phthr[c]	1.00E-05	0.00210386498938649	0.01999	1.00E-05	0.02	0.01999	1.00E-05	0.02	0.01999
cpd_pi[c]	1.00E-05	0.00097013265280.00096013265280.00056777792810.00225885457491.6E-03	0.00038546892840.00324807574500.00286260681700						
cpd_pi[e]	1.00E-05	0.01356474	0.01355474	5.68E-05	0.01356474	0.01350796429	3.85E-05	0.01356474	0.013526194844
cpd_pi[p]	1.00E-05	0.01356473511	0.01355473511	5.68E-05	0.01356473534	0.01350795865	3.85E-05	0.01356473543	0.013526189229
cpd_pmcoa[c]	1.00E-05	0.01999998264	0.01998998264	1.00E-05	0.01999998339	0.01998998339	1.00E-05	0.01999998359	0.01998998359
cpd_pmcoa[e]	1.00E-05	0.02	0.01998999999	1.00E-05	0.02	0.01998999999	1.00E-05	0.02	0.01998999999
cpd_pmcoa[p]	1.00E-05	0.01999999132	0.01998999132	1.00E-05	0.01999999165	0.01998999165	1.00E-05	0.01999999179	0.01998999179
cpd_pnto-R[c]	1.19E-07	1.19E-05	1.17E-05	1.19E-07	1.19E-05	1.17E-05	1.19E-07	1.19E-05	1.17E-05
cpd_ppa[c]	1.00E-05	0.02	0.01999	1.00E-05	0.02	0.01999	1.00E-05	0.02	0.01999
cpd_ppa[e]	1.00E-05	0.02	0.01999	1.00E-05	0.02	0.01999	1.00E-05	0.02	0.01999
cpd_ppa[p]	1.00E-05	0.02	0.01999	1.00E-05	0.02	0.01999	1.00E-05	0.02	0.01999
cpd_ppbng[c]	1.00E-05	0.02	0.01999	1.00E-05	0.02	0.01999	1.00E-05	0.02	0.01999

cpd_ppcoa[c]	1.00E-05	0.02	0.01999	1.00E-05	0.02	0.01999	1.00E-05	0.02	0.01999
cpd_pphn[c]	1.00E-05	0.02	0.01999	1.00E-05	0.02	0.01999	1.00E-05	0.02	0.01999
cpd_ppi[c]	1.00E-05	4.99E-05	3.99E-05	1.00E-05	1.99E-05	9.95E-06	1.00E-05	2.90E-05	1.90E-05
cpd_ppp9[c]	1.00E-05	0.02	0.01999	1.00E-05	0.02	0.01999	1.00E-05	0.02	0.01999
cpd_ppppg9[c]	1.00E-05	0.02	0.01999	1.00E-05	0.02	0.01999	1.00E-05	0.02	0.01999
cpd_pram[c]	1.00E-05	0.02	0.01999	1.00E-05	0.02	0.01999	1.00E-05	0.02	0.01999
cpd_pran[c]	1.00E-05	0.02	0.01999	1.00E-05	0.02	0.01999	1.00E-05	0.02	0.01999
cpd_prbamp[c]	1.00E-05	0.02	0.01999	1.00E-05	0.02	0.01999	1.00E-05	0.02	0.01999
cpd_prbatp[c]	1.00E-05	0.02	0.01999	1.00E-05	0.02	0.01999	1.00E-05	0.02	0.01999
cpd_prfp[c]	1.00E-05	0.02	0.01999	1.00E-05	0.02	0.01999	1.00E-05	0.02	0.01999
cpd_prlp[c]	1.00E-05	0.02	0.01999	1.00E-05	0.02	0.01999	1.00E-05	0.02	0.01999
cpd_pro-gly[c]	1.00E-05	0.02	0.01999	NA	NA	NA	1.00E-05	0.02	0.01999
cpd_pro-L[c]	1.00E-05	0.02	0.01999	1.00E-05	0.02	0.01999	1.00E-05	0.02	0.01999
cpd_pro-L[e]	1.00E-05	0.02	0.01999	1.00E-05	0.02	0.01999	1.00E-05	0.02	0.01999
cpd_pro-L[p]	1.00E-05	0.02	0.01999	1.00E-05	0.02	0.01999	1.00E-05	0.02	0.01999
cpd_protein_macro[c]	1.00E-05	0.02	0.01999	1.00E-05	0.02	0.01999	1.00E-05	0.02	0.01999
cpd_protrna[c]	1.00E-05	0.02	0.01999	1.00E-05	0.02	0.01999	1.00E-05	0.02	0.01999
cpd_prpp[c]	1.00E-05	0.02	0.01999	1.00E-05	0.02	0.01999	1.00E-05	0.02	0.01999
cpd_ps[c]	1.00E-05	0.02	0.01999	1.00E-05	0.02	0.01999	1.00E-05	0.02	0.01999

cpd_psd5p[c]	1.00E-05	0.02	0.01999	1.00E-05	0.02	0.01999	1.00E-05	0.02	0.01999
cpd_pser-L[c]	1.00E-05	0.02	0.01999	1.00E-05	0.02	0.01999	1.00E-05	0.02	0.01999
cpd_ptdca[c]	1.00E-05	0.02	0.01999	NA	NA	NA	1.00E-05	0.02	0.01999
cpd_ptrc[c]	1.00E-05	0.02	0.01999	1.00E-05	0.02	0.01999	1.00E-05	0.02	0.01999
cpd_ptrc[e]	1.00E-05	0.02	0.01999	1.00E-05	0.02	0.01999	1.00E-05	0.02	0.01999
cpd_ptrc[p]	1.00E-05	0.02	0.01999	1.00E-05	0.02	0.01999	1.00E-05	0.02	0.01999
cpd_pyam5p[c]	1.00E-05	0.02	0.01999	1.00E-05	0.02	0.01999	1.00E-05	0.02	0.01999
cpd_pydx5p[c]	1.00E-05	0.00011594141 27	0.00010594141 27	1.00E-05	0.02	0.01999	1.00E-05	0.02	0.01999
cpd_pyr[c]	1.00E-05	0.02	0.01999	1.00E-05	0.02	0.01999	1.00E-05	0.02	0.01999
cpd_pyr[e]	1.00E-05	0.02	0.01999	1.00E-05	0.02	0.01999	1.00E-05	0.02	0.01999
cpd_pyr[p]	1.00E-05	0.02	0.01999	1.00E-05	0.02	0.01999	1.00E-05	0.02	0.01999
cpd_quln[c]	1.00E-05	0.02	0.01999	1.00E-05	0.02	0.01999	1.00E-05	0.02	0.01999
cpd_r1p[c]	1.00E-05	0.00050801810 06	0.00049801810 06	1.00E-05	0.00058448499 94	0.00057448499 94	1.00E-05	0.00062078587 46	0.00061078587 46
cpd_r5p[c]	0.00039368675 99	0.02	0.01960631324	0.00034218157 91	0.02	0.01965781842	0.00032217227 9	0.02	0.01967782772
cpd_rb15bp[c]	1.00E-05	0.02	0.01999	1.00E-05	0.02	0.01999	1.00E-05	0.02	0.01999
cpd_rhcys[c]	1.00E-05	0.02	0.01999	1.00E-05	0.02	0.01999	1.00E-05	0.02	0.01999
cpd_rib-d[c]	1.00E-05	0.02	0.01999	1.00E-05	0.02	0.01999	1.00E-05	0.02	0.01999
cpd_rib-d[e]	NA	NA	NA	NA	NA	NA	1.00E-05	0.02	0.01999
cpd_ribflv[c]	1.00E-05	0.02	0.01999	1.00E-05	0.02	0.01999	1.00E-05	0.02	0.01999

cpd_rna_macro[c]	1.00E-05	0.02	0.01999	1.00E-05	0.02	0.01999	1.00E-05	0.02	0.01999
cpd_ru5p-D[c]	1.00E-05	0.013953120118	0.013943120118	1.00E-05	0.014146215112	0.014136215112	1.00E-05	0.014230013885	0.014220013885
cpd_s7p[c]	0.00049712728889	0.02	0.019502872771	0.00042825820870	0.02	0.019571741779	0.00040167530930	0.02	0.019598324669
cpd_sbzcoa[c]	1.00E-05	0.02	0.01999	1.00E-05	0.02	0.01999	1.00E-05	0.02	0.01999
cpd_seln[c]	1.00E-05	0.02	0.01999	1.00E-05	0.02	0.01999	1.00E-05	0.02	0.01999
cpd_selnp[c]	1.00E-05	0.02	0.01999	1.00E-05	0.02	0.01999	1.00E-05	0.02	0.01999
cpd_ser-L[c]	1.00E-05	0.02	0.01999	1.00E-05	0.02	0.01999	1.00E-05	0.02	0.01999
cpd_ser-L[e]	1.00E-05	0.02	0.01999	1.00E-05	0.02	0.01999	1.00E-05	0.02	0.01999
cpd_ser-L[p]	1.00E-05	0.02	0.01999	1.00E-05	0.02	0.01999	1.00E-05	0.02	0.01999
cpd_sertrna[c]	1.00E-05	0.02	0.01999	1.00E-05	0.02	0.01999	1.00E-05	0.02	0.01999
cpd_shcl[c]	1.00E-05	0.02	0.01999	1.00E-05	0.02	0.01999	1.00E-05	0.02	0.01999
cpd_sheme[c]	1.00E-05	0.02	0.01999	1.00E-05	0.02	0.01999	1.00E-05	0.02	0.01999
cpd_skm[c]	1.00E-05	0.02	0.01999	1.00E-05	0.02	0.01999	1.00E-05	0.02	0.01999
cpd_skm5p[c]	1.00E-05	0.02	0.01999	1.00E-05	0.02	0.01999	1.00E-05	0.02	0.01999
cpd_sl26da[c]	1.00E-05	0.02	0.01999	1.00E-05	0.02	0.01999	1.00E-05	0.02	0.01999
cpd_sl2a6o[c]	1.00E-05	0.00023325347650	0.00022325347650	1.00E-05	0.00036952398560	0.00035952398560	1.00E-05	0.00045030859140	0.00044030859140
cpd_slcys[c]	1.00E-05	0.02	0.01999	1.00E-05	0.02	0.01999	1.00E-05	0.02	0.01999
cpd_so3[c]	1.00E-05	0.02	0.01999	1.00E-05	0.02	0.01999	1.00E-05	0.02	0.01999
cpd_so3[e]	1.00E-05	0.02	0.01999	1.00E-05	0.02	0.01999	1.00E-05	0.02	0.01999

cpd_so3[p]	1.00E-05	0.02	0.01999	1.00E-05	0.02	0.01999	1.00E-05	0.02	0.01999
cpd_so4[c]	1.00E-05	0.566237304	0.566227304	1.00E-05	0.566237304	0.566227304	1.00E-05	0.566237304	0.566227304
cpd_so4[e]	1.00E-05	0.566237304	0.566227304	1.00E-05	0.566237304	0.566227304	1.00E-05	0.566237304	0.566227304
cpd_so4[p]	1.00E-05	0.566237058 3	0.566227058 3	1.00E-05	0.566237067 7	0.566227067 7	1.00E-05	0.566237071 7	0.566227071 7
cpd_spmd[c]	1.00E-05	0.02	0.01999	1.00E-05	0.02	0.01999	1.00E-05	0.02	0.01999
cpd_sprm[c]	NA	NA	NA	NA	NA	NA	1.00E-05	0.02	0.01999
cpd_srch[c]	1.00E-05	0.02	0.01999	1.00E-05	0.02	0.01999	1.00E-05	0.02	0.01999
cpd_ssaltpp[c]	1.00E-05	0.02	0.01999	1.00E-05	0.02	0.01999	1.00E-05	0.02	0.01999
cpd_suc6p[c]	1.00E-05	0.02	0.01999	1.00E-05	0.02	0.01999	1.00E-05	0.02	0.01999
cpd_sucarg[c]	1.00E-05	0.02	0.01999	1.00E-05	0.02	0.01999	1.00E-05	0.02	0.01999
cpd_sucbz[c]	1.00E-05	0.02	0.01999	1.00E-05	0.02	0.01999	1.00E-05	0.02	0.01999
cpd_succ[c]	1.00E-05	0.02	0.01999	4.67E-05	0.02	0.019953259 52	2.91E-05	0.02	0.019970913 03
cpd_succ[e]	1.00E-05	0.02	0.01999	1.00E-05	0.02	0.01999	1.00E-05	0.019999991 779	0.019989991 779
cpd_succ[p]	1.00E-05	0.02	0.01999	1.00E-05	0.02	0.01999	1.00E-05	0.02	0.01999
cpd_succoa[c]	0.000857436 3093	0.02	0.019142563 69	0.000541236 8555	0.02	0.01945876 314	0.000444139 8716	0.02	0.019555860 13
cpd_sucglu[c]	1.00E-05	0.02	0.01999	1.00E-05	0.02	0.01999	1.00E-05	0.02	0.01999
cpd_sucgsa[c]	1.00E-05	0.02	0.01999	1.00E-05	0.02	0.01999	1.00E-05	0.02	0.01999
cpd_suchms[c]	1.00E-05	0.02	0.01999	1.00E-05	0.02	0.01999	1.00E-05	0.02	0.01999
cpd_sucorn[c]	1.00E-05	0.02	0.01999	1.00E-05	0.02	0.01999	1.00E-05	0.02	0.01999

cpd_sucr[c]	1.00E-05	0.02	0.01999	1.00E-05	0.02	0.01999	1.00E-05	0.02	0.01999
cpd_sucr[p]	1.00E-05	0.02	0.01999	1.00E-05	0.02	0.01999	1.00E-05	0.02	0.01999
cpd_sucsal[c]	1.00E-05	0.02	0.01999	1.00E-05	0.02	0.01999	1.00E-05	0.02	0.01999
cpd_tcynt[c]	1.00E-05	0.02	0.01999	NA	NA	NA	1.00E-05	0.02	0.01999
cpd_thbpt[c]	1.00E-05	0.02	0.01999	1.00E-05	0.02	0.01999	1.00E-05	0.02	0.01999
cpd_thdp[c]	0.00085743630 93	0.02	0.01914256369	0.00054123685 55	0.02	0.01945876314	0.00044139871 6	0.02	0.01955586013
cpd_thf[c]	1.00E-05	0.00230060365 4	0.00229060365 4	1.00E-05	0.01227190984	0.01226190984	1.00E-05	0.02	0.01999
cpd_thglu[c]	1.00E-05	0.02	0.01999	NA	NA	NA	NA	NA	NA
cpd_thmmp[c]	1.00E-05	0.02	0.01999	1.00E-05	0.02	0.01999	1.00E-05	0.02	0.01999
cpd_thmpp[c]	1.00E-05	0.02	0.01999	1.00E-05	0.02	0.01999	1.00E-05	0.02	0.01999
cpd_thr-L[c]	1.00E-05	0.00176820525 4	0.00175820525 4	1.00E-05	0.02	0.01999	1.00E-05	0.02	0.01999
cpd_thr-L[e]	1.00E-05	0.02	0.01999	1.00E-05	0.02	0.01999	1.00E-05	0.02	0.01999
cpd_thr-L[p]	1.00E-05	0.02	0.01999	1.00E-05	0.02	0.01999	1.00E-05	0.02	0.01999
cpd_thr-LA[c]	1.00E-05	0.02	0.01999	1.00E-05	0.02	0.01999	1.00E-05	0.02	0.01999
cpd_thrtrna[c]	1.00E-05	0.02	0.01999	1.00E-05	0.02	0.01999	1.00E-05	0.02	0.01999
cpd_thym[c]	1.00E-05	0.02	0.01999	1.00E-05	0.02	0.01999	1.00E-05	0.02	0.01999
cpd_thym[e]	1.00E-05	0.02	0.01999	1.00E-05	0.02	0.01999	1.00E-05	0.02	0.01999
cpd_thymd[c]	1.00E-05	0.02	0.01999	1.00E-05	0.02	0.01999	1.00E-05	0.02	0.01999
cpd_thymd[e]	1.00E-05	0.02	0.01999	1.00E-05	0.02	0.01999	1.00E-05	0.02	0.01999

cpd_thymd[p]	1.00E-05	0.02	0.01999	1.00E-05	0.02	0.01999	1.00E-05	0.02	0.01999
cpd_tma[e]	1.00E-05	0.02	0.01999	1.00E-05	0.02	0.01999	1.00E-05	0.02	0.01999
cpd_tma[p]	1.00E-05	0.02	0.01999	1.00E-05	0.02	0.01999	1.00E-05	0.02	0.01999
cpd_tmao[e]	1.00E-05	0.02	0.01999	1.00E-05	0.02	0.01999	1.00E-05	0.02	0.01999
cpd_tmao[p]	1.00E-05	0.02	0.01999	1.00E-05	0.02	0.01999	1.00E-05	0.02	0.01999
cpd_trace_macro[c]	1.00E-05	0.02	0.01999	1.00E-05	0.02	0.01999	1.00E-05	0.02	0.01999
cpd_trdox[c]	1.00E-05	0.02	0.01999	1.00E-05	0.02	0.01999	1.00E-05	0.02	0.01999
cpd_trdrd[c]	1.00E-05	0.02	0.01999	1.00E-05	0.02	0.01999	1.00E-05	0.02	0.01999
cpd_trehalose[c]	1.00E-05	0.02	0.01999	1.00E-05	0.02	0.01999	1.00E-05	0.02	0.01999
cpd_trehalose[p]	1.00E-05	0.02	0.01999	1.00E-05	0.02	0.01999	1.00E-05	0.02	0.01999
cpd_trehalose6p[c]	1.00E-05	0.02	0.01999	1.00E-05	0.02	0.01999	1.00E-05	0.02	0.01999
cpd_trnaala[c]	1.00E-05	0.02	0.01999	1.00E-05	0.02	0.01999	1.00E-05	0.02	0.01999
cpd_trnaarg[c]	1.00E-05	0.02	0.01999	1.00E-05	0.02	0.01999	1.00E-05	0.02	0.01999
cpd_trnaasn[c]	1.00E-05	0.02	0.01999	1.00E-05	0.02	0.01999	1.00E-05	0.02	0.01999
cpd_trnaasp[c]	1.00E-05	0.02	0.01999	1.00E-05	0.02	0.01999	1.00E-05	0.02	0.01999
cpd_trnacys[c]	1.00E-05	0.02	0.01999	1.00E-05	0.02	0.01999	1.00E-05	0.02	0.01999

cpd_tr nagln[c]	1.00E-05	0.02	0.01999	1.00E-05	0.02	0.01999	1.00E-05	0.02	0.01999
cpd_tr naglu[c]	1.00E-05	0.02	0.01999	1.00E-05	0.02	0.01999	1.00E-05	0.02	0.01999
cpd_tr nagly[c]	1.00E-05	0.02	0.01999	1.00E-05	0.02	0.01999	1.00E-05	0.02	0.01999
cpd_tr nahis[c]	1.00E-05	0.02	0.01999	1.00E-05	0.02	0.01999	1.00E-05	0.02	0.01999
cpd_tr naile[c]	1.00E-05	0.02	0.01999	1.00E-05	0.02	0.01999	1.00E-05	0.02	0.01999
cpd_tr naleu[c]	1.00E-05	0.02	0.01999	1.00E-05	0.02	0.01999	1.00E-05	0.02	0.01999
cpd_tr nalys[c]	1.00E-05	0.02	0.01999	1.00E-05	0.02	0.01999	1.00E-05	0.02	0.01999
cpd_tr namet[c]	1.00E-05	0.02	0.01999	1.00E-05	0.02	0.01999	1.00E-05	0.02	0.01999
cpd_tr naphe[c]	1.00E-05	0.02	0.01999	1.00E-05	0.02	0.01999	1.00E-05	0.02	0.01999
cpd_tr napro[c]	1.00E-05	0.02	0.01999	1.00E-05	0.02	0.01999	1.00E-05	0.02	0.01999
cpd_tr naser[c]	1.00E-05	0.02	0.01999	1.00E-05	0.02	0.01999	1.00E-05	0.02	0.01999
cpd_tr nathr[c]	1.00E-05	0.02	0.01999	1.00E-05	0.02	0.01999	1.00E-05	0.02	0.01999
cpd_tr natrp[c]	1.00E-05	0.02	0.01999	1.00E-05	0.02	0.01999	1.00E-05	0.02	0.01999
cpd_tr natyr[c]	1.00E-05	0.02	0.01999	1.00E-05	0.02	0.01999	1.00E-05	0.02	0.01999

cpd_trnaval[c]	1.00E-05	0.02	0.01999	1.00E-05	0.02	0.01999	1.00E-05	0.02	0.01999
cpd_trp-L[c]	1.00E-05	0.02	0.01999	1.00E-05	0.02	0.01999	1.00E-05	0.02	0.01999
cpd_trp-L[e]	1.00E-05	0.02	0.01999	1.00E-05	0.02	0.01999	1.00E-05	0.019999991799	0.019989991799
cpd_trp-L[p]	1.00E-05	0.02	0.01999	1.00E-05	0.02	0.01999	1.00E-05	0.02	0.01999
cpd_trptrna[c]	1.00E-05	0.02	0.01999	1.00E-05	0.02	0.01999	1.00E-05	0.02	0.01999
cpd_tsul[c]	1.00E-05	0.02	0.01999	1.00E-05	0.02	0.01999	1.00E-05	0.02	0.01999
cpd_tsul[e]	1.00E-05	0.02	0.01999	1.00E-05	0.02	0.01999	1.00E-05	0.02	0.01999
cpd_tsul[p]	1.00E-05	0.02	0.01999	1.00E-05	0.02	0.01999	1.00E-05	0.02	0.01999
cpd_ttdcan[e]	1.00E-05	0.02	0.01999	1.00E-05	0.02	0.01999	1.00E-05	0.02	0.01999
cpd_ttdcan[p]	1.00E-05	0.02	0.01999	1.00E-05	0.02	0.01999	1.00E-05	0.02	0.01999
cpd_tttnt[e]	1.00E-05	0.02	0.01999	1.00E-05	0.02	0.01999	1.00E-05	0.02	0.01999
cpd_tttnt[p]	1.00E-05	0.02	0.01999	1.00E-05	0.02	0.01999	1.00E-05	0.02	0.01999
cpd_tyr-L[c]	1.00E-05	0.02	0.01999	1.00E-05	0.02	0.01999	1.00E-05	0.02	0.01999
cpd_tyr-L[e]	1.00E-05	0.02	0.01999	1.00E-05	0.02	0.01999	1.00E-05	0.019999991799	0.019989991799
cpd_tyr-L[p]	1.00E-05	0.02	0.01999	1.00E-05	0.02	0.01999	1.00E-05	0.02	0.01999
cpd_tyrtrna[c]	1.00E-05	0.02	0.01999	1.00E-05	0.02	0.01999	1.00E-05	0.02	0.01999
cpd_u23ga[c]	1.00E-05	0.02	0.01999	1.00E-05	0.02	0.01999	1.00E-05	0.02	0.01999
cpd_u3aga[c]	1.00E-05	0.02	0.01999	1.00E-05	0.02	0.01999	1.00E-05	0.02	0.01999
cpd_u3hga[c]	1.00E-05	0.02	0.01999	1.00E-05	0.02	0.01999	1.00E-05	0.02	0.01999

cpd_uaagmda[c]	1.00E-05	0.02	0.01999	1.00E-05	0.02	0.01999	1.00E-05	0.02	0.01999
cpd_uaccg[c]	1.00E-05	0.02	0.01999	1.00E-05	0.02	0.01999	1.00E-05	0.02	0.01999
cpd_uacgam[c]	1.00E-05	0.02	0.01999	1.00E-05	0.02	0.01999	1.00E-05	0.02	0.01999
cpd_uagmda[c]	1.00E-05	0.02	0.01999	1.00E-05	0.02	0.01999	1.00E-05	0.02	0.01999
cpd_uama[c]	1.00E-05	0.02	0.01999	1.00E-05	0.02	0.01999	1.00E-05	0.02	0.01999
cpd_uamag[c]	1.00E-05	0.02	0.01999	1.00E-05	0.02	0.01999	1.00E-05	0.02	0.01999
cpd_uamr[c]	1.00E-05	0.02	0.01999	1.00E-05	0.02	0.01999	1.00E-05	0.02	0.01999
cpd_ubq8[c]	1.00E-05	0.02	0.01999	1.00E-05	0.02	0.01999	1.00E-05	0.02	0.01999
cpd_ubq8h2[c]	1.00E-05	0.02	0.01999	1.00E-05	0.02	0.01999	1.00E-05	0.02	0.01999
cpd_udcpdp[c]	1.00E-05	0.02	0.01999	1.00E-05	0.02	0.01999	1.00E-05	0.02	0.01999
cpd_udcpp[c]	1.00E-05	0.02	0.01999	1.00E-05	0.02	0.01999	1.00E-05	0.02	0.01999
cpd_udp[c]	1.00E-05	0.02	0.01999	1.00E-05	0.02	0.01999	1.00E-05	0.02	0.01999
cpd_udpg[c]	4.24E-05	0.02	0.01995760666	4.01E-05	0.02	0.01995988093	3.92E-05	0.02	0.01996082040
cpd_udpgal[c]	1.00E-05	0.00471772232 1	0.00470772232 1	1.00E-05	0.00498516098 1	0.00497516098 1	1.00E-05	0.00510469745 7	0.00509469745 7
cpd_ugmd[c]	1.00E-05	0.02	0.01999	1.00E-05	0.02	0.01999	1.00E-05	0.02	0.01999
cpd_ugmda[c]	1.00E-05	0.02	0.01999	1.00E-05	0.02	0.01999	1.00E-05	0.02	0.01999
cpd_ump[c]	1.00E-05	0.02	0.01999	1.00E-05	0.02	0.01999	1.00E-05	0.02	0.01999
cpd_uppg3[c]	1.00E-05	0.02	0.01999	1.00E-05	0.02	0.01999	1.00E-05	0.02	0.01999
cpd_ura[c]	1.00E-05	0.02	0.01999	1.00E-05	0.02	0.01999	1.00E-05	0.02	0.01999

cpd_ura[e]	1.00E-05	0.02	0.01999	1.00E-05	0.02	0.01999	1.00E-05	0.02	0.01999
cpd_ura[p]	1.00E-05	0.02	0.01999	1.00E-05	0.02	0.01999	1.00E-05	0.02	0.01999
cpd_urate[c]	1.00E-05	0.02	0.01999	1.00E-05	0.02	0.01999	1.00E-05	0.02	0.01999
cpd_urcan[c]	1.00E-05	0.02	0.01999	1.00E-05	0.02	0.01999	1.00E-05	0.02	0.01999
cpd_urdglyc[c]	1.00E-05	0.02	0.01999	NA	NA	NA	NA	NA	NA
cpd_urdio[e]	1.00E-05	0.02	0.01999	1.00E-05	0.02	0.01999	1.00E-05	0.02	0.01999
cpd_urea[c]	1.00E-05	0.02	0.019989999999	1.00E-05	0.02	0.019989999999	1.00E-05	0.02	0.019989999999
cpd_urea[e]	1.00E-05	0.019999998264	0.019989982644	1.00E-05	0.019999998333	0.019989983333	1.00E-05	0.019999998359	0.019989983589
cpd_urea[p]	1.00E-05	0.019999999132	0.019989991322	1.00E-05	0.019999999165	0.019989991665	1.00E-05	0.019999999179	0.019989991799
cpd_uri[c]	1.00E-05	0.02	0.01999	1.00E-05	0.02	0.01999	1.00E-05	0.02	0.01999
cpd_uri[e]	1.00E-05	0.02	0.01999	1.00E-05	0.02	0.01999	1.00E-05	0.02	0.01999
cpd_uri[p]	1.00E-05	0.02	0.01999	1.00E-05	0.02	0.01999	1.00E-05	0.02	0.01999
cpd_urnyl[e]	1.00E-05	0.02	0.01999	1.00E-05	0.02	0.01999	1.00E-05	0.02	0.01999
cpd_utp[c]	1.00E-05	0.02	0.01999	1.00E-05	0.02	0.01999	1.00E-05	0.02	0.01999
cpd_val-L[c]	1.00E-05	0.02	0.01999	1.00E-05	0.02	0.01999	1.00E-05	0.02	0.01999
cpd_val-L[e]	1.00E-05	0.02	0.01999	1.00E-05	0.02	0.01999	1.00E-05	0.02	0.01999
cpd_val-L[p]	1.00E-05	0.02	0.01999	1.00E-05	0.02	0.01999	1.00E-05	0.02	0.01999
cpd_valtrna[c]	1.00E-05	0.02	0.01999	1.00E-05	0.02	0.01999	1.00E-05	0.02	0.01999
cpd_wo4[c]	1.00E-05	0.02	0.01999	1.00E-05	0.02	0.01999	1.00E-05	0.02	0.01999

cpd_wo4[p]	1.00E-05	0.02	0.01999	1.00E-05	0.02	0.01999	1.00E-05	0.02	0.01999
cpd_xan[c]	1.00E-05	0.02	0.01999	1.00E-05	0.02	0.01999	1.00E-05	0.02	0.01999
cpd_xan[e]	1.00E-05	0.02	0.01999	1.00E-05	0.02	0.01999	1.00E-05	0.02	0.01999
cpd_xan[p]	1.00E-05	0.02	0.01999	1.00E-05	0.02	0.01999	1.00E-05	0.02	0.01999
cpd_xmp[c]	1.00E-05	0.00101916235656	0.00100916235656	1.00E-05	0.00270348526666	0.00269348526666	1.00E-05	0.00411145049191	0.00410145049191
cpd_xtp[c]	1.00E-05	0.02	0.01999	NA	NA	NA	1.00E-05	0.02	0.01999
cpd_xtsn[c]	1.00E-05	0.02	0.01999	1.00E-05	0.02	0.01999	1.00E-05	0.02	0.01999
cpd_xu5p-D[c]	1.00E-05	0.00362073306868	0.00361073306868	1.00E-05	0.00453098704646	0.00452098704646	1.00E-05	0.00464719865	0.00463719865

Data S2 Table B Reaction Gibbs Free Energy Ranges from TMFA simulations.

Reaction ID	Lower Bound 4	Upper Bound 4	Range 4	Lower Bound 15	Upper Bound 15	Range 15	Lower Bound 20	Upper Bound 20	Range 20
2MAHMP	NA	NA	NA	NA	NA	NA	NA	NA	NA
4HBASink	NA	NA	NA	NA	NA	NA	NA	NA	NA
4HBTE	-64.4185	-22.1306	42.2879	NA	NA	NA	-66.9613	-20.6287	46.3326
5DOAN	-40.86333653	-1.00E-06	40.86333553	-42.6114697	-1.00E-06	42.6114687	-43.40607569	-1.00E-06	43.40607469
5DRIB_Sink	NA	NA	NA	NA	NA	NA	NA	NA	NA
5HPUDICDCr	NA	NA	NA	NA	NA	NA	NA	NA	NA
5HPUDICDCs	-100.489237	-47.94374791	52.54548906	NA	NA	NA	NA	NA	NA
A5PISO	-19.1914	0	19.1914	-19.8866	0	19.8866	-20.2026	0	20.2026
AACPS10	-12.65284383	43.59693911	56.24978294	NA	NA	NA	-15.68631977	43.96936233	59.6556821
AACPS11	-20.17025009	36.07953285	56.24978294	NA	NA	NA	-23.20372603	36.45195607	59.6556821
AACPS12	-27.68765635	28.56212659	56.24978294	NA	NA	NA	-30.72113229	28.93454981	59.6556821
AACPS13	-35.20506261	21.04472033	56.24978294	NA	NA	NA	-38.23853855	21.41714355	59.6556821
AACPS14	-90.64793863	-34.39815569	56.24978294	NA	NA	NA	-93.68141457	-34.02573246	59.6556821
AACPS15	-105.6771705	-49.42738759	56.24978294	NA	NA	NA	-108.7106465	-49.05496437	59.65568211

AACPS16	2.687952891	58.93773583	56.24978294	NA	NA	NA	-0.3455230499	59.31015906	59.6556821
AACPS3	-27.38167215	28.8681108	56.24978294	NA	NA	NA	-30.41514809	29.24053402	59.6556821
AACPS4	-98.1608145	-41.91103156	56.24978294	NA	NA	NA	-101.1942904	-41.53860833	59.6556821
AACPS5	-113.195627	-56.94584408	56.24978294	NA	NA	NA	-116.229103	-56.57342085	59.65568211
AACPS6	-19.86426589	36.38551705	56.24978294	NA	NA	NA	-22.89774183	36.75794028	59.6556821
AACPS7	-34.89907841	21.35070454	56.24978294	NA	NA	NA	-37.93255435	21.72312776	59.6556821
AACPS8	-42.41648467	13.83329828	56.24978294	NA	NA	NA	-45.44996061	14.2057215	59.6556821
AACPS9	-5.135437573	51.11434537	56.24978294	NA	NA	NA	-8.168913513	51.48676859	59.6556821
AACPSFA130OH	154.0287383	210.2785213	56.24978294	NA	NA	NA	150.9952624	210.6509445	59.65568211
AACPSFA1718	-105.6780387	-49.4282558	56.24978294	NA	NA	NA	-108.7115147	-49.0558258	59.65568211
AACPSFA1817	-113.1967377	-56.9469474	56.24978294	NA	NA	NA	-116.2302136	-56.5753152	59.6556821
ABTA	-4.293637385	43.06255138	47.35618876	-13.3563189	44.45289452	57.80921342	-14.9263368	45.08486867	60.01180235
ACACCB	-51.7833	8.0199	59.8032	-45.3486	9.4102	54.7588	-46.8413	10.0422	56.8835
ACACCT	-27.8450954	42.21555634	70.06065174	-29.23544154	34.73589364	63.97133518	-29.8674169	36.40178274	66.26919843

ACACT10R	-51.86859757	7.934547476	59.80314504	-45.43394789	9.324890615	54.7588385	-46.92662445	9.956866477	56.88348922
ACALDi	-13.85096249	24.24685889	38.09782138	-14.26330693	22.41235735	36.67566429	-14.45073623	24.15492457	38.6056608
ACBIPGT	NA	NA	NA	NA	NA	NA	NA	NA	NA
ACCOAC	-653.3880696	-580.5406005	72.84746909	-641.1533464	-576.8756429	64.27770358	-642.5613294	-575.2097538	67.35157562
ACGAMK	-41.91556521	-1.00E-06	41.91556421	-41.84425091	-1.00E-06	41.84424991	-43.75346183	-1.00E-06	43.75346083
ACGAt2	-19.62666603	-1.00E-06	19.62666503	-20.40564257	-1.00E-06	20.40564157	-20.75972282	-1.00E-06	20.75972182
ACGK	-11.82424835	-1.00E-06	11.82424735	-11.87972326	-1.00E-06	11.87972226	-13.84656564	-1.00E-06	13.84656464
ACGS	-51.95567528	-12.04887005	39.90680523	-52.70632176	-5.354317363	47.3520044	-54.98915122	-3.861640799	51.12751042
ACHBS	-72.58725492	-2.526602184	70.06065274	-73.97759806	-1.136259044	72.84133902	-74.60957422	-0.5042848902	74.10528933
ACKr	-25.5324	0	25.5324	-25.3959	0	25.3959	-26.2242	0	26.2242
ACLS	-77.57848499	-7.517832244	70.06065274	-78.96882812	-6.127489105	72.84133902	-79.60080428	-5.495514951	74.10528933
ACMAT1	-49.30282406	32.61901665	81.92184072	-51.74612881	30.49258054	82.23870935	-52.85672387	33.71936275	86.57608662
ACNAMS	-100.4158672	-37.32831131	63.08755592	-83.15557086	-34.189835	48.96573586	-84.08957319	-32.76325485	51.32631833
ACOAD10	21.3352	66.7813	45.4461	18.575	58.304	39.729	17.3204	59.5679	42.2475
ACOAD8	NA	NA	NA	NA	NA	NA	17.32035	59.56793237	42.24758237

ACOAD9	30.5382	75.9843	45.4461	27.778	67.507	39.729	26.5234	68.771	42.2476
ACOATA	-39.0692	20.7339	59.8031	-40.4595	14.2993	54.7588	-41.0915	15.792	56.8835
ACODA	-51.69786893	-1.00E-06	51.69786793	-53.44600561	-1.00E-06	53.44600461	-54.2406116	-1.00E-06	54.2406106
ACONT	-9.6076	0	9.6076	-10.3027	0	10.3027	-10.6187	0	10.6187
ACOTA	0	28.1356	28.1356	0	29.5259	29.5259	0	30.1579	30.1579
ACPS1	NA	NA	NA	NA	NA	NA	NA	NA	NA
ACPSc	NA	NA	NA	NA	NA	NA	NA	NA	NA
ACS	-52.81533485	-6.823064605	45.99227024	-36.9960749	-7.791242303	29.20483259	-38.2646615	-6.450638382	31.81402312
ACt6	0	17.5152	17.5152	0	19.5957	19.5957	0	20.6633	20.6633
ADA	-43.08249921	-13.29683876	29.78566046	-41.61670135	-12.97996257	28.63673878	-44.46986163	-12.83592793	31.6339337
ADCL	-145.9567335	-100.3127801	45.64395344	-148.1813966	-100.7258484	47.45554821	-149.192607	-100.9136067	48.27900037
ADCOBAK	NA	NA	NA	NA	NA	NA	NA	NA	NA
ADCS	-46.5283167	-1.00E-06	46.5283157	-52.03174103	-1.00E-06	52.03174003	-52.6637158	-1.00E-06	52.6637142
ADHMCYSSYN	-8.566205888	-1.00E-06	8.566204888	-10.31433906	-1.00E-06	10.31433806	-11.10894505	-1.00E-06	11.10894405
ADK1	-19.5198	0	19.5198	-17.1295	0	17.1295	-20.351	0	20.351
ADK3	-19.5198	25.3731	44.8929	-17.1295	26.4158	43.5453	-20.351	26.8898	47.2408
ADK4	-17.2786	27.7196	44.9982	-16.2231	28.7623	44.9854	-18.1097	29.2363	47.346

ADMDC	-424.0064	-378.434	45.5724	-417.8256	-378.0966	39.729	-420.1908	-377.9433	42.2475
ADNCYC	-73.87152105	-52.65206548	21.21945557	-75.61965423	-55.75515105	19.86450318	-76.41426022	-55.29046903	21.12379119
ADNK1	-35.22340813	-14.83726695	20.38614118	-33.13557425	-13.92080991	19.21476434	-35.81678209	-12.613896	23.20288609
ADNt2	-22.82117884	8.566203888	31.38738273	-23.72694459	10.10151943	33.82846402	-24.1386563	11.647548	35.7864111
ADPT	-51.4170126	-12.68239334	38.73461926	-52.80735574	-13.65057404	39.1567817	-53.43932989	-12.30997012	41.12935977
ADSK	-82.50244394	-36.06793363	46.43451031	-82.55791885	-36.20443819	46.35348066	-84.52476123	-35.37614319	49.14861804
ADSL1r	-0.4158	0	0.4158	-2.1639	0	2.1639	-2.9585	0	2.9585
ADSL2r	-7.8843	0	7.8843	-9.6324	0	9.6324	-10.427	0	10.427
ADSS	-63.59568227	-1.00E-06	63.59568127	-52.41392075	-1.00E-06	52.41391975	-54.3005226	-1.00E-06	54.3005216
AGDC	-44.50194915	-1.00E-06	44.50194815	-46.25008533	-1.00E-06	46.25008433	-47.04469132	-1.00E-06	47.04469032
AGMAHYD	-95.40728602	-42.86179696	52.54548906	-97.1554192	-42.52441543	54.63100376	-97.95002519	-42.37106019	55.578965
AGPR	4.4515	67.1049	62.6534	1.1443	41.7299	40.5856	0	42.5533	42.5533
AHAI	-47.02909992	-1.00E-06	47.02909892	-37.53450923	-1.00E-06	37.53450823	-38.9899068	-1.00E-06	38.9899058
AHCYSNS	-60.69971182	-17.10317956	43.59653226	-62.447845	-15.71283642	46.73500857	-63.24245098	-15.08086227	48.16158872
AICART	-12.5319	0	12.5319	-17.0402	0	17.0402	-19.0894	0	19.0894
AIRC2	-642.9146004	-570.0671313	72.84746909	-630.6798773	-566.4021737	64.27770358	-632.0878602	-564.7362846	67.3515757562

AIRC3	13.5964	48.6268	35.0304	12.9013	49.3219	36.4206	12.5853	49.6379	37.0526
AKGD	-34.84826271	12.66619995	47.51446266	-43.25214516	4.884083984	48.13622914	-44.82276194	6.464019369	51.28678131
ALAALA	-84.3679	-11.8165	72.5514	-72.1332	-8.1515	63.9817	-73.5412	-6.4856	67.0556
ALAD_L	6.207624801	48.25941945	42.05179465	3.069148485	42.65013357	39.58098509	1.642568342	43.74212943	42.09956109
ALAGLYX	-31.636	0	31.636	-38.6162	0	38.6162	-39.2482	0	39.2482
ALAR	-17.3671	0	17.3671	-18.0623	0	18.0623	-18.3783	0	18.3783
ALATA_D2	-17.19787684	40.84641017	58.04428701	-30.45656644	42.23675331	72.69331974	-31.08854059	42.86872746	73.95726805
ALATA_L	-11.8328	32.129	43.9618	-20.8955	36.7657	57.6612	-22.4661	37.3977	59.8638
ALATA_L2	-17.19787784	37.60011214	54.79798998	-30.45656743	42.23675231	72.69331974	-31.08854159	42.86872646	73.95726805
ALATRS	NA	NA	NA	NA	NA	NA	NA	NA	NA
ALA_Dt4	-28.12719299	-1.00E-06	28.12719199	-23.72694359	-1.00E-06	23.72694259	-50.37949806	20.515244	70.89474206
ALAt4	-27.97917171	35.03032637	63.00949808	-23.57892231	36.42066951	59.99959182	-50.23147678	20.66326627	70.89474306
ALCD2x	6.8892	46.7455	39.8563	-1.4608	38.2682	39.729	-2.7155	39.5321	42.2476
ALDD2x	-74.17943208	-34.32314651	39.85628557	-76.67076265	-37.21060965	39.460153	NA	NA	NA
ALLNRAC	-17.5152	17.5152	35.0304	-18.2103	18.2103	36.4206	-18.5263	18.5263	37.0526
ALLTC	-3.2926	49.2529	52.5455	NA	NA	NA	NA	NA	NA

ALLTN	-36.8973	-1.867	35.0303	-37.5925	-1.1718	36.4207	-37.9085	-0.8559	37.0526
AMAA	-37.28047944	15.11699034	52.39746978	-39.02861262	15.45437187	54.48298449	-39.82321861	15.60772711	55.43094572
AMALT1	-13.13713199	56.92352275	70.06065474	-14.52747513	58.31386589	72.84134102	-15.15944928	58.94584005	74.10528933
AMALT2	-84.24366906	-14.18301432	70.06065474	-85.6340122	-12.79267118	72.84134102	-86.26598636	-12.16069703	74.10528933
AMALT3	-39.05385832	31.00679642	70.06065474	-40.44420146	32.39713956	72.84134102	-41.07617561	33.02911372	74.10528933
AMALT4	-58.32693936	11.73371538	70.06065474	-59.7172825	13.12405852	72.84134102	-60.34925665	13.75603268	74.10528933
AMAOT	-28.6943	0	28.6943	-22.1557	0	22.1557	-24.3583	0	24.3583
AMMQT7_2	-41.70578185	-1.00E-06	41.70578085	-36.22018602	-1.00E-06	36.22018502	-38.90139387	-1.00E-06	38.90139287
AMOB_Sink	NA	NA	NA	NA	NA	NA	NA	NA	NA
AMPMS2	-248.8589507	-168.3825104	80.47644033	-253.7250509	-177.575378	76.14967288	-255.9369164	-176.6366934	79.30022304
AMPTASECG	-23.6304	23.3253	46.9557	NA	NA	NA	-31.7629	23.816	55.5789
AMPTASEPG	-7.6945	39.2612	46.9557	NA	NA	NA	-15.827	39.7519	55.5789
ANPRT	-92.48203845	-36.23225551	56.24978294	-93.87238159	-37.5872079	56.28517369	-94.50435574	-36.32791989	58.17643585
ANS1	-162.9663216	-81.54881394	81.41750767	-169.5227075	-81.070297	88.45241054	-170.6333006	-80.91694176	89.71635885
AOXS	-48.0064	0	48.0064	-50.4497	0	50.4497	-51.5603	0	51.5603

APRAUR	-39.39005795	-1.00E-06	39.39005695	-29.87780661	-1.00E-06	29.87780561	-33.39175847	-1.00E-06	33.39175747
ARBABC	NA	NA	NA	NA	NA	NA	-79.7103	-30.885	48.8253
ARGDC	-42.65864024	-1.00E-06	42.65863924	-44.40677342	-1.00E-06	44.40677242	-45.20138141	-1.00E-06	45.20138041
ARGSL	-33.7945	0	33.7945	-35.5426	0	35.5426	-36.3372	0	36.3372
ARGSS	-53.32722583	-1.00E-06	53.32722483	-55.41274054	-2.332918772	53.07982176	-56.36070177	-0.4463169197	55.91438485
ARGTRS	NA	NA	NA	NA	NA	NA	NA	NA	NA
ASAD	0	65.4666	65.4666	0	40.0916	40.0916	0	40.915	40.915
ASNN	-42.55286739	-4.729735479	37.82313191	NA	NA	NA	-41.65688717	-4.268824657	37.38806252
ASNS1	-117.8396286	-50.17547165	67.66415699	-125.0911861	-54.87725023	70.21393591	-126.5177663	-53.15328021	73.36448607
ASNTRS	NA	NA	NA	NA	NA	NA	NA	NA	NA
ASP1DC	-61.10786476	-9.473863049	51.63400171	-62.85599794	-9.776178175	53.07981976	-63.65060593	-8.071638932	55.578967
ASPCT	-55.59452319	-1.00E-06	55.59452219	-47.51842489	-1.00E-06	47.51842389	-49.02213162	-1.00E-06	49.02213062
ASPK	-16.6037	0	16.6037	-16.6592	0	16.6592	-18.626	0	18.626
ASPO3	-165.6887379	-102.9647923	62.72394566	-157.7140713	-102.2141458	55.4999255	-159.3933324	-100.0309876	59.3623479
ASPO5	-39.03395663	13.01580042	52.04975706	-37.78285759	13.76644691	51.5493045	-39.98544652	15.94960506	55.9350558

ASPO6	24.12094053	63.88659779	39.76565726	23.69733573	84.55942278	60.86208706	23.48043609	86.74258094	63.26214485
ASPO8	12.02167906	81.17084646	69.1491674	10.63133592	81.92149294	71.29015702	9.999361763	84.10465109	74.10528933
ASPO9	-50.07812517	19.07104223	69.1491674	-51.46846831	19.82168871	71.29015702	-52.10044246	22.00484687	74.10528933
ASPTA1	0	37.0429	37.0429	0	37.7935	37.7935	0	39.9767	39.9767
ASPTA4	-33.8155	13.5407	47.3562	-42.8782	14.9311	57.8093	-44.4488	15.563	60.0118
ASPTRS	NA	NA	NA	NA	NA	NA	NA	NA	NA
ASPt2	-21.9096915	17.51516269	39.42485418	-22.17576059	19.59565182	41.77141241	-24.1386563	20.66326827	44.80192457
AST	-44.93934752	-2.651366163	42.28798136	-46.32969066	-1.261023024	45.06866764	-46.9616648	-0.6290488694	46.33261594
ATPM	NA	NA	NA	NA	NA	NA	NA	NA	NA
ATPPRT	-130.0262654	-91.2916461	38.7346192	-131.4166085	-93.3417701	38.0748384	-132.0485827	-92.3984691	39.6501135
ATPS4r	36.2814	72.5014	36.22	33.7328	60.7769	27.0441	32.5744	62.3999	29.8255
BPNT	-45.94371061	-17.4707287	28.4729819	-38.01481004	-14.3325241	23.6825763	-39.5854281	-12.9056726	26.6797525
BTS4	-282.0341	-190.9646	91.0695	-277.0991	-190.0614	87.0377	-280.0306	-189.6508	90.3798
BUTSUCCCOA	-40.5398	19.2633	59.8031	-38.2357	21.3489	59.5846	-39.9597	22.2968	62.2565
Biomass_WP2	NA	NA	NA	NA	NA	NA	NA	NA	NA
C120SN	-572.4687948	-278.8955539	293.5732409	-517.4962345	-270.195705	247.3005295	-532.3847584	-266.2412263	266.1435321
C130ISN	-468.5809223	-264.8334189	203.7475034	-433.8420049	-259.9672179	173.874787	-443.3782789	-257.7553083	185.6229705

C130OHISN	-231.97495	-32.90121926	199.0737307	-204.0157807	-30.14099368	173.874787	-212.4126442	-26.78967366	185.6229705
C140ISN	-618.9361751	-358.9496131	259.9865621	-572.3858948	-352.6930689	219.6928259	-584.9955977	-349.8491852	235.1464125
C140SN	-719.8347365	-373.0117481	346.8229885	-656.0401244	-362.9215561	293.1185683	-674.0020772	-358.3351032	315.6669741
C150ISN	-618.9361751	-358.9496131	259.9865621	-572.3858948	-352.6930689	219.6928259	-584.9955977	-349.8491852	235.1464125
C150SN	-769.291428	-453.0658072	316.2256207	-710.9297847	-445.41892	265.5108647	-726.6129166	-441.9430621	284.6698545
C151SN	NA	NA	NA	-718.1248452	-425.006277	293.1185683	-735.7419956	-420.0750215	315.6669741
C160ISN	-769.291428	-453.0658072	316.2256207	-710.9297847	-445.41892	265.5108647	-726.6129166	-441.9430621	284.6698545
C160SN	-867.2006783	-467.1279423	400.072736	-794.5840142	-455.6474071	338.9366071	-815.6193961	-450.42898	365.190416
C161SN	-870.149404	-492.8486296	377.3007743	-807.7225022	-482.5897469	325.1327553	-827.6184736	-477.9266173	349.6918562
C170ISN	-769.291428	-453.0658072	316.2256207	-710.9297847	-445.41892	265.5108647	-726.6129166	-441.9430621	284.6698545
C170SN	-919.6466808	-547.1820014	372.4646794	-849.4736746	-538.144771	311.3289035	-868.2302354	-534.036939	334.1932964
C171SN	NA	NA	NA	-856.6687351	-517.732128	338.9366071	-877.3593145	-512.1688984	365.190416
C171n8SN	-932.3603192	-525.3583726	407.0019466	-856.6685531	-517.731946	338.9366071	-877.3591325	-512.1687164	365.190416
C180SN	-1000	-561.2441365	438.7558636	-933.1279041	-548.3732582	384.754646	-957.2367149	-542.5228569	414.713858

C181SN	NA	NA	NA	-946.2663921	-575.3155979	370.9507942	-969.2357924	-570.0204942	399.2152982
C181n7SN	-1000	-586.9646418	413.0353582	-946.2662101	-575.3154159	370.9507942	-969.2356104	-570.0203122	399.2152982
C205SN	-670.6194738	-214.8778036	455.7416702	-612.3427944	-209.3778131	402.9649812	-633.8279817	-200.5878014	433.2401803
C50SN	-30.20312763	50.37112309	80.57425072	-12.26690786	51.76146623	64.02837409	-15.6563239	52.39344039	68.04976429
C60ISN	-38.02651809	42.54773263	80.57425072	-20.09029832	43.93807577	64.02837409	-23.4791437	44.57004992	68.04976429
C70ISN	-45.54392435	-1.00E-06	45.54392335	-27.60770458	-1.00E-06	27.60770358	-30.9912063	-1.00E-06	30.9911963
CAT	-446.2387709	-434.9451364	11.29363447	-478.3666774	-434.1637416	44.2029358	-478.5200326	-433.7842101	44.7382252
CBL1abc	-81.11913149	-23.0869139	58.03221759	-69.29943816	-19.87589392	49.42354424	-70.89442533	-18.37543838	52.5189695
CBLAT	NA	NA	NA	NA	NA	NA	NA	NA	NA
CBPS	-704.0902612	-609.1570175	94.93324365	-696.3818842	-605.3233697	91.05851455	-699.9193414	-603.5808014	96.33853992
CDPG46D	-122.4585694	-87.42824206	35.03032737	-123.153741	-86.73307049	36.42067051	-123.4697281	-86.41708341	37.05264466
CDPMEK	-44.01937305	-1.00E-06	44.01937205	-44.07484796	-1.00E-06	44.07484696	-46.0419034	-1.00E-06	46.0418934
CHOLDH1	-22.1824915	47.87816325	70.06065474	NA	NA	NA	NA	NA	NA
CHOLDH2	4.494441371	49.94055434	45.44611296	NA	NA	NA	NA	NA	NA
CHOLDH3	4.188786113	61.99107516	57.80228905	NA	NA	NA	NA	NA	NA

CHOLDH4	-6.643924802	63.41672994	70.06065474	NA	NA	NA	NA	NA	NA
CHOLDH5	-68.74372903	1.316925715	70.06065474	NA	NA	NA	NA	NA	NA
CHOLt4	-31.09301608	32.06450328	63.15751936	-26.67368676	33.47392634	60.1476131	-54.54936199	16.49340235	71.04276434
CHORM	-62.21213306	-28.15081415	34.06131891	-62.90730463	-27.45564258	35.45166205	-63.22329171	-27.1396555	36.0836362
CHORS	-97.36412163	-52.76073786	44.60338377	-89.43522105	-50.67522315	38.75999791	-91.00583583	-49.72726192	41.27857391
CHRPL	-157.4047494	-105.8282668	51.5764826	-159.1528826	-105.4908853	53.66199731	-159.9474886	-105.3375301	54.6095854
CKDOAS	-17.9331914	-1.00E-06	17.9331904	-21.38854391	-1.00E-06	21.38854291	-22.95915869	-1.00E-06	22.95915769
CO2t	0	17.5152	17.5152	0	18.2103	18.2103	-18.5263	18.5263	37.0526
COBALTt3	7.731589963	18.34361827	10.61202831	6.745622384	20.54947418	13.80385179	6.202783075	21.70134239	15.49855931
COBALTt5	0	10.612	10.612	0	13.8039	13.8039	0	15.4986	15.4986
CONFALDD	-56.41247403	-10.96636107	45.44611296	NA	NA	NA	-60.42728266	-18.17970029	42.24758237
CPPPGO	-423.0592931	-347.3518252	75.70746797	424.5358596	343.9122572	80.62360231	425.2313821	343.4429149	81.78846718
CPPPGOAN	NA	NA	NA	NA	NA	NA	NA	NA	NA
CS	-64.3643256	-12.4728192	51.8955063	65.7587569	18.9075316	46.8514409	66.3907485	17.4145504	48.9758981
CSND	-56.6149522	-17.8803276	38.7346926	57.2926294	17.5635657	39.7290637	59.6670431	17.4192194	42.2475858237

CSNt2	-22.8212	17.5152	40.3364	-23.7269	19.5957	43.3226	-24.1387	20.6633	44.802
CTPS2	-91.01820164	-8.908459014	82.10974262	83.9495213	-5.780186695	78.16933435	85.83612316	-4.358245103	81.47787805
CU2t	-97.74818872	-40.61594202	57.13224669	-85.73436098	-37.96578667	47.76857431	-87.22461224	-36.76226822	50.46234402
CYCPOe	-430.795873	-343.2200545	87.57581843	NA	NA	NA	NA	NA	NA
CYOO2	-195.8081391	-112.3120474	83.49609166	-199.3068531	-108.7705277	90.53632546	-201.1532329	-107.7077948	93.44543807
CYOR7	69.47949492	189.3693119	119.889817	61.85270997	182.9321936	121.0794836	57.89823121	185.3103403	127.4121091
CYSS	-91.39503677	-21.33438503	70.06065174	-92.78538291	-19.94404189	72.84134102	-93.41735406	-19.31206774	74.10528633
CYSTL	-50.513842	-3.213017857	47.30082414	-52.24431453	-2.200970097	50.04334443	-55.09747481	-1.740948388	53.35652643
CYSTRS	NA	NA	NA	NA	NA	NA	NA	NA	NA
CYTBD	-56.2679934	-14.22745085	42.04054255	-59.0715359	-20.74611247	38.32542343	-60.60192857	-18.9520797	41.64984887
CYTD	-49.46348694	-10.72886768	38.73461926	-50.14099786	-10.41199149	39.72900637	-52.51553923	-10.26795686	42.24758237
CYTDH	-41.0337	11.5118	52.5455	-42.7819	11.8492	54.6311	-43.5765	12.0025	55.579
CYTDK1	-54.11228381	-15.66204553	38.45023828	-54.16775872	-15.10337852	39.06438019	-56.1346011	-13.95909545	42.17550565
CYTDK2	-54.11228281	7.858895294	61.971781	-54.16775772	-9.944410003	64.11216772	-56.1346001	10.89237123	67.02697133
CYTDK3	-51.87100715	10.20537605	62.0763832	-53.26135029	12.29089076	65.55224105	-53.89332445	13.23885199	67.13217644

CYTDt2	-22.821 17884	17.515 16269	40.336 34152	-23.726 94459	19.595 65182	43.322 59641	-24.138 6563	20.663 26827	44.801 92457
CYTK1	-23.600 5	0	23.600 5	-24.351 2	0	24.351 2	-26.634	0	26.634
CYTK2	-33.553 3	12.881 2	46.434 5	-33.608 8	12.744 7	46.353 5	-35.575 7	13.573	49.148 7
CampHydrolyase	-30.256 1652	-12.325 24817	17.930 91703	-30.951 33677	-10.577 115	20.374 22178	-31.267 32385	-9.7825 09008	21.484 81484
Clt	-25.956 7	0	25.956 7	-27.123 7	0	27.123 7	-27.653 6	0	27.653 6
DADA	-48.475 2617	-9.7406 42445	38.734 61926	-49.152 77262	-9.4237 66255	39.729 00637	-51.527 314	-9.2797 31623	42.247 58237
DADK	-28.759 2	17.675 3	46.434 5	-28.814 6	17.538 8	46.353 4	-30.781 5	18.367 1	49.148 6
DADNt2	-22.821 17884	17.515 16269	40.336 34152	-23.726 94459	19.595 65182	43.322 59641	-24.138 6563	20.663 26827	44.801 92457
DAGK	-48.608 87555	-2.1743 65233	46.434 51031	NA	NA	NA	-50.631 19284	-1.4825 74299	49.148 61854
DAHPS	-105.60 73943	-45.413 00538	60.194 38889	-91.240 26492	-47.879 82919	43.360 43573	-92.174 26675	-44.566 64719	47.607 61956
DAPDC	-94.489 99234	-41.944 50329	52.545 48906	-96.238 12552	-41.607 12176	54.631 00376	-97.032 73351	-41.453 76651	55.578 967
DAPE	-18.193	0	18.193	-18.888 1	0	18.888 1	-19.204 1	0	19.204 1
DASYN	-73.849	-25.583 5	48.265 5	-75.934 5	-26.938 5	48.996	-76.882 5	-25.679 2	51.203 3
DB4PS	-124.49 60748	-72.780 21795	51.715 85681	-126.24 42059	-72.442 83642	53.801 36952	-127.03 88119	-72.289 48118	54.749 33075

DBTSr	-68.3352	0	68.3352	-56.1005	0	56.1005	-57.5085	0	57.5085
DCYTD	-47.65409604	-8.919476788	38.73461926	-48.33160696	-8.602600597	39.72900637	-50.70614834	-8.458565966	42.24758237
DCYTt2	-22.82117884	17.51516269	40.33634152	-23.72694459	19.59565182	43.32259641	-24.1386563	20.66326827	44.80192457
DGK1	-34.3005	12.134	46.4345	-34.356	11.9975	46.3535	-36.3228	12.8258	49.1486
DHAD1	-60.4438502	-25.41352283	35.03032737	-61.13902177	-24.71835126	36.42067051	-61.45500884	-24.40236418	37.05264466
DHAD2	-60.44366364	-25.41333627	35.03032737	-61.13883521	-24.7181647	36.42067051	-61.45482229	-24.40217762	37.05264466
DHDPRy	-47.64922158	-0.1044422296	47.54477935	-38.84980246	-1.00E-06	38.84980146	-40.6211871	-1.00E-06	40.6211861
DHDPS	-124.1191145	-71.57362348	52.54549106	-124.4564961	-69.8254903	54.63100576	-124.6098513	-69.03088431	55.578967
DHFR	-60.3523	-7.5333	52.819	-50.8577	-1.8033	49.0544	-52.3131	0	52.3131
DHFS	-67.40123661	-1.00E-06	67.40123561	-55.16651348	-1.00E-06	55.16651248	-56.57449642	-1.00E-06	56.57449542
DHNAOT7	-144.5773395	-60.39660932	84.18073022	-149.0856537	-72.93597878	76.14967487	-151.1348893	-71.8346623	79.30022704
DHNPA	-44.79589825	-1.00E-06	44.79589725	-46.54403142	-1.00E-06	46.54403042	-47.33863741	-1.00E-06	47.33863641
DHORD2	-191.800005	-127.0011376	64.79886739	-183.9091414	-125.4002021	58.50893933	-185.6264949	-124.6725042	60.95399072
DHORD4i	-14.08958799	57.13450114	71.22408913	-15.56373424	58.73543661	74.29917084	-16.23380071	59.46313454	75.69693526

DHORD8	-76.18939221	-4.96530308	71.22408913	-77.66353846	-3.364367619	74.29917084	-78.33360494	-2.636669682	75.69693526
DHORTS	0	18.6786	18.6786	0	19.6682	19.6682	0	20.118	20.118
DHPPDA2	-4.472168516	-1.00E-06	4.472167516	-5.149679434	-1.00E-06	5.149678434	-7.524220809	-1.00E-06	7.524219809
DHPRx	12.2777	57.7238	45.4461	20.755	60.484	39.729	19.491	61.7386	42.2476
DHPS3	-72.27202075	-22.92377542	49.34824533	-72.91191409	-23.80219796	49.10971613	-73.2027747	-22.32630547	50.87646922
DHPTPE	-17.5152	17.5152	35.0304	-18.2103	18.2103	36.4206	-18.5263	18.5263	37.0526
DHQD1	-22.5473	0	22.5473	-23.2425	0	23.2425	-23.5584	0	23.5584
DHQS	-168.9309128	-123.3585206	45.5723923	-161.0020122	-121.2730059	39.7290637	-162.572627	-120.3250446	42.24758237
DKMPPD3	-144.235107	-60.31597994	83.9191271	-141.4891848	-76.93317348	64.55601133	-145.4156997	-74.25192162	71.16377812
DMATT	-129.2996734	-73.04989049	56.24978294	-130.6900166	-74.40484288	56.28517369	-131.3219907	-73.14555488	58.17643585
DMOCT	-68.69157496	-12.44179202	56.24978294	-70.0819181	-13.79674441	56.28517369	-70.7139225	-12.5374564	58.17643585
DMPPS	-88.30840697	-42.862294	45.44611296	-79.83111943	-40.10211307	39.7290637	-81.09506774	-38.84748537	42.24758237
DMQMT	-27.95364537	-1.00E-06	27.95364437	-21.43807805	-1.00E-06	21.43807705	-23.5658107	-1.00E-06	23.5658107
DMSOR3e	NA	NA	NA	NA	NA	NA	NA	NA	NA
DMSOR4e	NA	NA	NA	NA	NA	NA	NA	NA	NA

DNA_SYNTHESIS	NA	NA	NA	NA	NA	NA	NA	NA	NA
DNMPPA	-62.75384641	-17.18145418	45.57239223	-54.82494584	-15.09593947	39.72900637	-56.39556061	-14.14797824	42.24758237
DNTPPA	-86.4669899	-47.73237064	38.73461926	-88.21512307	-50.14028464	38.07483844	-89.00972906	-49.35961555	39.65011352
DPCOAK	-34.32856931	-1.00E-06	34.32856831	-34.38404422	-1.00E-06	34.38404322	-36.3508866	-1.00E-06	36.3508856
DPR	-53.36073539	-1.00E-06	53.36073439	-43.8661447	-1.00E-06	43.8661437	-45.32154227	-1.00E-06	45.32154127
DRBK	-51.24237905	-7.089571757	44.15280729	-51.98353693	-5.630056266	46.35348066	-53.95037931	-4.801760767	49.14861854
DRPA	-16.82948172	-1.00E-06	16.82948072	-9.265439885	30.46356648	39.72900637	-11.63066065	30.61692172	42.24758237
DTMPK	-32.3726	0	32.3726	-32.4281	0	32.4281	-34.3949	0	34.3949
DURIK1	-49.88737801	-3.452868193	46.43450981	-49.94285292	-3.589372758	46.35348016	-51.9096953	-2.761076759	49.14861854
DURIPP	-13.88	34.4766	48.3566	-17.0185	40.9208	57.9393	-18.4451	42.3288	60.7739
DURIt2	-22.82117884	17.51516269	40.33634152	-23.72694459	19.59565182	43.32259641	-24.1386563	20.66326827	44.80192457
DUTPDP	-103.1609062	-64.73160175	38.42930449	-104.9090394	-67.48710153	37.42193789	-105.7036454	-66.86442597	38.83921943
DXPRI	-50.8325	0	50.8325	-41.3379	0	41.3379	-42.7933	0	42.7933
DXPS	-59.00815286	-1.00E-06	59.00815186	-68.33073379	-10.39139417	57.93933962	-68.9627095	-8.188805242	60.7739047

E4PD	-53.0771	-14.7303	38.3468	62.9366	-32.1212	30.8154	-64.1912	-30.8573	33.3339
ECOAH2C	-2.8905	32.1398	35.0303	-3.5857	32.835	36.4207	-3.9016	33.151	37.0526
ECOAH9	2.0136	37.044	35.0304	1.3185	37.7391	36.4206	1.0025	38.0551	37.0526
EDA	-27.09809057	-1.00E-06	27.09808957	-13.94422435	25.78478201	39.72900637	-16.30944512	25.93813726	42.24758237
EDTXS5	NA	NA	NA	NA	NA	NA	NA	NA	NA
EDTXS6	NA	NA	NA	NA	NA	NA	NA	NA	NA
ENO	-21.4955	13.5349	35.0304	-12.5451	0	12.5451	-14.2737	0	14.2737
EPPP2	-68.8105	-23.2381	45.5724	-60.8816	-21.1526	39.729	-62.4522	-20.2046	42.2476
EX_cpd_CrOH3[e]	NA	NA	NA	NA	NA	NA	NA	NA	NA
EX_cpd_ac[e]	NA	NA	NA	NA	NA	NA	NA	NA	NA
EX_cpd_acgam[e]	NA	NA	NA	NA	NA	NA	NA	NA	NA
EX_cpd_adn[e]	NA	NA	NA	NA	NA	NA	NA	NA	NA
EX_cpd_akg[e]	NA	NA	NA	NA	NA	NA	NA	NA	NA
EX_cpd_ala-D[e]	NA	NA	NA	NA	NA	NA	NA	NA	NA
EX_cpd_ala-L[e]	NA	NA	NA	NA	NA	NA	NA	NA	NA
EX_cpd_asn-L[e]	NA	NA	NA	NA	NA	NA	NA	NA	NA
EX_cpd_asp-L[e]	NA	NA	NA	NA	NA	NA	NA	NA	NA

EX_cpd_bgl[e]	NA	NA	NA	NA	NA	NA	NA	NA	NA
EX_cpd_ca2[e]	NA	NA	NA	NA	NA	NA	NA	NA	NA
EX_cpd_cbl1[e]	NA	NA	NA	NA	NA	NA	NA	NA	NA
EX_cpd_chitin[e]	NA	NA	NA	NA	NA	NA	NA	NA	NA
EX_cpd_cl[e]	NA	NA	NA	NA	NA	NA	NA	NA	NA
EX_cpd_co2[e]	NA	NA	NA	NA	NA	NA	NA	NA	NA
EX_cpd_cobalt2[e]	NA	NA	NA	NA	NA	NA	NA	NA	NA
EX_cpd_cobalt3[e]	NA	NA	NA	NA	NA	NA	NA	NA	NA
EX_cpd_cro4[e]	NA	NA	NA	NA	NA	NA	NA	NA	NA
EX_cpd_cu2[e]	NA	NA	NA	NA	NA	NA	NA	NA	NA
EX_cpd_cytd[e]	NA	NA	NA	NA	NA	NA	NA	NA	NA
EX_cpd_dad-2[e]	NA	NA	NA	NA	NA	NA	NA	NA	NA
EX_cpd_damp[e]	NA	NA	NA	NA	NA	NA	NA	NA	NA
EX_cpd_dcmp[e]	NA	NA	NA	NA	NA	NA	NA	NA	NA
EX_cpd_dcyt[e]	NA	NA	NA	NA	NA	NA	NA	NA	NA
EX_cpd_dgmp[e]	NA	NA	NA	NA	NA	NA	NA	NA	NA

EX_cpd_dgsn[e]	NA	NA	NA	NA	NA	NA	NA	NA	NA
EX_cpd_dms[e]	NA	NA	NA	NA	NA	NA	NA	NA	NA
EX_cpd_dmso[e]	NA	NA	NA	NA	NA	NA	NA	NA	NA
EX_cpd_dna[e]	NA	NA	NA	NA	NA	NA	NA	NA	NA
EX_cpd_dodcan[e]	NA	NA	NA	NA	NA	NA	NA	NA	NA
EX_cpd_dtmp[e]	NA	NA	NA	NA	NA	NA	NA	NA	NA
EX_cpd_duri[e]	NA	NA	NA	NA	NA	NA	NA	NA	NA
EX_cpd_etoh[e]	NA	NA	NA	NA	NA	NA	NA	NA	NA
EX_cpd_fe2[e]	NA	NA	NA	NA	NA	NA	NA	NA	NA
EX_cpd_fe3[e]	NA	NA	NA	NA	NA	NA	NA	NA	NA
EX_cpd_for[e]	NA	NA	NA	NA	NA	NA	NA	NA	NA
EX_cpd_fum[e]	NA	NA	NA	NA	NA	NA	NA	NA	NA
EX_cpd_gal[e]	NA	NA	NA	NA	NA	NA	NA	NA	NA
EX_cpd_galactan[e]	NA	NA	NA	NA	NA	NA	NA	NA	NA
EX_cpd_glc-D[e]	NA	NA	NA	NA	NA	NA	NA	NA	NA

EX_cpd_gln-L[e]	NA	NA	NA	NA	NA	NA	NA	NA	NA
EX_cpd_glu-L[e]	NA	NA	NA	NA	NA	NA	NA	NA	NA
EX_cpd_gly-asp-L[e]	NA	NA	NA	NA	NA	NA	NA	NA	NA
EX_cpd_gly-glu-L[e]	NA	NA	NA	NA	NA	NA	NA	NA	NA
EX_cpd_gly[e]	NA	NA	NA	NA	NA	NA	NA	NA	NA
EX_cpd_glyc-R[e]	NA	NA	NA	NA	NA	NA	NA	NA	NA
EX_cpd_glyc[e]	NA	NA	NA	NA	NA	NA	NA	NA	NA
EX_cpd_glyclt[e]	NA	NA	NA	NA	NA	NA	NA	NA	NA
EX_cpd_h2o2[e]	NA	NA	NA	NA	NA	NA	NA	NA	NA
EX_cpd_h2o[e]	NA	NA	NA	NA	NA	NA	NA	NA	NA
EX_cpd_h2s[e]	NA	NA	NA	NA	NA	NA	NA	NA	NA
EX_cpd_h[e]	NA	NA	NA	NA	NA	NA	NA	NA	NA
EX_cpd_hdcan[e]	NA	NA	NA	NA	NA	NA	NA	NA	NA
EX_cpd_hxan[e]	NA	NA	NA	NA	NA	NA	NA	NA	NA
EX_cpd_ile-L[e]	NA	NA	NA	NA	NA	NA	NA	NA	NA

EX_cpd_indole[e]	NA	NA	NA	NA	NA	NA	NA	NA	NA
EX_cpd_ins[e]	NA	NA	NA	NA	NA	NA	NA	NA	NA
EX_cpd_k[e]	NA	NA	NA	NA	NA	NA	NA	NA	NA
EX_cpd_lac-D[e]	NA	NA	NA	NA	NA	NA	NA	NA	NA
EX_cpd_lac-L[e]	NA	NA	NA	NA	NA	NA	NA	NA	NA
EX_cpd_lami[e]	NA	NA	NA	NA	NA	NA	NA	NA	NA
EX_cpd_leu-L[e]	NA	NA	NA	NA	NA	NA	NA	NA	NA
EX_cpd_lys-L[e]	NA	NA	NA	NA	NA	NA	NA	NA	NA
EX_cpd_mal-L[e]	NA	NA	NA	NA	NA	NA	NA	NA	NA
EX_cpd_malt[e]	NA	NA	NA	NA	NA	NA	NA	NA	NA
EX_cpd_malthp[e]	NA	NA	NA	NA	NA	NA	NA	NA	NA
EX_cpd_malthx[e]	NA	NA	NA	NA	NA	NA	NA	NA	NA
EX_cpd_maltpt[e]	NA	NA	NA	NA	NA	NA	NA	NA	NA
EX_cpd_malttr[e]	NA	NA	NA	NA	NA	NA	NA	NA	NA
EX_cpd_malttttr[e]	NA	NA	NA	NA	NA	NA	NA	NA	NA

EX_cpd_met-L[e]	NA	NA	NA	NA	NA	NA	NA	NA	NA
EX_cpd_mg2[e]	NA	NA	NA	NA	NA	NA	NA	NA	NA
EX_cpd_mn2[e]	NA	NA	NA	NA	NA	NA	NA	NA	NA
EX_cpd_mn4o[e]	NA	NA	NA	NA	NA	NA	NA	NA	NA
EX_cpd_mobd[e]	NA	NA	NA	NA	NA	NA	NA	NA	NA
EX_cpd_na1[e]	NA	NA	NA	NA	NA	NA	NA	NA	NA
EX_cpd_nh4[e]	NA	NA	NA	NA	NA	NA	NA	NA	NA
EX_cpd_no2[e]	NA	NA	NA	NA	NA	NA	NA	NA	NA
EX_cpd_no3[e]	NA	NA	NA	NA	NA	NA	NA	NA	NA
EX_cpd_o2[e]	NA	NA	NA	NA	NA	NA	NA	NA	NA
EX_cpd_ocdcan[e]	NA	NA	NA	NA	NA	NA	NA	NA	NA
EX_cpd_panose[e]	NA	NA	NA	NA	NA	NA	NA	NA	NA
EX_cpd_pi[e]	NA	NA	NA	NA	NA	NA	NA	NA	NA
EX_cpd_pmcoa[e]	NA	NA	NA	NA	NA	NA	NA	NA	NA
EX_cpd_ppa[e]	NA	NA	NA	NA	NA	NA	NA	NA	NA

EX_cpd_pro-L[e]	NA	NA	NA	NA	NA	NA	NA	NA	NA
EX_cpd_ptrc[e]	NA	NA	NA	NA	NA	NA	NA	NA	NA
EX_cpd_pyr[e]	NA	NA	NA	NA	NA	NA	NA	NA	NA
EX_cpd_ser-L[e]	NA	NA	NA	NA	NA	NA	NA	NA	NA
EX_cpd_so3[e]	NA	NA	NA	NA	NA	NA	NA	NA	NA
EX_cpd_so4[e]	NA	NA	NA	NA	NA	NA	NA	NA	NA
EX_cpd_succ[e]	NA	NA	NA	NA	NA	NA	NA	NA	NA
EX_cpd_thr-L[e]	NA	NA	NA	NA	NA	NA	NA	NA	NA
EX_cpd_thym[e]	NA	NA	NA	NA	NA	NA	NA	NA	NA
EX_cpd_thymd[e]	NA	NA	NA	NA	NA	NA	NA	NA	NA
EX_cpd_tma[e]	NA	NA	NA	NA	NA	NA	NA	NA	NA
EX_cpd_tmao[e]	NA	NA	NA	NA	NA	NA	NA	NA	NA
EX_cpd_trp-L[e]	NA	NA	NA	NA	NA	NA	NA	NA	NA
EX_cpd_tsul[e]	NA	NA	NA	NA	NA	NA	NA	NA	NA
EX_cpd_ttdcan[e]	NA	NA	NA	NA	NA	NA	NA	NA	NA

EX_cpd_tttnt[e]	NA	NA	NA	NA	NA	NA	NA	NA	NA
EX_cpd_tyr-L[e]	NA	NA	NA	NA	NA	NA	NA	NA	NA
EX_cpd_ura[e]	NA	NA	NA	NA	NA	NA	NA	NA	NA
EX_cpd_urdio[e]	NA	NA	NA	NA	NA	NA	NA	NA	NA
EX_cpd_urea[e]	NA	NA	NA	NA	NA	NA	NA	NA	NA
EX_cpd_uri[e]	NA	NA	NA	NA	NA	NA	NA	NA	NA
EX_cpd_urnyl[e]	NA	NA	NA	NA	NA	NA	NA	NA	NA
EX_cpd_val-L[e]	NA	NA	NA	NA	NA	NA	NA	NA	NA
EX_cpd_xan[e]	NA	NA	NA	NA	NA	NA	NA	NA	NA
FAO4	-661.3492362	-490.1296282	171.2196079	-659.5412522	-530.5806134	128.9606387	-660.3838844	-521.8863305	138.4975538
FAO5	-780.071212	-583.8061372	196.2650748	-779.0976132	-632.0392383	147.0583749	-779.764697	-621.76502	157.999677
FAO6	-898.7931878	-677.4826461	221.3105418	-898.6539742	-733.4978632	165.156111	-899.1455097	-721.6437095	177.5018002
FAO7	-1000	-771.159155	228.840845	-1000	-834.9564881	165.0435119	-1000	-821.522399	178.477601
FBA	0	30.9618	30.9618	-7.7441	31.9849	39.729	0	32.1382	32.1382
FBP	-46.42415307	-10.70936098	35.71479209	-39.25749399	-8.623846272	30.63364772	-40.82810876	-7.675885041	33.15222372
FCLT	NA	NA	NA	NA	NA	NA	NA	NA	NA

FDH10	-112.3172064	-42.25655362	70.06065274	-113.7075485	-40.86621148	72.84133702	-114.3395237	-40.23423632	74.10528733
FDH9	-50.21740213	19.84325061	70.06065274	-51.60774427	21.23359275	72.84133702	-52.23971943	21.8655679	74.10528733
FE2abc	-88.2029433	-50.16118743	38.04175587	-75.81026765	-47.88988	27.92038765	-77.12831531	-46.85856514	30.26975017
FFSD	-59.20014374	-13.85580847	45.34433527	-60.94827692	-13.51842694	47.42984998	-61.7428829	-13.3650717	48.37781121
FGLU	-62.26147998	-14.90529122	47.35618876	-68.12269434	-14.56790969	53.55478466	-68.91730033	-14.41455445	54.50274589
FMETTRS	NA	NA	NA	NA	NA	NA	NA	NA	NA
FMNAT	NA	NA	NA	NA	NA	NA	NA	NA	NA
FMNRx	-41.28868886	4.157424104	45.44611296	-32.81140133	6.91760504	39.72900637	-34.07534963	8.172232738	42.24758237
FNOR	NA	NA	NA	NA	NA	NA	NA	NA	NA
FORt	-17.5152	17.5152	35.0304	0	18.2103	18.2103	0	18.5263	18.5263
FRD10	NA	NA	NA	NA	NA	NA	NA	NA	NA
FRD11	NA	NA	NA	NA	NA	NA	NA	NA	NA
FRTT	-126.9991073	-70.74932435	56.24978294	-128.3894504	-72.10427673	56.28517369	-129.0214246	-70.84498873	58.17643585
FRUK	-43.69473799	-6.355586327	37.33915166	-43.7502129	-6.492091391	37.25812151	-45.71705528	-5.663795892	40.05325939
FTHFD	-67.08738942	-37.04036571	30.0470237	-59.92933241	-33.58501321	26.3443192	-61.18396011	-32.01439843	29.16956167
FTHFL	-35.46107235	-1.00E-06	35.46107135	-26.3443202	-1.00E-06	26.3443192	-29.16956267	-1.00E-06	29.16956167
FUM	-3.7711	0	3.7711	-5.5193	0	5.5193	0	15.171	15.171

FUMACA	-96.03625586	-60.59017514	35.44608072	-97.78438903	-59.199832	38.58455703	-98.57899502	-58.56785785	40.01113717
G1PACT	-59.16242094	-2.555053442	56.6063675	-60.55276408	-8.990703121	51.56206096	-61.18473824	-7.498026557	53.68671168
G1PCT	-32.5559	16.4928	49.0487	-33.9462	15.1378	49.084	NA	NA	NA
G1PTMT	-29.19109902	19.85752813	49.04862715	NA	NA	NA	-31.21341631	19.76186375	50.97528006
G1SATi	-26.83700724	-1.00E-06	26.83700624	-27.53217881	-1.00E-06	27.53217781	-27.84816588	-1.00E-06	27.84816488
G35DP	-58.07579575	-19.3411765	38.73461926	-59.82392893	-21.74909049	38.07483844	-60.61853492	-20.9684214	39.65011352
G3PD2	5.658	55.476	49.818	3.7412	46.6766	42.9354	2.8699	48.448	45.5781
G3PD4	-5.174682239	56.90170096	62.0763832	NA	NA	NA	-7.196999533	59.9351769	67.13217644
G3PD8	-67.27448646	-5.198103261	62.0763832	NA	NA	NA	-69.29680376	-2.16462732	67.13217644
G5SD	-75.16082754	-6.816473634	68.34435391	-53.73382885	-3.509306552	50.2245223	-54.55725226	-2.006047787	52.55120448
G6PDA	-20.72409751	-1.00E-06	20.72409651	-21.40160843	-1.00E-06	21.40160743	-23.7761498	-1.00E-06	23.7761488
G6PDHy	-26.8753	0	26.8753	-28.7921	0	28.7921	-29.6634	15.6867	45.3501
GAL1PURI	NA	NA	NA	NA	NA	NA	-44.54677606	1.206259925	45.75303599
GALKr	-43.7896	2.6449	46.4345	-43.8451	2.5084	46.3535	-45.8119	3.3367	49.1486

GALU	-25.2044	0	25.2044	-26.5947	0	26.5947	-27.2267	0	27.2267
GAPD	1.5279	56.8304	55.3025	-3.3083	0	3.3083	-5.1949	0	5.1949
GARFT	-43.2905	0	43.2905	-44.6808	0	44.6808	-45.3128	0	45.3128
GBEZ	-61.04278936	46.835 0071	107.8777965	-48.09248616	52.60588793	100.6983741	-49.17520543	55.22901485	104.4042203
GCALDD	-91.97430444	-46.52819147	45.44611296	-94.73448537	-55.00547901	39.72900637	-95.98911307	-53.7415307	42.24758237
GGLUGABDH	-59.45888238	-1.656593335	57.80228905	-61.37570633	-11.15118402	50.2245223	-62.24699094	-9.695786458	52.55120448
GGLUGABH	-49.4686984	-2.112509635	47.35618876	-55.32991276	-1.775128103	53.55478466	-56.12451875	-1.621772861	54.50274589
GGLUPTS	-80.32164119	-12.87135107	67.45029012	-68.08691807	-5.709591384	62.37732668	-69.49490101	-4.598998318	64.89590269
GGTT	-126.9991073	-70.74932435	56.24978294	-128.3894504	-72.10427673	56.28517369	-129.0214246	-70.84498873	58.17643585
GHMT	0	29.968	29.968	0	31.3583	31.3583	0	31.9903	31.9903
GK1	-35.2302	0	35.2302	-35.2857	0	35.2857	-37.2525	0	37.2525
GLCGSD	-99.03446713	-11.4586487	87.57581843	NA	NA	NA	NA	NA	NA
GLCP	NA	NA	NA	20.77989025	96.26028678	75.48039654	16.50014981	101.1068892	84.60673934
GLCS1	-172.7609379	-46.1454648	126.6154731	-171.2551129	-41.61664534	129.6384675	-178.337153	-39.5580 9305	138.77906
GLCt2	-22.82117884	17.51516269	40.33634152	-23.72694459	19.59565182	43.32259641	-24.1386563	20.66326827	44.80192457

GLGC	-40.32378219	-8.790318722	31.53346347	-41.71412533	-10.84044268	30.87368265	-42.34609948	-9.897141754	32.44895773
GLNS	-66.3856216	-16.45049516	49.93512644	-54.13039313	-6.912853315	47.21753981	-55.52905546	-4.064331825	51.46472363
GLNTRS	NA	NA	NA	NA	NA	NA	NA	NA	NA
GLU5K	-4.974660059	34.41840202	39.39306208	-5.030134971	40.06777676	45.09791173	-6.996977353	40.80197274	47.79895009
GLUCYSL	-90.80132571	-23.35103559	67.45029012	-78.56660258	-16.1892759	62.37732668	-79.97458553	-15.07868283	64.89590269
GLUDx	5.7146	18.0405	12.3259	2.5761	23.9647	21.3886	1.1495	24.1087	22.9592
GLUN	NA	NA	NA	NA	NA	NA	-46.82626691	-5.654905646	41.17136126
GLUPRT	-113.7693612	-45.19371686	68.57564433	-120.3257471	-46.90645928	73.41928784	-121.4363402	-45.80980311	75.62653707
GLUR	0	16.4389	16.4389	0	17.1341	17.1341	0	17.4501	17.4501
GLUSy	-76.4636041	-11.52475596	64.93884815	-76.14126869	-8.912760444	67.22850825	-76.9646921	-7.725488756	69.23920335
GLUTRR	NA	NA	NA	NA	NA	NA	NA	NA	NA
GLUTRS	NA	NA	NA	NA	NA	NA	NA	NA	NA
GLUt2	-17.63187654	17.51516269	35.14703923	-22.65072348	-19.59565182	42.2463753	-23.06243519	20.66326827	43.72570346
GLUt4i	-22.9378907	35.03032637	57.96821707	-22.65072248	-36.42066951	59.07139199	-49.30327696	20.66326627	69.96654323
GLYAT	-6.0288	48.1845	54.2133	-7.4192	47.3397	54.7589	-7.6175	48.8323	56.4498
GLYBt4	-28.1272	35.0303	63.1575	-23.7269	-36.4207	60.1476	-50.3795	20.6633	71.0428

GLYCL	-26.15190162	43.67235329	69.82425491	-29.9855495	41.10176634	71.08731584	-31.72811873	42.50974928	74.23786801
GLYCLTDXR	NA	NA	NA	NA	NA	NA	NA	NA	NA
GLYCOGEN_SYNTHESIS	NA	NA	NA	NA	NA	NA	NA	NA	NA
GLYCRt2	NA	NA	NA	NA	NA	NA	-24.1387	20.6633	44.802
GLYC_T	-17.5152	17.5152	35.0304	-18.2103	18.2103	36.4206	-18.5263	18.5263	37.0526
GLYK	-47.34160038	-8.891361599	38.45023878	48.09224686	-9.027866164	39.06438069	-50.37507632	-8.199571165	42.17550515
GLYOX	-69.48562983	-16.94013878	52.54549106	-71.23376301	-16.60275725	54.63100576	-72.028369	-16.449402	55.578967
GLYTRS	NA	NA	NA	NA	NA	NA	NA	NA	NA
GLYt4	-22.5373686	35.03032637	57.56769497	-23.72694359	36.42066951	60.1476131	-50.37949806	20.66326627	71.04276434
GMHEPAT	-77.13125202	-38.39663276	38.73461926	-78.52159516	-40.44675672	38.07483844	-79.15356931	-39.50345579	39.65011352
GMHEPK	-37.89225339	-0.4591480359	37.43310536	-37.9477283	-0.5956531002	37.3520752	-39.91457069	-1.00E-06	39.91456969
GMHEPPA	-54.19584772	-8.623455483	45.57239223	-46.26694714	-6.537940774	39.72900637	-47.83756191	-5.589979543	42.24758237
GPDDA2	-74.42010677	-29.85888726	44.56121952	-76.86341152	-29.52150572	47.3419058	-77.97400459	-29.36815048	48.6058541
GPDDA4	-87.69864485	-43.13742534	44.56121952	-90.1419496	-42.8000438	47.3419058	-91.25254267	-42.64668856	48.6058541
GRTT	-126.9991073	-70.74932435	56.24978294	-128.3894504	-72.10427673	56.28517369	-129.0214246	-70.84498873	58.17643585

GSHPO	-439.9176093	-381.725301	58.19230829	NA	NA	NA	NA	NA	NA
GSNK	-48.47019354	-2.035683722	46.43450981	-48.52566845	-2.172188286	46.35348016	-50.49251083	-1.343892287	49.14861854
GTHRD	-0.5922	74.7252	75.3174	-2.1512	66.2836	68.4348	-2.8599	68.2176	71.0775
GTHRDH	-35.1797	17.3658	52.5455	-36.9278	17.7032	54.631	-37.7224	17.8565	55.5789
GTHS	-94.89262288	-27.63497768	67.2576452	-82.65789976	-18.38019667	64.27770308	-84.0658827	-16.71430707	67.35157562
GTPCI	-128.3719196	-75.82642857	52.54549106	-130.1200508	-75.48904703	54.63100376	-130.9146568	-75.33569179	55.578965
GTPCII	-149.6008027	-106.3940159	43.20678677	-152.3842348	-109.1597199	43.22451487	-155.716014	-108.5416827	47.17433133
GTPDPK	-67.36321284	-28.62859358	38.73461926	-68.75355598	-29.59677428	39.1567817	-69.38553013	-28.25617036	41.12935977
GUAD	0	31.7804	31.7804	0	32.0973	32.0973	0	32.2413	32.2413
GUAPRT	-61.11490721	-4.865124267	56.24978294	-62.50525035	-6.220076656	56.28517369	-63.1372245	-4.960788653	58.17643585
Growth	NA	NA	NA	NA	NA	NA	NA	NA	NA
H2Ot5	NA	NA	NA	NA	NA	NA	NA	NA	NA
HACD8	-10.4683	34.9778	45.4461	-13.2285	26.5005	39.729	-14.4831	27.7645	42.2476
HACOADr	-224.1081129	-178.6619999	45.44611296	-226.8682938	-187.1392875	39.72900637	-228.1229215	-185.8753392	42.24758237
HBZOPT	-126.3019814	-70.05219843	56.24978294	-127.6923245	-71.40715082	56.28517369	-128.3242987	-70.14786282	58.17643585
HCO3E	NA	NA	NA	NA	NA	NA	NA	NA	NA
HEMEOS	-116.2882875	-60.03850452	56.24978294	-117.6786306	-61.3934569	56.28517369	-118.3106048	-60.1341689	58.17643585

HEPTT	-126.9991073	-70.74932435	56.24978294	-128.3894504	-72.10427673	56.28517369	-129.0214246	-70.84498873	58.17643585
HEX1	-47.16708931	-7.933735285	39.23335402	-47.22256422	-8.070239349	39.15232487	-49.1894066	-7.241944435	41.94746225
HEXTT	-126.9991073	-70.74932435	56.24978294	-128.3894504	-72.10427673	56.28517369	-129.0214246	-70.84498873	58.17643585
HIBHR	-66.49906386	-24.2110825	42.28798136	-68.24719703	-23.1785294	45.06866764	-69.04180302	-22.70918708	46.33261594
HISD1	-26.39308829	12.34153097	38.73461926	-27.07059921	12.65840716	39.72900637	-29.44514058	12.80244179	42.24758237
HISTD	-58.45537709	-2.593478533	55.86189856	-63.28056739	-20.24322517	43.03734222	-65.47383571	-18.03131563	47.44252008
HISTP	-58.93037299	-13.35798076	45.57239223	-51.00147242	-11.27246605	39.72900637	-52.57208719	-10.32450482	42.24758237
HISTRS	NA	NA	NA	NA	NA	NA	NA	NA	NA
HMBS	-183.335903	-80.94291706	102.392986	-182.8870619	-78.60204219	104.2850197	-190.9493706	-77.53800816	113.4113625
HMGDx	-24.99871583	20.44739714	45.44611296	-27.75889676	-11.9701096	39.72900637	-29.0132446	-13.23405791	42.24758237
HMGL	-60.82791386	-8.282422802	52.54549106	NA	NA	NA	NA	NA	NA
HMGSs	-29.9953	22.5502	52.5455	NA	NA	NA	-30.486	25.0929	55.5789
HOXPRx	11.9305	57.3766	45.4461	NA	NA	NA	NA	NA	NA
HPPDO1	-515.1392119	-456.9469056	58.19230629	NA	NA	NA	NA	NA	NA
HPPK	-49.85763296	-11.12301371	38.73461926	-51.2479761	-12.0911944	39.1567817	-51.8795026	-10.7505059048	41.12935977

HPYRRx	-55.4164	-9.9703	45.4461	-46.9391	-7.2101	39.729	-48.203	-5.9555	42.2475
HPYRRy	-67.4669	-9.6646	57.8023	-57.9723	-7.7478	50.2245	-59.4277	-6.8765	52.5512
HSDy	0	57.6318	57.6318	0	48.1373	48.1373	0	49.5927	49.5927
HSK	-46.53006312	-0.09555330969	46.43450981	-46.58553803	-0.232057374	46.35348066	-48.55238042	-1.00E-06	48.55237942
HSST	-55.52934212	-13.24136076	42.28798136	-56.91968526	-11.85101762	45.06866764	-57.55165941	-11.21904347	46.33261594
HSTPT	-27.24489209	-1.00E-06	27.24489109	-28.63523522	-1.00E-06	28.63523422	-29.26720938	-1.00E-06	29.26720838
HTHBPD	-167.3353885	-132.3050611	35.03032737	-168.03056	-131.6098895	36.42067051	-168.3465471	-131.2939024	37.05264466
HXAD	-46.97359908	-0.8171336373	46.15646544	-48.72173226	-0.7333305271	47.98840173	-49.51633824	-0.6952382043	48.82110004
HXPRT	-53.40097816	-4.01068129	49.39029687	-56.85633066	-5.365633679	51.49069698	-58.42694544	-4.1063045675	54.32059976
ICDHxi	-39.57163894	-0.1230046588	39.44859235	-43.38478148	-2.0507043829	41.33403765	-45.11803009	-0.9974535719	44.12057652
ICDHy	-39.8773	8.6055	48.4828	-42.8471	0	42.8471	-44.197	0	44.197
ICHORSi	-16.54615623	-1.00E-06	16.54615523	-17.2413278	-1.00E-06	17.2413268	-17.5731487	-1.00E-06	17.5731387
ICL	-30.00764439	-1.00E-06	30.00764339	-28.06137378	-1.00E-06	28.06137278	-29.9497563	15.12098903	45.06896466
IG3PS	-133.9216826	-61.16602181	72.75566076	-140.4780685	-59.0805071	81.3975614	-141.5886616	-58.13254587	83.4561157

IGPDH	-65.43835926	-30.40803189	35.03032737	-66.13353083	-29.71286032	36.42067051	-66.44951791	-29.39687324	37.05264466
IGPS	-99.07502378	-46.52953472	52.54548906	-100.823157	-46.19215319	54.63100376	-101.6177649	-46.03879795	55.578967
ILEDH2	0	39.1945	39.1945	0	30.3389	30.3389	0	31.4309	31.4309
ILETA	-18.0405	23.0641	41.1046	-23.9647	24.4545	48.4192	-24.1087	25.0865	49.1952
ILETRS	NA	NA	NA	NA	NA	NA	NA	NA	NA
ILEt4	-28.12719299	35.03032637	63.15751936	-23.72694359	36.42066951	60.1476131	-50.37949806	20.66326627	71.04276434
IMPC	0	12.5319	12.5319	0	16.6581	16.6581	0	17.9128	17.9128
IMPD	-10.65567861	-1.00E-06	10.65567761	-13.41585955	-1.00E-06	13.41585855	-14.67048725	-1.00E-06	14.67048625
INDOLEt2	NA	NA	NA	NA	NA	NA	-24.1387	20.6633	44.802
INSK	-46.36477748	-6.789753743	39.57502374	-48.48526176	-6.926257807	41.55900395	-51.39074476	-6.097962308	45.29278246
IPDPS	-83.70651924	-38.26040628	45.44611296	-75.22923171	-35.50022534	39.72900637	-76.49318002	-34.24559764	42.24758237
IPMD	-10.43866729	-1.00E-06	10.43866629	-13.19884823	-1.00E-06	13.19884723	-14.45347593	-1.00E-06	14.45347493
IPPMIa	NA	NA	NA	NA	NA	NA	NA	NA	NA
IPPMIb	0	28.6112	28.6112	0	29.3064	29.3064	0	29.6224	29.6224
IPPS	-57.47428678	-1.00E-06	57.47428578	-58.86462992	-4.105791413	54.7588385	-59.49660407	-2.613114849	56.88348922
IZPN	2.787275112	37.81760249	35.03032737	2.092100355	38.51277406	36.42067051	1.776116473	38.82876114	37.05264466
KARA2i	-47.02924301	-1.00E-06	47.02924201	-37.53465233	-1.00E-06	37.53465133	-38.99004989	-1.00E-06	38.99004889

KAS15	-53.34169859	-1.00E-06	53.34169759	-55.78500334	-1.00E-06	55.78500234	-56.8955984	-1.00E-06	56.8955974
KAS16	NA	NA	NA	NA	NA	NA	NA	NA	NA
KDOPP	-56.48590758	-10.91351535	45.57239223	-48.55700701	-8.828000641	39.72900637	-50.12762178	-7.88003941	42.24758237
KDOPS	-99.86215002	-36.77459411	63.08755592	-82.60185315	-33.63611779	48.96573536	-83.53585548	-32.20953765	51.32631783
Kt2i	-27.92964436	-1.00E-06	27.92964336	-28.90137106	-1.00E-06	28.90137006	-29.34361358	-1.00E-06	29.34361258
Kt3	-10.61202931	23.5235991	34.13562841	-11.03321767	25.88880409	36.92202177	-11.22466693	27.09947045	38.32413738
LDH_Dir	-48.5755	-3.1294	45.4461	-40.0982	-0.3692	39.729	-41.3622	0.8854	42.2476
LEUTA	-12.7631	34.5931	47.3562	-21.8258	35.9834	57.8092	-23.3964	36.6154	60.0118
LEUTRS	NA	NA	NA	NA	NA	NA	NA	NA	NA
LEUt4	-28.12719299	35.03032637	63.15751936	-23.72694359	36.42066951	60.1476131	-50.37949806	20.66326627	71.04276434
LIPID_SYNTHESIS	NA	NA	NA	NA	NA	NA	NA	NA	NA
LLEUDr	5.2774	50.7235	45.4461	2.1389	41.8679	39.729	0.7123	42.9599	42.2476
LPADSS	-37.25045085	-1.00E-06	37.25044985	-38.64079399	-1.00E-06	38.64079299	-39.27276814	-1.00E-06	39.27276714
LPSSYN_core	NA	NA	NA	NA	NA	NA	NA	NA	NA
LPS_SYNTHESIS	NA	NA	NA	NA	NA	NA	NA	NA	NA
LYSTRS	NA	NA	NA	NA	NA	NA	NA	NA	NA
LYSt3	NA	NA	NA	-23.72694359	19.59565182	43.32259541	NA	NA	NA

MACPD	-62.61051106	-15.71899772	46.89151335	-64.35864424	-18.5406054	45.81803884	-65.15325223	-15.62981027	49.52344196
MALS	-64.26768347	-18.20857817	46.0591053	-65.65802661	-23.83069808	41.82732853	-62.93462817	-9.406511546	53.52811662
MAN1PT2	-27.50150076	35.58605515	63.08755592	-19.21481015	38.72453147	57.93934162	-20.62279309	40.15111161	60.7739047
MCITD	-35.13998591	-0.1096585406	35.03032737	NA	NA	NA	-36.15114456	0.9015001062	37.05264466
MCITS	-78.02632856	-18.22318351	59.80314504	-79.4166717	-16.1366881	63.27900289	-80.04864585	-15.1897070757	64.85893828
MCOATA	-36.8311	0	36.8311	-38.2214	0	38.2214	-38.8534	0	38.8534
MDH	21.6659	53.368	31.7021	17.8527	44.8907	27.038	3.907	42.7992	38.8922
MDRPD	-68.82602993	-33.79570256	35.03032737	-69.5212015	-33.10053099	36.42067051	-69.83718858	-32.78454392	37.05264466
ME2	-26.5493618	-1.00E-06	26.5493608	-30.57210896	-1.00E-06	30.57210796	-44.61309262	23.10906159	67.72215421
MEAMP1_GLU-ASP	-36.4166	10.0281	46.4447	-41.6381	10.3655	52.0036	-43.9839	10.5188	54.5027
MEAMP1_GLY-ASP	-32.4102	13.634	46.0442	-39.1084	13.9714	53.0798	-41.4542	14.1248	55.579
MEAMP1_GLY-GLU	-34.5909	7.1755	41.7664	-46.0419	7.5129	53.5548	-46.8365	7.6662	54.5027
MECDPDH	NA	NA	NA	NA	NA	NA	NA	NA	NA
MECDPS	NA	NA	NA	NA	NA	NA	NA	NA	NA
MEPCT	-81.74548876	-25.49570582	56.24978294	-83.1358319	-26.8506582	56.28517369	-83.76780605	-25.5913702	58.17643585

MET-LABC	-83.04350293	-34.68429585	48.35920708	-63.23766926	-32.07230033	31.16536893	-66.37889881	-30.88503015	35.49386867
METAT	-10.54206586	-1.00E-06	10.54206486	-3.308336855	-1.00E-06	3.308335855	-5.194938708	-1.00E-06	5.194937708
METGL	130.8151361	180.0918202	49.27668412	NA	NA	NA	126.2315033	173.6740233	47.44252008
METS	-197.7808822	-151.8218591	45.95902306	-192.2952863	-146.6183734	45.67691291	-194.9764942	-144.8162381	50.16025603
METTRS	NA	NA	NA	NA	NA	NA	NA	NA	NA
MGCH	-6.389072136	28.64125523	35.03032737	NA	NA	NA	NA	NA	NA
MGt3	6.557278194	25.24674965	18.68947146	6.27036433	27.72658876	21.45622443	6.142143179	29.00299512	22.86085194
MGt5	0	11.5835	11.5835	0	12.3168	12.3168	0	12.6491	12.6491
MI1PP	-78.93434857	-33.36195634	45.57239223	-71.005448	-31.27644163	39.72900637	-72.57606277	-30.3284804	42.24758237
MICITH	0.1083910332	35.1387184	35.03032737	-0.5867805365	35.8338997	36.4206751	-0.9027676136	36.1498705	37.0526466
MICITL	-29.8867	22.6587	52.5454	-27.9405	22.9961	50.9366	-29.8271	23.1495	52.9766
MLACI	-17.51516369	17.51516369	35.03032737	NA	NA	NA	NA	NA	NA
MLTS	NA	NA	NA	NA	NA	NA	NA	NA	NA
MLTSp	-58.71155731	-6.166066258	52.54549106	-60.45969049	-5.828684725	54.63100576	-61.25429648	-5.675329483	55.578967
MMSDHir	156.5228115	226.7417401	70.21892864	152.3722874	218.9596241	66.58733675	150.4856835	220.5395595	70.05387598
MNabc	-100.6286311	-34.68429785	65.94433321	-89.17288633	-29.30166721	59.87121912	-90.93495037	-26.61113776	64.3238126
MOAT3	NA	NA	NA	NA	NA	NA	NA	NA	NA

MOBDabc	-83.11462422	-41.58627238	41.52835184	-70.96375376	-39.24821423	31.71553953	-72.40985155	-38.18546053	34.22439102
MOHMT	-34.49307503	-1.00E-06	34.49307403	-35.88341817	-1.00E-06	35.88341717	-36.51539232	-1.00E-06	36.51539132
MTAN	-50.43636613	-1.00E-06	50.43636513	-52.18449931	-1.00E-06	52.18449831	-52.9791053	-1.00E-06	52.9791043
MTHFC	0	10.5131	10.5131	0	11.2082	11.2082	0	11.5242	11.5242
MTHFD	0	37.8675	37.8675	0	28.3729	28.3729	0	29.8283	29.8283
MTHFR2	-65.78456131	-20.33844834	45.44611296	-57.30727377	-17.57826741	39.72900637	-58.57122208	-16.32363971	42.24758237
MTHPTGHM	-217.7308218	-166.7884951	50.94232673	NA	NA	NA	NA	NA	NA
MTRI	-18.7369	0	18.7369	-19.432	0	19.432	-19.748	0	19.748
MTRK	-46.33188364	-1.00E-06	46.33188264	-46.38735855	-0.03387789075	46.35348066	-48.35420093	-1.00E-06	48.35419993
NADH11	NA	NA	NA	NA	NA	NA	NA	NA	NA
NADH12	-199.2645687	-160.2436775	39.02089122	-181.4222714	-157.4834966	23.93877485	-183.7335067	-156.2288689	27.50463783
NADH13	NA	NA	NA	NA	NA	NA	NA	NA	NA
NADH14	NA	NA	NA	NA	NA	NA	NA	NA	NA
NADH4	-21.55415177	23.8919612	45.44611296	-13.07686423	26.65214213	39.72900637	-14.34081254	27.90676983	42.24758237
NADK	-30.17185515	-1.00E-06	30.17185415	-31.59716786	-0.4317989278	31.16536893	-34.18666378	-1.00E-06	34.18666278

NADS1	-3.704292886	-1.00E-06	3.704291886	-3.308336855	-1.00E-06	3.308335855	-5.194938708	-1.00E-06	5.194937708
NAabcO	-90.01660075	-41.58743023	48.42917052	NA	NA	NA	NA	NA	NA
NAt3	-22.82117784	5.306014153	28.12719199	-23.72694359	-1.00E-06	23.72694259	2.00E-06	33.99012167	33.99011967
NAt3_2	-28.12719299	-1.00E-06	28.12719199	-29.24355293	1.385331556	30.62886849	-5.612331964	36.12706762	41.73939958
NAt9	0	47.4768	47.4768	0	49.4537	49.4537	0	33.9901	33.9901
NDPK1	-34.9251	0	34.9251	-34.9806	0	34.9806	-36.9474	0	36.9474
NDPK2	-37.9426	0	37.9426	-37.9981	0	37.9981	-39.965	0	39.965
NDPK3	-24.8224	0	24.8224	-24.8779	0	24.8779	-26.8448	0	26.8448
NDPK4	-24.3049	0	24.3049	-24.3604	0	24.3604	-26.3272	0	26.3272
NDPK5	-34.0476	12.3869	46.4345	-34.1031	12.2504	46.3535	-36.07	13.0787	49.1487
NDPK6	-27.7287	18.7058	46.4345	-27.7841	18.5693	46.3534	-29.751	19.3976	49.1486
NDPK7	-25.3033	21.1312	46.4345	-25.3588	20.9947	46.3535	-27.3257	21.823	49.1487
NDPK8	-26.6557	19.7788	46.4345	-26.7112	19.6423	46.3535	-28.6781	20.4706	49.1487
NH4t	0	16.9985	16.9985	0	17.6732	17.6732	0	17.9799	17.9799
NIt3	-9.9848	18.342	28.3268	-10.6547	20.5478	31.2025	-10.9581	21.6997	32.6578

NNAT	-63.60232926	-38.6785818	24.92374746	-63.9015448	-40.72870576	23.17283904	-66.10413373	-39.78540484	26.31872889
NNDPR	-74.61810095	-0.8531563203	73.76494463	-77.06140569	-2.565898746	74.49550695	-78.17200076	-1.469242578	76.70275818
NODOx	-98.24281995	-6.47274515	91.7700748	-87.81164724	3.902560225	91.71420746	-88.23616992	6.430412824	94.66658275
NODOy	-110.2933408	-6.1670 89891	104.1262509	-98.84486491	3.36485849	102.2097234	-99.46083685	5.509368002	104.9702049
NPHS	-102.5307822	-60.2428008	42.28798136	-104.2789153	-59.2102477	45.06866764	-105.0735213	-58.7490538	46.33261594
NTD1	-57.64438743	-12.0719952	45.57239223	-49.0625868	-9.986480489	39.07610631	-50.47520804	-9.038519257	41.43668878
NTD10	-28.33751391	-1.00E-06	28.33751291	-31.09603594	-1.00E-06	31.09603494	-33.60529134	-1.00E-06	33.60529034
NTD11	-54.30750188	-15.59459572	38.71290616	-46.3786013	-11.44407165	34.93452966	-47.94921608	-9.557469794	38.39174629
NTD12	-71.7369	-26.1646	45.5723	NA	NA	NA	NA	NA	NA
NTD2	-59.02978001	-13.45738778	45.57239223	-51.10087944	-11.37187307	39.72900637	-52.67149421	-10.42391184	42.24758237
NTD3	NA	NA	NA	NA	NA	NA	NA	NA	NA
NTD3_P	-61.30809679	-9.6572 91259	51.65080553	-58.89580455	-9.3554 19485	49.54038507	-60.56214396	-9.218205043	51.34393891
NTD4	-45.43521009	-7.8470 89399	37.58812069	-38.20148109	-5.76157469	32.4399064	-40.08808294	-4.813613459	35.27446948
NTD5	NA	NA	NA	NA	NA	NA	NA	NA	NA
NTD5_P	-54.24028367	-2.5894 7814	51.65080553	-51.82799143	-2.287606366	49.54038507	-53.49433084	-2.150391924	51.34393891
NTD6	NA	NA	NA	NA	NA	NA	NA	NA	NA

NTD6_P	-59.54120535	-7.890399819	51.65080553	-57.12891311	-7.588528046	49.54038507	-58.79525252	-7.451313604	51.34393891
NTD7	-46.25998817	-29.93223547	16.3277527	-37.22016268	-26.79375916	10.42640353	-38.47479038	-25.36717901	13.10761137
NTD8	NA	NA	NA	NA	NA	NA	NA	NA	NA
NTD8_P	-72.10905483	-20.4582493	51.65080553	-69.69676259	-20.15637752	49.54038507	-71.36310199	-20.01916308	51.34393891
NTD9	-59.0615719	-13.48917967	45.57239223	-51.13267133	-11.40366496	39.72900637	-52.7032861	-10.45570373	42.24758237
NTPP10	-92.38523199	-53.65061273	38.73461926	NA	NA	NA	-94.92797116	-55.27785764	39.65011352
NTPP11	-92.40247724	-64.23163595	28.1708413	NA	NA	NA	-94.94521641	-61.74840783	33.19680858
NTPP9	-68.19702115	-36.32188797	31.87513318	NA	NA	NA	-73.74341031	-37.94913288	35.79427743
NTR4	-217.7750121	-147.7143574	70.06065474	-219.1653553	-146.3240143	72.84134102	-219.7973294	-145.6920401	74.10528933
NTR5	-155.6752079	-85.61455317	70.06065474	-157.0655511	-84.22421003	72.84134102	-157.6975252	-83.59223588	74.10528933
O2t	-5.6468	0	5.6468	-7.7823	0	7.7823	-7.6832	0	7.6832
OAADC	-65.42474893	-24.37162348	41.05312545	-67.17288211	-22.5110298	44.66185231	-67.9674901	-12.3885231	55.578967
OBTFL	-38.00577141	-1.00E-06	38.00577041	-40.09128412	-1.00E-06	40.09128312	-41.03924535	-1.00E-06	41.03924435
OCBT	-60.1488	0	60.1488	-51.8621	0	51.8621	-53.2701	0	53.2701
OHPBAT	-12.3259	0	12.3259	-20.8156	36.9936	57.8092	-21.4476	38.5642	60.0118

OHPHM	-27.93756381	-1.00E-06	27.93756281	-22.45196798	-1.00E-06	22.45196698	-25.13317582	-1.00E-06	25.13317482
OIVD1i	-59.68569521	-1.00E-06	59.68569421	-60.90256903	-1.00E-06	60.90256803	-62.12329843	-1.00E-06	62.12329743
OIVD2	-54.00922691	16.20970173	70.21892864	-58.15975099	8.427585761	66.58733675	-60.04635484	10.00752115	70.05387598
OIVD3	-54.00908072	16.20984792	70.21892864	-58.15960479	8.427731951	66.58733675	-60.04620865	10.00766734	70.05387598
OMBZLM	-15.91200035	-1.00E-06	15.91199935	-10.42640453	-1.00E-06	10.42640353	-13.10761237	-1.00E-06	13.10761137
OMCDC	-47.7345582	-2.265566537	45.46899166	-51.54770074	-1.928185005	49.61951574	-53.28094935	-1.774829763	51.50611959
OMMBLHX	-220.3037822	-184.0532105	36.25057166	-214.1559222	-181.6280507	32.52787143	-216.5482768	-181.0727542	35.47552263
OMMBLHXAN	-148.7949854	-64.3480797	84.4469057	-120.2301896	-68.99171935	51.23847027	-126.3592935	-65.98520382	60.37408966
OMPDC	-40.84856599	-1.00E-06	40.84856499	-42.59669916	-1.00E-06	42.59669816	-43.39130715	-1.00E-06	43.39130615
OMPHHX	-220.3045561	-184.0539844	36.25057166	-214.1566961	-181.6288246	32.52787143	-216.5490507	-181.0735281	35.47552263
OMPHHXAN	-148.7957593	-64.3485358	84.4469057	-120.2309635	-68.99249323	51.23847027	-126.3600674	-65.98509787	60.37408866
OMP_AC	0	17.5152	17.5152	0	18.2103	18.2103	0	18.5263	18.5263
OMP_ACGAM	-14.3207	0	14.3207	-14.889	0	14.889	-15.1474	0	15.1474
OMP_ADN	-17.5152	17.5152	35.0304	-18.2103	18.2103	36.4206	NA	NA	NA

OMP_ALA-D	-17.5152	17.5152	35.0304	-18.2103	18.2103	36.4206	0	18.5263	18.5263
OMP_ALA-L	-17.5152	17.5152	35.0304	-18.2103	18.2103	36.4206	-18.5263	18.5263	37.0526
OMP_ASP-L	-17.5152	17.5152	35.0304	-18.2103	18.2103	36.4206	-18.5263	18.5263	37.0526
OMP_CA2	-22.2301	0	22.2301	-23.1124	0	23.1124	-23.5134	0	23.5134
OMP_CBL1	-17.5152	0	17.5152	-18.2103	0	18.2103	-18.5263	0	18.5263
OMP_CHITOB	-17.5152	17.5152	35.0304	-18.2103	18.2103	36.4206	-18.5263	18.5263	37.0526
OMP_CHOL	-17.5152	17.5152	35.0304	-18.2103	18.2103	36.4206	-18.5263	18.5263	37.0526
OMP_CIT	-17.5152	17.5152	35.0304	-18.2103	18.2103	36.4206	-18.5263	18.5263	37.0526
OMP_CL	-25.9567	0	25.9567	-27.1237	0	27.1237	-27.6536	0	27.6536
OMP_CO2	0	17.5152	17.5152	0	18.2103	18.2103	-18.5263	18.5263	37.0526
OMP_COBALT2	-10.612	0	10.612	-11.0332	0	11.0332	-11.2247	0	11.2247
OMP_CU2	-17.5152	0	17.5152	-18.2103	0	18.2103	-18.5263	0	18.5263
OMP_CYTD	-17.5152	17.5152	35.0304	-18.2103	18.2103	36.4206	NA	NA	NA
OMP_DAD-2	-17.5152	17.5152	35.0304	-18.2103	18.2103	36.4206	NA	NA	NA

OMP_DAMP	-17.5152	17.5152	35.0304	-18.2103	18.2103	36.4206	NA	NA	NA
OMP_DCMP	-17.5152	17.5152	35.0304	-18.2103	18.2103	36.4206	NA	NA	NA
OMP_DCYT	-17.5152	17.5152	35.0304	-18.2103	18.2103	36.4206	NA	NA	NA
OMP_DGMP	-17.5152	17.5152	35.0304	-18.2103	18.2103	36.4206	NA	NA	NA
OMP_DGSN	-17.5152	17.5152	35.0304	-18.2103	18.2103	36.4206	NA	NA	NA
OMP_DMS	-17.5152	17.5152	35.0304	-18.2103	18.2103	36.4206	-18.5263	18.5263	37.0526
OMP_DMSO	-17.5152	17.5152	35.0304	-18.2103	18.2103	36.4206	-18.5263	18.5263	37.0526
OMP_DODCA	-17.5152	17.5152	35.0304	-18.2103	18.2103	36.4206	-18.5263	18.5263	37.0526
OMP_DTMP	-17.5152	17.5152	35.0304	-18.2103	18.2103	36.4206	NA	NA	NA
OMP_DURI	-17.5152	17.5152	35.0304	-18.2103	18.2103	36.4206	NA	NA	NA
OMP_FE2	-7.9699	0	7.9699	-8.2862	0	8.2862	-8.43	0	8.43
OMP_FOR	-17.5152	17.5152	35.0304	0	18.2103	18.2103	0	18.5263	18.5263
OMP_FUM	-17.5152	17.5152	35.0304	-18.2103	18.2103	36.4206	-18.5263	18.5263	37.0526
OMP_GLU-L	-17.5152	17.5152	35.0304	-18.2103	18.2103	36.4206	-18.5263	18.5263	37.0526

OMP_GLY	-17.5152	17.5152	35.0304	-18.2103	18.2103	36.4206	-18.5263	18.5263	37.0526
OMP_GLY-ASP-L	-17.5152	17.5152	35.0304	-18.2103	18.2103	36.4206	-18.5263	18.5263	37.0526
OMP_GLY-GLU-L	-17.5152	17.5152	35.0304	-18.2103	18.2103	36.4206	-18.5263	18.5263	37.0526
OMP_GLYB	-17.5152	17.5152	35.0304	-18.2103	18.2103	36.4206	-18.5263	18.5263	37.0526
OMP_GLYCLT	-17.5152	17.5152	35.0304	-18.2103	18.2103	36.4206	-18.5263	18.5263	37.0526
OMP_GTHRD	-17.5152	17.5152	35.0304	-18.2103	18.2103	36.4206	-18.5263	18.5263	37.0526
OMP_H	NA	NA	NA	NA	NA	NA	NA	NA	NA
OMP_H2	-17.5152	17.5152	35.0304	-18.2103	18.2103	36.4206	-18.5263	18.5263	37.0526
OMP_H2O	NA	NA	NA	NA	NA	NA	NA	NA	NA
OMP_H2O2	-17.5152	17.5152	35.0304	-18.2103	18.2103	36.4206	-18.5263	18.5263	37.0526
OMP_H2S	-17.5152	17.5152	35.0304	-18.2103	18.2103	36.4206	-18.5263	18.5263	37.0526
OMP_HDCA	-17.5152	17.5152	35.0304	-18.2103	18.2103	36.4206	-18.5263	18.5263	37.0526
OMP_ILE-L	-17.5152	17.5152	35.0304	-18.2103	18.2103	36.4206	-18.5263	18.5263	37.0526
OMP_INDOLE	-17.5152	17.5152	35.0304	-18.2103	18.2103	36.4206	-18.5263	18.5263	37.0526
OMP_INOSHP	-17.5152	17.5152	35.0304	-18.2103	18.2103	36.4206	-18.5263	18.5263	37.0526

OMP_INOSPP1	-17.5152	17.5152	35.0304	-18.2103	18.2103	36.4206	-18.5263	18.5263	37.0526
OMP_K	-19.6578	0	19.6578	-20.438	0	20.438	-20.7927	0	20.7927
OMP_LAC-D	-17.5152	17.5152	35.0304	-18.2103	18.2103	36.4206	-18.5263	18.5263	37.0526
OMP_LAC-L	-17.5152	17.5152	35.0304	-18.2103	18.2103	36.4206	-18.5263	18.5263	37.0526
OMP_LEU-L	-17.5152	17.5152	35.0304	-18.2103	18.2103	36.4206	-18.5263	18.5263	37.0526
OMP_LYS-L	-17.5152	17.5152	35.0304	-18.2103	18.2103	36.4206	-18.5263	18.5263	37.0526
OMP_MAL-L	-17.5152	17.5152	35.0304	-18.2103	18.2103	36.4206	-18.5263	18.5263	37.0526
OMP_MET-L	-17.5152	17.5152	35.0304	-18.2103	18.2103	36.4206	-18.5263	18.5263	37.0526
OMP_MG2	-11.5835	0	11.5835	-12.3168	0	12.3168	-12.6491	0	12.6491
OMP_MN2	-17.5152	0	17.5152	-18.2103	0	18.2103	-18.5263	0	18.5263
OMP_MOBD	-10.6132	0	10.6132	-11.0344	0	11.0344	-11.2259	0	11.2259
OMP_NH4	0	16.9985	16.9985	0	17.6732	17.6732	0	17.9799	17.9799
OMP_NMN	-17.5152	17.5152	35.0304	-18.2103	18.2103	36.4206	-18.5263	18.5263	37.0526
OMP_NO2	-17.5152	17.5152	35.0304	-18.2103	18.2103	36.4206	-18.5263	18.5263	37.0526

OMP_NO3	-17.5152	17.5152	35.0304	-18.2103	18.2103	36.4206	-18.5263	18.5263	37.0526
OMP_O2	-5.6468	0	5.6468	-7.7823	0	7.7823	-7.6832	0	7.6832
OMP_OCDCA	-17.5152	17.5152	35.0304	-18.2103	18.2103	36.4206	-18.5263	18.5263	37.0526
OMP_PI	-16.6205	0	16.6205	-13.1197	0	13.1197	-14.2913	0	14.2913
OMP_PMCOA	-17.5152	0	17.5152	-18.2103	0	18.2103	-18.5263	0	18.5263
OMP_PPA	-17.5152	17.5152	35.0304	-18.2103	18.2103	36.4206	-18.5263	18.5263	37.0526
OMP_PRO-L	-17.5152	17.5152	35.0304	-18.2103	18.2103	36.4206	-18.5263	18.5263	37.0526
OMP_PTRC	-17.5152	17.5152	35.0304	-18.2103	18.2103	36.4206	-18.5263	18.5263	37.0526
OMP_PYR	-17.5152	17.5152	35.0304	-18.2103	18.2103	36.4206	-18.5263	18.5263	37.0526
OMP_SER-L	-17.5152	17.5152	35.0304	-18.2103	18.2103	36.4206	-18.5263	18.5263	37.0526
OMP_SO3	-17.5152	17.5152	35.0304	-18.2103	18.2103	36.4206	-18.5263	18.5263	37.0526
OMP_SO4	-25.2193	0	25.2193	-26.2202	0	26.2202	-26.6752	0	26.6752
OMP_SUCC	-17.5152	17.5152	35.0304	-18.2103	18.2103	36.4206	0	18.5263	18.5263
OMP_THR-L	-17.5152	17.5152	35.0304	-18.2103	18.2103	36.4206	-18.5263	18.5263	37.0526

OMP_THYMD	-17.5152	17.5152	35.0304	-18.2103	18.2103	36.4206	NA	NA	NA
OMP_TMA	-17.5152	17.5152	35.0304	-18.2103	18.2103	36.4206	-18.5263	18.5263	37.0526
OMP_TMAO	-17.5152	17.5152	35.0304	-18.2103	18.2103	36.4206	-18.5263	18.5263	37.0526
OMP_TRP-L	-17.5152	17.5152	35.0304	-18.2103	18.2103	36.4206	-18.5263	18.5263	37.0526
OMP_TSUL	-17.5152	17.5152	35.0304	-18.2103	18.2103	36.4206	-18.5263	18.5263	37.0526
OMP_TTDCA	-17.5152	17.5152	35.0304	-18.2103	18.2103	36.4206	-18.5263	18.5263	37.0526
OMP_TTTNT	-17.5152	17.5152	35.0304	-18.2103	18.2103	36.4206	-18.5263	18.5263	37.0526
OMP_TYR-L	-17.5152	17.5152	35.0304	-18.2103	18.2103	36.4206	-18.5263	18.5263	37.0526
OMP_URA	-17.5152	17.5152	35.0304	-18.2103	18.2103	36.4206	-18.5263	18.5263	37.0526
OMP_UREA	0	17.5152	17.5152	0	18.2103	18.2103	0	18.5263	18.5263
OMP_URI	-17.5152	17.5152	35.0304	-18.2103	18.2103	36.4206	NA	NA	NA
OMP_VAL-L	-17.5152	17.5152	35.0304	-18.2103	18.2103	36.4206	-18.5263	18.5263	37.0526
OMP_XAN	-17.5152	17.5152	35.0304	-18.2103	18.2103	36.4206	NA	NA	NA
OMP_na1	-28.8907	28.8907	57.7814	-30.0374	30.0374	60.0748	-30.5586	30.5586	61.1172

OPHBDC	-55.20370214	-2.658213084	52.54548906	-56.95183532	-2.320831552	54.63100376	-57.74644331	-2.16747631	55.578967
OPHHX	-221.9127433	-184.0590074	37.85373599	-221.9456507	-181.6338476	40.31180316	-221.9727846	-181.078551	40.89423359
OPHHXAN	-150.4039466	-64.35387653	86.05007003	-128.0199182	-68.99751618	59.022402	-131.7838013	-65.99100065	65.79280062
ORNCD	-58.0923	-19.3577	38.7346	-58.7698	-19.0408	39.729	-61.1444	-18.8968	42.2476
ORPT	31.8036	88.0534	56.2498	33.1585	89.4437	56.2852	31.8992	90.0757	58.1765
OXGDC2	-56.34518573	-1.00E-06	56.34518473	-62.92483116	-1.00E-06	62.92483016	-63.55680732	-1.00E-06	63.55680632
P5CD	-51.60428013	-11.34746946	40.25681067	-58.47754225	-19.824757	38.65278526	-59.73216995	-18.56080869	41.17136126
P5CR	-85.31878708	-27.51649803	57.80228905	-75.82419639	-25.59967409	50.2245223	-77.27959395	-24.72838948	52.55120448
PANTS	-109.7590089	-60.41322778	49.34578112	-112.2500295	-62.06093213	50.18909738	-113.3823116	-61.02920259	52.353109
PAP	-58.92288989	-13.35049766	45.57239223	-50.99398931	-11.26498295	39.72900637	-52.56460409	-10.31702172	42.24758237
PAPPT3	-22.68656852	-1.00E-06	22.68656752	-24.07691166	-1.00E-06	24.07691066	-24.70888581	-1.00E-06	24.70888481
PAPSR	NA	NA	NA	NA	NA	NA	NA	NA	NA
PASYN_WP2	NA	NA	NA	NA	NA	NA	NA	NA	NA
PDH	-59.39909981	0.1164649096	59.51556472	-60.86440586	-5.978408323	54.88599754	-61.53045607	-4.398472937	57.13198313
PDX5PO	-5.6468	0	5.6468	-6.0704	56.3428	62.4132	-6.2873	56.9748	63.2621
PDX5PS	-293.6012177	-219.6403632	73.96085445	-305.4901468	-226.0321361	79.45801073	-308.3153913	-223.8202265	84.49516474

PEPTIDOXe	NA	NA	NA	NA	NA	NA	NA	NA	NA
PEPTIDO_SYNTHESIS	NA	NA	NA	NA	NA	NA	NA	NA	NA
PERD	-10.4158	0	10.4158	-13.176	26.553	39.729	-14.4306	27.817	42.2476
PFL	-46.8513	0	46.8513	-40.4167	0	40.4167	-41.9094	0	41.9094
PGAMT	0	14.3184	14.3184	0	15.0136	15.0136	0	15.3295	15.3295
PGCD	12.4027505	57.84886346	45.44611296	13.92507738	44.00850305	30.08342567	11.25782844	45.27245136	34.01462291
PGDH	-40.83674873	19.9133052	60.75005393	-43.80653428	-1.00E-06	43.80653328	-45.1564398	25.09145276	70.24789256
PGDHY	-58.78049256	-23.75016519	35.03032737	-59.47566413	-23.05499362	36.42067051	-59.79165121	-22.73900655	37.05264466
PGI	0	12.858	12.858	0	13.5531	13.5531	0	13.8691	13.8691
PGK	-30.3344	16.1001	46.4345	-8.5648	0	8.5648	-10.2934	0	10.2934
PGL	-40.3257264	-5.295399029	35.03032737	-41.02089797	-4.600227459	36.42067051	-41.33688505	-4.284240382	37.05264466
PGLYCP	-83.44680607	-37.87441383	45.57239223	-75.51790549	-35.78889912	39.72900637	-77.08852027	-34.84093789	42.24758237
PGM	-12.1521	22.8782	35.0303	-8.5648	0	8.5648	-10.2934	0	10.2934
PGMT	0	10.314	10.314	0	11.0092	11.0092	0	11.3252	11.3252
PGPPH	-48.49752343	-10.90940273	37.58812069	-41.26379442	-8.823888025	32.4399064	-43.15039627	-7.875926794	35.27446948
PGSA	-9.5309	0	9.5309	-10.9212	0	10.9212	-11.5532	0	11.5532

PHE4MO	-459.4631406	-383.7556686	75.70747197	NA	NA	NA	NA	NA	NA
PHEAL	-33.97897042	4.755648838	38.73461926	-34.65648134	5.072525029	39.72900637	-37.03102271	5.21655966	42.24758237
PHEMEabc	-90.0166	-34.6843	55.3323	-78.1397	-32.0723	46.0674	NA	NA	NA
PHETA1	0	34.572	34.572	0	35.9624	35.9624	0	36.5944	36.5944
PHETRS	NA	NA	NA	NA	NA	NA	NA	NA	NA
PIabc	-89.12191623	-46.89344588	42.22847035	NA	NA	NA	NA	NA	NA
PIt6	-21.9265	0	21.9265	-13.1197	0	13.1197	-14.2913	0	14.2913
PMANM	-23.2768	11.7535	35.0303	NA	NA	NA	-24.2879	12.7647	37.0526
PMCOAt	0	17.5152	17.5152	0	18.2103	18.2103	0	18.5263	18.5263
PMDPHT	-58.66256958	-13.09017735	45.57239223	-50.733669	-11.00466264	39.72900637	-52.30428378	-10.05670141	42.24758237
PNTK	-35.30479657	-1.00E-06	35.30479557	-34.68074784	-1.00E-06	34.68074684	-36.33871584	-1.00E-06	36.33871484
PPA	-42.99057045	-18.20214884	24.78842161	-20.98517266	-14.36850095	6.616671711	-23.01580915	-12.62593373	10.38987542
PPAtNa	-28.1272	35.0303	63.1575	-23.7269	-36.4207	60.1476	-50.3795	20.6633	71.0428
PPBNGS	-115.2512853	-62.7057942	52.54549106	-115.5886668	-60.95766102	54.63100576	-115.742022	-60.16305503	55.578967
PPC	-70.73309089	-7.645536974	63.08755392	-53.47279402	-4.507060658	48.96573336	-54.40679685	-3.080478514	51.32631833

PPCDC	-59.45451867	-6.909029611	52.54548906	-61.20265184	-6.571648078	54.63100376	-61.99725983	-6.418292836	55.578967
PPCK	-54.31383623	9.635835268	63.9496715	-55.42227275	2.108215672	57.53048842	-57.86773604	3.516198612	61.38393466
PPM	0	9.0513	9.0513	0	9.7465	9.7465	0	10.0625	10.0625
PPM2	-16.926	0	16.926	-21.942	14.4787	36.4207	-22.258	14.7947	37.0527
PPNCL	-99.04676434	-11.13677554	87.9099888	-86.81204122	-7.303127656	79.50891356	-88.22002416	-5.560560436	82.65946372
PPND	-129.5634442	-66.60216957	62.9627465	-133.3765868	-75.4374714	57.93933962	-135.1098354	-74.33593067	60.7739047
PPNDH	-132.7949456	-80.24945658	52.54548906	-134.5430788	-79.91207505	54.63100376	-135.3376868	-79.75871981	55.578967
PPPGFUM	-156.2466059	-67.42352747	88.82307846	-151.1029657	-64.64284119	86.46012447	-157.0787583	-63.37889289	93.69986541
PPPGMEN	-3.079698886	137.0416106	140.1213095	-5.860385138	139.8222969	145.682682	-7.124333447	141.0862452	148.2105787
PPPGNO3	-551.3137532	-411.1924437	140.1213095	-554.0944394	-408.4117574	145.682682	-555.3583877	-407.1478091	148.2105787
PPPGO	-619.1996191	-575.6990659	43.50055322	-617.9079981	-569.8139297	48.09406845	-617.3574257	-568.7800142	48.57741145
PPS	-59.80161405	-13.81346847	45.98814558	-52.56788504	-17.42220532	35.14567972	-54.45448689	-14.98030693	39.47417996
PPTGSe	NA	NA	NA	NA	NA	NA	NA	NA	NA
PPTT	-126.9991073	-70.74932435	56.24978294	-128.3894504	-72.10427673	56.28517369	-129.0214246	-70.84498873	58.17643585
PRAGS	-87.37295473	-20.11530953	67.2576452	-75.1382316	-10.86052852	64.27770308	-76.54621454	-9.194638421	67.3515762

PRAIS	-104.2521281	-48.91982223	55.3323059	-92.37519505	-46.30782672	46.06736833	-93.94580982	-45.12055603	48.82525379
PRAIi	-22.88655267	-1.00E-06	22.88655167	-23.58172424	-1.00E-06	23.58172324	-23.89771132	-1.00E-06	23.89771032
PRAMPC	NA	NA	NA	NA	NA	NA	NA	NA	NA
PRASCS	-86.5678	-34.0226	52.5452	-75.386	-30.8841	44.5019	-77.2726	-29.4575	47.8151
PRATPP	-88.20068033	-49.46606107	38.73461926	-89.9488135	-51.87397507	38.07483844	-90.74341949	-51.09330598	39.65011352
PRFGS	-52.61041779	-1.00E-06	52.61041679	-45.54173746	-1.00E-06	45.54173646	-47.42833931	-1.00E-06	47.42833831
PRKIN	-49.43970088	-3.83482531	45.60487557	-49.49517579	-3.97129374	45.52384641	-51.46201817	-3.14303375	48.31898429
PRMICIi	-22.86047664	-1.00E-06	22.86047564	-23.55564821	-1.00E-06	23.55564721	-23.87163529	-1.00E-06	23.87163429
PRO1q	-161.0266299	-97.39119687	63.635433	-153.0519632	-96.00085373	57.051095	-154.7312244	-95.36887957	59.36234479
PROTRS	NA	NA	NA	NA	NA	NA	NA	NA	NA
PROT_SYNTHESIS	NA	NA	NA	NA	NA	NA	NA	NA	NA
PROt4	-28.12719299	35.03032637	63.15751936	-23.72694359	36.42066951	60.1476131	-50.37949806	20.66326627	71.04276434
PRPPS	-41.3736	-11.1028	30.2708	-42.764	-12.071	30.693	-43.396	-10.7304	32.6656
PSCVT	-71.1917	-8.1042	63.0875	-53.9314	-4.9657	48.9657	-54.8654	-3.5391	51.3263
PSD	-61.69031672	-9.14482766	52.54548906	-63.43844989	-8.807446127	54.63100376	-64.23305788	-8.654090885	55.578967

PSERT	-45.46206064	1.894128123	47.35618876	-46.85240378	10.95680964	57.80921342	-47.48437793	12.52742442	60.01180235
PSP_L	-53.12770627	-7.555314036	45.57239223	-45.19880569	-5.469799327	39.72900637	-46.76942047	-4.521838096	42.24758237
PSSA	-27.031	0	27.031	-28.4214	0	28.4214	-29.0533	0	29.0533
PSUDS	-42.67864851	1.40302139	44.0816699	-43.01603004	3.151154566	46.1671846	-43.16938528	3.945760556	47.11514584
PTAr	0	35.3173	35.3173	-20.6512	0	20.6512	-22.0778	0	22.0778
PTPATi	-97.29665296	-58.56946198	38.72719098	-98.69442437	-60.61958594	38.07483844	-99.32639853	-59.67628501	39.65011352
PUNP1	0	34.3486	34.3486	0	26.2205	26.2205	0	27.6285	27.6285
PUNP2	-13.3263	35.5841	48.9104	-16.4647	41.4746	57.9393	-17.8913	42.8826	60.7739
PUNP3	0	36.4987	36.4987	0	31.6206	31.6206	0	33.0286	33.0286
PUNP4	-7.0697	41.8407	48.9104	-10.2081	47.7312	57.9393	-11.6347	49.1392	60.7739
PUNP5	-20.325	34.1402	54.4652	-23.4635	26.0121	49.4756	-24.89	27.4201	52.3101
PUNP6	-17.0909	31.8195	48.9104	-20.2294	37.71	57.9394	-21.656	39.118	60.774
PUNP7	-19.4348	0	19.4348	-22.5733	0	22.5733	-23.9999	0	23.9999
PYAM5PO	-2.499874861	24.36639794	26.8662728	-2.905819012	62.8157879	65.72160691	-5.181272795	63.27580961	68.45708256
PYDXL5PSYN	-357.57978	-296.114616	61.46516398	-365.2325915	-295.3146211	69.91797046	-366.9428958	-292.0014391	74.94145672

PYK	-40.03025933	6.404250982	46.43451031	-32.86042927	-1.00E-06	32.86042827	-34.43104405	-1.00E-06	34.43104305
PYNP2	-22.3457	32.1194	54.4651	-25.4842	23.9913	49.4755	-26.9108	25.3993	52.3101
PYRt2	-22.8212	17.5152	40.3364	-23.7269	19.5957	43.3226	-24.1387	20.6633	44.802
QULNS	-255.8811691	-197.3191823	58.5619868	-252.1200476	-194.180706	57.93934162	-253.5280306	-192.7541259	60.7739047
RBFK	NA	NA	NA	NA	NA	NA	NA	NA	NA
RBFSa	-170.0349388	-106.9473829	63.08755592	-161.7482482	-103.8089065	57.93934162	-163.1562311	-102.3823264	60.7739047
RBFSb	-65.10866714	-1.00E-06	65.10866614	-66.49901028	-1.00E-06	66.49900928	-67.13098443	-1.00E-06	67.13098343
RBK	-53.63505168	-15.66436303	37.97068865	-53.69052659	-15.80086709	37.8896595	-55.65736898	-14.9725716	40.6847979738
RHCCE	-59.09636411	-15.49983186	43.59653226	-60.84449729	-14.10948872	46.73500857	-61.63910328	-13.47751456	48.1615858872
RIBabc	NA	NA	NA	NA	NA	NA	-79.7103	-30.885	48.8253
RNA_SYNTHESIS	NA	NA	NA	NA	NA	NA	NA	NA	NA
RNDR1	NA	NA	NA	NA	NA	NA	NA	NA	NA
RNDR2	NA	NA	NA	NA	NA	NA	NA	NA	NA
RNDR3	NA	NA	NA	NA	NA	NA	NA	NA	NA
RNDR4	NA	NA	NA	NA	NA	NA	NA	NA	NA
RNTR1	NA	NA	NA	NA	NA	NA	NA	NA	NA
RNTR2	NA	NA	NA	NA	NA	NA	NA	NA	NA
RNTR3	NA	NA	NA	NA	NA	NA	NA	NA	NA
RNTR4	NA	NA	NA	NA	NA	NA	NA	NA	NA
RPE	-19.0801	0	19.0801	-19.7753	0	19.7753	-20.0913	0	20.0913

RPI	-16.6855	0	16.6855	-17.3807	0	17.3807	-17.6967	0	17.6967
S7PI	-8.5138	0	8.5138	-9.2089	0	9.2089	-9.5249	0	9.5249
SADH	-153.3882467	-93.43417386	59.95407283	-155.1010586	-93.85338309	61.24767548	-160.0127752	-94.04393274	65.96884241
SADT2	-73.58330992	-1.00E-06	73.58330892	-62.70732181	-1.00E-06	62.70732081	-64.73291158	-1.00E-06	64.73291058
SDPDS	-28.14370013	-1.00E-06	28.14369913	-25.95665717	-1.00E-06	25.95665617	-27.84325903	-1.00E-06	27.84325803
SDPTA	0	24.532	24.532	0	25.9567	25.9567	0	27.5655	27.5655
SELNPS	NA	NA	NA	NA	NA	NA	NA	NA	NA
SERAT	-41.8223	0	41.8223	-43.2126	0	43.2126	-43.8446	0	43.8446
SERD_L	-64.09292616	-25.3583069	38.73461926	-64.77043708	-25.04143071	39.72900637	-67.14497545	-24.89739608	42.24757937
SERGLYX	-28.1947	36.2762	64.4709	-30.1125	37.6665	67.779	-30.7445	38.2985	69.043
SERTRS	NA	NA	NA	NA	NA	NA	NA	NA	NA
SERt4	-28.12719299	35.03032637	63.15751936	-23.72694359	36.42066951	60.1476131	-50.37949806	20.66326627	71.04276434
SERt6	-22.82117884	17.51516269	40.33634152	-23.72694459	19.59565182	43.32259641	-24.1386563	20.66326827	44.80192457
SFGTH	-67.5029	-14.9574	52.5455	-69.2511	-14.6201	54.631	-70.0457	-14.4667	55.579
SGDS	-37.28455502	10.07163374	47.35618876	-39.45136559	10.40901528	49.86038087	-41.33796744	10.56237052	51.90033796
SGSAD	-61.58958763	-16.14347467	45.44611296	-64.34976857	-24.6207622	39.72900637	-65.60439627	-23.3568139	42.24758237

SHCHCS2	-124.5353267	-37.92851671	86.60680997	-126.9786314	-36.89596361	90.08266782	-128.0892245	-36.42662129	91.6626032
SHCHD2	-33.01355822	-1.00E-06	33.01355722	-35.77373916	-1.00E-06	35.77373816	-37.02836686	-1.00E-06	37.02836586
SHCHF	NA	NA	NA	NA	NA	NA	NA	NA	NA
SHK3D	-78.8012	-20.9989	57.8023	-69.3066	-19.0821	50.2245	-70.762	-18.2108	52.5512
SHKK	-38.02374597	-1.00E-06	38.02374497	-38.07922088	-1.00E-06	38.07921988	-40.04606326	-1.00E-06	40.04606226
SHSL1	-100.4611916	-30.40053689	70.06065474	-98.15713098	-29.01019375	69.14693723	-99.881101	-28.3782196	71.5028814
SLCYSS	-670.2071914	-600.1465397	70.06065174	-671.5975376	-598.7561966	72.84134102	-672.2295117	-598.1242224	74.10528933
SO4t2	-30.52527797	-1.00E-06	30.52527697	-31.73681714	-1.00E-06	31.73681614	-32.28751676	-1.00E-06	32.28751576
SOD	66.32736294	112.6513248	46.32396184	62.53000498	124.943276	62.41327106	61.89803082	125.1601757	63.26214485
SOTA	-17.91525647	29.4409323	47.35618876	-26.97793798	30.83127544	57.80921342	-28.5485276	31.46324959	60.01180235
SPA	-28.19467666	38.47165977	66.66633643	-30.11248516	39.86200291	69.97448807	-30.7445931	40.49397707	71.23843638
SPMS	NA	NA	NA	NA	NA	NA	NA	NA	NA
SPRS	NA	NA	NA	NA	NA	NA	350.6392923	424.7445816	74.10528933
SSALx	-63.00136985	-17.55525689	45.44611296	-62.067147	-26.03254442	36.03460258	-64.4137056	-24.7685911	39.64517445
SUCBZL	-67.5605109 8	-21.5682377 3	45.9927324	-70.3419726	-22.5364184 3	47.8047788 2	-71.6051455 6	-21.1958145 1	50.4093310 5
SUCBZS	-72.4255304	-37.3952257	35.0303273 7	-73.1207246 1	-36.700054 1	36.4206705 1	-73.4367116 9	-36.3840670 2	37.0526446 6

SUCCtex	-22.821 17884	17.515 16269	40.336 34152	-23.726 94459	14.247 0801	37.974 02469	-24.138 6553	-1.00E-06	24.138 6543
SUCD7	-144.58 56983	-98.049 67566	46.536 02266	-136.61 10317	-99.300 7747	37.310 25698	-138.29 02928	-97.098 18577	41.192 10704
SUCOAS	-26.750 7	0	26.750 7	-14.515 9	0	14.515 9	-15.923 9	0	15.923 9
SUCP	-27.062 4	28.824	55.886 4	-30.200 9	20.537 3	50.738 2	-31.627 5	21.945 3	53.572 8
SUCRPTS	-89.751 24022	-19.690 58548	70.060 65474	-85.476 31296	-18.300 24234	67.176 07062	-87.520 90885	-17.668 26819	69.852 64066
SULR	NA	NA	NA	NA	NA	NA	NA	NA	NA
TAL	0	16.839 6	16.839 6	0	12.605	12.605	0	14.807 6	14.807 6
TDP3AAAT	-1.3723 05984	45.983 88278	47.356 18876	-2.7626 49124	55.046 5643	57.809 21342	-3.3946 23278	56.617 17907	60.011 80235
TDPDRE	-17.515 2	17.515 2	35.030 4	-18.210 3	18.210 3	36.420 6	-18.526 3	18.526 3	37.052 6
TDPDRR	-10.169 1	47.633 2	57.802 3	-12.085 9	38.138 6	50.224 5	-12.957 2	39.594	52.551 2
TDPGDH	-97.649 96124	-62.619 63387	35.030 32737	-98.345 13281	-61.924 4623	36.420 67051	-98.661 11989	-61.608 47522	37.052 64466
TDSK	NA	NA	NA	NA	NA	NA	NA	NA	NA
THD2	-21.333 47116	22.466 30442	43.799 77558	-13.803 85279	-1.00E-06	13.803 85179	-15.498 56081	-1.00E-06	15.498 55981
THD5	-22.466 30642	10.721 44085	33.187 74727	-11.033 21767	2.7706 34121	13.803 85179	-11.224 66693	4.2738 92885	15.498 55981
THDPS	-7.2576 54987	-1.00E-06	7.2576 53987	-8.6479 98126	-1.00E-06	8.6479 97126	-9.2799 7228	-1.00E-06	9.2799 7128
THMDt2	-22.821 17884	17.515 16269	40.336 34152	-23.726 94459	19.595 65182	43.322 59641	-24.138 6563	20.663 26827	44.801 92457

THRA	0	11.9253	11.9253	-42.3683	12.2627	54.631	-43.1629	7.6175	50.7804
THRD	-4.123101346	35.73318723	39.85628857	-12.47310667	27.25589969	39.72900637	-13.72773437	28.519848	42.24758237
THRD_L	-56.31473489	-23.16994003	33.14479487	-62.5820702	-22.85306384	39.72900637	-64.95661158	-22.70902921	42.24758237
THRHT	NA	NA	NA	-23.7269	19.5957	43.3226	0	20.6633	20.6633
THRLAD	-19.8496	9.5909	29.4405	-44.7027	9.9283	54.631	-45.4973	10.0816	55.5789
THRS	-65.13246849	-25.14990065	39.98256784	-57.20356791	-17.47456155	39.72900637	-58.31365878	-16.52660031	41.78705846
THRTRS	NA	NA	NA	NA	NA	NA	NA	NA	NA
THRt3	-17.23135445	17.51516269	34.74651713	NA	NA	NA	-24.1386563	4.273890885	28.41254718
THRt4	-28.12719299	29.44050198	57.56769497	-23.72694359	36.42066951	60.1476131	-33.99012067	-1.00E-06	33.99011967
THZPSN	-361.7855687	-235.6231543	126.1624144	-366.6721782	-236.6117435	130.0604347	-368.8933663	-235.2804161	133.6129502
TKT1	0	19.7747	19.7747	0	24.9094	24.9094	0	25.5413	25.5413
TKT2	0	16.8396	16.8396	0	18.23	18.23	0	18.8619	18.8619
TMAOR3e	NA	NA	NA	NA	NA	NA	NA	NA	NA
TMDK1	-53.29148176	-6.85697195	46.43450981	-53.34695668	-6.9934076015	46.35348066	-55.31379906	-6.1651680516	49.14861854
TMDPP	-14.9111	33.9993	48.9104	-18.0496	39.8898	57.9394	-19.4761	41.2978	60.7739

TMDS	-89.14713157	-19.08647683	70.06065474	-90.53747471	-17.69613369	72.84134102	-91.16944887	-17.06415954	74.10528933
TMPKr	-29.9467	0	29.9467	-30.0022	0	30.0022	-31.969	0	31.969
TMPPP	-55.71468461	-1.00E-06	55.71468361	-57.10502775	-0.8198540538	56.28517369	-57.7370019	-1.00E-06	57.7370009
TPI	0	23.4352	23.4352	3.2973	24.816	21.5187	1.4107	25.132	23.7213
TRACE_ELEMENTS	NA	NA	NA	NA	NA	NA	NA	NA	NA
TRDR	NA	NA	NA	NA	NA	NA	NA	NA	NA
TRE6PP	-59.9412375	-14.36884527	45.57239223	-52.01233692	-12.28333056	39.72900637	-53.5829517	-11.33536933	42.24758237
TREH	-50.26436007	2.281130988	52.54549106	-52.01249324	2.61851252	54.63100576	-52.80709923	2.771867762	55.578967
TREHtex	-79.70947919	-9.64882445	70.06065474	-75.43455193	-8.25848131	67.17607062	-77.47914782	-7.62607156	69.85264066
TRPOR	-430.2718187	-328.6076962	101.6641225	-430.4516761	-322.704415	107.7472611	-430.5572329	-321.115203	109.4420299
TRPS2	-63.02805512	-10.48256406	52.54549106	-63.36543665	-8.734430887	54.63100576	-63.51879189	-7.939824898	55.578967
TRPS3	-71.39800248	-19.53819439	51.85980809	-58.24413625	-18.51512989	39.72900637	-60.60935702	-18.36177465	42.24758237
TRPTRS	NA	NA	NA	NA	NA	NA	NA	NA	NA
TRPt6	NA	NA	NA	-23.7269	19.5957	43.3226	-24.1387	20.6633	44.802
TSULST	14.71628894	84.77694368	70.06065474	NA	NA	NA	12.69397165	86.79926097	74.10528933
TYRTA	NA	NA	NA	NA	NA	NA	NA	NA	NA
TYRTRS	NA	NA	NA	NA	NA	NA	NA	NA	NA

TYRt6	NA	NA	NA	-23.7269	19.5957	43.3226	-24.1387	20.6633	44.802
U23GAAT	-287.9337952	-217.8731405	70.06065474	-289.3241384	-216.4827973	72.84134102	-289.9561125	-215.8508232	74.10528933
UAAGDS	-91.0948136	-18.24734401	72.84746959	-78.86009048	-14.58238689	64.27770358	-80.26807342	-12.9164973	67.35157612
UAGAAT	-280.0932	-210.0326	70.0606	-281.4836	-208.6422	72.8414	-282.1155	-208.0102	74.1053
UAGCVT	-79.06563659	-15.97808068	63.08755592	-61.80534022	-12.83960436	48.96573586	-62.73934255	-11.41302422	51.32631833
UAGDP	-66.1319392	-9.882156259	56.24978294	-67.52228234	-11.23710865	56.28517369	-68.15425649	-9.977820644	58.17643585
UAGPT3	-39.98823527	-1.00E-06	39.98823427	-41.37857841	-1.00E-06	41.37857741	-42.01055256	-1.00E-06	42.01055156
UAMAGS	-86.45956788	-14.6883194	71.77124848	-74.22484476	-11.02336228	63.20148247	-75.6328277	-9.357472685	66.27535501
UAMAS	-87.61843941	-14.9189911	72.69944831	-75.38371628	-11.25403448	64.1296818	-76.79169922	-9.588144379	67.20355484
UAPGR	-88.03493344	-30.23264439	57.80228905	-78.54034275	-28.31582045	50.2245223	-79.99574032	-27.44453584	52.55120448
UDCPDP	-75.71351687	-30.14112464	45.57239223	-67.78461629	-28.05560993	39.72900637	-69.35523107	-27.1076487	42.24758237
UDCPDPS	-893.3867125	-688.6007406	204.7859719	-899.6432566	-704.3065607	195.336696	-902.4871403	-696.4441662	206.0429742
UDPG4E	-14.1867	0	14.1867	-14.8819	0	14.8819	-15.1979	0	15.1979
UDPHEXURI	NA	NA	NA	NA	NA	NA	-43.84312839	1.206260925	45.04938932

UGMDDS	-90.86917248	-18.02170289	72.84746959	-78.63444936	-14.35674578	64.27770358	-80.0424323	-12.69085618	67.35157612
UHGADA	-48.00225786	-1.00E-06	48.00225686	-49.75039404	-1.00E-06	49.75039304	-50.54500003	-1.00E-06	50.54499903
UMPK	-30.7861	0	30.7861	-30.8416	0	30.8416	-32.8084	0	32.8084
UNK3	-184.4116122	-144.0285222	40.38308994	-177.8730547	-134.9658407	42.90721402	-180.0756437	-133.395226	46.68041773
UPP3MT	NA	NA	NA	NA	NA	NA	NA	NA	NA
UPP3S	-260.0267694	-224.996442	35.03032737	-260.7219409	-224.3012704	36.42067051	-261.037928	-223.9852834	37.05264466
UPPDC1	-166.122969	-61.03199492	105.0909741	-171.029987	-61.7679835	109.2620035	-173.2604578	-62.10252376	111.157934
UPPRT	-53.5174603	2.73232264	56.24978294	-54.9078044	1.377370251	56.28517369	-55.5397776	2.636658254	58.17643585
UQOR	-234.2948941	-139.0196189	95.27527521	-217.8429399	-146.4502799	71.39266003	-188.0073946	-94.17331352	93.83408109
URAt6	-22.8212	17.5152	40.3364	-23.7269	19.5957	43.3226	-24.1387	20.6633	44.802
URCN	-23.3641684	11.66591053	35.03032737	-24.0595884	12.361 0821	36.42067051	-24.3757549	12.67706917	37.05264466
URHYDROX	-365.0867	-313.9938	51.0929	-355.2849	-307.7736	47.5113	-355.9712	-306.0404	49.9308
URIDK2	0	19.062	19.062	0	18.9255	18.9255	0	19.7538	19.7538
URIH	-48.1852	4.3603	52.5455	-49.9333	4.6977	54.631	-50.7279	4.851	55.5789
URIK1	-48.50198542	-2.06747511	46.43451031	-48.5574603 3	-2.203979674	46.35348066	-50.5243027 2	-1.375684174	49.14861854

URIK2	-48.50198442	21.45346521	69.95544964	-48.55745933	22.84380835	71.40126769	-50.52430172	23.47578251	74.00008422
URIK3	-46.26070877	23.79994597	70.06065474	-47.65105191	25.19028911	72.84134102	-48.28302607	25.82226326	74.10528933
URIt2	-22.82117884	17.51516269	40.33634152	-23.72694459	19.59565182	43.32259641	-24.1386563	20.66326827	44.80192457
USHD	-47.23801136	-1.00E-06	47.23801036	-48.98614454	-1.00E-06	48.98614354	-49.78075052	-1.00E-06	49.78074952
UreaExp	-17.5152	0	17.5152	-18.2103	0	18.2103	-18.5263	0	18.5263
VALALAMOB	-37.1834	29.4829	66.6663	-41.8201	30.8732	72.6933	-42.4521	31.5052	73.9573
VALDHr	0.6602	46.1063	45.4461	0	37.2507	37.2507	0	38.3427	38.3427
VALTA	-17.3803	29.9759	47.3562	-23.9647	31.3663	55.331	-24.1087	31.9982	56.1069
VALTRS	NA	NA	NA	NA	NA	NA	NA	NA	NA
VALt4	-30.46738506	38.89611935	69.36350441	-26.29680976	41.87145504	68.1682648	-50.59072322	26.97007614	77.56079936
WO4abc	-90.0166	-34.6843	55.3323	-78.1397	-32.0723	46.0674	-79.7103	-30.885	48.8253
XAND	-71.4291	-25.983	45.4461	-74.1893	-34.4603	39.729	-75.4439	-33.1963	42.2476
XANt	-17.5152	17.5152	35.0304	-18.2103	18.2103	36.4206	-18.5263	18.5263	37.0526
XPK	-75.08154939	-34.63655396	40.44499543	-70.16927479	-32.65947424	37.50980055	-72.53760242	-32.02750008	40.51010234

Data S2 Table C Reaction Fluxes Normalized by the biomass flux in each simulation

Reaction ID	4C Normalized Lower Bound	4C Normalized Upper Bound	15C Normalized Lower Bound	15C Normalized Upper Bound	20C Normalized Lower Bound	20C Normalized Upper Bound
2MAHMP	-0.000252	-0.000252	-0.000252	-0.000252	-0.000252	-0.000252
4HBASink	0.000252	0.000252	0.000252	0.000252	0.000252	0.000252
4HBTE	0	0	NA	NA	0	0
5DOAN	2.00E-06	2.00E-06	2.00E-06	2.00E-06	2.00E-06	2.00E-06
5DRIB_Sink	2.00E-06	2.00E-06	2.00E-06	2.00E-06	2.00E-06	2.00E-06
5HPUDICDCr	0	0	0	0	0	0
5HPUDICDCs	0	0	NA	NA	NA	NA
A5PISO	0.011934	0.011934	0.011934	0.011934	0.011934	0.011934
AACPS10	0	0	NA	NA	0	0
AACPS11	0	0	NA	NA	0	0
AACPS12	0	0	NA	NA	0	0
AACPS13	0	0	NA	NA	0	0
AACPS14	0	0	NA	NA	0	0
AACPS15	0	0	NA	NA	0	0
AACPS16	0	0	NA	NA	0	0
AACPS3	0	0	NA	NA	0	0
AACPS4	0	0	NA	NA	0	0
AACPS5	0	0	NA	NA	0	0
AACPS6	0	0	NA	NA	0	0
AACPS7	0	0	NA	NA	0	0
AACPS8	0	0	NA	NA	0	0
AACPS9	0	0	NA	NA	0	0
AACPSFA130OH	0	0	NA	NA	0	0
AACPSFA1718	0	0	NA	NA	0	0
AACPSFA1817	0	0	NA	NA	0	0
ABTA	0	0	0	0	0	0
ACACCB	0	0	0	0	0	0
ACACCT	0	0	0	0	0	0
ACACT10R	0	0	0	0	0	0
ACALDi	0	0	0	0	0	0.990343
ACBIPGT	0	0	NA	NA	NA	NA
ACCOAC	5.068387	5.068387	5.068387	5.068387	5.068387	5.068387
ACGAMK	45.160359	45.160359	19.628974	19.628974	53.547053	53.547053

ACGAt2	45.160359	45.160359	19.628974	19.628974	53.547053	53.547053
ACGK	0.376736	0.376736	0.376736	0.376736	0.376737	0.376737
ACGS	0.376736	0.376736	0.376736	0.376736	0.376737	0.376737
ACHBS	0.268394	0.268394	0.268394	0.268394	0.268394	0.268394
ACKr	111.500203	111.500203	31.889046	31.889046	122.364024	122.364024
ACLS	0.799812	0.799812	0.799812	0.799812	0.799812	0.799812
ACMAT1	0	0.661538	0	0.661538	0	0.661538
ACNAMS	0	0	0	0	0	0
ACOAD10	0	0	0	0	0	0
ACOAD8	NA	NA	NA	NA	0	0
ACOAD9	0	0	0	0	0	0
ACOATA	0	0.661538	0	0.661538	0	0.661538
ACODA	0.376736	0.376736	0.376736	0.376736	0.376737	0.376737
ACONT	2.336425	2.336425	1.832539	1.832539	0.842196	0.842196
ACOTA	-0.376736	-0.376736	-0.376736	-0.376736	-0.376737	-0.376737
ACPS1	0	0	0	0	0	0
ACPSc	0	0	0	0	0	0
ACS	0	0	0	0	0	0
ACt6	-157.211901	-157.211901	-52.06936	-52.06936	-176.462418	-176.462418
ADA	0	0	0	0	0	0
ADCL	0.000252	0.000252	0.000252	0.000252	0.000252	0.000252
ADCOBAK	0	0	NA	NA	NA	NA
ADCS	0.000252	0.000252	0.000252	0.000252	0.000252	0.000252
ADHMCYSSYN	0.001514	0.001514	0.001514	0.001514	0.001514	0.001514
ADK1	0	18.866261	0	13.852294	0	13.852294
ADK3	-8.58965	10.276611	-8.58965	5.262644	-8.58965	5.262644
ADK4	-0.503885	0	0	0	0	0
ADMDC	0.007633	0.007633	0.007633	0.007633	0.007633	0.007633
ADNCYC	0	0	0	0	0	0
ADNK1	0.00915	0.513035	0.00915	0.00915	0.00915	0.00915
ADNt2	0	0	0	0	0	0
ADPT	0	0	0	0	0	0
ADSK	0.150736	0.150736	0.150736	0.150736	0.150736	0.150736

ADSL1r	0.16639	0.16639	0.16639	0.16639	0.16639	0.16639
ADSL2r	0.150541	0.150541	0.150541	0.150541	0.150541	0.150541
ADSS	0.16639	0.16639	0.16639	0.16639	0.16639	0.16639
AGDC	45.160359	45.160359	19.628974	19.628974	53.547053	53.547053
AGMAHYD	0.045289	0.045289	0.045289	0.045289	0.045289	0.045289
AGPR	-0.376736	-0.376736	-0.376736	-0.376736	-0.376737	-0.376737
AHAI	0.799812	0.799812	0.799812	0.799812	0.799812	0.799812
AHCYSNS	0	0	0	0	0	0
AICART	0.238914	0.238914	0.238914	0.238914	0.238914	0.238914
AIRC2	0.150541	0.150541	0.150541	0.150541	0.150541	0.150541
AIRC3	-0.150541	-0.150541	-0.150541	-0.150541	-0.150541	-0.150541
AKGD	0	0	0	0	0	0
ALAALA	0.02772	0.02772	0.02772	0.02772	0.02772	0.02772
ALAD_L	0	0	0	0	0	0
ALAGLYX	1.494481	1.494481	0.990595	0.990595	0.000252	0.000252
ALAR	0.02772	0.02772	0.02772	0.02772	0.05544	0.05544
ALATA_D2	0	0	0	0	0	0
ALATA_L	-2.168105	4.01504	-1.664219	4.518673	-0.701596	5.509016
ALATA_L2	0	0	0	0	0	0
ALATRS	0.346091	0.346091	0.346091	0.346091	0.346091	0.346091
ALA_Dt4	0.02772	0.02772	0.02772	0.02772	0	0
ALAt4	0	0	0	0	0	0
ALCD2x	0	0	0	0	0	0
ALDD2x	0	0	0	0	NA	NA
ALLNRAC	0	0	0	0	0	0
ALLTC	0	0	NA	NA	NA	NA
ALLTN	0	0	0	0	0	0
AMAA	0	0	0	0	0	0
AMALT1	0	0	0	0	0	0
AMALT2	0	0	0	0	0	0
AMALT3	0	0	0	0	0	0
AMALT4	0	0	0	0	0	0
AMAOT	2.00E-06	2.00E-06	2.00E-06	2.00E-06	2.00E-06	2.00E-06
AMMQT7_2	0.000252	0.000252	0.000252	0.000252	0.000252	0.000252
AMOB_Sink	2.00E-06	2.00E-06	2.00E-06	2.00E-06	2.00E-06	2.00E-06
AMPMS2	0.000252	0.000252	0.000252	0.000252	0.000252	0.000252
AMPTASECG	0	0	NA	NA	0	0

AMPTASEPG	0	0	NA	NA	0	0
ANPRT	0.049387	0.049387	0.049387	0.049387	0.049387	0.049387
ANS1	0.049387	0.049387	0.049387	0.049387	0.049387	0.049387
AOXS	2.00E-06	2.00E-06	2.00E-06	2.00E-06	2.00E-06	2.00E-06
APRAUR	0.000505	0.000505	0.000505	0.000505	0.000505	0.000505
ARBABC	NA	NA	NA	NA	0	0
ARGDC	0.045289	0.045289	0.045289	0.045289	0.045289	0.045289
ARGSL	0.221268	0.221268	0.221268	0.221268	0.221268	0.221268
ARGSS	0.221268	0.221268	0.221268	0.221268	0.221268	0.221268
ARGTRS	0.175979	0.175979	0.175979	0.175979	0.175979	0.175979
ASAD	-0.35446	-0.35446	-0.858345	-0.858345	-1.848688	-1.848688
ASNN	0	0	NA	NA	0	0
ASNS1	0.175627	0.175627	0.175627	0.175627	0.175627	0.175627
ASNTRS	0.175627	0.175627	0.175627	0.175627	0.175627	0.175627
ASP1DC	0.000615	0.000615	0.000615	0.000615	0.000615	0.000615
ASPCT	0.141483	0.141483	0.141482	0.141482	0.141482	0.141482
ASPK	0.35446	0.35446	0.858345	0.858345	1.848688	1.848688
ASPO3	0	0.002579	0	0.002579	0	0.002579
ASPO5	0	0.002579	0	0.002579	0	0.002579
ASPO6	0	0	0	0	0	0
ASPO8	0	0	0	0	0	0
ASPO9	0	0	0	0.002579	0	0.002579
ASPTA1	-1.445588	-1.445588	-1.949474	-1.949474	-2.939817	-2.939817
ASPTA4	0	0	0	0	0	0
ASPTRS	0.232626	0.232626	0.232626	0.232626	0.232626	0.232626
ASPt2	0	0	0	0	0	0
AST	0	0	0	0	0	0
ATPM	25.173328	25.173328	3.877508	3.877508	84.468623	84.468623
ATPPRT	0.088373	0.088373	0.088373	0.088373	0.088373	0.088373
ATPS4r	0	0	-7.40024	-7.398726	0	0
BPNT	0.150736	0.150736	0.150736	0.150736	0.150736	0.150736
BTS4	2.00E-06	2.00E-06	2.00E-06	2.00E-06	2.00E-06	2.00E-06
BUTSUCCCOA	0	0	0	0	0	0
Biomass_WP2	1	1	1	1	1	1
C120SN	0.101504	0.101504	0.101504	0.101504	0.101504	0.101504
C130ISN	0.051761	0.051761	0.051761	0.051761	0.051761	0.051761
C130OHISN	0.012763	0.012763	0.012763	0.012763	0.012763	0.012763

C140ISN	0	0	0	0	0	0
C140SN	0.067949	0.067949	0.067949	0.067949	0.067949	0.067949
C150ISN	0.028362	0.028362	0.028362	0.028362	0.028362	0.028362
C150SN	0	0	0	0	0	0
C151SN	NA	NA	0	0	0	0
C160ISN	0	0	0	0	0	0
C160SN	0.09005	0.09005	0.09005	0.09005	0.09005	0.09005
C161SN	0.27086	0.27086	0.27086	0.27086	0.27086	0.27086
C170ISN	0	0	0	0	0	0
C170SN	0	0	0	0	0	0
C171SN	NA	NA	0	0	0	0
C171n8SN	0.011345	0.011345	0.011345	0.011345	0.011345	0.011345
C180SN	0.014181	0.014181	0.014181	0.014181	0.014181	0.014181
C181SN	NA	NA	0	0	0	0
C181n7SN	0.066651	0.066651	0.066651	0.066651	0.066651	0.066651
C205SN	0.050343	0.050343	0.050343	0.050343	0.050343	0.050343
C50SN	0	0	0	0	0	0
C60ISN	0	0	0	0	0	0
C70ISN	0.092886	0.092886	0.092886	0.092886	0.092886	0.092886
CAT	0.000126	0.000126	0	0	0	0
CBL1abc	0.000252	0.000252	0.000252	0.000252	0.000252	0.000252
CBLAT	0.000252	0.000252	0.000252	0.000252	0.000252	0.000252
CBPS	0.362751	0.362751	0.362751	0.362751	0.362751	0.362751
CDPG46D	0	0	0	0	0	0
CDPMEK	0.004471	0.004471	0.004471	0.004471	0.004471	0.004471
CHOLDH1	0	0	NA	NA	NA	NA
CHOLDH2	0	0	NA	NA	NA	NA
CHOLDH3	0	0	NA	NA	NA	NA
CHOLDH4	0	0	NA	NA	NA	NA
CHOLDH5	0	0	NA	NA	NA	NA
CHOLt4	0	0	0	0	0	0
CHORM	0.29381	0.29381	0.29381	0.29381	0.29381	0.29381
CHORS	0.344207	0.344207	0.344207	0.344207	0.344207	0.344207
CHRPL	0.000252	0.000252	0.000252	0.000252	0.000252	0.000252
CKDOAS	0.011934	0.011934	0.011934	0.011934	0.011934	0.011934
CO2t	-6.406695	-6.406695	-0.753705	-0.753705	0	0
COBALTt3	0	0	0	0	0	0
COBALTt5	-2.70E-05	-2.70E-05	-2.70E-05	-2.70E-05	-2.70E-05	-2.70E-05
CONFALDD	0	0	NA	NA	0	0
CPPPGO	0.000252	0.000252	0.000252	0.000252	0.000252	0.000252

CPPPGOAN	0	0	0	0	0	0
CS	2.336425	2.336425	1.832539	1.832539	0.842196	0.842196
CSND	0	0	0	0	0	0
CSNt2	0	0	0	0	0	0
CTPS2	0.067309	0.067309	0.067308	0.067308	0.067309	0.067309
CU2t	0.000763	0.000763	0.000763	0.000763	0.000763	0.000763
CYCPOe	0	0	NA	NA	NA	NA
CYOO2	0	0	0	0	0	0
CYOR7	0	0	0	0	0	0
CYSS	0.150736	0.150736	0.150736	0.150736	0.150736	0.150736
CYSTL	0.108051	0.108051	0.108051	0.108051	0.108051	0.108051
CYSTRS	0.041816	0.041816	0.041815	0.041815	0.041816	0.041816
CYTBD	1.63818	1.638937	2.020205	2.020962	5.008139	5.008139
CYTD	0	0	0	0	0	0
CYTDH	0	0	0	0	0	0
CYTDK1	0	0	0	0	0	0
CYTDK2	0	0	0	0	0	0
CYTDK3	0	0	0	0	0	0
CYTDt2	0	0	0	0	0	0
CYTK1	0.090071	0.090071	0.090071	0.090071	0.090071	0.090071
CYTK2	0	0	0	0	0	0
CampHydrolyase	0	0	0	0	0	0
Clt	0.005605	0.005605	0.005605	0.005605	0.005605	0.005605
DADA	0	0	0	0	0	0
DADK	-0.503885	0	0	0	0	0
DADNt2	0	0	0	0	0	0
DAGK	0	0	NA	NA	0	0
DAHPS	0.344207	0.344207	0.344207	0.344207	0.344207	0.344207
DAPDC	0.218689	0.218689	0.218689	0.218689	0.218689	0.218689
DAPE	0.246409	0.246409	0.246409	0.246409	0.246409	0.246409
DASYN	0.073667	0.073667	0.073667	0.073667	0.073667	0.073667
DB4PS	0.00101	0.00101	0.00101	0.00101	0.00101	0.00101
DBTSr	2.00E-06	2.00E-06	2.00E-06	2.00E-06	2.00E-06	2.00E-06
DCYTD	0	0	0	0	0	0
DCYTt2	0	0	0	0	0	0
DGK1	-0.503885	0	0	0	0	0
DHAD1	0.799812	0.799812	0.799812	0.799812	0.799812	0.799812
DHAD2	0.268394	0.268394	0.268394	0.268394	0.268394	0.268394
DHDPRy	0.246409	0.246409	0.246409	0.246409	0.246409	0.246409

DHDPS	0.246409	0.246409	0.246409	0.246409	0.246409	0.246409
DHFR	0.022996	0.022996	0.022996	0.022996	0.022996	0.022996
DHFS	0.000252	0.000252	0.000252	0.000252	0.000252	0.000252
DHNAOT7	0.000252	0.000252	0.000252	0.000252	0.000252	0.000252
DHNPA	0.000252	0.000252	0.000252	0.000252	0.000252	0.000252
DHORD2	0	0.141483	0	0.141482	0	0.141482
DHORD4i	0	0.141483	0	0.141482	0	0.141482
DHORD8	0	0	0	0.141482	0	0.141482
DHORTS	-0.141483	-0.141483	-0.141482	-0.141482	-0.141482	-0.141482
DHPPDA2	0.000505	0.000505	0.000505	0.000505	0.000505	0.000505
DHPRx	0	0	0	0	0	0
DHPS3	0.000252	0.000252	0.000252	0.000252	0.000252	0.000252
DHPTPE	0	0	0	0	0	0
DHQD1	0.344207	0.344207	0.344207	0.344207	0.344207	0.344207
DHQS	0.344207	0.344207	0.344207	0.344207	0.344207	0.344207
DKMPPD3	0.007633	0.007633	0.007633	0.007633	0.007633	0.007633
DMATT	0.000567	0.000567	0.000567	0.000567	0.000567	0.000567
DMOCT	0.011934	0.011934	0.011934	0.011934	0.011934	0.011934
DMPPS	0.000567	0.000567	0.000567	0.000567	0.000567	0.000567
DMQMT	0.000252	0.000252	0.000252	0.000252	0.000252	0.000252
DMSOR3e	0	0	0	0	0	0
DMSOR4e	0	0	0	0	0	0
DNA_SYNTHESIS	0.05	0.05	0.05	0.05	0.05	0.05
DNMPPA	0.000252	0.000252	0.000252	0.000252	0.000252	0.000252
DNTPPA	0.000252	0.000252	0.000252	0.000252	0.000252	0.000252
DPCOAK	0.000615	0.000615	0.000615	0.000615	0.000615	0.000615
DPR	0.000615	0.000615	0.000615	0.000615	0.000615	0.000615
DRBK	0	0	0	0	0	0
DRPA	0.503885	0.503885	0	0	0	0
DTMPK	0.022744	0.022744	0.022744	0.022744	0.022744	0.022744
DURIK1	0	0	0	0	0	0
DURIPP	0	0.503885	0	0	0	0
DURIt2	0	0	0	0	0	0
DUTPDP	0	0	0	0	0	0
DXPRI	0.004471	0.004471	0.004471	0.004471	0.004471	0.004471
DXPS	0.004975	0.004975	0.004723	0.004723	0.004723	0.004723
E4PD	0.000252	0.000252	0	0	0	0
ECOAH2C	0	0	0	0	0	0
ECOAH9	0	0	0	0	0	0
EDA	5.898494	11.21305	0	0	0	0

EDTXS5	0.011934	0.011934	0.011934	0.011934	0.011934	0.011934
EDTXS6	0.011934	0.011934	0.011934	0.011934	0.011934	0.011934
ENO	0	0	18.089124	18.089124	30.249697	30.249697
EPPP2	0	0	0	0	0	0
EX_cpd_CrOH3[e]	0	0	0	0	0	0
EX_cpd_ac[e]	157.211901	157.211901	52.06936	52.06936	176.462418	176.462418
EX_cpd_acgam[e]	-45.160359	-45.160359	-19.628974	-19.628974	-53.547053	-53.547053
EX_cpd_adn[e]	0	0	0	0	0	0
EX_cpd_akg[e]	0	0	0	0	0	0
EX_cpd_ala-D[e]	0	0	0	0	0.02772	0.02772
EX_cpd_ala-L[e]	0	0	0	0	0	0
EX_cpd_asn-L[e]	0	0	0	0	0	0
EX_cpd_asp-L[e]	0	0	0	0	0	0
EX_cpd_bgl[e]	0	0	0	0	0	0
EX_cpd_ca2[e]	-0.005605	-0.005605	-0.005605	-0.005605	-0.005605	-0.005605
EX_cpd_cbl1[e]	-0.000252	-0.000252	-0.000252	-0.000252	-0.000252	-0.000252
EX_cpd_chitin[e]	0	0	0	0	0	0
EX_cpd_cl[e]	-0.005605	-0.005605	-0.005605	-0.005605	-0.005605	-0.005605
EX_cpd_co2[e]	6.406695	6.406695	0.753705	0.753705	0	0
EX_cpd_cobalt2[e]	-2.70E-05	-2.70E-05	-2.70E-05	-2.70E-05	-2.70E-05	-2.70E-05
EX_cpd_cobalt3[e]	0	0	0	0	0	0
EX_cpd_cro4[e]	0	0	0	0	0	0
EX_cpd_cu2[e]	-0.000763	-0.000763	-0.000763	-0.000763	-0.000763	-0.000763
EX_cpd_cytd[e]	0	0	0	0	0	0
EX_cpd_dad-2[e]	0	0	0	0	0	0
EX_cpd_damp[e]	0	0	0	0	0	0
EX_cpd_dcmp[e]	0	0	0	0	0	0
EX_cpd_dcyt[e]	0	0	0	0	0	0
EX_cpd_dgmp[e]	0	0	0	0	0	0
EX_cpd_dgsn[e]	0	0	0	0	0	0
EX_cpd_dms[e]	0	0	0	0	0	0
EX_cpd_dmso[e]	0	0	0	0	0	0
EX_cpd_dna[e]	0	0	0	0	0	0

EX_cpd_dodcan[e]	0	0	0	0	0	0
EX_cpd_dtmp[e]	0	0	0	0	0	0
EX_cpd_duri[e]	0	0	0	0	0	0
EX_cpd_etoh[e]	0	0	0	0	0	0
EX_cpd_fe2[e]	-0.007735	-0.007735	-0.007735	-0.007735	-0.007735	-0.007735
EX_cpd_fe3[e]	0	0	0	0	0	0
EX_cpd_for[e]	0	0	11.686996	11.686996	9.937768	9.937768
EX_cpd_fum[e]	0	0	0	0	0	0
EX_cpd_gal[e]	0	0	0	0	0	0
EX_cpd_galactan[e]	0	0	0	0	0	0
EX_cpd_glc-D[e]	0	0	0	0	0	0
EX_cpd_gln-L[e]	0	0	0	0	0	0
EX_cpd_glu-L[e]	0	0	0	0	0	0
EX_cpd_gly-asp-L[e]	0	0	0	0	0	0
EX_cpd_gly-glu-L[e]	0	0	0	0	0	0
EX_cpd_gly[e]	0	0	0	0	0	0
EX_cpd_glyc-R[e]	0	0	0	0	0	0
EX_cpd_glyc[e]	0	0	0	0	0	0
EX_cpd_glyclt[e]	0	0	0	0	0	0
EX_cpd_h2o2[e]	0	0	0	0	0	0
EX_cpd_h2o[e]	-65.605843	-65.605843	-20.196064	-20.196064	-82.513634	-82.513634
EX_cpd_h2s[e]	0	0	0	0	0	0
EX_cpd_h[e]	105.511916	105.511916	37.587756	37.587756	138.830372	138.830372
EX_cpd_hdcan[e]	0	0	0	0	0	0
EX_cpd_hxan[e]	0	0	0	0	0	0
EX_cpd_ile-L[e]	0	0	0	0	0	0
EX_cpd_indole[e]	0	0	0	0	0	0
EX_cpd_ins[e]	0	0	0	0	0	0
EX_cpd_k[e]	-0.21017	-0.21017	-0.21017	-0.21017	-0.21017	-0.21017
EX_cpd_lac-D[e]	0	0	0	0	0	0
EX_cpd_lac-L[e]	0	0	0	0	0	0
EX_cpd_lami[e]	0	0	0	0	0	0
EX_cpd_leu-L[e]	0	0	0	0	0	0

EX_cpd_lys-L[e]	0	0	0	0	0	0
EX_cpd_mal-L[e]	0	0	0	0	0	0
EX_cpd_malt[e]	0	0	0	0	0	0
EX_cpd_malthp[e]	0	0	0	0	0	0
EX_cpd_malthx[e]	0	0	0	0	0	0
EX_cpd_maltpt[e]	0	0	0	0	0	0
EX_cpd_malttr[e]	0	0	0	0	0	0
EX_cpd_maltttr[e]	0	0	0	0	0	0
EX_cpd_met-L[e]	0	0	0	0	0	0
EX_cpd_mg2[e]	-0.009341	-0.009341	-0.009341	-0.009341	-0.009341	-0.009341
EX_cpd_mn2[e]	-0.000745	-0.000745	-0.000745	-0.000745	-0.000745	-0.000745
EX_cpd_mn4o[e]	0	0	0	0	0	0
EX_cpd_mobd[e]	-8.00E-06	-8.00E-06	-8.00E-06	-8.00E-06	-8.00E-06	-8.00E-06
EX_cpd_na1[e]	0	0	0	0	0	0
EX_cpd_nh4[e]	38.124593	38.124593	12.593208	12.593208	46.483567	46.483567
EX_cpd_no2[e]	0	0	0	0	0	0
EX_cpd_no3[e]	0	0	0	0	0	0
EX_cpd_o2[e]	-0.820226	-0.820226	-1.010734	-1.010734	-2.5047	-2.5047
EX_cpd_ocdcan[e]	0	0	0	0	0	0
EX_cpd_panose[e]	0	0	0	0	0	0
EX_cpd_pi[e]	-0.421062	-0.421062	-0.421062	-0.421062	-0.421062	-0.421062
EX_cpd_pmcoa[e]	-2.00E-06	-2.00E-06	-2.00E-06	-2.00E-06	-2.00E-06	-2.00E-06
EX_cpd_ppa[e]	0	0	0	0	0	0
EX_cpd_pro-L[e]	0	0	0	0	0	0
EX_cpd_ptrc[e]	0	0	0	0	0	0
EX_cpd_pyr[e]	0	0	0	0	0	0
EX_cpd_ser-L[e]	0	0	0	0	0	0
EX_cpd_so3[e]	0	0	0	0	0	0
EX_cpd_so4[e]	-0.155406	-0.155406	-0.155406	-0.155406	-0.155406	-0.155406
EX_cpd_succ[e]	0	0	0	0	6.244573	6.244573
EX_cpd_thr-L[e]	0	0	0	0	0	0
EX_cpd_thym[e]	0	0	0	0	0	0
EX_cpd_thymd[e]	0	0	0	0	0	0
EX_cpd_tma[e]	0	0	0	0	0	0
EX_cpd_tmao[e]	0	0	0	0	0	0

EX_cpd_trp-L[e]	0	0	0	0	0	0
EX_cpd_tsul[e]	0	0	0	0	0	0
EX_cpd_ttdcan[e]	0	0	0	0	0	0
EX_cpd_tttnt[e]	0	0	0	0	0	0
EX_cpd_tyr-L[e]	0	0	0	0	0	0
EX_cpd_ura[e]	0	0	0	0	0	0
EX_cpd_urdio[e]	0	0	0	0	0	0
EX_cpd_urea[e]	0.045289	0.045289	0.045289	0.045289	0.045289	0.045289
EX_cpd_uri[e]	0	0	0	0	0	0
EX_cpd_urnyl[e]	0	0	0	0	0	0
EX_cpd_val-L[e]	0	0	0	0	0	0
EX_cpd_xan[e]	0	0	0	0	0	0
FAO4	0	0	0	0	0	0
FAO5	0	0	0	0	0	0
FAO6	0	0	0	0	0	0
FAO7	0	0	0	0	0	0
FBA	-43.620508	-43.620508	0	0	-21.757506	-21.757506
FBP	43.620508	43.620508	0	0	21.757506	21.757506
FCLT	0.000252	0.000252	0.000252	0.000252	0.000252	0.000252
FDH10	0	0	0	0	0	0
FDH9	0	0	0	0	0	0
FE2abc	0.007735	0.007735	0.007735	0.007735	0.007735	0.007735
FFSD	0	0	0	0	0	0
FGLU	0	0	0	0	0	0
FMETTRS	0	0	0	0	0	0
FMNAT	0.000252	0.000252	0.000252	0.000252	0.000252	0.000252
FMNRx	0	0	0	0	0	0
FNOR	0	0	0	0	0	0
FORt	0	0	-11.686996	-11.686996	-9.937768	-9.937768
FRD10	0	0.14224	0	1.028151	6.099865	11.250243
FRD11	NA	NA	0	0.144062	0	0.144062
FRTT	0.000505	0.000505	0.000505	0.000505	0.000505	0.000505
FRUK	0	0.000505	0	0	0	0
FTHFD	0	0	0	0	0	0
FTHFL	1.079494	1.079494	1.079494	1.079494	1.079494	1.079494

FUM	2.032317	2.032317	1.528431	1.528431	-5.706485	-5.706485
FUMACA	0	0	0	0	0	0
G1PACT	0.079308	0.079308	0.079308	0.079308	0.079308	0.079308
G1PCT	0	0	0	0	NA	NA
G1PTMT	0	0	NA	NA	0	0
G1SATi	0.004038	0.004038	0.004038	0.004038	0.004038	0.004038
G35DP	0	0	0	0	0	0
G3PD2	-0.19153	-0.19153	-0.19153	-0.19153	-0.19153	-0.19153
G3PD4	0	0	NA	NA	0	0
G3PD8	0	0	NA	NA	0	0
G5SD	0	0	0	0	0	0
G6PDA	45.081051	45.081051	19.549666	19.549666	53.467745	53.467745
G6PDHy	11.21305	11.21305	0.165955	0.165955	0	0
GAL1PURI	NA	NA	NA	NA	0	0
GALKr	0	0	0	0	0	0
GALU	0.039197	0.039197	0.039197	0.039197	0.039197	0.039197
GAPD	0	0	18.089124	18.089124	30.249697	30.249697
GARFT	0.150793	0.150793	0.150793	0.150793	0.150793	0.150793
GBEZ	0	0	0	0	0	0
GCALDD	0.000252	0.000252	0.000252	0.000252	0.000252	0.000252
GGLUGABDH	0	0	0	0	0	0
GGLUGABH	0	0	0	0	0	0
GGLUPTS	0	0	0	0	0	0
GGTT	0.000505	0.000505	0.000505	0.000505	0.000505	0.000505
GHMT	-0.556611	-0.556611	-0.556611	-0.556611	-0.556611	-0.556611
GK1	0.072524	0.576409	0.072524	0.072524	0.072524	0.072524
GLCGSD	0	0	NA	NA	NA	NA
GLCP	NA	NA	0	0	0	0
GLCS1	0.115515	0.115515	0.115515	0.115515	0.115515	0.115515
GLCt2	0	0	0	0	0	0
GLGC	0.46206	0.46206	0.46206	0.46206	0.46206	0.46206
GLNS	1.229981	1.229981	1.230233	1.230233	1.230233	1.230233
GLNTRS	0.184695	0.184695	0.184695	0.184695	0.184695	0.184695
GLU5K	0	0	0	0	0	0
GLUCYSL	0	0	0	0	0	0
GLUDx	-6.183145	0	-6.182892	0	-6.210613	0

GLUN	NA	NA	NA	NA	0	0
GLUPRT	0.150793	0.150793	0.150793	0.150793	0.150793	0.150793
GLUR	-0.02772	-0.02772	-0.02772	-0.02772	-0.02772	-0.02772
GLUSy	0	0	0	0	0	0
GLUTRR	0.004038	0.004038	0.004038	0.004038	0.004038	0.004038
GLUTRS	0.252539	0.252539	0.252539	0.252539	0.252539	0.252539
GLUt2	0	0	0	0	0	0
GLUt4i	0	0	0	0	0	0
GLYAT	0	0	0	0	-0.990343	0
GLYBt4	0	0	0	0	0	0
GLYCL	0	0	0	0	0	0
GLYCLTDXR	0.000252	0.000252	0.000252	0.000252	0.000252	0.000252
GLYCOGEN_SYNTHESIS	0.077	0.077	0.077	0.077	0.077	0.077
GLYCRt2	NA	NA	NA	NA	0	0
GLYC_T	0	0	0	0	0	0
GLYK	0	0	0	0	0	0
GLYOX	0	0	0	0	0	0
GLYTRS	0.283191	0.283191	0.283191	0.283191	0.283191	0.283191
GLYt4	0	0	0	0	0	0
GMHEPAT	0.011934	0.011934	0.011934	0.011934	0.011934	0.011934
GMHEPK	0.011934	0.011934	0.011934	0.011934	0.011934	0.011934
GMHEPPA	0.011934	0.011934	0.011934	0.011934	0.011934	0.011934
GPDDA2	0	0	0	0	0	0
GPDDA4	0	0	0	0	0	0
GRTT	0.000567	0.000567	0.000567	0.000567	0.000567	0.000567
GSHPO	0	0	NA	NA	NA	NA
GSNK	0.072524	0.576409	0.072524	0.072524	0.072524	0.072524
GTHRD	0	0	0	0	0	0
GTHRDH	0	0	0	0	0	0
GTHS	0	0	0	0	0	0
GTPCI	0.000252	0.000252	0.000252	0.000252	0.000252	0.000252
GTPCII	0.000505	0.000505	0.000505	0.000505	0.000505	0.000505
GTPDPK	0	0	0	0	0	0
GUAD	-0.072524	-0.072524	-0.072524	-0.072524	-0.072524	-0.072524
GUAPRT	0	0	0	0	0	0
Growth	1	1	1	1	1	1
H2Ot5	65.605843	65.605843	20.196064	20.196064	82.513634	82.513634

HACD8	0	0	0	0	0	0
HACOADr	0	0	0	0	0	0
HBZOPT	0.000252	0.000252	0.000252	0.000252	0.000252	0.000252
HCO3E	5.581679	5.581679	5.581679	5.581679	5.581679	5.581679
HEMEOS	0	0	0	0	0	0
HEPTT	0.000252	0.000252	0.000252	0.000252	0.000252	0.000252
HEX1	0	0	0	0	0	0
HEXTT	0.000505	0.000505	0.000505	0.000505	0.000505	0.000505
HIBHR	0	0	0	0	0	0
HISD1	0	0	0	0	0	0
HISTD	0.088373	0.088373	0.088373	0.088373	0.088373	0.088373
HISTP	0.088373	0.088373	0.088373	0.088373	0.088373	0.088373
HISTRS	0.088373	0.088373	0.088373	0.088373	0.088373	0.088373
HMBS	0.000505	0.000505	0.000505	0.000505	0.000505	0.000505
HMGDx	0	0	0	0	0	0
HMGL	0	0	NA	NA	NA	NA
HMGSs	0	0	NA	NA	0	0
HOXPRx	0	0	NA	NA	NA	NA
HPPDO1	0	0	NA	NA	NA	NA
HPPK	0.000252	0.000252	0.000252	0.000252	0.000252	0.000252
HPYRRx	0	0	0	0	0	0
HPYRRy	0	0	0	0	0	0
HSDy	-0.108051	-0.108051	-0.611937	-0.611937	-1.60228	-1.60228
HSK	0	0	0.503885	0.503885	1.494229	1.494229
HSST	0.108051	0.108051	0.108051	0.108051	0.108051	0.108051
HSTPT	0.088373	0.088373	0.088373	0.088373	0.088373	0.088373
HTHBPD	0	0	0	0	0	0
HXAD	0	0	0	0	0	0
HXPRT	0	0	0	0	0	0
ICDHxi	0	9.795027	0	0	0	0
ICDHy	-8.952831	0.842196	0.842196	0.842196	0.842196	0.842196
ICHORSi	0.000252	0.000252	0.000252	0.000252	0.000252	0.000252
ICL	1.494229	1.494229	0.990343	0.990343	0	0
IG3PS	0.088373	0.088373	0.088373	0.088373	0.088373	0.088373
IGPDH	0.088373	0.088373	0.088373	0.088373	0.088373	0.088373
IGPS	0.049387	0.049387	0.049387	0.049387	0.049387	0.049387
ILEDH2	-6.183145	0	-6.182892	0	-6.210613	0

ILETA	-0.268394	5.914751	-0.268394	5.914498	-0.268394	5.942219
ILETRS	0.268394	0.268394	0.268394	0.268394	0.268394	0.268394
ILEt4	0	0	0	0	0	0
IMPC	-0.238914	-0.238914	-0.238914	-0.238914	-0.238914	-0.238914
IMPD	0.072524	0.072524	0.072524	0.072524	0.072524	0.072524
INDOLEt2	NA	NA	NA	NA	0	0
INSK	0	0	0	0	0	0
IPDPS	0.003904	0.003904	0.003904	0.003904	0.003904	0.003904
IPMD	0.526852	0.526852	0.526852	0.526852	0.526852	0.526852
IPPMIa	-0.526852	-0.526852	-0.526852	-0.526852	-0.526852	-0.526852
IPPMIb	-0.526852	-0.526852	-0.526852	-0.526852	-0.526852	-0.526852
IPPS	0.526852	0.526852	0.526852	0.526852	0.526852	0.526852
IZPN	0	0	0	0	0	0
KARA2i	0.268394	0.268394	0.268394	0.268394	0.268394	0.268394
KAS15	0	0.661538	0	0.661538	0	0.661538
KAS16	0.047735	0.047735	0.047735	0.047735	0.047735	0.047735
KDOPP	0.011934	0.011934	0.011934	0.011934	0.011934	0.011934
KDOPS	0.011934	0.011934	0.011934	0.011934	0.011934	0.011934
Kt2i	0.21017	4.728404	0.21017	0.21017	0.21017	0.21017
Kt3	0	4.518233	0	0	0	0
LDH_Dir	0	0	0	0	0	0
LEUTA	-0.433966	5.749179	-0.433966	5.748927	-0.433966	5.776647
LEUTRS	0.433966	0.433966	0.433966	0.433966	0.433966	0.433966
LEUt4	0	0	0	0	0	0
LIPID_SYNTHESIS	0.175	0.175	0.175	0.175	0.175	0.175
LLEUDr	-6.183145	0	-6.182892	0	-6.210613	0
LPADSS	0.011934	0.011934	0.011934	0.011934	0.011934	0.011934
LPSSYN_core	0.011934	0.011934	0.011934	0.011934	0.011934	0.011934
LPS_SYNTHESIS	0.034	0.034	0.034	0.034	0.034	0.034
LYSTRS	0.218689	0.218689	0.218689	0.218689	0.218689	0.218689
LYSt3	NA	NA	0	0	NA	NA
MACPD	0	0	0	0	0	0
MALS	0	0	0	0	0	0
MAN1PT2	0	0	0	0	0	0
MCITD	0	0	NA	NA	0	0

MCITS	0	0	0	0	0	0
MCOATA	5.068387	5.068387	5.068387	5.068387	5.068387	5.068387
MDH	0	0	0	0	-5.706485	-5.706485
MDRPD	0.007633	0.007633	0.007633	0.007633	0.007633	0.007633
ME2	2.032317	2.032317	1.528431	1.528431	0	0
MEAMP1_GLU-ASP	0	0	0	0	0	0
MEAMP1_GLY-ASP	0	0	0	0	0	0
MEAMP1_GLY-GLU	0	0	0	0	0	0
MECDPDH	0.004471	0.004471	0.004471	0.004471	0.004471	0.004471
MECDPS	0.004471	0.004471	0.004471	0.004471	0.004471	0.004471
MEPCT	0.004471	0.004471	0.004471	0.004471	0.004471	0.004471
MET-LABC	0	0	0	0	0	0
METAT	0.009404	0.009404	0.009404	0.009404	0.009404	0.009404
METGL	0	0	NA	NA	0	0
METS	0.109566	0.109566	0.109566	0.109566	0.109566	0.109566
METTRS	0.107797	0.107797	0.107796	0.107796	0.107796	0.107796
MGCH	0	0	NA	NA	NA	NA
MGt3	0	0	0	0	0	0
MGt5	-0.009341	-0.009341	-0.009341	-0.009341	-0.009341	-0.009341
MI1PP	0	0	0	0	0	0
MICITH	0	0	0	0	0	0
MICITL	0	0	0	0	0	0
MLACI	0	0	NA	NA	NA	NA
MLTS	0	0	NA	NA	NA	NA
MLTSp	0	0	0	0	0	0
MMSDHir	0	0	0	0	0	0
MNabc	0.000745	0.000745	0.000745	0.000745	0.000745	0.000745
MOAT3	0.011934	0.011934	0.011934	0.011934	0.011934	0.011934
MOBDabc	8.00E-06	8.00E-06	8.00E-06	8.00E-06	8.00E-06	8.00E-06
MOHMT	0.000615	0.000615	0.000615	0.000615	0.000615	0.000615
MTAN	0.007633	0.007633	0.007633	0.007633	0.007633	0.007633
MTHFC	-0.689787	-0.689787	-0.689787	-0.689787	-0.689787	-0.689787
MTHFD	-0.689787	-0.689787	-0.689787	-0.689787	-0.689787	-0.689787
MTHFR2	0.109818	0.109818	0.109818	0.109818	0.109818	0.109818
MTHPTGHM	0	0	NA	NA	NA	NA
MTRI	0.007633	0.007633	0.007633	0.007633	0.007633	0.007633
MTRK	0.007633	0.007633	0.007633	0.007633	0.007633	0.007633

NADH11	NA	NA	0	0.885911	0	5.008139
NADH12	0	0	0	0	0	0
NADH13	NA	NA	0	0.885911	6.099865	11.108003
NADH14	0	0	0	0	0	0
NADH4	0	0	0	0	0	0
NADK	0.000506	0.000506	0.000506	0.000506	0.000506	0.000506
NADS1	0.002579	0.002579	0.002579	0.002579	0.002579	0.002579
NAabcO	0	0	NA	NA	NA	NA
NAt3	0	4.540349	0.022115	0.022115	0	0
NAt3_2	0	3.026899	0	0	0	0
NAt9	-0.005605	-0.005605	-0.005605	-0.005605	-0.005605	-0.005605
NDPK1	0	18.866261	0	13.852294	0	13.852294
NDPK2	0.233848	0.760477	0.233848	0.256592	0.233848	0.256592
NDPK3	0.06209	0.090686	0.06209	0.090686	0.06209	0.090686
NDPK4	0.022744	0.022744	0.022744	0.022744	0.022744	0.022744
NDPK5	-0.503885	0.028596	0	0.028596	0	0.028596
NDPK6	-0.526629	0	-0.022744	0	-0.022744	0
NDPK7	0	0.028596	0	0.028596	0	0.028596
NDPK8	-0.503885	0.022744	0	0.022744	0	0.022744
NH4t	-38.124593	-38.124593	-12.593208	-12.593208	-46.483567	-46.483567
NIt3	0	0	0	0	0	0
NNAT	0.002579	0.002579	0.002579	0.002579	0.002579	0.002579
NNDPR	0.002579	0.002579	0.002579	0.002579	0.002579	0.002579
NODOx	0	0	0	0	0	0
NODOy	0	0	0	0	0	0
NPHS	0.000252	0.000252	0.000252	0.000252	0.000252	0.000252
NTD1	0	0.503885	0	0	0	0
NTD10	0.072524	0.072524	0.072524	0.072524	0.072524	0.072524
NTD11	0	0	0	0	0	0
NTD12	0	0	NA	NA	NA	NA
NTD2	0	0	0	0	0	0
NTD3	0	0	0	0	0	0
NTD3_P	0	0	0	0	0	0

NTD4	0	0	0	0	0	0
NTD5	0	0	0	0	0	0
NTD5_P	0	0	0	0	0	0
NTD6	0	0.503885	0	0	0	0
NTD6_P	0	0	0	0	0	0
NTD7	0	0	0	0	0	0
NTD8	0	0.503885	0	0	0	0
NTD8_P	0	0	0	0	0	0
NTD9	0	0	0	0	0	0
NTPP10	0	0	NA	NA	0	0
NTPP11	0	0	NA	NA	0	0
NTPP9	0	0	NA	NA	0	0
NTR4	0	0	0	0	0	0
NTR5	0	0	0	0	0	0
O2t	0.820226	0.820226	1.010734	1.010734	2.5047	2.5047
OAADC	0	0	0	0	0	0
OBTFL	0.011345	0.011345	0.011345	0.011345	0.011345	0.011345
OCBT	0.221268	0.221268	0.221268	0.221268	0.221268	0.221268
OHPBAT	0.000252	0.000252	0	0	0	0
OHPHM	0.000252	0.000252	0.000252	0.000252	0.000252	0.000252
OIVD1i	0.092886	0.092886	0.092886	0.092886	0.092886	0.092886
OIVD2	0	0	0	0	0	0
OIVD3	0	0	0	0	0	0
OMBZLM	0.000252	0.000252	0.000252	0.000252	0.000252	0.000252
OMCDC	0.526852	0.526852	0.526852	0.526852	0.526852	0.526852
OMMBLHX	0.000252	0.000252	0	0.000252	0.000252	0.000252
OMMBLHXAN	0	0	0	0.000252	0	0
OMPDC	0.141483	0.141483	0.141482	0.141482	0.141482	0.141482
OMPHHX	0.000252	0.000252	0	0.000252	0.000252	0.000252
OMPHHXAN	0	0	0	0.000252	0	0
OMP_AC	-157.211901	-157.211901	-52.06936	-52.06936	-176.462418	-176.462418
OMP_ACGAM	45.160359	45.160359	19.628974	19.628974	53.547053	53.547053
OMP_ADN	0	0	0	0	NA	NA
OMP_ALA-D	0	0	0	0	-0.02772	-0.02772
OMP_ALA-L	0	0	0	0	0	0
OMP_ASP-L	0	0	0	0	0	0
OMP_CA2	0.005605	0.005605	0.005605	0.005605	0.005605	0.005605
OMP_CBL1	0.000252	0.000252	0.000252	0.000252	0.000252	0.000252

OMP_CHITOB	0	0	0	0	0	0
OMP_CHOL	0	0	0	0	0	0
OMP_CIT	0	0	0	0	0	0
OMP_CL	0.005605	0.005605	0.005605	0.005605	0.005605	0.005605
OMP_CO2	-6.406695	-6.406695	-0.753705	-0.753705	0	0
OMP_COBALT2	2.70E-05	2.70E-05	2.70E-05	2.70E-05	2.70E-05	2.70E-05
OMP_CU2	0.000763	0.000763	0.000763	0.000763	0.000763	0.000763
OMP_CYTD	0	0	0	0	NA	NA
OMP_DAD-2	0	0	0	0	NA	NA
OMP_DAMP	0	0	0	0	NA	NA
OMP_DCMP	0	0	0	0	NA	NA
OMP_DCYT	0	0	0	0	NA	NA
OMP_DGMP	0	0	0	0	NA	NA
OMP_DGSN	0	0	0	0	NA	NA
OMP_DMS	0	0	0	0	0	0
OMP_DMSO	0	0	0	0	0	0
OMP_DODCA	0	0	0	0	0	0
OMP_DTMP	0	0	0	0	NA	NA
OMP_DURI	0	0	0	0	NA	NA
OMP_FE2	0.007735	0.007735	0.007735	0.007735	0.007735	0.007735
OMP_FOR	0	0	-11.686996	-11.686996	-9.937768	-9.937768
OMP_FUM	0	0	0	0	0	0
OMP_GLU-L	0	0	0	0	0	0
OMP_GLY	0	0	0	0	0	0
OMP_GLY-ASP-L	0	0	0	0	0	0
OMP_GLY-GLU-L	0	0	0	0	0	0
OMP_GLYB	0	0	0	0	0	0
OMP_GLYCLT	0	0	0	0	0	0
OMP_GTHRD	0	0	0	0	0	0
OMP_H	-105.511916	-105.511916	-37.587756	-37.587756	-138.830372	-138.830372
OMP_H2	0	0	0	0	0	0
OMP_H2O	65.605843	65.605843	20.196064	20.196064	82.513634	82.513634
OMP_H2O2	0	0	0	0	0	0
OMP_H2S	0	0	0	0	0	0
OMP_HDCA	0	0	0	0	0	0

OMP_ILE-L	0	0	0	0	0	0
OMP_INDOLE	0	0	0	0	0	0
OMP_INOSHP	0	0	0	0	0	0
OMP_INOSPP1	0	0	0	0	0	0
OMP_K	0.21017	0.21017	0.21017	0.21017	0.21017	0.21017
OMP_LAC-D	0	0	0	0	0	0
OMP_LAC-L	0	0	0	0	0	0
OMP_LEU-L	0	0	0	0	0	0
OMP_LYS-L	0	0	0	0	0	0
OMP_MAL-L	0	0	0	0	0	0
OMP_MET-L	0	0	0	0	0	0
OMP_MG2	0.009341	0.009341	0.009341	0.009341	0.009341	0.009341
OMP_MN2	0.000745	0.000745	0.000745	0.000745	0.000745	0.000745
OMP_MOBD	8.00E-06	8.00E-06	8.00E-06	8.00E-06	8.00E-06	8.00E-06
OMP_NH4	-38.124593	-38.124593	-12.593208	-12.593208	-46.483567	-46.483567
OMP_NMN	0	0	0	0	0	0
OMP_NO2	0	0	0	0	0	0
OMP_NO3	0	0	0	0	0	0
OMP_O2	0.820226	0.820226	1.010734	1.010734	2.5047	2.5047
OMP_OCDCA	0	0	0	0	0	0
OMP_PI	0.421062	0.421062	0.421062	0.421062	0.421062	0.421062
OMP_PMCOA	2.00E-06	2.00E-06	2.00E-06	2.00E-06	2.00E-06	2.00E-06
OMP_PPA	0	0	0	0	0	0
OMP_PRO-L	0	0	0	0	0	0
OMP_PTRC	0	0	0	0	0	0
OMP_PYR	0	0	0	0	0	0
OMP_SER-L	0	0	0	0	0	0
OMP_SO3	0	0	0	0	0	0
OMP_SO4	0.155406	0.155406	0.155406	0.155406	0.155406	0.155406
OMP_SUCC	0	0	0	0	-6.244573	-6.244573
OMP_THR-L	0	0	0	0	0	0
OMP_THYMD	0	0	0	0	NA	NA
OMP_TMA	0	0	0	0	0	0
OMP_TMAO	0	0	0	0	0	0
OMP_TRP-L	0	0	0	0	0	0
OMP_TSUL	0	0	0	0	0	0
OMP_TTDCA	0	0	0	0	0	0
OMP_TTTNT	0	0	0	0	0	0

OMP_TYR-L	0	0	0	0	0	0
OMP_URA	0	0	0	0	0	0
OMP_UREA	-0.045289	-0.045289	-0.045289	-0.045289	-0.045289	-0.045289
OMP_URI	0	0	0	0	NA	NA
OMP_VAL-L	0	0	0	0	0	0
OMP_XAN	0	0	0	0	NA	NA
OMP_na1	0	0	0	0	0	0
OPHBDC	0.000252	0.000252	0.000252	0.000252	0.000252	0.000252
OPHHX	0.000252	0.000252	0	0.000252	0.000252	0.000252
OPHHXAN	0	0	0	0.000252	0	0
ORNCD	0.155468	0.155468	0.155468	0.155468	0.155468	0.155468
ORPT	-0.141483	-0.141483	-0.141482	-0.141482	-0.141482	-0.141482
OXGDC2	0.000252	0.000252	0.000252	0.000252	0.000252	0.000252
P5CD	0	0	0	0	0	0
P5CR	0	0	0	0	0	0
PANTS	0.000615	0.000615	0.000615	0.000615	0.000615	0.000615
PAP	0.101276	0.101276	0.101276	0.101276	0.101276	0.101276
PAPPT3	0.02772	0.02772	0.02772	0.02772	0.02772	0.02772
PAPSR	0.150736	0.150736	0.150736	0.150736	0.150736	0.150736
PASYN_WP2	0.175	0.175	0.175	0.175	0.175	0.175
PDH	0	5.314555	0	0	6.647166	6.647166
PDX5PO	0.000252	0.000252	0	0	0	0
PDX5PS	0.000252	0.000252	0	0	0	0
PEPTIDOXe	0.02772	0.02772	0.02772	0.02772	0.02772	0.02772
PEPTIDO_SYNTHESIS	0.025	0.025	0.025	0.025	0.025	0.025
PERD	0.000252	0.000252	0	0	0	0
PFL	1.058245	1.058245	12.745241	12.745241	10.996012	10.996012
PGAMT	-0.079308	-0.079308	-0.079308	-0.079308	-0.079308	-0.079308
PGCD	0	0	0	0	0	0
PGDH	0	5.314555	0.165955	0.165955	0	0
PGDHY	5.898494	11.21305	0	0	0	0
PGI	-11.714307	-11.714307	-0.667212	-0.667212	-0.501257	-0.501257
PGK	0	0	18.089124	18.089124	30.249697	30.249697

PGL	11.21305	11.21305	0.165955	0.165955	0	0
PGLYCP	0	0	0	0	0	0
PGM	0	0	18.089124	18.089124	30.249697	30.249697
PGMT	-0.501257	-0.501257	-0.501257	-0.501257	-0.501257	-0.501257
PGPPH	0.01653	0.01653	0.01653	0.01653	0.01653	0.01653
PGSA	0.01653	0.01653	0.01653	0.01653	0.01653	0.01653
PHE4MO	0	0	NA	NA	NA	NA
PHEAL	0	0	0	0	0	0
PHEMEabc	0	0	0	0	NA	NA
PHETA1	-0.166877	-0.166877	-0.166877	-0.166877	-0.166877	-0.166877
PHETRS	0.166877	0.166877	0.166877	0.166877	0.166877	0.166877
PIabc	0	0	NA	NA	NA	NA
PIt6	0.421062	0.421062	0.421062	0.421062	0.421062	0.421062
PMANM	0	0	NA	NA	0	0
PMCOAt	-2.00E-06	-2.00E-06	-2.00E-06	-2.00E-06	-2.00E-06	-2.00E-06
PMDPHT	0.000505	0.000505	0.000505	0.000505	0.000505	0.000505
PNTK	0.000615	0.000615	0.000615	0.000615	0.000615	0.000615
PPA	6.160486	6.160486	6.160486	6.160486	6.160486	6.160486
PPAtNa	0	0	0	0	0	0
PPBNGS	0.002019	0.002019	0.002019	0.002019	0.002019	0.002019
PPC	3.782013	3.782013	3.782013	3.782013	9.488498	9.488498
PPCDC	0.000615	0.000615	0.000615	0.000615	0.000615	0.000615
PPCK	0	0	0	0	0	0
PPM	-0.511521	-0.511521	-0.007635	-0.007635	-0.007635	-0.007635
PPM2	0.503885	0.503885	0	0	0	0
PPNCL	0.000615	0.000615	0.000615	0.000615	0.000615	0.000615
PPND	0.126933	0.126933	0.126933	0.126933	0.126933	0.126933
PPNDH	0.166877	0.166877	0.166877	0.166877	0.166877	0.166877
PPPGFUM	0	0.000252	0	0.000252	0	0.000252
PPPGMEN	0	0.000252	0	0.000252	0	0.000252
PPPGNO3	0	0	0	0	0	0
PPPGO	0	0.000252	0	0	0	0
PPS	4.510081	4.510081	0	0	0	0
PPTGSe	0.02772	0.02772	0.02772	0.02772	0.02772	0.02772
PPTT	0.000505	0.000505	0.000505	0.000505	0.000505	0.000505
PRAGS	0.150793	0.150793	0.150793	0.150793	0.150793	0.150793
PRAIS	0.150793	0.150793	0.150793	0.150793	0.150793	0.150793

PRAIi	0.049387	0.049387	0.049387	0.049387	0.049387	0.049387
PRAMPC	0.088373	0.088373	0.088373	0.088373	0.088373	0.088373
PRASCS	0.150541	0.150541	0.150541	0.150541	0.150541	0.150541
PRATPP	0.088373	0.088373	0.088373	0.088373	0.088373	0.088373
PRFGS	0.150793	0.150793	0.150793	0.150793	0.150793	0.150793
PRKIN	0	0	0	0	0	0
PRMICIi	0.088373	0.088373	0.088373	0.088373	0.088373	0.088373
PRO1q	0	0	0	0	0	0
PROTRS	0.155468	0.155468	0.155468	0.155468	0.155468	0.155468
PROT_SYNTHESIS	0.528	0.528	0.528	0.528	0.528	0.528
PROt4	0	0	0	0	0	0
PRPPS	0.432615	0.432615	0.432615	0.432615	0.432615	0.432615
PSCVT	0.344207	0.344207	0.344207	0.344207	0.344207	0.344207
PSD	0.057136	0.057136	0.057136	0.057136	0.057136	0.057136
PSERT	0	0	0	0	0	0
PSP_L	0	0	0	0	0	0
PSSA	0.057136	0.057136	0.057136	0.057136	0.057136	0.057136
PSUDS	0	0	0	0	0	0
PTAr	-8.142054	-2.827499	4.048828	4.048828	10.927451	10.927451
PTPATi	0.000615	0.000615	0.000615	0.000615	0.000615	0.000615
PUNP1	-0.511521	-0.007635	-0.007635	-0.007635	-0.007635	-0.007635
PUNP2	0	0.503885	0	0	0	0
PUNP3	-0.576409	-0.072524	-0.072524	-0.072524	-0.072524	-0.072524
PUNP4	0	0.503885	0	0	0	0
PUNP5	0	0	0	0	0	0
PUNP6	0	0	0	0	0	0
PUNP7	0.072524	0.072524	0.072524	0.072524	0.072524	0.072524
PYAM5PO	0	0	0	0	0	0
PYDXL5PSYN	0	0	0.000252	0.000252	0.000252	0.000252
PYK	0	0	13.579043	13.579043	20.033131	20.033131
PYNP2	-0.503885	0	0	0	0	0
PYRt2	0	0	0	0	0	0
QULNS	0.002579	0.002579	0.002579	0.002579	0.002579	0.002579
RBFK	0.000252	0.000252	0.000252	0.000252	0.000252	0.000252
RBFSa	0.00101	0.00101	0.00101	0.00101	0.00101	0.00101
RBFSb	0.000505	0.000505	0.000505	0.000505	0.000505	0.000505

RBK	0	0	0	0	0	0
RHCCE	0	0	0	0	0	0
RIBabc	NA	NA	NA	NA	0	0
RNA_SYNTHESIS	0.09	0.09	0.09	0.09	0.09	0.09
RNDR1	0	0.526629	0	0.022744	0	0.022744
RNDR2	0	0.532482	0	0.028596	0	0.028596
RNDR3	0	0.028596	0	0.028596	0	0.028596
RNDR4	0	0.526629	0	0.022744	0	0.022744
RNTR1	0	0.526629	0	0.022744	0	0.022744
RNTR2	0	0.532482	0	0.028596	0	0.028596
RNTR3	0	0.028596	0	0.028596	0	0.028596
RNTR4	0	0.526629	0	0.022744	0	0.022744
RPE	37.352383	42.666938	8.969698	8.969698	36.724513	36.724513
RPI	37.365327	37.365327	8.816687	8.816687	36.737457	36.737457
S7PI	0.011934	0.011934	0.011934	0.011934	0.011934	0.011934
SADH	0	0	0	0	0	0
SADT2	0.150736	0.150736	0.150736	0.150736	0.150736	0.150736
SDPDS	0.246409	0.246409	0.246409	0.246409	0.246409	0.246409
SDPTA	-0.246409	-0.246409	-0.246409	-0.246409	-0.246409	-0.246409
SELNPS	0	0	0	0	0	0
SERAT	0.150736	0.150736	0.150736	0.150736	0.150736	0.150736
SERD_L	0	0	0	0	0	0
SERGLYX	0	0	0	0	0	0
SERTRS	0.299352	0.299352	0.299352	0.299352	0.299352	0.299352
SERt4	0	0	0	0	0	0
SERt6	0	0	0	0	0	0
SFGTH	0	0	0	0	0	0
SGDS	0	0	0	0	0	0
SGSAD	0	0	0	0	0	0
SHCHCS2	0.000252	0.000252	0.000252	0.000252	0.000252	0.000252
SHCHD2	0.000252	0.000252	0.000252	0.000252	0.000252	0.000252
SHCHF	0.000252	0.000252	0.000252	0.000252	0.000252	0.000252
SHK3D	0.344207	0.344207	0.344207	0.344207	0.344207	0.344207
SHKK	0.344207	0.344207	0.344207	0.344207	0.344207	0.344207
SHSL1	0.108051	0.108051	0.108051	0.108051	0.108051	0.108051
SLCYSS	0	0	0	0	0	0
SO4t2	0.155406	0.155406	0.155406	0.155406	0.155406	0.155406
SOD	0	0	0	0	0	0

SOTA	0	0	0	0	0	0
SPA	0	0	0	0	0	0
SPMS	0.007633	0.007633	0.007633	0.007633	0.007633	0.007633
SPRS	NA	NA	NA	NA	0	0
SSALx	0	0	0	0	0	0
SUCBZL	0.000252	0.000252	0.000252	0.000252	0.000252	0.000252
SUCBZS	0.000252	0.000252	0.000252	0.000252	0.000252	0.000252
SUCCtex	0	0	0	0	6.244573	6.244573
SUCD7	1.494118	1.638937	0.990989	2.020962	0	5.008139
SUCOAS	0.354571	0.354571	0.354571	0.354571	0.354571	0.354571
SUCP	0	0	0	0	0	0
SUCRPTS	0	0	0	0	0	0
SULR	-0.150736	-0.150736	-0.150736	-0.150736	-0.150736	-0.150736
TAL	-38.321396	-38.321396	-9.269123	-9.269123	-37.189893	-37.189893
TDP3AAAT	0	0	0	0	0	0
TDPDRE	0	0	0	0	0	0
TDPDRR	0	0	0	0	0	0
TDPGDH	0	0	0	0	0	0
TDSK	0.011934	0.011934	0.011934	0.011934	0.011934	0.011934
THD2	0	4.518233	11.926671	11.926671	15.767699	15.767699
THD5	0	9.79427	0	0	0	0
THDPS	0.246409	0.246409	0.246409	0.246409	0.246409	0.246409
THMDt2	0	0	0	0	0	0
THRA	-0.503885	-0.503885	0	0	0	0.990343
THRD	0	0	0	0	0	0.990343
THRD_L	0.279739	0.279739	0.279739	0.279739	0.279739	0.279739
THRHT	NA	NA	0	0	-0.005605	-0.005605
THRLAD	0	0	0	0	0	0
THRS	0	0	0.503885	0.503885	1.494229	1.494229
THRTRS	0.224147	0.224147	0.224147	0.224147	0.224147	0.224147
THRt3	0	4.518233	NA	NA	0	0
THRt4	0	4.518233	0	0	0.005605	0.005605
THZPSN	0.000252	0.000252	0.000252	0.000252	0.000252	0.000252

TKT1	-38.309463	-38.309463	-9.25719	-9.25719	-37.17796	-37.17796
TKT2	-38.665856	-38.665856	-9.61333	-9.61333	-37.5341	-37.5341
TMAOR3e	0	0	0	0	0	0
TMDK1	0	0	0	0	0	0
TMDPP	0	0	0	0	0	0
TMDS	0.022744	0.022744	0.022744	0.022744	0.022744	0.022744
TMPKr	0.000252	0.000252	0.000252	0.000252	0.000252	0.000252
TMPPP	0.000252	0.000252	0.000252	0.000252	0.000252	0.000252
TPI	-43.814618	-43.814618	-0.19411	-0.19411	-21.951615	-21.951615
TRACE_ELEMENTS	0.021	0.021	0.021	0.021	0.021	0.021
TRDR	0.757301	0.757301	0.253416	0.253416	0.253416	0.253416
TRE6PP	0	0	0	0	0	0
TREH	0	0	0	0	0	0
TREHtex	0	0	0	0	0	0
TRPOR	0	0	0	0	0	0
TRPS2	0.049387	0.049387	0.049387	0.049387	0.049387	0.049387
TRPS3	0.049387	0.049387	0.049387	0.049387	0.049387	0.049387
TRPTRS	0.049387	0.049387	0.049387	0.049387	0.049387	0.049387
TRPt6	NA	NA	0	0	0	0
TSULST	0	0	NA	NA	0	0
TYRTA	-0.126933	-0.126933	-0.126933	-0.126933	-0.126933	-0.126933
TYRTRS	0.126681	0.126681	0.126681	0.126681	0.126681	0.126681
TYRt6	NA	NA	0	0	0	0
U23GAAT	0.023868	0.023868	0.023868	0.023868	0.023868	0.023868
UAAGDS	0.02772	0.02772	0.02772	0.02772	0.02772	0.02772
UAGAAT	0.023868	0.023868	0.023868	0.023868	0.023868	0.023868
UAGCVT	0.02772	0.02772	0.02772	0.02772	0.02772	0.02772
UAGDP	0.079308	0.079308	0.079308	0.079308	0.079308	0.079308
UAGPT3	0.02772	0.02772	0.02772	0.02772	0.02772	0.02772
UAMAGS	0.02772	0.02772	0.02772	0.02772	0.02772	0.02772
UAMAS	0.02772	0.02772	0.02772	0.02772	0.02772	0.02772
UAPGR	0.02772	0.02772	0.02772	0.02772	0.02772	0.02772
UDCPDP	0.02772	0.02772	0.02772	0.02772	0.02772	0.02772
UDCPDPS	6.20E-05	6.20E-05	6.20E-05	6.20E-05	6.20E-05	6.20E-05

UDPG4E	0.035802	0.035802	0.035801	0.035801	0.035801	0.035801
UDPHEXURI	NA	NA	NA	NA	0	0
UGMDDS	0.02772	0.02772	0.02772	0.02772	0.02772	0.02772
UHGADA	0.023868	0.023868	0.023868	0.023868	0.023868	0.023868
UMPK	0.19307	0.696956	0.19307	0.19307	0.19307	0.19307
UNK3	0.007633	0.007633	0.007633	0.007633	0.007633	0.007633
UPP3MT	0.000252	0.000252	0.000252	0.000252	0.000252	0.000252
UPP3S	0.000505	0.000505	0.000505	0.000505	0.000505	0.000505
UPPDC1	0.000252	0.000252	0.000252	0.000252	0.000252	0.000252
UPPRT	0	0	0	0	0	0
UQOR	0	0	0	0	0	0
URAt6	0	0	0	0	0	0
URCN	0	0	0	0	0	0
URHYDROX	0	0	0	0	0	0
URIDK2	-0.526629	-0.022744	-0.022744	-0.022744	-0.022744	-0.022744
URIH	0	0	0	0	0	0
URIK1	0	0.503885	0	0	0	0
URIK2	0	0.503885	0	0	0	0
URIK3	0	0.503885	0	0	0	0
URIt2	0	0	0	0	0	0
USHD	0.011934	0.011934	0.011934	0.011934	0.011934	0.011934
UreaExp	0.045289	0.045289	0.045289	0.045289	0.045289	0.045289
VALALAMOB	-0.272345	5.9108	-0.272345	5.910547	-0.272345	5.938268
VALDHr	-6.183145	0	-6.182892	0	-6.210613	0
VALTA	-2.168105	5.9108	-1.664219	5.910547	-0.701596	5.938268
VALTRS	0.272345	0.272345	0.272345	0.272345	0.272345	0.272345
VALt4	0	0	0	0	0	0
WO4abc	0	0	0	0	0	0
XAND	0	0	0	0	0	0
XANt	0	0	0	0	0	0
XPK	114.327702	119.642257	27.840218	27.840218	111.436574	111.436574

Appendix V Data S3 for Manuscript II

Data S3 Index

Each page in the workbook represents a unique comparison between two transcriptomes. The name of the tab is in the format of {condition 1}_{condition 2}_{growth phase}	
Table A: Comparison between early log phase samples from 15°C and 4°C cultures.	
Table B: Comparison between late log phase samples from 15°C and 4°C cultures.	
Table C: Comparison between stationary phase samples from 15°C and 4°C cultures.	
Table D: Comparison between early log phase samples from 20°C and 15°C cultures.	
Table E: Comparison between late log phase samples from 20°C and 15°C cultures.	
Table F: Comparison between stationary phase samples from 20°C and 15°C cultures.	
Table G: Comparison between early log phase samples from 20°C and 4°C cultures.	
Table H: Comparison between late log phase samples from 20°C and 4°C cultures.	
Table I: Comparison between stationary phase samples from 20°C and 4°C cultures.	
Column Descriptions	
gene	Refseq locus tag
log2FoldChange	Log2 Fold change calculated by DESeq2. Negative log 2 fold changes indicate that the expression of the gene was higher in condition 1. Positive log2 fold changes indicate that expression was higher in condition 2.
padj	P-value of the log2 fold change adjusted for multiple testing calcualted by DESeq2
name	Gene name based on EggNOG functional annotation
cats	COG functional category based on EggNOG functional annotation

Data S3 Table A: Comparison between early log phase samples from 15°C and 4°C cultures.

gene	log2FoldChange (<0 higher in 4, >0 higher in 15)	padj	name	cats
sps_RS00915	2.45713272	4.55E-08	oligopeptidase A	Amino Acid metabolism and transport
sps_RS03160	-2.009881016	0.000229053 9501	PLP-dependent cysteine synthase family protein	Amino Acid metabolism and transport
sps_RS06490	3.260427248	6.51E-13	ATP phosphoribosyltransferase	Amino Acid metabolism and transport
sps_RS06495	3.114438403	1.64E-07	histidinol dehydrogenase	Amino Acid metabolism and transport
sps_RS06500	2.763546765	6.04E-05	histidinol-phosphate transaminase	Amino Acid metabolism and transport
sps_RS06505	2.279887361	0.000888896 4923	bifunctional histidinol-phosphatase/imidazoleglycerol-phosphate dehydratase HisB	Amino Acid metabolism and transport
sps_RS06510	2.690921544	2.09E-05	imidazole glycerol phosphate synthase subunit HisH	Amino Acid metabolism and transport
sps_RS07005	-3.714884653	6.25E-10	1-aminocyclopropane-1-carboxylate deaminase	Amino Acid metabolism and transport
sps_RS09130	-2.582720492	3.05E-08	aminotransferase class V-fold PLP-dependent enzyme	Amino Acid metabolism and transport
sps_RS09555	2.195978181	6.87E-09	branched-chain amino acid ABC transporter permease	Amino Acid metabolism and transport
sps_RS11505	2.33616171	2.08E-07	pyrroline-5-carboxylate reductase	Amino Acid metabolism and transport
sps_RS12080	2.245453489	5.03E-07	glutamate synthase large subunit	Amino Acid metabolism and transport

sps_RS12085	2.121024505	1.12E-06	glutamate synthase small subunit	Amino Acid metabolism and transport
sps_RS12610	-3.127205126	8.68E-08	aspartate aminotransferase family protein	Amino Acid metabolism and transport
sps_RS13315	-3.846667565	1.78E-16	EamA/RhaT family transporter	Amino Acid metabolism and transport
sps_RS15440	2.039009776	0.0005674527167	ketol-acid reductoisomerase	Amino Acid metabolism and transport
sps_RS16205	2.094814937	1.32E-05	3-isopropylmalate dehydratase small subunit	Amino Acid metabolism and transport
sps_RS16210	2.412388933	3.26E-13	3-isopropylmalate dehydratase large subunit	Amino Acid metabolism and transport
sps_RS16215	2.824060037	3.47E-24	3-isopropylmalate dehydrogenase	Amino Acid metabolism and transport
sps_RS16220	2.11633424	1.17E-11	2-isopropylmalate synthase	Amino Acid metabolism and transport
sps_RS17470	2.304780343	1.57E-09	cysteine synthase A	Amino Acid metabolism and transport
sps_RS21065	-2.574248589	7.60E-09	EamA/RhaT family transporter	Amino Acid metabolism and transport
sps_RS22050	3.655180789	1.94E-23	5-methyltetrahydropteroyltriglutamate--homocysteine S-methyltransferase	Amino Acid metabolism and transport
sps_RS24965	-2.079652744	4.38E-05	type 1 glutamine amidotransferase	Amino Acid metabolism and transport
sps_RS19520	-2.576775722	4.51E-07	allantoinase PuuE	Carbohydrate metabolism and transport
sps_RS00455	-2.679431123	4.61E-13	hypothetical protein	Cell motility
sps_RS00460	-2.845272074	1.71E-09	flagellar motor stator protein MotA	Cell motility

sps_RS00475	-3.61274973	2.14E-14	flagellar hook-length control protein FliK	Cell motility
sps_RS00485	-2.55181689	0.0007239463908	flagellar export chaperone FliS	Cell motility
sps_RS00490	-2.13382262	8.66E-09	flagellar hook protein FliD	Cell motility
sps_RS00530	-2.291305737	1.34E-05	flagellar basal-body rod protein FlgG	Cell motility
sps_RS00610	-2.170766019	2.49E-06	OmpA family protein	Cell motility
sps_RS11495	2.009659766	2.38E-09	type IV pili twitching motility protein PilT	Cell motility
sps_RS27410	2.423594944	5.36E-06	EscN/YscN/HrcN family type III secretion system ATPase	Cell motility
sps_RS09045	2.110708275	1.41E-08	energy transducer TonB	Cell wall/membrane/envelope biogenesis
sps_RS10100	2.76022882	8.46E-14	outer membrane protein OmpW	Cell wall/membrane/envelope biogenesis
sps_RS11770	2.455559926	0.0002404438064	OmpA family protein	Cell wall/membrane/envelope biogenesis
sps_RS12490	2.24682787	6.80E-06	hypothetical protein	Cell wall/membrane/envelope biogenesis
sps_RS14445	2.240185628	2.52E-05	transporter	Cell wall/membrane/envelope biogenesis
sps_RS15300	2.527244614	7.07E-20	OmpA family protein	Cell wall/membrane/envelope biogenesis
sps_RS18185	-3.204180978	2.70E-13	glycosyl transferase	Cell wall/membrane/envelope biogenesis

sps_RS18190	-2.060551892	4.80E-06	nucleotidyl transferase	Cell wall/membrane/envelope biogenesis
sps_RS18195	-2.175613766	0.000327639818	CDP-glycerol glycerophosphotransferase	Cell wall/membrane/envelope biogenesis
sps_RS24070	-2.275403605	2.29E-08	energy transducer TonB	Cell wall/membrane/envelope biogenesis
sps_RS13240	-2.344482639	3.36E-11	type 3 dihydrofolate reductase	Coenzyme metabolism
sps_RS20075	2.044034077	9.43E-09	glutamate--cysteine ligase	Coenzyme metabolism
sps_RS24100	-2.09186263	9.24E-06	heme anaerobic degradation radical SAM methyltransferase ChuW/HutW	Coenzyme metabolism
sps_RS03735	2.198386721	2.30E-07	hypothetical protein	Energy production and conversion
sps_RS04545	2.415320991	1.05E-10	cytochrome-c oxidase, cbb3-type subunit III	Energy production and conversion
sps_RS04550	2.631593818	6.20E-08	cbb3-type cytochrome c oxidase subunit 3	Energy production and conversion
sps_RS04555	2.299061615	2.63E-07	cytochrome-c oxidase, cbb3-type subunit II	Energy production and conversion
sps_RS07560	-3.143398846	2.99E-07	hydrogenase	Energy production and conversion
sps_RS09325	2.395606052	0.000634247 2103	cytochrome C	Energy production and conversion
sps_RS10985	2.371120945	4.95E-09	isocitrate dehydrogenase	Energy production and conversion
sps_RS15885	-2.410901992	0.000157089 0195	NADH-dependent alcohol dehydrogenase	Energy production and conversion

sps_RS20125	3.000126405	4.95E-09	sodium ion-translocating decarboxylase subunit beta	Energy production and conversion
sps_RS23415	-3.586962671	9.10E-15	alkene reductase	Energy production and conversion
sps_RS26460	2.155907803	6.40E-06	pyruvate dehydrogenase complex dihydrolipoyllysine-residue acetyltransferase	Energy production and conversion
sps_RS27670	2.039050411	0.000122375 6457	NAD(P)H-dependent glycerol-3-phosphate dehydrogenase	Energy production and conversion
sps_RS27845	2.815960909	2.81E-07	F0F1 ATP synthase subunit epsilon	Energy production and conversion
sps_RS27850	2.428804031	4.76E-05	F0F1 ATP synthase subunit beta	Energy production and conversion
sps_RS27855	2.22246063	0.000227161 9999	F0F1 ATP synthase subunit gamma	Energy production and conversion
sps_RS00060	-2.325339247	3.01E-05	LysE family translocator	Function Unknown
sps_RS00385	-2.378343078	0.000156718 6126	collagenase	Function Unknown
sps_RS00675	-3.316985444	0.000399051 909	methyltransferase domain-containing protein	Function Unknown
sps_RS00870	-2.320278104	0.000109240 6723	VUT family protein	Function Unknown
sps_RS01100	3.268112626	4.27E-08	hypothetical protein	Function Unknown
sps_RS02165	-2.1134215	1.15E-08	ABC transporter ATP-binding protein	Function Unknown
sps_RS02645	-2.104132255	1.98E-05	hypothetical protein	Function Unknown
sps_RS04630	-2.47485543	0.000601054 3627	hypothetical protein	Function Unknown
sps_RS05145	2.021261061	7.06E-05	type VI secretion system protein TssA	Function Unknown

sps_RS06735	2.741663981	7.00E-13	23S rRNA accumulation protein YceD	Function Unknown
sps_RS07010	-2.320203194	5.31E-13	YccF domain-containing protein	Function Unknown
sps_RS07015	-2.905274387	2.34E-09	ABC transporter	Function Unknown
sps_RS07580	-2.900963985	7.82E-11	DUF1566 domain-containing protein	Function Unknown
sps_RS07765	3.099944953	6.14E-10	curlin	Function Unknown
sps_RS08435	2.144324267	1.95E-20	cytotoxic necrotizing factor	Function Unknown
sps_RS08545	-2.581440896	0.0002538308085	N-acetyltransferase	Function Unknown
sps_RS08925	-2.623670774	7.64E-07	NADP-dependent oxidoreductase	Function Unknown
sps_RS09140	-2.005382677	3.18E-07	ATPase	Function Unknown
sps_RS09320	2.507647862	0.0001206541052	cytochrome C	Function Unknown
sps_RS09560	2.454958194	5.18E-13	AzlD domain-containing protein	Function Unknown
sps_RS09605	-3.000053821	0.0004109779478	N-acetyltransferase	Function Unknown
sps_RS09770	-2.557121675	5.75E-10	hypothetical protein	Function Unknown
sps_RS09930	-2.276670047	3.38E-08	tetratricopeptide repeat protein	Function Unknown
sps_RS10070	2.363379476	2.81E-17	protease	Function Unknown
sps_RS10625	3.285501204	1.57E-15	hypothetical protein	Function Unknown
sps_RS11140	2.910318722	9.49E-07	peptidase	Function Unknown
sps_RS11145	2.663661131	7.59E-07	hypothetical protein	Function Unknown

sps_RS11540	-3.114629175	1.92E-15	DUF2884 domain-containing protein	Function Unknown
sps_RS12620	-2.137517816	0.0003125748346	cupin domain-containing protein	Function Unknown
sps_RS12860	4.04554213	1.62E-06	hypothetical protein	Function Unknown
sps_RS13245	-3.791128466	7.89E-24	hypothetical protein	Function Unknown
sps_RS13250	-2.139561478	7.89E-24	threonine/serine exporter	Function Unknown
sps_RS13985	-2.051357857	0.0007026331602	transposase	Function Unknown
sps_RS14360	4.29282835	1.09E-19	hypothetical protein	Function Unknown
sps_RS14370	2.589832235	6.77E-07	hypothetical protein	Function Unknown
sps_RS14450	2.156297008	0.0001647730646	curli production assembly protein CsgF	Function Unknown
sps_RS15065	2.161897004	1.06E-07	adhesin	Function Unknown
sps_RS15070	2.225578094	4.57E-07	type I secretion system permease/ATPase	Function Unknown
sps_RS15570	3.02008577	7.77E-06	hypothetical protein	Function Unknown
sps_RS16965	-3.367050745	4.34E-10	hypothetical protein	Function Unknown
sps_RS16980	-4.565918914	1.04E-06	hypothetical protein	Function Unknown
sps_RS16990	-4.591236083	3.91E-05	DUF1320 domain-containing protein	Function Unknown
sps_RS17000	-4.224126326	7.95E-12	hypothetical protein	Function Unknown
sps_RS17005	-5.270994358	2.99E-08	hypothetical protein	Function Unknown

sps_RS17010	-2.266293376	4.21E-06	hypothetical protein	Function Unknown
sps_RS18960	3.189448525	1.42E-25	hypothetical protein	Function Unknown
sps_RS19515	-2.933489535	1.14E-08	OHCU decarboxylase	Function Unknown
sps_RS20300	-2.943676939	5.70E-17	hypothetical protein	Function Unknown
sps_RS20305	-2.279077482	1.03E-09	KR domain-containing protein	Function Unknown
sps_RS20565	-2.918390286	0.0001862942119	PAP2 family protein	Function Unknown
sps_RS20570	-2.455213805	0.0003100562264	putative porin	Function Unknown
sps_RS21070	-3.083071127	6.02E-06	hypothetical protein	Function Unknown
sps_RS21845	3.064626644	1.34E-13	hypothetical protein	Function Unknown
sps_RS22705	-2.468617537	5.42E-05	NADPH-dependent oxidoreductase	Function Unknown
sps_RS22710	-2.163684133	4.30E-09	VOC family protein	Function Unknown
sps_RS23235	-2.030421318	1.06E-05	DUF3560 domain-containing protein	Function Unknown
sps_RS23400	-4.850839012	4.43E-16	SRPBCC family protein	Function Unknown
sps_RS23405	-3.737165435	4.43E-16	hypothetical protein	Function Unknown
sps_RS23410	-3.747356102	4.92E-25	patatin	Function Unknown
sps_RS24525	2.156384047	4.61E-12	ABC transporter ATP-binding protein	Function Unknown

sps_RS25345	-2.031275252	0.0002184192448	hypothetical protein	Function Unknown
sps_RS25710	-2.834571272	6.20E-06	hypothetical protein	Function Unknown
sps_RS27290	2.685658705	1.25E-06	hypothetical protein	Function Unknown
sps_RS27295	2.702226015	1.15E-08	hypothetical protein	Function Unknown
sps_RS27350	3.866868937	2.80E-16	hypothetical protein	Function Unknown
sps_RS27355	3.37408373	9.73E-14	hypothetical protein	Function Unknown
sps_RS27360	3.583291849	8.10E-18	CesD/SycD/LcrH family type III secretion system chaperone	Function Unknown
sps_RS27365	2.679317552	1.25E-11	hypothetical protein	Function Unknown
sps_RS27395	2.862846899	1.35E-07	type III secretion chaperone SycN	Function Unknown
sps_RS27405	3.285092458	2.26E-15	YopN family type III secretion system gatekeeper subunit	Function Unknown
sps_RS06925	-2.046694039	4.03E-07	MFS transporter	Inorganic ion transport and metabolism
sps_RS07025	-3.472683352	6.12E-14	cytochrome C biogenesis protein CcsA	Inorganic ion transport and metabolism
sps_RS09050	2.445187092	3.82E-06	biopolymer transporter ExbD	Inorganic ion transport and metabolism
sps_RS09125	-2.893352327	2.04E-12	Anion transporter	Inorganic ion transport and metabolism
sps_RS13780	2.139624449	4.85E-15	phosphoadenylyl-sulfate reductase	Inorganic ion transport and metabolism
sps_RS14125	-2.738476475	8.82E-05	hypothetical protein	Inorganic ion transport and metabolism
sps_RS17560	3.040985233	7.93E-10	TonB-dependent receptor	Inorganic ion transport and metabolism

sps_RS24090	-2.467218552	6.99E-06	iron ABC transporter permease	Inorganic ion transport and metabolism
sps_RS24125	-2.102169321	3.53E-07	TonB-dependent siderophore receptor	Inorganic ion transport and metabolism
sps_RS24165	-2.128555483	6.35E-07	potassium transporter Kef	Inorganic ion transport and metabolism
sps_RS09055	2.13759388	1.50E-06	MotA/TolQ/ExbB proton channel family protein	Intracellular trafficking and secretion
sps_RS14610	-2.197646936	4.79E-05	type II secretion system F family protein	Intracellular trafficking and secretion
sps_RS14615	-2.376254269	1.67E-10	type II secretion system protein F	Intracellular trafficking and secretion
sps_RS17775	2.514705164	1.01E-05	protein translocase subunit SecF	Intracellular trafficking and secretion
sps_RS17780	2.366819311	2.53E-07	protein translocase subunit SecD	Intracellular trafficking and secretion
sps_RS17785	2.464028679	2.09E-06	preprotein translocase subunit YajC	Intracellular trafficking and secretion
sps_RS26490	2.121021748	3.75E-33	prepilin-type N-terminal cleavage/methylation domain-containing protein	Intracellular trafficking and secretion
sps_RS27675	2.643534633	6.38E-05	protein-export chaperone SecB	Intracellular trafficking and secretion
sps_RS01105	2.232537794	7.89E-05	hypothetical protein	Lipid metabolism
sps_RS01110	2.758928133	1.28E-06	hypothetical protein	Lipid metabolism
sps_RS01115	3.981614128	1.48E-14	hypothetical protein	Lipid metabolism
sps_RS17815	-2.495064631	0.000915568 9982	acyltransferase	Lipid metabolism
sps_RS25165	-2.169923008	4.27E-08	enoyl-CoA hydratase	Lipid metabolism

sps_RS04270	2.273771002	2.08E-07	adenylosuccinate synthetase	Nucleotide metabolism and transport
sps_RS05160	2.256914587	0.000276839344	type VI secretion system ATPase TssH	Post-translational modification, protein turnover, chaperone functions
sps_RS06895	-2.961022307	2.71E-05	serine protease	Post-translational modification, protein turnover, chaperone functions
sps_RS06900	-2.225241703	5.04E-11	hypothetical protein	Post-translational modification, protein turnover, chaperone functions
sps_RS07585	-2.437743222	0.000118156 8298	hypothetical protein	Post-translational modification, protein turnover, chaperone functions
sps_RS07830	2.101954459	9.32E-07	protease HtpX	Post-translational modification, protein turnover, chaperone functions
sps_RS08175	2.630809385	7.37E-09	co-chaperone YbbN	Post-translational modification, protein turnover, chaperone functions
sps_RS08180	2.824484546	1.45E-07	molecular chaperone HtpG	Post-translational modification, protein turnover, chaperone functions
sps_RS09205	2.200073671	1.79E-06	peptidylprolyl isomerase	Post-translational modification, protein turnover, chaperone functions
sps_RS09215	2.368383867	8.94E-09	endopeptidase La	Post-translational modification, protein turnover,

				chaperone functions
sps_RS11045	2.113414063	3.39E-08	nucleotide exchange factor GrpE	Post-translational modification, protein turnover, chaperone functions
sps_RS18045	-2.186030638	3.63E-05	peptidylprolyl isomerase	Post-translational modification, protein turnover, chaperone functions
sps_RS20985	2.147358962	1.70E-07	ATP-dependent zinc metalloprotease FtsH	Post-translational modification, protein turnover, chaperone functions
sps_RS21055	2.243681874	6.80E-07	molecular chaperone DnaJ	Post-translational modification, protein turnover, chaperone functions
sps_RS21060	2.480593716	0.000173408 0891	molecular chaperone DnaK	Post-translational modification, protein turnover, chaperone functions
sps_RS21670	2.295689314	1.87E-06	ATP-dependent chaperone ClpB	Post-translational modification, protein turnover, chaperone functions
sps_RS22460	2.96625476	1.49E-15	glutathione-dependent disulfide-bond oxidoreductase	Post-translational modification, protein turnover, chaperone functions
sps_RS25550	2.499198482	3.08E-14	DegQ family serine endoprotease	Post-translational modification, protein turnover, chaperone functions
sps_RS25925	2.199007706	0.000136018 5061	chaperonin GroEL	Post-translational modification, protein turnover,

				chaperone functions
sps_RS25930	2.413216383	1.49E-05	co-chaperone GroES	Post-translational modification, protein turnover, chaperone functions
sps_RS26410	2.555464875	2.86E-11	ATP-dependent protease subunit HslV	Post-translational modification, protein turnover, chaperone functions
sps_RS26415	2.819966262	2.78E-10	ATP-dependent protease ATPase subunit HslU	Post-translational modification, protein turnover, chaperone functions
sps_RS26850	2.405959738	1.28E-06	Hsp33 family molecular chaperone HslO	Post-translational modification, protein turnover, chaperone functions
sps_RS27340	4.109557853	4.76E-21	hypothetical protein	Post-translational modification, protein turnover, chaperone functions
sps_RS04595	-2.212634899	9.56E-11	replication endonuclease	Replication and repair
sps_RS06160	-2.528312853	1.11E-05	integrase	Replication and repair
sps_RS13310	-5.911961778	1.11E-07	IS256 family transposase	Replication and repair
sps_RS22930	-2.565929582	8.22E-17	hypothetical protein	Replication and repair
sps_RS22990	-2.117581492	7.41E-07	IS30 family transposase	Replication and repair
sps_RS23700	-2.247459919	3.46E-08	IS21 family transposase	Replication and repair

sps_RS15280	2.22318351	1.24E-07	tandem-95 repeat protein	Secondary Structure
sps_RS00605	-2.337190459	6.51E-13	sigma-54-dependent Fis family transcriptional regulator	Signal Transduction
sps_RS11800	-2.097144291	3.25E-05	PAS domain-containing protein	Signal Transduction
sps_RS22745	-2.930965139	4.02E-11	response regulator	Signal Transduction
sps_RS00465	-2.758941847	2.36E-09	RNA polymerase sigma factor FliA	Transcription
sps_RS09570	2.535515435	3.66E-30	YafY family transcriptional regulator	Transcription
sps_RS09575	3.320131148	4.94E-10	AraC family transcriptional regulator	Transcription
sps_RS09965	-3.190037743	2.36E-16	GntR family transcriptional regulator	Transcription
sps_RS13295	-3.014560719	4.43E-05	cold-shock protein	Transcription
sps_RS14655	-2.606226722	1.57E-09	LysR family transcriptional regulator	Transcription
sps_RS17430	-2.36366177	4.00E-12	transcriptional regulator BetI	Transcription
sps_RS23225	-2.450195094	4.28E-09	hypothetical protein	Transcription
sps_RS27370	3.314103238	4.02E-07	hypothetical protein	Transcription
sps_RS00180	-2.413961322	7.27E-06	ribonuclease P protein component	Translation
sps_RS01780	2.010760518	9.40E-06	30S ribosomal protein S12	Translation
sps_RS01785	2.427431551	1.05E-05	30S ribosomal protein S7	Translation
sps_RS01790	2.461686147	2.18E-07	elongation factor G	Translation
sps_RS11855	2.246113936	0.000127326 6449	ribosome-associated translation inhibitor RaiA	Translation

sps_RS11900	2.88007929	2.98E-06	50S ribosomal protein L19	Translation
sps_RS11905	2.762139477	9.14E-09	tRNA (guanosine(37)-N1)-methyltransferase TrmD	Translation
sps_RS11910	2.475032146	2.75E-05	ribosome maturation factor RimM	Translation
sps_RS11915	2.218756959	2.21E-05	30S ribosomal protein S16	Translation
sps_RS14235	2.112294145	1.29E-07	30S ribosomal protein S6--L-glutamate ligase	Translation
sps_RS17790	2.223167295	2.31E-05	tRNA guanosine(34) transglycosylase Tgt	Translation
sps_RS19945	2.304867096	2.68E-05	ribosome-associated translation inhibitor RaiA	Translation
sps_RS20990	2.487934622	1.33E-08	23S rRNA (uridine(2552)-2'-O)-methyltransferase RlmE	Translation

Data S3 Table B: Comparison between late log phase samples from 15°C and 4°C cultures.

gene	log2FoldChange (<0 higher in 4, >0 higher in 15)	padj	name	cats
sps_RS05410	-2.251297573	1.17E-07	serine dehydratase	Amino Acid metabolism and transport
sps_RS05415	-2.188101251	6.08E-10	DSD1 family PLP-dependent enzyme	Amino Acid metabolism and transport
sps_RS07005	-2.204573376	0.000833329333979	1-aminocyclopropane-1-carboxylate deaminase	Amino Acid metabolism and transport
sps_RS11430	-2.295816048	6.81E-08	low-specificity L-threonine aldolase	Amino Acid metabolism and transport
sps_RS11890	-2.799793394	8.19E-07	3-deoxy-7-phosphoheptulonate synthase	Amino Acid metabolism and transport
sps_RS14555	-2.78520259	3.89E-06	methylenetetrahydrofolate reductase	Amino Acid metabolism and transport
sps_RS16775	-2.651691747	1.42E-21	dihydrodipicolinate synthase family protein	Amino Acid metabolism and transport
sps_RS11765	2.474339026	1.44E-13	phosphoketolase family protein	Carbohydrate metabolism and transport
sps_RS19520	-2.450764521	2.89E-06	allantoinase PuuE	Carbohydrate metabolism and transport
sps_RS20810	2.227328424	5.89E-07	sugar ABC transporter substrate-binding protein	Carbohydrate metabolism and transport
sps_RS17255	-3.349087296	3.79E-06	hypothetical protein	Cell motility
sps_RS27270	2.006547001	4.59E-05	HrpE/YscL family type III secretion apparatus protein	Cell motility

sps_RS27410	4.017940358	1.62E-15	EscN/YscN/HrcN family type III secretion system ATPase	Cell motility
sps_RS27425	2.963367258	1.83E-11	YscQ/HrcQ family type III secretion apparatus protein	Cell motility
sps_RS09335	2.929797642	4.44E-09	hypothetical protein	Cell wall/membrane/envelope biogenesis
sps_RS10100	2.751039948	9.01E-14	outer membrane protein OmpW	Cell wall/membrane/envelope biogenesis
sps_RS12855	3.766171284	4.18E-11	LrgB family protein	Cell wall/membrane/envelope biogenesis
sps_RS00660	2.123457099	8.79E-06	oxygen-independent coproporphyrinogen III oxidase	Coenzyme metabolism
sps_RS01075	2.57099078	4.36E-06	hypothetical protein	Energy production and conversion
sps_RS03745	-4.054348131	3.46E-26	isocitrate lyase	Energy production and conversion
sps_RS03765	2.118466909	3.11E-09	bifunctional acetaldehyde-CoA/alcohol dehydrogenase	Energy production and conversion
sps_RS04555	2.232442027	7.83E-07	cytochrome-c oxidase, cbb3-type subunit II	Energy production and conversion
sps_RS04560	2.069631451	5.32E-08	cytochrome-c oxidase, cbb3-type subunit I	Energy production and conversion
sps_RS08005	-2.306217513	9.53E-09	citrate synthase	Energy production and conversion

sps_RS08860	-3.028955554	1.09E-06	malate synthase	Energy production and conversion
sps_RS09325	3.726408731	2.44E-08	cytochrome C	Energy production and conversion
sps_RS09330	3.660893039	2.91E-06	cystathionine beta-synthase	Energy production and conversion
sps_RS11115	2.058018349	0.0003319023347	NADH:ubiquinone reductase (Na(+)-transporting) subunit D	Energy production and conversion
sps_RS11120	2.33482692	4.95E-06	Na(+)-translocating NADH-quinone reductase subunit C	Energy production and conversion
sps_RS11125	3.096698864	2.49E-05	NADH:ubiquinone reductase (Na(+)-transporting) subunit B	Energy production and conversion
sps_RS11130	3.126630001	7.93E-12	Na(+)-translocating NADH-quinone reductase subunit A	Energy production and conversion
sps_RS11370	2.156652566	3.22E-05	L-threonine dehydrogenase	Energy production and conversion
sps_RS15005	-3.030073652	1.47E-07	SDR family NAD(P)-dependent oxidoreductase	Energy production and conversion
sps_RS15135	2.412280418	0.0003170011745	fumarate reductase flavoprotein subunit	Energy production and conversion
sps_RS17575	2.451146051	1.85E-07	formate C-acetyltransferase	Energy production and conversion
sps_RS18985	-3.955351693	1.89E-19	malate synthase A	Energy production and conversion

sps_RS19370	-2.479899085	4.41E-08	dicarboxylate/amino acid:cation symporter	Energy production and conversion
sps_RS27115	2.92511801	2.58E-08	coproporphyrinogen III oxidase family protein	Energy production and conversion
sps_RS27125	2.030416571	0.000246518657 4	4Fe-4S dicluster domain-containing protein	Energy production and conversion
sps_RS27130	3.058889745	1.63E-09	formate dehydrogenase	Energy production and conversion
sps_RS27670	2.260576312	2.16E-05	NAD(P)H-dependent glycerol-3-phosphate dehydrogenase	Energy production and conversion
sps_RS27795	2.467801715	6.70E-06	cytochrome o ubiquinol oxidase subunit III	Energy production and conversion
sps_RS27800	2.68423386	3.20E-11	cytochrome o ubiquinol oxidase subunit I	Energy production and conversion
sps_RS27805	2.088397482	1.09E-05	ubiquinol oxidase subunit II	Energy production and conversion
sps_RS00895	2.133987127	2.41E-19	putative sulfate exporter family transporter	Function Unknown
sps_RS01100	5.208157253	1.64E-14	hypothetical protein	Function Unknown
sps_RS01375	3.719617102	6.93E-30	ATPase P	Function Unknown
sps_RS01385	3.281145695	3.20E-07	DUF2057 domain-containing protein	Function Unknown
sps_RS02265	2.52552984	9.71E-08	hypothetical protein	Function Unknown
sps_RS02275	2.006963933	6.56E-07	phytochelatin synthase	Function Unknown

sps_RS04385	-2.500539512	3.88E-06	hypothetical protein	Function Unknown
sps_RS04390	-2.808524718	7.53E-12	N-acetyltransferase	Function Unknown
sps_RS04880	-2.000214882	5.14E-05	type III secretion apparatus	Function Unknown
sps_RS05225	-3.210814348	4.16E-09	META domain-containing protein	Function Unknown
sps_RS05430	-2.041015208	4.77E-07	YtoQ family protein	Function Unknown
sps_RS06230	2.985365231	3.41E-05	hypothetical protein	Function Unknown
sps_RS06235	3.54904298	4.98E-19	hypothetical protein	Function Unknown
sps_RS07520	2.515603667	0.0005832515331	anaerobic C4-dicarboxylate transporter	Function Unknown
sps_RS09320	4.116488482	3.07E-11	cytochrome C	Function Unknown
sps_RS09560	2.184493683	1.23E-09	AzlD domain-containing protein	Function Unknown
sps_RS09825	-2.125806196	1.32E-09	GNAT family N-acetyltransferase	Function Unknown
sps_RS10625	2.748262219	5.02E-11	hypothetical protein	Function Unknown
sps_RS12860	4.768188285	8.68E-09	hypothetical protein	Function Unknown
sps_RS13860	2.450838133	0.0001561433071	oxidative stress defense protein	Function Unknown
sps_RS14205	-2.34496438	4.95E-06	hypothetical protein	Function Unknown
sps_RS14420	2.472539876	0.0001269622273	collagenase	Function Unknown
sps_RS15065	2.172604671	1.24E-07	adhesin	Function Unknown
sps_RS15070	2.553243551	1.28E-08	type I secretion system permease/ATPase	Function Unknown

sps_RS15285	2.114713559	2.71E-12	type I secretion system permease/ATPase	Function Unknown
sps_RS15570	3.3791067	5.09E-07	hypothetical protein	Function Unknown
sps_RS17000	-2.598562794	5.12E-05	hypothetical protein	Function Unknown
sps_RS17005	-3.377431967	0.0004890462935	hypothetical protein	Function Unknown
sps_RS18820	3.100621417	1.99E-22	methyl-accepting chemotaxis protein	Function Unknown
sps_RS19515	-2.752274116	1.98E-07	OHCU decarboxylase	Function Unknown
sps_RS20500	2.23184764	2.38E-05	MipA/OmpV family protein	Function Unknown
sps_RS20505	2.327663668	3.41E-05	DUF3019 domain-containing protein	Function Unknown
sps_RS21080	3.03966257	1.68E-13	hypothetical protein	Function Unknown
sps_RS23400	-3.116756196	1.77E-07	SRPBCC family protein	Function Unknown
sps_RS27275	2.686319692	5.37E-10	hypothetical protein	Function Unknown
sps_RS27285	3.005269776	7.44E-10	EscI/YscI/HrpB family type III secretion system inner rod protein	Function Unknown
sps_RS27290	3.556104216	4.78E-11	hypothetical protein	Function Unknown
sps_RS27295	4.25002937	8.77E-22	hypothetical protein	Function Unknown
sps_RS27310	3.392255294	1.83E-21	EscD/YscD/HrpQ family type III secretion system inner membrane ring protein	Function Unknown
sps_RS27350	3.866446239	6.10E-17	hypothetical protein	Function Unknown

sps_RS27355	4.058696582	2.02E-20	hypothetical protein	Function Unknown
sps_RS27360	4.504790823	1.63E-31	CesD/SycD/LcrH family type III secretion system chaperone	Function Unknown
sps_RS27365	3.760290094	1.33E-23	hypothetical protein	Function Unknown
sps_RS27385	3.670547054	1.38E-11	hypothetical protein	Function Unknown
sps_RS27395	4.850126293	8.77E-22	type III secretion chaperone SycN	Function Unknown
sps_RS27400	4.705800356	8.37E-07	TyeA family type III secretion system gatekeeper subunit	Function Unknown
sps_RS27405	3.946578186	9.28E-24	YopN family type III secretion system gatekeeper subunit	Function Unknown
sps_RS27455	3.153070749	7.81E-30	hypothetical protein	Function Unknown
sps_RS27760	3.936749821	0.0005128497368	DUF2061 domain-containing protein	Function Unknown
sps_RS01365	2.029749504	4.43E-05	AcrB/AcrD/AcrF family protein	Inorganic ion transport and metabolism
sps_RS01370	2.950226404	5.10E-19	efflux RND transporter periplasmic adaptor subunit	Inorganic ion transport and metabolism
sps_RS01620	2.180320034	2.66E-08	catalase	Inorganic ion transport and metabolism
sps_RS02090	2.411588947	1.01E-07	ABC transporter permease	Inorganic ion transport and metabolism

sps_RS06305	2.098316747	5.90E-07	sodium/proton antiporter NhaB	Inorganic ion transport and metabolism
sps_RS08845	-2.269209062	1.03E-06	rhodanese-like domain-containing protein	Inorganic ion transport and metabolism
sps_RS14015	2.551774014	9.18E-07	catalase	Inorganic ion transport and metabolism
sps_RS15640	-2.411088447	0.000101525 1418	C4-dicarboxylate ABC transporter substrate-binding protein	Inorganic ion transport and metabolism
sps_RS17570	2.91015431	2.02E-09	formate transporter FocA	Inorganic ion transport and metabolism
sps_RS21625	2.564272938	2.98E-06	DNA starvation/stationary phase protection protein	Inorganic ion transport and metabolism
sps_RS27280	3.314108907	8.77E-22	EscJ/YscJ/HrcJ family type III secretion inner membrane ring protein	Intracellular trafficking and secretion
sps_RS27300	3.272136692	2.47E-07	EscF/YscF/HrpA family type III secretion system needle major subunit	Intracellular trafficking and secretion
sps_RS27315	3.70202654	1.33E-43	EscC/YscC/HrcC family type III secretion system outer membrane ring protein	Intracellular trafficking and secretion
sps_RS27380	3.905493093	5.12E-37	EscV/YscV/HrcV family type III secretion system export apparatus protein	Intracellular trafficking and secretion

sps_RS27390	3.878461197	1.95E-19	YscX family type III secretion protein	Intracellular trafficking and secretion
sps_RS27415	3.575094311	4.46E-06	hypothetical protein	Intracellular trafficking and secretion
sps_RS27420	3.152413258	5.40E-15	type III secretion system needle length determinant	Intracellular trafficking and secretion
sps_RS27430	3.105151559	4.23E-07	EscR/YscR/HrcR family type III secretion system export apparatus protein	Intracellular trafficking and secretion
sps_RS27435	3.464001301	1.18E-05	EscS/YscS/HrcS family type III secretion system export apparatus protein	Intracellular trafficking and secretion
sps_RS01090	2.575788805	4.13E-06	hypothetical protein	Lipid metabolism
sps_RS01105	3.240604938	4.65E-09	hypothetical protein	Lipid metabolism
sps_RS01110	3.476868577	9.24E-10	hypothetical protein	Lipid metabolism
sps_RS01115	3.961007549	4.11E-14	hypothetical protein	Lipid metabolism
sps_RS08835	-2.387161901	1.62E-09	transporter	Lipid metabolism
sps_RS20665	2.146523738	0.0005552829819	hypothetical protein	Lipid metabolism
sps_RS21950	-2.570844826	3.97E-08	alpha/beta hydrolase	Lipid metabolism
sps_RS04270	2.365655531	6.08E-08	adenylosuccinate synthetase	Nucleotide metabolism and transport
sps_RS01955	2.137531674	3.06E-05	heme ABC transporter permease	Post-translational modification, protein turnover,

				chaperone functions
sps_RS03850	-2.310811973	6.44E-05	peptide-methionine (S)-S-oxide reductase	Post-translational modification, protein turnover, chaperone functions
sps_RS20670	2.655385553	1.05E-05	U32 family peptidase	Post-translational modification, protein turnover, chaperone functions
sps_RS20675	2.114799468	0.0001430359177	U32 family peptidase	Post-translational modification, protein turnover, chaperone functions
sps_RS20985	2.062360328	7.47E-07	ATP-dependent zinc metalloprotease FtsH	Post-translational modification, protein turnover, chaperone functions
sps_RS22460	2.155503673	2.33E-08	glutathione-dependent disulfide-bond oxidoreductase	Post-translational modification, protein turnover, chaperone functions
sps_RS24220	2.111736663	0.0001086729567	alkyl hydroperoxide reductase subunit F	Post-translational modification, protein turnover, chaperone functions
sps_RS24225	3.250360652	5.00E-05	peroxiredoxin	Post-translational

				modification, protein turnover, chaperone functions
sps_RS26850	2.055703911	6.91E-05	Hsp33 family molecular chaperone HslO	Post-translational modification, protein turnover, chaperone functions
sps_RS27340	3.604478108	3.14E-17	hypothetical protein	Post-translational modification, protein turnover, chaperone functions
sps_RS01085	2.603124452	2.74E-06	hypothetical protein	Secondary Structure
sps_RS01095	3.301386047	8.68E-09	hypothetical protein	Secondary Structure
sps_RS06040	2.359080321	1.30E-10	copper resistance system multicopper oxidase	Secondary Structure
sps_RS15280	2.448583378	4.99E-09	tandem-95 repeat protein	Secondary Structure
sps_RS03040	-2.292840491	0.0003158951979	PrkA family serine protein kinase	Signal Transduction
sps_RS11275	2.221007313	9.67E-15	methyl-accepting chemotaxis protein	Signal Transduction
sps_RS20510	2.696642555	1.45E-05	DNA-binding response regulator	Signal Transduction
sps_RS27835	2.005497069	0.000949293563737	hypothetical protein	Signal Transduction
sps_RS09570	2.258567275	1.33E-23	YafY family transcriptional regulator	Transcription

sps_RS22055	-2.413152654	2.11E-08	LysR family transcriptional regulator	Transcription
sps_RS27370	3.423565507	1.22E-07	hypothetical protein	Transcription
sps_RS27375	2.55325427	0.000877193685	hypothetical protein	Transcription
sps_RS20540	3.127015948	4.56E-48	threonine--tRNA ligase	Translation

Data S3 Table C: Comparison between stationary phase samples from 15°C and 4°C cultures.

gene	log2FoldChange (<0 higher in 4, >0 higher in 15)	padj	name	cats
sps_RS03105	4.37910112	6.38E-15	amino acid transporter	Amino Acid metabolism and transport
sps_RS08280	2.087042264	2.98E-06	anthranilate synthase component 1	Amino Acid metabolism and transport
sps_RS08295	2.031765077	2.61E-05	bifunctional indole-3-glycerol-phosphate synthase TrpC/phosphoribosylanthranilate isomerase TrpF	Amino Acid metabolism and transport
sps_RS09555	2.259261662	5.81E-09	branched-chain amino acid ABC transporter permease	Amino Acid metabolism and transport
sps_RS19340	2.067555755	2.70E-12	sodium/glutamate symporter	Amino Acid metabolism and transport
sps_RS26675	-2.288195952	0.000210855542	ornithine carbamoyltransferase	Amino Acid metabolism and transport
sps_RS26680	-3.111911488	1.79E-06	acetylglutamate kinase	Amino Acid metabolism and transport
sps_RS26685	-2.85621217	1.95E-10	N-acetyl-gamma-glutamyl-phosphate reductase	Amino Acid metabolism and transport
sps_RS02380	2.257975208	0.000692731902 7	gluconokinase	Carbohydrate metabolism and transport
sps_RS06180	2.829391151	5.15E-05	carbohydrate ABC transporter	Carbohydrate metabolism and transport

			substrate-binding protein	
sps_RS11340	2.004652578	7.34E-06	glycogen/starch/alpha-glucan phosphorylase	Carbohydrate metabolism and transport
sps_RS11685	2.588920966	5.41E-22	rRNA (guanine-N1)-methyltransferase	Cell motility
sps_RS18555	2.17870521	1.24E-15	flagellar biosynthesis protein FlhA	Cell motility
sps_RS18630	2.232872733	1.11E-05	flagellar basal body M-ring protein FliF	Cell motility
sps_RS18675	2.088934191	0.0002582292625	flagellin	Cell motility
sps_RS18690	2.054108501	4.02E-05	flagellar hook-associated protein FlgK	Cell motility
sps_RS18705	2.184230157	2.64E-07	flagellar biosynthesis protein FlgH	Cell motility
sps_RS26085	2.027632119	5.75E-07	chemotaxis protein CheD	Cell motility
sps_RS27410	2.092808444	0.0001831414108	EscN/YscN/HrcN family type III secretion system ATPase	Cell motility
sps_RS08020	2.319638101	4.34E-06	efflux RND transporter periplasmic adaptor subunit	Cell wall/membrane/envelope biogenesis
sps_RS09305	2.885430188	1.93E-05	hypothetical protein	Cell wall/membrane/envelope biogenesis
sps_RS11360	2.000094358	7.45E-05	porin	Cell wall/membrane/envelope biogenesis
sps_RS15945	4.099235757	1.72E-06	porin family protein	Cell wall/membrane/envelope biogenesis

sps_RS05830	-2.409758079	8.03E-06	thiamine biosynthesis protein ThiS	Coenzyme metabolism
sps_RS00020	2.019700949	0.0008342275041	cytochrome-c oxidase	Energy production and conversion
sps_RS09300	3.083648602	6.06E-07	cystathionine beta-synthase	Energy production and conversion
sps_RS09310	2.966842289	1.35E-07	cytochrome C	Energy production and conversion
sps_RS13470	2.276821633	7.68E-13	cytochrome d terminal oxidase subunit 1	Energy production and conversion
sps_RS17485	2.273372901	5.85E-10	NADH-quinone oxidoreductase subunit A	Energy production and conversion
sps_RS17495	2.884528314	0.0002949246513	NADH-quinone oxidoreductase subunit NuoC/D	Energy production and conversion
sps_RS17510	2.39658358	0.0002122783829	NADH dehydrogenase (quinone) subunit G	Energy production and conversion
sps_RS17520	3.168413939	0.0008716647841	NADH-quinone oxidoreductase subunit NuoI	Energy production and conversion
sps_RS17525	2.356696929	0.0001642400804	NADH:ubiquinone oxidoreductase subunit J	Energy production and conversion
sps_RS18985	-2.254085342	1.56E-06	malate synthase A	Energy production and conversion
sps_RS00990	2.078960086	1.04E-05	acylase	Function Unknown
sps_RS01625	2.211969529	2.04E-07	phospholipase	Function Unknown
sps_RS01630	2.466513696	0.0002707205235	hypothetical protein	Function Unknown
sps_RS03620	2.82566494	3.49E-15	pilus assembly protein	Function Unknown

sps_RS04390	-2.364565947	3.18E-08	N-acetyltransferase	Function Unknown
sps_RS04940	2.802345908	6.70E-05	hypothetical protein	Function Unknown
sps_RS04950	2.125889945	6.04E-05	hypothetical protein	Function Unknown
sps_RS04955	2.223263065	9.76E-05	secretion protein	Function Unknown
sps_RS04960	3.237935951	1.57E-09	pathogenicity island effector protein	Function Unknown
sps_RS04965	2.924395747	2.47E-06	type III secretion system translocon protein	Function Unknown
sps_RS04970	2.717640935	6.23E-05	CesD/SycD/LcrH family type III secretion system chaperone	Function Unknown
sps_RS04975	2.329453385	0.0001197691047	secretion protein EspA	Function Unknown
sps_RS06080	2.310693691	2.05E-07	hypothetical protein	Function Unknown
sps_RS08435	2.049643337	9.55E-18	cytotoxic necrotizing factor	Function Unknown
sps_RS09560	2.887529069	1.24E-15	AzlD domain-containing protein	Function Unknown
sps_RS09805	2.048842281	0.0001566709439	DUF4136 domain-containing protein	Function Unknown
sps_RS10070	2.522915853	2.48E-18	protease	Function Unknown
sps_RS10785	2.786006729	1.92E-09	penicillin acylase family protein	Function Unknown
sps_RS10795	2.894915251	2.75E-16	hypothetical protein	Function Unknown
sps_RS12620	-2.282292448	0.0006227120577	cupin domain-containing protein	Function Unknown

sps_RS12860	3.381831849	0.000236449413	hypothetical protein	Function Unknown
sps_RS13850	2.0480048	4.44E-05	hypothetical protein	Function Unknown
sps_RS14010	2.211041965	5.53E-06	UPF0016 domain-containing protein	Function Unknown
sps_RS15070	2.293237294	4.67E-07	type I secretion system permease/ATPase	Function Unknown
sps_RS15400	3.269553257	1.52E-10	hydrolase	Function Unknown
sps_RS15570	2.582318308	0.000274530257	hypothetical protein	Function Unknown
sps_RS15625	4.943870692	1.56E-13	HlyD family secretion protein	Function Unknown
sps_RS15895	-2.332942153	5.21E-09	phasin family protein	Function Unknown
sps_RS19160	2.298046955	1.91E-05	DUF2219 domain-containing protein	Function Unknown
sps_RS20500	2.013106444	0.000207613988	MipA/OmpV family protein	Function Unknown
sps_RS20505	2.517833068	1.19E-05	DUF3019 domain-containing protein	Function Unknown
sps_RS21020	2.413610054	0.000403549381	hypothetical protein	Function Unknown
sps_RS21315	3.390832229	6.25E-15	hypothetical protein	Function Unknown
sps_RS21730	2.677035022	1.87E-05	GTP pyrophosphokinase	Function Unknown
sps_RS23400	-2.455679562	6.40E-05	SRPBCC family protein	Function Unknown
sps_RS24450	3.052074741	5.08E-08	multidrug transporter	Function Unknown
sps_RS24545	2.354940588	2.10E-09	ABC transporter permease	Function Unknown

sps_RS27295	2.397746348	9.01E-07	hypothetical protein	Function Unknown
sps_RS27350	2.384724326	1.79E-06	hypothetical protein	Function Unknown
sps_RS27355	2.701208446	6.84E-09	hypothetical protein	Function Unknown
sps_RS27395	2.501578215	1.09E-05	type III secretion chaperone SycN	Function Unknown
sps_RS27760	4.71684529	2.22E-05	DUF2061 domain-containing protein	Function Unknown
sps_RS01620	3.550908801	4.10E-21	catalase	Inorganic ion transport and metabolism
sps_RS09075	2.817201186	9.47E-13	TonB-dependent receptor	Inorganic ion transport and metabolism
sps_RS14015	3.775448563	4.17E-14	catalase	Inorganic ion transport and metabolism
sps_RS14130	-2.07521329	0.000793566722	sorbose reductase	Inorganic ion transport and metabolism
sps_RS15620	3.96478885	2.37E-08	MFS transporter	Inorganic ion transport and metabolism
sps_RS17675	-2.332152706	1.25E-10	TonB-dependent receptor	Inorganic ion transport and metabolism
sps_RS21625	3.709462096	1.87E-12	DNA starvation/stationary phase protection protein	Inorganic ion transport and metabolism
sps_RS22160	2.378253811	2.47E-07	MFS transporter	Inorganic ion transport and metabolism
sps_RS11695	2.049920962	1.72E-06	prepilin-type N-terminal cleavage/methylation domain-containing protein	Intracellular trafficking and secretion

sps_RS11700	2.446822552	1.68E-06	type IV pilus modification protein PilV	Intracellular trafficking and secretion
sps_RS15755	2.111968534	3.32E-05	signal peptidase I	Intracellular trafficking and secretion
sps_RS27315	2.029832054	1.94E-12	EscC/YscC/HrcC family type III secretion system outer membrane ring protein	Intracellular trafficking and secretion
sps_RS08835	-2.188103952	6.99E-08	transporter	Lipid metabolism
sps_RS08910	-2.494691249	1.27E-15	anaerobic ribonucleoside-triphosphate reductase	Nucleotide metabolism and transport
sps_RS10470	-2.129270999	1.43E-07	UMP kinase	Nucleotide metabolism and transport
sps_RS04945	2.760738177	2.92E-07	CesD/SycD/LcrH family type III secretion system chaperone	Post-translational modification, protein turnover, chaperone functions
sps_RS09315	2.586989251	0.0004368057725	hypothetical protein	Post-translational modification, protein turnover, chaperone functions
sps_RS17270	-2.830498216	0.0006998881985	thiol peroxidase	Post-translational modification, protein turnover, chaperone functions
sps_RS19150	3.526383355	2.45E-14	organic hydroperoxide resistance protein	Post-translational modification, protein

				turnover, chaperone functions
sps_RS24220	4.311808106	1.15E-17	alkyl hydroperoxide reductase subunit F	Post-translational modification, protein turnover, chaperone functions
sps_RS24225	5.195197967	7.21E-12	peroxiredoxin	Post-translational modification, protein turnover, chaperone functions
sps_RS06255	2.305425729	4.51E-07	hypothetical protein	Replication and repair
sps_RS16750	2.050949431	1.16E-05	group II intron reverse transcriptase/maturase	Replication and repair
sps_RS16235	-2.537149585	2.02E-10	hypothetical protein	Secondary Structure
sps_RS02065	2.219170531	3.75E-06	GHKL domain-containing protein	Signal Transduction
sps_RS02070	2.383263365	6.87E-09	DNA-binding response regulator	Signal Transduction
sps_RS03915	2.380049497	3.79E-07	DNA-binding response regulator	Signal Transduction
sps_RS04570	2.805093996	6.79E-08	DUF3369 domain-containing protein	Signal Transduction
sps_RS18155	2.540207047	8.43E-05	fused response regulator/phosphatase	Signal Transduction
sps_RS20510	2.552528657	5.49E-05	DNA-binding response regulator	Signal Transduction
sps_RS21025	2.726417378	2.56E-06	methyl-accepting	Signal Transduction

			chemotaxis protein	
sps_RS09570	2.157886905	1.16E-20	YafY family transcriptional regulator	Transcription
sps_RS08515	-2.069896604	4.52E-12	N-acetyltransferase	Translation

Data S3 Table D: Comparison between early log phase samples from 20°C and 15°C cultures.

gene	log2FoldChange (<0 higher in 15, >0 higher in 20)	padj	name	cats
sps_RS10195	-4.493246407	2.27E-25	type VI secretion system tube protein Hcp	Function Unknown
sps_RS19095	-4.340308176	2.07E-22	type VI secretion system tube protein Hcp	Function Unknown
sps_RS14360	-4.261139454	1.23E-18	hypothetical protein	Function Unknown
sps_RS24400	-4.049696994	4.25E-15	type VI secretion system tube protein Hcp	Function Unknown
sps_RS08860	-3.197028386	2.24E-06	malate synthase	Energy production and conversion
sps_RS19090	-3.013362157	5.06E-07	type VI secretion system tip protein VgrG	Cell wall/membrane/ envelope biogenesis
sps_RS10190	-2.921998632	3.38E-06	type VI secretion system tip protein VgrG	Cell wall/membrane/ envelope biogenesis
sps_RS10180	-2.604685919	5.03E-05	LysM domain-containing protein	Function Unknown
sps_RS19080	-2.561880809	1.59E-05	LysM peptidoglycan-binding domain-containing protein	Function Unknown
sps_RS22050	-2.541738045	1.00E-10	5-methyltetrahydropteroyltriglutamate--homocysteine S-	Amino Acid metabolism and transport

			methyltransferase	
sps_RS19085	-2.534230144	5.03E-05	DUF4123 domain-containing protein	Function Unknown
sps_RS24405	-2.397993379	1.90E-05	type VI secretion system tip protein VgrG	Cell wall/membrane/envelope biogenesis
sps_RS04175	-2.276038852	4.25E-15	hypothetical protein	Function Unknown
sps_RS18235	-2.001295119	0.0007779570947	sulfate adenylyltransferase subunit CysD	Inorganic ion transport and metabolism
sps_RS04420	2.244682356	0.000669685164	bacterioferritin	Inorganic ion transport and metabolism
sps_RS10355	2.706572509	1.55E-08	DUF1611 domain-containing protein	Function Unknown
sps_RS10360	2.717091443	7.43E-13	dipeptide epimerase	Cell wall/membrane/envelope biogenesis

Data S3 Table E: Comparison between late log phase samples from 20°C and 15°C cultures.

gene	log2FoldChange (<0 higher in 15, >0 higher in 20)	padj	name	cats
sps_RS03160	2.002902784	0.0005389051566	PLP-dependent cysteine synthase family protein	Amino Acid metabolism and transport
sps_RS13055	-2.356820823	6.17E-05	HAAAP family serine/threonine permease	Amino Acid metabolism and transport
sps_RS05545	-2.302160549	6.72E-06	pyruvate kinase	Carbohydrate metabolism and transport
sps_RS11765	-3.03084186	1.16E-19	phosphoketolase family protein	Carbohydrate metabolism and transport
sps_RS01230	2.763101264	0.0002980966925	PAS domain-containing protein	Cell motility
sps_RS09080	-2.396033577	6.17E-05	porin	Cell wall/membrane/envelope biogenesis
sps_RS10100	-2.435155977	1.60E-10	outer membrane protein OmpW	Cell wall/membrane/envelope biogenesis
sps_RS10360	2.21563557	5.77E-08	dipeptide epimerase	Cell wall/membrane/envelope biogenesis
sps_RS15350	-2.545028021	1.11E-06	efflux RND transporter periplasmic adaptor subunit	Cell wall/membrane/envelope biogenesis
sps_RS15940	-2.043748495	5.58E-07	porin family protein	Cell wall/membrane/envelope biogenesis
sps_RS15945	-3.694176774	3.30E-05	porin family protein	Cell wall/membrane/envelope biogenesis

sps_RS00660	-2.702930697	9.66E-09	oxygen-independent coproporphyrinogen III oxidase	Coenzyme metabolism
sps_RS07855	2.090386533	6.75E-14	8-amino-7-oxononanoate synthase	Coenzyme metabolism
sps_RS00020	2.139152844	0.0008788133428	cytochrome-c oxidase	Energy production and conversion
sps_RS01610	-2.488865061	0.0008504568413	aldehyde dehydrogenase	Energy production and conversion
sps_RS03765	-2.429140979	1.36E-11	bifunctional acetaldehyde-CoA/alcohol dehydrogenase	Energy production and conversion
sps_RS09300	2.373869782	0.0003897082731	cystathionine beta-synthase	Energy production and conversion
sps_RS11130	-2.34283737	1.46E-06	Na(+)-translocating NADH-quinone reductase subunit A	Energy production and conversion
sps_RS17495	2.802754881	0.0009148957977	NADH-quinone oxidoreductase subunit NuoC/D	Energy production and conversion
sps_RS17505	3.745847465	0.0007394794554	NADH oxidoreductase (quinone) subunit F	Energy production and conversion
sps_RS17510	2.269945306	0.0009737284262	NADH dehydrogenase (quinone) subunit G	Energy production and conversion
sps_RS17575	-2.995452748	1.39E-10	formate C-acetyltransferase	Energy production and conversion
sps_RS22755	3.230782563	1.74E-05	MFS transporter	Energy production and conversion
sps_RS27130	-2.760980488	1.56E-07	formate dehydrogenase	Energy production and conversion

sps_RS27790	-3.648404321	0.0003628254105	cytochrome o ubiquinol oxidase subunit IV	Energy production and conversion
sps_RS27795	-2.601057005	8.21E-06	cytochrome o ubiquinol oxidase subunit III	Energy production and conversion
sps_RS27800	-2.758814428	2.96E-11	cytochrome o ubiquinol oxidase subunit I	Energy production and conversion
sps_RS01305	2.439577113	2.33E-06	cell division protein	Function Unknown
sps_RS01375	-2.801855816	7.15E-17	ATPase P	Function Unknown
sps_RS02895	2.133959769	8.36E-05	DUF1302 domain-containing protein	Function Unknown
sps_RS04175	-2.333335158	5.37E-17	hypothetical protein	Function Unknown
sps_RS04695	-2.297335684	5.35E-10	hypothetical protein	Function Unknown
sps_RS06230	-2.659744863	0.000591312282	hypothetical protein	Function Unknown
sps_RS08025	2.057553817	0.0006772532111	AcrB/AcrD/AcrF family protein	Function Unknown
sps_RS10195	-4.359549727	1.51E-23	type VI secretion system tube protein Hcp	Function Unknown
sps_RS10355	2.486115417	2.20E-07	DUF1611 domain-containing protein	Function Unknown
sps_RS10625	-2.667382642	4.15E-10	hypothetical protein	Function Unknown
sps_RS15000	-5.424390691	3.06E-09	phasin family protein	Function Unknown
sps_RS15400	-2.36610819	2.08E-05	hydrolase	Function Unknown
sps_RS17010	2.122715965	4.30E-05	hypothetical protein	Function Unknown

sps_RS17130	2.170363817	5.65E-06	regulatory protein GemA	Function Unknown
sps_RS17135	2.913125883	2.23E-07	DUF3164 domain-containing protein	Function Unknown
sps_RS17145	2.747405263	3.15E-06	XRE family transcriptional regulator	Function Unknown
sps_RS17220	2.675985673	0.0005826238301	hypothetical protein	Function Unknown
sps_RS18820	-2.273770317	7.25E-12	methyl-accepting chemotaxis protein	Function Unknown
sps_RS19095	-3.388696805	9.55E-14	type VI secretion system tube protein Hcp	Function Unknown
sps_RS19180	2.167682679	0.0005941234571	nitrate ABC transporter substrate-binding protein	Function Unknown
sps_RS19895	2.406790088	0.0007923666871	hypothetical protein	Function Unknown
sps_RS21080	-2.050962492	4.13E-06	hypothetical protein	Function Unknown
sps_RS21730	-2.675888793	3.25E-05	GTP pyrophosphokinase	Function Unknown
sps_RS21780	2.536479667	2.56E-05	tripartite tricarboxylate transporter substrate binding protein	Function Unknown
sps_RS24400	-4.095666081	1.17E-15	type VI secretion system tube protein Hcp	Function Unknown
sps_RS25235	-2.178851194	1.22E-05	hypothetical protein	Function Unknown
sps_RS27295	-2.180390919	8.94E-06	hypothetical protein	Function Unknown
sps_RS27310	-2.446701824	5.24E-11	EscD/YscD/HrpQ family type III secretion	Function Unknown

			system inner membrane ring protein	
sps_RS27360	-2.435979426	1.98E-09	CesD/SycD/LcrH family type III secretion system chaperone	Function Unknown
sps_RS27365	-2.555238641	9.45E-11	hypothetical protein	Function Unknown
sps_RS27455	-2.004950638	4.88E-12	hypothetical protein	Function Unknown
sps_RS01370	-3.343544121	3.99E-23	efflux RND transporter periplasmic adaptor subunit	Inorganic ion transport and metabolism
sps_RS09075	2.446132199	1.60E-09	TonB-dependent receptor	Inorganic ion transport and metabolism
sps_RS17570	-2.26191516	1.31E-05	formate transporter FocA	Inorganic ion transport and metabolism
sps_RS19860	2.355978361	9.49E-05	arylsulfatase	Inorganic ion transport and metabolism
sps_RS21625	-2.078827136	0.0005141959835	DNA starvation/stationary phase protection protein	Inorganic ion transport and metabolism
sps_RS21785	2.276824723	3.22E-05	porin	Inorganic ion transport and metabolism
sps_RS15075	2.473440211	0.0003197411383	HlyD family type I secretion periplasmic adaptor subunit	Intracellular trafficking and secretion
sps_RS27280	-2.102622866	9.30E-09	EscJ/YscJ/HrcJ family type III secretion inner membrane ring protein	Intracellular trafficking and secretion
sps_RS27390	-2.333410461	1.20E-07	YscX family type III secretion protein	Intracellular trafficking and secretion

sps_RS14995	-2.657754139	1.18E-11	class I poly(R)-hydroxyalkanoic acid synthase	Lipid metabolism
sps_RS08910	-2.410888623	2.44E-14	anaerobic ribonucleoside-triphosphate reductase	Nucleotide metabolism and transport
sps_RS15525	-2.314489454	2.73E-10	uridine phosphorylase	Nucleotide metabolism and transport
sps_RS20865	-2.24876896	0.000927061373	purine-nucleoside phosphorylase	Nucleotide metabolism and transport
sps_RS20875	-2.211874837	8.33E-10	thymidine phosphorylase	Nucleotide metabolism and transport
sps_RS01600	2.854376416	9.67E-05	YjjW family glycine radical enzyme activase	Post-translational modification, protein turnover, chaperone functions
sps_RS17580	-2.222543587	1.60E-09	pyruvate formate lyase 1-activating protein	Post-translational modification, protein turnover, chaperone functions
sps_RS19150	-2.254056794	1.94E-05	organic hydroperoxide resistance protein	Post-translational modification, protein turnover, chaperone functions
sps_RS24220	-2.410502007	1.34E-05	alkyl hydroperoxide reductase subunit F	Post-translational modification, protein turnover, chaperone functions
sps_RS13960	2.255830454	1.14E-05	group II intron reverse	Replication and repair

			transcriptase/maturase	
sps_RS16750	2.044192656	1.71E-05	group II intron reverse transcriptase/maturase	Replication and repair
sps_RS17155	3.223893077	2.78E-13	ATP-binding protein	Replication and repair
sps_RS17160	2.436528703	8.40E-16	hypothetical protein	Replication and repair
sps_RS21135	2.699576704	5.07E-08	DNA polymerase IV	Replication and repair
sps_RS23425	-2.035180285	5.56E-06	universal stress protein	Signal Transduction
sps_RS27835	-2.157084295	0.000619188804	hypothetical protein	Signal Transduction
sps_RS17125	2.796093484	2.56E-07	transcriptional regulator	Transcription
sps_RS20540	-2.36599461	6.96E-27	threonine--tRNA ligase	Translation

Data S3 Table F: Comparison between stationary phase samples from 20°C and 15°C cultures.

gene	log2FoldChange (<0 higher in 15, >0 higher in 20)	padj	name	cats
sps_RS03105	-3.202635613	4.24E-08	amino acid transporter	Amino Acid metabolism and transport
sps_RS06470	-3.51141094	6.30E-13	branched-chain amino acid ABC transporter permease	Amino Acid metabolism and transport
sps_RS15460	2.927916676	8.82E-11	serine O-acetyltransferase	Amino Acid metabolism and transport
sps_RS17470	2.213409416	2.43E-08	cysteine synthase A	Amino Acid metabolism and transport
sps_RS09960	-2.394133885	8.78E-06	methylisocitrate lyase	Carbohydrate metabolism and transport
sps_RS19520	-2.222460122	7.05E-05	allantoinase PuuE	Carbohydrate metabolism and transport
sps_RS05125	-4.020323389	4.81E-19	type VI secretion system tip protein VgrG	Cell wall/membrane/envelope biogenesis
sps_RS10190	-2.855824577	1.89E-06	type VI secretion system tip protein VgrG	Cell wall/membrane/envelope biogenesis
sps_RS15945	-3.723078464	3.45E-05	porin family protein	Cell wall/membrane/envelope biogenesis
sps_RS19090	-3.015459977	1.43E-07	type VI secretion system tip protein VgrG	Cell wall/membrane/envelope biogenesis
sps_RS24405	-2.061743998	0.0002146792024	type VI secretion system tip protein VgrG	Cell wall/membrane/envelope biogenesis

sps_RS25955	-2.372619478	7.94E-07	efflux RND transporter periplasmic adaptor subunit	Cell wall/membrane/ envelope biogenesis
sps_RS26230	-2.174644658	0.0004259479866	TolC family protein	Cell wall/membrane/ envelope biogenesis
sps_RS10360	2.833433804	2.13E-14	dipeptide epimerase	Cell wall/membrane/ envelope biogenesis
sps_RS07040	-2.435262652	1.80E-09	4-hydroxyphenylpyruvate dioxygenase	Coenzyme metabolism
sps_RS13735	3.525070299	4.29E-19	uroporphyrinogen-III C-methyltransferase	Coenzyme metabolism
sps_RS01075	2.390514104	5.67E-05	hypothetical protein	Energy production and conversion
sps_RS08485	-2.332244017	0.0009908320601	(Fe-S)-binding protein	Energy production and conversion
sps_RS08490	-2.243610425	3.16E-05	iron-sulfur cluster-binding protein	Energy production and conversion
sps_RS09955	-2.1819561	1.51E-07	2-methylcitrate synthase	Energy production and conversion
sps_RS15885	-3.353221008	2.44E-07	NADH-dependent alcohol dehydrogenase	Energy production and conversion
sps_RS00895	2.417088107	2.64E-23	putative sulfate exporter family transporter	Function Unknown
sps_RS01100	2.886649995	8.05E-06	hypothetical protein	Function Unknown
sps_RS01625	-2.472383773	5.52E-09	phospholipase	Function Unknown
sps_RS04960	-2.388386624	3.67E-05	pathogenicity island effector protein	Function Unknown

sps_RS04965	-2.398345673	0.0003323225098	type III secretion system translocon protein	Function Unknown
sps_RS05115	-2.020156919	2.79E-06	hypothetical protein	Function Unknown
sps_RS05120	-2.928372778	3.87E-08	DUF4123 domain-containing protein	Function Unknown
sps_RS05130	-3.16543868	3.71E-05	type VI secretion system tube protein Hcp	Function Unknown
sps_RS06460	-2.077520069	3.06E-05	serine dehydratase subunit alpha family protein	Function Unknown
sps_RS08925	-4.082910269	5.62E-15	NADP-dependent oxidoreductase	Function Unknown
sps_RS10195	-3.907036734	3.91E-17	type VI secretion system tube protein Hcp	Function Unknown
sps_RS10795	-2.009449356	3.54E-08	hypothetical protein	Function Unknown
sps_RS10355	3.216066082	6.30E-13	DUF1611 domain-containing protein	Function Unknown
sps_RS13850	-2.07151457	7.04E-05	hypothetical protein	Function Unknown
sps_RS14010	-3.219900954	9.29E-12	UPF0016 domain-containing protein	Function Unknown
sps_RS15400	-3.649446034	6.03E-13	hydrolase	Function Unknown
sps_RS15625	-4.645200008	4.73E-12	HlyD family secretion protein	Function Unknown
sps_RS19080	-2.24641819	0.0001193099063	LysM peptidoglycan-binding	Function Unknown

			domain-containing protein	
sps_RS19085	-2.253073626	0.0001731110496	DUF4123 domain-containing protein	Function Unknown
sps_RS19095	-4.438315573	9.32E-23	type VI secretion system tube protein Hcp	Function Unknown
sps_RS19160	-2.443556432	8.55E-06	DUF2219 domain-containing protein	Function Unknown
sps_RS19515	-2.085128805	0.0003682687763	OHCU decarboxylase	Function Unknown
sps_RS21730	-2.345662758	0.0004798922473	GTP pyrophosphokinase	Function Unknown
sps_RS24400	-3.628176643	4.94E-12	type VI secretion system tube protein Hcp	Function Unknown
sps_RS24450	-2.699696138	3.15E-06	multidrug transporter	Function Unknown
sps_RS27285	-2.180590953	8.98E-05	EscI/YscI/HrpB family type III secretion system inner rod protein	Function Unknown
sps_RS27350	-3.501607706	2.94E-13	hypothetical protein	Function Unknown
sps_RS27355	-3.430098658	5.30E-14	hypothetical protein	Function Unknown
sps_RS27360	-2.031476666	1.10E-05	CesD/SycD/LcrH family type III secretion system chaperone	Function Unknown
sps_RS27760	-4.109080184	0.0005655501856	DUF2061 domain-containing protein	Function Unknown

sps_RS13780	2.323269975	8.67E-14	phosphoadenyl l-sulfate reductase	Inorganic ion transport and metabolism
sps_RS13785	2.967518488	3.24E-17	NADPH-dependent assimilatory sulfite reductase hemoprotein subunit	Inorganic ion transport and metabolism
sps_RS13790	3.247360256	4.70E-14	assimilatory sulfite reductase (NADPH) flavoprotein subunit	Inorganic ion transport and metabolism
sps_RS18235	2.737406565	2.32E-07	sulfate adenylyltransfer ase subunit CysD	Inorganic ion transport and metabolism
sps_RS01620	-3.046111367	7.12E-16	catalase	Inorganic ion transport and metabolism
sps_RS14015	-4.27679358	5.18E-18	catalase	Inorganic ion transport and metabolism
sps_RS15620	-3.663188551	4.99E-07	MFS transporter	Inorganic ion transport and metabolism
sps_RS21625	-4.947268525	7.50E-21	DNA starvation/statio nary phase protection protein	Inorganic ion transport and metabolism
sps_RS22160	-2.24007972	2.22E-06	MFS transporter	Inorganic ion transport and metabolism
sps_RS15755	-2.254390719	1.73E-05	signal peptidase I	Intracellular trafficking and secretion
sps_RS01090	2.776272702	1.07E-06	hypothetical protein	Lipid metabolism
sps_RS01105	2.068371728	0.00093453084 02	hypothetical protein	Lipid metabolism
sps_RS01110	2.314568826	0.00023215793 57	hypothetical protein	Lipid metabolism
sps_RS01115	2.638873631	3.14E-06	hypothetical protein	Lipid metabolism

sps_RS05895	-2.063500883	0.0001628752387	acyl-CoA dehydrogenase	Lipid metabolism
sps_RS10265	-2.138572107	0.0001780601691	succinyl-CoA--3-ketoacid-CoA transferase	Lipid metabolism
sps_RS06940	2.608649332	0.0001196876498	heat-shock protein	Post-translational modification, protein turnover, chaperone functions
sps_RS22460	2.67185539	2.34E-12	glutathione-dependent disulfide-bond oxidoreductase	Post-translational modification, protein turnover, chaperone functions
sps_RS19150	-4.579618501	8.27E-23	organic hydroperoxide resistance protein	Post-translational modification, protein turnover, chaperone functions
sps_RS24220	-4.81913761	4.25E-22	alkyl hydroperoxide reductase subunit F	Post-translational modification, protein turnover, chaperone functions
sps_RS24225	-5.640077394	7.62E-14	peroxiredoxin	Post-translational modification, protein turnover, chaperone functions
sps_RS27340	-2.104825219	1.65E-05	hypothetical protein	Post-translational modification, protein turnover,

				chaperone functions
sps_RS17155	2.179774499	4.75E-06	ATP-binding protein	Replication and repair
sps_RS01085	2.118191426	0.000479348642	hypothetical protein	Secondary Structure
sps_RS01095	2.387248928	0.000152620548	hypothetical protein	Secondary Structure
sps_RS02070	-2.450966683	3.14E-09	DNA-binding response regulator	Signal Transduction
sps_RS03040	-2.701132009	3.00E-05	PrkA family serine protein kinase	Signal Transduction
sps_RS03915	-3.371103351	1.37E-13	DNA-binding response regulator	Signal Transduction
sps_RS08920	-2.348014489	9.49E-08	MarR family transcriptional regulator	Transcription
sps_RS06465	-2.654320948	4.06E-05	RidA family protein	Translation

Data S3 Table G: Comparison between early log phase samples from 20°C and 4°C cultures.

gene	log2FoldChange (<0 higher in 4, >0 higher in 20)	padj	name	cats
sps_RS00915	2.473297838	3.70E-08	oligopeptidase A	Amino Acid metabolism and transport
sps_RS05300	2.504603871	0.0004756484313	alanine dehydrogenase	Amino Acid metabolism and transport
sps_RS06490	2.371543739	4.19E-07	ATP phosphoribosyltransferase	Amino Acid metabolism and transport
sps_RS06495	2.131181472	0.0006412357818	histidinol dehydrogenase	Amino Acid metabolism and transport
sps_RS06510	2.471111565	0.0001107199133	imidazole glycerol phosphate synthase subunit HisH	Amino Acid metabolism and transport
sps_RS07005	-3.533727838	4.73E-09	1-aminocyclopropane-1-carboxylate deaminase	Amino Acid metabolism and transport
sps_RS08295	2.09839961	6.74E-06	bifunctional indole-3-glycerol-phosphate synthase TrpC/phosphoribosylanthranilate isomerase TrpF	Amino Acid metabolism and transport
sps_RS08300	2.24429259	5.59E-09	tryptophan synthase subunit beta	Amino Acid metabolism and transport
sps_RS08305	2.461791484	2.12E-07	tryptophan synthase subunit alpha	Amino Acid metabolism and transport
sps_RS09555	2.668739053	6.87E-13	branched-chain amino acid ABC transporter permease	Amino Acid metabolism and transport
sps_RS11505	2.521527885	1.58E-08	pyrroline-5-carboxylate reductase	Amino Acid metabolism and transport
sps_RS12080	2.564517547	6.28E-09	glutamate synthase large subunit	Amino Acid metabolism and transport

sps_RS12085	2.305569872	9.62E-08	glutamate synthase small subunit	Amino Acid metabolism and transport
sps_RS12610	-2.378197835	7.42E-05	aspartate aminotransferase family protein	Amino Acid metabolism and transport
sps_RS13315	-2.741720974	6.31E-09	EamA/RhaT family transporter	Amino Acid metabolism and transport
sps_RS21065	-2.489422486	2.57E-08	EamA/RhaT family transporter	Amino Acid metabolism and transport
sps_RS05520	2.540519755	1.65E-09	keto-deoxy-phosphogluconate aldolase	Carbohydrate metabolism and transport
sps_RS05525	2.319023414	4.28E-07	phosphogluconate dehydratase	Carbohydrate metabolism and transport
sps_RS18005	-2.285462679	7.36E-09	MFS transporter	Carbohydrate metabolism and transport
sps_RS19520	-3.65110482	2.04E-13	allantoinase PuuE	Carbohydrate metabolism and transport
sps_RS00455	-2.317242626	5.48E-10	hypothetical protein	Cell motility
sps_RS00460	-2.139791625	6.07E-06	flagellar motor stator protein MotA	Cell motility
sps_RS00475	-2.807469452	1.69E-09	flagellar hook-length control protein FliK	Cell motility
sps_RS00490	-2.029521657	5.49E-08	flagellar hook protein FliD	Cell motility
sps_RS00610	-2.480335439	1.23E-07	OmpA family protein	Cell motility
sps_RS27410	3.212737634	5.31E-10	EscN/YscN/HrcN family type III secretion system ATPase	Cell motility
sps_RS09045	2.500768282	9.42E-12	energy transducer TonB	Cell wall/membrane/envelope biogenesis
sps_RS10190	-2.733619814	2.07E-06	type VI secretion system tip protein VgrG	Cell wall/membrane/envelope biogenesis

sps_RS10360	2.995531524	1.34E-16	dipeptide epimerase	Cell wall/membrane/envelope biogenesis
sps_RS11770	3.249946574	4.50E-07	OmpA family protein	Cell wall/membrane/envelope biogenesis
sps_RS12490	2.130852348	2.15E-05	hypothetical protein	Cell wall/membrane/envelope biogenesis
sps_RS15300	2.261167563	6.41E-16	OmpA family protein	Cell wall/membrane/envelope biogenesis
sps_RS15350	-2.053291975	6.16E-05	efflux RND transporter periplasmic adaptor subunit	Cell wall/membrane/envelope biogenesis
sps_RS18185	-2.625036349	2.54E-09	glycosyl transferase	Cell wall/membrane/envelope biogenesis
sps_RS18190	-2.436568113	5.58E-08	nucleotidyl transferase	Cell wall/membrane/envelope biogenesis
sps_RS18195	-2.169826984	0.0003674356292	CDP-glycerol glycerophosphotransferase	Cell wall/membrane/envelope biogenesis
sps_RS19090	-2.645529721	2.27E-06	type VI secretion system tip protein VgrG	Cell wall/membrane/envelope biogenesis
sps_RS24405	-2.06836203	5.78E-05	type VI secretion system tip protein VgrG	Cell wall/membrane/envelope biogenesis
sps_RS07850	2.149056974	1.11E-11	methyltransferase domain-containing protein	Coenzyme metabolism
sps_RS07860	2.151726239	1.34E-16	biotin synthase BioB	Coenzyme metabolism
sps_RS07865	2.019542502	8.92E-07	adenosylmethionine--8-amino-7-oxononanoate transaminase	Coenzyme metabolism
sps_RS13240	-2.382932423	3.16E-11	type 3 dihydrofolate reductase	Coenzyme metabolism
sps_RS03745	-2.69362479	1.19E-11	isocitrate lyase	Energy production and conversion
sps_RS04550	2.124920332	2.28E-05	cbb3-type cytochrome c oxidase subunit 3	Energy production and conversion

sps_RS04555	2.254032868	4.63E-07	cytochrome-c oxidase, cbb3-type subunit II	Energy production and conversion
sps_RS07560	-2.789205715	5.90E-06	hydrogenase	Energy production and conversion
sps_RS08860	-2.247658685	0.0004819105477	malate synthase	Energy production and conversion
sps_RS10985	2.206294141	6.15E-08	isocitrate dehydrogenase	Energy production and conversion
sps_RS15885	-2.9442779	2.45E-06	NADH-dependent alcohol dehydrogenase	Energy production and conversion
sps_RS20125	3.32189275	6.36E-11	sodium ion-translocating decarboxylase subunit beta	Energy production and conversion
sps_RS23415	-3.720547178	8.57E-16	alkene reductase	Energy production and conversion
sps_RS26460	2.881707815	5.31E-10	pyruvate dehydrogenase complex dihydrolipoyllysine-residue acetyltransferase	Energy production and conversion
sps_RS26465	2.340016067	6.57E-06	pyruvate dehydrogenase (acetyl-transferring), homodimeric type	Energy production and conversion
sps_RS27670	2.814399213	3.47E-08	NAD(P)H-dependent glycerol-3-phosphate dehydrogenase	Energy production and conversion
sps_RS27845	2.939690752	7.27E-08	F0F1 ATP synthase subunit epsilon	Energy production and conversion
sps_RS27850	2.568897463	1.41E-05	F0F1 ATP synthase subunit beta	Energy production and conversion
sps_RS27855	2.452899459	3.62E-05	F0F1 ATP synthase subunit gamma	Energy production and conversion
sps_RS00385	-2.438451695	0.0001001691601	collagenase	Function Unknown
sps_RS00480	-3.357865272	2.93E-06	hypothetical protein	Function Unknown
sps_RS00675	-3.410372752	0.0002700512618	methyltransferase domain-containing protein	Function Unknown
sps_RS00870	-2.09140705	0.0005627293187	VUT family protein	Function Unknown
sps_RS01010	-2.068994411	9.02E-09	multidrug efflux protein	Function Unknown
sps_RS01100	3.452451363	5.98E-09	hypothetical protein	Function Unknown

sps_RS01525	-2.364678586	0.0002818308048	hypothetical protein	Function Unknown
sps_RS02490	2.054339731	6.53E-07	tol-pal system-associated acyl-CoA thioesterase	Function Unknown
sps_RS02645	-2.382569799	1.20E-06	hypothetical protein	Function Unknown
sps_RS04175	-2.739588519	3.48E-23	hypothetical protein	Function Unknown
sps_RS05145	2.021617602	6.90E-05	type VI secretion system protein TssA	Function Unknown
sps_RS05175	2.04013844	0.0008367984236	type VI secretion system lipoprotein TssJ	Function Unknown
sps_RS06735	2.72571405	1.13E-12	23S rRNA accumulation protein YceD	Function Unknown
sps_RS07010	-2.248587365	3.89E-12	YccF domain-containing protein	Function Unknown
sps_RS07015	-3.016140716	5.36E-10	ABC transporter	Function Unknown
sps_RS07765	2.613046822	2.82E-07	curlin	Function Unknown
sps_RS08245	2.125520543	9.54E-08	lipase	Function Unknown
sps_RS08545	-2.604867121	0.0002716976324	N-acetyltransferase	Function Unknown
sps_RS08915	-2.177334425	1.03E-05	hypothetical protein	Function Unknown
sps_RS08925	-3.099947187	3.64E-09	NADP-dependent oxidoreductase	Function Unknown
sps_RS09040	2.22689469	0.0002845607299	hypothetical protein	Function Unknown
sps_RS09560	2.99160466	3.75E-19	AzlD domain-containing protein	Function Unknown
sps_RS09565	2.675003278	0.0003468422222	NIPSNAP family protein	Function Unknown
sps_RS09770	-2.207295056	8.63E-08	hypothetical protein	Function Unknown
sps_RS09985	2.542558234	1.47E-09	ABC-F family ATPase	Function Unknown
sps_RS10070	2.49292302	2.99E-19	protease	Function Unknown
sps_RS10180	-2.362245241	4.66E-05	LysM domain-containing protein	Function Unknown
sps_RS10195	-4.320452293	3.72E-24	type VI secretion system tube protein Hcp	Function Unknown

sps_RS10355	2.948049625	4.21E-11	DUF1611 domain-containing protein	Function Unknown
sps_RS11140	3.386515655	6.90E-09	peptidase	Function Unknown
sps_RS11145	2.581952277	1.85E-06	hypothetical protein	Function Unknown
sps_RS11485	2.073199428	0.000112307 7603	hypothetical protein	Function Unknown
sps_RS11540	-2.679444292	1.68E-11	DUF2884 domain-containing protein	Function Unknown
sps_RS13245	-3.274027702	4.44E-19	hypothetical protein	Function Unknown
sps_RS13420	-2.035543108	2.74E-07	NINE protein	Function Unknown
sps_RS13985	-2.35758331	0.000131888 119	transposase	Function Unknown
sps_RS15065	2.31914063	8.94E-09	adhesin	Function Unknown
sps_RS15070	2.236929601	4.08E-07	type I secretion system permease/ATPase	Function Unknown
sps_RS15570	2.787310859	4.34E-05	hypothetical protein	Function Unknown
sps_RS16965	-2.189085415	2.51E-05	hypothetical protein	Function Unknown
sps_RS16980	-3.26305389	0.000311931 7043	hypothetical protein	Function Unknown
sps_RS17000	-3.829160263	5.31E-10	hypothetical protein	Function Unknown
sps_RS17005	-3.833000674	8.19E-06	hypothetical protein	Function Unknown
sps_RS17010	-2.182859691	1.05E-05	hypothetical protein	Function Unknown
sps_RS17325	2.219727118	3.42E-05	DUF2919 domain-containing protein	Function Unknown
sps_RS18960	2.373636069	2.22E-14	hypothetical protein	Function Unknown
sps_RS19080	-2.319984805	1.81E-05	LysM peptidoglycan-binding domain-containing protein	Function Unknown
sps_RS19085	-2.833388455	2.46E-07	DUF4123 domain-containing protein	Function Unknown
sps_RS19095	-3.346506632	9.82E-14	type VI secretion system tube protein Hcp	Function Unknown
sps_RS19145	-2.023061679	2.05E-07	DoxX family protein	Function Unknown

sps_RS19515	-3.855546301	3.01E-14	OHCU decarboxylase	Function Unknown
sps_RS19870	2.107869645	0.0008726340514	DUF3604 domain-containing protein	Function Unknown
sps_RS20300	-2.32652502	5.38E-11	hypothetical protein	Function Unknown
sps_RS21070	-2.457959302	0.0004616929371	hypothetical protein	Function Unknown
sps_RS21845	2.073556007	1.49E-06	hypothetical protein	Function Unknown
sps_RS23235	-2.391021966	1.36E-07	DUF3560 domain-containing protein	Function Unknown
sps_RS23400	-4.548249722	1.93E-14	SRPBCC family protein	Function Unknown
sps_RS23405	-3.751341329	4.14E-16	hypothetical protein	Function Unknown
sps_RS23410	-3.769934146	3.42E-25	patatin	Function Unknown
sps_RS24400	-3.085092994	2.58E-09	type VI secretion system tube protein Hcp	Function Unknown
sps_RS24525	2.135759473	9.42E-12	ABC transporter ATP-binding protein	Function Unknown
sps_RS25410	-3.142198139	0.0008686277586	hypothetical protein	Function Unknown
sps_RS27290	2.862005667	2.04E-07	hypothetical protein	Function Unknown
sps_RS27295	3.619354663	3.29E-15	hypothetical protein	Function Unknown
sps_RS27310	2.105398212	3.57E-08	EscD/YscD/HrpQ family type III secretion system inner membrane ring protein	Function Unknown
sps_RS27350	5.094906906	3.28E-28	hypothetical protein	Function Unknown
sps_RS27355	5.07287112	8.24E-31	hypothetical protein	Function Unknown
sps_RS27360	4.388459415	5.86E-27	CesD/SycD/LcrH family type III secretion system chaperone	Function Unknown
sps_RS27365	3.40333133	1.42E-18	hypothetical protein	Function Unknown
sps_RS27385	2.063279245	0.0001625410229	hypothetical protein	Function Unknown
sps_RS27395	3.457498409	8.19E-11	type III secretion chaperone SycN	Function Unknown

sps_RS27405	3.724153559	1.23E-19	YopN family type III secretion system gatekeeper subunit	Function Unknown
sps_RS27665	2.163219059	1.50E-07	NAD(P)/FAD-dependent oxidoreductase	Function Unknown
sps_RS07025	-3.452734497	1.09E-13	cytochrome C biogenesis protein CcsA	Inorganic ion transport and metabolism
sps_RS09050	2.401619441	5.75E-06	biopolymer transporter ExbD	Inorganic ion transport and metabolism
sps_RS09125	-2.539404115	1.13E-09	Anion transporter	Inorganic ion transport and metabolism
sps_RS10800	2.248756185	7.73E-09	TonB-dependent receptor	Inorganic ion transport and metabolism
sps_RS11650	2.308530962	1.21E-05	TonB-dependent receptor	Inorganic ion transport and metabolism
sps_RS12845	-2.173465158	3.82E-06	alkaline phosphatase	Inorganic ion transport and metabolism
sps_RS17560	2.756478238	3.32E-08	TonB-dependent receptor	Inorganic ion transport and metabolism
sps_RS24705	-2.058354598	7.37E-05	ion transporter	Inorganic ion transport and metabolism
sps_RS27765	-2.246593006	4.59E-09	phosphate ABC transporter substrate-binding protein	Inorganic ion transport and metabolism
sps_RS09055	2.537202941	6.31E-09	MotA/TolQ/ExbB proton channel family protein	Intracellular trafficking and secretion
sps_RS17775	2.133086832	0.000254887 5961	protein translocase subunit SecF	Intracellular trafficking and secretion
sps_RS17780	2.455758424	7.86E-08	protein translocase subunit SecD	Intracellular trafficking and secretion
sps_RS17785	2.300615414	1.12E-05	preprotein translocase subunit YajC	Intracellular trafficking and secretion

sps_RS27280	2.186301508	1.69E-09	EscJ/YscJ/HrcJ family type III secretion inner membrane ring protein	Intracellular trafficking and secretion
sps_RS27300	2.749933851	2.76E-05	EscF/YscF/HrpA family type III secretion system needle major subunit	Intracellular trafficking and secretion
sps_RS27315	2.273483267	2.76E-16	EscC/YscC/HrcC family type III secretion system outer membrane ring protein	Intracellular trafficking and secretion
sps_RS27390	2.597053944	1.28E-08	YscX family type III secretion protein	Intracellular trafficking and secretion
sps_RS27675	2.645334886	6.07E-05	protein-export chaperone SecB	Intracellular trafficking and secretion
sps_RS01105	2.119231787	0.0002012402357	hypothetical protein	Lipid metabolism
sps_RS01110	3.0303685	7.94E-08	hypothetical protein	Lipid metabolism
sps_RS01115	3.94073512	3.01E-14	hypothetical protein	Lipid metabolism
sps_RS26895	-2.36426423	0.0007969741748	PAP2 family protein	Lipid metabolism
sps_RS04270	2.757608805	1.51E-10	adenylosuccinate synthetase	Nucleotide metabolism and transport
sps_RS05160	2.183503379	0.0004640365808	type VI secretion system ATPase TssH	Post-translational modification, protein turnover, chaperone functions
sps_RS07585	-2.900592623	5.54E-06	hypothetical protein	Post-translational modification, protein turnover, chaperone functions
sps_RS07830	2.096191537	1.01E-06	protease HtpX	Post-translational modification, protein turnover, chaperone functions
sps_RS08180	2.625310775	1.20E-06	molecular chaperone HtpG	Post-translational modification, protein turnover,

				chaperone functions
sps_RS09205	2.567339524	1.49E-08	peptidylprolyl isomerase	Post-translational modification, protein turnover, chaperone functions
sps_RS09215	2.381433794	6.90E-09	endopeptidase La	Post-translational modification, protein turnover, chaperone functions
sps_RS10150	2.223985425	0.000358126277	peroxiredoxin	Post-translational modification, protein turnover, chaperone functions
sps_RS11045	2.106795419	3.79E-08	nucleotide exchange factor GrpE	Post-translational modification, protein turnover, chaperone functions
sps_RS17270	-2.779791093	0.0006265155215	thiol peroxidase	Post-translational modification, protein turnover, chaperone functions
sps_RS18045	-2.098696208	8.47E-05	peptidylprolyl isomerase	Post-translational modification, protein turnover, chaperone functions
sps_RS19150	-2.88489726	3.40E-09	organic hydroperoxide resistance protein	Post-translational modification, protein turnover, chaperone functions
sps_RS20985	2.359155945	6.53E-09	ATP-dependent zinc metalloprotease FtsH	Post-translational modification, protein turnover, chaperone functions
sps_RS21055	2.552907327	1.00E-08	molecular chaperone DnaJ	Post-translational modification, protein turnover,

				chaperone functions
sps_RS22460	2.697848607	6.26E-13	glutathione-dependent disulfide-bond oxidoreductase	Post-translational modification, protein turnover, chaperone functions
sps_RS25550	2.364603931	8.99E-13	DegQ family serine endoprotease	Post-translational modification, protein turnover, chaperone functions
sps_RS25925	2.327738644	4.53E-05	chaperonin GroEL	Post-translational modification, protein turnover, chaperone functions
sps_RS25930	2.377174616	1.96E-05	co-chaperone GroES	Post-translational modification, protein turnover, chaperone functions
sps_RS26410	2.895426261	2.45E-14	ATP-dependent protease subunit HslV	Post-translational modification, protein turnover, chaperone functions
sps_RS26415	2.721968851	1.31E-09	ATP-dependent protease ATPase subunit HslU	Post-translational modification, protein turnover, chaperone functions
sps_RS26850	2.326135273	3.09E-06	Hsp33 family molecular chaperone HslO	Post-translational modification, protein turnover, chaperone functions
sps_RS27340	5.015286757	2.62E-31	hypothetical protein	Post-translational modification, protein turnover, chaperone functions
sps_RS06160	-2.365701168	4.55E-05	integrase	Replication and repair
sps_RS07065	-2.048744908	3.59E-05	hypothetical protein	Replication and repair

sps_RS07090	-3.306453599	0.0006033836821	hypothetical protein	Replication and repair
sps_RS13310	-4.057716061	0.0002515286607	IS256 family transposase	Replication and repair
sps_RS14690	-2.202480566	5.78E-05	endonuclease I	Replication and repair
sps_RS22645	2.07799625	6.73E-07	DNA polymerase III subunit chi	Replication and repair
sps_RS22930	-2.537815092	2.25E-16	hypothetical protein	Replication and repair
sps_RS22990	-2.553880839	1.69E-09	IS30 family transposase	Replication and repair
sps_RS25405	-2.239026615	0.0005858109063	phage N-6-adenine-methyltransferase	Replication and repair
sps_RS01095	2.110059204	0.0004072403602	hypothetical protein	Secondary Structure
sps_RS08660	2.304565309	2.27E-06	reductase	Secondary Structure
sps_RS08665	2.668936075	3.42E-07	thioesterase	Secondary Structure
sps_RS15280	2.074222371	9.55E-07	tandem-95 repeat protein	Secondary Structure
sps_RS00605	-2.423661829	2.99E-13	sigma-54-dependent Fis family transcriptional regulator	Signal Transduction
sps_RS03915	-2.08519072	9.05E-06	DNA-binding response regulator	Signal Transduction
sps_RS05180	2.253665936	0.0002012560198	type VI secretion system-associated FHA domain protein TagH	Signal Transduction
sps_RS11275	2.118380441	2.04E-13	methyl-accepting chemotaxis protein	Signal Transduction
sps_RS11800	-2.498305045	1.03E-06	PAS domain-containing protein	Signal Transduction
sps_RS22745	-2.076660325	3.52E-06	response regulator	Signal Transduction
sps_RS00465	-2.723170359	5.29E-09	RNA polymerase sigma factor FliA	Transcription
sps_RS01930	2.058575598	3.32E-05	DNA-directed RNA polymerase subunit alpha	Transcription
sps_RS09550	2.215989432	1.94E-06	AraC family transcriptional regulator	Transcription
sps_RS09570	3.044029388	5.92E-44	YafY family transcriptional regulator	Transcription

sps_RS09575	2.789269135	2.65E-07	AraC family transcriptional regulator	Transcription
sps_RS09965	-3.292570998	3.47E-17	GntR family transcriptional regulator	Transcription
sps_RS12545	2.326682345	4.72E-06	RNA polymerase sigma factor RpoD	Transcription
sps_RS14655	-2.173970549	7.04E-07	LysR family transcriptional regulator	Transcription
sps_RS17430	-3.588847108	4.27E-25	transcriptional regulator BetI	Transcription
sps_RS23225	-2.595386474	5.31E-10	hypothetical protein	Transcription
sps_RS27330	2.14769305	1.26E-09	AraC family transcriptional regulator	Transcription
sps_RS27370	3.135921594	1.93E-06	hypothetical protein	Transcription
sps_RS01750	2.064605896	5.34E-05	50S ribosomal protein L11	Translation
sps_RS01755	2.118288641	0.0008767055618	50S ribosomal protein L1	Translation
sps_RS01780	2.012603546	8.86E-06	30S ribosomal protein S12	Translation
sps_RS01790	2.569529472	5.49E-08	elongation factor G	Translation
sps_RS01915	2.190065274	8.98E-05	30S ribosomal protein S13	Translation
sps_RS06555	2.448467325	6.46E-10	phenylalanine--tRNA ligase subunit beta	Translation
sps_RS06560	3.10283222	5.49E-08	phenylalanine--tRNA ligase subunit alpha	Translation
sps_RS09255	2.130282884	4.57E-11	cysteine--tRNA ligase	Translation
sps_RS11905	2.400582141	8.38E-07	tRNA (guanosine(37)-N1)-methyltransferase TrmD	Translation
sps_RS11910	2.424002401	4.11E-05	ribosome maturation factor RimM	Translation
sps_RS11915	2.211626603	2.28E-05	30S ribosomal protein S16	Translation
sps_RS12360	2.156367875	9.78E-07	tyrosine--tRNA ligase	Translation
sps_RS12530	2.10071334	0.0005898512769	30S ribosomal protein S21	Translation
sps_RS14235	2.453785596	5.31E-10	30S ribosomal protein S6--L-glutamate ligase	Translation

sps_RS19945	2.115698622	0.0001369153752	ribosome-associated translation inhibitor RaiA	Translation
sps_RS20940	2.307679905	1.55E-06	translation initiation factor IF-2	Translation
sps_RS20990	2.589762127	2.98E-09	23S rRNA (uridine(2552)-2'-O)-methyltransferase RlmE	Translation
sps_RS24155	2.162200772	5.73E-08	lysine--tRNA ligase	Translation
sps_RS26400	2.476358676	5.44E-13	arginine--tRNA ligase	Translation

Data S3 Table H: Comparison between late log phase samples from 20°C and 4°C cultures.

gene	log2FoldChange (<0 higher in 4, >0 higher in 20)	padj	name	cats
sps_RS02585	2.432967432	3.68E-16	FAD-binding oxidoreductase	Amino Acid metabolism and transport
sps_RS02815	-2.62325148	6.55E-09	cystathionine beta-lyase	Amino Acid metabolism and transport
sps_RS03160	2.082832257	7.00E-05	PLP-dependent cysteine synthase family protein	Amino Acid metabolism and transport
sps_RS03450	-2.146479288	4.12E-17	sarcosine oxidase subunit gamma family protein	Amino Acid metabolism and transport
sps_RS04490	-2.889406809	1.16E-07	aspartate/tyrosine/aromatic aminotransferase	Amino Acid metabolism and transport
sps_RS06510	2.237174457	0.000431487391	imidazole glycerol phosphate synthase subunit HisH	Amino Acid metabolism and transport
sps_RS07005	-2.308603	0.000248975345	1-aminocyclopropane-1-carboxylate deaminase	Amino Acid metabolism and transport
sps_RS08380	2.152438385	0.000293422871	GMC family oxidoreductase	Amino Acid metabolism and transport
sps_RS09555	3.530787099	2.74E-22	branched-chain amino acid ABC transporter permease	Amino Acid metabolism and transport
sps_RS10075	-2.10549464	1.66E-05	homoserine O-succinyltransferase	Amino Acid metabolism and transport
sps_RS11430	-2.942693883	9.00E-13	low-specificity L-threonine aldolase	Amino Acid metabolism and transport
sps_RS11825	-2.929936891	1.45E-09	bifunctional aspartate kinase/homoserine dehydrogenase I	Amino Acid metabolism and transport

sps_RS11890	-2.495200904	9.94E-06	3-deoxy-7-phosphoheptulonate synthase	Amino Acid metabolism and transport
sps_RS14555	-3.141433946	7.97E-08	methylenetetrahydrofolate reductase	Amino Acid metabolism and transport
sps_RS14565	-2.753095133	3.08E-07	O-succinylhomoserine (thiol)-lyase	Amino Acid metabolism and transport
sps_RS14755	-2.426600049	7.04E-05	HAD-IB family hydrolase	Amino Acid metabolism and transport
sps_RS15425	-2.377008819	4.75E-10	branched-chain amino acid transaminase	Amino Acid metabolism and transport
sps_RS15430	-3.153787209	3.68E-14	acetolactate synthase 2 small subunit	Amino Acid metabolism and transport
sps_RS15435	-2.122386236	0.0001858064363	acetolactate synthase 2 catalytic subunit	Amino Acid metabolism and transport
sps_RS15440	-2.991516746	9.42E-08	ketol-acid reductoisomerase	Amino Acid metabolism and transport
sps_RS16220	-2.172148186	2.42E-12	2-isopropylmalate synthase	Amino Acid metabolism and transport
sps_RS16775	-3.277195875	2.41E-31	dihydrodipicolinate synthase family protein	Amino Acid metabolism and transport
sps_RS20350	-2.288885307	1.20E-07	serine hydroxymethyltransferase	Amino Acid metabolism and transport
sps_RS22605	-3.937882589	3.82E-06	LysE family translocator	Amino Acid metabolism and transport
sps_RS26665	-2.821317124	6.38E-09	argininosuccinate lyase	Amino Acid metabolism and transport
sps_RS26670	-2.160753368	8.98E-06	argininosuccinate synthase	Amino Acid metabolism and transport
sps_RS03280	2.427088679	5.25E-05	glucan 1,4-alpha-glucosidase	Carbohydrate metabolism and transport

sps_RS19520	-2.66578705	1.75E-07	allantoinase PuuE	Carbohydrate metabolism and transport
sps_RS20400	-2.335405937	1.54E-07	chitinase	Carbohydrate metabolism and transport
sps_RS26405	2.219417589	9.36E-11	sporulation protein	Cell cycle control and mitosis
sps_RS01230	3.049676229	1.20E-05	PAS domain-containing protein	Cell motility
sps_RS03520	2.155648326	0.0001935587614	flagellin	Cell motility
sps_RS17255	-5.320852604	1.63E-14	hypothetical protein	Cell motility
sps_RS21855	2.06242213	2.54E-05	hypothetical protein	Cell motility
sps_RS27410	3.29631472	1.38E-10	EscN/YscN/HrcN family type III secretion system ATPase	Cell motility
sps_RS27425	2.362221446	1.40E-07	YscQ/HrcQ family type III secretion apparatus protein	Cell motility
sps_RS01180	2.322175038	3.00E-24	LTA synthase family protein	Cell wall/membrane/envelope biogenesis
sps_RS05215	2.21295443	9.58E-10	efflux RND transporter periplasmic adaptor subunit	Cell wall/membrane/envelope biogenesis
sps_RS05385	-2.097023326	0.0003800328242	hypothetical protein	Cell wall/membrane/envelope biogenesis
sps_RS06170	-2.290620345	2.27E-08	D-alanine--D-alanine ligase	Cell wall/membrane/envelope biogenesis
sps_RS07000	2.184837644	6.05E-15	mechanosensitive ion channel protein MscS	Cell wall/membrane/envelope biogenesis
sps_RS09080	-2.505318639	7.29E-06	porin	Cell wall/membrane/envelope biogenesis
sps_RS09305	2.70757643	4.37E-05	hypothetical protein	Cell wall/membrane/envelope biogenesis

sps_RS12855	2.851965957	9.41E-07	LrgB family protein	Cell wall/membrane/envelope biogenesis
sps_RS15080	3.507014058	1.10E-15	agglutination protein	Cell wall/membrane/envelope biogenesis
sps_RS15295	2.112759757	4.43E-06	channel protein TolC	Cell wall/membrane/envelope biogenesis
sps_RS20885	-2.838836009	4.43E-06	hypothetical protein	Cell wall/membrane/envelope biogenesis
sps_RS05830	-3.098180536	1.02E-07	thiamine biosynthesis protein ThiS	Coenzyme metabolism
sps_RS07040	-2.168044418	1.42E-07	4-hydroxyphenylpyruvate dioxygenase	Coenzyme metabolism
sps_RS07850	2.01750249	3.89E-10	methyltransferase domain-containing protein	Coenzyme metabolism
sps_RS07855	2.670996484	2.09E-23	8-amino-7-oxononanoate synthase	Coenzyme metabolism
sps_RS07860	2.24594267	9.39E-18	biotin synthase BioB	Coenzyme metabolism
sps_RS01075	2.883998093	1.04E-07	hypothetical protein	Energy production and conversion
sps_RS01610	-4.303511554	3.61E-11	aldehyde dehydrogenase	Energy production and conversion
sps_RS03745	-3.62477364	4.27E-21	isocitrate lyase	Energy production and conversion
sps_RS04705	-3.494286572	1.56E-10	alcohol dehydrogenase	Energy production and conversion
sps_RS05675	2.420291361	2.46E-12	electron transport complex subunit RsxB	Energy production and conversion
sps_RS05680	2.054928972	2.98E-08	electron transport complex subunit RsxC	Energy production and conversion
sps_RS05685	2.437428107	7.09E-10	electron transport complex subunit RsxD	Energy production and conversion
sps_RS08005	-2.707442742	4.83E-12	citrate synthase	Energy production and conversion

sps_RS08860	-3.31396699	4.71E-08	malate synthase	Energy production and conversion
sps_RS09300	3.427884457	1.08E-08	cystathionine beta-synthase	Energy production and conversion
sps_RS09310	2.277455159	4.83E-05	cytochrome C	Energy production and conversion
sps_RS15005	-4.50922875	6.16E-16	SDR family NAD(P)-dependent oxidoreductase	Energy production and conversion
sps_RS17495	2.887194427	0.0001779416287	NADH-quinone oxidoreductase subunit NuoC/D	Energy production and conversion
sps_RS17505	3.883386137	0.000116816013	NADH oxidoreductase (quinone) subunit F	Energy production and conversion
sps_RS17510	2.1576288	0.0006500355765	NADH dehydrogenase (quinone) subunit G	Energy production and conversion
sps_RS17520	3.834237896	2.94E-05	NADH-quinone oxidoreductase subunit NuoI	Energy production and conversion
sps_RS18985	-2.606652119	6.55E-09	malate synthase A	Energy production and conversion
sps_RS19850	2.891238878	6.15E-07	hypothetical protein	Energy production and conversion
sps_RS27670	2.592397258	4.16E-07	NAD(P)H-dependent glycerol-3-phosphate dehydrogenase	Energy production and conversion
sps_RS27870	2.101067784	6.14E-07	F0F1 ATP synthase subunit B	Energy production and conversion
sps_RS00050	-2.577267	0.0009825280082	SDR family NAD(P)-dependent oxidoreductase	Function Unknown
sps_RS00895	2.826129795	8.34E-34	putative sulfate exporter family transporter	Function Unknown
sps_RS01100	4.389501481	2.23E-10	hypothetical protein	Function Unknown
sps_RS01275	2.22923224	7.32E-06	SURF1 family protein	Function Unknown
sps_RS02200	-2.079402124	1.53E-10	DUF4336 domain-containing protein	Function Unknown
sps_RS02895	3.426785493	2.42E-12	DUF1302 domain-containing protein	Function Unknown

sps_RS03030	-3.221569136	4.89E-09	SpoVR family protein	Function Unknown
sps_RS03035	-3.317282472	1.84E-07	hypothetical protein	Function Unknown
sps_RS03135	2.077704014	2.11E-06	AcrB/AcrD/AcrF family protein	Function Unknown
sps_RS03275	2.052588717	1.14E-10	hypothetical protein	Function Unknown
sps_RS04300	2.017569937	2.78E-12	hypothetical protein	Function Unknown
sps_RS04385	-3.34560232	1.24E-10	hypothetical protein	Function Unknown
sps_RS04390	-2.436963057	2.87E-09	N-acetyltransferase	Function Unknown
sps_RS04635	-2.088956496	3.30E-05	KR domain-containing protein	Function Unknown
sps_RS04880	-2.465666497	4.94E-07	type III secretion apparatus	Function Unknown
sps_RS05080	2.246990291	0.0004842217867	type VI secretion system PAAR protein	Function Unknown
sps_RS05130	-2.745409498	0.0001387996399	type VI secretion system tube protein Hcp	Function Unknown
sps_RS05225	-2.73255384	5.52E-07	META domain-containing protein	Function Unknown
sps_RS05430	-2.220155774	2.84E-08	YtoQ family protein	Function Unknown
sps_RS06130	-2.663820908	9.15E-05	DUF2975 domain-containing protein	Function Unknown
sps_RS07015	-2.153968555	1.88E-05	ABC transporter	Function Unknown
sps_RS07205	-2.022633894	4.40E-05	hypothetical protein	Function Unknown
sps_RS07690	-2.379338868	0.0005612003088	hypothetical protein	Function Unknown
sps_RS07765	2.437462568	1.98E-06	curlin	Function Unknown
sps_RS08035	2.285969608	1.00E-06	MBL fold metallo-hydrolase	Function Unknown
sps_RS08150	2.070443021	9.16E-08	hypothetical protein	Function Unknown
sps_RS08245	2.170047659	4.44E-08	lipase	Function Unknown

sps_RS08455	-2.220241886	2.31E-06	hypothetical protein	Function Unknown
sps_RS08545	-3.12456507	5.36E-05	N-acetyltransferase	Function Unknown
sps_RS09320	2.793261752	1.14E-05	cytochrome C	Function Unknown
sps_RS09560	3.337708202	6.90E-23	AzlD domain-containing protein	Function Unknown
sps_RS09565	2.478001394	0.000926664586	NIPSNAP family protein	Function Unknown
sps_RS09620	-2.560594684	0.000169350742	amphi-Trp domain-containing protein	Function Unknown
sps_RS09825	-2.025967941	4.92E-09	GNAT family N-acetyltransferase	Function Unknown
sps_RS10070	2.229095898	1.19E-15	protease	Function Unknown
sps_RS10195	-5.611808363	2.89E-40	type VI secretion system tube protein Hcp	Function Unknown
sps_RS10335	2.021844539	1.88E-05	acyltransferase	Function Unknown
sps_RS10355	2.488481358	4.64E-08	DUF1611 domain-containing protein	Function Unknown
sps_RS11140	3.48294448	1.83E-09	peptidase	Function Unknown
sps_RS11145	3.0291171	8.07E-09	hypothetical protein	Function Unknown
sps_RS11150	2.135676497	4.06E-05	PKD domain-containing protein	Function Unknown
sps_RS11395	2.498869509	3.15E-09	hypothetical protein	Function Unknown
sps_RS11550	-3.418547846	3.16E-05	DUF469 domain-containing protein	Function Unknown
sps_RS11785	2.140951315	6.37E-05	DUF3545 domain-containing protein	Function Unknown
sps_RS12740	2.12418513	2.76E-08	flotillin	Function Unknown
sps_RS12840	-2.016008953	1.27E-05	hypoxanthine phosphoribosyltransferase	Function Unknown
sps_RS12860	3.113128985	0.000285968946	hypothetical protein	Function Unknown
sps_RS13330	-2.018703658	3.91E-20	hypothetical protein	Function Unknown

sps_RS14215	-2.068149672	0.000328713946	DUF5062 domain-containing protein	Function Unknown
sps_RS15000	-7.381744578	1.16E-17	phasin family protein	Function Unknown
sps_RS15065	3.92002712	3.00E-24	adhesin	Function Unknown
sps_RS15070	4.219326456	1.96E-23	type I secretion system permease/ATPase	Function Unknown
sps_RS15285	2.791402817	1.39E-21	type I secretion system permease/ATPase	Function Unknown
sps_RS15895	-2.473354916	4.73E-10	phasin family protein	Function Unknown
sps_RS17000	-2.286215213	0.000254401923 7	hypothetical protein	Function Unknown
sps_RS17110	-2.862382028	8.66E-07	DUF1851 domain-containing protein	Function Unknown
sps_RS17135	2.807805055	1.91E-07	DUF3164 domain-containing protein	Function Unknown
sps_RS17295	-2.612633074	0.000589106850 3	MBL fold metallo-hydrolase	Function Unknown
sps_RS18960	2.014079869	1.53E-10	hypothetical protein	Function Unknown
sps_RS19095	-4.420059061	4.93E-24	type VI secretion system tube protein Hcp	Function Unknown
sps_RS19515	-3.072554762	3.44E-09	OHCU decarboxylase	Function Unknown
sps_RS19855	2.295386358	2.14E-06	hypothetical protein	Function Unknown
sps_RS19865	2.270814515	7.08E-07	hypothetical protein	Function Unknown
sps_RS19870	3.309789244	2.70E-08	DUF3604 domain-containing protein	Function Unknown
sps_RS19875	2.509553636	1.63E-16	peptidyl-prolyl cis-trans isomerase	Function Unknown
sps_RS19880	4.256968734	4.53E-11	hypothetical protein	Function Unknown
sps_RS20500	2.15708208	3.05E-05	MipA/OmpV family protein	Function Unknown
sps_RS20505	2.140126738	0.000114529085 5	DUF3019 domain-containing protein	Function Unknown
sps_RS21315	2.146389124	1.81E-06	hypothetical protein	Function Unknown

sps_RS21770	2.033422272	0.000886193053	tripartite tricarboxylate transporter TctA	Function Unknown
sps_RS21780	2.509567189	6.14E-06	tripartite tricarboxylate transporter substrate binding protein	Function Unknown
sps_RS21845	2.132905791	6.51E-07	hypothetical protein	Function Unknown
sps_RS21990	-2.385598881	1.57E-05	GNAT family N-acetyltransferase	Function Unknown
sps_RS22115	2.41744448	0.000135260721 9	hypothetical protein	Function Unknown
sps_RS22275	-3.089386699	0.000673064006 7	DUF4255 domain-containing protein	Function Unknown
sps_RS22465	2.046785643	9.42E-08	hypothetical protein	Function Unknown
sps_RS22815	2.458659705	1.58E-06	HlyD family secretion protein	Function Unknown
sps_RS23400	-4.066881676	3.61E-11	SRPBCC family protein	Function Unknown
sps_RS23405	-2.204859237	4.00E-06	hypothetical protein	Function Unknown
sps_RS23410	-2.791142135	1.21E-13	patatin	Function Unknown
sps_RS23810	-2.332394833	0.000201295758 4	hypothetical protein	Function Unknown
sps_RS24400	-4.365802519	2.43E-18	type VI secretion system tube protein Hcp	Function Unknown
sps_RS24685	-3.551423386	6.93E-07	DUF2170 domain-containing protein	Function Unknown
sps_RS24695	-2.358368825	1.32E-10	hypothetical protein	Function Unknown
sps_RS24890	-2.149314594	4.87E-05	TAT leader-containing periplasmic protein	Function Unknown
sps_RS26975	3.373281861	1.45E-06	DUF692 domain-containing protein	Function Unknown
sps_RS26980	4.121123102	1.68E-05	DUF2282 domain-containing protein	Function Unknown
sps_RS27290	2.532643793	4.64E-06	hypothetical protein	Function Unknown
sps_RS27295	2.069638451	1.30E-05	hypothetical protein	Function Unknown

sps_RS27350	2.285903194	2.44E-06	hypothetical protein	Function Unknown
sps_RS27355	2.433883181	1.14E-07	hypothetical protein	Function Unknown
sps_RS27360	2.068811397	5.89E-07	CesD/SycD/LcrH family type III secretion system chaperone	Function Unknown
sps_RS27385	2.761816979	8.17E-07	hypothetical protein	Function Unknown
sps_RS27395	2.863663393	8.73E-08	type III secretion chaperone SycN	Function Unknown
sps_RS27405	2.051835412	8.80E-07	YopN family type III secretion system gatekeeper subunit	Function Unknown
sps_RS07025	-2.008958713	4.23E-05	cytochrome C biogenesis protein CcsA	Inorganic ion transport and metabolism
sps_RS08845	-2.708764964	2.87E-09	rhodanese-like domain-containing protein	Inorganic ion transport and metabolism
sps_RS09075	3.800714138	2.09E-23	TonB-dependent receptor	Inorganic ion transport and metabolism
sps_RS10800	2.203399361	1.62E-08	TonB-dependent receptor	Inorganic ion transport and metabolism
sps_RS10900	-2.419258938	5.87E-10	phosphate-binding protein	Inorganic ion transport and metabolism
sps_RS19860	3.172991497	8.56E-09	arylsulfatase	Inorganic ion transport and metabolism
sps_RS27765	-2.301580733	1.83E-09	phosphate ABC transporter substrate-binding protein	Inorganic ion transport and metabolism
sps_RS11690	2.696052531	0.000448934316 8	pilus assembly protein PilX	Intracellular trafficking and secretion
sps_RS11700	2.988940453	3.33E-08	type IV pilus modification protein PilV	Intracellular trafficking and secretion
sps_RS15075	4.492391622	2.29E-13	HlyD family type I secretion periplasmic adaptor subunit	Intracellular trafficking and secretion

sps_RS26330	2.15873685	1.46E-09	type II/IV secretion system protein	Intracellular trafficking and secretion
sps_RS26340	2.241358532	1.04E-06	AAA family ATPase	Intracellular trafficking and secretion
sps_RS26495	2.90865955	3.32E-15	type IV-A pilus assembly ATPase PilB	Intracellular trafficking and secretion
sps_RS27300	2.40843268	0.0002030993653	EscF/YscF/HrpA family type III secretion system needle major subunit	Intracellular trafficking and secretion
sps_RS27315	2.09414861	8.37E-14	EscC/YscC/HrcC family type III secretion system outer membrane ring protein	Intracellular trafficking and secretion
sps_RS27380	2.74244719	4.54E-18	EscV/YscV/HrcV family type III secretion system export apparatus protein	Intracellular trafficking and secretion
sps_RS27415	2.981590005	0.0001654802532	hypothetical protein	Intracellular trafficking and secretion
sps_RS27435	3.439431307	8.71E-06	EscS/YscS/HrcS family type III secretion system export apparatus protein	Intracellular trafficking and secretion
sps_RS01090	2.708564244	6.74E-07	hypothetical protein	Lipid metabolism
sps_RS01105	3.443090214	2.70E-10	hypothetical protein	Lipid metabolism
sps_RS01110	3.589755078	1.53E-10	hypothetical protein	Lipid metabolism
sps_RS01115	3.726402891	1.26E-12	hypothetical protein	Lipid metabolism
sps_RS08835	-3.283606596	5.99E-18	transporter	Lipid metabolism
sps_RS14995	-3.442924677	2.31E-20	class I poly(R)-hydroxyalkanoic acid synthase	Lipid metabolism
sps_RS21950	-2.107992015	6.45E-06	alpha/beta hydrolase	Lipid metabolism

sps_RS08910	-2.435155858	3.14E-15	anaerobic ribonucleoside-triphosphate reductase	Nucleotide metabolism and transport
sps_RS01600	3.319766854	8.45E-07	YjjW family glycine radical enzyme activase	Post-translational modification, protein turnover, chaperone functions
sps_RS02470	-2.485172135	1.34E-08	alkyl hydroperoxide reductase	Post-translational modification, protein turnover, chaperone functions
sps_RS03850	-2.710025025	9.99E-07	peptide-methionine (S)-S-oxide reductase	Post-translational modification, protein turnover, chaperone functions
sps_RS06075	3.222826849	4.64E-08	DsbA family protein	Post-translational modification, protein turnover, chaperone functions
sps_RS07320	-3.581504335	0.000668663748 2	hypothetical protein	Post-translational modification, protein turnover, chaperone functions
sps_RS09315	2.917125964	2.78E-05	hypothetical protein	Post-translational modification, protein turnover, chaperone functions
sps_RS17270	-3.921602293	4.28E-07	thiol peroxidase	Post-translational modification, protein turnover, chaperone functions
sps_RS27340	2.092243845	3.27E-06	hypothetical protein	Post-translational modification, protein turnover, chaperone functions
sps_RS00375	3.235764735	3.55E-09	DNA-protecting protein DprA	Replication and repair
sps_RS06065	2.327830814	3.79E-07	exodeoxyribonuclease V subunit beta	Replication and repair
sps_RS06070	2.513452333	2.20E-07	exodeoxyribonuclease V subunit alpha	Replication and repair
sps_RS07515	2.113235101	2.69E-05	PKD domain-containing protein	Replication and repair
sps_RS08100	2.014379309	2.13E-07	transcription-repair coupling factor	Replication and repair

sps_RS08570	2.296125413	4.00E-08	DNA topoisomerase III	Replication and repair
sps_RS10920	-2.688446282	6.67E-06	recombination-associated protein RdgC	Replication and repair
sps_RS13310	-3.998922105	0.000636249829 7	IS256 family transposase	Replication and repair
sps_RS13960	2.487163749	2.13E-07	group II intron reverse transcriptase/maturase	Replication and repair
sps_RS13980	2.508998287	0.000761393464 6	hypothetical protein	Replication and repair
sps_RS16750	3.612384475	6.28E-17	group II intron reverse transcriptase/maturase	Replication and repair
sps_RS17155	2.503316519	2.68E-09	ATP-binding protein	Replication and repair
sps_RS19405	2.451203332	0.000114499791	hypothetical protein	Replication and repair
sps_RS23060	3.113012122	7.04E-06	IS66 family transposase	Replication and repair
sps_RS01085	2.80898152	1.97E-07	hypothetical protein	Secondary Structure
sps_RS01095	3.353664761	3.44E-09	hypothetical protein	Secondary Structure
sps_RS08660	2.625786757	5.81E-08	reductase	Secondary Structure
sps_RS08665	2.031948858	0.000139398789 6	thioesterase	Secondary Structure
sps_RS15280	2.710056353	4.62E-11	tandem-95 repeat protein	Secondary Structure
sps_RS03040	-3.650389943	5.43E-10	PrkA family serine protein kinase	Signal Transduction
sps_RS05495	-2.371953436	1.23E-06	GGDEF domain-containing protein	Signal Transduction
sps_RS07805	-2.119680762	7.86E-05	ANTAR domain-containing protein	Signal Transduction
sps_RS11275	2.472278492	2.37E-18	methyl-accepting chemotaxis protein	Signal Transduction
sps_RS20510	2.659090494	1.27E-05	DNA-binding response regulator	Signal Transduction

sps_RS20515	2.532492669	7.37E-07	two-component sensor histidine kinase	Signal Transduction
sps_RS20610	2.374815581	1.62E-05	HDOD domain-containing protein	Signal Transduction
sps_RS07760	2.376809105	0.000275196531	helix-turn-helix transcriptional regulator	Transcription
sps_RS09550	3.207724158	1.03E-12	AraC family transcriptional regulator	Transcription
sps_RS09570	3.795111604	5.06E-68	YafY family transcriptional regulator	Transcription
sps_RS09575	2.577525217	2.21E-06	AraC family transcriptional regulator	Transcription
sps_RS14035	2.530147865	2.16E-08	DNA-binding response regulator	Transcription
sps_RS15345	-2.045666298	3.99E-05	TetR family transcriptional regulator	Transcription
sps_RS17125	2.954632007	8.07E-09	transcriptional regulator	Transcription
sps_RS22055	-2.586561867	1.04E-09	LysR family transcriptional regulator	Transcription
sps_RS24690	-2.158612464	3.79E-20	phage shock protein A	Transcription
sps_RS26965	2.975601593	0.000425360056	RNA polymerase sigma factor	Transcription
sps_RS27370	2.858287534	1.09E-05	hypothetical protein	Transcription
sps_RS08515	-2.384737104	2.09E-15	N-acetyltransferase	Translation
sps_RS10475	-2.252301132	4.95E-07	elongation factor Ts	Translation

Data S3 Table I: Comparison between stationary phase samples from 20°C and 4°C cultures.

gene	log2FoldChange (<0 higher in 4, >0 higher in 20)	padj	name	cats
sps_RS11825	-2.086325517	5.10E-05	bifunctional aspartate kinase/homoserine dehydrogenase I	Amino Acid metabolism and transport
sps_RS13170	-2.285955658	2.01E-17	PKD domain-containing protein	Amino Acid metabolism and transport
sps_RS08280	2.536604478	2.90E-09	anthranilate synthase component 1	Amino Acid metabolism and transport
sps_RS08285	2.188972053	3.85E-05	type 1 glutamine amidotransferase	Amino Acid metabolism and transport
sps_RS08290	2.051732685	8.95E-05	anthranilate phosphoribosyltransferase	Amino Acid metabolism and transport
sps_RS08295	2.775880405	1.12E-09	bifunctional indole-3-glycerol-phosphate synthase TrpC/phosphoribosylanthranilate isomerase TrpF	Amino Acid metabolism and transport
sps_RS08300	2.672895499	1.98E-12	tryptophan synthase subunit beta	Amino Acid metabolism and transport
sps_RS08305	2.425779528	5.33E-07	tryptophan synthase subunit alpha	Amino Acid metabolism and transport
sps_RS09545	2.059004842	1.31E-07	chorismate mutase	Amino Acid metabolism and transport
sps_RS09555	3.043292443	2.00E-16	branched-chain amino acid ABC transporter permease	Amino Acid metabolism and transport
sps_RS15460	2.651690661	2.96E-09	serine O-acetyltransferase	Amino Acid metabolism and transport
sps_RS15655	-2.43738487	3.68E-13	S9 family peptidase	Amino Acid metabolism and transport

sps_RS18555	2.715688136	5.30E-25	flagellar biosynthesis protein FlhA	Cell motility
sps_RS16775	-2.251720936	1.09E-14	dihydrodipicolinate synthase family protein	Amino Acid metabolism and transport
sps_RS24885	-2.365114513	4.36E-13	FAD-binding protein	Amino Acid metabolism and transport
sps_RS26680	-2.651808388	3.95E-05	acetylglutamate kinase	Amino Acid metabolism and transport
sps_RS26685	-2.768358045	3.58E-10	N-acetyl-gamma-glutamyl-phosphate reductase	Amino Acid metabolism and transport
sps_RS02600	-2.242443129	1.15E-07	glycoside hydrolase	Carbohydrate metabolism and transport
sps_RS19520	-3.558352271	7.96E-13	allantoinase PuuE	Carbohydrate metabolism and transport
sps_RS05125	-3.001026181	6.12E-11	type VI secretion system tip protein VgrG	Cell wall/membrane/envelope biogenesis
sps_RS10190	-2.053258727	0.000740723 2578	type VI secretion system tip protein VgrG	Cell wall/membrane/envelope biogenesis
sps_RS14350	-2.766353924	3.79E-13	porin	Cell wall/membrane/envelope biogenesis
sps_RS15350	-2.741884285	4.19E-08	efflux RND transporter periplasmic adaptor subunit	Cell wall/membrane/envelope biogenesis
sps_RS00715	-2.602991744	2.44E-12	glycine C-acetyltransferase	Coenzyme metabolism
sps_RS05830	-2.30005303	6.48E-06	thiamine biosynthesis protein ThiS	Coenzyme metabolism
sps_RS01395	-2.310842263	1.76E-05	cytochrome C	Energy production and conversion
sps_RS01610	-2.829686908	4.79E-05	aldehyde dehydrogenase	Energy production and conversion
sps_RS18575	2.118374688	0.000580118 4741	flagellar type III secretion system protein FliQ	Cell motility
sps_RS03945	-2.124259834	0.000773479 6049	NADPH-dependent 2,4-dienoyl-CoA reductase	Energy production and conversion

sps_RS18580	2.258650385	5.66E-14	flagellar biosynthetic protein FliP	Cell motility
sps_RS08005	-2.113956873	2.09E-07	citrate synthase	Energy production and conversion
sps_RS12775	-2.275217671	3.95E-05	ammonia-forming cytochrome c nitrite reductase	Energy production and conversion
sps_RS18610	2.012594933	1.07E-06	flagellar export protein FliJ	Cell motility
sps_RS14135	-2.864031186	1.78E-06	nitrate reductase catalytic subunit NapA	Energy production and conversion
sps_RS14140	-2.469483652	0.0003596614777	nitrate reductase	Energy production and conversion
sps_RS15885	-2.520782686	0.0001269834222	NADH-dependent alcohol dehydrogenase	Energy production and conversion
sps_RS18615	2.064429679	3.13E-06	flagellar protein export ATPase FliI	Cell motility
sps_RS18985	-2.293926767	6.29E-07	malate synthase A	Energy production and conversion
sps_RS18620	2.043344521	7.31E-11	flagellar assembly protein FliH	Cell motility
sps_RS18630	2.564368176	1.92E-07	flagellar basal body M-ring protein FliF	Cell motility
sps_RS18695	2.571054518	3.99E-15	flagellar assembly peptidoglycan hydrolase FlgJ	Cell motility
sps_RS18705	2.259513619	5.16E-08	flagellar biosynthesis protein FlgH	Cell motility
sps_RS08020	3.028216055	2.62E-10	efflux RND transporter periplasmic adaptor subunit	Cell wall/membrane/envelope biogenesis
sps_RS10360	3.035660556	3.93E-17	dipeptide epimerase	Cell wall/membrane/envelope biogenesis
sps_RS07860	2.052389225	1.07E-14	biotin synthase BioB	Coenzyme metabolism
sps_RS13735	3.09273994	3.21E-15	uroporphyrinogen-III C-methyltransferase	Coenzyme metabolism
sps_RS23415	-2.339187067	1.84E-06	alkene reductase	Energy production and conversion
sps_RS02200	-2.337950535	3.84E-13	DUF4336 domain-containing protein	Function Unknown
sps_RS03030	-3.66950723	9.54E-12	SpoVR family protein	Function Unknown

sps_RS03035	-3.634735125	7.13E-09	hypothetical protein	Function Unknown
sps_RS04390	-2.219934553	1.31E-07	N-acetyltransferase	Function Unknown
sps_RS01075	2.75998547	5.63E-07	hypothetical protein	Energy production and conversion
sps_RS09300	2.286414353	0.000321129 6218	cystathionine beta-synthase	Energy production and conversion
sps_RS09310	2.116248143	0.000277059 7889	cytochrome C	Energy production and conversion
sps_RS13470	3.449003903	1.17E-30	cytochrome d terminal oxidase subunit 1	Energy production and conversion
sps_RS13475	2.350299934	9.41E-09	cytochrome d ubiquinol oxidase subunit II	Energy production and conversion
sps_RS00895	3.386665164	8.63E-47	putative sulfate exporter family transporter	Function Unknown
sps_RS01100	4.518717602	9.69E-13	hypothetical protein	Function Unknown
sps_RS05725	2.450446706	4.49E-13	hypothetical protein	Function Unknown
sps_RS06080	2.641648686	4.53E-10	hypothetical protein	Function Unknown
sps_RS08925	-2.511887893	4.87E-06	NADP-dependent oxidoreductase	Function Unknown
sps_RS10180	-2.339326925	0.000108069 4783	LysM domain-containing protein	Function Unknown
sps_RS10195	-4.724486792	1.44E-25	type VI secretion system tube protein Hcp	Function Unknown
sps_RS08025	2.542095536	3.25E-06	AcrB/AcrD/AcrF family protein	Function Unknown
sps_RS09540	2.303232347	2.41E-13	hypothetical protein	Function Unknown
sps_RS10625	-2.13771009	7.36E-07	hypothetical protein	Function Unknown
sps_RS12850	-2.131682055	4.38E-08	CBS domain-containing protein	Function Unknown
sps_RS09560	3.65703157	5.50E-26	AzlD domain-containing protein	Function Unknown
sps_RS09565	2.997703539	6.66E-05	NIPSNAP family protein	Function Unknown
sps_RS13420	-2.158078468	3.00E-08	NINE protein	Function Unknown
sps_RS15000	-3.941554963	2.80E-06	phasin family protein	Function Unknown

sps_RS15695	-2.1291936	0.0007344572115	hypothetical protein	Function Unknown
sps_RS15895	-3.653886357	7.92E-22	phasin family protein	Function Unknown
sps_RS15990	-2.50548815	0.0002795540374	nitrous oxide-stimulated promoter family protein	Function Unknown
sps_RS10355	3.259831866	1.33E-13	DUF1611 domain-containing protein	Function Unknown
sps_RS13465	2.230827052	0.0006130758117	DoxX family protein	Function Unknown
sps_RS14330	2.517665813	1.11E-09	hypothetical protein	Function Unknown
sps_RS15070	2.098789981	3.63E-06	type I secretion system permease/ATPase	Function Unknown
sps_RS18780	2.328864675	1.27E-09	flagellar biosynthesis protein FlgT	Function Unknown
sps_RS20505	2.096420537	0.0003383132647	DUF3019 domain-containing protein	Function Unknown
sps_RS21780	2.033904608	0.0004009834389	tripartite tricarboxylate transporter substrate binding protein	Function Unknown
sps_RS19095	-4.431498858	3.77E-23	type VI secretion system tube protein Hcp	Function Unknown
sps_RS19515	-3.650844014	5.71E-13	OHCU decarboxylase	Function Unknown
sps_RS21295	-2.19513035	1.33E-11	DUF2804 domain-containing protein	Function Unknown
sps_RS26885	2.289110257	1.07E-10	hypothetical protein	Function Unknown
sps_RS23400	-3.020956044	3.83E-07	SRPBCC family protein	Function Unknown
sps_RS23405	-2.559922242	8.68E-08	hypothetical protein	Function Unknown
sps_RS01540	2.949123937	4.76E-07	MFS transporter	Inorganic ion transport and metabolism
sps_RS23410	-2.490494981	2.26E-11	patatin	Function Unknown
sps_RS23905	-2.309484558	0.0003141161291	DUF3144 domain-containing protein	Function Unknown
sps_RS13780	2.681608289	8.21E-19	phosphoadenylyl-sulfate reductase	Inorganic ion transport and metabolism
sps_RS24400	-3.752421059	4.31E-13	type VI secretion system tube protein Hcp	Function Unknown

sps_RS24890	-2.100698947	0.0001185384367	TAT leader-containing periplasmic protein	Function Unknown
sps_RS27585	-2.011851802	1.90E-05	acyl-CoA thioesterase	Function Unknown
sps_RS27595	-2.117141526	7.88E-16	acyl-CoA thioesterase	Function Unknown
sps_RS06210	-2.85664545	0.0001749211018	reductase	Inorganic ion transport and metabolism
sps_RS14130	-3.634810536	1.24E-09	sorbose reductase	Inorganic ion transport and metabolism
sps_RS04040	-2.954407519	7.02E-08	acyl-CoA dehydrogenase	Lipid metabolism
sps_RS05895	-3.777084186	3.24E-15	acyl-CoA dehydrogenase	Lipid metabolism
sps_RS13785	2.885336025	1.27E-16	NADPH-dependent assimilatory sulfite reductase hemoprotein subunit	Inorganic ion transport and metabolism
sps_RS13790	2.916258709	8.41E-12	assimilatory sulfite reductase (NADPH) flavoprotein subunit	Inorganic ion transport and metabolism
sps_RS11695	2.220477484	9.18E-08	prepilin-type N-terminal cleavage/methylation domain-containing protein	Intracellular trafficking and secretion
sps_RS11700	2.620763421	1.25E-07	type IV pilus modification protein PilV	Intracellular trafficking and secretion
sps_RS01090	3.152922698	4.39E-09	hypothetical protein	Lipid metabolism
sps_RS01105	2.852160291	3.53E-07	hypothetical protein	Lipid metabolism
sps_RS01110	3.323991059	3.71E-09	hypothetical protein	Lipid metabolism
sps_RS01115	3.984054049	2.91E-14	hypothetical protein	Lipid metabolism
sps_RS22460	2.651852912	1.72E-12	glutathione-dependent disulfide-bond oxidoreductase	Post-translational modification, protein turnover, chaperone functions
sps_RS01085	2.222729616	8.12E-05	hypothetical protein	Secondary Structure

sps_RS07490	-3.319249274	2.06E-14	acyl-CoA dehydrogenase	Lipid metabolism
sps_RS08785	-3.16374189	4.58E-13	acetyl-CoA C-acyltransferase FadI	Lipid metabolism
sps_RS08835	-3.759680308	3.77E-23	transporter	Lipid metabolism
sps_RS19255	-3.212734622	4.68E-08	acyl-CoA dehydrogenase	Lipid metabolism
sps_RS21950	-2.143255876	9.71E-06	alpha/beta hydrolase	Lipid metabolism
sps_RS04270	-2.095991154	2.80E-06	adenylosuccinate synthetase	Nucleotide metabolism and transport
sps_RS01095	3.455227412	1.02E-09	hypothetical protein	Secondary Structure
sps_RS07710	-2.037883931	2.97E-11	histidine triad nucleotide-binding protein	Nucleotide metabolism and transport
sps_RS05405	2.159857347	4.87E-12	IclR family transcriptional regulator	Transcription
sps_RS18865	-2.318961237	2.71E-09	IMP dehydrogenase	Nucleotide metabolism and transport
sps_RS09550	2.987652795	5.16E-11	AraC family transcriptional regulator	Transcription
sps_RS02470	-2.050190978	6.40E-06	alkyl hydroperoxide reductase	Post-translational modification, protein turnover, chaperone functions
sps_RS08535	-2.564478514	1.51E-12	disulfide bond formation protein B	Post-translational modification, protein turnover, chaperone functions
sps_RS09025	-2.056768145	1.02E-06	peptidylprolyl isomerase	Post-translational modification, protein turnover, chaperone functions
sps_RS17270	-3.124593296	0.000113597 6081	thiol peroxidase	Post-translational modification, protein turnover, chaperone functions

sps_RS03840	-2.23686316	2.76E-17	replication initiation negative regulator SeqA	Replication and repair
sps_RS11030	-2.066018398	0.0001545621337	exodeoxyribonuclease VII small subunit	Replication and repair
sps_RS16235	-2.867743323	1.84E-13	hypothetical protein	Secondary Structure
sps_RS03040	-3.601063732	1.06E-09	PrkA family serine protein kinase	Signal Transduction
sps_RS25995	-2.844543104	0.0002362524103	PhoH family protein	Signal Transduction
sps_RS00465	-2.077200509	1.69E-05	RNA polymerase sigma factor FliA	Transcription
sps_RS05555	-2.049872122	8.48E-19	TetR/AcrR family transcriptional regulator	Transcription
sps_RS09570	2.838227561	5.02E-37	YafY family transcriptional regulator	Transcription
sps_RS15345	-2.331821137	3.36E-06	TetR family transcriptional regulator	Transcription
sps_RS01785	-2.129566304	0.000186270355	30S ribosomal protein S7	Translation

Appendix VI Supplemental Tables for Manuscript III

Supplemental Table S1: List of compounds that are removed in the AP-filtered network representation.

Metabolite Name	KEGG Id	MetaCyc ID
ATP	C00002	ATP
ADP	C00008	ADP
NAD+	C00003	NAD
NADH	C00004	NADH
NADP+	C00006	NADP
NADPH	C00005	NADPH
FAD	C00016	FAD
FADH2	C01352	FADH2
H+	C00080	PROTON
Water	C00001	WATER
Orthophosphate	C00009	Pi
Carbon Dioxide	C00011	CARBON_DIOXIDE
Diphosphate	C00013	PPI
Ammonia	C00014	AMMONIUM

Supplemental Table S2: Highest degree nodes from KEGG networks for the FPP, AP, and AP-Filtered network representations with all elements. The percentage of networks where each node was in the top 5% of highest degree nodes is shown along with the average degree of the node across all of the networks.

AP		
Metabolite	**Percent Networks with metabolite in top 5% of nodes**	**Average Degree of Metabolite**
H2O	99.98%	228.04
H+	99.75%	121.64
Phosphate	99.75%	104.21
ATP	99.61%	115.36
ADP	99.29%	99.31
NAD+	98.76%	84.62
Diphosphate	98.67%	70.31
NADH	97.24%	83.83
NADP+	95.73%	52.04
Carbon Dioxide (CO2)	95.56%	58.45
NADPH	95.35%	51.09
Ammonia	94.61%	51.94
L-Glutamate	94.03%	50.00
AMP	92.80%	34.56
2-Oxoglutarate	91.47%	31.69
Coenzyme A (CoA)	90.15%	36.65
Pyruvate	89.69%	36.94
L-Glutamine	87.87%	22.91
5-Phospho-alpha-D-ribose 1-diphosphate (PRPP)	85.33%	19.31
Tetrahydrofolate	82.45%	19.25
GTP	79.28%	17.72
L-Aspartate	78.80%	19.04
Glyceraldehyde 3-phosphate	78.30%	17.72
Acetyl-CoA	75.86%	31.18
AP-Filtered		

Metabolite	Percent Networks with metabolite in top 5% of nodes	Average Degree of Metabolite
L-Glutamate	96.35%	40.14
AMP	95.02%	28.18
Pyruvate	95.00%	29.35
Glyceraldehyde 3-phosphate	94.32%	12.88
2-Oxoglutarate	92.76%	25.85
CoA	92.35%	28.23
5-Phospho-alpha-D-ribose 1-diphosphate (PRPP)	90.17%	14.60
L-Glutamine	88.86%	15.84
GTP	87.08%	13.27
Acetyl-CoA	85.23%	25.22
L-Aspartate	83.14%	12.99
CMP	78.99%	13.15
UMP	78.51%	14.03
Tetrahydrofolate	78.18%	11.55
FPP		
Metabolite	**Percent Networks with metabolite in top 5% of nodes**	**Average Degree of Metabolite**
H2O	99.90%	144.80
Phosphate	99.71%	66.60
ATP	99.65%	82.44
H+	99.56%	79.04
NADH	98.78%	56.93
Ammonia	97.68%	44.73
Diphosphate	97.22%	31.87
NADPH	96.18%	33.95
L-Glutamate	96.14%	43.28
Carbon Dioxide (CO2)	94.92%	44.41
2-Oxoglutarate	93.34%	28.09

5-Phospho-alpha-D-ribose 1-diphosphate (PRPP)	91.04%	15.61
Pyruvate	89.59%	26.07
GTP	86.19%	14.81
L-Glutamine	85.48%	15.20
Phosphoenolpyruvate	84.11%	12.30
L-Aspartate	84.03%	15.61
Acetyl-CoA	80.67%	26.01
Glycine	78.74%	15.70
CTP	78.66%	11.89
UTP	78.57%	11.37
UMP	78.26%	16.04
AMP	76.04%	16.05

Supplemental Table S3: Median network statistics values across all KEGG networks for the all-elements networks.

	FPP		
	25th Percentile	**Median**	**75th Percentile**
Number of Nodes	531.00	713.00	921.00
Number of Edges	1080.50	1489.00	1931.00
Average Degree	3.98	4.12	4.26
Density	0.00	0.01	0.01
Transitivity	0.04	0.05	0.05
Degree Assortativity	-0.15	-0.15	-0.13
Average Betweenness Centrality	728.75	988.14	1246.07
Average Closeness Centrality	0.27	0.28	0.28
Diameter	8.00	9.00	9.00
Average Shortest Path Length	3.68	3.73	3.80

	AP		
	25th Percentile	**Median**	**75th Percentile**
Number of Nodes	531.00	714.00	922.00
Number of Edges	1539.00	2102.00	2735.00
Average Degree	5.67	5.85	5.99
Density	0.01	0.01	0.01
Transitivity	0.04	0.05	0.06
Degree Assortativity	-0.23	-0.22	-0.21
Average Betweenness Centrality	541.90	737.68	947.54
Average Closeness Centrality	0.33	0.33	0.34
Diameter	7.00	7.00	8.00
Average Shortest Path Length	3.03	3.06	3.09

	AP-Filtered		
	25th Percentile	**Median**	**75th Percentile**
Number of Nodes	450.50	608.00	772.50
Number of Edges	743.00	1024.00	1318.00
Average Degree	3.24	3.33	3.43
Density	0.00	0.01	0.01
Transitivity	0.04	0.05	0.06

Degree Assortativity	-0.08	-0.05	-0.02
Average Betweenness Centrality	998.50	1324.23	1635.72
Average Closeness Centrality	0.19	0.19	0.20
Diameter	14.00	15.00	17.00
Average Shortest Path Length	5.16	5.32	5.50

Supplemental Table S4: Median network statistics values across all KEGG networks for the carbon filtered networks.

	FPP		
	25th Percentile	**Median**	**75th Percentile**
Number of Nodes	436.00	569.00	721.00
Number of Edges	605.00	820.00	1042.00
Average Degree	2.75	2.83	2.90
Density	0.00	0.00	0.01
Transitivity	0.05	0.06	0.07
Degree Assortativity	-0.05	-0.04	-0.02
Average Betweenness Centrality	1137.07	1431.66	1779.08
Average Closeness Centrality	0.16	0.17	0.18
Diameter	16.00	16.00	18.00
Average Shortest Path Length	5.88	6.04	6.28

	AP		
	25th Percentile	**Median**	**75th Percentile**
Number of Nodes	494.00	655.00	836.50
Number of Edges	1095.00	1469.00	1884.00
Average Degree	4.32	4.43	4.56
Density	0.01	0.01	0.01
Transitivity	0.05	0.05	0.06
Degree Assortativity	-0.18	-0.16	-0.15
Average Betweenness Centrality	685.28	910.10	1165.47
Average Closeness Centrality	0.27	0.27	0.28
Diameter	11.00	12.00	13.00
Average Shortest Path Length	3.70	3.77	3.84

	AP-Filtered		
	25th Percentile	**Median**	**75th Percentile**
Number of Nodes	434.00	571.00	722.00
Number of Edges	743.00	991.00	1246.00
Average Degree	3.29	3.39	3.48
Density	0.00	0.01	0.01
Transitivity	0.05	0.05	0.06
Degree Assortativity	-0.05	-0.04	-0.02

Average Betweenness Centrality	886.91	1146.38	1452.10
Average Closeness Centrality	0.20	0.21	0.21
Diameter	14.00	15.00	16.00
Average Shortest Path Length	4.92	5.06	5.21

Supplemental Table S5: Median network statistics values across all KEGG networks for the nitrogen filtered networks.

	FPP		
	25th Percentile	**Median**	**75th Percentile**
Number of Nodes	285.00	367.00	477.00
Number of Edges	356.00	478.00	622.00
Average Degree	2.52	2.60	2.66
Density	0.01	0.01	0.01
Transitivity	0.05	0.06	0.06
Degree Assortativity	-0.09	-0.07	-0.05
Average Betweenness Centrality	669.26	876.86	1292.81
Average Closeness Centrality	0.17	0.18	0.19
Diameter	16.00	18.00	26.00
Average Shortest Path Length	5.63	5.90	6.35

	AP		
	25th Percentile	**Median**	**75th Percentile**
Number of Nodes	318.00	433.00	540.75
Number of Edges	663.00	909.50	1154.00
Average Degree	4.07	4.21	4.33
Density	0.01	0.01	0.01
Transitivity	0.06	0.07	0.08
Degree Assortativity	-0.18	-0.17	-0.16
Average Betweenness Centrality	423.57	569.78	701.18
Average Closeness Centrality	0.28	0.29	0.29
Diameter	9.00	10.00	11.00
Average Shortest Path Length	3.53	3.59	3.66

	AP-Filtered		
	25th Percentile	**Median**	**75th Percentile**
Number of Nodes	279.00	379.00	487.00
Number of Edges	425.00	581.00	747.00
Average Degree	2.97	3.07	3.17
Density	0.01	0.01	0.01
Transitivity	0.05	0.05	0.06
Degree Assortativity	-0.11	-0.09	-0.06

Average Betweenness Centrality	531.11	714.76	902.13
Average Closeness Centrality	0.21	0.22	0.22
Diameter	12.00	13.00	15.00
Average Shortest Path Length	4.62	4.72	4.84

Supplemental Table S6: Median network statistics values across all KEGG networks for the phosphorus filtered networks.

	FPP		
	25th Percentile	**Median**	**75th Percentile**
Number of Nodes	207.00	249.00	302.00
Number of Edges	339.00	409.00	481.00
Average Degree	3.11	3.23	3.33
Density	0.01	0.01	0.02
Transitivity	0.06	0.06	0.07
Degree Assortativity	-0.19	-0.17	-0.16
Average Betweenness Centrality	310.91	376.59	612.01
Average Closeness Centrality	0.23	0.26	0.27
Diameter	15.00	16.00	23.00
Average Shortest Path Length	3.94	4.13	4.71

	AP		
	25th Percentile	**Median**	**75th Percentile**
Number of Nodes	226.00	288.00	342.00
Number of Edges	525.00	668.00	800.00
Average Degree	4.55	4.68	4.77
Density	0.01	0.02	0.02
Transitivity	0.07	0.07	0.08
Degree Assortativity	-0.23	-0.22	-0.21
Average Betweenness Centrality	241.66	307.35	377.91
Average Closeness Centrality	0.32	0.32	0.33
Diameter	8.00	9.00	10.00
Average Shortest Path Length	3.12	3.18	3.23

	AP-Filtered		
	25th Percentile	**Median**	**75th Percentile**
Number of Nodes	206.00	257.00	313.00
Number of Edges	352.25	437.00	524.00
Average Degree	3.32	3.38	3.44
Density	0.01	0.01	0.02
Transitivity	0.05	0.06	0.07
Degree Assortativity	-0.16	-0.15	-0.14
Average Betweenness Centrality	278.14	354.36	443.73

Average Closeness Centrality	0.27	0.27	0.28
Diameter	10.00	11.00	11.00
Average Shortest Path Length	3.70	3.81	3.90

Supplemental Table S7: Results of Multi-way ANOVA analysis of the effects of database, network representation, and phylum on network metrics. The degrees of freedom are provided for each factor in the DF column, the Sum of Squares and Mean Squares values are provided in the Sum Sq and Mean Sq columns. The F-statistic is provided in the F-value column and the P-value is provided in the p-value column. The results are shown for all three factors as well as the residuals.

Average Degree

	DF	**Sum Sq**	**Mean Sq**	**F-Value**	**p-value**
Network	2	16860	8430	201085.46	<0.001
Database	1	3	3	59.85	<0.001
Phylum	31	476	15	366.52	<0.001
Residuals	16759	703	0		

Density

	DF	**Sum Sq**	**Mean Sq**	**F-Value**	**p-value**
Network	2	0.03735	0.018674	1848.8	<0.001
Database	1	0.00941	0.00941	931.6	<0.001
Phylum	31	0.21009	0.006777	670.9	<0.001
Residuals	16759	0.16928	0.00001		

Transitivity

	DF	**Sum Sq**	**Mean Sq**	**F-Value**	**p-value**
Network	2	0.3278	0.16388	1415	<0.001
Database	1	0.1492	0.14921	1288.4	<0.001
Phylum	31	0.8232	0.02655	229.3	<0.001
Residuals	16759	1.9409	0.00012		

Degree Assortativity

	DF	**Sum Sq**	**Mean Sq**	**F-Value**	**p-value**
Network	2	68.93	34.47	49901.9	<0.001
Database	1	4.62	4.62	6694.8	<0.001
Phylum	31	2.88	0.09	134.6	<0.001
Residuals	16759	11.58	0		

Log(Average Betweenness Centrality)

	DF	**Sum Sq**	**Mean Sq**	**F-Value**	**p-value**
Network	2	775.3	387.7	4374.7	<0.001
Database	1	307.9	307.9	3474.2	<0.001
Phylum	31	1625.2	52.4	591.6	<0.001
Residuals	16759	1485.1	0.1		

Average Closeness Centrality

	DF	Sum Sq	Mean Sq	F-Value	p-value
Network	2	48.76	24.38	366486.08	<0.001
Database	1	2.2	2.204	33135.01	<0.001
Phylum	31	0.18	0.006	88.53	<0.001
Residuals	16759	1.11	0		

Diameter

	DF	Sum Sq	Mean Sq	F-Value	p-value
Network	2	175448	87724	53848.67	<0.001
Database	1	4266	4266	2618.51	0.002
Phylum	31	1025	33	20.29	<0.001
Residuals	16759	27302	2		

Average Shortest Path Length

	DF	Sum Sq	Mean Sq	F-Value	p-value
Network	2	11598	5799	130712.39	<0.001
Database	1	623	623	14037	<0.001
Phylum	31	61	2	44.32	<0.001
Residuals	16759	743	0		

Supplemental Table S8: Eta Square values for each factor in multi-way ANOVA analysis between KEGG and MetaCyc across three network types, representing the proportion of variance in the model explained by each of the factors.

Statistic	Network	Database	Phylum
Average Degree	0.943	0.000	0.026
Density	0.082	0.022	0.493
Transitivity	0.096	0.046	0.254
Degree Assortativity	0.791	0.053	0.033
Average Betweenness Centrality	0.166	0.073	0.388
Average Closeness Centrality	0.935	0.042	0.003
Diameter	0.841	0.021	0.005
Average Path Length	0.893	0.048	0.005

Supplemental Table S9: Genome-scale models used in the analysis of network metric differences between the KEGG, MetaCyc, and GEM based networks.

Organism	Model Name	KEGG Genome ID	MetaCyc ID	Excluded Reactions for FPP Prediction	Reference PMID
Salmonella typhimurium LT2	STM_v1.0	stm	sent99287cyc	biomass_iRR1083_metals, biomass_iRR1083, Ec_biomass_iAF1260_core_59p81M	21244678
Escherichia coli K-12 MG1655	iAF1260	eco	ecocyc	Ec_biomass_iAF1260_core_59p81M	17593909
Methanosarcina barkeri	iAF692	mba	mbar269797cyc	Mb_biomass_30	16738551
Clostridium beijerinckii NCIMB 8052	iCB925	cbe	cbei290402cyc	biomass	21846360
Synechocystis sp. PCC6803	iJN678	sys	ssp1080229cyc	Ec_biomass_SynHetero, Ec_biomass_SynAuto, Ec_biomass_SynMixo	22308420
Pseudomonas putida KT2440	iJN746	ppu	pput160488cyc	BiomassKT_TEMP	18793442
Escherichia coli K-12 MG1655	iJO1366	eco	ecocyc	Ec_biomass_iJO1366_core_53p95M	21988831
Escherichia coli K-12 MG1655	iJR904	eco	ecocyc	BiomassEcoli, LPLIPA3, LPLIPA4, LPLIPA5, LPLIPA6, LPSSYN_EC, PLIPA1, PLIPA2, PLIPA3, LPLIPA2, LPLIPA1	12952533

Methanosarcina acetivorans C2A	iMB745	mac	mace188937cyc	overall	22139506
Shewanella oneidensis MR-1	iMR1_799	son	sone211586cyc	SO_BIOMASSMACRO_DM_NOATP2, RNASYN_SON, DNASYN_SON, LPSSYN_SO, PASYN_SO_AEROBIC, PLIPPE_SO, PLIPPG_SO, PROTSYN_SON_AEROBIC	24621294
Mycobacterium tuberculosis H37Rv	iNJ661	mtv	mtbrvcyc	biomass_Mtb_9_60atp	17555602
Mycoplasma genitalium	iPS189	mge	mgen243273cyc	Biomass	19214212
Staphylococcus auresus N315	iSB619	sau	saur158879cyc	SA_biomass_1a, biomass_SA_2a, biomass_SA_2b, biomass_SA_3a, biomass_SA_3b, biomass_SA_4a, biomass_SA_5a, biomass_SA_6a, biomass_SA_6b, biomass_SA	15752426

				_7a, biomass_SA_7b, biomass_SA_8a, biomass_SA_lipids_only, biomass_SA_nuc_only, biomass_SA_only_AA, PASYN_SA	
Thermotoga maritima	iTZ479	tmw	tmar243274cyc	BiomassEcoli_TM, GLSe, GLS2e, AMYe, PULLe, GLYCOe, GLCMAN600a_e, GLCMAN600b_e, GLCMAN600c_e, AMYLe	19762644
Shewanella piezotolerans WP3	GEM-iWP3	swp	spie225849cyc	Core_Biomass, PASYN_WP3_20C, DNASYN, RNASYN, PROTSYN	28382331

Supplemental Table S10: Summary of the percentage of networks from each category that have small world properties.

	FPP	AP	AP-Filtered
All-elements	100.0%	99.9%	99.8%
Carbon	99.7%	99.9%	99.8%
Nitrogen	98.8%	99.9%	99.2%
Phosphorus	100.0%	99.9%	99.9%

Supplemental Table S11: Table showing media constraints used in random deletion simulations for the GEM-iWP3 GEM.

Compound ID	Lower Limit	Upper Limit	Compound Name	Compound Category
cpd_pro-L[e]	0	1000	L-Proline	Amino Acid
cpd_met-L[e]	0	1000	L-Methionine	Amino Acid
cpd_indole[e]	0	1000	Indole	Amino Acid
cpd_ala-D[e]	0	1000	D-Alanine	Amino Acid
cpd_ala-L[e]	0	1000	L-Alanine	Amino Acid
cpd_asp-L[e]	0	1000	L-Aspartate	Amino Acid
cpd_glu-L[e]	0	1000	L-Glutamate	Amino Acid
cpd_gly[e]	0	1000	Glycine	Amino Acid
cpd_gly-asp-L[e]	0	1000	glycyl-L-aspartic acid	Amino Acid
cpd_gly-glu-L[e]	0	1000	glycyl-L-glutamic acid	Amino Acid
cpd_ile-L[e]	0	1000	L-Isoleucine	Amino Acid
cpd_leu-L[e]	0	1000	L-Leucine	Amino Acid
cpd_ptrc[e]	0	1000	Putrescine	Amino Acid
cpd_ser-L[e]	0	1000	L-Serine	Amino Acid
cpd_thr-L[e]	0	1000	L-Threonine	Amino Acid
cpd_tyr-L[e]	0	1000	L-Tyrosine	Amino Acid
cpd_val-L[e]	0	1000	L-Valine	Amino Acid
cpd_lys-L[e]	0	1000	L-Lysine	Amino Acid
cpd_trp-L[e]	0	1000	L-Tryptophan	Amino Acid
cpd_akg[e]	0	1000	2-Oxoglutarate	Amino Acid
cpd_gln-L[e]	0	1000	L-Glutamine	Amino Acid
cpd_asn-L[e]	0	1000	L-Asparagine	Amino Acid
cpd_glyc-R[e]	-1000	1000	(R)-Glycerate	Carbohydrate
cpd_ac[e]	-1000	1000	Acetate	Carbohydrate
cpd_acgam[e]	-1000	1000	N-Acetyl-D-glucosamine	Carbohydrate
cpd_bgl[e]	-1000	1000	cellobiose	Carbohydrate
cpd_for[e]	-1000	1000	Formate	Carbohydrate
cpd_fum[e]	-1000	1000	Fumarate	Carbohydrate
cpd_galactan[e]	-1000	1000	Galactan	Carbohydrate
cpd_gal[e]	-1000	1000	D-Galactose	Carbohydrate
cpd_glc-D[e]	-1000	1000	D-Glucose	Carbohydrate
cpd_glyc[e]	-1000	1000	Glycerol	Carbohydrate

cpd_glyclt[e]	-1000	1000	Glycolate	Carbohydrate
cpd_lac-D[e]	-1000	1000	D-Lactate	Carbohydrate
cpd_lac-L[e]	-1000	1000	L-Lactate	Carbohydrate
cpd_lami[e]	-1000	1000	laminarin	Carbohydrate
cpd_mal-L[e]	-1000	1000	L-Malate	Carbohydrate
cpd_panose[e]	-1000	1000	Panose	Carbohydrate
cpd_malt[e]	-1000	1000	Maltose	Carbohydrate
cpd_malthp[e]	-1000	1000	Maltoheptaose	Carbohydrate
cpd_malthx[e]	-1000	1000	Maltohexaose	Carbohydrate
cpd_maltpt[e]	-1000	1000	Maltopentaose	Carbohydrate
cpd_malttr[e]	-1000	1000	Maltotriose	Carbohydrate
cpd_maltttr[e]	-1000	1000	Maltotetraose	Carbohydrate
cpd_pyr[e]	-1000	1000	Pyruvate	Carbohydrate
cpd_succ[e]	-1000	1000	Succinate	Carbohydrate
cpd_ppa[e]	-1000	1000	Propionate	Carbohydrate
cpd_chitin[e]	-1000	1000	chitin	Carbohydrate
cpd_etoh[e]	-1000	1000	Ethanol	Carbohydrate
cpd_na1[e]	-1000	1000	Sodium	Ions and Small Molecules
cpd_h2o2[e]	-1000	1000	Hydrogen peroxide	Ions and Small Molecules
cpd_CrOH3[e]	-1000	1000	Cr(OH)3	Ions and Small Molecules
cpd_ca2[e]	-1000	1000	Calcium	Ions and Small Molecules
cpd_cl[e]	-1000	1000	Chloride	Ions and Small Molecules
cpd_co2[e]	-1000	1000	CO2	Ions and Small Molecules
cpd_cobalt3[e]	-1000	1000	Co3+	Ions and Small Molecules
cpd_cobalt2[e]	-1000	1000	Co2+	Ions and Small Molecules
cpd_cro4[e]	-1000	1000	chromate	Ions and Small Molecules
cpd_cu2[e]	-1000	1000	Cu2+	Ions and Small Molecules
cpd_dms[e]	-1000	1000	Dimethyl sulfide	Ions and Small Molecules
cpd_dmso[e]	-1000	1000	Dimethyl sulfoxide	Ions and Small Molecules

cpd_fe2[e]	-1000	1000	Fe2+	Ions and Small Molecules
cpd_fe3[e]	-1000	1000	Fe3+	Ions and Small Molecules
cpd_h[e]	-1000	1000	H+	Ions and Small Molecules
cpd_h2o[e]	-1000	1000	H2O	Ions and Small Molecules
cpd_h2s[e]	-1000	1000	Hydrogen sulfide	Ions and Small Molecules
cpd_k[e]	-1000	1000	K+	Ions and Small Molecules
cpd_mg2[e]	-1000	1000	Mg	Ions and Small Molecules
cpd_mn2[e]	-1000	1000	Mn2+	Ions and Small Molecules
cpd_mn4o[e]	-1000	1000	Manganese(IV) oxide	Ions and Small Molecules
cpd_nh4[e]	-1000	1000	Ammonium	Ions and Small Molecules
cpd_no2[e]	-1000	1000	Nitrite	Ions and Small Molecules
cpd_no3[e]	-1000	1000	Nitrate	Ions and Small Molecules
cpd_o2[e]	-1000	1000	O2	Ions and Small Molecules
cpd_pi[e]	-1000	1000	Phosphate	Ions and Small Molecules
cpd_so3[e]	-1000	1000	Sulfite	Ions and Small Molecules
cpd_so4[e]	-1000	1000	Sulfate	Ions and Small Molecules
cpd_tma[e]	-1000	1000	Trimethylamine	Ions and Small Molecules
cpd_tmao[e]	-1000	1000	Trimethylamine N-oxide	Ions and Small Molecules
cpd_tsul[e]	-1000	1000	Thiosulfate	Ions and Small Molecules
cpd_tttnt[e]	-1000	1000	tetrathionate	Ions and Small Molecules
cpd_urdio[e]	-1000	1000	Uranium dioxide	Ions and Small Molecules
cpd_urnyl[e]	-1000	1000	Uranyl	Ions and Small Molecules

cpd_mobd[e]	-1000	1000	Molybdate	Ions and Small Molecules
cpd_urea[e]	-1000	1000	Urea	Ions and Small Molecules
cpd_dodcan[e]	0	1000	Dodecanoic acid (neutral)	Lipid
cpd_hdcan[e]	0	1000	hexadecanoate (n-C16:0) (neutral)	Lipid
cpd_ocdcan[e]	0	1000	octadecanoate (n-C18:0) neutral	Lipid
cpd_ttdcan[e]	0	1000	tetradecanoate (C14:0) (neutral)	Lipid
cpd_damp[e]	0	1000	dAMP	Nucleic Acids and Derivatives
cpd_dcmp[e]	0	1000	dCMP	Nucleic Acids and Derivatives
cpd_dgmp[e]	0	1000	dGMP	Nucleic Acids and Derivatives
cpd_dtmp[e]	0	1000	dTMP	Nucleic Acids and Derivatives
cpd_adn[e]	0	1000	Adenosine	Nucleic Acids and Derivatives
cpd_dad-2[e]	0	1000	Deoxyadenosine	Nucleic Acids and Derivatives
cpd_dgsn[e]	0	1000	Deoxyguanosine	Nucleic Acids and Derivatives
cpd_ura[e]	0	1000	Uracil	Nucleic Acids and Derivatives
cpd_cytd[e]	0	1000	Cytidine	Nucleic Acids and Derivatives
cpd_dcyt[e]	0	1000	Deoxycytidine	Nucleic Acids and Derivatives
cpd_dna[e]	0	1000	DNA	Nucleic Acids and Derivatives
cpd_duri[e]	0	1000	Deoxyuridine	Nucleic Acids and Derivatives
cpd_uri[e]	0	1000	Uridine	Nucleic Acids and Derivatives
cpd_thymd[e]	0	1000	Thymidine	Nucleic Acids and Derivatives
cpd_xan[e]	0	1000	Xanthine	Nucleic Acids and Derivatives

cpd_ins[e]	0	1000	Inosine	Nucleic Acids and Derivatives
cpd_thym[e]	0	1000	Thymine	Nucleic Acids and Derivatives
cpd_hxan[e]	0	1000	Hypoxanthine	Nucleic Acids and Derivatives
cpd_pmcoa[e]	-1000	1000	Pimeloyl-CoA	Vitamins
cpd_cbl1[e]	-1000	1000	Cob(I)alamin	Vitamins

Supplemental Table S12: Table showing media constraints used in random deletion simulations for the iTZ479 GEM.

Compound ID	Lower Limit	Upper Limit	Compound Name	Compound Category
ala_L	0	1000	L-Alanine	Amino Acid
ile_L	0	1000	L-Isoleucine	Amino Acid
leu_L	0	1000	L-Leucine	Amino Acid
ptrc	0	1000	Putrescine	Amino Acid
spmd	0	1000	Spermidine	Amino Acid
thr_L	0	1000	L-Threonine	Amino Acid
val_L	0	1000	L-Valine	Amino Acid
ac	-1000	1000	Acetate	Carbohydrate
amylose300	-1000	1000	amylose (n=300 repeat units, alpha-1,4-glc)	Carbohydrate
arab_L	-1000	1000	L-Arabinose	Carbohydrate
cell4	-1000	1000	cellulose (n=4 repeating units)	Carbohydrate
cell500	-1000	1000	celluose (n=500 repeating units, beta-1,4 glc)	Carbohydrate
cell6	-1000	1000	cellulose (n=6 repeating units)	Carbohydrate
cellb	-1000	1000	cellobiose	Carbohydrate
fru	-1000	1000	D-Fructose	Carbohydrate
gal	-1000	1000	D-Galactose	Carbohydrate
galman4	-1000	1000	galactomannan(n=4 repeat units mannose, alpha-1,4 man)	Carbohydrate
galman6	-1000	1000	galactomannan(n=6 repeat units mannose, alpha-1,4 man)	Carbohydrate
galman600	-1000	1000	galactomannan (n=600 repeat units mannose, alpha-1,4 man)	Carbohydrate
glc_D	-1000	1000	D-Glucose	Carbohydrate
glcman4	-1000	1000	glucomannan (n=4 repeat units, glc beta-1,4 man)	Carbohydrate

glcman6	-1000	1000	glucomannan (n=6 repeat units, glc beta-1,4 man)	Carbohydrate
glcman600	-1000	1000	glucomannan (n=600 repeat units, glc beta-1,4 man)	Carbohydrate
glucan1500	-1000	1000	beta-1,3/1,4-glucan (Barley, n=1500, Glc beta1->3,4 Glc)	Carbohydrate
glucan4	-1000	1000	beta-1,3/1,4-glucan (Barley, n=4, Glc beta1->3,4 Glc)	Carbohydrate
glucan6	-1000	1000	beta-1,3/1,4-glucan (Barley, n=6, Glc beta1->3,4 Glc)	Carbohydrate
glyc	-1000	1000	Glycerol	Carbohydrate
glyc3p	-1000	1000	Glycerol 3-phosphate	Carbohydrate
glycogen1500	-1000	1000	glycogen (n=1500 repeat units) (glc alpha 1,4/6 glc)	Carbohydrate
inost	-1000	1000	myo-Inositol	Carbohydrate
lac_L	-1000	1000	L-Lactate	Carbohydrate
lcts	-1000	1000	Lactose	Carbohydrate
lmn2	-1000	1000	Laminaribiose	Carbohydrate
lmn30	-1000	1000	laminarin (n=30 repeat units, beta -1,3 glc)	Carbohydrate
malt	-1000	1000	Maltose	Carbohydrate
malttr	-1000	1000	Maltotriose	Carbohydrate
maltttr	-1000	1000	Maltotetraose	Carbohydrate
man	-1000	1000	D-Mannose	Carbohydrate
manb	-1000	1000	Mannobiose (beta-1,4)	Carbohydrate
mantr	-1000	1000	mannotriose (beta-1,4)	Carbohydrate
manttr	-1000	1000	mannotetraose	Carbohydrate
melib	-1000	1000	Melibiose	Carbohydrate

pullulan1200	-1000	1000	pullulan (n=1200 repeat units, alpha-1,4 and alph-1,6 bounds)	Carbohydrate
raffin	-1000	1000	Raffinose	Carbohydrate
rib_D	-1000	1000	D-Ribose	Carbohydrate
rmn	-1000	1000	L-Rhamnose	Carbohydrate
starch1200	-1000	1000	starch n=1200 repeat units (300 repeat units amylose, 900 repeat units amylopectin, corresponds to potatoe starch)	Carbohydrate
sucr	-1000	1000	Sucrose	Carbohydrate
tre	-1000	1000	Trehalose	Carbohydrate
xyl3	-1000	1000	xylotriose	Carbohydrate
xyl_D	-1000	1000	D-Xylose	Carbohydrate
xylan12	-1000	1000	Xylan (12 backbone units, 3 glcur side chain)	Carbohydrate
xylan4	-1000	1000	Xylan (4 backbone units, 1 glcur side chain)	Carbohydrate
xylan8	-1000	1000	Xylan (8 backbone units, 2 glcur side chain)	Carbohydrate
xylb	-1000	1000	Xylobiose	Carbohydrate
co2	-1000	1000	CO2	Ions and Small Molecules
fe2	-1000	1000	Fe2+	Ions and Small Molecules
fe3	-1000	1000	Fe3+	Ions and Small Molecules
h	-1000	1000	H+	Ions and Small Molecules
h2	-1000	1000	H2	Ions and Small Molecules

h2o	-1000	1000	H2O	Ions and Small Molecules
h2s	-1000	1000	Hydrogen sulfide	Ions and Small Molecules
hco3	-1000	1000	Bicarbonate	Ions and Small Molecules
mg2	-1000	1000	magnesium	Ions and Small Molecules
na1	-1000	1000	Sodium	Ions and Small Molecules
nh4	-1000	1000	Ammonium	Ions and Small Molecules
pi	-1000	1000	Phosphate	Ions and Small Molecules
s	-1000	1000	Sulfur	Ions and Small Molecules
zn2	-1000	1000	Zinc	Ions and Small Molecules
csn	0	1000	Cytosine	Nucleic Acids and Derivatives
ura	0	1000	Uracil	Nucleic Acids and Derivatives
xan	0	1000	Xanthine	Nucleic Acids and Derivatives
xtsn	0	1000	Xanthosine	Nucleic Acids and Derivatives

Supplemental Table S13: Table showing media constraints used in random deletion simulations for the iJR904 GEM.

Compound ID	Lower Limit	Upper Limit	Compound Name	Compound Category
15dap	0	1000	_1,5-Diaminopentane	Amino Acid
akg	0	1000	_2-Oxoglutarate	Amino Acid
ala-D	0	1000	D-Alanine	Amino Acid
ala-L	0	1000	L-Alanine	Amino Acid
arg-L	0	1000	L-Arginine	Amino Acid
asn-L	0	1000	L-Asparagine	Amino Acid
asp-L	0	1000	L-Aspartate	Amino Acid
crn	0	1000	L-Carnitine	Amino Acid
cys-L	0	1000	L-Cysteine	Amino Acid
gbbtn	0	1000	gamma-butyrobetaine	Amino Acid
gln-L	0	1000	L-Glutamine	Amino Acid
glu-L	0	1000	L-Glutamate	Amino Acid
gly	0	1000	Glycine	Amino Acid
his-L	0	1000	L-Histidine	Amino Acid
ile-L	0	1000	L-Isoleucine	Amino Acid
indole	0	1000	Indole	Amino Acid
leu-L	0	1000	L-Leucine	Amino Acid
lys-L	0	1000	L-Lysine	Amino Acid
met-D	0	1000	D-Methionine	Amino Acid
met-L	0	1000	L-Methionine	Amino Acid
orn	0	1000	Ornithine	Amino Acid
phe-L	0	1000	L-Phenylalanine	Amino Acid
pro-L	0	1000	L-Proline	Amino Acid
ptrc	0	1000	Putrescine	Amino Acid
ser-D	0	1000	D-Serine	Amino Acid
ser-L	0	1000	L-Serine	Amino Acid
spmd	0	1000	Spermidine	Amino Acid
tartr-L	0	1000	L-tartrate	Amino Acid
taur	0	1000	Taurine	Amino Acid
thr-L	0	1000	L-Threonine	Amino Acid
trp-L	0	1000	L-Tryptophan	Amino Acid
tyr-L	0	1000	L-Tyrosine	Amino Acid

val-L	0	1000	L-Valine	Amino Acid
12ppd-S	-1000	1000	(S)-Propane-1,2-diol	Carbohydrate
2ddglcn	-1000	1000	_2-Dehydro-3-deoxy-D-gluconate	Carbohydrate
3hcinnm	-1000	1000	_3-hydroxycinnamic acid	Carbohydrate
3hpppn	-1000	1000	_3-(3-hydroxy-phenyl)propionate	Carbohydrate
4abut	-1000	1000	_4-Aminobutanoate	Carbohydrate
ac	-1000	1000	Acetate	Carbohydrate
acac	-1000	1000	Acetoacetate	Carbohydrate
acald	-1000	1000	Acetaldehyde	Carbohydrate
acgam	-1000	1000	N-Acetyl-D-glucosamine	Carbohydrate
acmana	-1000	1000	N-Acetyl-D-mannosamine	Carbohydrate
acnam	-1000	1000	N-Acetylneuraminate	Carbohydrate
arab-L	-1000	1000	L-Arabinose	Carbohydrate
but	-1000	1000	Butyrate (n-C4:0)	Carbohydrate
cit	-1000	1000	Citrate	Carbohydrate
for	-1000	1000	Formate	Carbohydrate
fru	-1000	1000	D-Fructose	Carbohydrate
fuc-L	-1000	1000	L-Fucose	Carbohydrate
fuc1p-L	-1000	1000	L-Fucose 1-phosphate	Carbohydrate
fum	-1000	1000	Fumarate	Carbohydrate
g6p	-1000	1000	D-Glucose 6-phosphate	Carbohydrate
gal	-1000	1000	D-Galactose	Carbohydrate
galct-D	-1000	1000	D-Galactarate	Carbohydrate
galctn-D	-1000	1000	D-Galactonate	Carbohydrate
galt	-1000	1000	Galactitol	Carbohydrate
galur	-1000	1000	D-Galacturonate	Carbohydrate

gam	-1000	1000	D-Glucosamine	Carbohydrate
glc-D	-1000	1000	D-Glucose	Carbohydrate
glcn	-1000	1000	D-Gluconate	Carbohydrate
glcr	-1000	1000	D-Glucarate	Carbohydrate
glcur	-1000	1000	D-Glucuronate	Carbohydrate
glyald	-1000	1000	D-Glyceraldehyde	Carbohydrate
glyc	-1000	1000	Glycerol	Carbohydrate
glyc3p	-1000	1000	Glycerol 3-phosphate	Carbohydrate
glyclt	-1000	1000	Glycolate	Carbohydrate
idon-L	-1000	1000	L-Idonate	Carbohydrate
lac-D	-1000	1000	D-Lactate	Carbohydrate
lac-L	-1000	1000	L-Lactate	Carbohydrate
lcts	-1000	1000	Lactose	Carbohydrate
mal-L	-1000	1000	L-Malate	Carbohydrate
malt	-1000	1000	Maltose	Carbohydrate
malthx	-1000	1000	Maltohexaose	Carbohydrate
maltpt	-1000	1000	Maltopentaose	Carbohydrate
malttr	-1000	1000	Maltotriose	Carbohydrate
maltttr	-1000	1000	Maltotetraose	Carbohydrate
man	-1000	1000	D-Mannose	Carbohydrate
man6p	-1000	1000	D-Mannose 6-phosphate	Carbohydrate
melib	-1000	1000	Melibiose	Carbohydrate
mnl	-1000	1000	D-Mannitol	Carbohydrate
pppn	-1000	1000	Phenylpropanoate	Carbohydrate
pyr	-1000	1000	Pyruvate	Carbohydrate
rib-D	-1000	1000	D-Ribose	Carbohydrate
rmn	-1000	1000	L-Rhamnose	Carbohydrate
sbt-D	-1000	1000	D-Sorbitol	Carbohydrate
succ	-1000	1000	Succinate	Carbohydrate
sucr	-1000	1000	Sucrose	Carbohydrate
tre	-1000	1000	Trehalose	Carbohydrate
xyl-D	-1000	1000	D-Xylose	Carbohydrate
26dap-M	0	1000	meso-2,6-Diaminoheptanedioate	Cell Wall
co2	-1000	1000	CO2	Ions and Small Molecules

cynt	-1000	1000	Cyanate	Ions and Small Molecules
dms	-1000	1000	Dimethyl sulfide	Ions and Small Molecules
dmso	-1000	1000	Dimethyl sulfoxide	Ions and Small Molecules
etoh	-1000	1000	Ethanol	Ions and Small Molecules
fe2	-1000	1000	Fe2+	Ions and Small Molecules
h	-1000	1000	H+	Ions and Small Molecules
h2o	-1000	1000	H2O	Ions and Small Molecules
k	-1000	1000	potassium	Ions and Small Molecules
na1	-1000	1000	Sodium	Ions and Small Molecules
nh4	-1000	1000	Ammonium	Ions and Small Molecules
no2	-1000	1000	Nitrite	Ions and Small Molecules
no3	-1000	1000	Nitrate	Ions and Small Molecules
o2	-1000	1000	O2	Ions and Small Molecules
pi	-1000	1000	Phosphate	Ions and Small Molecules
so4	-1000	1000	Sulfate	Ions and Small Molecules
tma	-1000	1000	trimethylamine	Ions and Small Molecules
tmao	-1000	1000	Trimethylamine N-oxide	Ions and Small Molecules
tsul	-1000	1000	Thiosulfate	Ions and Small Molecules
urea	-1000	1000	Urea	Ions and Small Molecules
hdca	0	1000	Hexadecanoate (n-C16:0)	Lipid
ocdca	0	1000	octadecanoate (n-C18:0)	Lipid
ttdca	0	1000	tetradecanoate (n-C14:0)	Lipid

ade	0	1000	Adenine	Nucleic Acids and Derivatives
adn	0	1000	Adenosine	Nucleic Acids and Derivatives
alltn	0	1000	Allantoin	Nucleic Acids and Derivatives
amp	0	1000	AMP	Nucleic Acids and Derivatives
csn	0	1000	Cytosine	Nucleic Acids and Derivatives
cytd	0	1000	Cytidine	Nucleic Acids and Derivatives
dad-2	0	1000	Deoxyadenosine	Nucleic Acids and Derivatives
dcyt	0	1000	Deoxycytidine	Nucleic Acids and Derivatives
dgsn	0	1000	Deoxyguanosine	Nucleic Acids and Derivatives
dha	0	1000	Dihydroxyacetone	Nucleic Acids and Derivatives
din	0	1000	Deoxyinosine	Nucleic Acids and Derivatives
duri	0	1000	Deoxyuridine	Nucleic Acids and Derivatives
gsn	0	1000	Guanosine	Nucleic Acids and Derivatives
gua	0	1000	Guanine	Nucleic Acids and Derivatives
hxan	0	1000	Hypoxanthine	Nucleic Acids and Derivatives
ins	0	1000	Inosine	Nucleic Acids and Derivatives
thymd	0	1000	Thymidine	Nucleic Acids and Derivatives
ura	0	1000	Uracil	Nucleic Acids and Derivatives
uri	0	1000	Uridine	Nucleic Acids and Derivatives
xan	0	1000	Xanthine	Nucleic Acids and Derivatives
xtsn	0	1000	Xanthosine	Nucleic Acids and Derivatives
cbl1	-1000	1000	Cob(I)alamin	Vitamins
chol	-1000	1000	Choline	Vitamins
glyb	-1000	1000	Glycine betaine	Vitamins

nac	-1000	1000	Nicotinate	Vitamins
nad	-1000	1000	Nicotinamide adenine dinucleotide	Vitamins
nmn	-1000	1000	NMN	Vitamins
pnto-R	-1000	1000	(R)-Pantothenate	Vitamins
thm	-1000	1000	Thiamin	Vitamins